LUMINESCENCE DATING OF WIND BLOWN SANDS FROM ARCHAEOLOGICAL SITES IN NORTHERN SCOTLAND

ANNE AMANDA SOMMERVILLE

DEPARTMENT OF GEOGRAPHY AND TOPOGRAPHIC SCIENCE

UNIVERSITY OF GLASGOW

Presented as a thesis for the degree of Doctor of Philosophy

in the University of Glasgow

February 2003

Abstract

The sheltered bays of the Orkney Islands are backed by extensive dune systems that commonly contain archaeological sites, many of which now protrude from cliffed sections due to coastal erosion. In an area where other dating techniques are often precluded due to a lack of organic dating material, this research establishes that optically stimulated luminescence (OSL) dating can provide a viable and robust alternative by dating wind blown sands within the sites to constrain the archaeological age. Since this is the case, the OSL chronology can also be applied to natural sites where no archaeological chronology exists and so be used in palaeoenvironmental reconstruction.

Six periods of increased sand movement are recorded in the Orkney Islands at the sites sampled; the Neolithic, the Bronze Age, two periods in the Iron Age, the Viking/Medieval period and the Little Ice Age. The phases of sand movement identified using OSL in the Orkney Islands are also identified at other sites in Scotland and north-west Europe and support the chronologies derived from other environmental indicators such as tree rings and peat bogs. It is suggested that at least two events may be related to the deterioration in climate subsequent to the eruption of Hekla 4 in the late Neolithic and Hekla 3 in the late Bronze Age.

However, OSL dating requires that the latent luminescence signal within quartz and feldspar is rapidly reduced to near zero by exposure to light, yet the rate and extent of bleaching depends on the length of time that the grains are exposed and the light intensity at the time of exposure. Bleaching experiments used here confirmed that not only is there a difference in the rate of bleaching between quartz and feldspar depending on the light intensity, but that there is also a difference in the rate of bleaching between samples from different geological areas and this needs to be taken into account in future research.

The residual levels from the Orcadian modern beach sands (<0.5 Gy) suggest that some samples collected for OSL dating may be partially bleached and a new technique, the psi (ψ) ratio, is proposed here to identify partially bleached sediments. This technique uses the shape of the natural and regenerated decay curves from associated feldspar and determines the ratio based on the differences between the two curves. The decay curve of samples well-bleached at deposition will be similar to the regenerated decay curve, whereas those partially bleached have a residual component which flattens the shape of the decay curve. Further analysis of such decay curves is required in future research.

Declaration

Except where specific reference is made to other sources, the work presented here in this thesis is the original work of the author. It has not been submitted, in part or in whole, for any other degree.

Anne A. Sommerville

Acknowledgements

This research was funded by the Physical Sciences Graduate School, Department of Archaeology and SUERC, and fieldwork was funded by RSGS, BGRG and Carnegie Trust. Thanks also to the School of History and Archaeology, SUERC and the Department of Geography and Topographic Science for their contributions towards attending conferences.

I would like to thank my supervisors Drs. Jim Hansom, Rupert Housley and David Sanderson for their help, guidance and encouragement throughout the research. I have finally submitted a thesis and I can only hope that it has contributed to all three departments in some way. Despite all the ups and downs it has been an enjoyable experience and I have gained so much over the past 4 (and a bit!) years.

This research has introduced the Orkney Islands and the Outer Hebrides to me, places that the Scottish do not tend to go. I will be back. Perhaps one of the more interesting field trips was the search for sand on Eday and I must thank Alistair Rennie who dug many test pits through thick peat deposits in the pouring rain. I would also like to thank Dr L. Carmichael, Dr. A. Cresswell, Simon Murphy, Colin Kerr, Iona Anthony and Ian Houston at SUERC for their advice and help during sample preparation and measurement. Thanks also to Steve Anderson for emailing diagrams when required.

I have spent much of my time at the Department of Geography and Topographic Science and I would like to thank all those who have contributed towards making it an enjoyable experience and have freely given help and advice when required. I would like to thank the staff and post-graduates for their patience and tolerance due to the inevitable ups and downs of writing a thesis. I would especially like to thank Ali Rennie, Stephen Thomson (a great office mate who has put up with the pacing and frustration for over three years – we have both finally submitted!) and Nicola Burns who has always managed to give me encouragement when most required.

Finally I would like to thank my husband and my family who have supported me from the beginning and encouraged me throughout this research. The past few months have been tough and I hope they realise how much they have helped, whether it be with drawing diagrams, proof-reading, or escaping for the odd pint!

Thank you to you all.

LIST OF FIGURES

Page

Chapter 2

Chapter 3

LIST OF TABLES

Chapter 2

Chapter 3

Chapter 4

Chapter 5

APPENDICES

Chapter 1 – Introduction

1.1 Introduction

Since Neolithic, or possibly even Mesolithic, times (approximately 6000 years ago) humans have inhabited the sheltered bays located within the windswept and rugged coastlines of the Orkney Islands. Today the islands are mostly devoid of native woodland and the cool and windy climate ensures that the vegetation is sparse and low-lying. However, during Neolithic times, the climate was warmer allowing both tree growth and a variety of crops to be grown in these northern locations (Dickson 2000). Such conditions have ensured that the Orkney Islands are rich in archaeological sites and the lack of industrial or residential development in these northern locations has also favoured the survival of numerous sites. In addition, many previously concealed archaeological sites have been discovered as they have been exposed in eroding clifflines. Although, originally situated inland the sites have emerged as the sea slowly encroached due to glacio-isostasy and rising sea levels. However, dating such sites is problematic due to a lack of preserved organic material, often precluding the use of radiocarbon dating (Campbell *et al.* in press). Wood is sometimes found within archaeological sites but it may not be local; driftwood from North America or mainland Europe washed up on the shore is likely to have been used for construction or fuel (Dickson 1992). Archaeological sites in Orkney are often dated based on the structure and form of the monument being excavated. The flagstone nature of the bedrock geology in Orkney is ideal for construction but, with few other dating methods available, many of the sites are placed within a wide age bracket reflecting broad periods of time.

This research addresses the problem of dating both archaeological and non-archaeological sites in the Orkney Islands by using wind blown sands deposited on these sites and sampled for optically stimulated luminescence (OSL) dating. OSL dating of the wind blown sands that bury and are found within these sites may prove to be a viable alternative dating method which can accurately date archaeological sites and provide the archaeologist with information on the construction, abandonment and re-occupation of multiphased sites. If this is the case then OSL dating can be applied to sites where archaeological dating is problematic or completely absent.

Throughout the Orkney Islands large sandy bays are often backed by dune systems, which have slowly encroached inland as sea level has risen since the last glaciation. The movement of sand over this period has caused sites to be slowly or rapidly engulfed by sand only to be subsequently subject to large storm events and coastal erosion. For example, the World Heritage Site of Skara Brae on Mainland Orkney was discovered in such a way about AD 1850, and is generally thought to have been abandoned during a sand storm in the Neolithic, that buried the village which was then further inland (Childe 1931). Many of such archaeological sites in the Orkney Islands have either been built directly onto wind-blown sand within dune systems or have inter-stratified sand layers suggesting some period of complete, or temporary, abandonment of the site.

Optically stimulated luminescence dating requires that sediments are well-bleached upon deposition due to their exposure to light during transportation (Aitken 1998). This should make OSL an ideal dating method to use on wind blown sands, however, the amount of light to which the sediment is exposed can vary due to cloud conditions, latitude and time of day and there is a chance that some sediments may be only partially bleached (Aitken 1998). In order to accept the OSL dates from the archaeological sites with confidence, it is important to understand the bleaching process in the study area and determine how spectral variations in natural light can affect the bleaching rate. Bleaching experiments undertaken here on sand collected from modern beaches should provide information on the extent and rate of such bleaching. The geology of the Orkney Islands is dominated by Old Red Sandstone and therefore to determine if the source of the sediment, i.e. the crystal structure, affects the rate of bleaching, samples were also collected from a comparable area characterised by a different geology (the Outer Hebrides which are mainly composed of Lewisian Gneiss).

It is hoped to show here that OSL dating of wind blown sands from archaeological sites and coastal sediments is a robust technique that has the potential to provide a chronostratigraphic framework that will aid both archaeological interpretation and climate reconstruction.

1.2 Aims of Research

- The main aim of this research is to establish whether OSL can provide a reliable and robust method for dating wind blown sands from archaeological sites in the Orkney Islands. OSL chronologies are powerful tools that allow dating to extend beyond sites occupied by humans into natural sites and so establish climatic trends and signatures. Using the OSL dates from the archaeological sites it is hoped to identify periods of increased storminess in the Holocene in the Orkney Islands that correlate with other periods of climatic instability elsewhere in north-west Europe.

- An essential requirement of successful and robust OSL dating of environmental change is that the sand is well-bleached prior to burial. In order to establish this, experiments have been undertaken to determine the extent of bleaching of modern beach sands from Orkney and a comparable area and the rate of bleaching of quartz and feldspar in controlled and natural conditions. An understanding of the controls on the rate and degree of bleaching is of vital importance in assigning degrees of confidence to any OSL date on sediments. This research addresses such questions.

1.3 Outline of the thesis

Chapter 2 starts by concentrating on the study area and introduces the geology, geomorphology and archaeology of the Orkney Islands and Outer Hebrides. This is followed by a review of the luminescence literature from the early experiments involving thermoluminescence to date marine sediments, through to the development of optically stimulated luminescence dating used today. The chapter continues by discussing the development of the Single Aliquot Regenerative (SAR) technique and concludes by examining the Orkney Islands as an ideal location to test both the SAR technique and the assumption that quartz grains bleach rapidly when exposed to natural light.

Chapter 3 concentrates on the fieldwork, sampling and laboratory methods used in the study and is split into two sections. The selection of the modern beaches and archaeological sites sampled in this research is discussed in Section 1 and includes a brief summary of the sample collection methodology. This is followed by a review of previous research and sampling of the individual archaeological sites and a brief summary of sample preparation methods. The rate and extent of bleaching is an integral part of the OSL dating

technique and the experimental procedures used to determine the residual levels and bleaching rates of the modern beach sands are outlined in Section 2 before the modified SAR procedure used to date the archaeological samples is introduced.

The results from the bleaching experiments and dating of archaeological samples are presented and discussed in Chapters 4 and 5. The first part of Chapter 4 examines the rate and extent of bleaching in high latitude areas and the effect this may have on dating sand from archaeological sites in these areas. This is followed by the introduction of a potential new method (the psi (ψ) ratio) to identify partially bleached samples based on the shape of associated feldspar decay curves.

In Chapter 5 the various aspects of the SAR procedure used in this research are discussed and assessed to determine whether it is robust enough to successfully date wind blown sands from archaeological and non-archaeological dune sites in the Orkney Islands. The remainder of the chapter presents and discusses the significance of the OSL dates obtained from the sites studied and how they can illuminate environmental changes both at these sites and adjacent areas.

Chapter 6 sets the Orkney OSL dating results into a wider context and discusses whether the periods of increased storminess that have been identified across northern Europe throughout history and prehistory are also recognised within the Orkney Islands. It goes on to assess the extent to which these events may have affected the local communities.

Chapter 7 forms the conclusions and presents ideas for future research.

Chapter 2 – Background to Study

2.1 Introduction

The aim of this chapter is to introduce the study area and to present the background literature on optically stimulated luminescence dating before outlining the main assumptions and problems associated with the technique.

It is important to understand why the Orkney Islands were chosen for the focus of this research and this is discussed briefly before presenting a short summary of the geological and glacial history of the islands. Samples from present day beaches in the Outer Hebrides are also included in the modern beach analysis discussed in Chapter 4, in order to allow the luminescence properties of quartz from a different bedrock geology to be compared with that of the Orkney Islands. Therefore, a brief background to the geology and glacial history of the Outer Hebrides has also been included. The archaeological history of the two island groups is also briefly summarised citing the most important sites and environmental information. This research concentrates on the movement of wind blown sands during the Holocene and how this may have impacted on the local population and therefore references to known historic and inferred prehistoric periods of increased sand movement within Scotland and northern Europe are presented.

The section on the background to optically stimulated luminescence dating includes the main principles behind luminescence dating and the more recent developments of the technique to include unheated sediments where light is used to optically stimulate the traps. The chapter concludes by outlining the main problems in luminescence dating that remain to be addressed and how this research aims to address some of these questions.

2.2 The Study Area

Although the core of the study area is the Orkney Islands, for comparative purposes the field area extends to the Outer Hebrides (Figure 2.1). Both areas are today characterised by treeless and windswept landscapes whose coasts are commonly backed by extensive aeolian depositional systems. A large number of archaeological sites exist within these dune areas, but the use of radiocarbon dating is frequently precluded due to a lack of

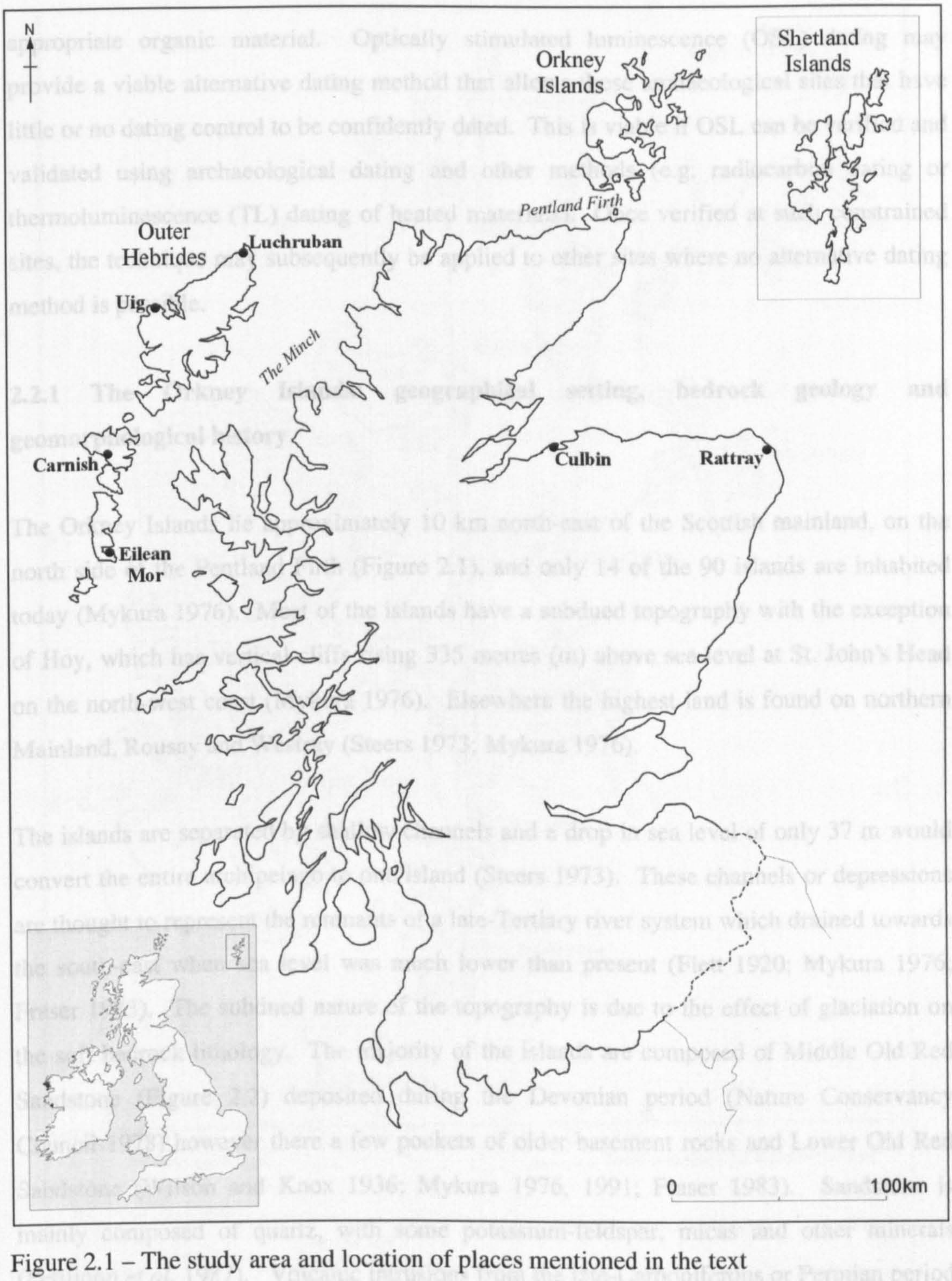

Figure 2.1 – The study area and location of places mentioned in the text

appropriate organic material. Optically stimulated luminescence (OSL) dating may provide a viable alternative dating method that allows those archaeological sites that have little or no dating control to be confidently dated. This is viable if OSL can be verified and validated using archaeological dating and other methods (e.g. radiocarbon dating or thermoluminescence (TL) dating of heated materials). Once verified at such constrained sites, the technique may subsequently be applied to other sites where no alternative dating method is possible.

2.2.1 The Orkney Islands: geographical setting, bedrock geology and geomorphological history

The Orkney Islands lie approximately 10 km north-east of the Scottish mainland, on the north side of the Pentland Firth (Figure 2.1), and only 14 of the 90 islands are inhabited today (Mykura 1976). Most of the islands have a subdued topography with the exception of Hoy, which has vertical cliffs rising 335 metres (m) above sea level at St. John's Head on the north-west coast (Mykura 1976). Elsewhere the highest land is found on northern Mainland, Rousay and Westray (Steers 1973; Mykura 1976).

The islands are separated by shallow channels and a drop in sea level of only 37 m would convert the entire archipelago to one island (Steers 1973). These channels or depressions are thought to represent the remnants of a late-Tertiary river system which drained towards the south-east when sea level was much lower than present (Flett 1920; Mykura 1976; Fraser 1983). The subdued nature of the topography is due to the effect of glaciation on the soft bedrock lithology. The majority of the islands are composed of Middle Old Red Sandstone (Figure 2.2) deposited during the Devonian period (Nature Conservancy Council 1978) however there a few pockets of older basement rocks and Lower Old Red Sandstone (Wilson and Knox 1936; Mykura 1976, 1991; Fraser 1983). Sandstone is mainly composed of quartz, with some potassium-feldspar, micas and other minerals (Pettijohn *et al.* 1987). Volcanic intrusions from the late-Carboniferous or Permian period occur throughout the southern and western parts of the Orkney archipelago although none appear in the Northern Isles (Mykura 1976; Fraser 1983).

During the Quaternary glacial period in Orkney the remnant river channels of the late-Tertiary river system are thought to have channelled ice flow (Fraser 1983). Throughout the past 120 years there have been various models to explain how and when the Orkney

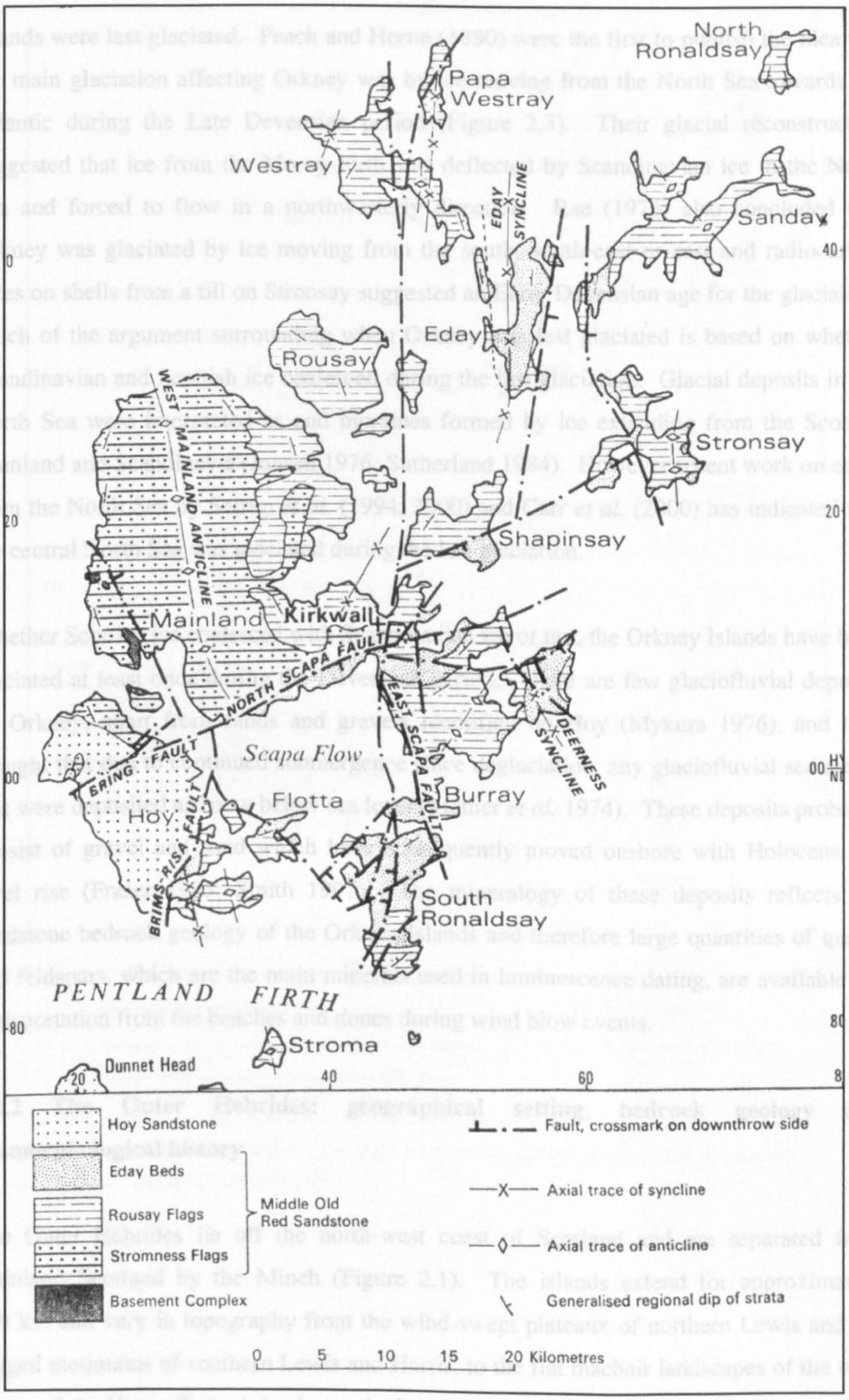

Figure 2.2 – Geology of the Orkney Islands (after Mykura 1976)

Islands were last glaciated. Peach and Horne (1880) were the first to publish the idea that the main glaciation affecting Orkney was by ice moving from the North Sea towards the Atlantic during the Late Devensian period (Figure 2.3). Their glacial reconstruction suggested that ice from the Moray Firth was deflected by Scandinavian ice in the North Sea and forced to flow in a northwesterly direction. Rae (1976) also concluded that Orkney was glaciated by ice moving from the south, south-east or east and radiocarbon dates on shells from a till on Stronsay suggested an Early Devensian age for the glaciation. Much of the argument surrounding when Orkney was last glaciated is based on whether Scandinavian and Scottish ice coalesced during the last glaciation. Glacial deposits in the North Sea were interpreted as end moraines formed by ice extending from the Scottish mainland and Scandinavia (Jansen 1976; Sutherland 1984). However recent work on cores from the North Sea by Sejrup *et al.* (1994, 2000) and Carr *et al.* (2000) has indicated that the central North Sea was glaciated during the last glaciation.

Whether Scottish ice coalesced with Scandinavian ice or not, the Orkney Islands have been glaciated at least once during the Devensian period. There are few glaciofluvial deposits on Orkney, apart from sands and gravels identified on Hoy (Mykura 1976), and it is thought that due to continued submergence since deglaciation, any glaciofluvial sediments that were deposited are now below sea level (Mather *et al.* 1974). These deposits probably consist of gravel and sand which have subsequently moved onshore with Holocene sea level rise (Fraser 1983; Smith 1997). The mineralogy of these deposits reflects the sandstone bedrock geology of the Orkney Islands and therefore large quantities of quartz and feldspars, which are the main minerals used in luminescence dating, are available for transportation from the beaches and dunes during wind blow events.

2.2.2 The Outer Hebrides: geographical setting, bedrock geology and geomorphological history

The Outer Hebrides lie off the north-west coast of Scotland and are separated from mainland Scotland by the Minch (Figure 2.1). The islands extend for approximately 200 km and vary in topography from the wind-swept plateaux of northern Lewis and the rugged mountains of southern Lewis and Harris, to the flat machair landscapes of the west coasts of the Uists. Today's landscape is the result of weathering processes, glaciation and sea level change acting on the bedrock geology.

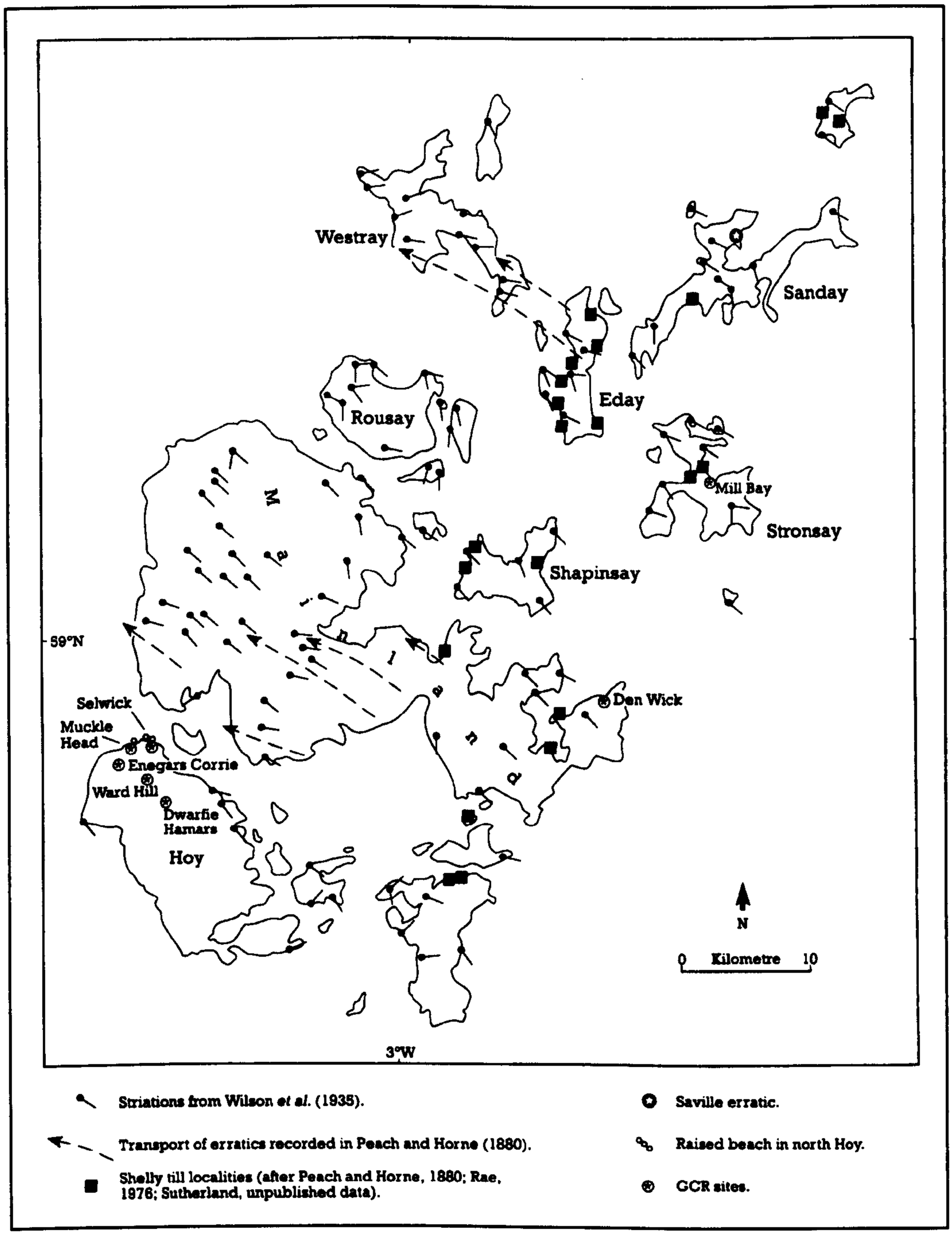

Figure 2.3 – Ice flow movements in the Orkney Islands during the last glaciation (after Sutherland and Gordon 1993).

Although sedimentary rocks surround Stornoway, and igneous intrusions occur in South Harris, the geology of the Outer Hebrides is dominated by Lewisian Gneiss (Figure 2.4) (Jehu and Craig 1933; Whittow 1992). Lewisian Gneiss is a hard and ancient crystalline rock mainly composed of quartz, feldspar and hornblende gneisses (T. Dempster *pers. comm.*) formed approximately 2900 million years (Ma) ago (Hall 1996). Originally sedimentary and igneous, they have since experienced at least two periods of intense metamorphism and deformation during phases of Precambrian mountain building (Whittow 1992).

The landscape seen today has been fundamentally influenced by Quaternary glaciation and weathering processes. Geikie (1873, 1878) was the first to suggest that the Outer Hebrides was overrun by ice from mainland Scotland, based on observations of roches moutonnées, striations and erratics throughout the island chain that appeared to represent ice movement from the south-east. Research by Sissons (1967) proposed that the highest ground in northern Harris may have supported its own local glaciers throughout the last glacial maximum. This was confirmed by Flinn (1978) and von Weymarn (1979) who mapped striations and glacially streamlined landforms that displayed a pattern of radial ice flow originating from three ice centres.

Very little work has been carried out on the deglaciation of the Outer Hebrides, however von Weymarn (1979) and Peacock (1981, 1984) noted glaciofluvial features, mainly eskers, kames, glaciolacustrine deltas and meltwater channels at Carnish (Grid ref: NB 030 323) and Uig (Grid ref: NB 055 333) (Figure 2.1). The mineralogy of these deposits will mainly be quartz, feldspars and hornblende, eroded from the bedrock by the action of ice, and it is these sediments and those brought onshore by a rising sea level to the beaches and machair which are transported inland by the wind.

2.2.3 Sea level change in the Holocene

Sea level during the last glacial maximum would have been much lower than present, and much of the ice margin was probably marine (Hall and Bent 1990). Both the Orkney Islands and Outer Hebrides were located on the periphery of the main Scottish ice centre and thought to be close to zero isobase, which marks the point at which land closer to the ice centre undergoes continual emergence, and land beyond which experiences continual submergence (Ballantyne and Dawson 1997; Figure 2.5). The deep embayments found on

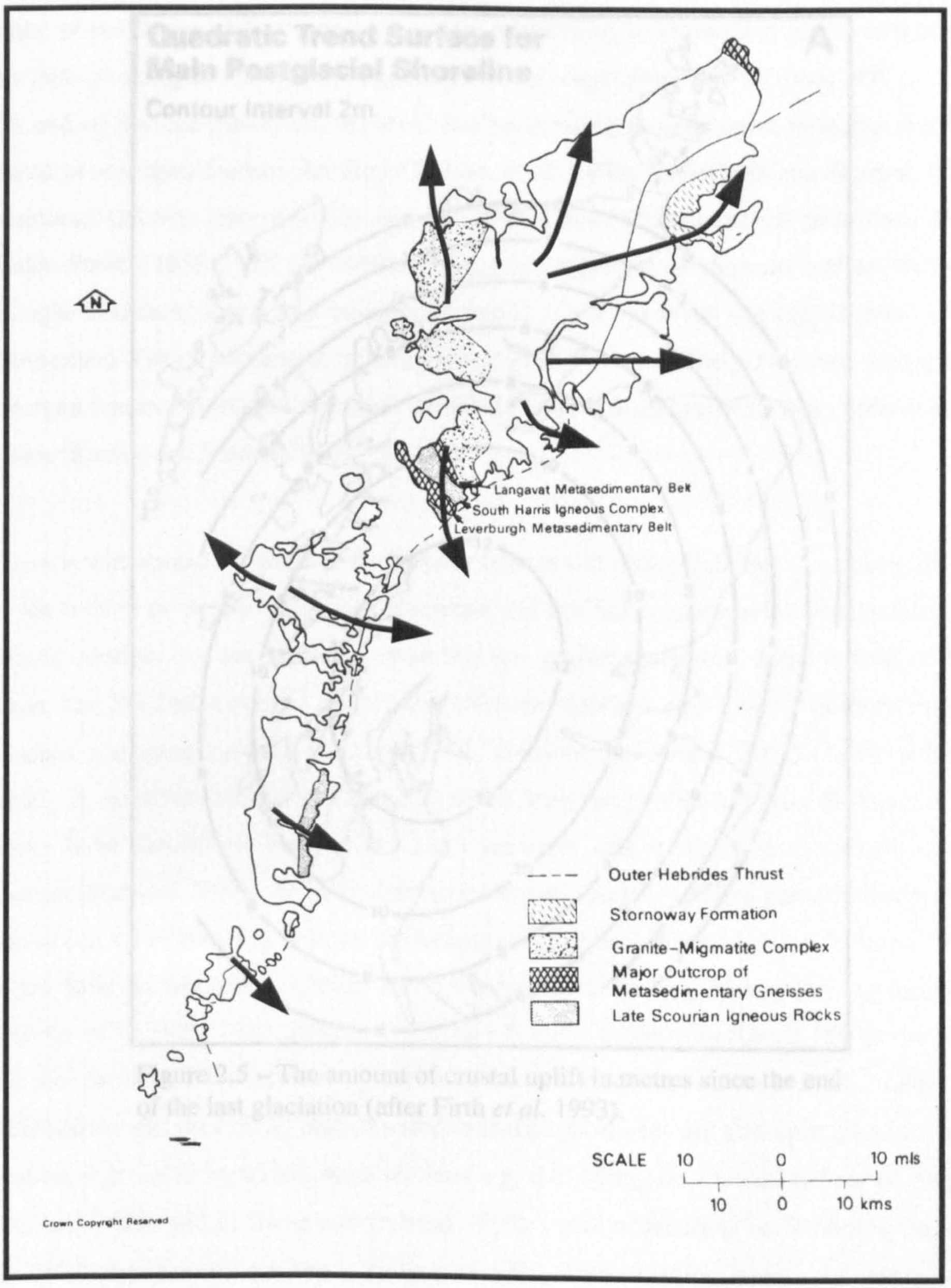

Figure 2.4 – Geology of the Outer Hebrides (after Nature Conservancy Council 1977) and the main ice flow directions during the last glaciation (after Sutherland and Gordon 1993). Lewisian gneiss is represented by the unshaded area.

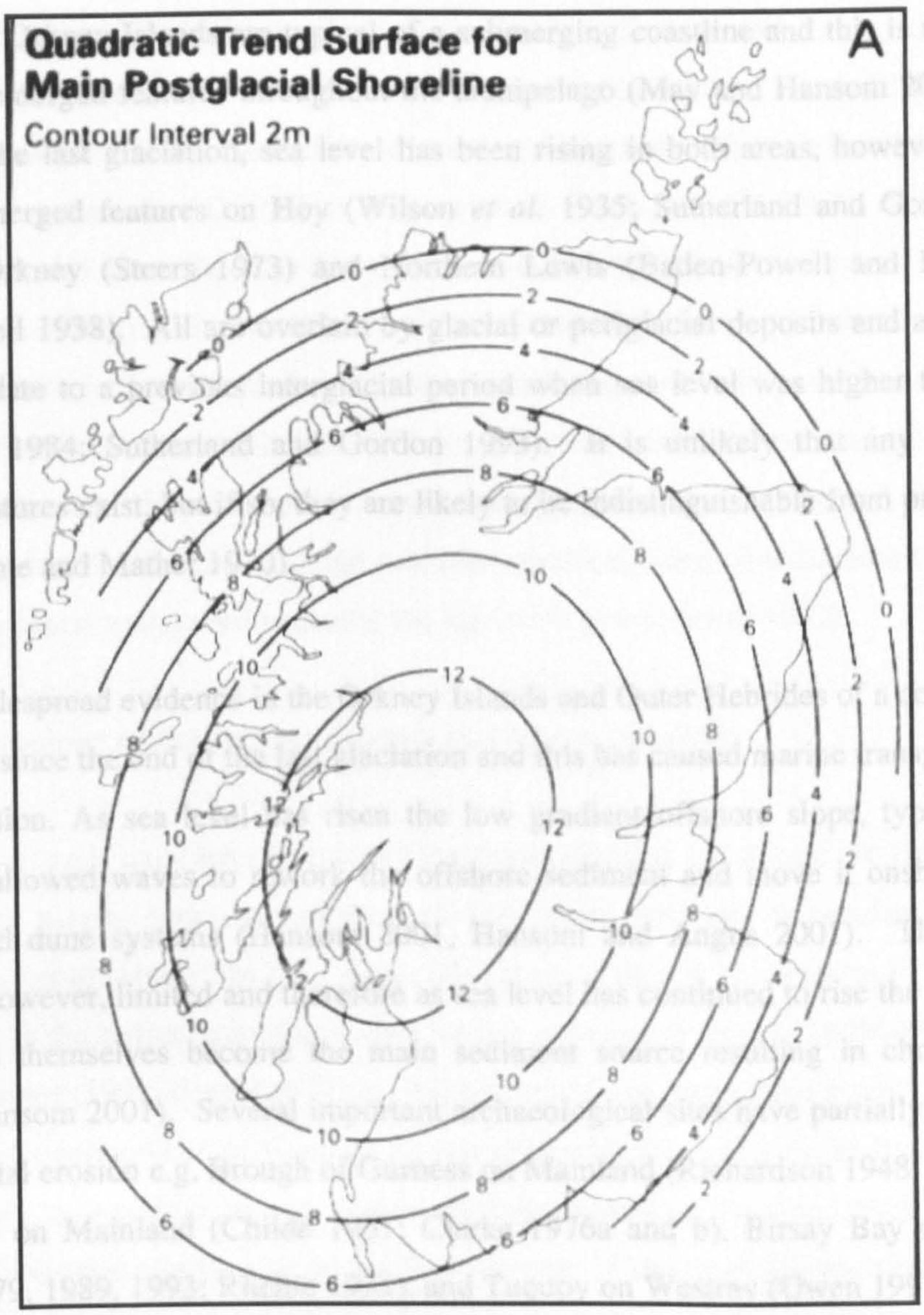

Figure 2.5 – The amount of crustal uplift in metres since the end of the last glaciation (after Firth *et al.* 1993).

many of the Orkney Islands are typical of a submerging coastline and this is reflected by the lack of emerged features throughout the archipelago (May and Hansom 2003). Since the end of the last glaciation, sea level has been rising in both areas, however there are traces of emerged features on Hoy (Wilson *et al.* 1935; Sutherland and Gordon 1993), Mainland Orkney (Steers 1973) and Northern Lewis (Baden-Powell and Elton 1937; Baden-Powell 1938). All are overlain by glacial or periglacial deposits and are therefore thought to date to a previous interglacial period when sea level was higher than present (Sutherland 1984; Sutherland and Gordon 1993). It is unlikely that any post-glacial emerged features exist, but if so, they are likely to be indistinguishable from present beach levels (Ritchie and Mather 1970).

There is widespread evidence in the Orkney Islands and Outer Hebrides of a consistent rise in sea level since the end of the last glaciation and this has caused marine transgression and coastal erosion. As sea level has risen the low gradient offshore slope, typical of both areas, has allowed waves to rework the offshore sediment and move it onshore to form beaches and dune systems (Hansom 2001, Hansom and Angus 2001). This sediment supply is, however, limited and therefore as sea level has continued to rise the beaches and dunes have themselves become the main sediment source resulting in chronic coastal erosion (Hansom 2001). Several important archaeological sites have partially disappeared due to coastal erosion e.g. Brough of Gurness on Mainland (Richardson 1948, Fojut 1993), Skara Brae on Mainland (Childe 1931; Clarke 1976a and b), Birsay Bay on Mainland (Morris 1979, 1989, 1993; Ritchie 1993), and Tuquoy on Westray (Owen 1993), and some are now protected from erosion by concrete barriers or sea walls (Fraser 1983). Other less well-known and previously undiscovered archaeological sites are also emerging as coastal erosion exposes them within dune sections e.g. the Viking boat burial at Scar on Sanday (Dalland 1992a and b; Owen and Dalland 1999), Links of Noltland on Westray (Clarke *et al.* 1978) and Galson on Lewis (Edwards 1924; Church 1998; Neighbour and Church 2001). These sites are unlikely to have been originally located so close to the coast. For example, at the Bay of Skaill on Mainland Orkney, Childe (1931) originally suggested that Skara Brae was located on a freshwater loch. Subsequently Vega Leinert *et al.* (2000) confirmed this through pollen analysis of peat exposed at low tide, which showed that freshwater deposits developed on top of glacial sediments. A dune ridge across the mouth of the bay retained the freshwater marsh (Vega Leinert *et al.* 2000) and therefore the coastline was originally located further to the west.

Other peat deposits exposed at low tide were found on Rousay and Sanday (Traill 1868) and Sissons (1967) identified nine locations of sub-tidal peat in the Orkney Islands. Some of the peat deposits contain the remains of trees and the most extensive forest was found at low tide after a storm in AD 1838 at Otterswick on Sanday (Traill 1868). Inter-tidal peat deposits have also been found in Northern Lewis and the Uists (Sutherland and Walker 1984; Ritchie 1985a). Those at Borve (North Uist) have been extensively studied and radiocarbon dating of the deposits suggests a rise in sea level of approximately 5 metres during the last 5000 years (Ritchie 1985a). The trees, peat and settlement sites would originally have been located further inland (Angus and Elliott 1992) and their location today at, or close to, the coastal edge provides good evidence of the amount of sea level change and coastal transgression during the last 5000 years (Armit 1992).

2.2.4 Archaeology of the Orkney Islands and Outer Hebrides

The Orkney Islands and Outer Hebrides have been occupied for at least the last 6000 years and possibly longer, however evidence of Mesolithic activities is problematic (Ritchie 1985b; Fojut *et al.* 1994). In the Outer Hebrides it is mostly in the form of vegetational disturbance in the pollen record and microscopic charcoal (Edwards 1996) and in Orkney Wickham-Jones (1994) describes lithics that are thought to date to this period. On Orkney, the Neolithic communities of Knap of Howar (Papa Westray) and Skara Brae (Mainland) are generally assumed to be the earliest definite human occupation (Berry 1985; Hall 1996). The Neolithic village at Skara Brae is one of the best known sites in Orkney, thought to have been occupied from approximately 3500 cal BC until 1900 cal BC at the latest, with one period of abandonment during this time due to sand inundation (Shepherd 1996). Although the two communities of Skara Brae and Knap of Howar are thought to have existed contemporaneously, they exhibit distinct material cultures in the form of different pottery styles, known respectively as Grooved Ware and Unstan Ware (Hedges 1986; Ritchie and Ritchie 1995).

Burial cairns, standing stones and stone circles also represent the Neolithic period in Scotland. In Orkney two types of chambered funerary tombs were constructed and reused over a long period of time (Schei and Moberg 1985; Ritchie 1995; Ritchie and Ritchie 1995). The Maes Howe type (e.g. Maes Howe, Quoyness, Quanterness) has a central chamber with a high corbelled roof and three or four side chambers often containing Grooved Ware (Ritchie 1985b, 1996; Hedges 1986). The stalled tomb (e.g. Midhowe,

Unstan and Isbister) has a main chamber that is divided into compartments by upright flagstones and Unstan Ware is normally associated (Schei and Moberg 1985; Ritchie 1985b; Hedges 1986).

The burial cairns, or passage graves, found in the Outer Hebrides are very different to those in Orkney, but again they were reused over many hundreds of years (Ritchie and Harman 1985). The oval or round chamber and the passage of the passage graves were initially constructed using large stones before being covered by a small circular cairn that supported the corbelled roofing. This cairn was then covered by a larger façade of small stones, which may only have been added after burials had ceased (Fojut *et al.* 1994).

Standing stones and stone circles are also associated with the Neolithic period in Scotland and appear to have had an important role in Neolithic society. Two of the most impressive stone circles in Orkney are the Ring of Brodgar and the Stones of Stenness, both situated on promontories separating the Lochs of Harray and Stenness (Figure 2.6). The Stones of Stenness are described as a typical henge monument with a circle of standing stones surrounded by a deep rock-cut ditch and outer bank (Ritchie 1975). Excavations in the 1970s revealed a hearth in the centre of the circle and the ditch contained the bones of cattle, sheep and dogs (Ritchie 1975). Calibrated radiocarbon dates from the bones suggest that the henge was built in the early 3rd millennium BC (Ritchie 1996). Cereal pollen grains were also found in the ditch surrounding the Stones (Caseldine and Whittington 1975) and because cereal crops are self-pollinating the presence of cereal pollen grains within the deposits indicates that arable farming was undertaken close to the site (Dickson and Dickson 2000). It is generally believed that the climate in Northern Scotland at the beginning of the Neolithic period was favourable for the growth of cereal crops, and grains have also been found in the oldest deposits at Skara Brae (Shepherd 1996) and in the ditch surrounding Maes Howe (Childe 1954). The Ring of Brodgar is thought to be slightly younger than the Stones of Stenness, although it has not been excavated and therefore it has not been possible to accurately date the monument (Ritchie 1996).

The best known prehistoric monument in the Outer Hebrides is the Callanish Stone Circle, which was constructed some time between 2900-2600 cal BC (Ashmore 1999). The pattern of stones is unique with a circle of stones, an avenue of 2 rows of stones towards the north and single rows of stones towards the south, east and west (Fojut *et al.* 1994).

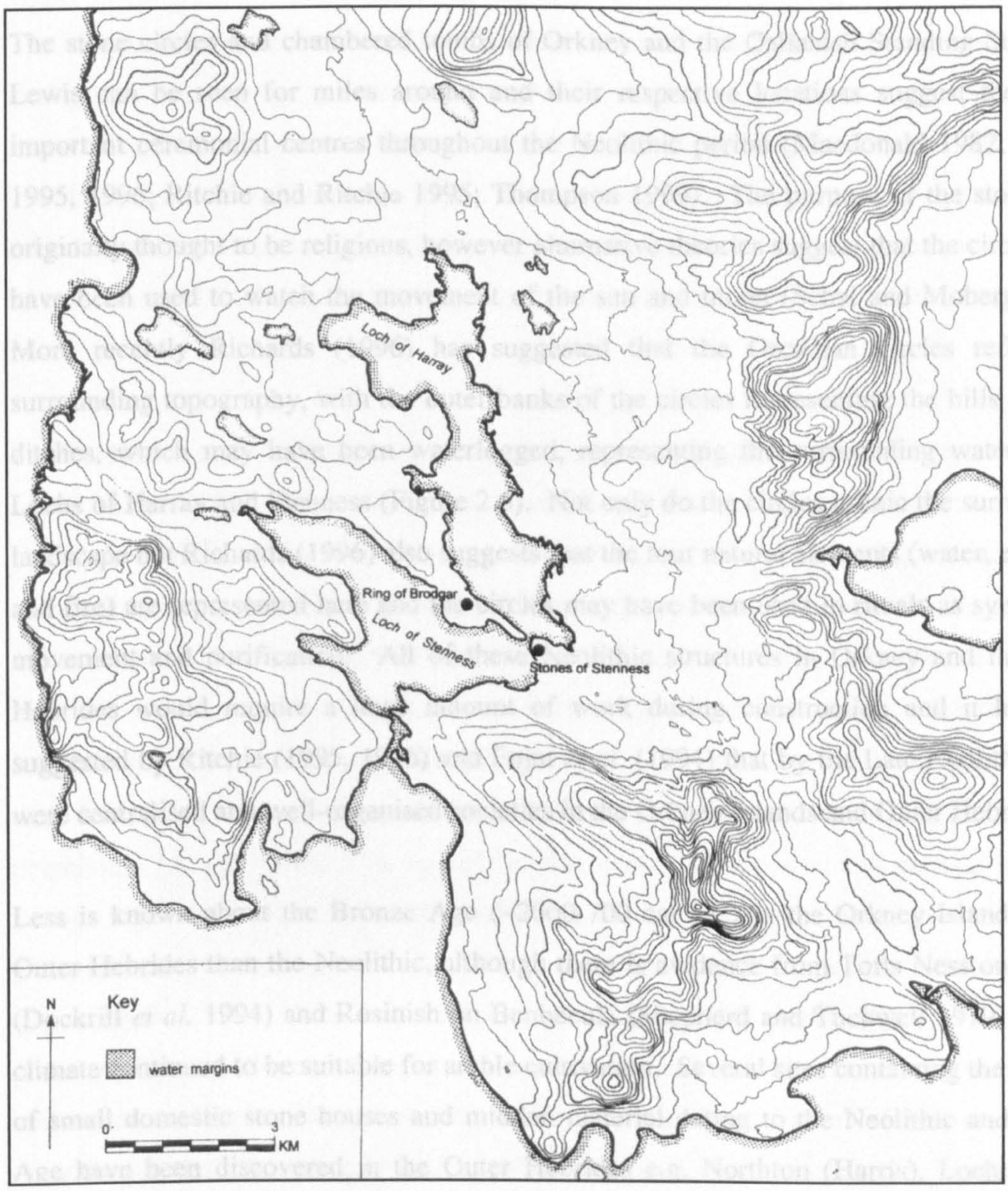

Figure 2.6 – Location of the Stones of Stenness and Ring of Brodgar on promontories between the Lochs of Stenness and Harray, west Mainland, Orkney. Contours in 50 ft intervals OD based on data from O.S. (after Richards 1996).

The stone circles and chambered tombs of Orkney and the Callanish Standing Stones on Lewis can be seen for miles around and their respective locations suggest they were important ceremonial centres throughout the Neolithic period (Macdonald 1982; Ritchie 1995, 1996; Ritchie and Ritchie 1995; Thompson 1999). The purpose of the stones was originally thought to be religious, however alternative theories suggest that the circles may have been used to watch the movement of the sun and moon (Schei and Moberg 1985). More recently Richards (1996) has suggested that the Orcadian circles reflect the surrounding topography, with the outer banks of the circles representing the hills, and the ditches, which may have been waterlogged, representing the surrounding water of the Lochs of Harray and Stenness (Figure 2.6). Not only do the circles mimic the surrounding landscape but Richards (1996) also suggests that the four natural elements (water, earth, air and fire) are represented here and the circles may have been used in rituals as symbols of movement and purification. All of these Neolithic structures in Orkney and the Outer Hebrides would require a huge amount of work during construction and it has been suggested by Ritchie (1995, 1996) and Fojut *et al.* (1994) that by the Late Neolithic there were centralised and well-organised societies in the Orkney Islands and Outer Hebrides.

Less is known about the Bronze Age (~2000-700 cal BC) in the Orkney Islands or the Outer Hebrides than the Neolithic, although there is evidence from Tofts Ness on Sanday (Dockrill *et al.* 1994) and Rosinish on Benbecula (Shepherd and Tuckwell 1979) that the climate continued to be suitable for arable cultivation. Several sites containing the remains of small domestic stone houses and midden material dating to the Neolithic and Bronze Age have been discovered in the Outer Hebrides e.g. Northton (Harris), Loch Olabhat (North Uist) and Allt Chrysal (Barra) (Fojut *et al.* 1994). It has been suggested that in Orkney there was an apparent dispersal of the people from the coastal villages to individual dwellings close to small streams and the appearance of 'burnt mounds' (Hedges 1986), but such interpretation depends on whether burnt mounds are envisaged as settlement loci. Burnt mounds are piles of midden material that contain a large proportion of burnt and broken stones (Fraser 1983). Traditionally the stones are thought to have been heated in a fire and then placed in water to cook food (Fraser 1983; Hedges 1986; Ritchie 1995, 1996), however it has also been suggested that they may have been used as saunas and steam baths (Barfield and Hodder 1987).

The impressive tombs used to house the dead during the Neolithic were no longer in use during the Bronze Age period and the dead were generally buried in individual cists, barrows or mounds, none of which were intended to be reused (Fraser 1983; Ritchie 1985b; Hedges 1986; Thompson 1999). Such burials are numerous throughout the Orkney Islands and Outer Hebrides and many are now being exposed along the coastline as a result of coastal erosion e.g. Bay of Lopness, Sanday (Figure 2.7) discovered during the course of this research.

Towards the end of the Bronze Age the climate started to deteriorate becoming cooler and wetter (Armit 1997). As a result of the deteriorating climate and the intensive agricultural practices throughout the Neolithic and Bronze Age, the soil started to deteriorate and marginal land was eventually abandoned as blanket peat and heathland developed (Armit 1997; Armit and Ralston 1997). Good agricultural land was at a minimum, possibly resulting in aggressive competition (Ritchie 1995) and it has been suggested the introduction of the roundhouse (brochs and duns) in the Iron Age (~700 cal BC-AD 300) may have been developed not only as a status symbol but also to deter threatening neighbours (Armit 1990). Brochs are circular, drystone structures that were at least two storeys high and unique to Scotland (Ritchie 1996). There was only one entrance at ground level, no windows, and stairs were constructed within the walls to allow access to upper levels (Ritchie 1995, 1996; Ritchie and Ritchie 1995; Armit 1997). Although the primary purpose of brochs is not known, many have enclosing ditches and ramparts or are located on loch islets suggesting that the broch may have been a defensive structure (Macdonald 1982; Ritchie and Ritchie 1995). Domestic settlements are commonly found both surrounding the brochs and within the defence structures e.g. Brough of Gurness and Midhowe (Richardson 1948; Fojut 1993), and they may have been part of a hierarchical system with the landowner or chief residing in the broch tower and those of lesser status in the village below (Hedges 1986; Armit 1997). Towards the end of the Iron Age the need for a defensive home had receded, possibly due to an amelioration in the climate (Turner 1981), and this resulted in the abandonment of the brochs and the subsequent construction of cellular buildings. In the Outer Hebrides these cellular buildings are referred to as wheelhouses as they were subdivided internally creating a wheel-like structure. Wheelhouses are common in the Outer Hebrides, however several have also been identified in Shetland e.g. Jarlshof (Fojut *et al.* 1994).

Figure 2.7 – Cist exposed by coastal erosion at the Bay of Lopness, Sanday

By the fourth century AD Northern Scotland was part of the Pictish Kingdom. The Pictish Orcadians were probably descended from the broch-builders and many of their farms were on the sites of abandoned brochs e.g. Gurness (Ritchie and Ritchie 1995). Little remains of the Pictish culture in Orkney partly due to the removal of the Pictish symbol stones (Ritchie 1996) which may have been used as tombstones, landmarks or monuments (Ritchie and Ritchie 1995). In the Outer Hebrides during this period, cellular structures started to be constructed often within abandoned wheelhouses e.g. Galson, Cnip and The Udal (Edwards 1924; Armit 1992; Church 1998; Neighbour and Church 2001). The walls of the structures were generally revetted and Armit (1992) suggests that this may indicate the need for insulation and also a lack of timber for construction. Similar structures have been recognised in the Orkney Islands at Buckquoy, Birsay and Gurness (Ritchie 1971, 1983; Morris 1991; Fojut 1993).

Christianity is thought to have arrived in Orkney and the Outer Hebrides about the sixth century AD and is recorded by the appearance of crosses on Pictish symbol stones and place names (Fojut *et al.* 1994; Ritchie 1995). The name Pabbay, or Papay, appears throughout Orkney and the Outer Hebrides and is derived from the Norse word for priest (Ritchie 1993; Fojut *et al.* 1994). Ruins of Pictish monasteries can be found at Brough of Deerness and Brough of Birsay on Orkney (Morris and Emery 1986; Morris 1996), however very few churches which pre-date the Viking raids are known from the Outer Hebrides (Fojut *et al.* 1994) and those that do survive were constructed in remote locations such as Eilean Mór or Luchruban (Figure 2.1) (Fojut *et al.* 1994).

The Vikings first appeared in Scotland in approximately AD 800 and although they are traditionally thought to have been a violent, unruly people, the archaeology in the Orkney Isles suggests that they settled and integrated well with the Orcadians (Hedges 1986). In contrast the Outer Hebrides were initially raided before a phase of settlement began approximately AD 840 (Fojut *et al.* 1994). Few Viking burials have been found in Orkney, nevertheless cemeteries were discovered at Pierowall (Westray) and Westness (Rousay) (Hedges 1986), and several individual burials, including the Viking boat burial at Scar, Sanday, have been found (Ritchie 1996). The Vikings had a huge impact on the Orkney Islands and Outer Hebrides and this is shown, amongst other things, by the numerous Scandinavian place names found throughout the islands (Ritchie 1993; Fojut *et al.* 1994; Graham-Campbell and Batey 1998). Throughout the Norse period the Orkney Islands were politically part of the Kingdom of Norway (Ritchie 1993). The Earls of Orkney

managed Orkney during this time and their political history is recorded in the 'Orkneyinga Saga', which covers the time period from about AD 900-1200. The climate during this period is referred to as the Medieval Climatic Optimum and it is thought to have been one of the warmest periods since the end of the last glaciation allowing oats and barley to be grown as far north as Iceland (Lamb 1977). Finally, in AD 1468 the Orkney Islands were given to Scotland as part of a marriage agreement between King James III of Scotland and King Christian I of Norway and Denmark (Ritchie and Ritchie 1995; Schei and Moberg 1985). The Outer Hebrides were also under the control of the Kingdom of Norway during the Norse period however there was an attempt by the Scots to reclaim the land in the twelve century and in AD 1266 the islands were ceded to Scotland under the Treaty of Perth (Macdonald 1982).

2.3 The impact of storm events in history and prehistory

Although storms have a large impact on small and large communities throughout the world, it is the island or coastal communities that frequently experience the worst conditions. This often leads to irreversible changes in the local environment, which in turn affects the local population. Satellite and radar images are used today to inform people of impending storms, e.g. strong wind forecasts for the 28th January 2002 in Scotland and 27/28th October 2002 in southern England, however storms still affect local communities today by, for example, causing trees to fall down, damage to buildings, flooding and electricity cuts.

Periods of increased storminess have been recognised within historical times e.g. the Little Ice Age (c. AD 1250-1850) and specific storms within that period which had a large impact on communities within the British Isles have been summarised by Lamb (1991) and Hickey (1997). Therefore only some of the storm events that have affected communities in northern Scotland will be mentioned here.

The movement of large quantities of sand is one of the more devastating effects of storms and has affected several communities in northern Scotland. One of the best known events is that of a storm in AD 1694 that blew large quantities of sand over the village of Culbin (Figure 2.1) leaving the houses and the surrounding land buried and causing the permanent abandonment of the village and large areas of prime agricultural land (Steers 1937; Edlin 1976; Willis 1986). As a result of the disaster, an Act was passed in Parliament the

following year forbidding the removal of bent, juniper and broom from sand dunes (Willis 1986). Several years later the villages of Siabaidh, Berneray and Udal, North Uist, and the farm of Middleton, Pabbay were covered by sand during a large storm in AD 1697 (Crawford 1967; Morrison 1967). Archaeological excavations at Udal have revealed that the site had been continuously settled for approximately 4000 years from the early Bronze Age up until its abandonment due to sand inundation in the late 17th century (Ashmore 1996). The storm and sand movement that caused the final abandonment of the site must have been very severe in comparison with other storms experienced by the local population. Layers of sand between the various occupational phases helped to preserve the structures (Crawford and Switsur 1977), and although these earlier events may have caused temporary abandonment of the site, no storm severe enough to cause permanent abandonment occurred until the 17th century.

Settlements have also been abandoned due to sand inundation permanently changing the local environment. In north-east Scotland, close to the Loch of Strathbeg, there are the remains of a chapel that was once part of the village of Rattray (Figure 2.1) (Willis 1986). This part of the Scottish coastline is very exposed and Rattray provided a safe harbour because it was protected from the North Sea by a prograding gravel ridge (Walton 1956; Willis 1986). The earliest historical records indicate that Rattray was settled at the end of the 13th century and flourished as a fishing village during the 16th and 17th centuries, but even during this time the inlet was shallowing due to sand deposition (Walton 1956). The entrance to the harbour is thought to have finally closed during a storm about AD 1720 due to the inundation of sand, and with no harbour to provide safe anchorage for fishing vessels, the settlement was abandoned (Walton 1956).

Other historical documents record the movement of sand onto agricultural land that often resulted in the land being abandoned. Some of the earliest records are those of Sir Henry Sinclair who catalogued the rents paid by the crofters in the Orkney Islands in AD 1492 and 1500 (Sinclair 1492; Peterkin 1820). Within the records, especially those for Westray, Papay and Sanday, Sinclair describes large tracts of land as 'blawin' and this refers to land covered in wind blown sand. For land that had been abandoned or was unoccupied due to the inundation of wind blown sands, the rent on this land was either reduced or completely removed. The movement of sand onto agricultural land was probably a gradual process which would have been accelerated during storm events but Thomson (1984) suggests that this land may have been abandoned prior to the inundation of sand because land that was

easily tilled had a high rental price. The land may also have been abandoned due to over-cultivation or due to the introduction of rabbits (Thomson 1984), but whatever the cause, the movement of sand onto agricultural land had an impact on the local community. Later historical records from the Harris Estate Papers AD 1724-1754 mention the abandonment of the farm of Middleton, Pabbay, after the AD 1697 storm mentioned above, and that in the 18th century the rent on the farm Lingay, Pabbay and also farms in Berneray and Luskintyre were reduced due to blowing sand (Morrison 1967).

Historical records provide details of how climate has changed throughout the past 500-600 years including the identification of the Little Ice Age, and the records also indicate how this cooler period affected local communities. Some of the current knowledge of prehistoric climatic changes is from information contained within ice cores and tree rings. Cores from polar ice caps record variations in oxygen isotope content and atmospheric gas content that vary as a result of temperature changes and environmental changes respectively (Robin 1977; Lowe and Walker 1984). Although the ice core record has enabled major changes in climate to be identified, more discrete changes in the climate can be detected through dendroclimatology. This uses the width of annual tree rings to determine how the trees responded to the surrounding environment, with narrow tree rings inferring that environmental stresses prevented substantial growth of the tree (LeMarche 1974; Baillie 1982; Lowe and Walker 1984).

The movement of large quantities of sand at the sites mentioned above all occurred during the Little Ice Age and therefore it is likely that in prehistoric times the local people experienced similar events. There is evidence of prehistoric sand movement at various sites throughout Northern Scotland, e.g. Skara Brae and the Udal, however these sand deposits rarely contain organic material and therefore with few dating controls it is difficult to extend the knowledge of storms and their impact beyond historical records. The effect of a large storm event on the local population in prehistoric times would have been much greater than today with the destruction of crops, boats and settlements having a major impact on their lives. Archaeological sites in the Orkney Islands often contain sand layers between occupation layers and these could be the result of sand movement during large storm events inundating the sites and causing temporary or permanent abandonment of the sites by the local people. To gain an understanding of the effect of these storm events on the local population it is important to try to date the abandonment and reoccupation of the sites. This can be done through the use of OSL dating of the sand layers in conjunction

with radiocarbon dating of organic material found within middens and TL dating of heated material.

Recent research (Wilson and Braley 1997; Wintle *et al.* 1998; Gilbertson *et al.* 1999; Clemmensen *et al.* 2001 a and b) has applied OSL dating to sand deposits throughout northern Europe and this has identified several periods of increased sand movement within the Holocene (Figure 2.8). There is some correlation between these northern European sites notably during the Little Ice Age, 3-4000 years before present (BP), 5-6000 years BP and approximately 7000 years BP. Similar periods of wetter weather have been identified from peat bogs in north-west Scotland (Anderson 1998) and this record is also shown in Figure 2.8. Most of the sites shown have at least one period of sand movement that is not identified elsewhere and this is perhaps expected as local conditions will affect the amount of sand available for aeolian transportation. Alternatively due to the continual shifting of sand the evidence for these stormier periods may no longer exist. One of the aims of this research is to enhance the climatic data shown in Figure 2.8 by the addition of Orkney data. The area covered by the Orkney Islands is probably small enough that any large storm event would affect the whole archipelago and a storm concentrated in the Northern Isles of Westray, Eday and Sanday would certainly affect all of these islands. OSL dating of sand layers from various sites within the Orcadian Northern Isles will provide some indication of the extent of the storms and the impact on the local island communities, with the identification of increased periods of storminess providing information on past climatic changes within the Orkney Islands.

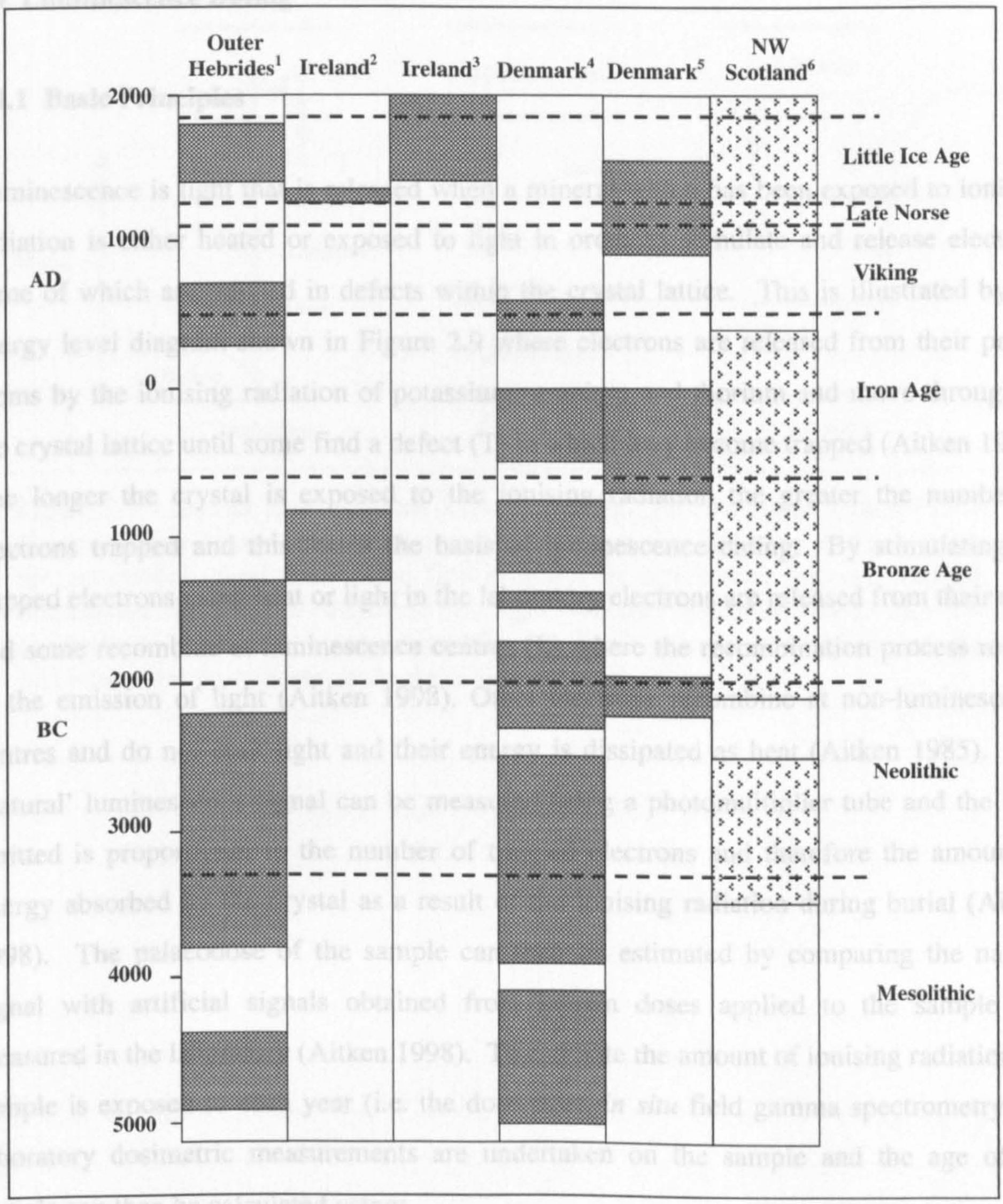

Figure 2.8 – Summary of phases of climatic instability (shaded areas) in the Holocene from several sites in north-west Europe: 1-5 – Increased sand movement; 6 – Phases of wetter conditions identified from peat bogs.
(after 1. Gilbertson *et al.* 1999; 2. Wilson and Braley 1997; 3. Wintle *et al.* 1998; 4. Clemmensen *et al.* 2001a; 5. Clemmensen *et al.* 2001b; 6. Anderson 1998).

2.4 Luminescence Dating

2.4.1 Basic Principles

Luminescence is light that is released when a mineral which has been exposed to ionising radiation is either heated or exposed to light in order to stimulate and release electrons some of which are trapped in defects within the crystal lattice. This is illustrated by the energy level diagram shown in Figure 2.9 where electrons are released from their parent atoms by the ionising radiation of potassium, uranium and thorium and move throughout the crystal lattice until some find a defect (T) in which they become trapped (Aitken 1998). The longer the crystal is exposed to the ionising radiation the greater the number of electrons trapped and this forms the basis of luminescence dating. By stimulating the trapped electrons using heat or light in the laboratory electrons are released from their traps and some recombine at luminescence centres (L) where the recombination process results in the emission of light (Aitken 1998). Other electrons recombine at non-luminescence centres and do not emit light and their energy is dissipated as heat (Aitken 1985). The 'natural' luminescence signal can be measured using a photomultiplier tube and the light emitted is proportional to the number of trapped electrons and therefore the amount of energy absorbed by the crystal as a result of the ionising radiation during burial (Aitken 1998). The palaeodose of the sample can then be estimated by comparing the natural signal with artificial signals obtained from known doses applied to the sample and measured in the laboratory (Aitken 1998). To estimate the amount of ionising radiation the sample is exposed to each year (i.e. the dose rate), *in situ* field gamma spectrometry and laboratory dosimetric measurements are undertaken on the sample and the age of the sample can then be calculated using:

$$Age = \frac{Palaeodose}{DoseRate}$$

The methods used to determine the palaeodose and dose rate are discussed in more detail in Chapter 3.

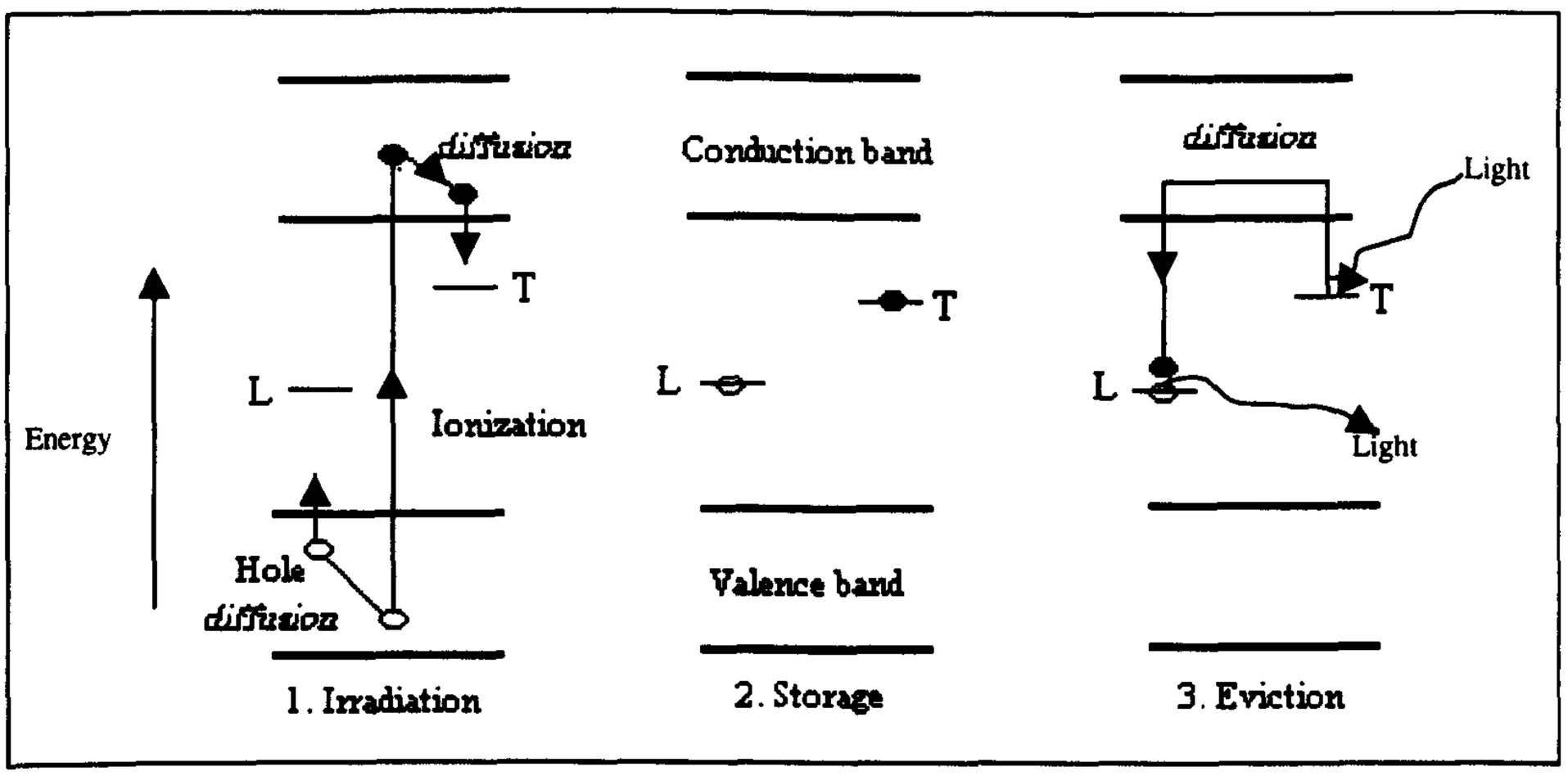

Figure 2.9 – Energy level diagram showing the OSL process (after Aitken 1985). Electrons are released from the parent atoms by ionising radiation and move into the conduction band until some find a defect in which they become trapped. Subsequent heating or exposure to light releases electrons back into the conduction band and some recombine at luminescence centres where the recombination process results in the release of luminescent light.

2.4.2 Sources of Natural Radiation

The ionising radiation that minerals are exposed to is mainly emitted from the natural radioisotopes of uranium and thorium (and their decay products) (Tables 2.1a, b and c) and potassium (Table 2.1d) although there are also small contributions from rubidium and cosmic radiation. Three types of radiation are emitted when a nucleus undergoes radioactive decay: alpha particles, beta particles and gamma rays. The extent to which these penetrate the sediment or heated material depends on the energy level of the various radiations and this is shown in Figure 2.10. Alpha particles are released from the radioactive decay of uranium and thorium, however the particles lose their energy rapidly because they are heavy (i.e. they are essentially helium ions) and travel in straight lines and therefore they travel very short distances (approximately 25μm) within the mineral. Beta particles are also released from uranium and thorium but also from the radioactive decay of potassium. These particles are essentially fast moving electrons that scatter throughout the material and as a result they can penetrate grains up to about 3 mm. In comparison gamma rays, which are essentially electromagnetic waves, are released from uranium, thorium and potassium and have an effective range of approximately 30-40 cm. Due to its extended range it is the major source of external radiation contributing to the dose rate of the sediment or heated artefact.

The contribution of cosmic radiation to the dose rate is usually quite small and therefore because the uncertainty on the cosmic dose rate is not vital, a standard is generally used in luminescence dating (Prescott and Stephan 1982). Cosmic radiation is composed of 'soft' and 'hard' components. The 'soft' component is mainly electrons which are easily attenuated in the top 50 cm of soil (Prescott and Stephan 1982; Aitken 1985, 1998) but the hard component is composed of muons which are particles similar to electrons but about 200 times heavier and created by secondary cosmic ray reactions about 15 km above the earth's surface (Burcham 1973). The hard component continues to penetrate well below 50 cm and it is this hard cosmic ray flux that contributes to a sample's dose rate. Prescott and Stephan (1982) evaluated the contribution of cosmic radiation to the environmental dose rate at various latitudes, altitudes and depths and their values are commonly used in luminescence dating.

Isotope	Emitted radiation	Half life	α-energy (MeV)	Maximum β-energy (MeV)	γ-energy (MeV)
^{238}U	α	4.47 x 10^9 y	4.19	-	0.0111
^{234}Th	β	24.1 days	-	0.162	0.0149
^{234}Pa	β	1.17 min	-	2.265	0.0112
^{234}U	α	2.45 x 10^5 y	4.76	-	0.0001
^{230}Th	α	75.4 x 10^3 y	4.66	-	0.004
^{226}Ra	α	1600 y	4.77	-	0.009
^{222}Rn	α	3.83 days	5.49	-	0.0004
^{218}Po	α	3.05 min	6.00	-	0.0001
^{214}Pb	β	26.8 min	-	0.724	0.2285
^{214}Bi	β	19.9 min	-	1.783	1.5088
^{214}Po	α	162 μs	7.69	-	0.0001
^{210}Pb	β	22.2 y	-	0.024	0.0019
^{210}Bi	β	5.01 days	-	1.161	-
^{210}Po	α	138.4 days	5.31	-	-
^{206}Pb					

Table 2.1a – Uranium-238 decay series (after Aitken 1985).

Isotope	Emitted radiation	Half life	α-energy (MeV)	Maximum β-energy (MeV)	γ-energy (MeV)
^{235}U	α	0.7 x 10^9 y	4.39	-	0.1485
^{231}Th	β	25.5 h	-	0.219	0.0151
^{231}Pa	α	32.8 x 10^3 y	4.92	-	0.0287
^{227}Ac	β	21.8 y	0.069	0.04	0.0099
^{227}Th	α	18.7 days	5.84	-	0.0988
^{223}Ra	α	11.43 days	5.82	-	0.0865
^{219}Rn	α	3.96 s	6.76	-	0.0576
^{215}Po	α	1.78 x 10^{-3} s	7.39	-	0.0003
^{211}Pb	β	36.1 min	-	1.323	0.0764
^{211}Bi	α	2.17 min	6.57	0.002	0.0491
^{207}Tl	β	4.77 min	-	1.434	0.0024
^{207}Pb					

Table 2.1b – Uranium-235 decay series (after Aitken 1985).

	Isotope	Emitted radiation	Half life	α-energy (MeV)	Maximum β-energy (MeV)	γ-energy (MeV)
	^{232}Th	α	14.1 x 10^9y	4.01		
	^{228}Ra	β	5.75 a		0.055	
	^{228}Ac	β	6.13 h		1.205	0.875
	^{228}Th	α	1.91 y	5.42		0.0024
	^{224}Ra	α	3.66 days	5.69		0.0099
	^{220}Rn	α	55.6 s	6.29		0.0002
	^{216}Po	α	0.15 s	6.78		
	^{212}Pb	β	10.64 h		0.371	0.1055
	^{212}Bi	β	60.6 min		1.336	0.1013
64% ^{212}Po		α	0.3 μs	5.63		
^{208}Pb				64% of 8.78(MeV)		
			60.6 min	2.18		0.0039
				(36% of 6.06(MeV)		
	36% ^{208}Tl	β	3.05 min		0.58	1.207
	^{208}Pb					

Table 2.1c – Thorium-232 decay series (after Aitken 1985).

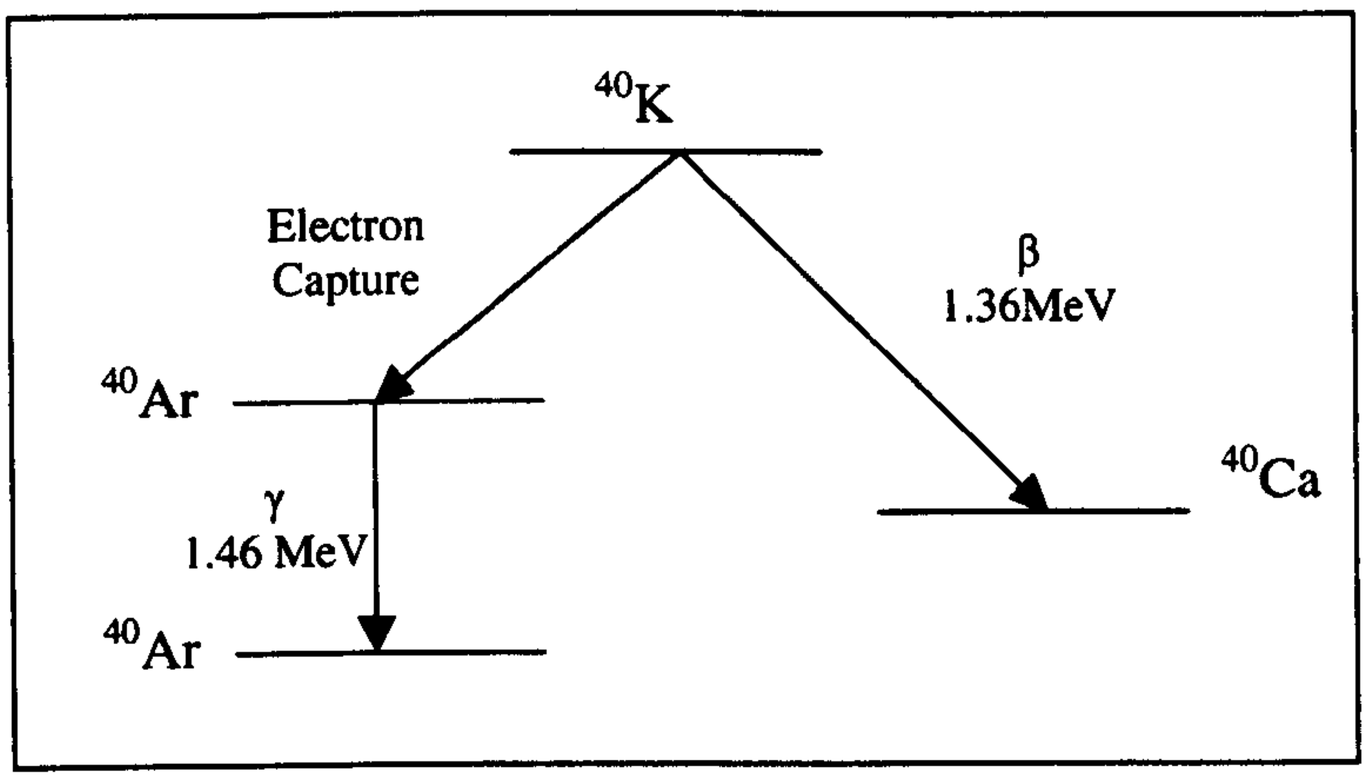

Table 2.1d – Potassium-40 decay series (after Fleming 1979)

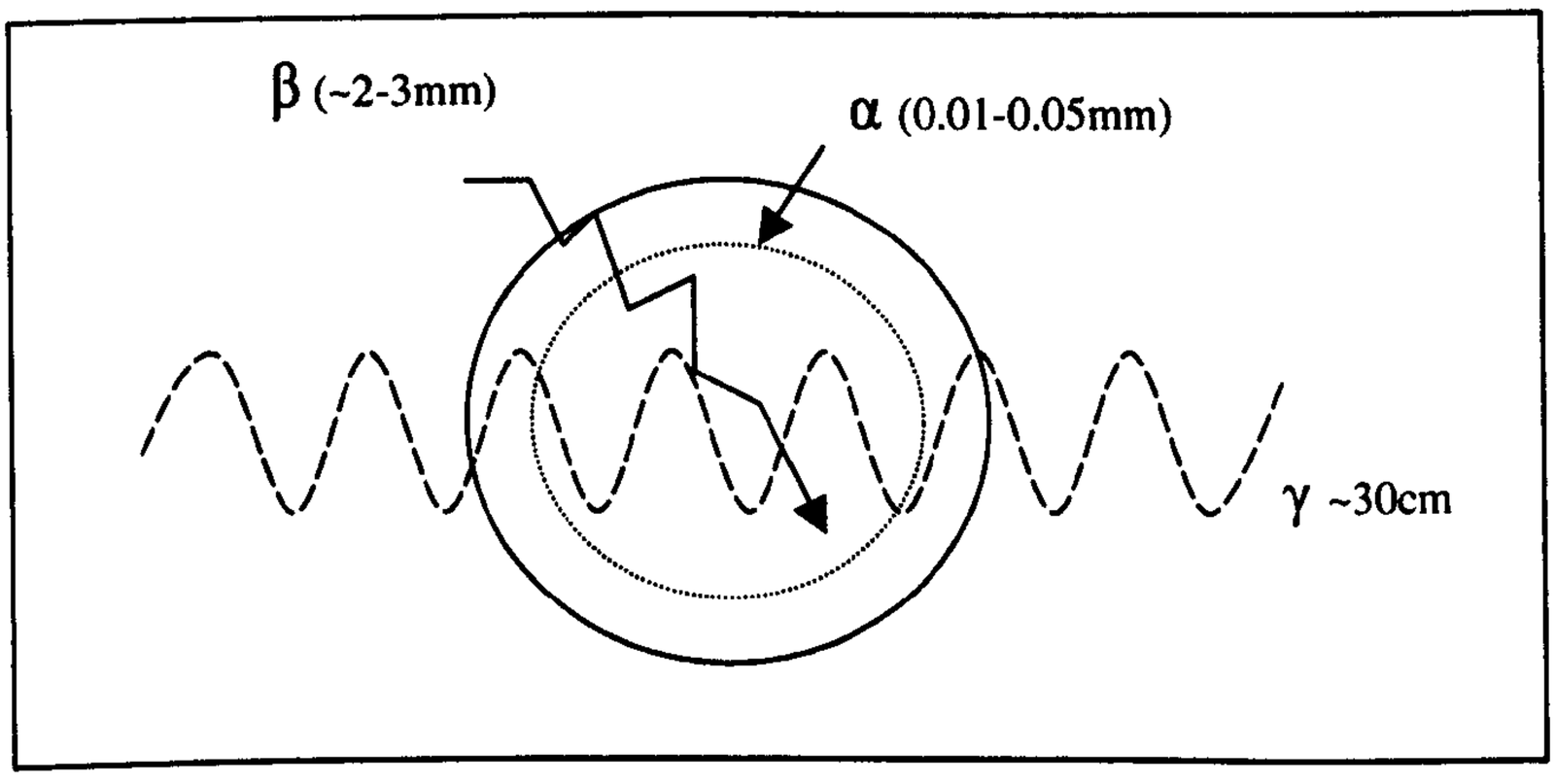

Figure 2.10 – Penetration depth of alpha (α), beta (β) and gamma (γ) radiation through a grain (after Aitken 1990).

The amount of radiation absorbed by a sample will vary due to the water content of the surrounding sediment. Water absorbs radiation and the amount of energy absorbed by the water per gram is greater by 50% for α-particles, 25% for β-particles and 14% for γ-radiation (Zimmerman 1971; Aitken 1974; Fleming 1979). Consequently an inaccurate estimate of the water content may result in an over- or under-estimation of the dose-rate, and hence age of the sample (Aitken 1990, 1998; Richardson 2001; Wintle 1991). In a well-drained or saturated environment the actual water content is generally seen as a good estimate to use (Aitken 1985, 1989, 1990). There are, however, many sites which have experienced a variable water content due to fluctuations in the water table as a result of climatic changes, sea level changes or human interference (Aitken 1989; Clarke and Rendell 2000), and so present day conditions may not be representative of the past (Rendell 1985). Where possible, historical records of water table fluctuations should be referred to (Wintle and Huntley 1980; Berger 1988) however the extent to which such records can be extrapolated remains unknown and the assumed uncertainty of the water content is an irreducible source of the final error in the luminescence age estimate.

2.4.3 History of luminescence dating

The luminescent properties of minerals was first scientifically recognised by Robert Boyle in AD 1663 who took a diamond to bed with him and after holding it against his body observed a 'glimmering light' (Boyle 1664). The knowledge that different minerals emitted different colours of light whilst they were being heated led to a geological use for this phenomenon (Daniels *et al.* 1953; McDougall 1968; McKeever 1985) which was aided by the development of the photomultiplier tube in the 1940's (Aitken 1985). Daniels *et al.* (1953) were the first to suggest that the thermoluminescence properties of minerals could potentially be used as a dating tool and Grögler *et al.* (1960) demonstrated that a natural TL signal could be measured from pottery. Thermoluminescence dating of archaeological pottery, burnt flint and heated sediments developed throughout the 1960's and was based on the principle that the heat generated during the final firing emptied the traps of all electrons, effectively 'zeroing' the age of the sample and starting the TL clock (Aitken *et al.* 1963; Tite 1966; Mejdahl and Wintle 1984). Subsequent exposure to ionising radiation trapped electrons in the defects until the signal was measured in the laboratory.

Initial TL dating work was relatively unsuccessful because large TL signals were observed in modern pottery samples which should have contained little or no signal (Tite and Waine 1962). Subsequent work showed that measuring the TL signals in a nitrogen atmosphere rather than air reduced the spurious TL in the modern samples resulting in low TL signals (Aitken *et al.* 1963; Tite 1966). However, the low penetrative power of alpha particles (~ 25μm) was not considered and therefore the first TL dates were based on the full dose rate from alpha, beta and gamma radiation, resulting in an underestimation of the true TL age. To solve this problem the 'quartz inclusion method' and the 'fine-grain technique' were developed by Fleming (1966, 1970) and Zimmerman (1967, 1971) respectively.

Fleming (1966, 1970) showed that the alpha, beta and gamma radiation within pottery mainly came from the clay matrix, and that the quartz grains embedded within the matrix were generally free of internal radioactivity. Alpha particles will only penetrate the surface of grains with a diameter of at least 100μm and therefore Fleming (1966) suggested that removing the outer skin of the grains using hydrofluoric acid would leave an inner core that was unaffected by alpha radiation. As a result the age of the sample could then be calculated using only the beta and gamma dose rates.

The second solution was proposed by Zimmerman (1967, 1971) who suggested that fine polymineral grains of between 1 and 8μm should be used for the TL measurements. The fine grains would have been fully exposed to alpha radiation and therefore the full dose rate (i.e. from alpha, beta and gamma radiation) could then be used to calculate the age of the sample. This technique has also been extensively used as an authenticity test for pottery, ceramics and the clay cores of bronze casts (Stoneham 1991; Roberts 1997). It has been especially important on pieces such as Chinese equestrian groups originally made in the Six Dynasties and Tang periods, but a modern rider is often added to a genuine horse to raise the asking price (Stoneham 1991).

In the early 1980s feldspar inclusions started to be used in TL dating (Guérin and Valladas 1980; Mejdahl and Winther-Nielsen 1982; Mejdahl 1983), although somewhat slowly given that Wintle (1973) had demonstrated that a few feldspars extracted from lavas collected from Naples, Iceland and the Massif Central exhibited various degrees of anomalous fading (i.e. a decay in luminescence with time). The anomalous fading

observed by Wintle (1973) was in the TL emission range of 620-720 K and therefore Guérin and Valladas (1980) measured the TL emission of plagioclase feldspar at 700-1000 K which they found to be unaffected by anomalous fading. Extensive fading tests were undertaken on feldspars from a variety of archaeological samples by Mejdahl (1983) and he demonstrated that the majority showed no evidence of significant anomalous fading. Mejdahl (1983) concluded that even if there was some fading (up to 4% for most samples) this would have little effect on the final age estimate. The literature on anomalous fading suggests that some feldspars will exhibit this phenomenon and others will not, nevertheless feldspars tend to be much brighter than quartz grains and saturate at much higher doses allowing them to date older artefacts.

Although much of the early thermoluminescence work was undertaken on pottery the technique is also used on a variety of other burnt materials such as burnt flint (e.g. Huxtable and Jacobi 1982; Mercier *et al.* 1995), burnt stones (Anthony *et al.* 2001) and volcanic deposits (Li and Yin 2001). In many circumstances thermoluminescence has helped to confirm radiocarbon dates that may have been slightly suspect (Roberts 1997) however the main contribution of TL dating to archaeology is its ability to date material from the Palaeolithic, which is beyond the scope of radiocarbon dating.

2.4.4 Luminescence dating of unheated sediments

The idea that natural luminescence signals could be used to date sediments was first recognised by Johnson and Blanchard (1967) who studied the radiation dosimetry from the natural thermoluminescence of fossil shells. Their results indicated that the older fossil shells had a higher dosimetric equivalent, and that in situations where there was a high dose of radiation the amount of thermoluminescence levelled off. The range of dosimetric values obtained from the fossil shells made it possible to differentiate between young and old samples, and they concluded that once the dose rate of the environment was known the age of the sample could be calculated (Johnson and Blanchard 1967). Further work by Bothner and Johnson (1969) used the natural thermoluminescence signals from calcitic foraminifera taken from deep-sea cores to determine if the dosimetry was related to age and radioactivity. Their results indicated that the natural signal did increase with depth, and therefore was proportional to age.

The potential to use thermoluminescence as a means to date marine sediments was discussed further by Huntley and Johnson (1976) and Wintle and Huntley (1979, 1980). Huntley and Johnson (1976) analysed siliceous fossils from two deep-sea cores and confirmed that the thermoluminescence signal did increase with depth. Equivalent doses were determined by giving the samples a variety of radiation doses in addition to their natural doses and extrapolating the growth curve to the dose axis (Figure 2.11) (Huntley and Johnson 1976). Preliminary age estimates were then calculated using the equivalent doses and an estimate of the radiation dose rate (Huntley and Johnson 1976).

Further work on deep-sea sediment cores by Wintle and Huntley (1979, 1980) confirmed that thermoluminescence dating was a viable technique for not only dating marine sediments, but also lake and wind blown sediments. Previous work by Johnson and Blanchard (1967), Bothner and Johnson (1969), and Huntley and Johnson (1976) thought that it was the siliceous material that gave off the luminescent light, however Wintle and Huntley (1979) found that the signal actually came from the inorganic material still attached to the radiolaria.

Despite the observation by Aitken *et al.* (1963) that exposure to sunlight effectively bleached the TL signal of pottery, Wintle and Huntley (1979) were surprised that TL signals from the top of marine cores, where fresh sediment had been deposited, were small. Wintle and Huntley (1979) expected the terrestrial material to be in saturation however low TL levels from young material were also recognised by workers in the USSR who also deduced that exposure to sunlight effectively emptied the TL traps (Dreimanis *et al.* 1978). Wintle and Huntley (1979, 1980) tested the theory by irradiating identical samples and then exposing them to a sunlamp for various amounts of time. They concluded that exposure for approximately 10 days reduced the TL signal to that measured from the top of the core, and therefore exposure to sunlight before deposition effectively zeroed the geological TL signal (Wintle and Huntley 1979, 1980). A small residual TL signal was measured after exposure to the sunlamp and Wintle and Huntley (1980) suggested that this was either due to traps that were unaffected by exposure to light or to biogenic silica that was not removed during the acid treatment.

Thermoluminescence dating was used throughout the early 1980's to date sediments from a variety of environments e.g. aeolian sand dunes, river and lake sediments and glacial sediments (Berger and Huntley 1982; Singhvi *et al.* 1982; Huntley *et al.* 1985; Kolstrup

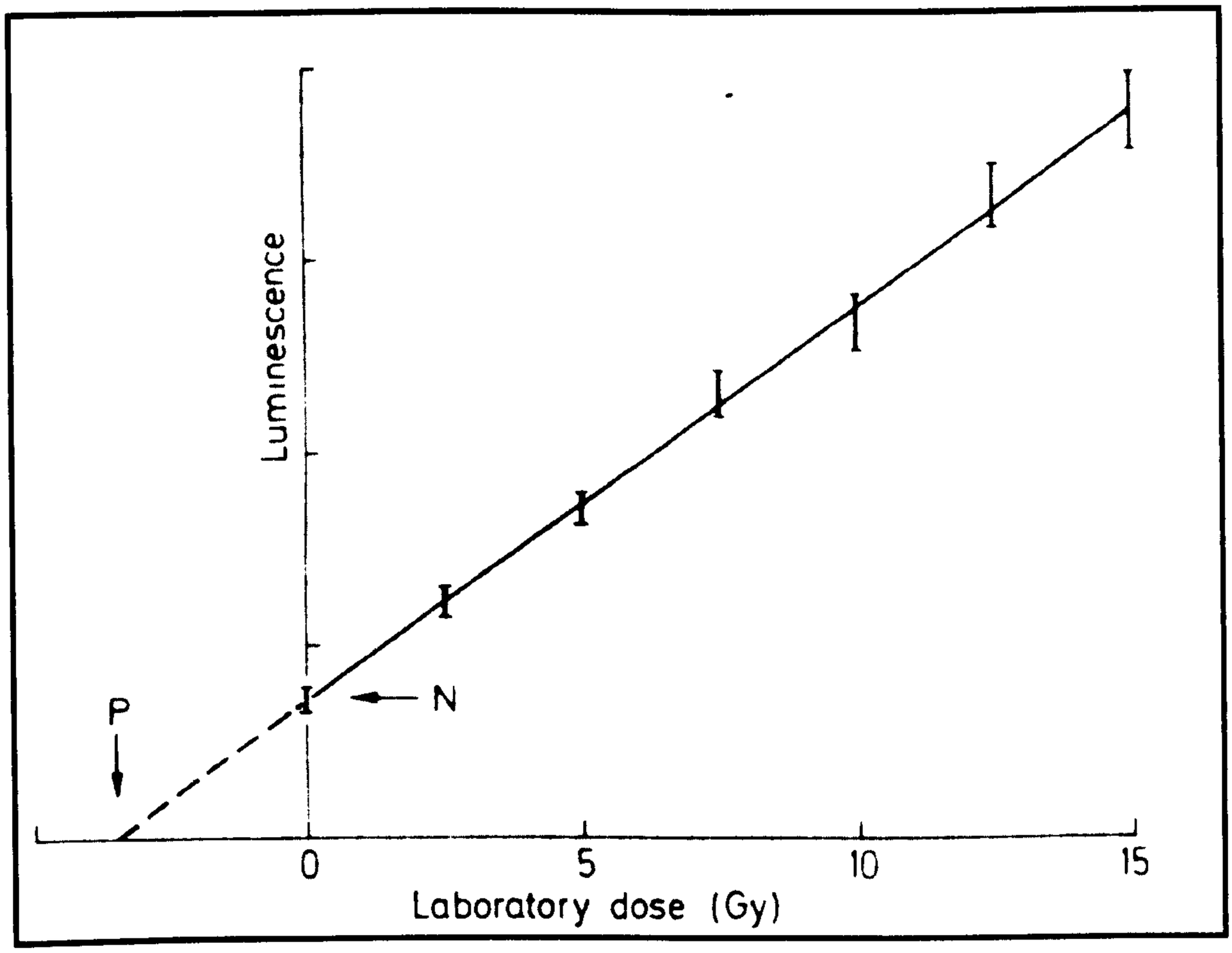

Figure 2.11 – Additive dose method of equivalent dose determination (after Aitken 1998).

and Mejdahl 1986). Much of the early work was undertaken on archaeological sites where the archaeology could be used to constrain the dates obtained (Singhvi *et al.* 1982; Prescott 1983; Rendell *et al.* 1983). As the technique developed, however, several problems arose that constrained the use of TL dating of sediments. The assumption that grains were well bleached upon deposition was tested by Prescott (1983) who measured a residual TL signal in surface grains, and therefore inclusion of these residuals in older samples would result in an overestimation of the sample age.

TL dating accesses both light sensitive and light insensitive traps and therefore even if a sample has been well bleached at deposition, a residual TL signal will still be observed (Wintle and Huntley 1980, 1982; Godfrey-Smith *et al.* 1988). The partial bleach method developed by Wintle and Huntley (1980) compensates for samples that may not have been fully bleached at deposition. The technique uses two sets of samples, one that has had laboratory irradiation added to the natural dose and another similar set that has had a short laboratory bleach after irradiation, but before TL measurement (Wintle and Huntley 1980, 1982). Both sets of measurements are plotted as TL growth curves and extrapolated until they intercept (Figure 2.12). The point on the dose axis immediately underneath the intercept is the equivalent dose (D_e) of the sample (Wintle and Huntley 1980, 1982). However, unless the laboratory bleaching time is less than that experienced before deposition, the laboratory bleach will reach traps that were not zeroed during deposition and therefore the D_e will be overestimated (Aitken 1985). Further techniques to identify partially bleached sediments using TL were proposed by Mejdahl (1985, 1988). The 'quartz-feldspar technique' successfully identified young partially bleached quartz samples however the age range of quartz restricted the method (Mejdahl 1988). Although the other technique, the 'plateau method', was successful for experiments undertaken in sunlight, the artificial light source (SOL 2) could not produce the same light spectrum and therefore the residual levels did not match those bleached by sunlight (Mejdahl 1988).

The knowledge that sunlight effectively bleached sediments before deposition led to the development of an optical dating technique by Huntley *et al.* (1985) which used light rather than heat to stimulate the trapped electrons. Stimulation by light ensured that only those traps that were light sensitive were measured (Huntley *et al.* 1985). These initial experiments were undertaken using a green (514.5 nm) beam from an argon-ion laser, which was used to stimulate trapped electrons within quartz grains. The luminescent light measured by the photomultiplier must be different to the stimulating light (Aitken 1989)

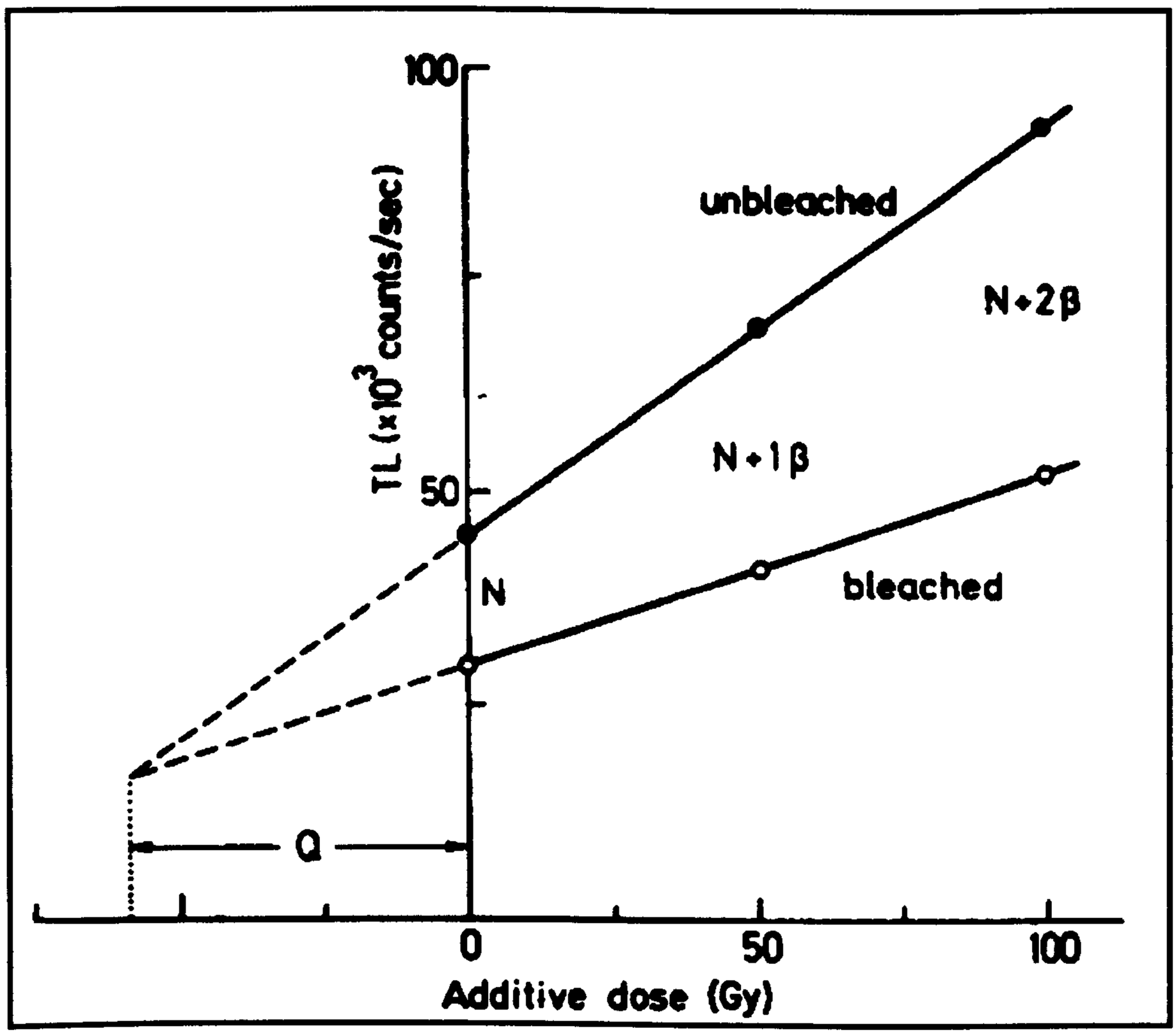

Figure 2.12 – The partial bleach method (after Aitken 1985).

and therefore blue filters (520 nm interference filter and Corning 3-70 and 3-71 glass filters) were used to absorb unwanted light (Huntley *et al.* 1985). Two experiments were undertaken by Huntley *et al.* (1985): the first to show that the light intensity did increase with age, and the second to compare the D_e using this technique with the D_e from partial bleach TL measurements. Their results confirmed that the light intensity did increase with age and two of their three samples correlated well with the partial bleach TL results. Huntley *et al.* (1985) concluded that optically stimulated luminescence was a viable method for dating sediments, especially those that may have only received a short exposure to sunlight before deposition.

2.4.5 Luminescence properties of quartz and feldspars

The luminescence properties of quartz and feldspars are determined during formation of the crystals and are largely dependent on the defects that form within the crystal structures. The minerals behave differently when stimulated by heat or light and therefore to allow the individual properties of each mineral to be highlighted they are discussed separately.

2.4.5.1 Quartz

Quartz is the most abundant silicate on the Earth's crust and although it has a relatively simple tetrahedral structure (SiO^{4+}, Figure 2.13) (Klein 2002) there are many different forms of quartz and the number of structural defects within the crystal is mainly controlled by the thermal conditions at the time of formation (Krbetschek *et al.* 1997). Defects within the quartz structure are sensitive to ionising radiation and the luminescence signal that is stored within these defects can be released by stimulating the trapped electrons using heat or light. When irradiated quartz is heated from room temperature to 500°C the subsequent glow curve is commonly composed of three or more distinct peaks (Figure 2.14). Fleming (1970) identified that the TL peak at 375°C would be most useful for dating purposes but he also suggested that the peak at 325°C (used in OSL dating) was 'malign' because it had an unreliable dose response. Both peaks do, however, exhibit supralinearity (Figure 2.15) which is an increase in the slope of the growth curve with an increase in dose (Aitken 1998) and it is thought to be due to competition for electrons by traps that do not produce thermoluminescence. Because these non-luminescence traps are saturated much earlier than the TL traps, the TL sensitivity will increase as they become saturated (Aitken 1985).

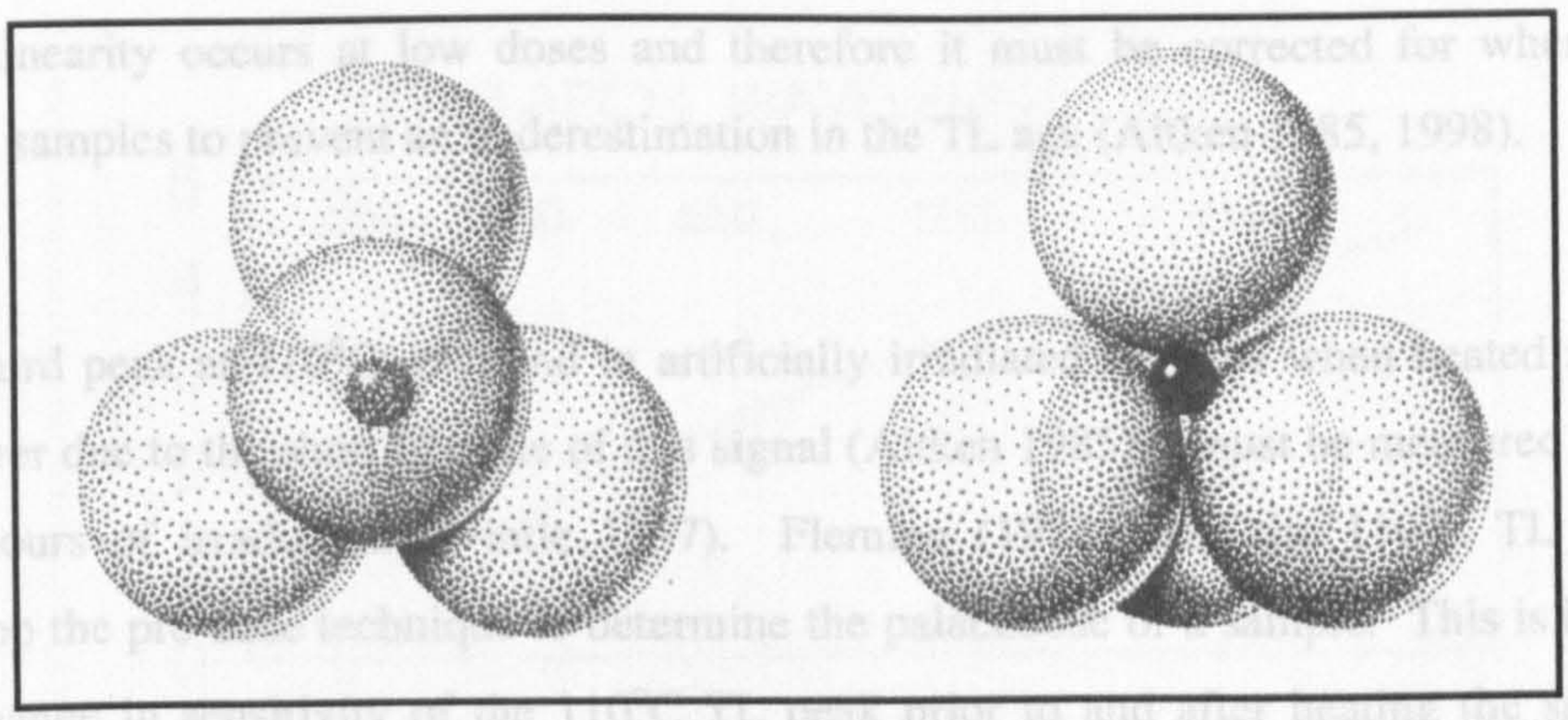

Figure 2.13 – Close packing representation of a $Si0_4$ tetrahedron (after Klein 2002).

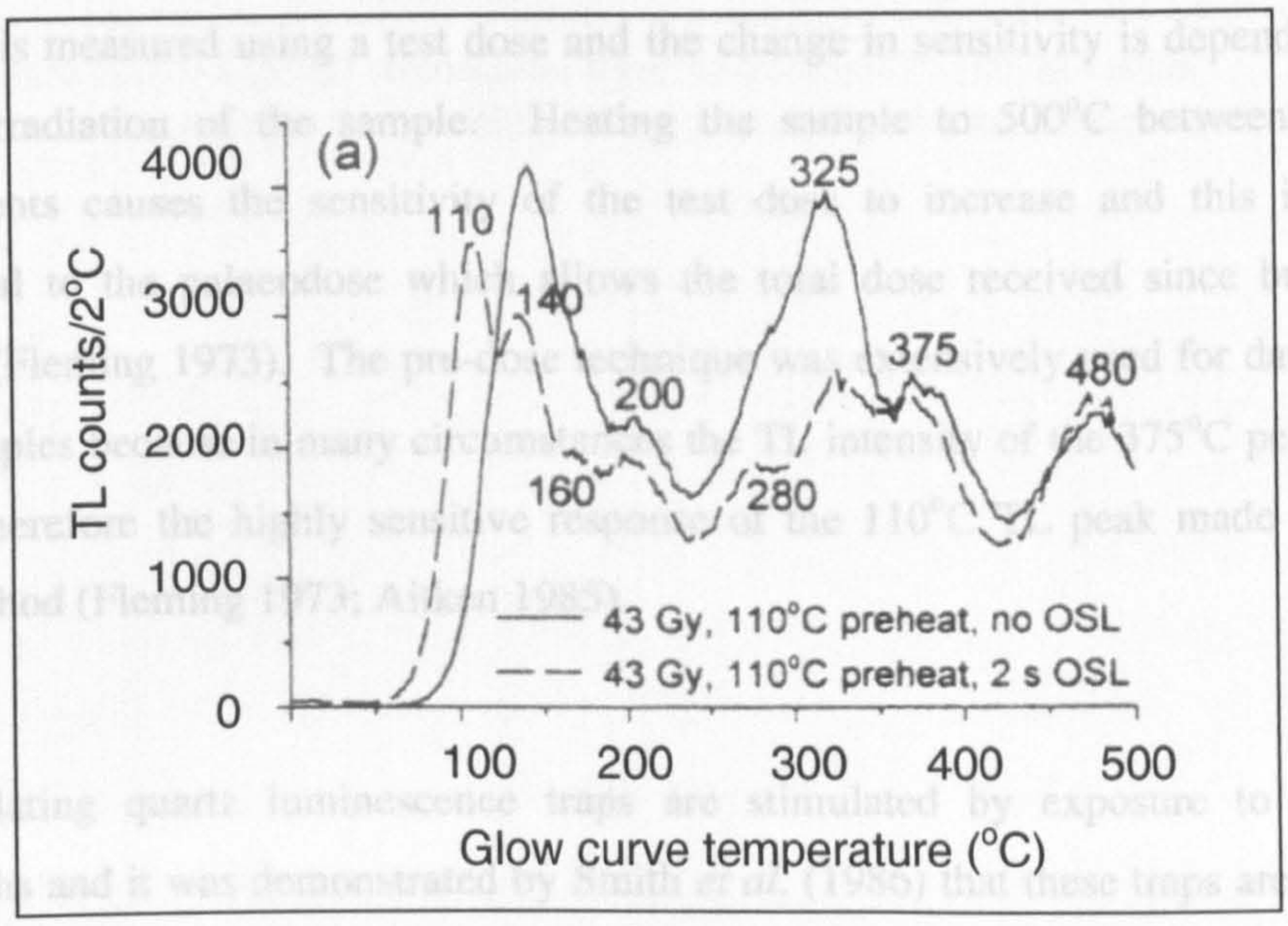

Figure 2.14 – TL glow curves of quartz (after Wintle and Murray 1997).

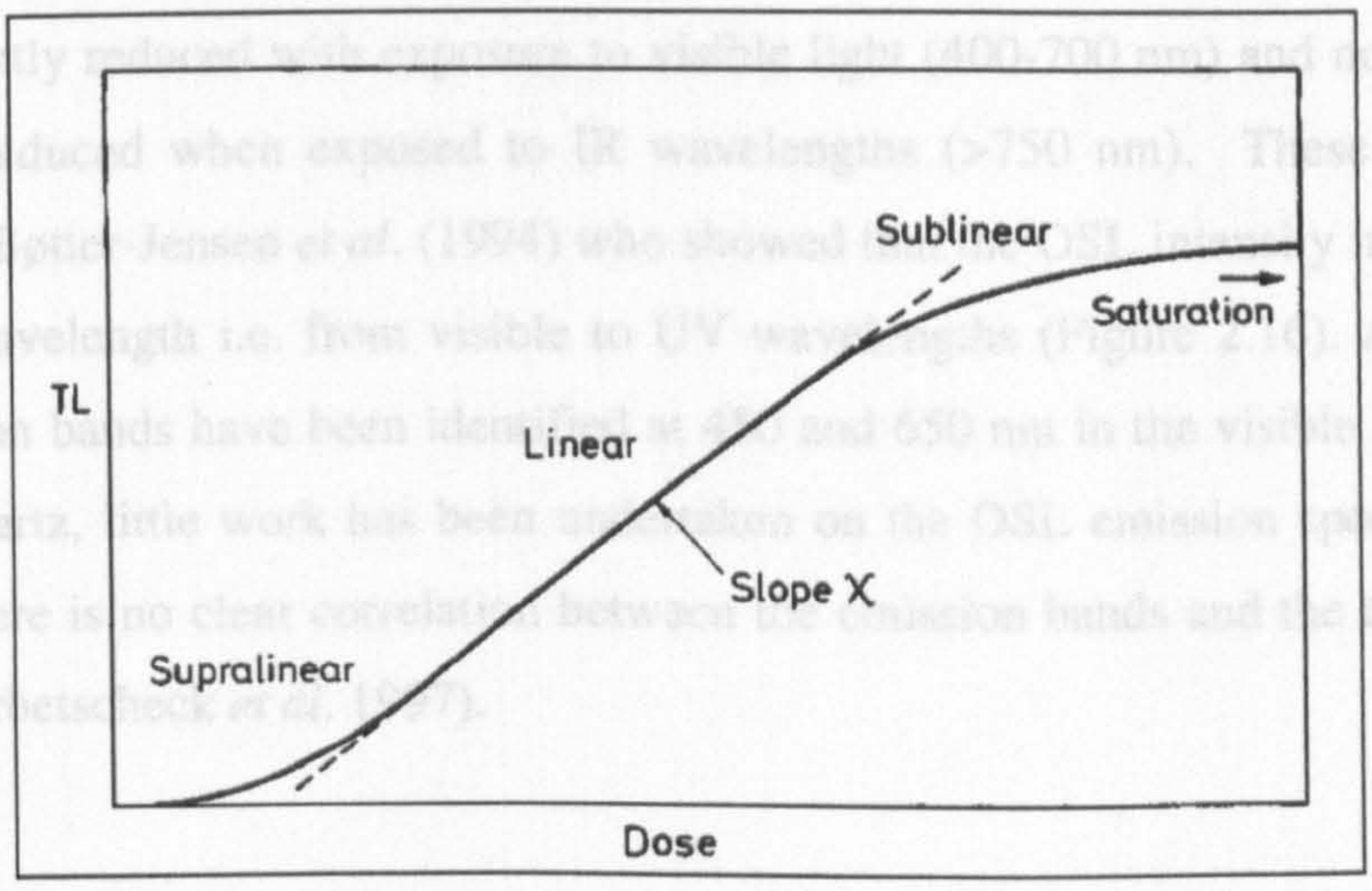

Figure 2.15 – Thermoluminescence growth characteristics showing supralinearity at low doses (after Aitken 1985).

Supralinearity occurs at low doses and therefore it must be corrected for when dating young samples to prevent an underestimation in the TL age (Aitken 1985, 1998).

The third peak at 110°C, is found in artificially irradiated samples when heated at 5°C/s, however due to the short lifetime of this signal (Aitken 1985) it must be measured within a few hours of irradiation (Wintle 1997). Fleming (1973) used the 110°C TL peak to develop the pre-dose technique to determine the palaeodose of a sample. This is based on the change in sensitivity of the 110°C TL peak prior to and after heating the sample to 500°C which unlocks the memory of the previous irradiation (Fleming 1973). The sensitivity is measured using a test dose and the change in sensitivity is dependent on the previous irradiation of the sample. Heating the sample to 500°C between test dose measurements causes the sensitivity of the test dose to increase and this increase is proportional to the palaeodose which allows the total dose received since burial to be estimated (Fleming 1973). The pre-dose technique was extensively used for dating young quartz samples because in many circumstances the TL intensity of the 375°C peak was too low and therefore the highly sensitive response of the 110°C TL peak made it an ideal dating method (Fleming 1973; Aitken 1985).

In OSL dating quartz luminescence traps are stimulated by exposure to green/blue wavelengths and it was demonstrated by Smith *et al.* (1986) that these traps are associated with the 325°C TL peak. Bleaching experiments by Spooner *et al.* (1988) showed that all TL peaks were reduced when exposed to UV light (< 400 nm) but that the 325°C TL peak was significantly reduced with exposure to visible light (400-700 nm) and none of the TL peaks were reduced when exposed to IR wavelengths (>750 nm). These results were reiterated by Bøtter-Jensen *et al.* (1994) who showed that the OSL intensity increased with decreasing wavelength i.e. from visible to UV wavelengths (Figure 2.16). Although two broad emission bands have been identified at 450 and 650 nm in the visible luminescence of natural quartz, little work has been undertaken on the OSL emission spectra of quartz and as yet there is no clear correlation between the emission bands and the defects within the grains (Krbetscheck *et al.* 1997).

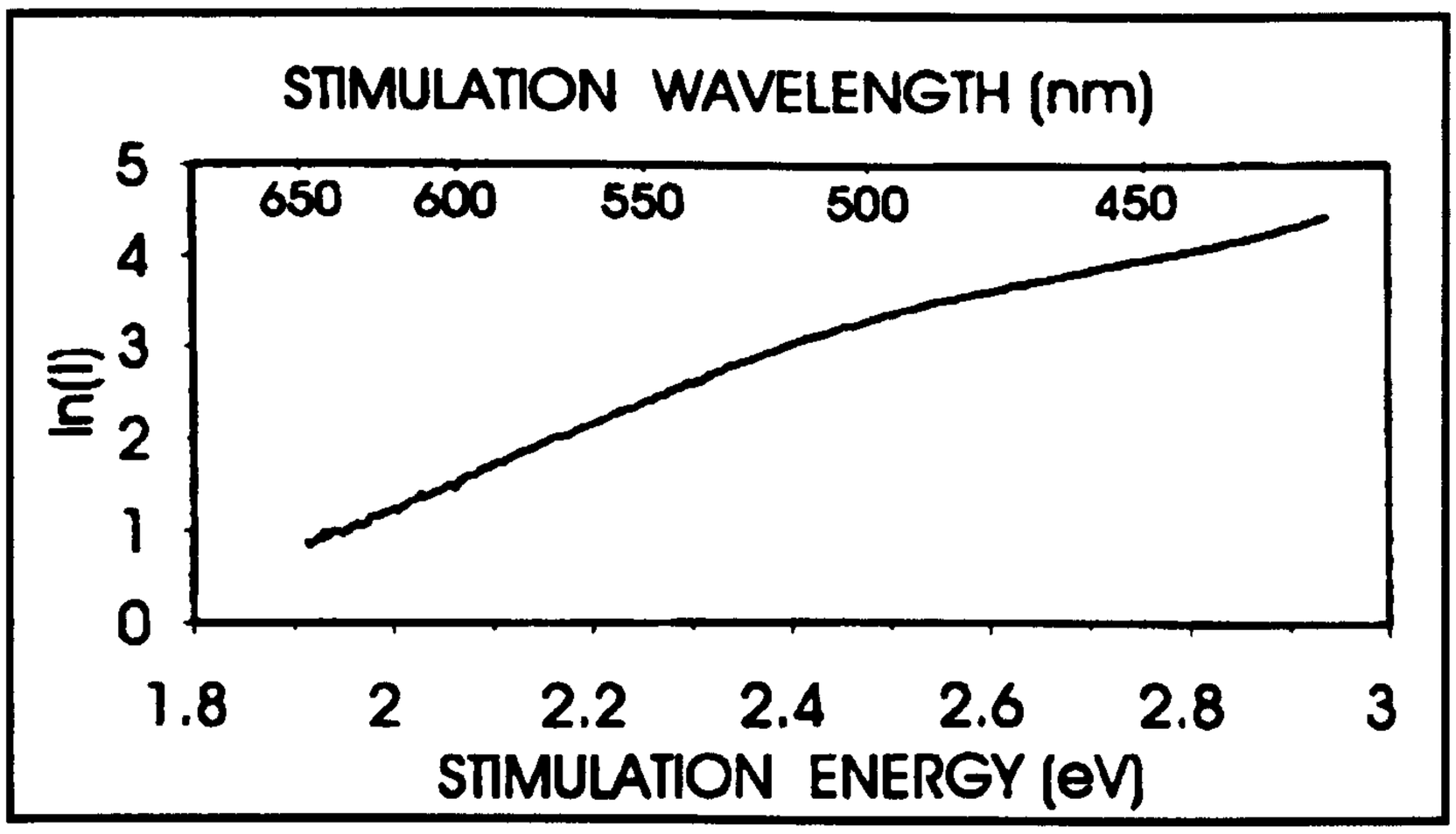

Figure 2.16 – Optical stimulation spectrum (intensity (ln(I)) versus stimulation energy) for a sedimentary quartz (after Bøtter-Jensen *et al.* 1994).

Experiments by Smith and Rhodes (1994) relating to charge movements in quartz demonstrated that the OSL signal is composed of at least two sources of charge when measured at 17°C, one from deep traps associated with the 325°C TL peak and the other from the unstable 110°C TL peak which grows rapidly during measurement as a result of phototransfer i.e. electrons evicted from deep traps are transferred to shallow traps prior to eviction (Figure 2.17). The combination of the two sources resulted in a non-exponential decay curve and although the measurements were repeated at 220°C to remove the unstable 110°C TL component, the decay curve was still non-exponential. Smith and Rhodes (1994) suggested that this was due to the signal originating in a range of trap depths with more than one mean life when optically stimulated and they identified three exponential components within the decay curve (Figure 2.18). Bailey *et al.* (1997) examined the 'fast', 'medium' and 'slow' components of the quartz OSL decay curve in more detail and found that the fast and medium components are associated with the 325°C TL peak but that the slow component is stable up to 650°C and they suggested that it could potentially be used as a long range dating tool. This was developed further by Singarayer *et al.* (2000) and although their initial results were encouraging they identified several potential problems with regard to sensitivity changes and thermal transfer. Recent work by Singarayer and Bailey (in press) using linear-modulated OSL has shown that some samples contain five or six components (Figure 2.19) and that the high dose response of their 'S3' component could be used to date quartz over 1 million years old.

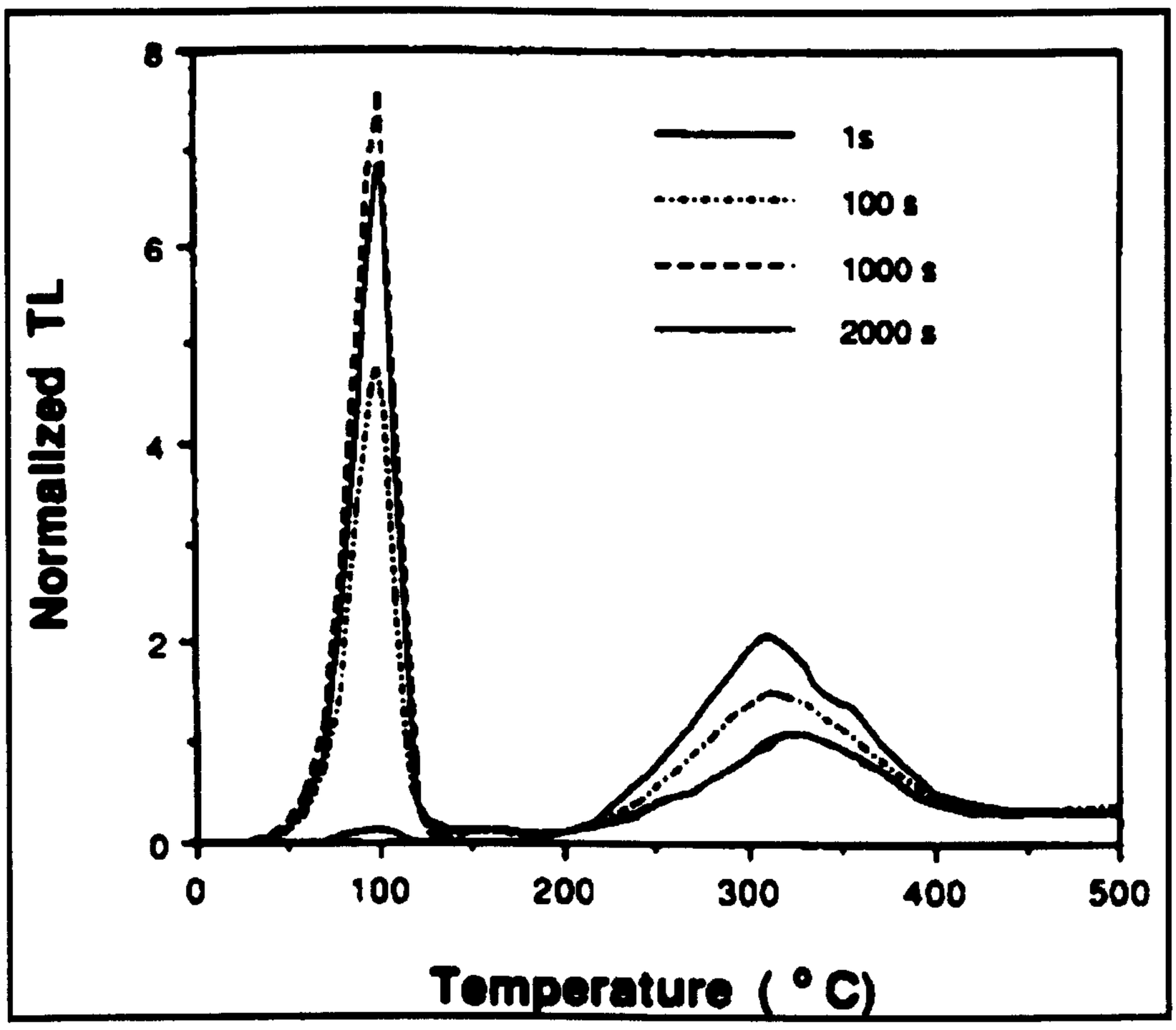

Figure 2.17 – TL measured after progressively longer exposures to green light. Phototransfer occuring between the high temperature 325°C peak and the 110°C TL peak (after Smith and Rhodes 1994).

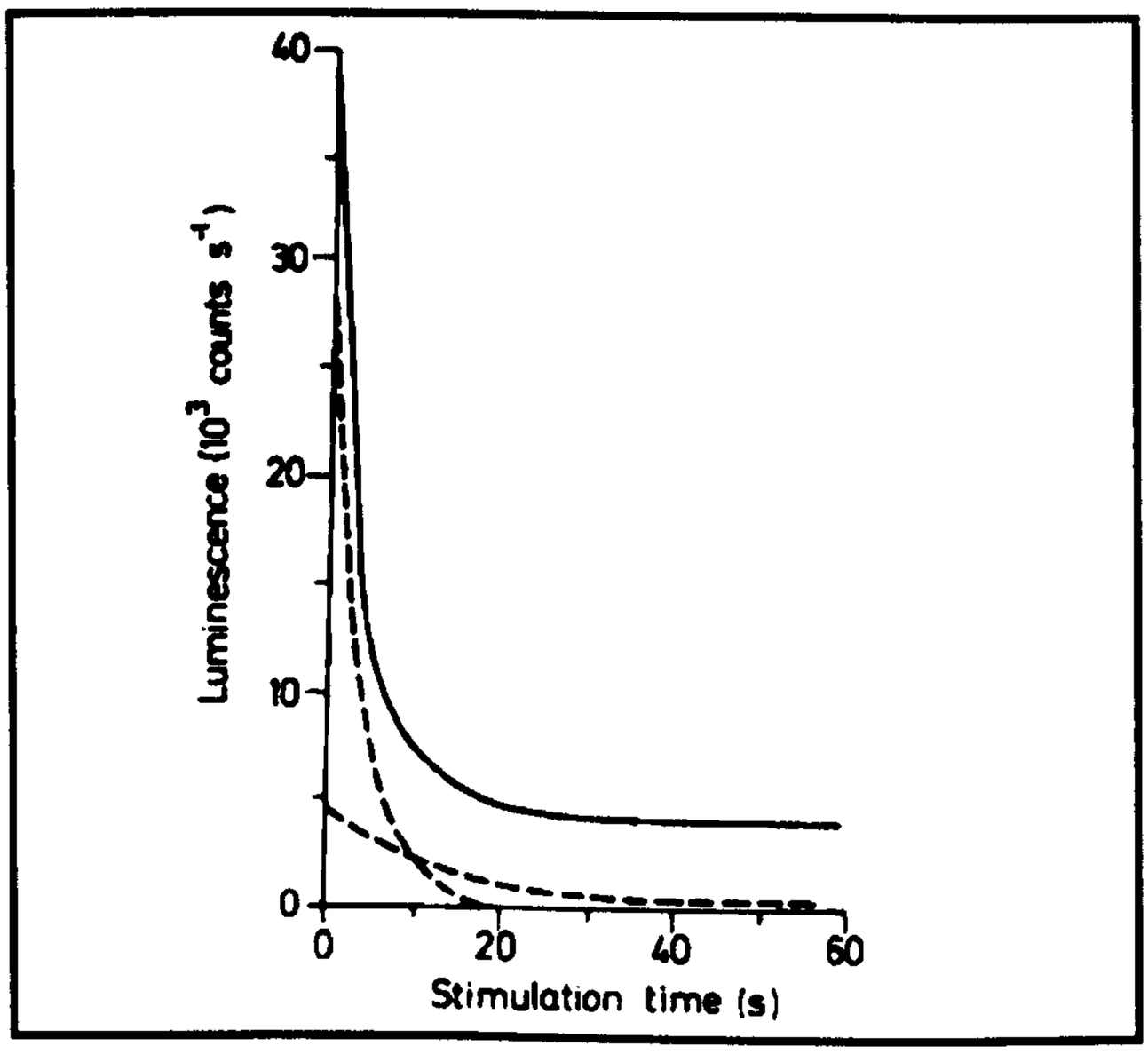

Figure 2.18 – The OSL decay curve from quartz. After subtraction of a long term, almost constant, component two exponential components (fast and medium) remain (after Smith and Rhodes 1994).

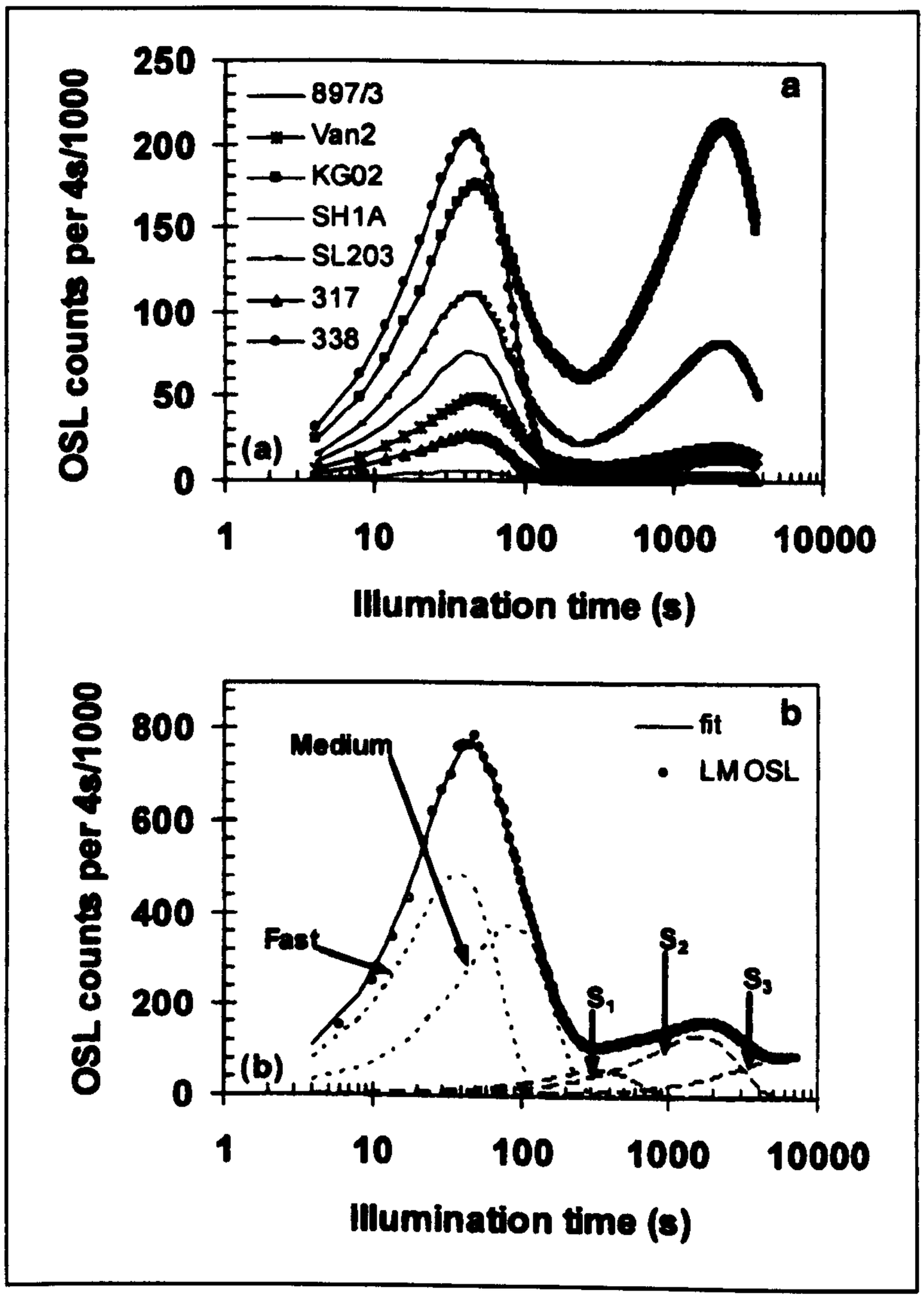

Figure 2.19 – a) Linear modulated OSL at 470 nm for seven quartz samples and b) linear modulated OSL of one sample with five fitted components (after Singarayer and Bailey (in press).

2.4.5.2 Feldspar

As discussed above, quartz is characterised by well-separated TL peaks and resolvable OSL components due to the relatively simple crystalline structure. In comparison, the crystal structure of feldspar is more complicated and depends on the temperature at which it crystallises and its subsequent thermal history (Klein 2002). Nevertheless, like quartz, the main structure is composed of SiO^{4+} tetrahedra but to allow cations like sodium (Na^{+}), potassium (K^{+}) and calcium (Ca^{+}), to enter into the lattice, some of the Si^{4+} are replaced by Al^{3+} (Klein 2002).

Krbetscheck *et al.* (1997) presented a summary of work undertaken on the TL emission of feldspar and they concluded that because TL is emitted in broad wavebands it is difficult to identify specific temperature ranges of emission that occur within a wide range of feldspars. However, two main TL peaks have been identified in potassium feldspars at 280 and 330°C and the heights of these peaks vary depending on whether the sample is from a region with a high ambient temperature (Duller 1997). The lower temperature peak tends to be smaller in such samples and is preferentially removed during preheating (Duller 1997). After irradiation a broad peak based at about 150-180°C was observed but as with the natural TL peaks the intensity of this peak varied presumably due to the variable geology (Duller 1997). Despite the identification of these peaks Duller (1997) concluded that due to sample variation it was not possible to apply the conclusions from one sample to another.

Feldspars were shown to be stimulated by a 514 nm line from an argon ion laser by Huntley *et al.* (1985) and Hütt *et al.* (1988) demonstrated that they were also stimulated by exposure to infrared wavelengths. Clark (1992) and Clark and Sanderson (1994) measured the excitation spectra of various feldspars and micas stimulated from 450-1200 nm using a scanning spectrometer. Their results indicated that the spectra of all the samples measured contained three main excitation bands (550-540 nm, 550-650 nm and 800-1000 nm, Figure 2.20) from the visible to the infra-red, but that the proportion of signal within each excitation band varied from sample to sample reflecting the different trap structures within the various feldspars (Figure 2.21) (Clark 1992; Clark and Sanderson 1994). Further experiments confirmed that the intensity of the luminescence signal depended on the

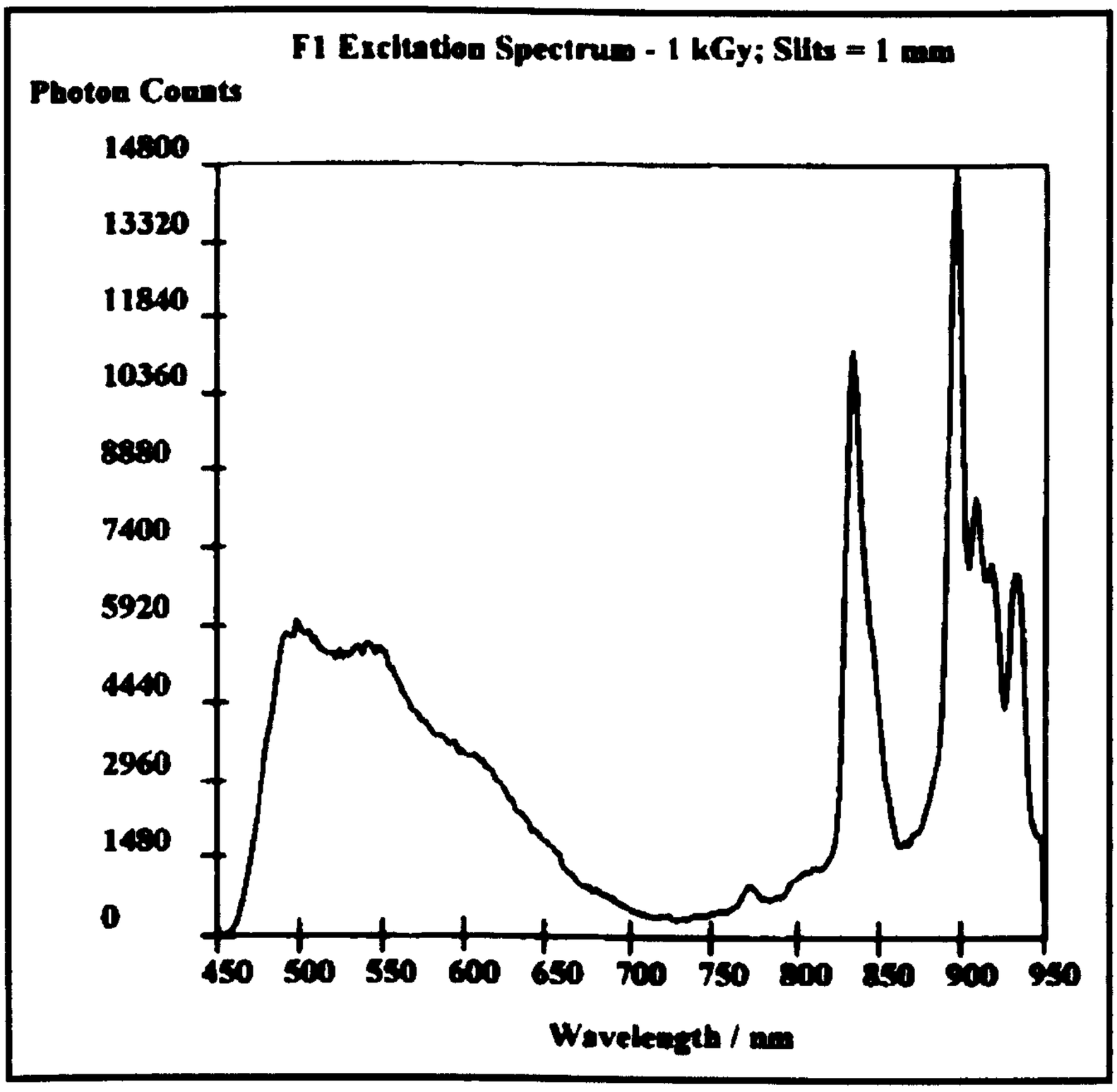

Figure 2.20 – Typical potassium feldspar excitation spectrum (after Clark 1992).

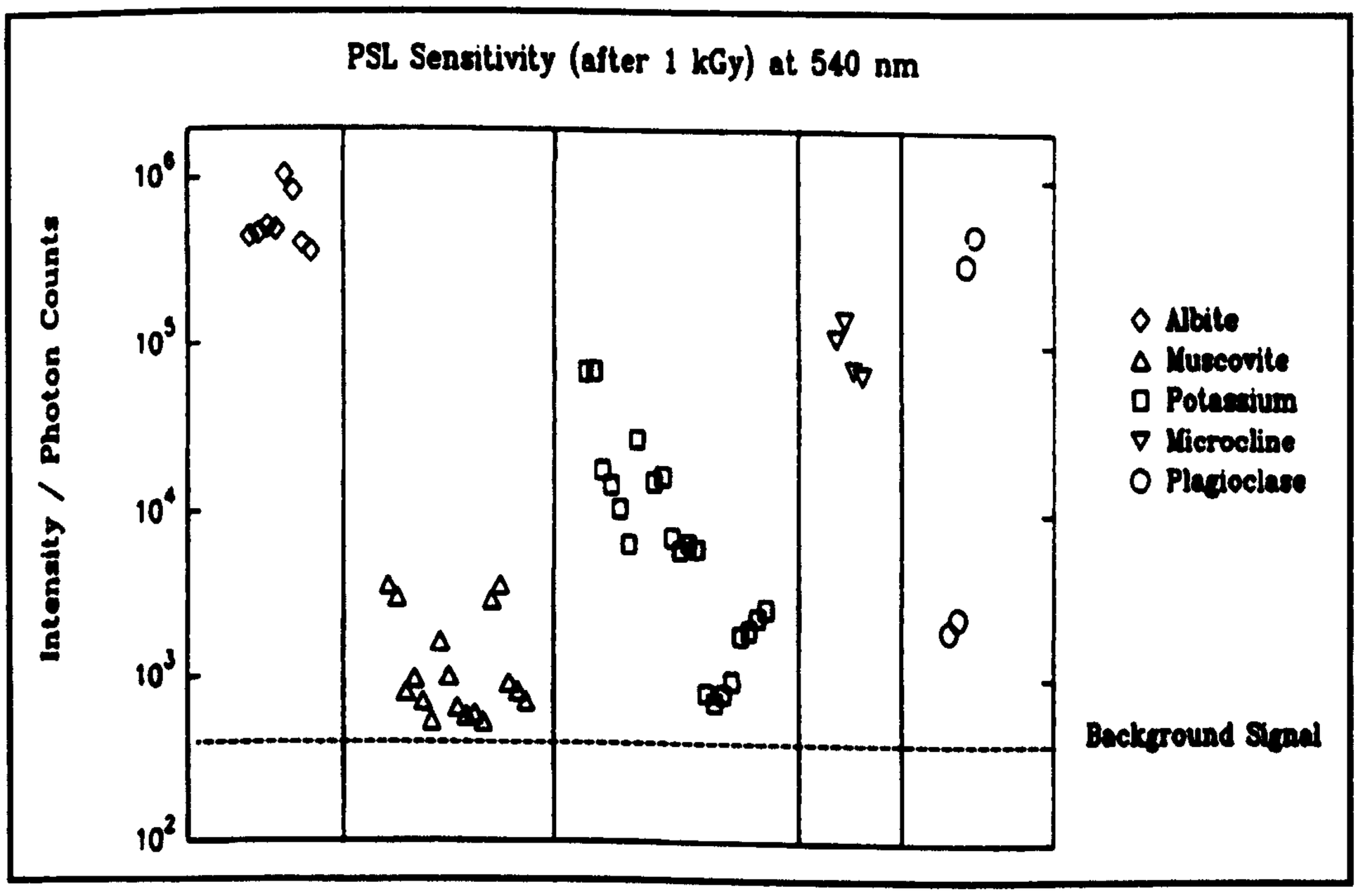

Figure 2.21- Variable feldspar sensitivities at 540 nm (after Clark 1992).

stimulating temperature, as initially demonstrated by Hütt *et al.* (1988), but the experiments by Clark and Sanderson (1994) also showed that the 500-540 nm excitation band was composed of two components, one of which was thermally assisted (Figure 2.22). Clark and Sanderson (1994) suggested that the ground state of the excitation band of the thermally assisted component could be less than 500 nm, in the UV region, and that potentially the sensitivity of this peak and the thermal stability could be used in IRSL dating of feldspars. Clark (1992) also explored a range of single and multiple aliquot approaches to measuring stored doses and showed using a series of samples irradiated to known doses that wavelengths from 500 to 900 nm could be used to recover stored doses successfully.

Further research on the IRSL emission spectra of feldspars by Clarke and Rendell (1997) showed that other emission bands of feldspar do exist at 335 and 400 nm for both natural and irradiated samples separated from detrital sediment. None of their samples showed an emission band at 290 nm for the natural measurement but this emission band was present after artificial irradiation (Figure 2.23) and Clarke and Rendell (1997) concluded that the traps related to this emission band were naturally thermally unstable and were therefore only filled by artificial irradiation. This was confirmed by preheating the samples at 220°C for at least a minute, which removed the 290 nm emission band. Krbetscheck *et al.* (1997) have presented a summary of work undertaken on the OSL and IRSL emission spectra of feldspar and although several clear emission bands are identified not all feldspars emit light at the same wavelengths and this reflects the complex crystal structure of feldspars.

The form of the feldspar decay curve is complex due to the various interactions that occur during measurement and therefore this results in a non-exponential decay curve that has many different components (Duller 1997). Time resolved OSL studies were undertaken on feldspars by Sanderson and Clark (1994) and Clark *et al.* (1997) and this technique measures the amount of luminescence as a function of time after very short pulses of optical stimulation. Sanderson and Clark (1994) identified three peaks, two of which (I and II, Figure 2.24) were unknown prior to these experiments and they concluded that the three peaks represent different recombination pathways within the crystal structure, with those giving rise to the first peak being closest to the recombination centres. In comparison Clark *et al.* (1997) produced a smooth decay curve (Figure 2.25) and a number of exponential components representing different trap lifetimes were fitted to the curve.

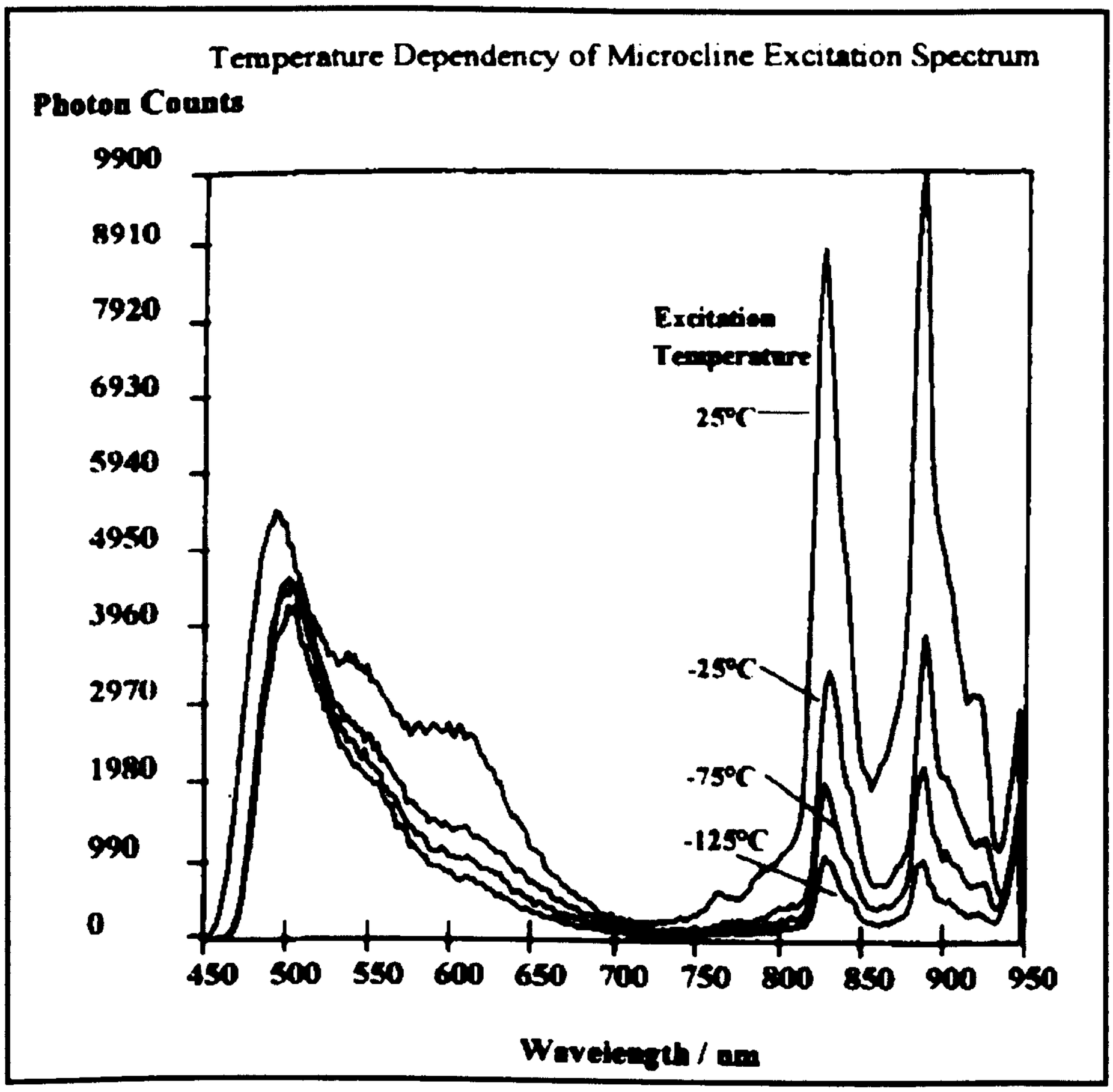

Figure 2.22 – Dependence of the feldspar excitation spectrum on excitation temperature, with the development of a thermally assisted peak in the 500-540 nm emission band (after Clark and Sanderson 1994).

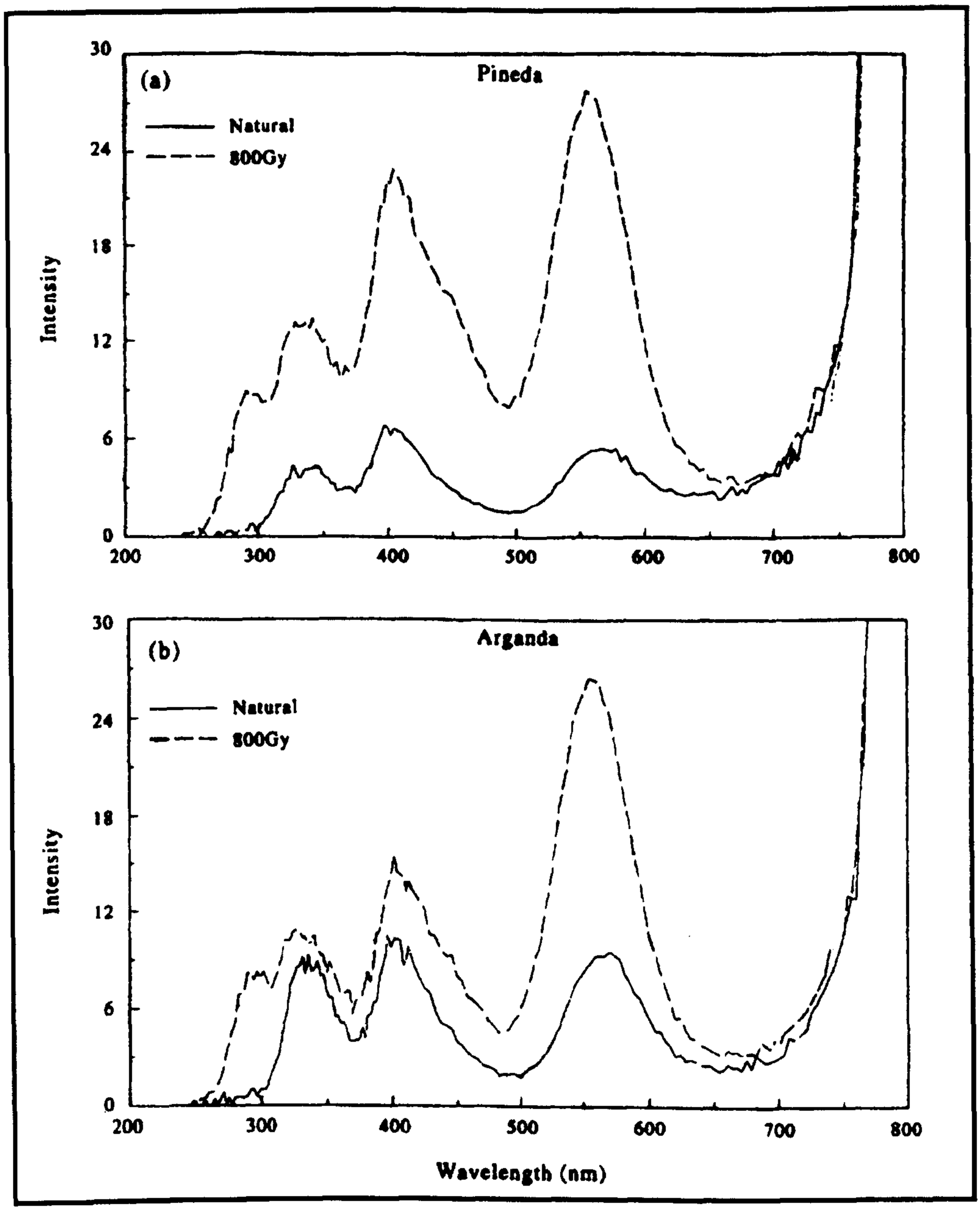

Figure 2.23 – The main emission bands of feldspar including the emission band at 290 nm that is not seen in the natural samples (after Clarke and Rendell 1997).

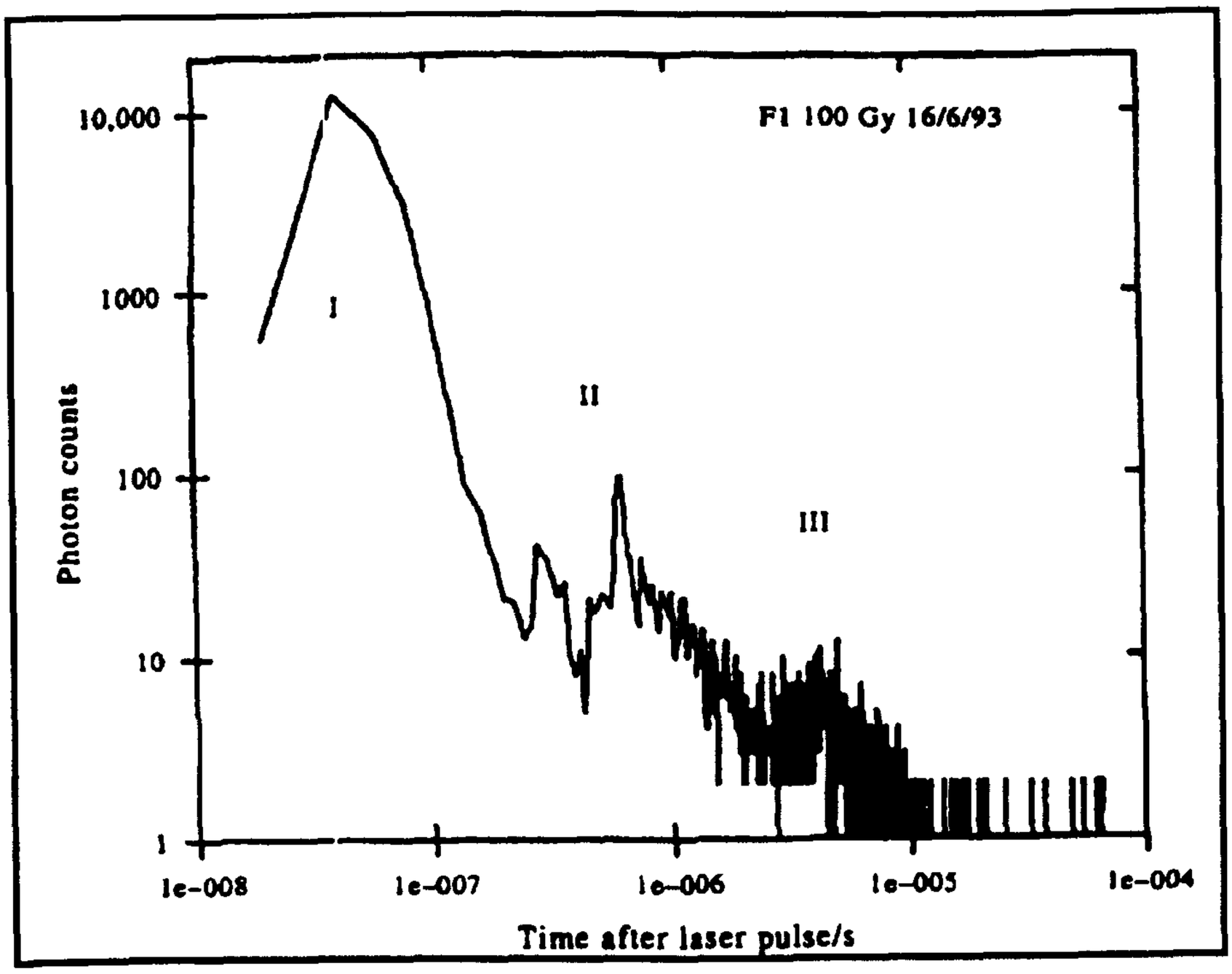

Figure 2.24 – Time resolved OSL spectrum for F1 feldspar (after Sanderson and Clark 1994).

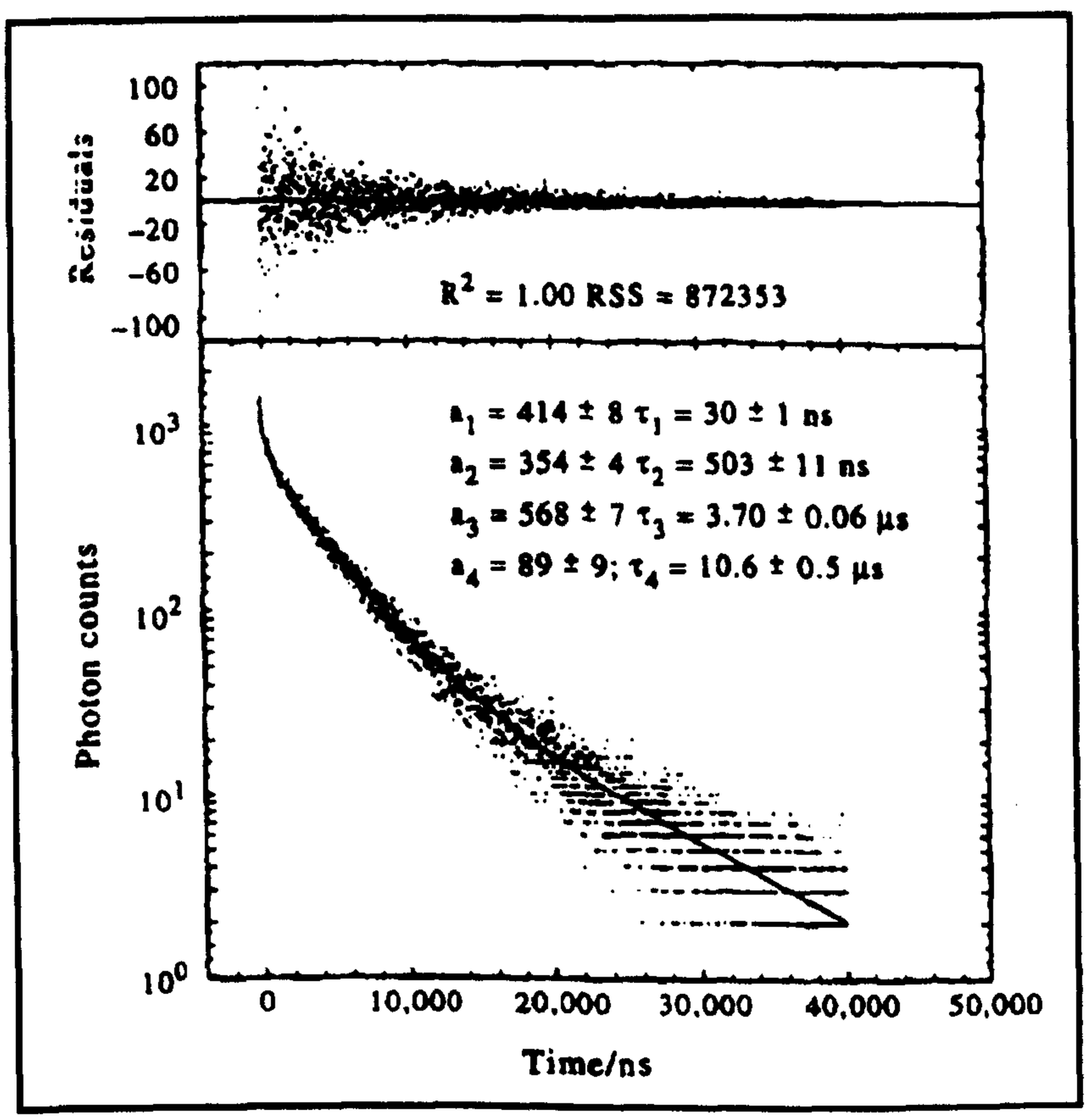

Figure 2.25 – Time resolved OSL from a moonstone with the characteristics of the different fitted components (after Clark *et al.* 1997).

Despite the apparent differences between the results the first three mean lives identified by Clark *et al.* (1997) correspond approximately to peaks I, II and III in Sanderson and Clark (1994).

2.4.5.3 Summary

Both quartz and feldspars have a number of emission bands and those that are most useful in OSL dating can be isolated using specific stimulation wavelengths and filters. Stimulation by IR wavelengths measures all four of the emission bands of feldspars however research on the OSL excitation spectroscopy of feldspars has shown that the UV emission band (~400 nm) is common in most feldspars and is therefore used in most IRSL dating studies (Krbetschek *et al.* 1997). Despite the substantial review by Krbetscheck *et al.* (1997) on spectral information from minerals relevant to the luminescence dating technique, further work is required to determine the emission bands associated with certain types of defects. This will further our understanding of the structure of quartz and feldspar grains and may provide an indication of grain provenance. Although certain stimulation wavelengths have been found to be successful in luminescence dating it should not be assumed that only these wavelengths bleach the luminescence signal and this is discussed in more detail below.

2.4.5.4 Sensitivity to bleaching

The sun's spectrum extends from ultra-violet (100-400 nm, short) to infrared (800-1000 nm, long) wavelengths and although all of these are measurable at the earth's surface the received flux will vary depending on the place, time of day and the weather (Twidell and Weir 1986). Clouds, dust and aerosols effectively scatter and absorb some of the incoming radiation and the amount that is absorbed or scattered will depend on the type of cloud cover (i.e. stratus, cumulus or cirrus) and the quantity of aerosols and dust in the atmosphere (Miller 1981). There is also a latitudinal effect with the highest levels of solar radiation reaching the earth's surface in the cloudless skies of the tropics and subtropics, but at higher latitudes the level of solar radiation reaching the earth's surface is severely restricted by cloud cover (Figure 2.26) (O'Hare and Sweeney 1986).

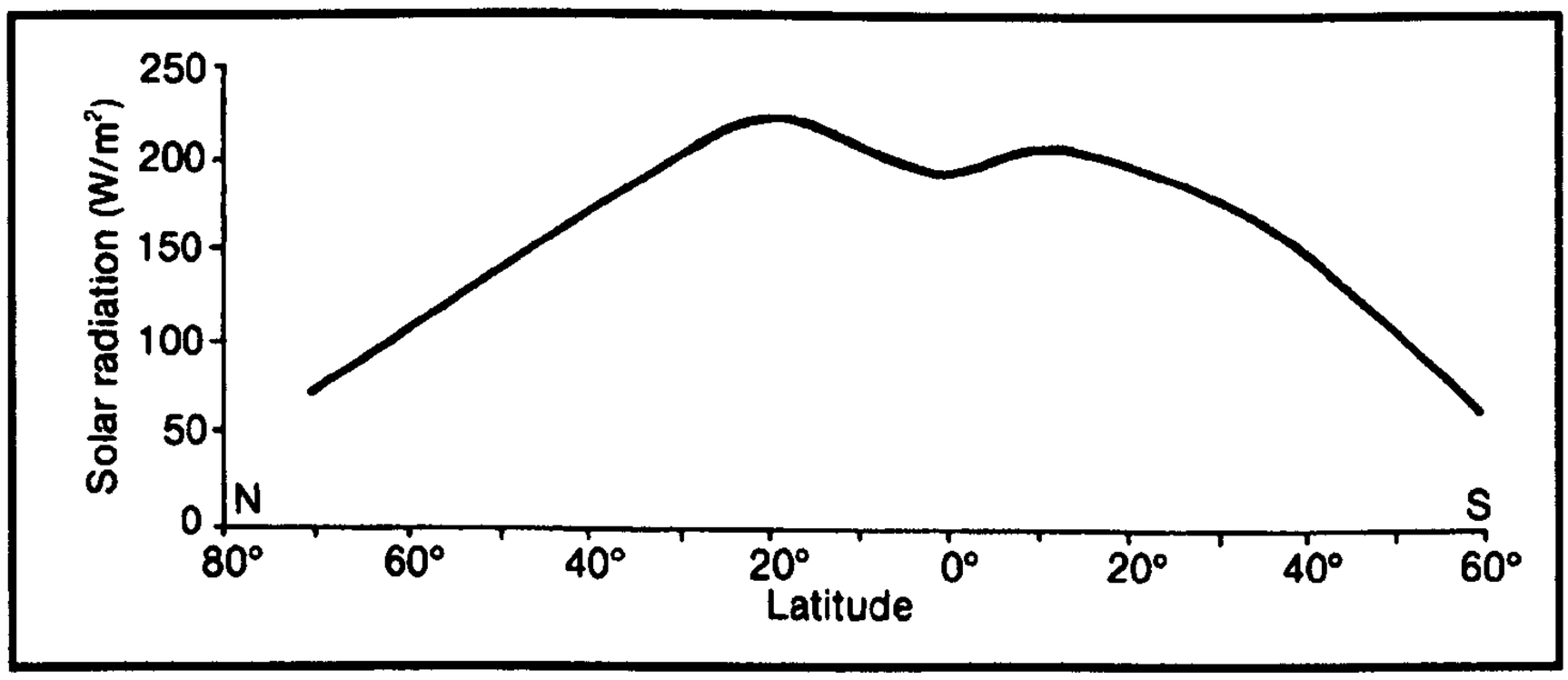

Figure 2.26 – Observed average latitudinal distribution of annual solar radiation received at the earth's surface (after O'Hare and Sweeney 1988).

Successful OSL dating requires the latent signal within quartz and feldspar grains to be removed prior to burial and it has been shown that the luminescence signal of both quartz and feldspar is bleached by exposure to sunlight (Godfrey-Smith *et al.* 1988). In their research they demonstrated that the OSL signal of both quartz and feldspar dropped rapidly within the first 20 seconds of exposure to sunlight (Figure 2.27) and that if the light intensity was reduced by 90%, the OSL signal from quartz bleached at a much slower rate (Godfrey-Smith *et al.* 1988). The luminescence traps in quartz used for OSL dating are stimulated mainly by short wavelengths (Godfrey-Smith *et al.* 1988) and therefore if clouds absorb or scatter this part of the spectrum there will be a reduction in the bleaching rate of these traps. In comparison feldspar is stimulated by both short and long wavelengths and therefore even if the light intensity is reduced the luminescence traps in feldspar will still be stimulated by the longer IR wavelengths. This was demonstrated by Clark (1992) who irradiated single aliquots of microcline feldspar to 100 Gy and then exposed one aliquot to 500 nm and the other to 880 nm. His results (Figure 2.28) showed that the green and infrared emission bands of feldspar are reduced by exposure to both wavelengths. The ease at which the feldspar luminescence signal is reduced by short or long wavelengths suggests that luminescence ages from feldspars should be more reliable than quartz because they should have lower residual levels. Despite this quartz is commonly used in OSL dating, more so than feldspars, because it is thought to bleach faster in optimal conditions. Aitken (1998, Table 6.1) refers to bleaching periods of between 2 and 130 seconds for quartz and 15-1100 seconds for feldspar signals to be bleached by a factor of 10 depending on the natural light intensity experienced by the samples. Although this provides a summary of bleaching rates for some minerals, Aitken (1998) points out that the term 'sunlight exposure' is very imprecise and will vary depending on the time of year, cloud cover etc. Many of the studies in Aitken's table are based on only a few samples and therefore although it does provide some indication on bleaching rates, variations in mineralogy will undoubtedly affect the rate of bleaching.

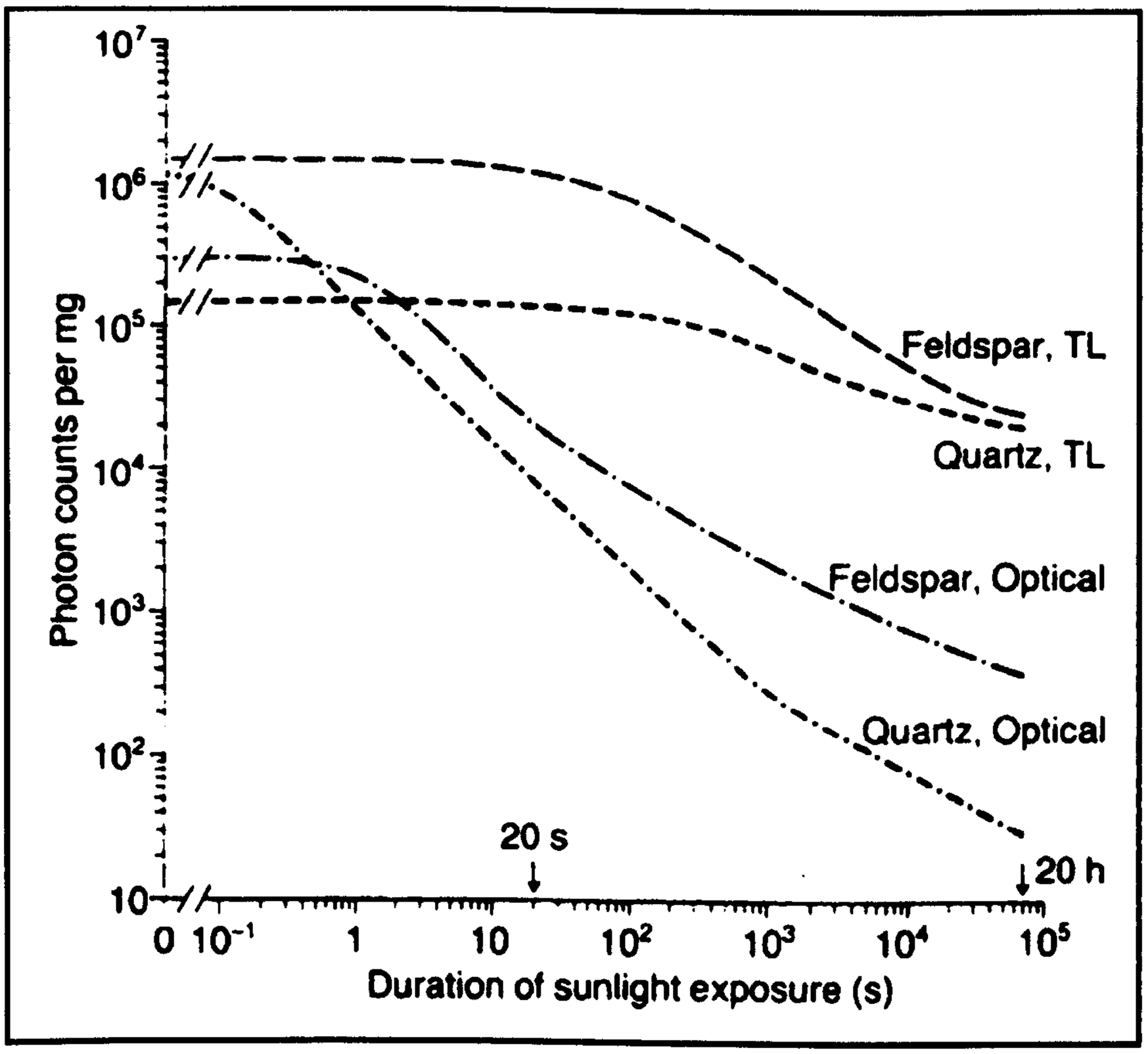

Figure 2.27 – Decay of TL and OSL signals from feldspar and quartz with exposure to sunlight (after Godfrey-Smith *et al.* 1988)

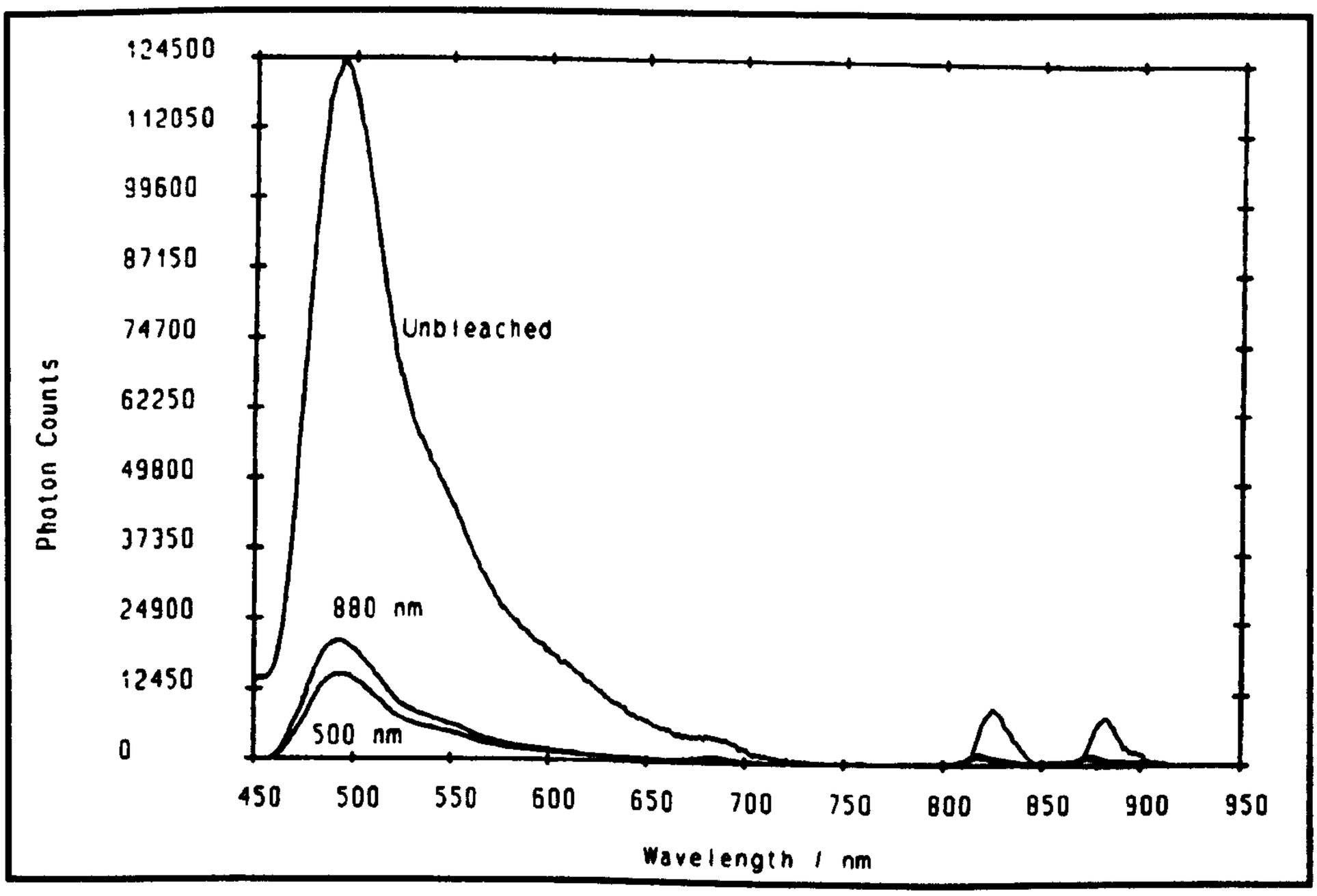

Figure 2.28 – The microcline excitation spectrum after bleaching with 500 nm and 880 nm light for 30 seconds (after Clark 1992).

2.4.6 Recent developments in OSL sediment dating

2.4.6.1 Development of detectors and automated systems

Initial OSL dating procedures (e.g. Huntley *et al.* 1985) used a green argon ion laser with a wavelength of 514 nm to stimulate traps within quartz and feldspar grains which have emission wavelengths of 365 nm and 410 nm respectively. The laser was ideal for stimulation because of its high intensity allowing measurements to be made quickly however the lasers were expensive and therefore a cheaper method of stimulation was sought leading to the use of light emitting diodes (LEDs) for stimulation. Hütt *et al.* (1988) identified traps within feldspars which could be stimulated by infra-red (IR) wavelengths and the ease at which the stimulating and emitting wavelengths were separated led to the first use of IR LEDs for stimulation (Poolton and Bailiff 1989). Smith *et al.* (1990) discovered that the traps in quartz grains did not appear to be stimulated by IR and this led to a further use of the IR LEDs in quartz OSL dating to determine if feldspars or other IR sensitive minerals contaminated the quartz.

Other sources of light such as halogen lamps and xenon lamps were used instead of the argon ion lasers for stimulation of quartz grains (Spooner and Questiaux 1989; Bøtter-Jensen and Duller 1992, Bøtter-Jensen 1997) however Galloway (1992) developed a green LED system based on the same arrangement as the IR diodes. Although the system was small and economic the samples had to be stimulated for much longer periods of time due to the low intensity of the green diodes (Galloway 1992; Galloway *et al.* 1997). The system was improved using a new mounting system for the LEDs and subsequent results indicated that the sensitivity was comparable to the argon ion lasers (Galloway *et al.* 1997).

The emission wavelength of quartz is concentrated between 360-380 nm and research by Bøtter-Jensen *et al.* (1994) concluded that stimulation at longer wavelengths effectively reduced the emission efficiency of the quartz OSL traps. This led to the development of the blue LED system which stimulates at a peak wavelength of 470 nm and uses a green long-pass GG-420 filter to reduce the intensity of the higher stimulating wavelengths and prevent scattered blue light reaching the photomultiplier (Bøtter-Jensen *et al.* 1999a and b). Due to the shorter stimulating wavelengths of the blue LEDs they provide more power and

are more efficient than the green LEDs (Bøtter-Jensen *et al.* 1999a and b) and are therefore commonly used in OSL dating of quartz today.

2.4.6.2 Palaeodose determination

The palaeodose of a sample is essentially determined by comparing the natural OSL signal with that of an induced OSL signal from a known dose of artificial irradiation (Aitken 1998). Early OSL dating work used a multiple aliquot additive dose procedure to determine the palaeodose, however a single aliquot regenerative technique is now used to date most unheated sediments. Both procedures are discussed in more detail in Sections 2.4.6.2.2 and 2.4.6.2.3, however multiple and single aliquot procedures require each aliquot to be given a preheat before the natural or regenerated doses are optically measured and this is discussed below.

2.4.6.2.1 Preheating

The OSL signal originates from the release of charge (electrons) from thermally stable and unstable traps and the subsequent interaction of the electrons with luminescence centres (Huntley *et al.* 1985; Aitken 1998). Preheating the quartz before optical stimulation ensures that electrons are ejected from the unstable traps, and therefore the OSL signal measured should be from light-sensitive thermally stable traps alone (Huntley *et al.* 1985). The low temperature unstable traps have short life-spans, e.g. the 110°C trap has a lifetime of 1.48×10^{-2} years (~5 days) at ambient temperatures (15°C), as demonstrated by Godfrey-Smith (1994), and due to thermal decay are generally not filled during burial (Rhodes 1988, Wintle and Murray 1998). These traps are, however, filled during artificial irradiation in the laboratory (Godfrey-Smith 1994), and unless they are emptied before the OSL measurement, the palaeodose, and hence age of the sample, may be over-estimated (Aitken 1998).

Rhodes (1988) suggested that during the preheat treatment there may be a thermal transfer of charge from less stable, harder to bleach traps to more stable, easy to bleach traps. He observed that the OSL signal of artificially irradiated samples increased as the preheat temperature was raised from 140°C to 210°C. Although also seen in natural samples the level of increase was much smaller, possibly due to charge transfer occurring during burial

(Rhodes 1988). Thermal transfer during burial is not restricted to light-sensitive traps and therefore preheating also completes any charge transfer between light-insensitive traps and the main OSL trap (Aitken 1998). It is important to try and replicate in the laboratory the amount of natural charge transfer, and therefore preheating of both natural and regenerated aliquots is required (Smith and Rhodes 1994; Murray and Roberts 1998; Murray and Mejdahl 1999).

It was also suggested by Rhodes (1988) that the increase in signal with higher preheat temperatures may be partly due to sensitivity changes in quartz, first reported by Aitken and Smith (1988). In their experiments the response of a small test dose preheated at 220°C and then 300°C was examined. After the 300°C preheat the test dose signal had increased by one-third in comparison to the 220°C preheat signal, and had increased by a factor of 3 after a preheat of 600°C (Aitken and Smith 1988). The 110°C TL peak was also measured throughout the experiment and found to reflect the increase in the OSL signal (Aitken and Smith 1988). Further work by Stoneham and Stokes (1991) concluded that dose related sensitivity changes in the 110°C TL peak reflected the sensitivity changes in the OSL signal, and therefore the 110°C TL peak could potentially be used to correct for sensitivity changes. This is discussed further in Section 2.4.6.2.3.

The introduction of the single aliquot regeneration method, discussed below, to determine the palaeodose of feldspars by Duller (1991) allowed small samples to be rapidly measured with high precision, however sensitivity changes were observed as a result of repeated preheating and bleaching. Jungner and Bøtter-Jensen (1994) discussed the effect of preheating at different temperatures using the regenerative technique. The quartz was zeroed before being irradiated and preheated over a range of temperatures from 150-320°C. Their results showed an increase in sensitivity between 200-250°C, but stable sensitivity above 250°C. Further, Murray and Roberts (1998) suggested that rather than thermal transfer being the cause of variation in D_e with preheat temperature, D_e variation was the result of a change in the probability of luminescence recombination. Recent research by Murray and Wintle (2000) and Murray-Wallace *et al.* (2002) indicates that D_e of young quartz samples appear to be independent of the preheat temperature. The majority of the preheat temperature dependence plots in their studies showed little or no increase in D_e with increasing preheat temperature, suggesting little, if any, charge transfer occurring. Although both ceramic and sediment samples from various sites throughout the world were used by Murray and Wintle (2000) other samples from different geological areas may not

be independent of preheat temperature and therefore preheat temperature dependence plots should be constructed for individual samples.

Various preheat temperatures have been used throughout the development and use of OSL dating. Although preheating is necessary to remove the unstable signal from artificially irradiated samples, a temperature must be found which does not thermally erode the main OSL trap (Smith *et al.* 1986). Rhodes (1988) established the preheat temperature range over which the ratio of the natural to natural+artificial OSL remained constant, indicating that a broad plateau of preheat temperatures could be used. However Rhodes (1988) continued to use a preheat of 220°C for 5 minutes as suggested by Smith *et al.* (1986). Further work by Stokes (1992, 1994) suggested longer preheats at lower temperatures (160°C for 16 hours) should be used, but samples measured by Roberts *et al.* (1994) using this preheat were underestimated by 10%-40%. They repeated their experiments using a preheat of 220°C for 5 minutes and the D_e they obtained agreed with independent age controls.

Murray *et al.* (1997) used a preheat temperature, obtained from constructing preheat plateau plots, or preheat temperature dependence plots, and an additive dose single aliquot protocol to determine the D_e of Australian sedimentary quartz. The results from the preheat temperature dependence plots indicated that samples from different environments in Australia require different preheat temperatures e.g. coastal dune sands between 160-200°C and wind blown quartz between 260-300°C (Murray *et al.* 1997). These results prompted Murray *et al.* (1997) to stress the importance of investigating the preheating behaviour prior to measurement of the D_e. Further preheat experiments by Wintle and Murray (1997), Murray and Roberts (1998), and Murray and Mejdahl (1999), on Australian sedimentary quartz and Scandinavian heated quartz from archaeological sites, concluded that preheat temperatures of between 160°C and 300°C could be used for OSL measurement. There was, however, a slight decrease in the OSL signal after the quartz was preheated to 280°C or above, prompting Wintle and Murray (1997) to suggest that lower temperatures should be used for younger samples to prevent thermal erosion of the OSL trap. Similar preheat temperatures should also be used for older samples however slight thermal erosion of the main OSL trap is unlikely to have a significant effect on the resultant age. Recent research by Murray and Wintle (2000), Banerjee *et al.* (2001) and Murray-Wallace *et al.* (2002) suggests that preheat temperatures of between 180°C and 270°C can be safely used in luminescence dating of unheated sediments.

2.4.6.2.2 Multiple aliquot additive dose procedure

The multiple aliquot additive dose method used in OSL dating to determine the palaeodose of a sample uses one set of discs to measure the natural signal and other groups of discs are given various doses of laboratory irradiation on top of the natural signal before measurement (Aitken 1998). A typical additive dose response curve is shown in Figure 2.11 and each point is the average dose response of the discs within each group. To determine the palaeodose of the sample the dose response curve is extrapolated back until it intercepts the dose axis. Extrapolation of the dose response curve can however be problematic with some samples, especially older samples, showing signs of sublinearity (i.e. as the dose increases the OSL response decreases) (Figure 2.15) and therefore extrapolation may only give a rough estimate of the palaeodose (Aitken 1998). For young samples supralinearity (i.e. an increase in sensitivity) can be a problem however this is unusual in OSL dating (Aitken 1998). Due to the problems associated with extrapolation this has led to the development of a single aliquot regenerative approach that uses interpolation rather than extrapolation to determine the palaeodose of the sample (Figure 2.29) and this is discussed in more detail below.

2.4.6.2.3 Development of single aliquot procedures

Single aliquot procedures were first developed for feldspars by Duller (1991), and subsequently for quartz by Stokes (1994) and Mejdahl and Bøtter-Jensen (1994), however all found that the changes in sensitivity were too severe for the technique to be viable. Mejdahl and Bøtter-Jensen (1994) tried to compensate for this by developing the SARA (Single Aliquot Regeneration Added dose) procedure, which Murray (1996) developed further with young fluvial sediments. SARA compensates for sensitivity changes by plotting the apparent doses from a regenerative protocol against added laboratory doses, however 4 aliquots are usually required and, as with multiple aliquot techniques it involves extrapolation of the regression line to calculate the D_e (Aitken 1998).

The first single aliquot procedure for quartz was proposed by Murray *et al.* (1997) using an additive dose protocol. A preheated aliquot was given a short shine (i.e. exposed for a short period of time to reduce the OSL signal by a negligible amount allowing many measurements on the same aliquot) before a laboratory dose was added and the procedure repeated several times. At the end of the cycle, preheating and short shine measurements

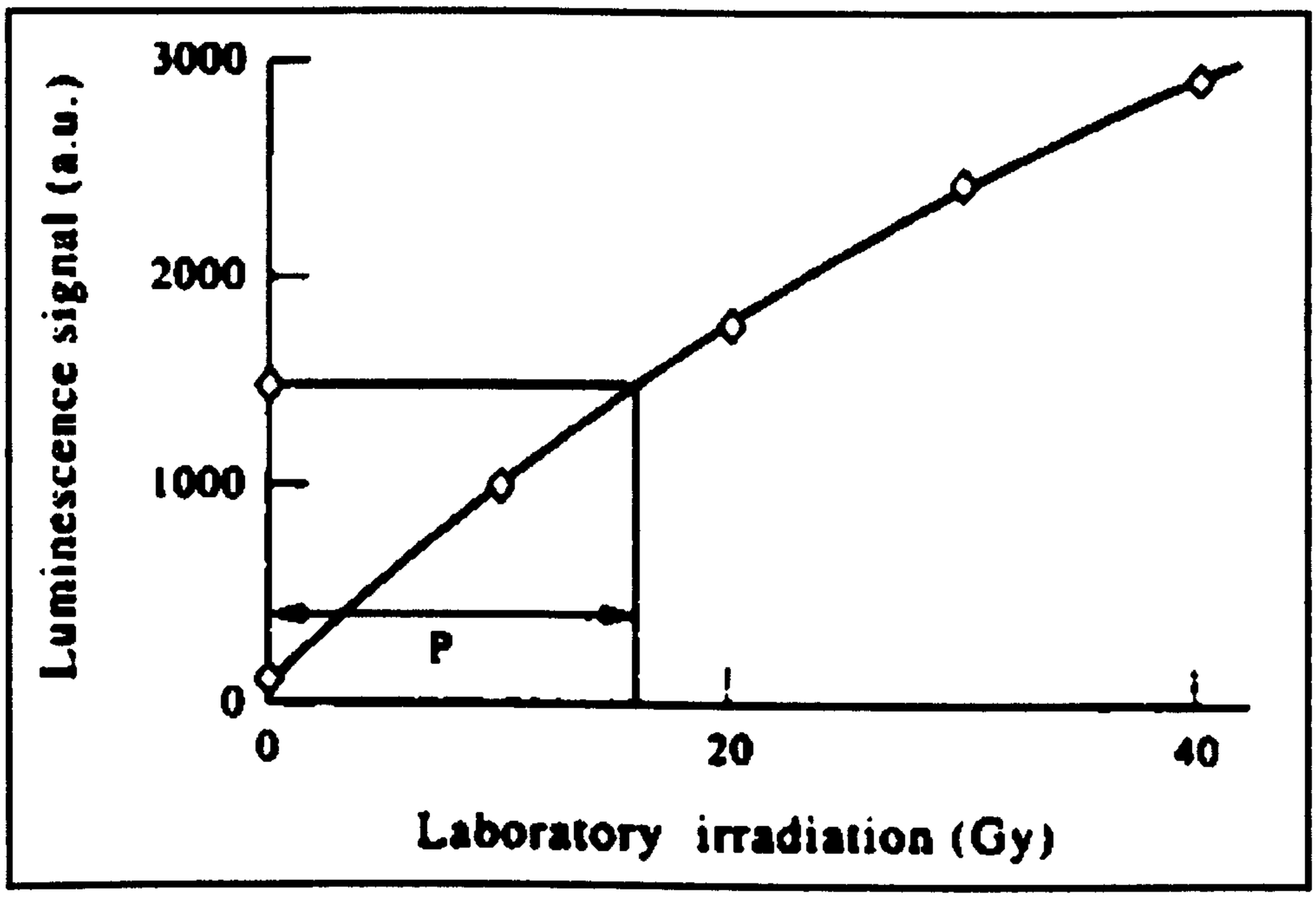

Figure 2.29 – The single aliquot regenerative technique to determine the D_e of a sample (after Wintle 1997)

were continued on the aliquot without further laboratory doses to allow the exponential decay rate of the OSL to be calculated and corrections made to the additive dose growth curve for sensitivity changes (Murray *et al.* 1997). However, it is not realistic to compare the natural signal of the aliquot with the signal at the end of the process as repeated irradiation, preheating and short-shine measurements on one aliquot will undoubtedly alter the behaviour of the quartz. This method also assumes that a constant fraction of the signal is removed at each stage, implying that the decay curve is a single exponential, however Smith and Rhodes (1994) and Bailey *et al.* (1997) have shown that there are at least three components to the quartz OSL signal. Another drawback of this technique is that because short shines are used to measure the OSL signal, samples must be highly sensitive (Aitken 1998) and therefore dim samples could not be dated in this way. Although the technique was successful for 10 of the 11 sites sampled (Murray *et al.* 1997), one of the sites could not be dated because the OSL signal did not decay exponentially. Murray *et al.* (1997) concluded that this was due to an increase in the efficiency of the luminescence signal, and hence sensitivity of the sample, during the preheat which could not be corrected for using the short shine measurements at the end of the cycle.

Fleming (1973) demonstrated that luminescence centres associated with the 110°C TL peak were thermally activated during preheating causing an increase in sensitivity and he used this in his pre-dose dating technique to determine the palaeodose of a sample. Further work by Aitken and Smith (1988) indicated that the sensitivity of the 110°C TL peak closely followed the OSL sensitivity changes of quartz. This was confirmed by Stoneham and Stokes (1991) who also suggested that the response of the 110°C TL to a test dose could be used to test whether any sensitivity changes occurred during the measurement procedure, and that potentially it could be used to correct for sensitivity changes. Based on the relationship between the 110°C TL peak and the OSL response Murray and Roberts (1998) proposed that sensitivity changes could be corrected for by dividing the OSL signal by the normalised 110°C TL peak area, measured during the following preheat. This allowed a single aliquot regenerative protocol to be developed. Further work by Murray and Mejdahl (1999) assumed that the sensitivity changes monitored by the OSL response of the test doses were proportional to the preceding natural or regenerated dose, and so sensitivity changes could be corrected for by dividing the natural or regenerated OSL signal by the subsequent test dose OSL response. Using the OSL test dose response to correct for sensitivity changes ensures that the same traps and centres are used for both the

regenerative and test dose signals however it does not allow the sensitivity to be measured prior to measurement of the natural signal.

Initial SAR work by Murray and Roberts (1998) and Murray and Mejdahl (1999) suggested that the test dose should be smaller than the natural dose to avoid contamination of the OSL trap by thermal transfer during the preheat from light insensitive traps. However, recent research by Murray and Wintle (2000) concluded that no significant variation in D_e occurred with the size of the test dose and that the test dose should be slightly greater or equal to the natural signal. Their conclusions were based on the response of two samples – a heated quartz and a sedimentary quartz- and although their results indicated that the D_e were insensitive to the size of the test dose it cannot be assumed that all samples will behave in a similar manner.

The SAR protocol currently used in OSL dating was developed by Murray and Wintle (2000) who considered in some detail sensitivity changes and correction procedures using the OSL response to the test dose, as suggested by Murray and Mejdahl (1999). At the end of the run, a low dose point was repeated to ensure that the test dose correction for sensitivity changes was satisfactory and that the D_e obtained were independent of preheat and stimulation temperature (Murray and Wintle 2000). It was also suggested by Murray and Wintle (2000) that only the initial part of the OSL signal should be used for D_e estimation in order to ensure that only the light-sensitive traps are measured, and that an enhanced signal-to-noise ratio is achieved.

A common problem when dating young samples using multiple grain single aliquots is that the D_e can be overestimated due to the potential mixture of bleached and partially bleached grains. Small aliquots of between 60 and 100 grains were used by Olley *et al.* (1998, 1999) to increase the likelihood of identifying a mixed dose population in young fluvial quartz. They plotted their results on histograms, which showed wide asymmetric dose distributions (Figure 2.30) and concluded that the aliquots with the lowest D_e were probably the best estimate of the true burial dose of the fluvial sand. Recent research by Spencer *et al.* (in press) has introduced the F-ratio to analyse D_e distributions from small aliquots and their initial results from four young sedimentary quartz samples is encouraging.

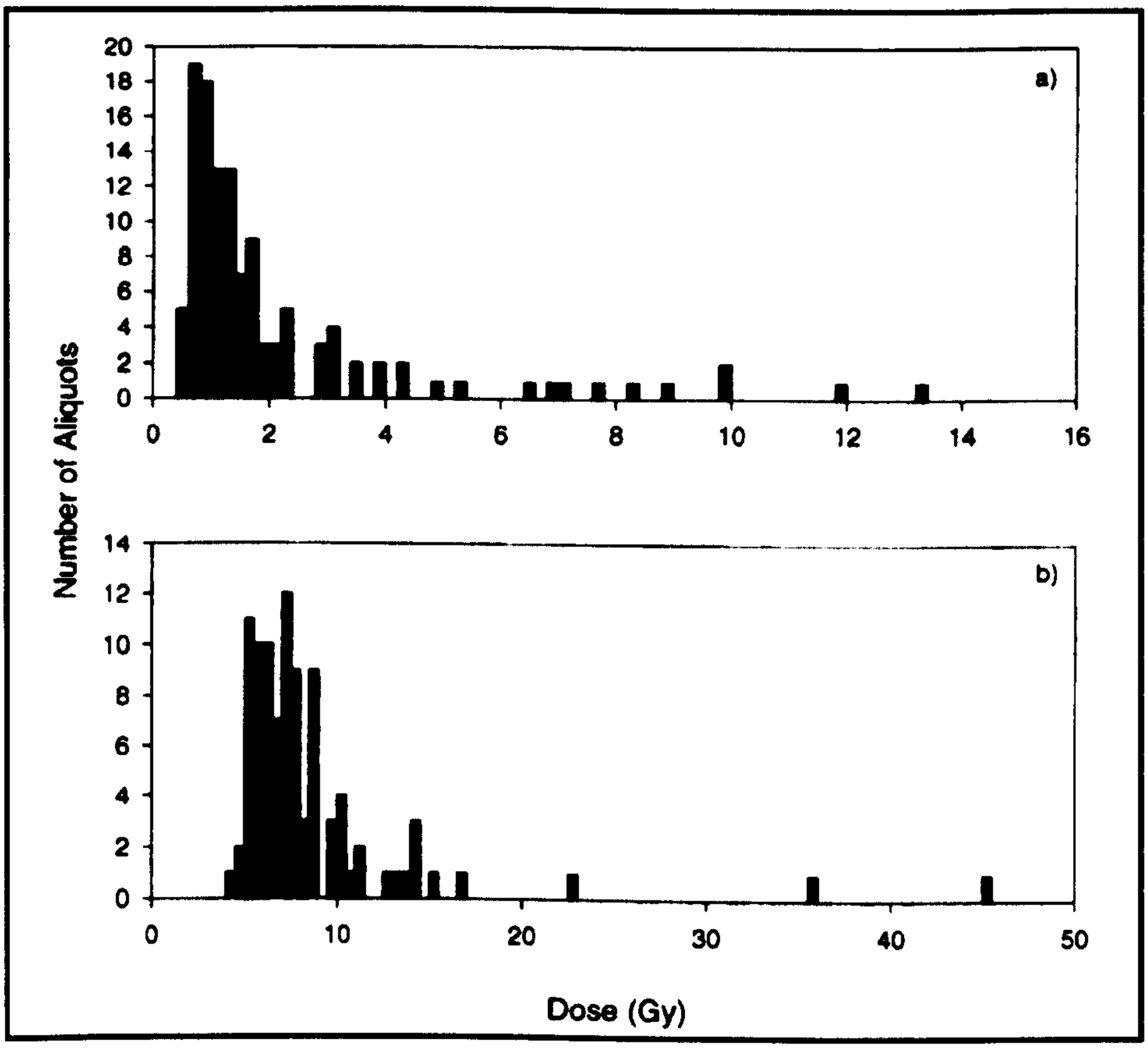

Figure 2.30 – D_e distribution histograms of small aliquots of quartz from fluvial sediments (after Olley *et al.* 1998, 1999).

2.4.7 Single grain measurements

As mentioned above, the luminescence signal from multiple grain aliquots can be quite varied and it has been suggested that this may be due to the number of 'bright' grains on each disc (Duller *et al.* 2000; McCoy *et al.* 2000). The majority of the OSL signal is thought to come from a few grains (McFee and Tite 1994) and therefore if the number of these 'bright' grains varies between discs then the luminescence signal will also vary. Recent developments in OSL dating of sediments have led to the introduction of single grain measurements which uses the SAR protocol on a single grain of quartz or feldspar to determine the age of the sample. The single grain technique was first proposed by Lamothe *et al.* (1994) who questioned whether all the grains within a sample were partially bleached or whether some were well-bleached and others only partially bleached. They concluded that based on the range of natural IRSL intensities from the individual grains the sample being dated was indeed partially bleached.

A large number of grains must be analysed in order to recognise any variability between the grains and this has led to the development of an attachment which allows the measurement of single grains to be made on a standard automatic reader. The grains are mounted on 9.7 mm discs which have had 64 holes drilled into them and the system has been developed to allow each grain to be individually stimulated, but all the grains to be irradiated and heated at the same time (Duller *et al.* 1999). Further details about single grain measurements and the single grain automated reader are given in Duller *et al.* (1999), Bøtter-Jensen *et al.* (2000), Duller *et al.* (2000) and McCoy *et al.* (2000).

2.4.8 Problems associated with OSL dating

OSL dating of unburnt sediments has developed considerably since the initial publication by Huntley *et al.* (1985). However, there remain concerns with regard to both the extent of bleaching prior to burial and the rate of bleaching when grains are initially exposed to light. Residual OSL signals have been identified in modern sediments that were expected to be well-bleached (e.g. Clarke 1996; Richardson 2001) and this has led to the development of several methods of analysis to identify partially bleached deposits e.g. the shine plateau (Huntley *et al.* 1985), D_e/ln plots (Clarke 1996), the use of a t-test (Colls *et al.* 2001) and signal component analysis (Bailey *et al.* 1997). The rate of bleaching is also assumed to be relatively quick with the majority of the signal thought to be depleted within

the first minute of exposure to sunlight (Aitken 1998). However, the rate of bleaching will vary quite considerably when, for example, latitude, length of daylight and cloud cover is taken into consideration. In addition some storms and burial events occur during darkness (especially in the long winter nights in Orkney) and so may retain a signal inherited from a previous event. As a result there is still a need to test modern sediments for residual signals in an environment similar to that being dated.

Few luminescence sediment studies have been undertaken in Scotland and those that have, have tended to concentrate on pre-Late Devensian or glacial deposits (e.g. Duller 1994, Duller *et al.* 1995, Hall *et al.* 1995, and Hall *et al.* 2002). Only one study to date, by Gilbertson *et al.* (1999), has concentrated on sand drift deposits on the Outer Hebrides and identified specific periods of increased sand movement throughout the last 14,000 years. The extensive sand deposits on the Orkney Islands and the exposure to the strong North Atlantic winds provide an ideal environment to test the viability of optically stimulated luminescence dating. Aeolian sediments are thought to be well bleached however the Orkney Islands are located at a relatively high latitude and therefore an ideal site to assess the rate and extent of bleaching of wind blown sands in an area which is often covered in cloud. Fieldwork was undertaken during 1999, 2000 and 2001 and involved the collection of sands from modern beaches and archaeological sites or landscapes, and the sites will be presented in the next chapter.

2.5 Summary of Chapter 2

This chapter has introduced the study area providing a summary of the geology, glacial history and archaeology of both the Orkney Islands and Outer Hebrides before presenting the background to luminescence dating. The Orkney Islands were chosen for this research because of the large number of archaeological sites that contain wind blown sand deposits, however OSL dating has not been undertaken in this area before and therefore it is not known whether such sand deposits can be successfully dated using this technique.

Many of the recent approaches in luminescence dating have been tested on one or two samples from an individual site and therefore there is a need to test these new approaches on samples from a variety of sites. Recent OSL applications have also tended to concentrate on sediment samples from pre-Holocene sites and many of these sites have few external dating controls. The development of sensitive automatic readers and advances in

the SAR procedure should enable much younger sediments to be accurately dated making it a useful dating technique for sediments deposited in the Holocene. This research will test these new techniques by dating young wind blown sand samples from the Orkney Islands that are constrained by the surrounding archaeology. Experiments have shown that when quartz is exposed to short wavelengths the luminescence signal is rapidly depleted however without determining the residual levels of modern beach sands in the study area it cannot be assumed that the quartz is indeed well bleached. A potential new technique to identify partially bleached samples using the shape of the natural and regenerated decay curves of feldspar is presented in Chapter 4. The following chapter presents the experimental procedures that will help to answer these questions and determine if quartz from the Orkney Islands can be accurately dated using OSL.

Chapter 3 – Methodology

3.1 Introduction

The previous chapter introduced the study area and the background to luminescence dating and therefore the aim of this chapter is to present details concerning the sites sampled and methods used for sample preparation and analysis. An outline of the procedures used to collect the modern beach and archaeological samples is given before individual archaeological sites are discussed. All of the samples were prepared in a similar manner and this is briefly described before the experimental procedures to test for residual levels and bleaching in the modern beach sands are outlined. A modified SAR protocol was used to determine the palaeodose of the archaeological samples and this is discussed in some detail before the methods used to determine the dose rates of the archaeological samples are presented.

3.2 Section 1 – Sample collection, site selection and background to sites

3.2.1 Modern beach sands

One of the main requirements in luminescence dating of sediments is that the sediment has been adequately bleached on deposition (Aitken 1998) and therefore the grains have little or no luminescence signal left within them. However, the degree of bleaching can differ not only for the sediment as a whole but also on a grain to grain basis (Aitken 1998). Although aeolian sediments are often considered to be well-bleached (Aitken 1998) it is not clear from the literature whether complete bleaching can be safely assumed for archaeological purposes. Moreover, the sensitivities of sands from the study area were unknown at the outset. With these points in mind a survey of modern beach sands was undertaken at the start of this study to assess luminescence sensitivities, ease of bleaching and residual signal levels prior to sampling archaeological deposits.

Present day beach samples were collected from the backshore of a wide range of beaches in the Orkney Islands and Outer Hebrides and the location of these beaches is shown in Figure 3.1a and b. The beaches have differing mineralogies, reflecting sediment provenance and underlying bedrock geology and therefore to ensure that these variables

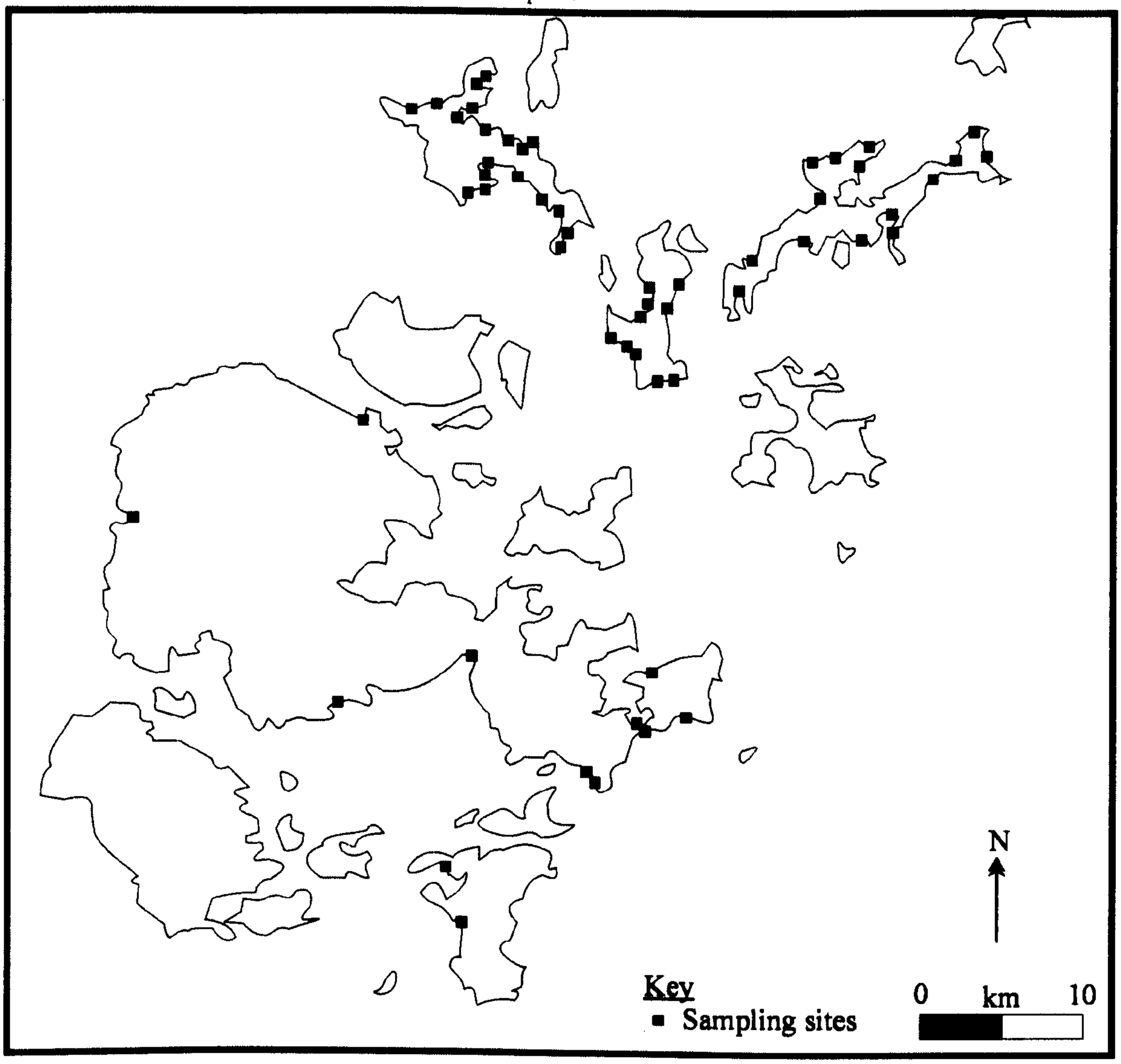

Figure 3.1a – Location of modern beaches sampled in the Orkney Islands

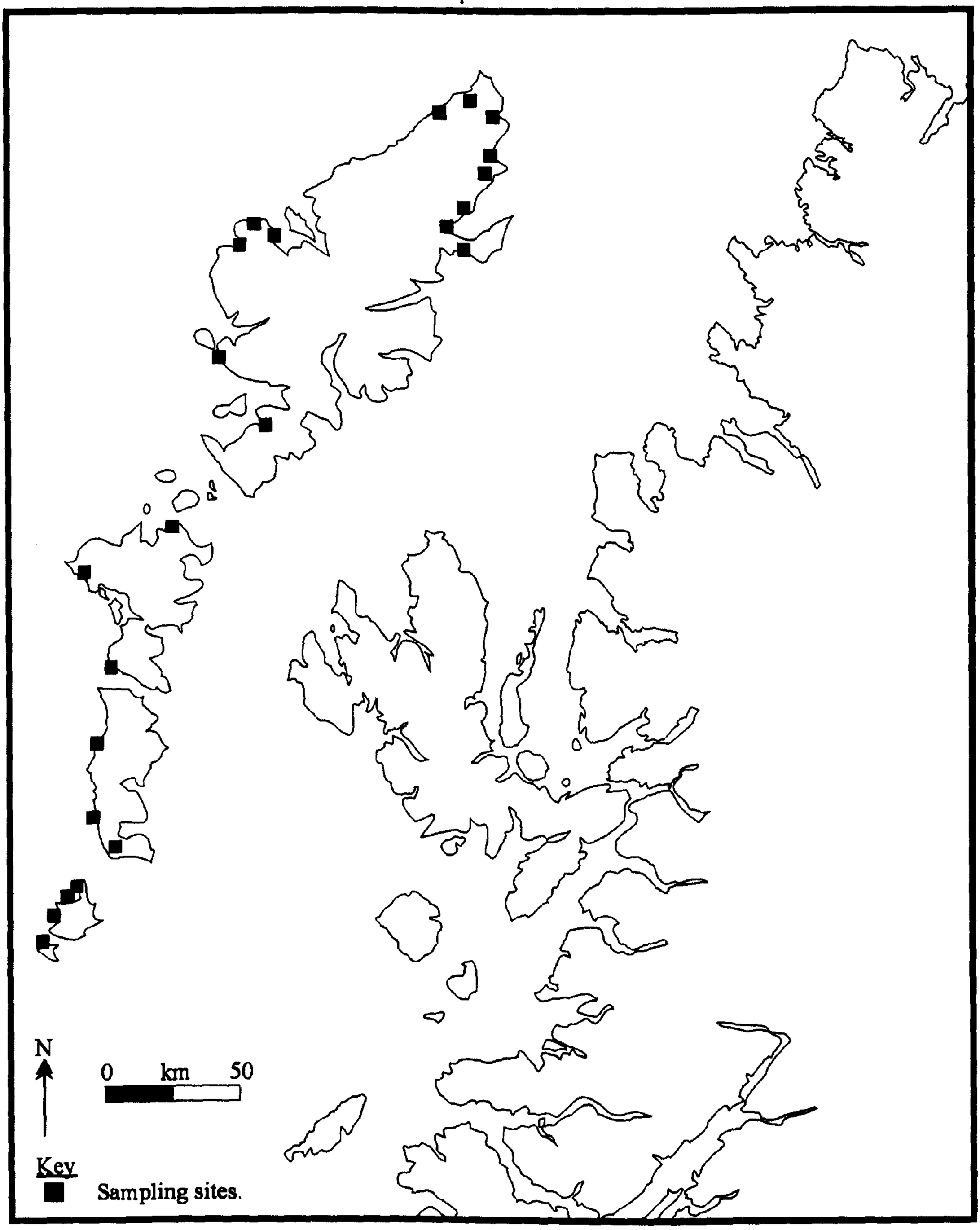

Figure 3.1b – Location of modern beaches sampled in the Outer Hebrides

are considered, modern beaches were sampled wherever possible. These beach systems in most cases represent the primary provenance of the aeolian sands that have been transported into the dunes behind and into adjacent archaeological sites (Schwenninger 1996; Gilbertson *et al.* 1999; Hansom 1999). The modern sand samples provide an opportunity to measure the residual levels of present day sands, establish the source characteristics of the aeolian sand in the sand dunes and provide the means to conduct bleaching experiments in the field and laboratory. If the modern sands have low residual levels then bleaching during the final transportation inland is not required and therefore the luminescence dates from the archaeological sites can be accepted with confidence.

The samples were collected during the day by skimming a trowel across the surface of the beach to a depth of approximately 1 cm. Further samples were taken using adhesive packing tape to ensure that only the surface layer was collected. All of the samples were immediately placed in black bags to prevent further exposure to light.

3.2.2 Archaeological sites

Six of the seven archaeological sites chosen for this study are concentrated in the Northern Isles of Orkney (Sanday, Eday and Westray), and the one remaining site is located close to the World Heritage site of Skara Brae on Mainland Orkney (Figure 3.2)[1]. The Northern Isles are topographically low in comparison with the other Orkney Islands (e.g. Hoy) and their flat land and good sandy soils have attracted settlers for thousands of years. As sea level has risen since the end of the last glaciation many of the settlement sites have been engulfed by sand that has been moved onshore and then blown inland during stormy conditions. Many such archaeological sites are now being exposed due to coastal erosion. Four of the archaeological sites sampled in this study were identified due to coastal erosion (Bay of Lopness (Sanday), Quoygrew (Westray), Evertaft (Westray) and Bay of Skaill (Mainland)). The site at Tofts Ness (Sanday) was known to have wind blown sands associated with it and the remaining sites at Pierowall (Westray) and Sandhill (Eday) were identified in the course of this research as sites affected by wind blown sands in the past.

[1] Two other sites were sampled during this research at Galson on Lewis and Amble in Northumberland (Sommerville *et al.* forthcoming). These sites have not been included in this work because it was felt that such a large study area could hinder the possible identification of specific storm events within the Orkney Islands. Further research on these sites will not only provide local climatic information but also contribute to a wider understanding of climatic events in Britain throughout the Holocene.

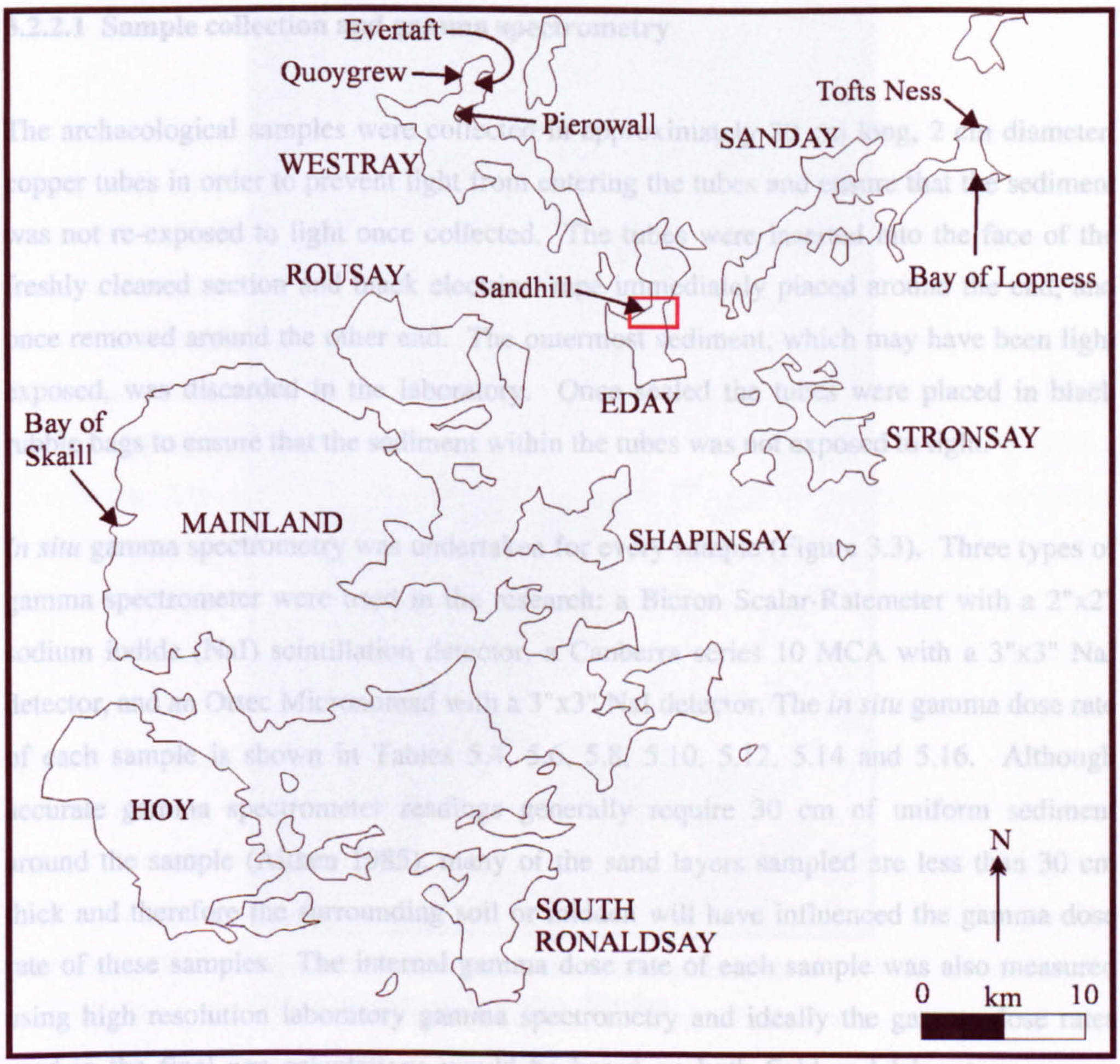

Figure 3.2 – Location of archaeological sites sampled in the Orkney Islands

3.2.2.1 Sample collection and gamma spectrometry

The archaeological samples were collected in approximately 20 cm long, 2 cm diameter, copper tubes in order to prevent light from entering the tubes and ensure that the sediment was not re-exposed to light once collected. The tubes were inserted into the face of the freshly cleaned section and black electrical tape immediately placed around the end, and once removed around the other end. The outermost sediment, which may have been light exposed, was discarded in the laboratory. Once sealed the tubes were placed in black rubble bags to ensure that the sediment within the tubes was not exposed to light.

In situ gamma spectrometry was undertaken for every sample (Figure 3.3). Three types of gamma spectrometer were used in the research: a Bicron Scalar-Ratemeter with a 2"x2" sodium iodide (NaI) scintillation detector, a Canberra series 10 MCA with a 3"x3" NaI detector, and an Ortec Micronomad with a 3"x3" NaI detector. The *in situ* gamma dose rate of each sample is shown in Tables 5.4, 5.6, 5.8, 5.10, 5.12, 5.14 and 5.16. Although accurate gamma spectrometer readings generally require 30 cm of uniform sediment around the sample (Aitken 1985), many of the sand layers sampled are less than 30 cm thick and therefore the surrounding soil or midden will have influenced the gamma dose rate of these samples. The internal gamma dose rate of each sample was also measured using high resolution laboratory gamma spectrometry and ideally the gamma dose rates used in the final age calculations would be based on both field and laboratory gamma spectrometer readings, but allowances may have to be made for the surrounding sediment. For samples that have similar *in situ* and high resolution gamma dose rates the gamma contribution to the working dose rate is calculated from the average of the two values. The similar values indicate that the external gamma dose rate of these samples is unaffected by the surrounding sediment. In comparison, samples that have *in situ* and high resolution gamma dose rates that are not within error of each other are likely to be surrounded by a different type of sediment that actively contributes to the *in situ* gamma dose rate of the sample. In these situations the *in situ* field gamma dose rate is used to determine the working dose rate of the sample, as this is a more realistic estimation of the dose rate affecting the sample. Laboratory high resolution gamma spectrometry was also used to cross-check internal beta dose rates and to determine the relative importance of uranium, thorium and potassium contributions to dosimetry.

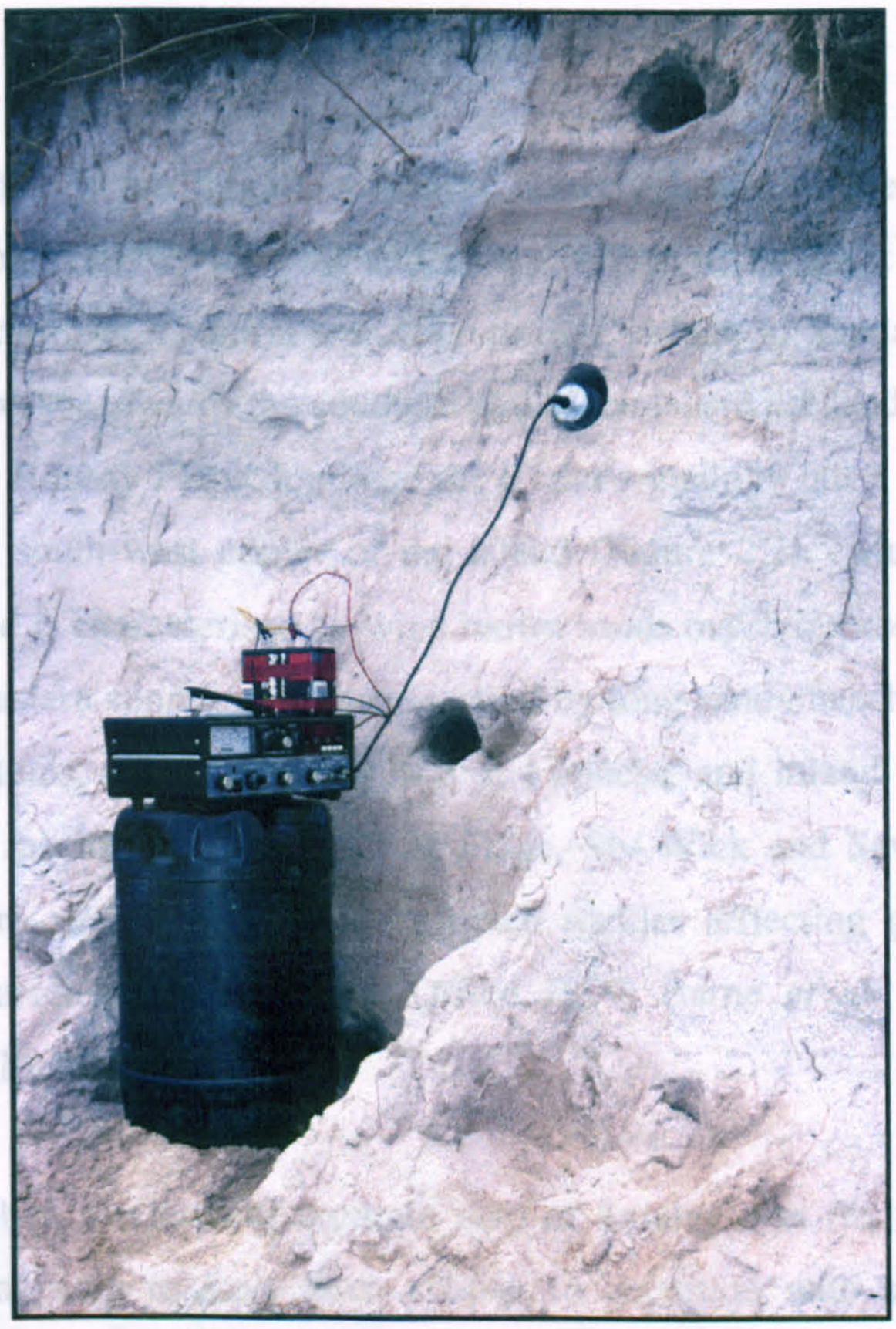

Figure 3.3 – Measuring the *in situ* gamma dose rate at the Bay of Lopness, Sanday

3.3 Sanday

The island of Sanday is the largest and most easterly island in the Northern Isles of Orkney. It is approximately 20 km long and 11 km wide at its broadest point and has three peninsulas protruding from a central area (Figure 3.4). Much of Sanday lies below 20 m above sea level, however towards the southern end of the island the land rises to a height of 65 m at The Wart. Rousay Flags dominate the island's geology but a small area of Eday Beds occurs in the south-west corner of the island (Figure 2.2). Much of the surficial geology of the island is characterised by wind blown sands overlying rock platforms and/or till deposits. The eastern shoreline is characterised by long sandy beaches often backed by extensive dune systems, e.g. Tres Ness, Bay of Lopness, and inland there are extensive areas of low-lying machair, e.g. at Plain of Fidge, Sty Wick and Saville (Mather *et al.* 1974). The western shoreline tends to be much rockier reflecting greater exposure to waves and tidal currents (Hydrographic Office 1899; Barne *et al.* 1997) and steeper offshore gradients (Mather *et al.* 1974).

Since AD 1750, when a relatively accurate map of Sanday was first published (Tindall 1981), the island appears to have been subject to accretion with several gravel spits overlain by dune sands joining what were originally several small offshore islands to the main landmass, e.g. Elsness and Tres Ness (Mather *et al.* 1974). During this process large bays were enclosed and infilled creating the large tidal flats of Cata Sand and Little Sea (Mather *et al.* 1974). Although there is evidence for sediment deposition along much of the Sanday coastline, sea level is continuing to rise, and there is historical evidence to support this. Traill (1868) discussed a 'forest' that once existed at Otterswick now represented by submerged peat and Stevenson (1818) mentioned that the older residents of Sanday remembered that the Start Point lighthouse, which today can only be reached by foot at low tide, was once permanently linked to Sanday. As a result of sea level rise many of the dune systems are actively eroding, often exposing archaeological sites within the dune sections e.g. Viking boat burial at Scar (Dalland 1992a and b; Owen and Dalland 1999), or on the beaches e.g. Bay of Lopness (see Section 3.3.2).

Two sites were sampled on Sanday (Figure 3.4) and were chosen for several reasons. Considerable archaeological work was undertaken at Tofts Ness in the 1980's and sand layers were identified during the excavations (Dockrill *et al.* 1994; Simpson 1998). In 1999 the site was being re-examined by Erika Guttmann (University of Stirling) who

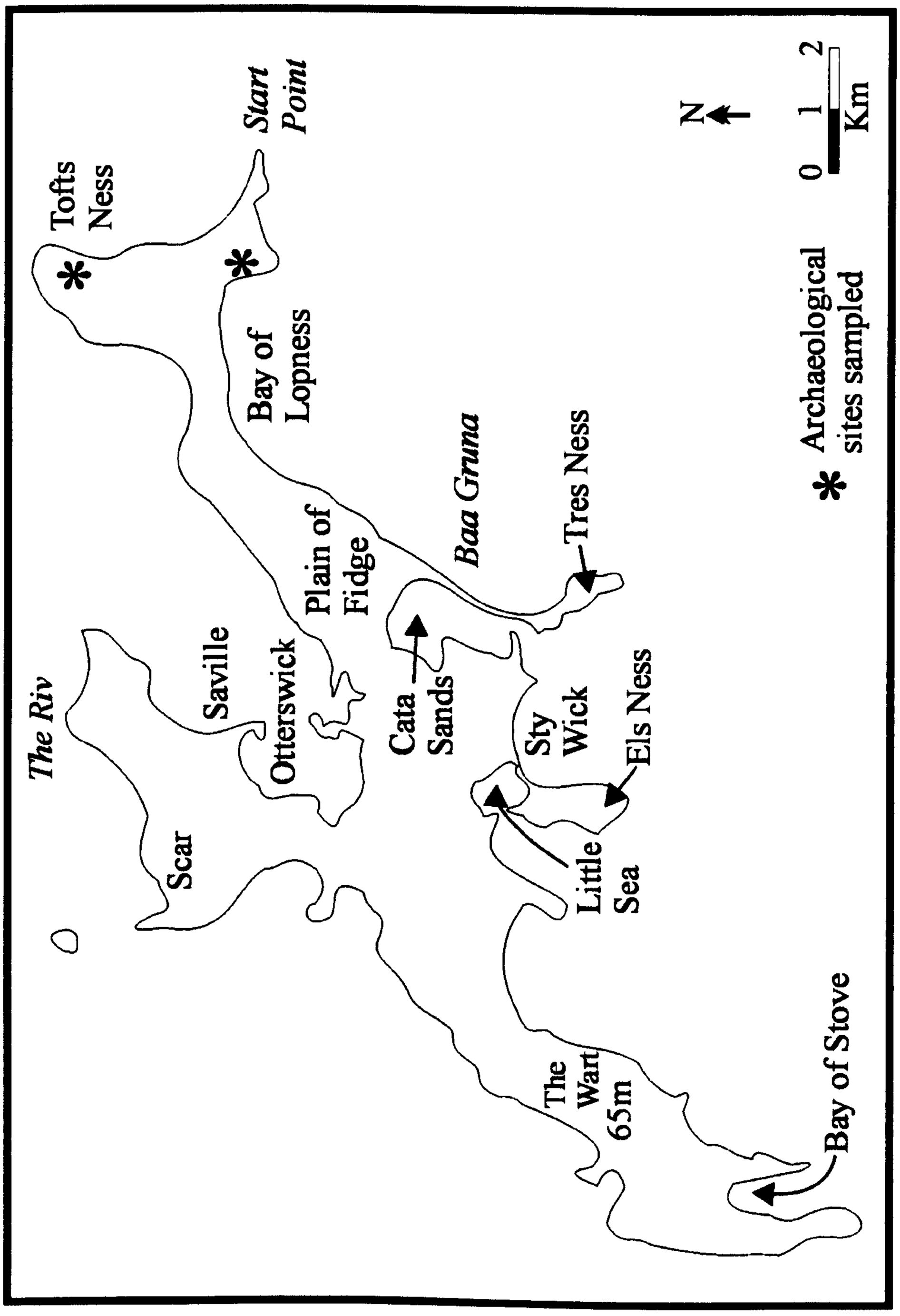

Figure 3.4 – The island of Sanday with location of places mentioned in the text and the archaeological sites sampled

planned to open test pits and sample the plaggen or anthropogenic soils for her Ph.D. research on agricultural land management in the Northern Isles. This provided an ideal opportunity to sample *in situ* sand layers on a site that was relatively well documented. In contrast, the Bay of Lopness was originally chosen because at the time of sampling the only known archaeology associated with the site was a midden deposit underlying wind blown sands. The midden deposit was subsequently radiocarbon dated providing a *terminus post quem* to the age of the overlying sand layers.

3.3.1 Tofts Ness, Sanday

Tofts Ness is located on a low-lying peninsula in the northeast of the island (Grid ref: HY 760 470) and Late Neolithic, Bronze Age and Iron Age settlement has been documented from the area.

Tofts Ness is first described by Daniell (1821) who visited Sanday in the early 19th century and after talking to locals he described an archaeological site that was covered in sand hills in the late 18th century. These were gradually eroded and dispersed at the beginning of the 19th century and little remained of the sand hills by the time of Daniell's visit. The first official record of Tofts Ness is in the New Statistical Account of 1845 by Dr Wood who described 'a chain of forts, which were connected by a stone wall' (New Stat. Acct. 1845 p136). Within the wall he identified buildings of different sizes, stone circles and many graves that were lined with stones. The Account also describes one of the 'forts' that had been exposed several years before Wood's visit to the site. Despite there being little evidence of these 'forts' today, the building that Wood saw was well preserved, with 8 ft high walls that were corbelled allowing the structure to be sealed with large flat stones (New Stat. Acct 1845).

The site was revisited in 1970 by the Ordnance Survey when six large mounds, several stony banks, a field system and over 50 smaller mounds were identified (NMRS No. HY74NE1). The larger mounds were composed of sand and stones and all had secondary structures on them, whereas the smaller mounds were thought to be burial cists.

The north-east area of the Tofts Ness peninsula was scheduled in 1991, however prior to this, between 1985 and 1988 excavation of an area outwith the scheduled area was undertaken by Steve Dockrill (University of Bradford). Mound 11 (Figure 3.5) was chosen

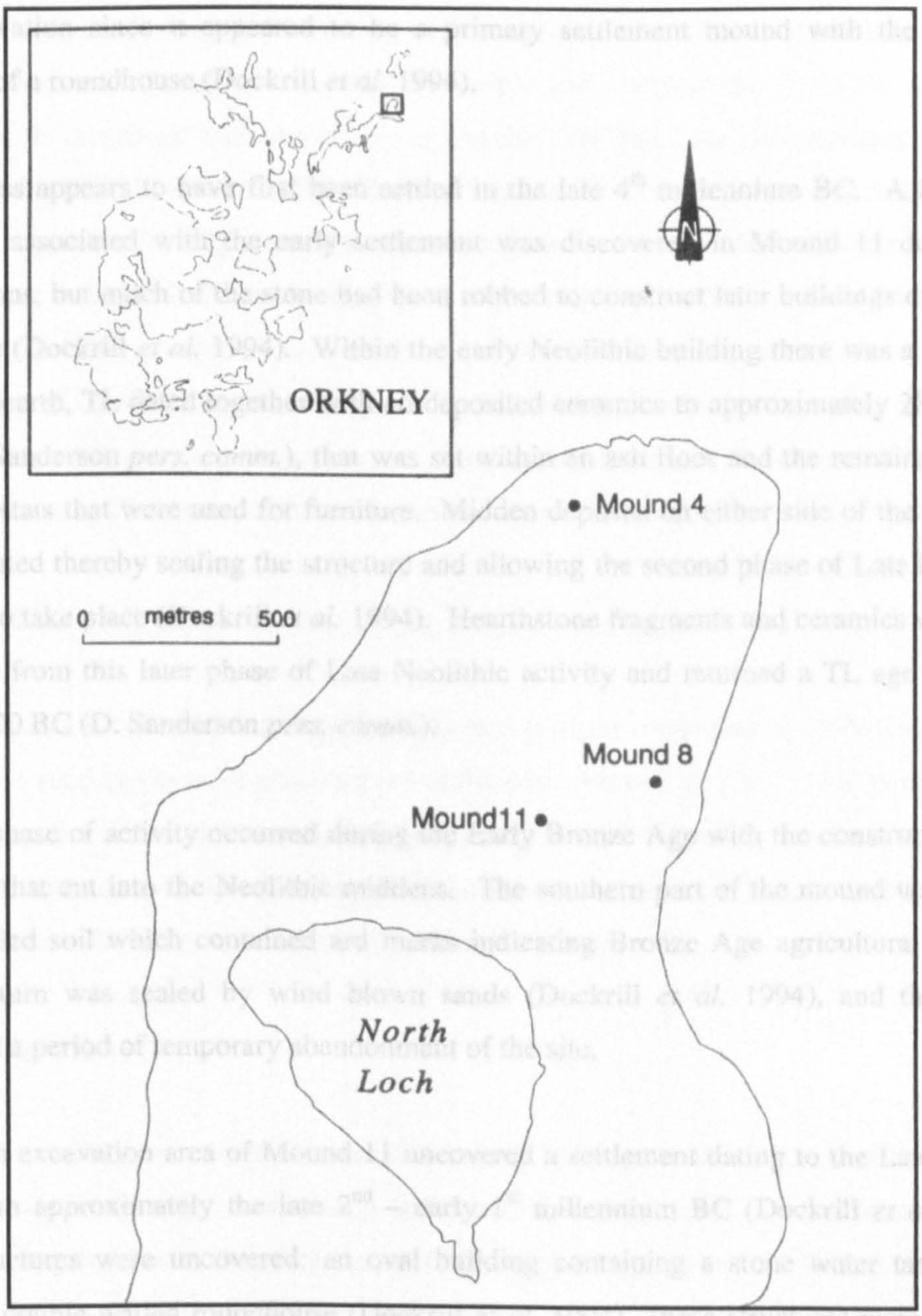

Figure 3.5 – Location of Mound 11 on the Tofts Ness peninsula (after Simpson and Dockrill 1996)

for excavation since it appeared to be a primary settlement mound with the exposed remains of a roundhouse (Dockrill *et al.* 1994).

Tofts Ness appears to have first been settled in the late 4th millennium BC. A Neolithic structure associated with the early settlement was discovered in Mound 11 during the excavations, but much of the stone had been robbed to construct later buildings during the Neolithic (Dockrill *et al.* 1994). Within the early Neolithic building there was a centrally located hearth, TL dated together with co-deposited ceramics to approximately 2800-2400 BC (D. Sanderson *pers. comm.*), that was set within an ash floor and the remains of slots for orthostats that were used for furniture. Midden deposits on either side of the structure accumulated thereby sealing the structure and allowing the second phase of Late Neolithic activity to take place (Dockrill *et al.* 1994). Hearthstone fragments and ceramics were also collected from this later phase of Late Neolithic activity and returned a TL age of about 2500-2000 BC (D. Sanderson *pers. comm.*).

The 3rd phase of activity occurred during the Early Bronze Age with the construction of a building that cut into the Neolithic middens. The southern part of the mound was sealed by a buried soil which contained ard marks indicating Bronze Age agricultural activity. This in turn was sealed by wind blown sands (Dockrill *et al.* 1994), and these may represent a period of temporary abandonment of the site.

The main excavation area of Mound 11 uncovered a settlement dating to the Late Bronze Age, from approximately the late 2nd – early 1st millennium BC (Dockrill *et al.* 1994). Two structures were uncovered: an oval building containing a stone water tank and a circular, double walled roundhouse (Dockrill *et al.* 1994). These structures were overlain by a sand-based soil, and this was overlain in turn by the exposed roundhouse dating to the early/mid 1st millennium BC. Within the central area of the roundhouse a vertical series of five hearthstones was uncovered. The lower, middle and upper hearthstones were TL dated and provided dates of 1120-960 BC, 1000-820 BC and 700-120 BC respectively (D. Sanderson *pers. comm*). These dates lend support to the late Bronze/early Iron Age archaeological interpretation. On abandonment the exposed roundhouse was infilled with wind blown sand and many of the internal features were well preserved (Dockrill *et al.* 1994).

In July 1999 Erika Guttmann (University of Stirling) and AOC (Scotland) returned to Tofts Ness to re-examine Mound 11 in order to sample and compare the Neolithic soil at the bottom of the sequence with the overlying Bronze Age and Late Bronze/Early Iron Age agricultural soils (Guttmann 2001). Much of the area lies below 5 m above sea level and there are deposits of shelly wind blown sands which have buried the landscape at various times, either as individual events or by dune encroachment (Dockrill *et al.* 1994; Simpson and Dockrill 1996; Simpson *et al.* 1998). Two test pits were dug within the established chronology of the 1986 excavation trenches and another seven pits were dug beyond the limits of excavation in an east-south-east direction to determine the extent of the buried soils (Figure 3.6) (Guttmann 2001) and to collect the OSL samples.

3.3.1.1 OSL samples

18 samples were collected from eight of the nine test pits excavated in 1999 (Figure 3.7). One or two sand layers were present in all of the pits, except Test Pit 1. All samples were medium grained sands and contained about 40%-75% shell fragments based on weight loss after HCl treatment. *In situ* gamma spectrometry was undertaken on all samples using a Canberra series 10 MCA with a 3"x3" NaI scintillation detector.

3.3.1.2 Test Pit 2

Test Pit 2 is within Area A which was excavated in 1986 under the direction of S. Dockrill. The pit is approximately 1 metre deep and is mainly composed of a complex midden and palaeosol sequence with many of the units thinning and pinching out within the section (Figure 3.7). At the base of the pit there is a very dark grey Neolithic agricultural soil with associated ard marks cutting into the underlying till, sealed by a thick sequence of Neolithic middens (Guttmann 2001). The middens (radiocarbon dated by Simpson *et al.* 1998) are overlain by a very dark brown Bronze Age soil, which is capped by an 8 cm thick deposit of very pale brown/light grey wind blown sand. Above the sand there is a 6.5 cm thick layer of sandy soil which may have been cultivated (Guttmann 2001), overlain by a modern soil. Three samples were collected from this pit (Figure 3.7); two from the wind blown sand layer (SUTL 602 and 603) and one from the sandy soil layer (SUTL 604). Based on the interpretation of the palaeosols by Guttmann (2001) the OSL samples are expected to be less than 2500 years old.

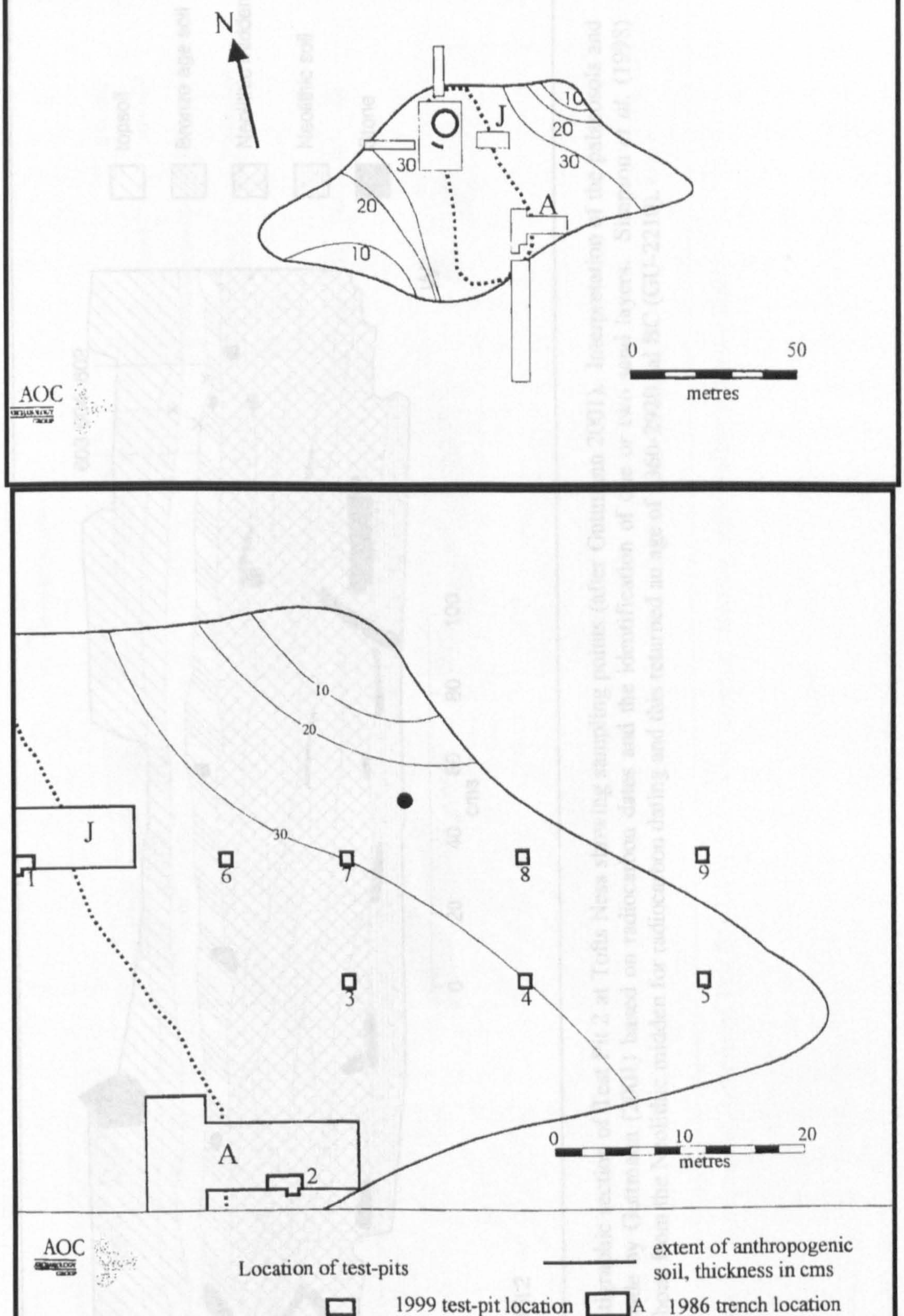

Figure 3.6 – 1986 trench layout and location of Test Pits 2-9 in 1999. Solid circle represents test pit from which samples for radiocarbon dating, discussed in Section 3.3.1.10, were collected (after Guttmann 2001 and courtesy of AOC Archaeology).

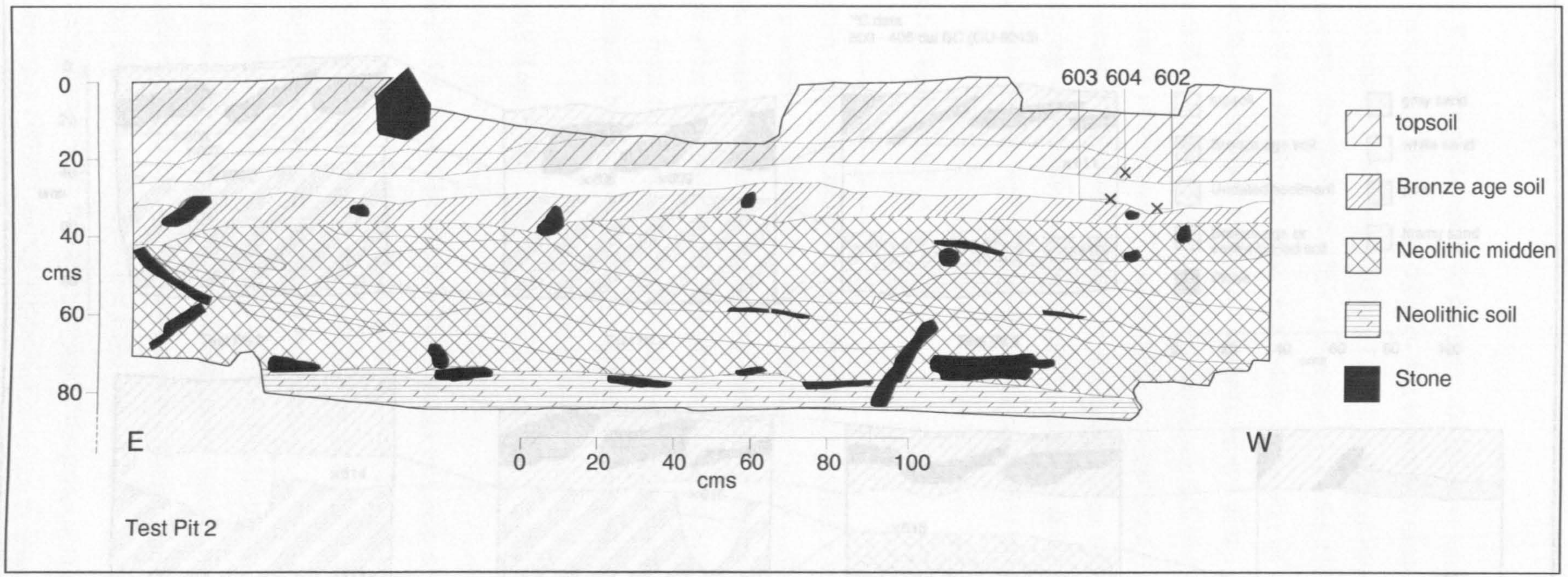

Figure 3.7 – Stratigraphic section of Test Pit 2 at Tofts Ness showing sampling points (after Guttmann 2001). Interpretation of the palaeosols and middens were made by Guttmann (2001) based on radiocarbon dates and the identification of one or two sand layers. Simpson *et al.* (1998) sampled animal bone from the Neolithic midden for radiocarbon dating and this returned an age of 3360-2920 cal BC (GU-2210).

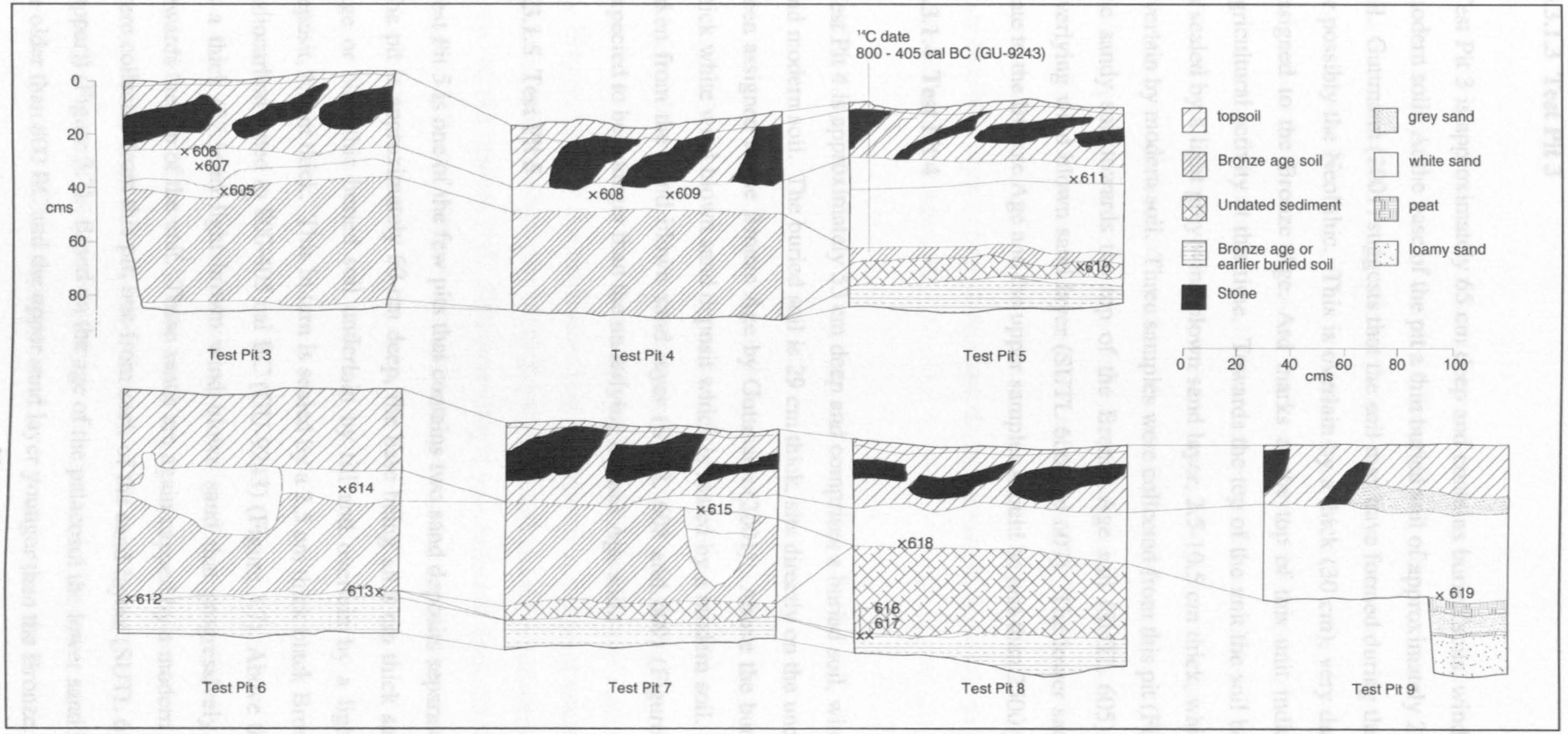

Figure 3.7 continued – Stratigraphic sections of Test Pits 3-9 at Tofts Ness showing sampling points (after Guttmann 2001).

3.3.1.3 Test Pit 3

Test Pit 3 is approximately 65 cm deep and contains buried soils, wind blown sands and a modern soil. At the base of the pit a thin buried soil of approximately 2.5 cm thick overlies till. Guttmann (2001) suggests that the soil may have formed during the early Bronze Age, or possibly the Neolithic. This is overlain by a thick (30 cm), very dark grey, buried soil assigned to the Bronze Age. Ard marks at the top of this unit indicate that there was agricultural activity at this time. Towards the top of the unit the soil becomes sandier and is sealed by a light grey wind blown sand layer, 2.5-10.5 cm thick, which in turn is finally overlain by modern soil. Three samples were collected from this pit (Figure 3.7); one from the sandy soil towards the top of the Bronze Age soil (SUTL 605) and two from the overlying wind blown sand layer (SUTL 606 and 607). The lower sample is expected to date to the Bronze Age and the upper samples should be less than 2500 years old.

3.3.1.4 Test Pit 4

Test Pit 4 is approximately 53 cm deep and comprises a buried soil, wind blown sand layer and modern soil. The buried soil is 29 cm thick, sits directly on the underlying till and has been assigned to the Bronze Age by Guttmann (2001). Above the buried soil is an 8 cm thick white wind blown sand deposit which is sealed by a modern soil. Two samples were taken from the wind blown sand layer (SUTL 608 and 609) (Figure 3.7) and both are expected to be younger than the underlying Bronze Age soil.

3.3.1.5 Test Pit 5

Test Pit 5 is one of the few pits that contains two sand deposits separated by a buried soil. The pit is approximately 60 cm deep, the base being an 8 cm thick sandy brown Bronze Age or Neolithic buried soil underlain by till and overlain by a light grey lower sand deposit, 6.5cm thick. This in turn is sealed by a 2.5 cm thick black Bronze Age buried soil radiocarbon dated to 800-405 cal BC (GU-9243) (Figure 3.7). Above the Bronze Age soil is a thick (22.5cm) light brown wind blown sand that progressively lightens in colour towards the top of the unit. These sands are again capped by a modern soil. Two samples were collected from this pit; one from each of the sand layers (SUTL 610 [lower] and 611 [upper]) (Figure 3.7). Based on the age of the palaeosol the lower sand layer is expected to be older than 800 BC and the upper sand layer younger than the Bronze Age.

3.3.1.6 Test Pit 6

Test Pit 6 also contains two sand layers separated by a buried soil (Figure 3.7). The pit is approximately 65 cm deep and at the base, directly above a till, is a 10.5 cm thick, very dark brown, Bronze Age or Neolithic buried soil. Above the soil is a thin (1.5 cm) sand layer which is light grey in colour, and this is sealed by a black Bronze Age buried soil, approximately 25 cm in thickness. The upper wind blown sand layer is 8.5 cm thick and is truncated by a linear cut feature which extends into the underlying Bronze Age buried soil. The infill of this cut is composed of a mixture of light brown sand and dark brown soil. The modern soil lies directly above the cut feature and upper sand layer, and Guttmann (2001) suggests that the cut is probably modern in age. Three samples were taken from this pit (Figure 3.7); two from the lower sand layer (SUTL 612 and 613) and one from the upper sand layer (SUTL 614). The lower samples may have been deposited during the Late Neolithic or early Bronze Age and the upper sample is thought to be younger than the underlying Bronze Age soil.

3.3.1.7 Test Pit 7

Test Pit 7 contains only one sand layer overlying a thick sequence of buried soils (Figure 3.7). The pit is approximately 60 cm deep and at the base is an 8 cm thick, very dark grey, Bronze Age or Neolithic buried soil. This is sealed by very dark grey sandy silt, 5 cm thick, and this in turn is overlain by a 25 cm thick Bronze Age buried soil. Within the Bronze Age soil is a cut feature that is sealed by a wedge of white wind blown sand. The sand extends across part of the Bronze Age soil and the remainder of the buried soil is sealed by the modern soil. Only one sample was collected from the sand sealing the cut feature (SUTL 615) (Figure 3.7) and it may have been deposited during the late Bronze Age.

3.3.1.8 Test Pit 8

Test Pit 8 contains two sand layers separated by a buried soil (Figure 3.7). The pit is 60 cm deep and at the base of the pit, overlying the till, is a 10.5 cm thick buried soil assigned to the Neolithic or Bronze Age by Guttmann (2001). The soil is separated from the upper buried soil on one side of the pit by a very thin (1.5 cm) layer of grey wind blown sand from which two OSL samples were collected (SUTL 616 and 617; Figure 3.7). The

remainder of the lower buried soil is sealed by the upper buried soil, which is 22.5 cm in thickness. Above the upper Bronze Age soil is a 13 cm thick wind blown sand layer, which is then overlain by the modern soil. A further sample was collected from the upper sand layer (SUTL 618) and this is expected to be younger than the underlying Bronze Age soil.

3.3.1.9 Test Pit 9

Although Test Pit 9 contained two sand layers, only one was sampled (Figure 3.7). The pit is approximately 85 cm deep and at the base of the pit, overlying the till, is a dark grey loamy sand, 22 cm thick, and interrupted by a dark brown palaeosol about 6 cm thick. Above the loamy sand unit there is a 6 cm thick palaeosol and this is sealed by a layer of white wind blown sand, approximately 55 cm in thickness, from which sample SUTL 619 was collected (Figure 3.7). Overlying the sand is a layer of cultivated sand and this in turn is overlain by the modern soil. The OSL sample is thought to be less than 2500 years old.

3.3.1.10 Summary of Tofts Ness

All of the buried soils have been assigned to the Neolithic or Bronze Age by Guttmann (2001) based on a radiocarbon date from midden material in Area A (3360-2920 cal BC, GU-2210) providing a *terminus ante quem* for the soil it sealed (Figure 3.7), radiocarbon dates of a palaeosol (900-795 cal BC, SRR-5256 and 1515-1315 cal BC, SRR-5247) collected from a test pit north-east (Figure 3.6) of the current investigation and dated by Simpson *et al.* (1998), and the identification of one or two sand layers within the 1999 test pits. A further sample for radiocarbon dating was collected during OSL sample collection from Test Pit 5 and this returned a ^{14}C age of 800-405 cal BC (GU-9243) (Figure 3.7). The links made by Guttmann (2001) between the various palaeosols are shown in Figure 3.7 although Test Pit 2 is not included as this was located south-west of the other test pits.

Ard marks in the Neolithic soil of Test Pit 2, and the Bronze Age soil in Test Pit 3, indicate the presence of agricultural activity on the site during these periods (Guttmann 2001). Although the area today is commonly used for grazing there is evidence for more intensive agriculture, with many of the modern soils in the test pits showing signs of recent ploughing (Figure 3.8). Some of the test pits contain two sand layers, which may suggest two depositional events, while others appear to only have one. Guttmann (2001) suggests

Figure 3.8 – Modern plough marks in Test Pit 3 at Tofts Ness

that the lower sandy layer in some of the test pits may have been reworked and mixed with the Bronze Age soil. Optical luminescence dating of the wind blown sands within the test pits should confirm whether these soils were indeed formed during the Neolithic or Bronze Age periods, and will test the linkage between the various test pits proposed by Guttmann (2001). This dating technique may also provide evidence to support the possible abandonment of the site for a short period of time during the Late Bronze Age (Dockrill *et al.* 1994; Guttmann 2001).

3.3.2 Bay of Lopness, Sanday

The site at the Bay of Lopness lies at the northern end of the bay close to Lopness Farm (Grid ref: HY758 439) (Figure 3.4). It was chosen because it had a vertical exposure of sand and midden, but did not have any known archaeological sites associated with it. During the sampling procedure in summer 2000, the landowner, Mr. Leslie, informed Dr. J. Hansom (University of Glasgow) and myself of upright slabs that had appeared on the beach at the front of the eroding section after storm activity during the previous winter. Dr. Hansom informed Julie Gibson (Orkney Archaeological Trust) of the cist and a rescue excavation was undertaken by Jane Downes (Orkney College), Judith Robertson (Orkney Archaeological Trust) and Mary Harris in September 2000. The cist, containing a crouched inhumation, was cut into clayey till and constructed with large beach flagstones (Figure 3.9) (Robertson and Downes 2000). The flagstones were held in place by internal paving and also externally by large boulders on the north and west of the cist (Robertson and Downes 2000). The upper deposits within the cist were mainly beach stones and sand, and one of the stones had crushed the skull and arm of the individual (Robertson and Downes 2000). Finer sands and clays and a limpet shell midden were found in the main fill of the cist. The shell midden had been deposited over the foot area of the inhumation and some small animal bones were also found beneath the shells. Surrounding the inhumation there were some lithics and pot sherds (Robertson and Downes 2000). Although the cist sits alone on the beach, two other areas with upright stones were investigated. One was a natural feature and the other was too eroded to be certain of its provenance (Robertson and Downes 2000). The cist was cut from a level above the till and may relate to midden deposits exposed in the cliff behind the cist. Radiocarbon dates from the left femur of the inhumation suggest that the cist was constructed between 1950-1730 cal BC (GU-9481).

Figure 3.9 – Crouched inhumation in a stone lined cist at the Bay of Lopness, subsequently radiocarbon dated to the Bronze Age

3.3.2.1 OSL samples

The vertical cliff section is cut into dunes and midden and lies approximately 2 m north of the cist and stands approximately 4 m high. Although there are 10 units within the section most of the contacts are gradational and the units are identified by changes in colour or textural composition of the sand (Figure 3.10).

3.3.2.2 Unit 1

At the base of the section, a poorly developed glacial till outcrops at beach level and lying above this there is a 1.1 metre thick layer of midden containing shells, bones, charcoal flecks, burnt stones and sand lenses. Radiocarbon dates from marine shells[2] and a sheep bone at the top of the midden indicate that this upper part accumulated between 200 cal BC and cal AD 430 (GU-9247, GU-9247A, GU-9248), and therefore the lower part of the midden would have been deposited earlier. Both the cist and midden overlie the till deposits and therefore the lower part of the midden may have been deposited as early as 1950 BC, however it is not known whether the midden and cist are contemporary. A sand lens at the top of the midden was sampled for OSL dating (SUTL 891) and the radiocarbon ages of the shells and bone will provide a direct age comparison.

3.3.2.3 Units 2-5

Unit 2 is 20 cm thick coarse sand with 57% shell content and sample SUTL 890 was collected from this unit (Figure 3.10). Contact with the underlying midden is sharp, and the upper contact with Unit 3 is gradational. Sample SUTL 889 was collected from Unit 3, which is darker in colour, and is medium-coarse grained. The unit is approximately 30 cm thick and has a slightly higher shell content of 63%. The contact with Unit 4 above is gradational, however there is a distinct colour change with Unit 4 being almost white. This sand is medium-fine grained and has the lowest shell content (46%) of all the sands within the section. The upper contact of Unit 4 grades into the medium-fine grained sand of Unit 5. There is banding throughout this unit, with alternating layers of dark and light sand. In

[2] The marine reservoir effect was taken into account before calibration of the radiocarbon dates from the marine shells (apparent age of 405 ± 40 years was subtracted from the conventional ^{14}C age prior to calibration (Harkness 1983)). It is not known whether the sheep bone is from a seaweed eating species and therefore the reservoir effect was not applied to this sample.

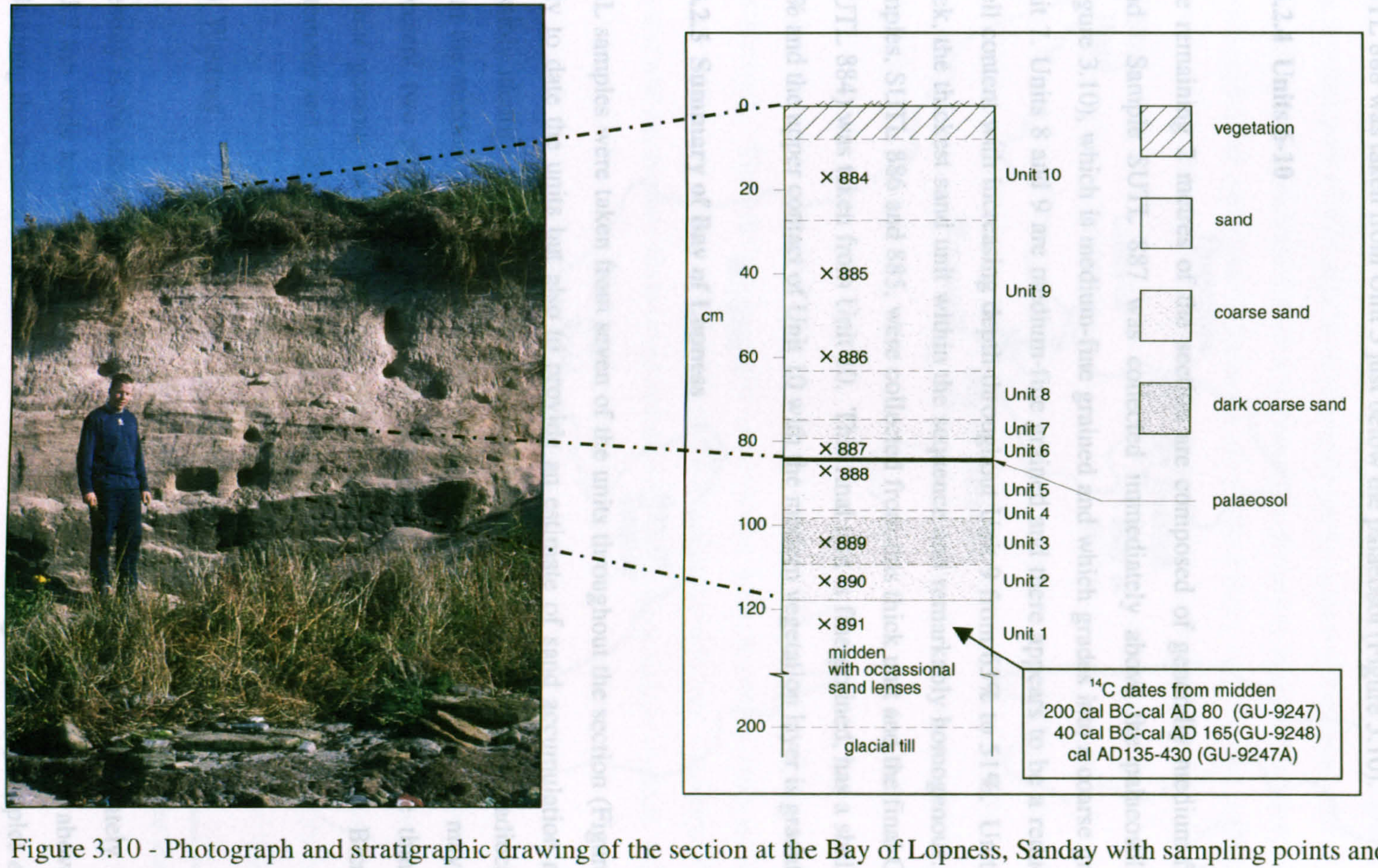

Figure 3.10 - Photograph and stratigraphic drawing of the section at the Bay of Lopness, Sanday with sampling points and radiocarbon dates

contrast to Unit 4, Unit 5 has the highest shell content within the section at 71%. The upper contact of Unit 5 is sharp and sealed by an old vegetation layer. It is thought that this may represent a former land surface and is referred to here as a palaeosol. Sample SUTL 888 was taken from Unit 5 just below the palaeosol (Figure 3.10).

3.3.2.4 Units 6-10

The remaining 2 metres of the section are composed of generally medium-fine grained sand. Sample SUTL 887 was collected immediately above the palaeosol in Unit 6 (Figure 3.10), which is medium-fine grained and which grades into a coarse grained sand, Unit 7. Units 8 and 9 are medium-fine grained and there appears to be a reduction in the shell content with increasing depth throughout Unit 9 from 63% to 51%. Unit 9 is 90 cm thick, the thickest sand unit within the sequence and remarkably homogenous. Two OSL samples, SUTL 886 and 885, were collected from this thick unit and the final OSL sample (SUTL 884) was taken from Unit 10. This final unit is fine grained, has a shell content of 60% and the upper contact of Unit 10 with the modern vegetation layer is gradational.

3.3.2.5 Summary of Bay of Lopness

OSL samples were taken from seven of the units throughout the section (Figure 3.10), not only to date the units but also to provide an estimate of sand accumulation rates and to possibly identify periods of increased sand blow activity. Based on the radiocarbon dates from the midden the sand is expected to be less than 2000 years old and may potentially represent two phases of increased aeolian movement separated by the thin palaeosol. *In situ* gamma spectrometry was undertaken on all samples using a Bicron Scalar-Ratemeter and a 2"x2" NaI scintillation detector.

3.4 Westray

Westray is the most northwesterly of the Orkney Islands. It is approximately 17 km long and 7 km wide and although the majority of the island lies below 30 m above sea level, hills along the western side of the island rise to 169 m (Figure 3.11) (Sharples *et al.* 1984). Bedrock outcrops at sea level along much of the coast and vertical cliffs dominate the west coast rising to a height of 76 m at Noup Head, a National Nature Reserve (Nature Conservancy Council 1978). The larger bays tend to be sandy and bordered by rocky

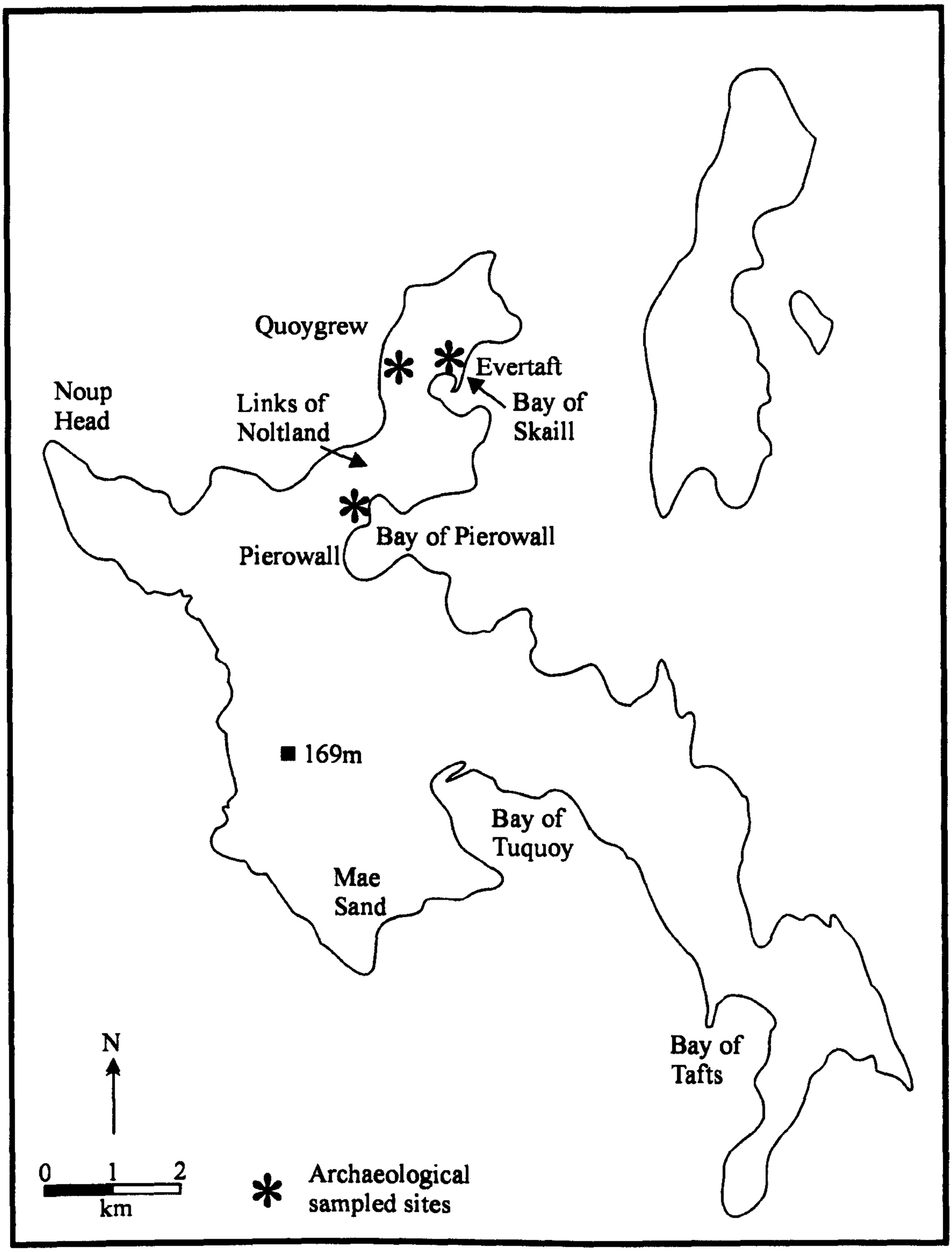

Figure 3.11 – The island of Westray with location of places mentioned in the text and archaeological sites sampled

headlands, e.g. Bay of Tuquoy, Bay of Tafts and Bay of Pierowall, with some areas of machair and wind blown sand. e.g. Mae Sand, Bay of Tafts and Bay of Skaill. The largest area of machair and wind blown sand stretches from Grobust on the west coast across the low saddle to the Bay of Pierowall on the east coast (Figure 3.11) (Mather *et al.* 1974). The western part of this area is also known as the Links of Noltland and it is currently undergoing severe erosion due to a combination of the waves and wind and excavation by rabbits and sand extraction (Clarke *et al.* 1978; Moore and Wilson 2000). The area contains an extensive prehistoric settlement and although much of it is now covered by wind blown sand, it is thought to be up to four times larger in area than the settlement at Skara Brae (Clarke *et al.* 1978). A recent survey of the area identified a scattering of human bones, settlement remains and a possible burial cairn all within the unstable dune system (Moore and Wilson 2000). All are thought to date to the Late Neolithic or Early Bronze Age and are under severe threat from erosion of one sort or another (Moore and Wilson 2000).

Three sites were sampled for OSL dating on Westray (Figure 3.11): Quoygrew, Pierowall, and Evertaft. The site at Quoygrew was chosen after reconnaissance work by James Barrett (University of York) in 1997 identified plaggen soils and sand layers throughout the site and excavation of the site provided an ideal opportunity to collect OSL samples. The second site was a test pit dug close to the ruined church of Lady Kirk at Pierowall after the local shopkeeper mentioned that his store was set into approximately 10 ft of wind blown sand deposits. Historical records also indicated that the northern end of the island had been inundated by sand after large storm events. This site provided an opportunity to OSL date sand deposits with no archaeological constraints but potentially connected to storm events. The final site on Westray was identified by Terry O'Connor (University of York) at Evertaft and despite little being known about the site, it was thought that the sand layers, which were interspersed within a walled structure and midden deposits, may represent more specific depositional events.

3.4.1 Quoygrew, Westray

The site at Quoygrew (Grid ref: HY 443 506) lies on the northern margin of Rack Wick Bay on the northwest coast of Westray (Figure 3.11). An abandoned croft occupying the site today lies on top of a large farm mound approximately 2 m high and 50 m in diameter (Barrett *et al.* 2000a). A second lower mound containing fish middens and walled

structures is exposed on the shore due to coastal erosion and was first recorded in 1978 by Sarah Colley (Barrett *et al.* 1997). Since then J. Barrett has excavated the site in 1997 and 1999-2002.

Reconnaissance work in 1997 confirmed the existence of the fish midden identified by Sarah Colley, establishing it stretched for 40 m along the shore and 15 m inland. A test trench within the midden revealed a drystone cellar with a flagstone floor and stone-lined drain that had been dug into the midden (Barrett *et al.* 1997, 2000a). The function of this feature is uncertain however it may have been used as a naust, a cold store or a semi-subterranean byre (Barrett *et al.* 1997, 2000a). Antler bone fragments, steatite vessel sherds and a bone pin found within the midden all suggest deposition between the 10th and 12th centuries AD, and radiocarbon dates on barley (1160-1290 cal AD, TO-7117) and a bone from a calf skeleton (995-1160 cal AD, TO-7529) from within the midden confirm this (Barrett *et al.* 2000b).

Excavations during 1999 and 2000 revealed a Viking Age and medieval rural settlement containing a house with undisturbed ash floors, a kitchen midden and a plaggen infield lying approximately 14 m inland from the fish midden (Barrett *et al.* 2000a). The exterior walls of the house are double faced and filled with rubble, and inside there are two rooms linked by stepping stones (Barrett *et al.* 2000a). The eastern room is well preserved and contains a stone built bench along one side of the room and a hearth in the centre of the room containing a cracked flagstone covered in pure peat ash (Barrett *et al.* 2000a). The floor is composed of ash, which has been placed on top of a flagstone floor overlying a lintelled drain (Barrett *et al.* 2000a). Coarse pottery sherds found within and on the floor have been dated to the 12th century AD (Barrett *et al.* 2000a).

Further excavations in a mound behind the Viking house identified a kitchen midden composed of predominantly mammal bones towards its base and fish bones and shells towards the top (Barrett *et al.* 2000a). A fragment of horse pelvis from between the two layers was radiocarbon dated to cal AD 1005-1260 (AA-39135), and this is consistent with the late Viking/early Middle Age date for the remainder of the site (Barrett *et al.* 2000a).

3.4.1.1 OSL samples

Ten samples were collected from 4 different pits on the Quoygrew site during 1999 and 2000. The locations of Test Pit 7, Area G and Test Pits 101 and 102 are shown in relation to the main Quoygrew excavation in Figure 3.12. To ensure continuity between this study and other work at this site the names of the various pits sampled are those used by the archaeologists excavating the site.

3.4.1.2 Test Pit 7

In summer 1999, an area approximately 550 m south-east of the main excavation was surveyed using EDM (Figure 3.12). This area is thought to be part of the plaggen infield identified by J. Barrett in 1997 (Barrett *et al.* 2000a), and a pit was dug to sample sand for OSL dating and soil for micromorphological analysis. The pit was approximately 1.8m deep and contained 12 units of interstratified layers of wind blown sand, silty loam, and midden (Figure 3.13).

3.4.1.2.1 Unit 1

Unit 1, at the base of the pit, is a dark greyish brown silty clay loam. This unit is approximately 36 cm thick and the shells, bones and charcoal within this layer indicate that it does not represent the natural substrate. Due to a lack of time and for health and safety reasons, work on the pit was not continued.

3.4.1.2.2 Unit 2

Unit 2, lies above Unit 1, is 14 cm thick and consists of a brown midden deposit with some wind blown sand. The amount of wind blown sand increases towards the top of the unit and grades into Unit 3 above.

3.4.1.2.3 Units 3-5

Unit 3 is 15 cm thick and is composed of a pale brown wind blown sand from which sample SUTL 702 was collected (Figure 3.13). The sand is medium grained and 80% of the sediment is composed of shell. At the top of the unit on the eastern side there are two

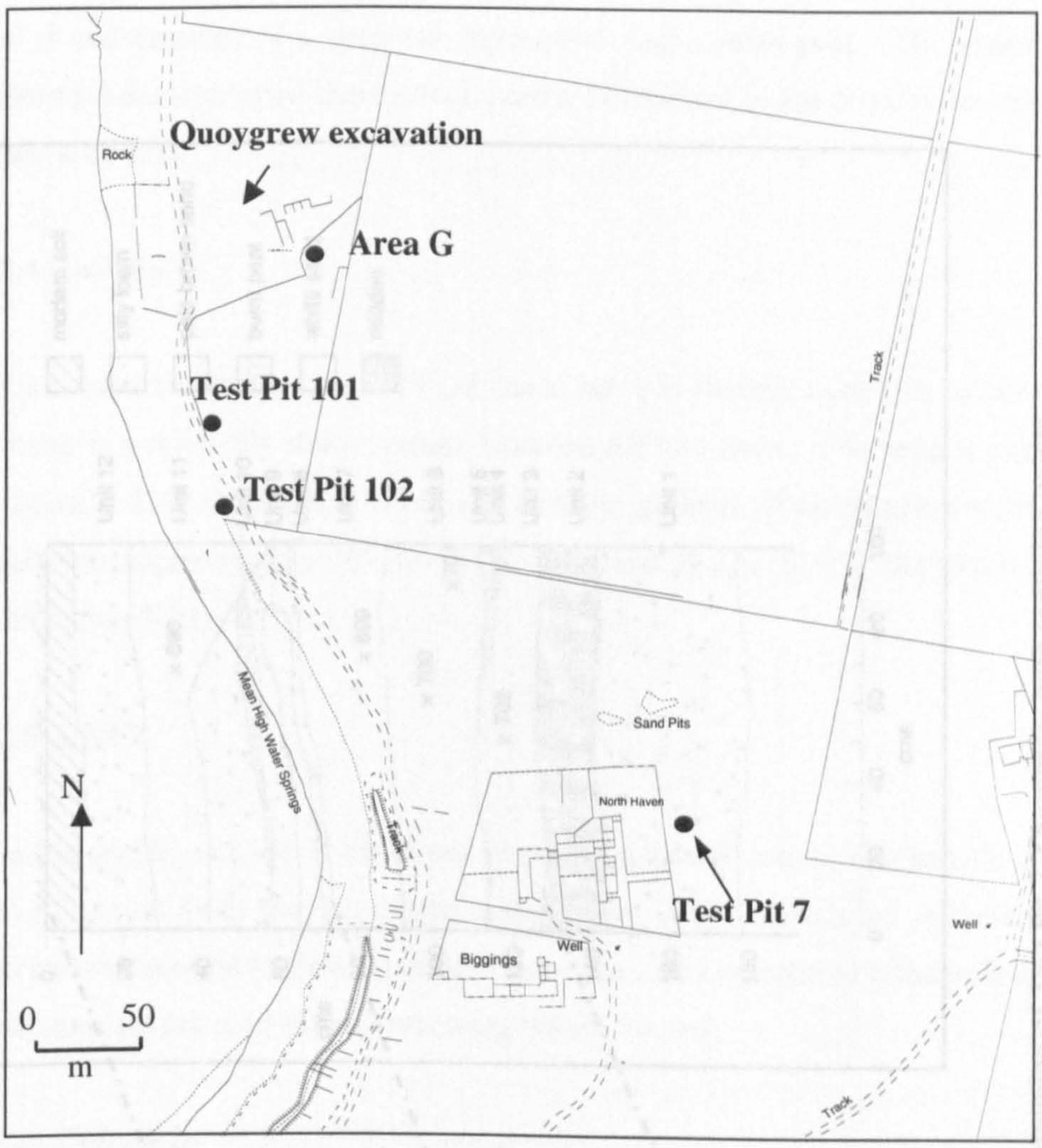

Figure 3.12 – Location of Test Pit 7, Area G and Test Pits 101 and 102 at Quoygrew

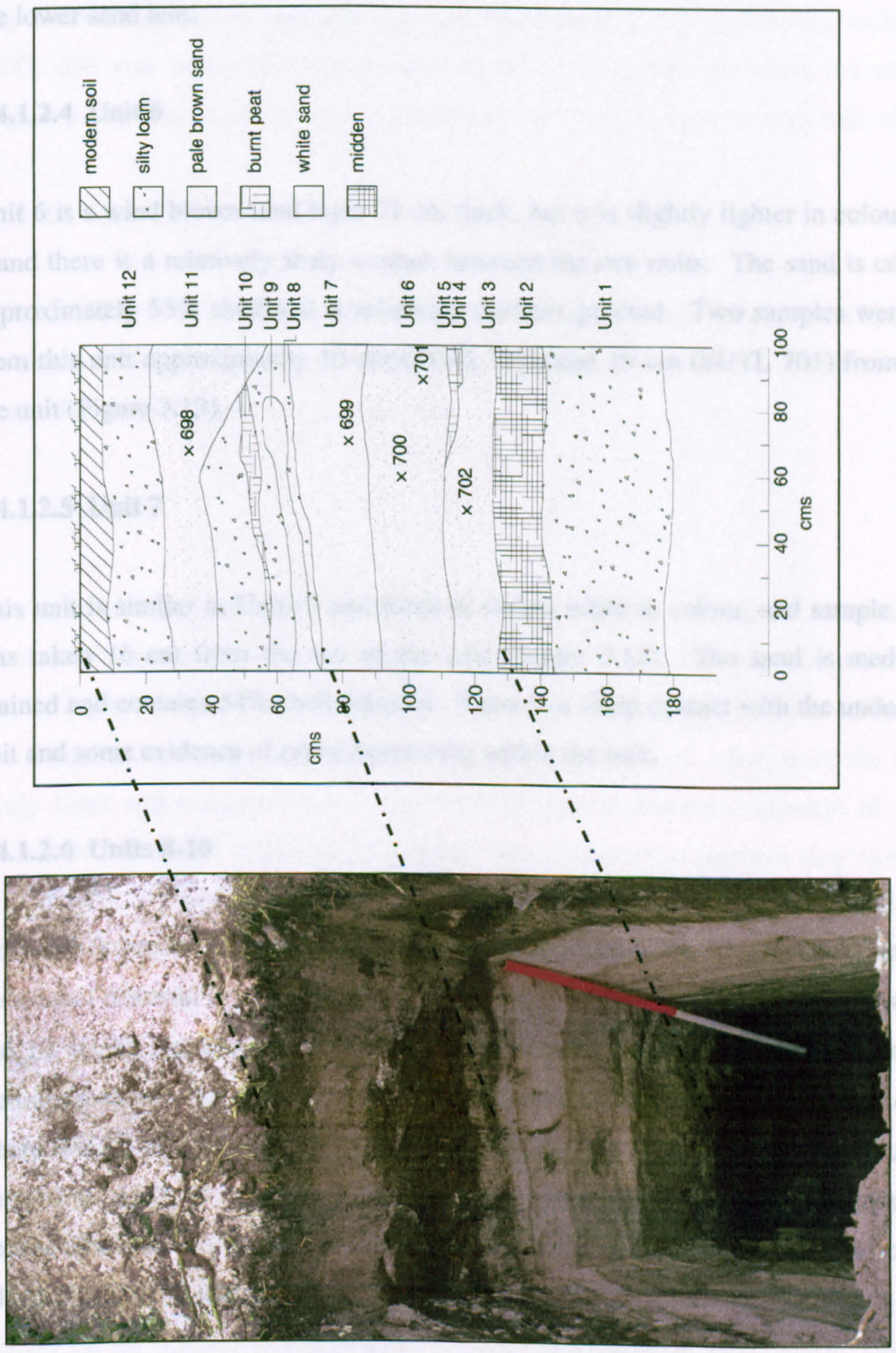

Figure 3.13 – Photograph and stratigraphic drawing of Test Pit 7, Quoygrew with sampling points

small lenses that continue outwith the pit section. Unit 4 (lens 1) is approximately 2 cm thick and composed of white wind blown sand. The other lens, Unit 5, lies directly on top of Unit 4 and consists of a grey ash layer with some burnt peat. The upper lens has undoubtedly been deposited there intentionally, however it is not possible to infer this for the lower sand lens.

3.4.1.2.4 Unit 6

Unit 6 is a wind blown sand layer 21 cm thick, but it is slightly lighter in colour than Unit 3 and there is a relatively sharp contact between the two units. The sand is composed of approximately 55% shell and is relatively medium grained. Two samples were collected from this unit approximately 10 cm (SUTL 700) and 19 cm (SUTL 701) from the top of the unit (Figure 3.13).

3.4.1.2.5 Unit 7

This unit is similar to Units 3 and 6 but is almost white in colour, and sample SUTL 699 was taken 16 cm from the top of the unit (Figure 3.13). The sand is medium-coarse grained and contains 54% shell material. There is a sharp contact with the underlying sand unit and some evidence of rabbit burrowing within the unit.

3.4.1.2.6 Units 8-10

Unit 8 is a brown layer of sandy silty loam approximately 32 cm thick, and contains occasional charcoal flecks, shells and bones. Within the unit there are two lenses, Units 9 and 10, which almost truncate the unit. Unit 9 is an 8 cm thick, pale brown sand that is medium grained. The contacts are undulating and the lens is oval shaped at its' eastern end where it stops abruptly in the silty loam of Unit 8. This feature may be the result of rabbit burrowing. Unit 10 is an orange-red burnt peat lens which contains some black charcoal flecks. The unit is truncated by the overlying unit (Unit 11), however it is not certain if this 'cut' is natural or man-made.

3.4.1.2.7 Unit 11

Unit 11 is 14-38 cm thick, composed of a pale brown, medium grained wind blown sand and 60% of the sediment is shell material. The unit thickens abruptly approximately half way across the section towards the east and truncates the underlying units. Sample SUTL 698 was taken 10 cm from the top of the unit close to where the unit thickens (Figure 3.13). The upper contact is gradational and there is some mixing with Unit 12.

3.4.1.2.8 Unit 12

Unit 12 is 18 cm thick and lies approximately 10 cm below the modern turf line. The unit is composed of a dark brown silty loam, which contains about 50% wind blown sand, some of which is from the underlying sand unit.

3.4.1.3 Area G

Two samples were collected from Area G (Figure 3.12) during the 1999 excavation. At the time of sampling, the pit was approximately 70 cm deep and was composed of a basal midden layer, an intervening sandy layer with some shells and an upper modern soil which also contained some shells (Figure 3.14). The samples were taken from the intervening sandy layer approximately 4 cm horizontally apart and were composed of a medium-grained brown sand. Although the samples were taken close together they varied in shell content with one sample having a shell content of 66% and the other 83%. Reasons for this variation in shell content are currently unclear.

3.4.1.4 Test Pits 101 and 102

D. Sanderson (SUERC) and R. Housley (University of Glasgow) collected the last three samples from two test pits prepared by J. Barrett and T. O'Connor during the 2000 excavation. Test Pit 101 is located approximately 70 m south-west of the main excavation (Figure 3.12) and contains four main units (Figure 3.15). At the base of the pit, lying directly on the underlying bedrock, is a 10 cm thick layer of wind blown sand (Unit 1). The sand is medium-coarse grained and 71% of it is composed of shell fragments. Sample SUTL 903 was taken from this layer (Figure 3.15). Unit 2, above the sand, is a dark greyish brown anthrosol or silty loam approximately 25 cm thick, and this is overlain by

Figure 3.14 – Sample collection from Area G. Another sample (SUTL 704) was taken approximately 4 cm left of the sample pictured.

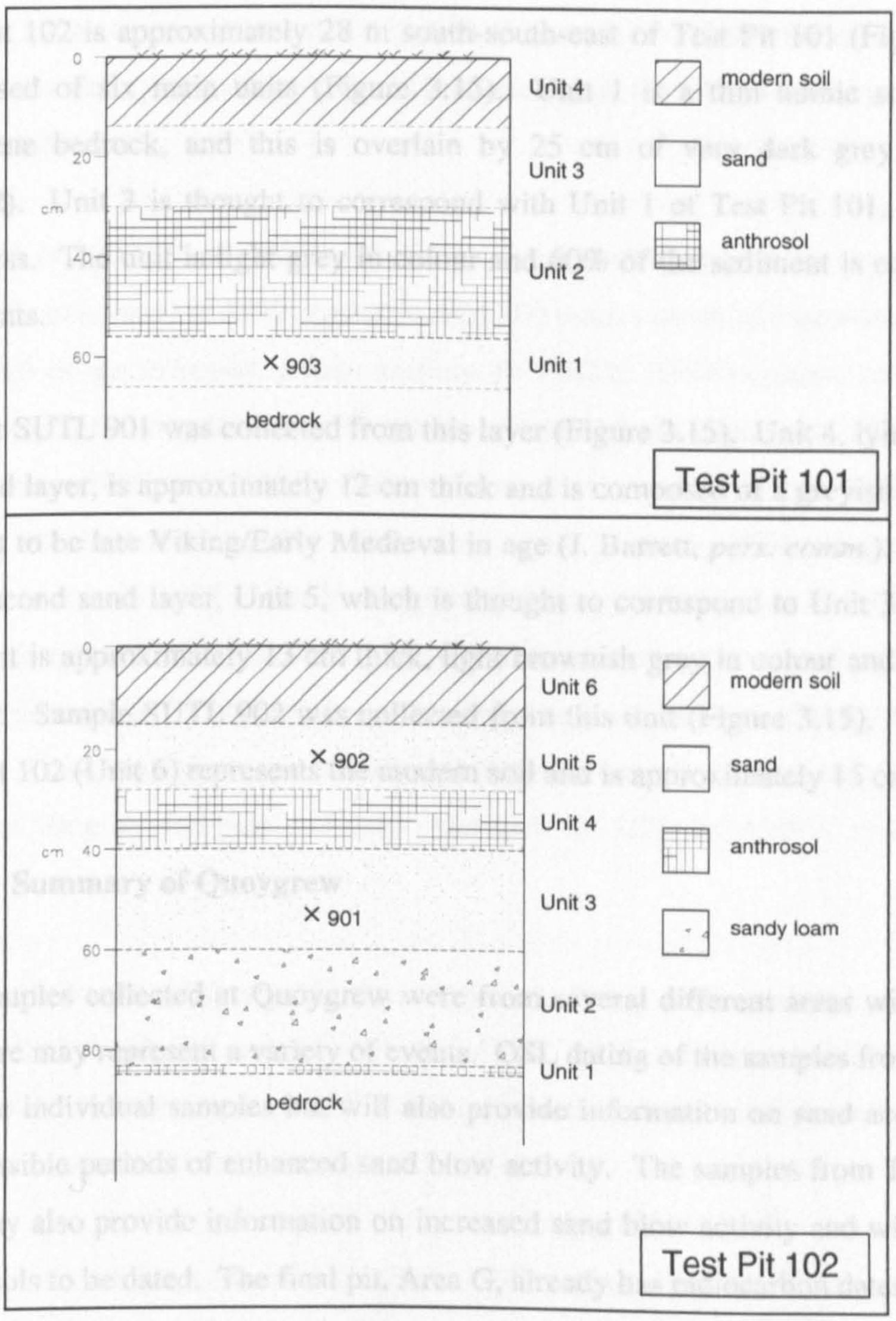

Figure 3.15 – Stratigraphic sections of Test Pits 101 and 102, Quoygrew with sampling points

Unit 3, which is 16 cm thick and composed of grey sand. The top unit (Unit 4) is 14 cm thick and represents the modern soil.

Test Pit 102 is approximately 28 m south-south-east of Test Pit 101 (Figure 3.12) and is composed of six main units (Figure 3.15). Unit 1 is a thin humic soil overlying the sandstone bedrock, and this is overlain by 25 cm of very dark grey sand-clay loam (Unit 2). Unit 3 is thought to correspond with Unit 1 of Test Pit 101, and is 20 cm in thickness. The unit is light grey in colour and 60% of the sediment is composed of shell fragments.

Sample SUTL 901 was collected from this layer (Figure 3.15). Unit 4, lying directly above the sand layer, is approximately 12 cm thick and is composed of a greyish brown anthrosol thought to be late Viking/Early Medieval in age (J. Barrett, *pers. comm.*). This is overlain by a second sand layer, Unit 5, which is thought to correspond to Unit 3 of Test Pit 101. The unit is approximately 13 cm thick, light brownish grey in colour and has a 57% shell content. Sample SUTL 902 was collected from this unit (Figure 3.15). The final unit in Test Pit 102 (Unit 6) represents the modern soil and is approximately 15 cm in thickness.

3.4.1.5 Summary of Quoygrew

The samples collected at Quoygrew were from several different areas within the site and therefore may represent a variety of events. OSL dating of the samples from Test Pit 7 will date the individual samples but will also provide information on sand accumulation rates and possible periods of enhanced sand blow activity. The samples from Test Pits 101 and 102 may also provide information on increased sand blow activity and will also allow the anthrosols to be dated. The final pit, Area G, already has radiocarbon dates associated with it and therefore the OSL dates should confirm the date of the midden. *In situ* gamma spectrometry was undertaken on all samples using a Canberra series 10 MCA or an Ortec Micronomad system (Test Pits 101 and 102) and a 3"x3" NaI scintillation detector.

3.4.2 Pierowall, Westray

The site at Pierowall (Grid ref: HY440 489) lies slightly north of the village in a field adjacent to the ruined church of Lady Kirk (Figure 3.11). The area north of Pierowall has produced a variety of archaeological finds relating to a Viking cemetery and an early Iron Age settlement.

Marwick (1931/32) first described in some detail five Viking graves that William Rendall originally excavated in 1839 approximately 400 metres north of Pierowall. Very little was published on the Pierowall graves until the RCAHMS (1946) summarised the excavations that took place during the mid-19th century. Rendall had continued to excavate in the area, and between 1839 and 1849 he discovered another nine Viking graves (RCAHMS 1946). Further details regarding the excavations were given by Thorsteinsson (1968), who mentioned that in 1855 James Farrer excavated yet another grave in the area and in 1863 he oversaw the final excavation. Well-preserved skeletons were found in most of the graves, the majority with their heads towards the south (Marwick 1931/32; Thorsteinsson 1968). Associated grave goods included daggers, swords, combs, shield bosses, tortoise brooches, ring-headed pins and axes (Marwick 1931/32; RCAHMS 1946; Thorsteinsson 1968).

During 1969 and 1970 construction workers building new council houses at Pierowall (Grid ref: HY 436 487 and HY 435 484) found kitchen middens of shells, animal bones and stones below approximately 2 ft (60 cm) of sand (Lamb 1983), however there is little information available on these sites.

Further excavations were undertaken in 1981 approximately 20 m north of Pierowall (Grid ref: HY 439 490) in Pierowall stone quarry where a large decorated stone was found during quarrying operations. The discovery of the stone led to a salvage excavation of a low mound at the edge of the quarry, which revealed a multi-period site (Sharples *et al.* 1984). The site was initially used during the Neolithic period as a chambered tomb and is thought to have had a structure similar to Maes Howe (Sharples *et al.* 1984). The tomb would have dominated the low lying landscape and the decorated stone was probably used in the tomb perhaps as a lintel above the main entrance to the passage (Sharples *et al.* 1984). Although there was no datable material within the tomb, Sharples *et al.* (1984) suggested that it was probably of a similar size and shape as that at Quanterness, and

therefore may have been in use approximately 3650-2900 cal BC. A radiocarbon date from an animal bone lying within the second occupation layer suggests that by the Late Neolithic, approximately 2890-2500 cal BC (GU-1583), this feature had fallen into disrepair and it was levelled and paved over (Sharples *et al.* 1984). A small platform was constructed adjacent to the paved area at this time and a rectangular structure was built on top of the platform. Large quantities of flaked stone were found within the structure and it is thought that during this phase it was used by a flint knapper and not as a living area (Lamb 1983; Sharples *et al.* 1984). It is not known when the structure was abandoned however a layer of wind blown sand, possibly representing the first event of this kind in eastern Westray at this time, covered the entire site (Sharples *et al.* 1984). In the early Iron Age, approximately 800-410 cal BC (GU-1580), a large roundhouse with 3 m thick walls was constructed over the original cairn. The construction of the roundhouse caused severe damage to the Neolithic chamber of the cairn (Sharples *et al.* 1984). Final occupation in the area is represented by plough furrows in wind blown sand deposits above the remains of the roundhouse. The cultivation layer is covered by yet another wind blown sand deposit, which lies directly below the modern turf (Sharples *et al.* 1984).

3.4.2.1 OSL samples

OSL samples were collected from a test pit dug in an adjacent field 20 m north-east of the ruined church of Lady Kirk (HY440 489). The pit was approximately 0.9 m deep and contained layers of sand and soil (Figure 3.16). A large flagstone at the base of the pit was not lifted and therefore it is not known if it lies on top of natural substrate. Above the flagstone was a layer of medium-grained brown sand with a shell content of 63% and sample SUTL 879 was collected from this unit (Figure 3.16). Contact with the overlying soil layer was undulating but relatively sharp, and the soil contained a few charcoal flecks. Two sand layers were identified above the soil (Figure 3.16). The lower layer was reddish brown in colour, medium grained and had a shell content of 69%. The colour of this layer became darker with depth and contact with the underlying soil was gradational. Contact between the reddish sand and the upper medium-grained white sand was also gradational and undulating, and sample SUTL 878 was taken just below the contact between the two sands. The upper sand had a shell content of 63%, and the final sample, SUTL 877, was taken from this unit. At the top of the section overlying the white sand was the modern soil and turf. The contact was relatively sharp and modern plough marks were noted (Figure 3.16).

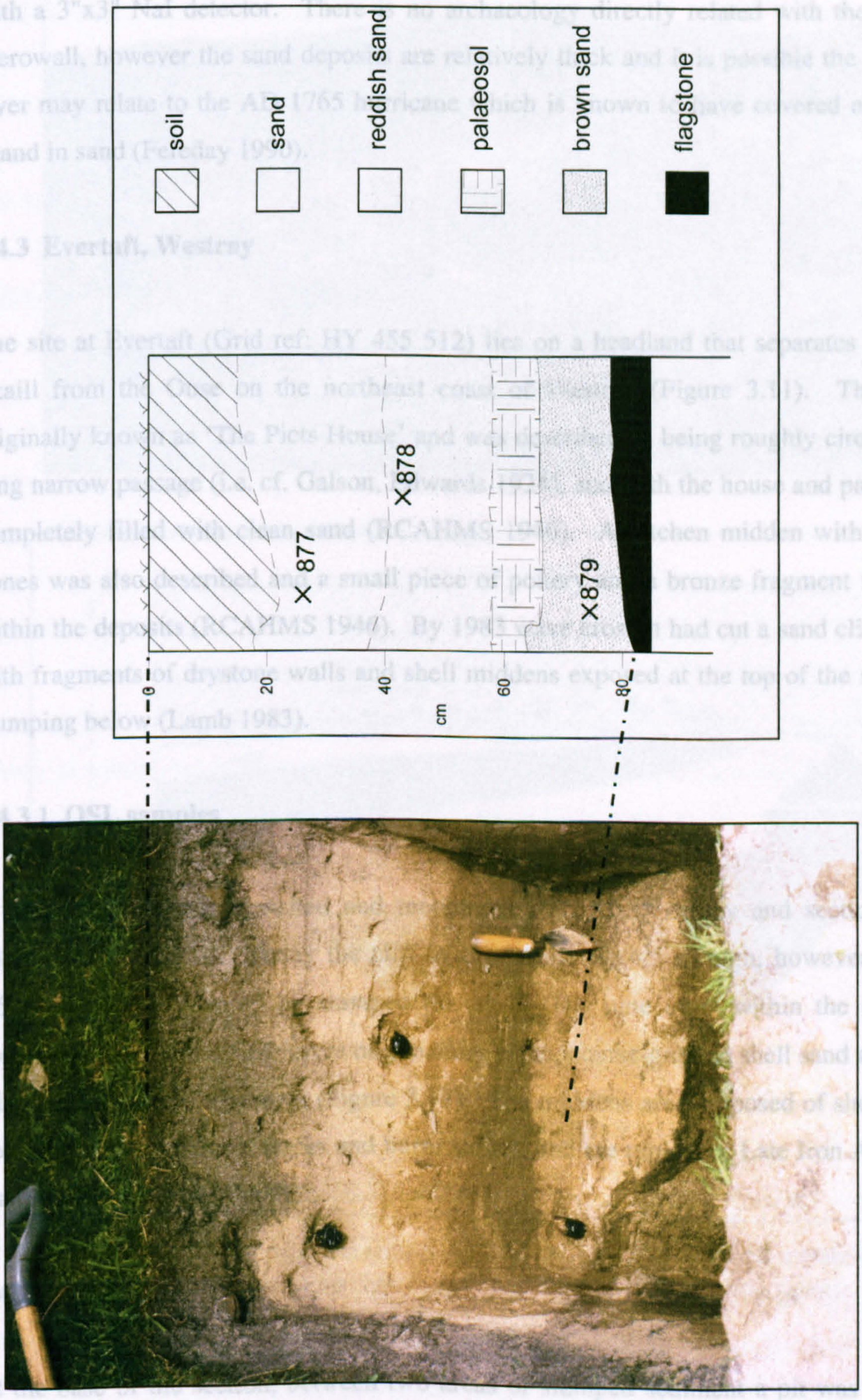

Figure 3.16 – Photograph and stratigraphic drawing of the test pit at Pierowall with sampling points

3.4.2.2 Summary of Pierowall

In situ gamma spectrometry was undertaken on all samples using an Ortec Micro-Nomad with a 3"x3" NaI detector. There is no archaeology directly related with the test pit at Pierowall, however the sand deposits are relatively thick and it is possible the upper sand layer may relate to the AD 1765 hurricane which is known to have covered much of the island in sand (Fereday 1990).

3.4.3 Evertaft, Westray

The site at Evertaft (Grid ref: HY 455 512) lies on a headland that separates the Bay of Skaill from the Ouse on the northeast coast of Westray (Figure 3.11). The site was originally known as 'The Picts House' and was described as being roughly circular with a long narrow passage (i.e. cf. Galson, Edwards 1924), and both the house and passage were completely filled with clean sand (RCAHMS 1946). A kitchen midden with shells and bones was also described and a small piece of pottery and a bronze fragment were found within the deposits (RCAHMS 1946). By 1983 wave erosion had cut a sand cliff 3m high, with fragments of drystone walls and shell middens exposed at the top of the section and slumping below (Lamb 1983).

3.4.3.1 OSL samples

In 2000 the site was revisited and recorded by an EDM survey and section drawing (Barrett *et al.* 2000a). Today the cliff is approximately 4.5 m high, however the lower 1.5 m is mostly covered by slumped material. The nine units within the section are composed of interstratified layers of generally clean, coarse-grained shell sand and midden with some drystone structures (Figure 3.17). The middens are composed of shells, stones, bone fragments, charcoal flecks and burnt stones, and are typical of Late Iron Age midden material (Barrett *et al.* 2000a).

3.4.3.2 Unit 1

At the base of the section, between two areas of slumped sediment a pit was dug below beach level (Figure 3.17). Unit 1 is at the base of this pit and is composed of a light yellow-grey fine-grained sand containing up to 51% of shell fragments. The layer extends

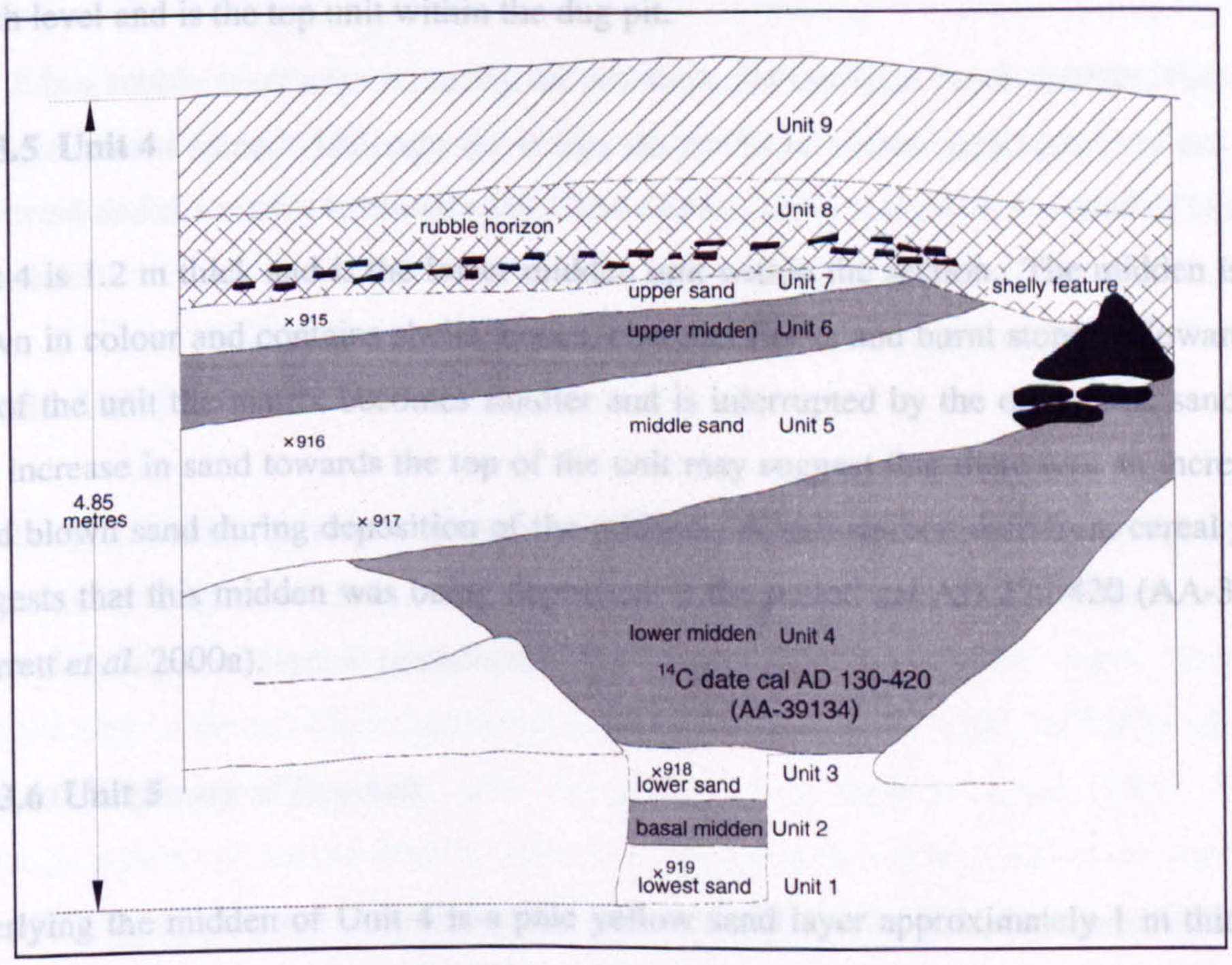

Figure 3.17 – Photograph and stratigraphic drawing of the exposed section at Evertaft, with multiple midden and sand deposits and the sampling points.

downwards for at least 80 cm, and one sample, SUTL 919, was collected from this layer for OSL dating.

3.4.3.3 Unit 2

Overlying this sand is a dark grey-brown basal midden containing charcoal, peat ash and some limpets and cobbles. The midden is approximately 20 cm thick and has sharp upper and lower contacts.

3.4.3.4 Unit 3

Unit 3 is a 15 cm thick sand unit similar to Unit 1 but slightly lighter in colour and sample SUTL 918 was collected from this unit (Figure 3.17). The sand is medium-fine grained and contains approximately 60% shell fragments. This unit is slightly exposed above the beach level and is the top unit within the dug pit.

3.4.3.5 Unit 4

Unit 4 is 1.2 m thick and is the lower midden unit within the section. The midden is dark brown in colour and contains shells, bones, charcoal flecks and burnt stones. Towards the top of the unit the matrix becomes sandier and is interrupted by the occasional sand lens. The increase in sand towards the top of the unit may suggest that there was an increase in wind blown sand during deposition of the midden. A radiocarbon date from cereal grains suggests that this midden was being deposited in the period cal AD 130-420 (AA-39134) (Barrett *et al.* 2000a).

3.4.3.6 Unit 5

Overlying the midden of Unit 4 is a pale yellow sand layer approximately 1 m thick and relatively fine-grained. Throughout the unit there is an increase in shell content with depth from approximately 37% to 51%. There is some evidence of banding throughout the unit, however it is reasonably homogeneous in colour and texture given the thickness of the unit. Two OSL samples were collected from this unit; SUTL 916 towards the top of the unit and SUTL 917 near the base (Figure 3.17).

3.4.3.7 Unit 6

Unit 6 is an upper midden, approximately 50 cm thick with a sharp underlying contact. The midden is brownish yellow in colour and contains shells, stones, bone fragments and black/orange flecks throughout.

3.4.3.8 Unit 7

Unit 7 is the final sand layer and sample SUTL 915 was collected from the middle of the unit (Figure 3.17). The sand is pale brown in colour, relatively fine grained and contains yellowish brown bands throughout. Approximately 60% of the sand is composed of shell fragments.

3.4.3.9 Unit 8

Unit 8 is a rubble layer approximately 60 cm thick and contains beach cobbles, flagstones and some burnt stone. Although the stones do not have a clear structure, they are clast-supported and the matrix is brown sand. The underlying contact with the sand of Unit 7 is gradational.

3.4.3.10 Unit 9

Overlying the rubble layer is a modern soil approximately 80 cm thick and composed of a medium-coarse grained sand with patches of limpet shells. The contact with the underlying flagstone layer is gradational.

3.4.3.11 Summary of Evertaft

Five OSL samples were collected from the site and *in situ* gamma spectrometry was undertaken for each sample using an Ortec Micro-Nomad with a 3"x3" NaI detector. There is little information available for this site and only one radiocarbon date from the lower midden material. Barrett *et al.* (2000a) did note that the contents and appearance of the upper midden (Unit 6) are very similar to the lower midden (Unit 4) and they have suggested that the upper midden may in fact be part of the lower midden that has been redeposited to try and stabilise the sand surface of Unit 5. OSL dating of the sand layers

will provide *terminus post quem* and *terminus ante quem* dates for the midden deposits, perhaps helping to assess whether the upper and lower middens are of a comparable age and they may also determine whether the site was temporarily abandoned due to sand inundation. The middle sand layer (Unit 5) should be less than 2000 years old based on the radiocarbon date from Unit 4 below, and therefore the sand and midden layers lying below Unit 4 are expected to be more than 2000 years old. Further radiocarbon dating of the other midden units would help to constrain the OSL dates, nevertheless the OSL dates will help to assess whether the stratigraphy is undisturbed providing a chronological context for future research at this site.

3.5 Eday

The island of Eday lies between Westray and Sanday, and is approximately 12 km long and 5 km wide. Topographically it is distinctive with steep offshore gradients and few beaches or flat machair areas. The island is almost bisected by a low tract of land, less than 10 m above sea level, stretching from the west to the east coast (Figure 3.18). The sandy beaches of Sands of Doomy and Bay of London border this low area, which is the most extensive area of blown sand, or machair, on the island (Mather *et al.* 1974). Smaller areas of machair are found at Sealskerry Bay, Sandyland and Bay of Doomy (Mather *et al.* 1974). The rest of the island is relatively high with hills in the north rising to 60 m and those in the south to 101 m at Ward Hill (Figure 3.18).

Eday Beds dominate the geology of the island and there are widespread till deposits, e.g. Fersness Bay, underlying the peat and heather moorland that extensively covers much of the island. Archaeologically, Eday is relatively rich in sites with many chambered tombs dating to the prehistoric period, and the remnants of stone walls, indicative of a once successful agricultural economy, now concealed by peat deposits (Lamb 1984). Despite the large number of archaeological sites on Eday, the palaeo-landscape of the island was sampled instead, concentrating on Sandhill, a small hill south of the low-lying land in the centre of the island (Figure 3.18).

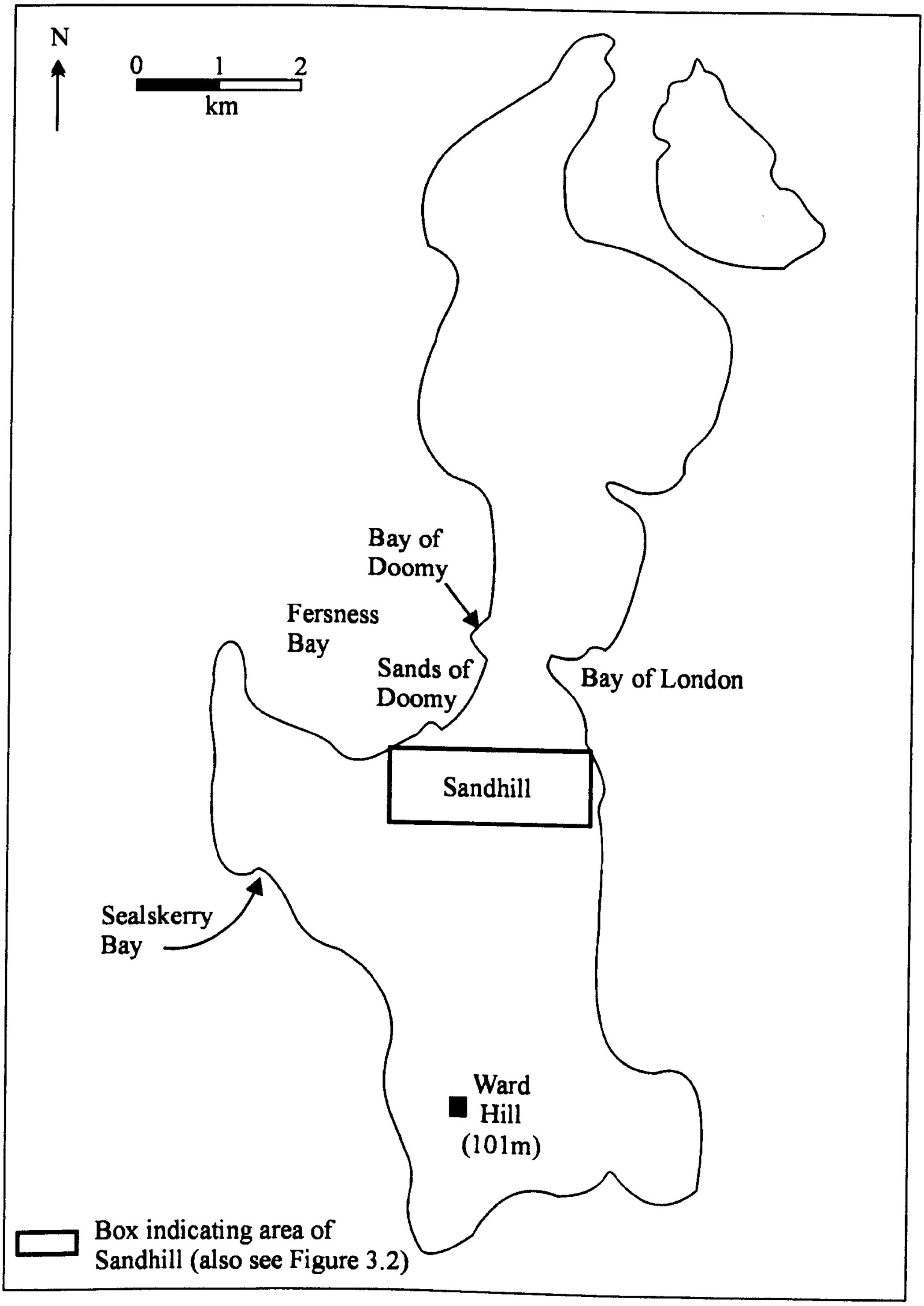

Figure 3.18 – The island of Eday including the location of places mentioned in the text and archaeological site sampled

3.5.1 Sandhill, Eday

Sandhill covers an area of land between Fersness Bay (Grid ref: HY554 334) and Skaill Farm (Grid ref: HY566 328) and, despite its name, is a peat and heather moorland with little sand outcropping at ground level. The main source of sand on Eday is located at Fersness Bay on the west coast, however sand was noted on the south-east flanks of Skaill Burnt Mound on the east coast (Figure 3.19) during sampling burnt stones for TL dating (Anthony *et al.* 2000; Robertson *et al.* 2000). The nearest source of modern sand is at Fersness Bay, about 1.5 km from Skaill Burnt Mound and movement of this sand across the island would involve a vertical elevation of 40-50 metres. This implies a very significant sand blow event or series of events if Fersness Bay was indeed the source of the sand. In order to test the hypothesis that the source of sand at Skaill Burnt Mound was Fersness Bay, a west to east transect of 10 pits were dug across Sandhill to establish the extent of sub-surface wind blown sand deposits (Figure 3.19).

Nine of the ten test pits were dug in October 2000 with the able help of A. Rennie (University of Glasgow). The pits varied in depth between 35 and 65 cm (Figure 3.20), the depth depending on the location of the sand layer within each pit. Peat samples were collected from beneath the sand layer in two of the pits and radiocarbon dating provided dates of cal AD 135-420 (GU-9240) and cal AD 885-1030 (GU-9242). The difference in age between the two basal peat deposits suggests that more than one sand blow event may be represented in this landscape. There was a sharp contact with the overlying sand layers, which varied in thickness between 7 and 23 cm and the thickness of the sand did not appear to be related to the topography (Figure 3.20). The upper contact of each sand layer with the overlying peat was sharp and the thickness of the upper peat varied between 17 and 45 cm. A radiocarbon date from the upper peat provided a date of cal AD 1525-1950 (GU-9241).

A sand sample for OSL dating was taken from the sand layer in each pit (Figure 3.21) and *in situ* gamma spectrometry was undertaken on each sample using a Bicron Scalar-Ratemeter and a 2"x2" NaI scintillation detector. All of the sand samples were fine grained and contained between 0 and 11% calcium carbonate content.

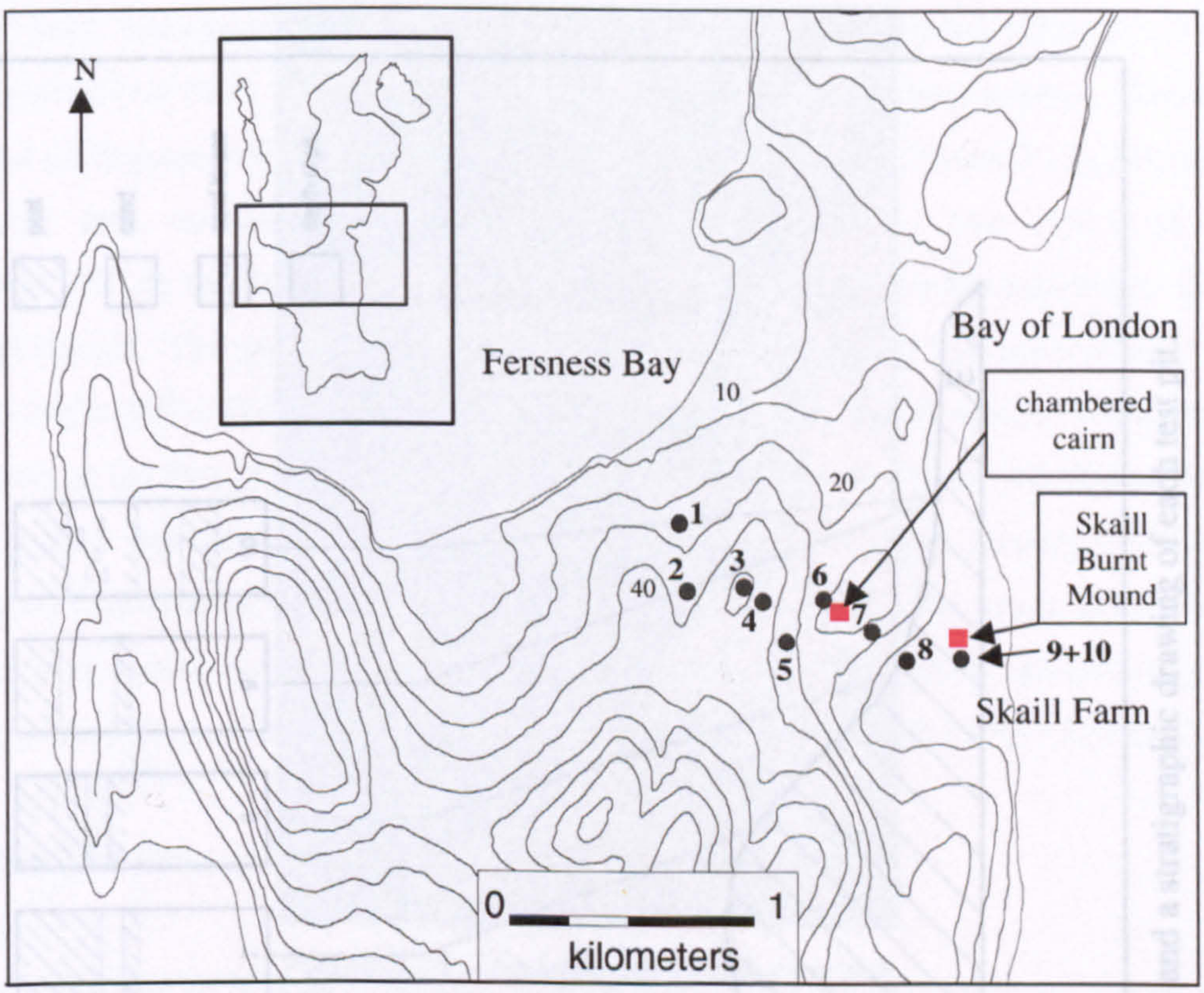

Figure 3.19 – Location of the test pits across Sandhill, Skaill Burnt Mound and the chambered cairn, Eday.

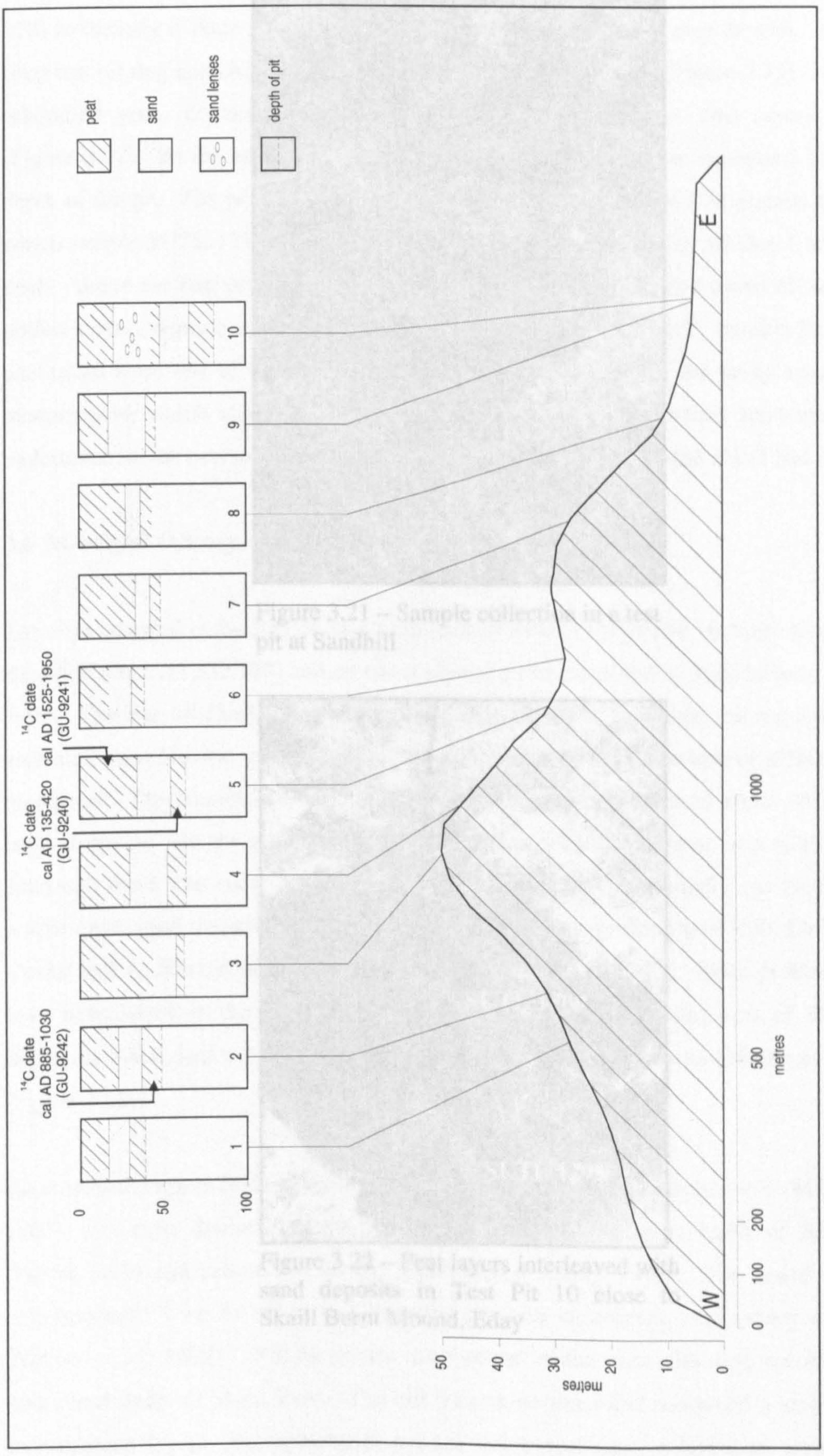

Figure 3.20 – Topographic profile showing the location of the test pits on Sandhill and a stratigraphic drawing of each test pit.

Figure 3.21 – Sample collection in a test pit at Sandhill

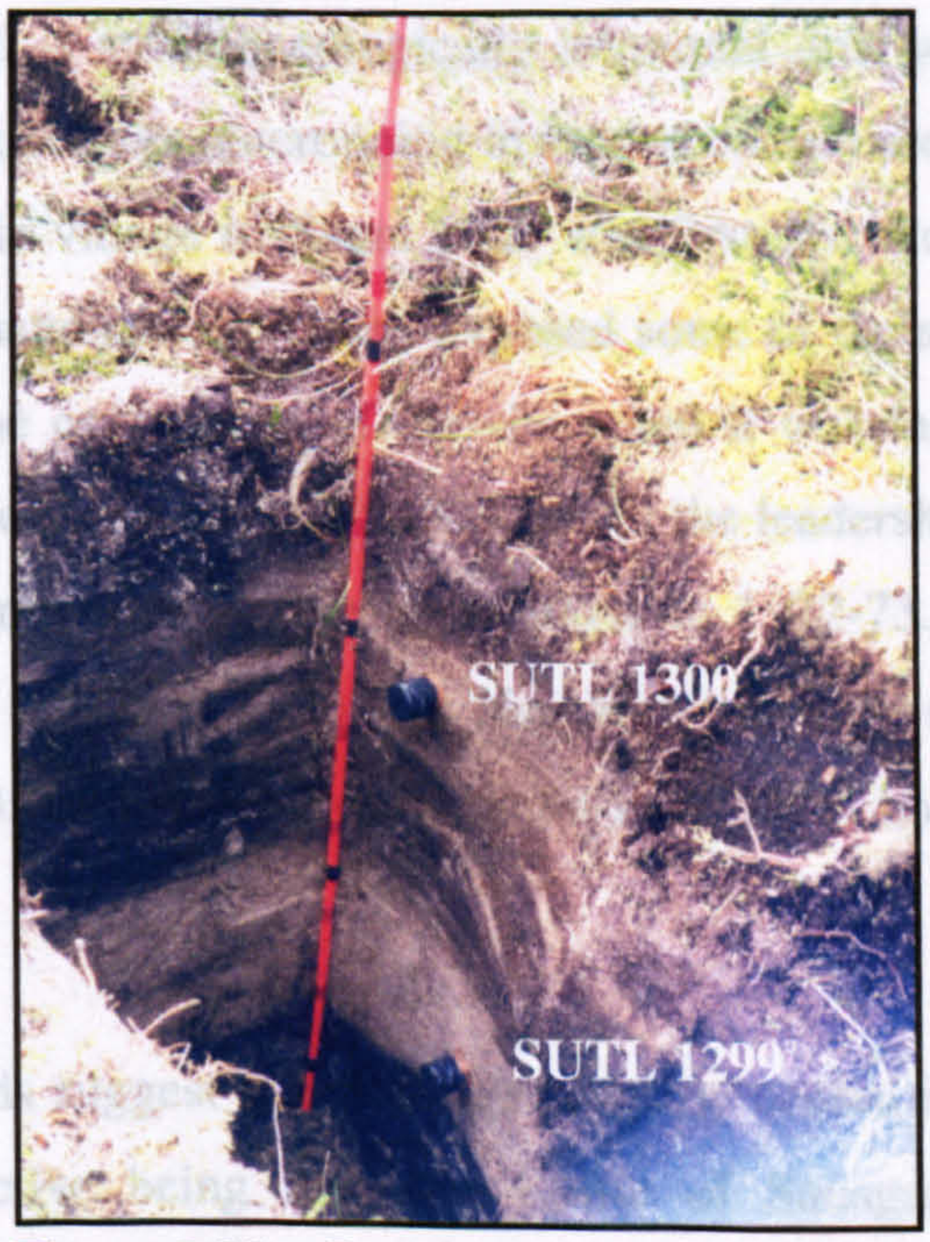

Figure 3.22 – Peat layers interleaved with sand deposits in Test Pit 10 close to Skaill Burnt Mound, Eday

Further work was carried out in July 2001 at the Skaill Burnt Mound (Grid ref: HY566 328) to identify if there was more than one sand layer within the peat deposit. An 85 cm deep test pit dug approximately 10 metres from the burnt mound (Figure 3.19), outside the scheduled area, contained three layers of peat separated by two layers of sand (Figure 3.22). At the base of the pit, a thick layer of peat 18.5 cm continued beyond the depth of the pit. The peat was overlain by a 17.5cm thick layer of fine grained sand from which sample SUTL 1299 was taken and this in turn was overlain by another 5 cm layer of peat. Above the thin peat layer was a second sand layer mainly composed of sand lenses within a peaty deposit and this layer was approximately 23 cm thick. Sample SUTL 1300 was taken from one of the fine grained sand lenses. Overlying the peaty sand was the modern peat, which supported the heather moorland. *In situ* gamma spectrometry was undertaken on the two samples using the Ortec Micro-nomad with the 3"x3" NaI detector.

3.6 Mainland Orkney – Bay of Skaill

The sites sampled at the Bay of Skaill are located west of the World Heritage Site of Skara Brae (Grid ref: HY232 187) and on either side of a cist identified by Julie Gibson (OAT) in 1994. The Bay of Skaill is an archaeologically important area with the remains of both prehistoric and historic structures outcropping in eroded coastal sections or within the dune hinterland. The Neolithic village of Skara Brae was first discovered about 1850 when a large storm cut into the sand dune cliff and exposed some of the structures (Childe 1931). Although there was some exploration of the site when it was initially exposed, the first proper excavation occurred between 1927-1930, under the leadership of V.G. Childe. D.V. Clarke and A. Ritchie undertook further excavations in 1972-73. Other prehistoric sites have been found in the area and include a Neolithic butchery site west of Skara Brae (Richards 1994) and a Bronze Age barrow mound near Skaill house (Morris *et al.* 1985) (Figure 3.23).

Later archaeological finds suggest that Vikings probably settled in the area (Morris *et al.* 1985), the most distinctive being near the Castle of Snusgar, north of Skara Brae (Figure 3.23) and referred to as the Skaill hoard (Greig 1940). The hoard contained approximately 7 kg of silver and included personal ornaments, ring-money and ingots (Morris *et al.* 1985). Viking graves also occur in the area, the first recorded being uncovered south of Skara Brae. The cist was stone lined and contained a male skeleton accompanied by an iron spearhead, a bone comb and case, a knife, an arrowhead, a

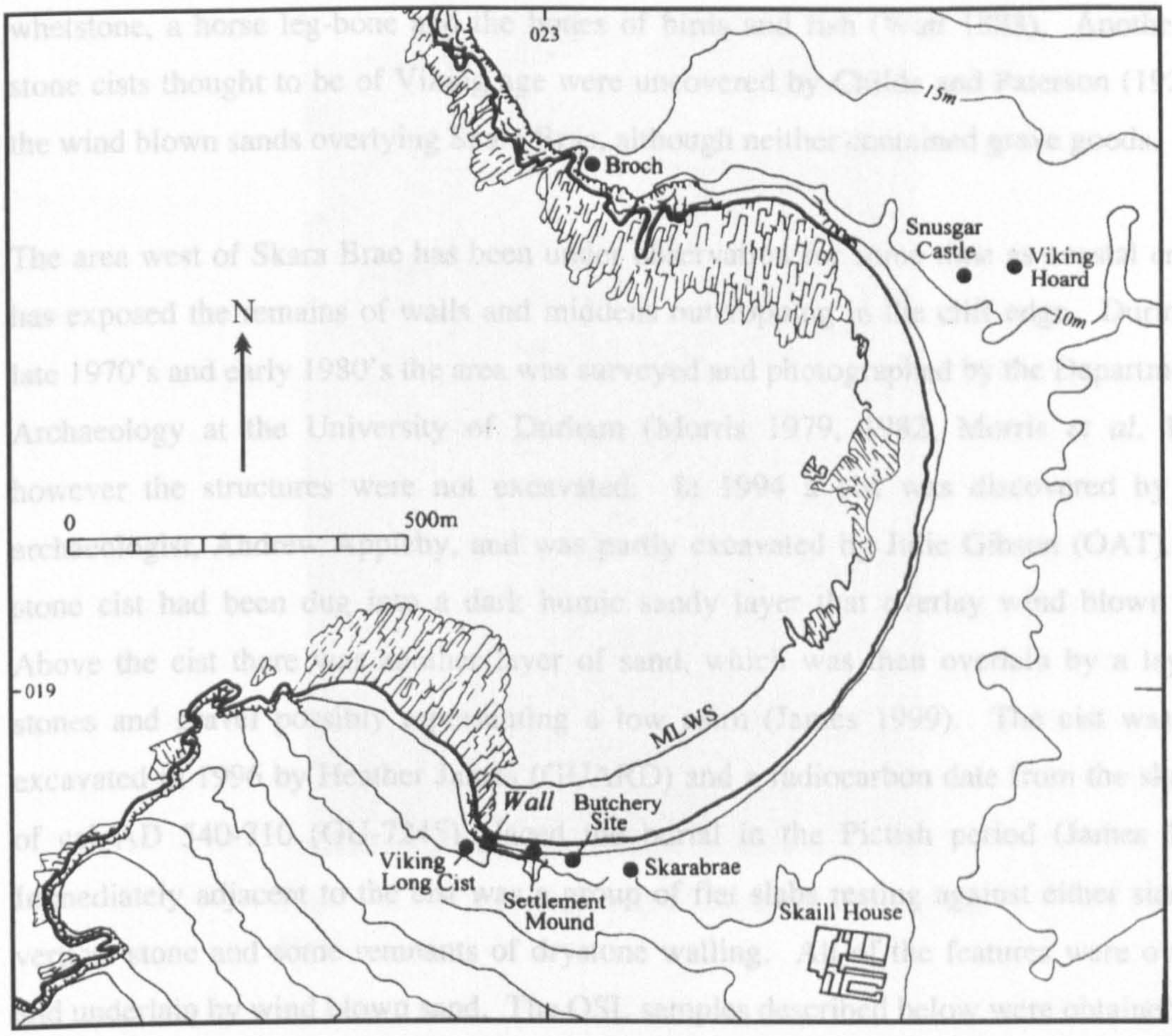

Figure 3.23 – Archaeological sites in the Bay of Skaill (after Simpson 1998).

whetstone, a horse leg-bone and the bones of birds and fish (Watt 1888). Another two stone cists thought to be of Viking age were uncovered by Childe and Paterson (1929) in the wind blown sands overlying Skara Brae, although neither contained grave goods.

The area west of Skara Brae has been under observation for some time as coastal erosion has exposed the remains of walls and middens outcropping in the cliff edge. During the late 1970's and early 1980's the area was surveyed and photographed by the Department of Archaeology at the University of Durham (Morris 1979, 1982; Morris *et al.* 1985), however the structures were not excavated. In 1994 a cist was discovered by local archaeologist, Andrew Appleby, and was partly excavated by Julie Gibson (OAT). The stone cist had been dug into a dark humic sandy layer that overlay wind blown sand. Above the cist there was another layer of sand, which was then overlain by a layer of stones and gravel possibly representing a low cairn (James 1999). The cist was fully excavated in 1996 by Heather James (GUARD) and a radiocarbon date from the skeleton of cal AD 540-710 (GU-7245) placed the burial in the Pictish period (James 1999). Immediately adjacent to the cist was a group of flat slabs resting against either side of a vertical stone and some remnants of drystone walling. All of the features were overlain and underlain by wind blown sand. The OSL samples described below were obtained from this section of the cliff.

3.6.1 OSL samples

Both sections had wind blown sands above and below walled structures that were eroding out of the coastal section, west of Skara Brae and close to the wall in Figure 3.23, providing good sampling points.

3.6.2 Section 1

Section 1 is approximately 4.25 m high, however much of the lower 1.25 metres of the section is covered by slumped material. Above the slumped material is a 90 cm thick deposit of medium grained wind blown sand that is capped by some *in situ* drystone walling (Figure 3.24). The contact between the underlying sand and the flagstones is sharp, however it is impossible to determine the height of the wall due to erosion and slumping above the wall which has clearly affected the top of the structure. Two samples were obtained for OSL dating from beneath the walled structure. The lower sample is

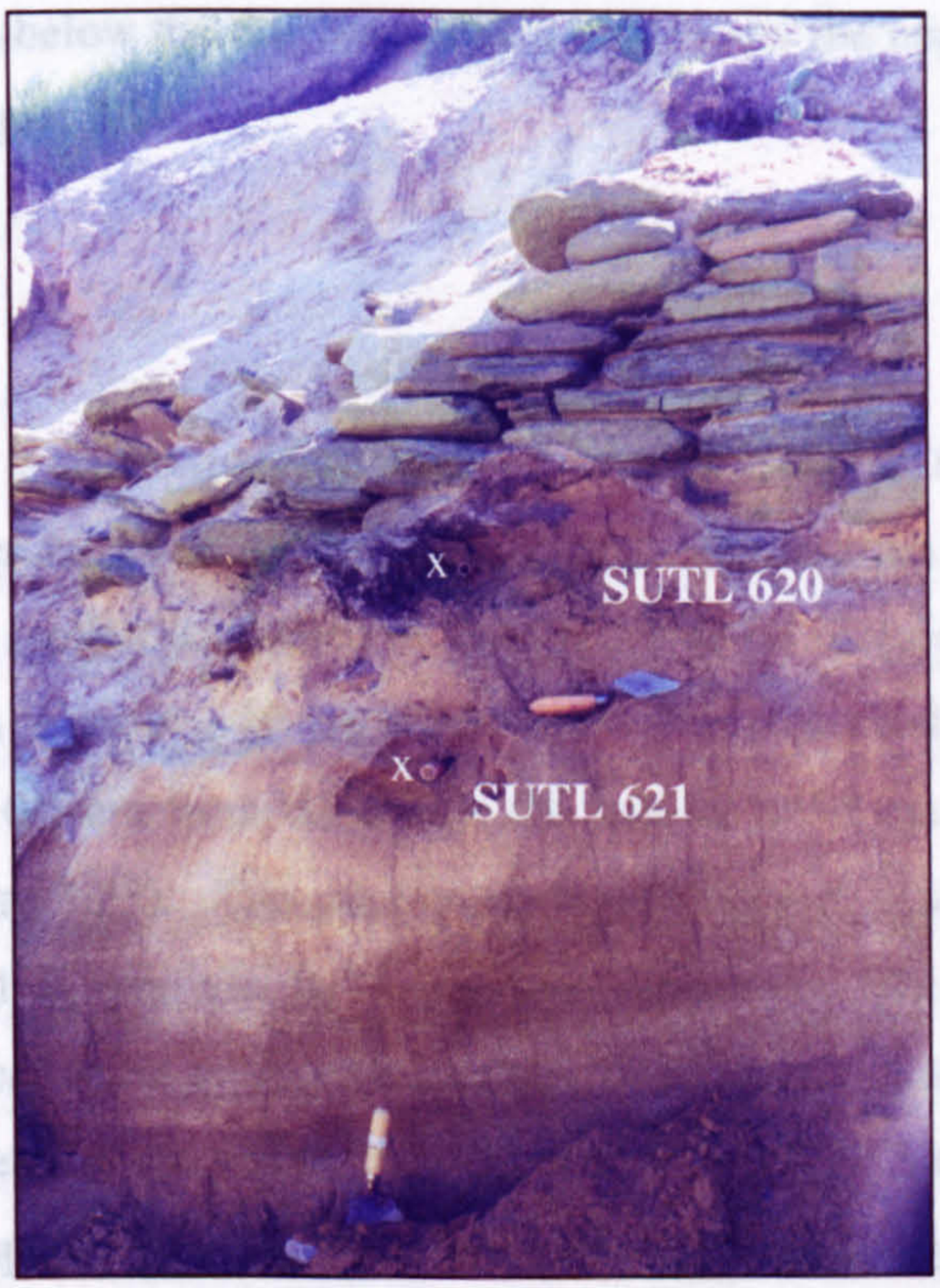

Figure 3.24 –Section 1, Bay of Skaill with sampling points

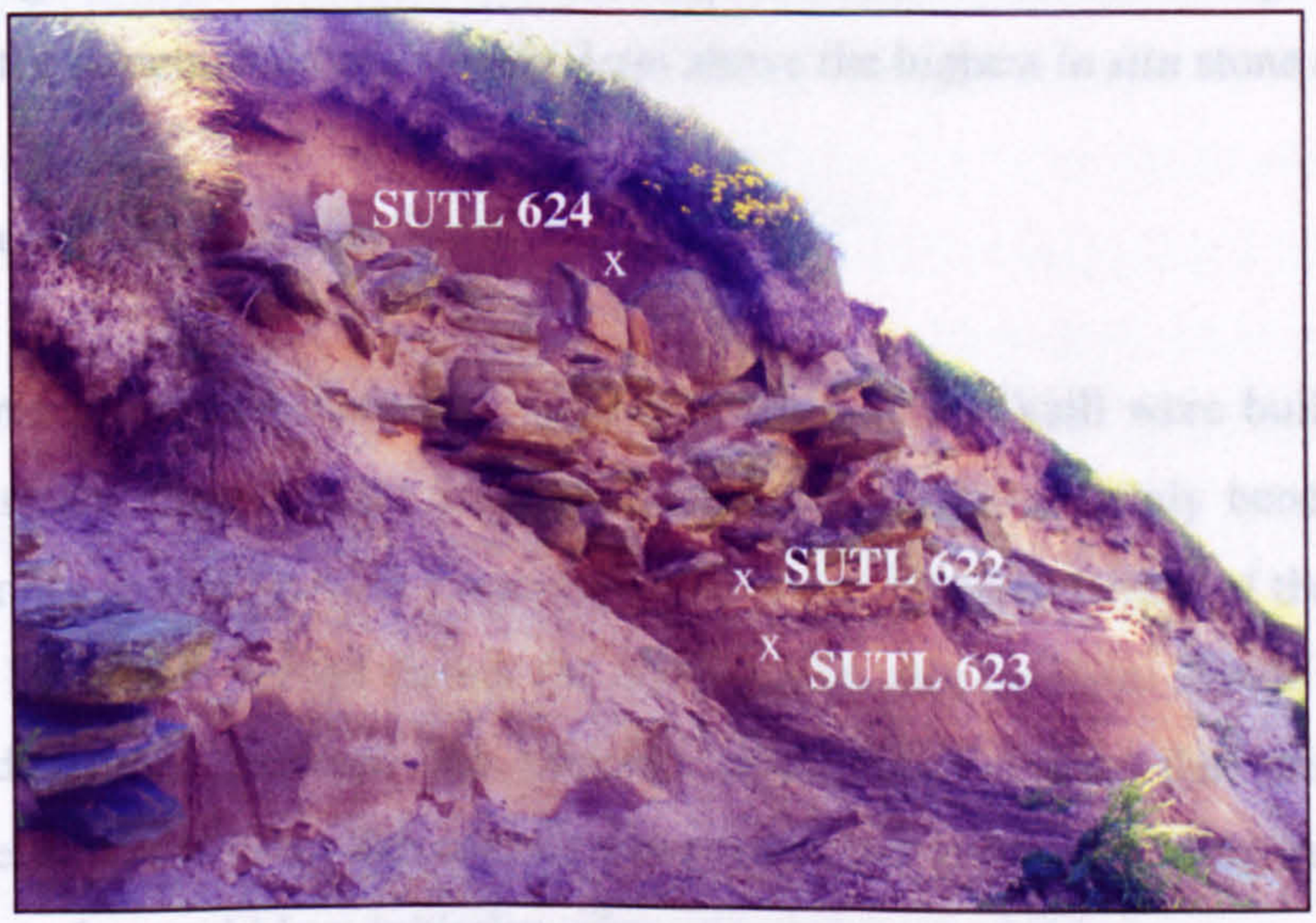

Figure 3.25 –Section 2, Bay of Skaill with sampling points

approximately 40 cm below the flagstones (SUTL 621) and the upper one 6 cm below the wall (SUTL 620) (Figure 3.24).

3.6.3 Section 2

The second section is approximately 10.5 m west of Section 1 and close to the cist excavated by Heather James in 1996 (James 1999). The section is 3.6 metres high and again the base of the section is covered in slumped material (Figure 3.25). Approximately 1.8 m up the section there is a 80 cm thick layer of *in situ* wind blown sands, which is interrupted briefly, 10.5 cm from the top of the unit by a 2.5 cm thick layer of medium grained gravel (Figure 3.25). The sand overlying the gravel is slightly coarser than the underlying sand and is overlain by a drystone structure. The flagstones within this structure do not appear to be as well set as those in Section 1, with a variety of sizes and shapes used and several of the stones are emplaced vertically. Although the walling does not appear to be complete, there is a layer of wind blown sands approximately 37 cm thick sealing the structure.

Two samples were obtained from beneath the structure 18.5 and 3 cm below the lowest course of flagstones (SUTL 623 and 622 respectively). A further sample was obtained from above the structure approximately 2 cm above the highest *in situ* stone (SUTL 624).

3.6.4 Summary of the Bay of Skaill

The structures protruding from the sections at the Bay of Skaill were built directly onto sand deposits and therefore the samples collected from immediately beneath the lowest course of stones should provide a *terminus post quem* for construction of the structures. If these sands have been zeroed during the construction process there should be a relatively large age difference between the samples immediately below the stones and those 18-40 cm below the stones. The sample from above the drystone walling in Section 2 may provide a date for sand blow initiation after abandonment of the structure. *In situ* gamma spectrometry was undertaken on all the samples using a Canberra series 10 MCA with 3"x3" NaI scintillation detector.

3.7 Section 2 – Laboratory methods and experimental procedures

3.8 Sample preparation

3.8.1 Water content

As discussed previously in Chapter 2, water affects the amount of radiation a sample will receive during burial (Aitken 1989, 1998) and therefore an estimate of the water content within the bulk sample must be established prior to further sample preparation.

Samples for this study were sealed immediately on extraction from the sections or pits, not only to prevent exposure to light, but also to prevent the sediment from drying out. In the laboratory, under safe light conditions (two 5W RS bulkhead fluorescent tubes) tested by Anthony *et al.* (1999/2000), a small amount of sediment was extracted from the end of the tubes to ensure that the remaining sediment used for analysis had not been exposed to light. The samples were then weighed in their tubes, saturated with de-ionised water and then re-weighed, before being emptied into plastic beakers and placed in a 50°C oven to dry. Once dried the samples were re-weighed and this allowed the actual and saturated water contents to be calculated using:

$$\text{Actual water content} = \left(\left(\frac{w}{dw}\right)-1\right)*100$$

$$\text{Saturated water content} = \left(\left(\frac{sw}{dw}\right)-1\right)*100$$

where w = sediment weight as submitted in grams

dw = dried sediment weight in grams

sw = saturated sediment weight in grams

Previous research has used various estimates of water content in the final age calculation based on the type of sediment used and location of the site. Both Berger (1988) and Prasad and Gupta (1999) suggest that the water content used in the age calculations should be an average of the 'as-found' and saturated water contents, however Wintle *et al.* (1998) suggest that it should be based on the field position of the sample. For this study the water content estimates used in the final age calculations are a mean of the actual and saturated

water contents. The samples were mainly collected during the drier summer months, however some of the sites e.g. Tofts Ness do flood during the winter indicating complete saturation of the ground. The mean of the actual and saturated water contents of the samples is thus a good estimate of the average water content experienced by samples throughout the year.

3.8.2 Mineral Separation

The size fraction used for luminescence dating often depends upon the size distribution of each sample. Fine grains (4-11μm) have the advantage that they remain longer in suspension either in air or water and once deposited they receive the full alpha dose (Aitken 1985, 1998), however they can infiltrate down through coarser sediment and contaminate an older sample (Aitken 1985, 1998; Wintle 1997). Coarser grains (>100μm) tend to be more abundant in beach sands but dunes are finer and positively skewed (Briggs 1977; Vega Leinert *et al.* 2000). Due to the different bleaching rates in coastal subaqueous and subaerial environments (Rink 1999), these larger grains may not be fully bleached upon deposition (Aitken 1998).

Twenty grams of bulk dried sediment from each sample were put aside for beta and gamma dosimetry (see Section 3.10.3) and the remainder was sieved for 15 minutes using a 'Fritch' siever with 4 mesh sizes: 500 μm, 250 μm, 125 μm and 90 μm. Most of the modern beach samples were relatively coarse with 52% having a dominant grain size of 250-500 μm (Figure 3.26a). The archaeological samples were also coarse grained with the 250-500 μm fraction being dominant in 70% of the samples and the 125-250 μm fraction in 28% of the samples (Figure 3.26b). Very few of the samples had sediment finer than 125 μm. The 125-250 μm fraction was used where possible for luminescence dating, and in the event of this not being possible, the 250-500 μm fraction was used.

The samples consisted mainly of a mixture of quartz, feldspar and shell fragments and were initially treated with 10% Hydrochloric Acid (HCl) for 30 minutes to dissolve any calcium carbonate (Aitken 1985; Mejdahl and Christiansen 1994) and the results are presented in Chapter 5. For samples that contained a large percentage of shell material the HCl was replaced after 15 minutes to ensure that all shell material was dissolved.

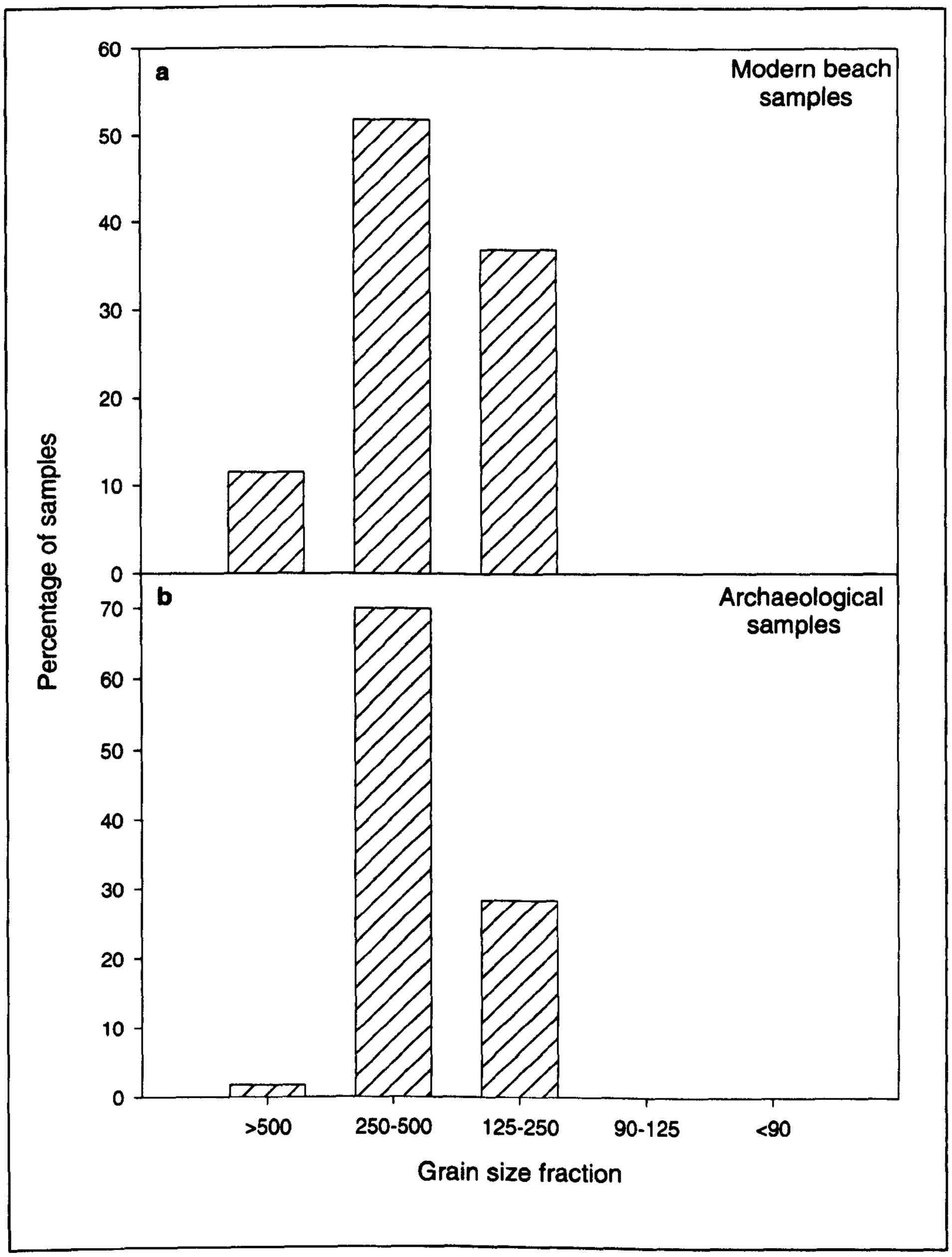

Figure 3.26 a and b – Grain size analysis of modern beach and archaeological samples. Approximately 50% of the modern beach sands are mainly composed of coarse sand (250-500 μm) whereas coarse sand is prevalent in up to 70% of the archaeological samples. This may suggest that the archaeological samples have a different sediment provenance (see Section 5.2.3.1).

After the HCl wash, 15% Hydrofluoric Acid (HF) was added for 15 minutes to clean the feldspars and slightly etch the grains, and a further 30 minutes of 10% HCl ensured that any fluorides that may have developed during the HF treatment were removed. The samples were washed three times with de-ionised water between each acid treatment and the 15% HF was neutralised using 10% ammonia.

Quartz and plagioclase feldspars (2.62-2.74 gcm^{-3}) and alkali feldspars (2.51-2.58 gcm^{-3}) were obtained by heavy liquid separation using sodium polytungstate solutions of 2.51, 2.58, 2.62 and 2.74 gcm^{-3}. A 'Clandon T-51' centrifuge was used for several minutes to settle the heavier grains and each fraction was washed 3 times with de-ionised water and then given an acetone wash.

Once the quartz/plagioclase feldspar fraction was dry, it was washed in 40% HF for 40 minutes to remove the plagioclase feldspar and etch the quartz grains. Etching is thought to dissolve the outside of the grains that may have been affected by alpha radiation (Fleming 1970; Aitken 1985; Berger 1988; Mejdahl and Christiansen 1994; Wintle 1997) removing the need to actively measure the alpha contribution for the dose rate (Aitken 1998). However, quartz tends to etch along dislocation lines (Lang and Miuscov 1967) and experiments by Bell and Zimmerman (1978) confirmed that etching attacks some grains more severely than others and therefore not all of the alpha-irradiated layer may be removed. Despite this, etching should also dissolve any plagioclase feldspar or other minerals that may not have been separated during the density separation and could contribute to the OSL signal if not removed (Aitken 1985). A further 10% HCl wash for 30 minutes should ensure that there was no build up of insoluble fluorides during the HF wash (Aitken 1985; Murray *et al.* 1995). Again 10% ammonia was used to neutralise the acid and the samples were washed 3 times with de-ionised water.

3.8.3 Dispensing

After the etched quartz was dried it was ready for dispensing. The quartz was dispensed onto 10 mm or 9.6 mm aluminium discs that had been cleaned with acetone and sprayed with a layer of 'Electrolube' silicon grease to allow the grains to adhere to them. Due to the non-uniformity of dose given by laboratory radiation sources, the sediment was concentrated, when possible, in the middle of the disc as a monolayer (Aitken 1998). Each disc was weighed before and after the quartz was added to potentially account for disc to

disc variations in the luminescence signal. The majority of discs had approximately 4 mg of quartz dispensed onto them, however samples that used the 250-500μm fraction were slightly heavier.

3.9 Experimental procedures undertaken on the modern beach sands

3.9.1 Residual levels of modern beach sands

To establish the degree of solar re-setting of luminescence at the time of deposition, present-day wind blown sands were collected from the back edges of a wide range of beaches in the Outer Hebrides and Orkney Islands (Figure 3.1a and b). The sand was collected during the day by skimming a trowel across the surface to a depth of approximately 1 cm, and further samples were taken using adhesive packing tape to ensure that only the surface layer was collected.

A comparative study of the Outer Hebrides and Orkney beach samples was conducted using TL, blue OSL and IRSL (Sommerville *et al.* 2001). The modern beach sands were tested using 125-250 μm polymineral samples, which had been treated with 10% hydrochloric acid for 30 minutes to remove any calcite. Three discs per sample were dispensed and measured to allow a comparison of TL, blue OSL and IR stimulated luminescence. Three runs were completed on each disc: the natural signal, 5 Gy and 5 Gy + 1 hour bleaching in a light box. This allowed the sensitivity of the samples to be measured, the residual levels to be determined and a comparison to be made between the samples and the stimulation methods used. The discs were irradiated using a 1.85 GBq Strontium-90 source and bleached in a light box constructed at SUERC. The light box contains four 40W 'Artificial Daylight' tubes with a total power density of 7.292mWcm^{-2}, and high reflectance paint, TiO_2, was used to cover the inside of the box to ensure that the light spectrum is evenly spread (Sanderson *et al.* 1992).

TL measurements were made using a manual reader fitted with a Corning (Kopp) 7-59 and a Schott KG1 filter[3]. The heater plate was ramped from 0-400°C at a rate of 5°C/s. The

---

[3] Corning (Kopp) 7-59 filter has a peak transmission at 365 nm with the main transmission band in the near UV/Visible (320-430 nm) and a secondary transmission in the near IR. Schott KG1 filter has a main transmission band in the visible and near-UV and is a heat absorbing filter. In TL measurements the Schott KG1 helps to suppress IR sensitivity of the Corning 7-59 filter and to reduce sensitivity to black body radiation.

blue OSL measurements were made using a SUERC-built PSL reader using gallium-nitride LEDs with a peak wavelength of 470 nm for sample stimulation (Sanderson *et al.* 2001). Each disc was given a 30 second preheat at 260°C and measured at 125°C for 100 seconds. The IRSL measurements were conducted using a SURRC pulsed PSL reader (Sanderson 1990, 1991; Sanderson *et al.* 1994, 1996) using 180mW IR diodes with a peak wavelength of 880 nm and a 50 mm diameter measurement chamber. Each disc was measured for 100 seconds.

To determine the residual level of grains lying on the surface of the beaches, twenty-one of the adhesive packing tape samples, selected at random, were prepared as above and two polymineral discs per sample were dispensed before being measured on an automated Riso TL/OSL (TL-DA-15) system. One disc from each sample was preheated at 150°C for 10 seconds, stimulated by 1W of IR laser operated at 60% power at 830 nm for 120 seconds at 50°C, followed by 25mW blue LED array stimulation at 60% power using a Schott GG420 longpass filter[4] at 125°C for 120 seconds. A 0.5 Gy test dose was administered and the procedure repeated. The other disc from each sample was preheated at 260°C for 30 seconds before being stimulated with blue LEDs at an elevated temperature of 125°C for 120 seconds and again a 0.5 Gy test dose was administered before the procedure was repeated. The variable stimulation methods allow a comparison to be made between the residual levels of quartz and feldspar grains and it may provide some indication as to the rate of bleaching of quartz and feldspar minerals in Orcadian light. In addition, the response of the adhesive packing tape samples to the 0.5 Gy test dose will allow the sensitivity of these samples to be compared with the sensitivity of the modern beach bulk samples.

3.9.2 Bleaching experiments

Although it was hoped that the residual levels of the modern beach sands would be low, indicating well bleached deposits, it was felt important to establish the bleaching rate of traps associated with IR, blue OSL and TL stimulation. Successful luminescence dating of sediment depends on the grains being well bleached by natural light during transportation

---

[4] The Schott GG420 is a longpass filter with 50% transmission at 420 nm, 90-99% transmission between 430-700 nm and >99% transmission in the near IR. When used in combination with Nichea blue LED stimulation the filter blocks stimulation below 400-420 nm from entering the sample chamber. A PMT filtered with a UG11 bandpass filter (main transmission band 280-380 nm) can detect luminescence in near UV emission bands without experiencing elevated background from the stimulation source.

and deposition, before being buried by other sediment. The amount of natural light reaching the Earth's surface varies depending on the thickness and extent of cloud cover (Barry and Chorley 1971, Critchfield 1983, O'Hare and Sweeney 1986). Between 27%-80% of the incoming radiation is reflected back to space by clouds (Barry and Chorley 1971), and therefore the amount and thickness of the cloud cover will have a direct impact on the bleaching rate of the various traps associated with IR, blue OSL and TL stimulation. For quartz to be rapidly bleached it needs to be exposed to UV and visible wavelengths (Godfrey-Smith *et al.* 1988) however the natural light intensity will vary and mineralogical variations will also affect the rate of bleaching. Feldspars are bleached by exposure to both long and short wavelengths and therefore any latent luminescence signal should be removed even in cloudy conditions. There has been little systematic work to determine the rate of bleaching of quartz and feldspar and it is not known whether exposure to visible wavelengths alone will quickly deplete the OSL signal of quartz. Bleaching experiments were undertaken to identify how quickly grains are bleached in controlled and natural conditions by exposing irradiated samples to light for different periods of time. Using this data it may also be possible to identify poorly bleached samples by comparing the shape of the shine down curves of the bleaching experiments and the archaeological samples described above.

3.9.2.1 Laboratory bleaching experiment 1 - Multiple stimulation of F1 feldspar

To test the bleaching rate of the traps associated with IR, blue OSL and TL stimulation, twelve discs of F1 feldspar were each given a 5 Gy dose and bleached in the light box at SUERC described in Section 3.9.1. The F1 feldspar used in the luminescence laboratory at SUERC is from the International Atomic Energy Agency (IAEA) and was obtained by D. Sanderson in 1986. F1 is an analytical standard made from ground Canadian Pegmatites and homogenised in a large volume. It was chosen for this study because it is very sensitive to artificial irradiation and its spectral properties are well known due to previous studies at SUERC (Clark and Sanderson 1994; Sanderson and Clark 1994). The discs were bleached over periods of 0, 10, 19 and 37 seconds, 1¼, 2½, 5, 10, 20 and 40 minutes, 1 hour 20 minutes and 2 hours 40 minutes.

After bleaching, each disc underwent multiple stimulation using an automated Riso TL/OSL (TL-DA-15) system. Each disc was preheated at 220°C for 20 seconds before being stimulated by IR for 60 seconds at an elevated temperature of 50°C. This was

followed by blue stimulation for 60 seconds at 125°C, and finally the TL of each disc was measured from 0-500°C with a heating rate of 5°C/second. The discs were then given another 5 Gy dose and the multiple stimulation run repeated, to allow the initial measurements on the discs to be normalised.

The experiment was repeated using a Schott GG495 longpass filter[5] placed on top of the discs during the bleaching process in the light box. This filter blocks wavelengths below 495 nm in the blue and violet region of the visible spectrum allowing only those wavelengths above 495 nm through to the grains on the discs. By blocking the shorter wavelengths in this way cloudy conditions are simulated under controlled laboratory conditions.

3.9.2.2 Laboratory bleaching experiment 2 – Quartz

The bleaching experiment described above for F1 feldspar was repeated in the laboratory using quartz from 4 modern beaches and two archaeological samples (SUTL 605 and 623). Comparing the bleaching rate of quartz with that of the F1 feldspar will provide information on the rate of bleaching of the two minerals and determine if quartz does indeed bleach faster than feldspar in controlled laboratory conditions. All of the quartz aliquots were given a dose of 15 Gy using the Sr/Y-90 beta source in the automated TL/OSL Riso (TL-DA-15) reader and then left overnight before bleaching in a light box using four 40W artificial daylight lamps. Discs were bleached for 0, 10, 19, and 37 seconds, 1, 1¼, 2½, 5, 10, 20 and 40 minutes and 1 hour 20 minutes, 2 hours 40 minutes, 5 hours 20 minutes and 10 hrs 40 minutes.

After bleaching each disc was preheated at 260°C for 30 seconds followed by blue stimulation at 125°C for 120 seconds. A test dose of 15 Gy was administered to each disc and the preheat and measurement repeated.

The laboratory bleaching experiments described above were then repeated using a Schott GG495 long pass filter placed on top of the discs to simulate cloudy conditions in the light box.

---

[5] The Schott GG495 is a longpass filter with 90% transmission at wavelengths >540 nm and 50% cut-off at 495 nm. This modifies the daylight source to exclude the blue and near UV components which are present in direct sunlight. The resulting illumination spectrum may be considered as a first approximation of the effects of overcast daylight or the natural spectrum under turbid water.

3.9.2.3 Field experiment

In order to determine how natural light conditions affected the rate of bleaching of quartz and feldspar grains an experiment was undertaken in Orkney, in June 2001, to determine the time required to bleach artificially irradiated sand samples to an acceptable residual level. Four bulk samples, collected previously from modern beaches on the Outer Hebrides, Orkney and Shetland[6], were placed in a light box in the laboratory at SUERC for several weeks to ensure that they were fully bleached. Although they were not tested for zero OSL, the sands were mixed several times a day and this ensured that all grains were exposed to light for what is thought to have been a sufficient length of time. The samples were chosen based on their good sensitivity to artificial irradiation and their different lithology. These bulk samples were then irradiated for a total of 15 minutes using the 'Hotspot' irradiator which has a Cobalt-60 source and a working dose rate of 1.08 Gy min^{-1} at the Veterinary School, University of Glasgow. The samples were exposed 5 times for three-minute exposures and between each exposure the samples were shaken to ensure uniform irradiation. Once irradiated they were placed in dark containers and thick black bags to make certain that there was no exposure to light, in readiness for the field experiment in Orkney.

In Orkney, each sample was split into nine parts, of approximately 25 grams, and each part was bleached by exposure to daylight for different time intervals. One part from each sample was retained unbleached and should have retained the 16 Gy dose, whilst the others were bleached over periods of 1, 5, 15 and 30 minutes, 1, 12 and 24 hours and 4 days of summer light conditions in Sanday. Throughout the experiment the weather varied with occasional clear skies, however for the majority of the experiment the sky was overcast with some rain. Two glass Petri dishes were used per sample for each bleaching time and the dishes were placed in rectangular Perspex containers which were half filled with local sand to stabilise them (Figure 3.27). The local sand underneath and around the dishes also allowed light to be absorbed or reflected by the sand grains as if in a natural beach environment. The Perspex containers were covered with cling film to prevent contamination of the samples and carried in thick black bags to and from the bleaching site, an exposed area of grassed sand on Sanday. After the allotted bleaching period the samples were transferred to small plastic blacked-out tubes and carefully labelled.

[6] Two samples were used from Shetland due to their high sensitivity and their different bedrock geology.

Figure 3.27 – Field bleaching experiment. Two glass petri dishes per sample in a perspex container filled with sand and covered with cling-film to prevent contamination of the samples.

In the laboratory, the samples were wet sieved to obtain the 125-250 μm fraction and washed in 10% HCl for 30 minutes to remove calcite, 15% HF for 15 minutes to slightly etch the grains and a further 30 minutes of HCl to dissolve any fluorides that might have formed. Between each acid treatment the samples were washed three times in de-ionised water, and the HF was neutralised using 10% ammonia.

Two discs per sample were dispensed, the polymineral nature of the prepared samples providing the opportunity to run an IRSL/post IR blue stimulation protocol first discussed by Clark and Sanderson (1994) and further developed by Banerjee *et al.* (2001). Using this combination of IRSL followed by (post IR) blue stimulation, two individual signals and estimated doses can be obtained from a single aliquot. The initial IR exposure stimulates and zeros the IRSL signal from the feldspars, and the subsequent blue exposure stimulates and zeros the signal from quartz and feldspar grains (Roberts and Wintle 2001). Both Banerjee *et al.* (2001) and Roberts and Wintle (2001) observed that the IRSL D_e were higher than the post IR blue stimulation D_e for the majority of their samples, however the post IR blue results tended to be more consistent.

An automated Riso TL/OSL system (TL-DA-15) was used for all measurements. Each disc in the IRSL/post IR blue run was given a preheat at 150°C for 10 seconds, followed by IR stimulation at 50°C for 120 seconds and then blue OSL stimulation at 125°C for 120 seconds. The discs were then irradiated for four seconds to produce a test dose of about 0.5 Gy and the preheat, IRSL and blue OSL stimulation procedure repeated.

The samples had enough prepared polymineral sediment to allow the remainder to be etched for 40 minutes using 40% HF producing pure quartz samples. A blue stimulation run was adopted to allow a comparison between the polymineral and quartz results. Two discs per sample were dispensed and each disc was preheated to 260°C for 30 seconds before being stimulated using blue diodes for 120 seconds at 125°C. Again, a 0.5 Gy test dose was given to each disc and the procedure repeated.

3.10 Analysis of archaeological samples

3.10.1 The SAR procedure

The SAR procedure used (Figure 3.28) is a modified version of that proposed by Murray and Wintle (2000) and discussed in Section 2.4.6.2.3, Chapter 2. Natural aliquots are preheated to 240-280°C and held at these temperatures for 30 seconds. Subsequently they are stimulated with blue light for 100 seconds at 125°C to measure the natural OSL (L_0). A test dose of 0.5 Gy is then applied to each aliquot and again preheated to 240-280°C for 30 seconds and measured to give T_0. Next, a regeneration dose of 1 Gy is applied followed by the preheat and measurement of the regenerated OSL (L_1). The test dose is repeated, preheated and measured to give T_1. The sequence is repeated using regenerative doses of 2-6 Gy (L_2-L_6) and test doses (T_2-T_6) are completed between each regenerative dose. At the end of the sequence, a further regenerative dose of 1 Gy and associated test dose are used to check that the test dose normalisation successfully corrects for any sensitivity changes that may have occurred during the run. In the following sections the features of the SAR protocol used in this study will be briefly summarised.

3.10.1.1 Preheating

The present study used four preheat temperatures for each sample. For most samples, 16 discs were dispensed per sample and divided into 4 portions, with each portion being preheated at 250°C, 260°C, 270°C or 280°C for 30 seconds. Samples with only 4 discs were preheated at 260°C and those with 8 or 12 discs at 250/260°C and 250/260/270°C respectively. Although recent work suggests slightly lower and shorter preheats (e.g. 240°C for 10 seconds (Murray and Clemmensen 2001), 200°C for 10 seconds (Bluszcz 2001)), the preheats used here follow those suggested by Murray and Wintle (2000). It is acknowledged that ideas on preheat temperature have changed over the past few years, however it was decided to continue using these preheat temperatures to ensure continuity between samples. Preheat temperature dependence plots have been constructed for each sample and the results of these tests are discussed in Chapter 5.

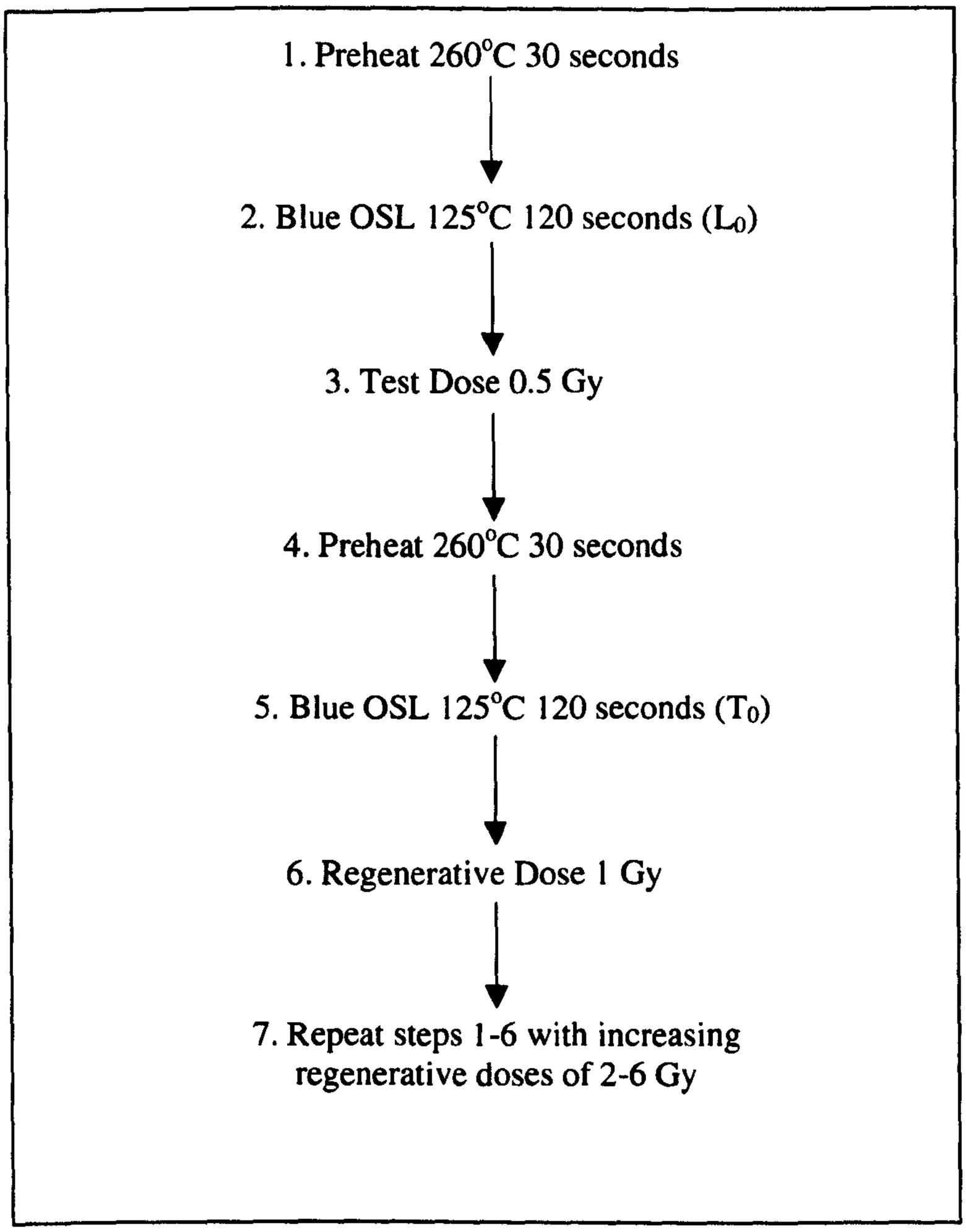

Figure 3.28 – The SAR procedure

3.10.1.2 OSL Measurement - Equipment and OSL stimulation

Unless previously stated, all luminescence measurements were undertaken on an automated TL/OSL Riso (TL-DA-15) system. The system was developed at the Riso National Laboratory in Denmark and uses blue LEDs with a wavelength of 470 nm and a 1W infrared laser diode emitting at 830 nm for stimulation, and a Sr/Y-90 beta source for irradiation (Bøtter-Jensen *et al.* 2000). A green longpass Schott GG420 filter is placed in front of each blue LED cluster to minimise scattered blue light reaching the photomultiplier and a Schott RG-715 longpass filter[7] is used in front of the IR laser to reduce the background counts of the photomultiplier (Bøtter-Jensen *et al.* 2000). More details regarding the Riso system are discussed by Bøtter-Jensen *et al.* (1999a, b, 2000).

Background counts of 10 seconds were recorded before and after the blue LEDs were switched on, and each aliquot was optically stimulated for 100 seconds during the regenerative and test dose measurements. The relatively long stimulation time was felt necessary to empty traps associated with the slow component of the OSL signal. Smith and Rhodes (1994) recognised three components which they called 'fast', 'medium' and 'slow', within the quartz OSL signal relating to the decay rate of the components during optical stimulation. The slowly decaying component is enhanced by optical stimulation at longer wavelengths (Smith and Rhodes 1994), however Bailey *et al.* (1997) demonstrated that it is also activated during the preheat procedure. The majority of the OSL signal comes from the fast and medium components (Bailey *et al.* 1997), however there may be some contribution from the slow component which may contaminate the subsequent regenerative or test dose signal. Therefore the aim of a long exposure time is to ensure that the medium component is fully bleached and to try and bleach the slow component.

During optical stimulation the samples were held at a temperature of 125°C to prevent re-trapping in the unstable 110°C TL trap which would contribute to the OSL signal if not removed (Murray and Wintle 1998). Stimulation at 125°C also increases the decay rate of the luminescence and Murray and Wintle (1998) suggest that as a result most of the OSL signal is released within the first 10 seconds of optical stimulation allowing shorter integration times.

---

[7]The Schott RG-715 filter has 90% transmittance at wavelengths >750 nm. When used in combination with IR stimulation using LEDs this filter removes the low intensity visible tail of the LED emission at 700-800 nm and eliminates cross-talk with a PMT filtered with BG39 filters (main emission band 340-610 nm).

3.10.1.3 Regenerative Doses

The SAR protocol proposed by Murray and Roberts (1998) using three samples of laboratory bleached Australian sedimentary quartz suggested that regenerative doses should be similar to the natural dose to avoid non-linearity in the dose-response curve. Further work by Murray and Mejdahl (1999) on 16 samples of heated quartz from 11 archaeological sites determined that because the sensitivity monitored by the test doses was proportional to the preceding natural or regenerated dose, sensitivity changes could be corrected for by dividing the natural/regenerative dose with the response from the subsequent test dose. The protocol was developed further by Murray and Wintle (2000) using six heated and six sedimentary samples and they suggested that because only one regenerative dose is needed to define the relationship between the test dose and the regenerative dose, multiple regenerative dose measurements would define a sensitivity corrected dose response curve.

To accurately determine the dose response curve, six regenerative doses of between 1 and 6 Gy were used for this research using the Sr/Y-90 source within the automated TL/OSL Riso (TL-DA-15) system for irradiation. The doses are relatively low, however the samples tested are thought to have been deposited during the Holocene and therefore large natural doses, and hence D_e, are not expected.

3.10.1.4 Test Dose

It was determined by Murray and Wintle (2000) that there was no significant variation in D_e with size of test dose and therefore because the D_e for the sites sampled here are not expected to be large, a test dose of 0.5 Gy was used throughout. Murray and Roberts (1998) suggested that the test dose should be preheated to 160°C allowing the 110°C TL peak to be measured. Further research by Murray and Wintle (2000) tested whether the D_e was dependent on the test dose preheat temperature and their results indicated that although there was a small increase in D_e above 220°C, the average was consistent over the range of test dose preheat temperatures studied. Recent research by Choi *et al.* (2003) on marine terrace sediments suggests that a cut-heat of 220°C should be used for the test dose to ensure that the thermally unstable component of the OSL signal is completely removed before measurement.

Although the current literature suggests that cut-heats of 160°C or 220°C should be used for the test dose it cannot be assumed that all samples will behave in a similar manner. For the research reported here, the test doses were treated in exactly the same manner as the regenerative doses with each aliquot preheated at 240-280°C for 30 seconds after each test dose was administered, and then stimulated at 125°C for 100 seconds. If the preheat temperatures used for the test doses thermally erode the main OSL trap then a decrease in D_e with increasing temperatures should be reflected in the preheat temperature dependent plots discussed in Chapter 5.

To test whether the test dose successfully corrects for sensitivity changes the first regeneration dose (1 Gy) was repeated at the end of each run. The ratio of the normalised last regeneration dose with that of the first dose indicates a successful correction for sensitivity changes (Murray and Wintle 2000). It is possible that some aliquots rejected on this basis are rejected because the quartz does not respond well to artificial irradiation preventing accurate measurement of the test dose. The 'Analyst' program, written by G. Duller (University of Aberystwyth) was used to analyse the data and this programme accepts aliquots that have low recycling ratios but large errors therefore discs with low sensitivity are not rejected unnecessarily. The results of the recycling ratio tests are discussed in Chapter 5.

3.10.1.5 Summary of SAR procedure

The SAR procedure used is based on that proposed by Murray and Wintle (2000), but due to the expected low D_e of the samples, it was felt necessary to include extra regenerative doses to accurately assess the D_e of the individual discs. All of the regenerated and test doses were preheated at 240-280°C for 30 seconds before 100 seconds of blue stimulation at 125°C. A 1 Gy regenerative dose was repeated at the end of the run to ensure that the test doses accurately corrected for sensitivity changes.

3.10.2 Contamination of quartz by IR sensitive minerals

Although the sample preparation involves density separation and etching, it is possible that feldspar and/or zircon grains may still be within the quartz fraction either as micro-inclusions or due to inadequate etching (Short and Huntley 1992; Jain and Singhvi 2001). These minerals have a higher sensitivity to radiation than quartz and zircon also has high

internal radioactivity, therefore it is important to check whether the prepared quartz contains any significant quantities of these IR sensitive minerals because both green/blue and infrared wavelengths stimulate the trapped electrons within these minerals, (Krbetschek *et al.* 1997). Contamination by these minerals might have a significant impact on the D_e due to their higher internal radioactivity and their potential higher residual signals if they bleach more slowly than quartz. Both could contribute to the natural OSL signal. To determine the amount of IR sensitive minerals on the prepared quartz discs an IRSL test was undertaken on all discs at the end of each SAR run. This test is based on the presumption that quartz has little or no response to infrared stimulation (Smith *et al.* 1990; Short and Huntley 1992; Spooner 1994; Jain and Singhvi 2001).

Each 'quartz' disc was given a 1 Gy dose, preheated to 150°C for 10 seconds and then measured on the Riso using IR diodes at a temperature of 50°C and 60% power. A background count of 10 seconds was conducted before the IR diodes were turned on for a further 10 seconds, allowing the actual IR signal from the individual discs to be calculated by subtracting the background counts. The 1 Gy IR and blue OSL signals from the 'quartz' discs were then compared with the responses of two separated feldspar aliquots per sample to a 1 Gy dose stimulated by blue OSL or IR. The feldspar discs were prepared as in Sections 3.82 and 3.83 using the 2.51-2.58 g cm^{-3} fraction obtained from the heavy liquid separation. The feldspar aliquot stimulated by blue light was preheated at 260°C for 30 seconds, stimulated at 125°C for 100 seconds and the procedure repeated once a 1 Gy dose had been administered. The IR feldspar disc was preheated at 150°C for 10 seconds, stimulated by IR at 50°C for 100 seconds followed by a blue stimulation at 125°C for 100 seconds and again the procedure repeated after a 1 Gy dose.

The amount of blue OSL arising from the quartz fraction on the 'quartz' disc was calculated using:

$$\text{Blue quartz} = \text{BlueOSL(mixed)} - \left[\text{IR(mixed)} * \left(\frac{\text{blue(feldspar)}}{\text{IR(feldpsar)}} \right) \right]$$

and the results are discussed in Chapter 5, Section 5.2.4.4.

3.10.3 Laboratory beta counting and high resolution gamma spectrometry

The internal dosimetry of each sample was measured using Thick Source Beta Counting (TSBC) and high-resolution laboratory gamma spectrometry on 20 grams of bulk sediment that was laid aside before each sample was sieved. The TSBC was used in conjunction with the *in situ* gamma field dosimetry to determine the initial working dose rate of each sample. The high-resolution laboratory gamma spectrometry determined the internal gamma and beta dosimetry of each sample and provided that these were within error of the TSBC and field gamma spectrometry, an average of all measurements was used to obtain the working dose rate. However, many of the sand layers sampled are interleaved by peat, midden or palaeosols and these may have different levels of radioactivity (Aitken 1985) resulting in larger or smaller field gamma dose rates than those measured in the laboratory. Where this is the case, only the field gamma dose rate is used for the gamma contribution of the working dose rate, as this is a more realistic estimate of the dose rate experienced by the sample.

3.10.3.1 Beta Counting

A SURRC built Thick Source Beta Counter (TSBC) as described by Sanderson (1988) was used to measure the internal beta dose rate of each sample. Background counts of 6 x 300 seconds were measured at the start and end of each day followed by measurement of a standard for 6 x 100 seconds. Each sample was measured for 10 x 300 seconds and the averages of the background, standard and sample were used to calculate the beta dose rate and its uncertainties in an Microsoft Excel spreadsheet using:

$$D_s = \Psi * (C_s - B)$$

$$\text{where, } \Psi = \text{Mean Sensitivity} = \frac{D_{std}}{C_{std} - B}$$

B = Background

D_{std} = Dose rate of Standard

C_{std} = Count rate of Standard

C_s = Count rate of sample

The TSBC dose rate for each sample is shown in Tables 5.4, 5.6, 5.8, 5.10, 5.12, 5.14 and 5.16.

3.10.3.2 High resolution laboratory gamma spectrometry

After the samples were measured on the Thick Source Beta Counter, they were sealed in petri dishes using Araldite adhesive and left for 3 weeks to allow the build up of radon resulting from the radioactive decay of Uranium and Thorium. If radon gas is allowed to escape, this can result in an underestimate of the dose rate (Aitken 1985) and therefore sealing the cylinders prevents this from happening. Using an Ortec 'n' type Gamma Spectrometer with a 50% relative efficiency Germanium detector at SUERC, each sample was measured for 100,000 seconds. Background and Shap granite standard counts of between 25,000-200,000 seconds were measured after every 5-6 samples. Ideally a longer measurement time would be given for these small samples of 20 grams, however due to the large number of samples that had to be measured, the measurement time was kept to 100,000 seconds. The Shap granite used for the standard is from a block of granite from Shap Wells in Cumbria, 3 kg of which were homogenised by D. Sanderson in 1986. Working values of potassium, uranium and thorium were determined by high resolution gamma spectrometry relative to Canmet and NBL standards. Twenty grams of the standard was placed in a container identical to those used for the samples, sealed using Araldite and subsequently used for all standard measurements.

Once the sample was measured, the Ortec 919 ADCAM mulitchannel analyser and Maestro software were used to analyse the spectra. The decay chains of the uranium, thorium and potassium were initially analysed using the JEF-2.2 Decay Data from the O.E.C.D./NEA Data Bank to identify the line intensities of selected nuclides. Table 3.1 shows the radionuclides, their half lives and the energy (keV) of their principal gamma ray used in this analysis.

Uranium series	Half life	Energy (keV)
234-Thorium	24.1 days	62
226-Radium	1599 years	185.99
214-Lead	26.8 minutes	241.91
214-Bismuth	19.9 minutes	609.3
210-Lead	22 years	45

Thorium series	Half Life	Energy (keV)
228-Actinium	6.15 hours	338.7
224-Radium	3.62 days	240.99
212-Lead	10.64 hours	238.63
212-Bismuth	1.01 hours	727.2
208-Thallium	3.06 minutes	277.36

Potassium	Half Life	Energy (keV)
40-Potassium	1.28×10^9 years	1460.8

Table 3.1 – Radionuclides, their half lives and energy (keV) of the principal gamma ray used in this analysis

Once identified, the Maestro program was used to generate regions of interest and the relevant intensities of the radioactive parents and associated daughter products within these regions of interest were noted. These were then entered into a Microsoft Excel spreadsheet designed to calculate the working dose rate and age of each sample. Using the concentration (part per million, ppm) of uranium, thorium and potassium and the intensities of the various radionuclides, the internal beta and gamma dose rates for each sample were calculated. The beta dose rate was compared with that measured by TSBC and the mean of these was generally used in the working dose rate. The internal and *in situ* field gamma dose rates were also compared and if within error, an average of these was used in the working dose rate. The mean of the actual and saturated water content and its associated error was also taken into consideration in the final working dose rate, and the contribution from cosmic radiation was also included based on the values determined by Prescott and Stephan (1982). The beta and gamma dose rates used in the final working dose rate for each sample are shown in Tables 5.4, 5.6, 5.8, 5.10, 5.12, 5.14 and 5.16.

3.10.4 Stored dose calculation and age calculation

The individual D_e value for each disc was calculated using late light subtraction. The initial signal bleaches the most readily and therefore to prevent the inclusion of the slowly decaying signal which is likely to accumulate with each regenerative cycle it is appropriate to subtract a background that will include this slowly decaying signal (Murray and Wintle 2000). The first 10 seconds of blue stimulation (Figure 3.29) are used for the initial signal and although this is somewhat longer than that suggested by Banerjee *et al.* (2000) for dim samples (1-2 seconds) it was felt necessary to use this integral due to the low sensitivity of some samples. The background is the counts from the next 90 seconds of stimulation (21-110 seconds, Figure 3.29) divided by nine to provide a 10 second background average that is subtracted from the initial signal. The normalised errors on the natural and regenerative normalised doses of each sample were calculated using:

$$\frac{L_0}{T_0} \times \sqrt{\left(\left(\frac{L_{0err}}{L_0}\right)^2 + \left(\frac{T_{0err}}{T_0}\right)^2\right)}$$

where L_0 = Natural signal (or regenerative)

T_0 = Test Dose

L_{0err} = error on the natural signal defined by $\frac{1}{\sqrt{\text{natural}}}$

T_{0err} = error on the test dose signal defined by $\frac{1}{\sqrt{\text{testdose}}}$

and the dose response curves with associated normalised errors were plotted using Sigmaplot5. An exponential $\left(y = a\left(1 - e^{-bx}\right)\right)$ or linear fit $\left(y = b + ax\right)$ was plotted through each dose response curve and the 'a' and 'b' values noted (Figure 3.30). For some discs the regenerative data was so scattered that an exponential or linear line could not be plotted and therefore these discs were rejected from further analysis. For discs that did allow an exponential or linear line to be fitted, the 'a' and 'b' values and the normalised natural values were inserted into a Microsoft Excel spreadsheet to calculate the estimated dose of each disc.

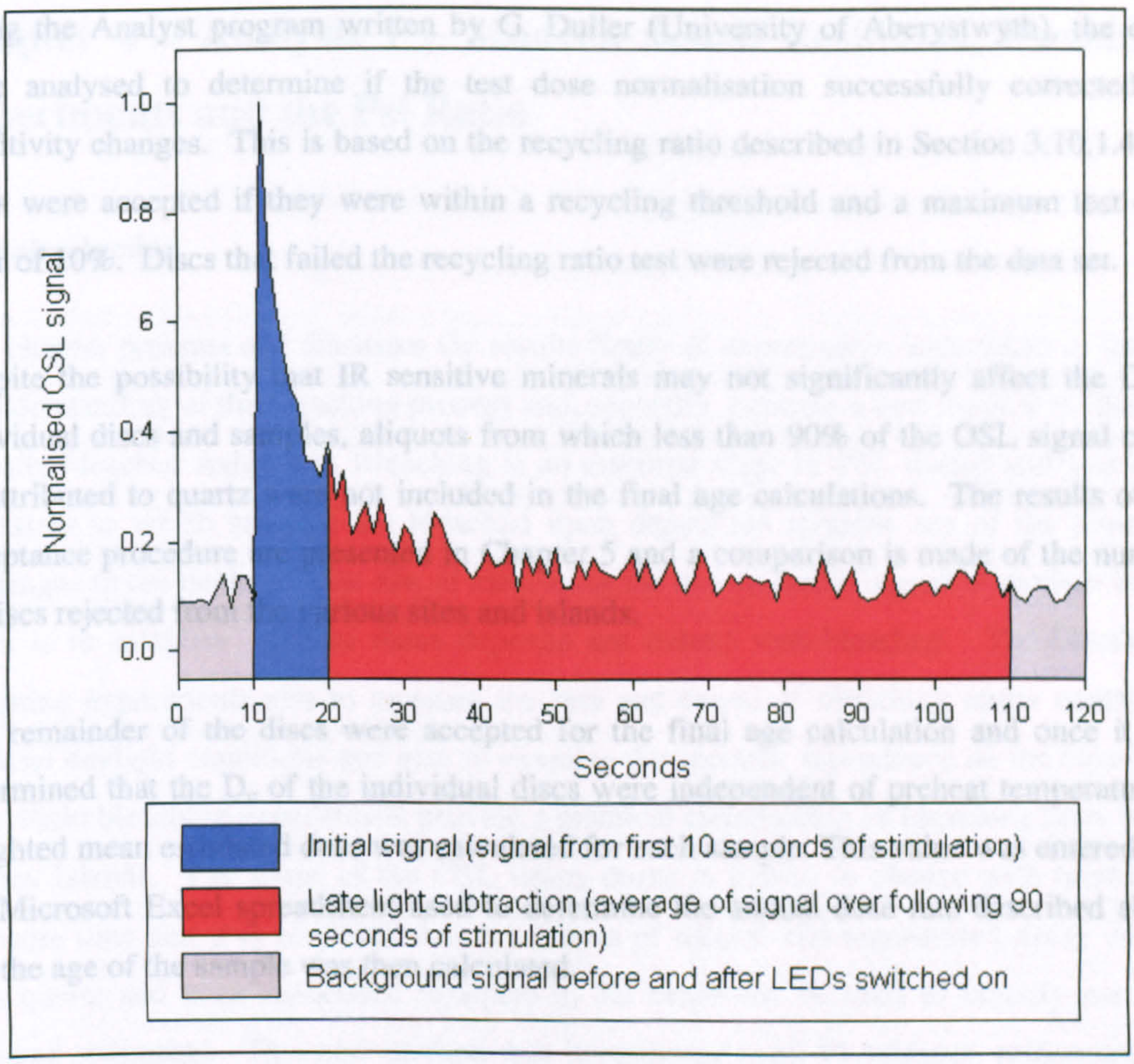

Figure 3.29 – Late light subtraction. The initial 10 seconds of stimulation is used as the main signal and the background subtracted is an average of the signal over the next 90 seconds of stimulation.

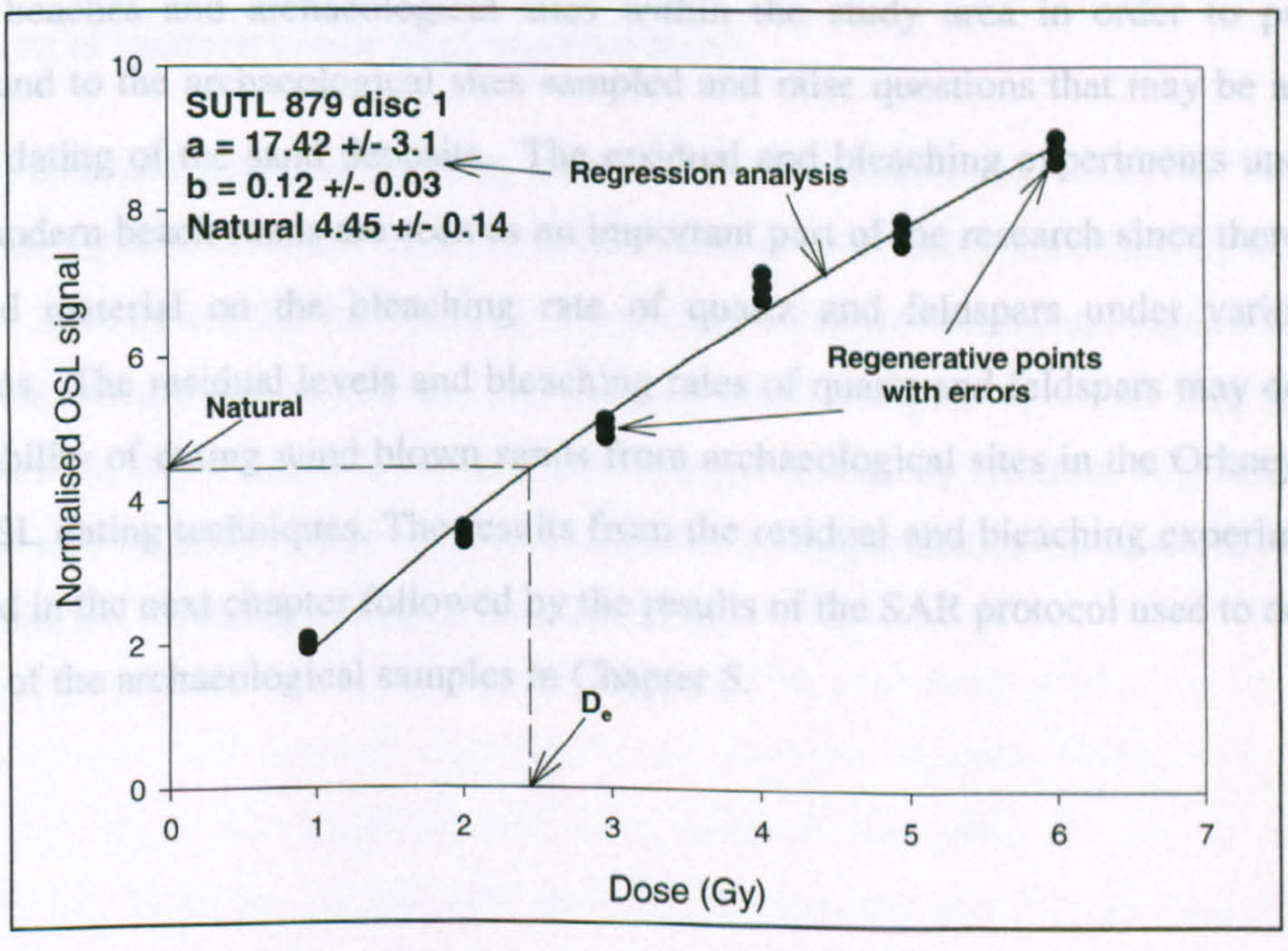

Figure 3.30 – Regenerative dose response curve with regression analysis

Using the Analyst program written by G. Duller (University of Aberystwyth), the discs were analysed to determine if the test dose normalisation successfully corrected for sensitivity changes. This is based on the recycling ratio described in Section 3.10.1.4 and discs were accepted if they were within a recycling threshold and a maximum test dose error of 10%. Discs that failed the recycling ratio test were rejected from the data set.

Despite the possibility that IR sensitive minerals may not significantly affect the D_e of individual discs and samples, aliquots from which less than 90% of the OSL signal could be attributed to quartz were not included in the final age calculations. The results of the acceptance procedure are presented in Chapter 5 and a comparison is made of the number of discs rejected from the various sites and islands.

The remainder of the discs were accepted for the final age calculation and once it was determined that the D_e of the individual discs were independent of preheat temperature, a weighted mean estimated dose was calculated for each sample. This value was entered into the Microsoft Excel spreadsheet used to determine the annual dose rate described above and the age of the sample was then calculated.

3.11 Summary of Chapter 3

This chapter has presented the methods used to collect and analyse samples from both modern beaches and archaeological sites within the study area in order to provide a background to the archaeological sites sampled and raise questions that may be answered by OSL dating of the sand deposits. The residual and bleaching experiments undertaken on the modern beach sands are seen as an important part of the research since there is little published material on the bleaching rate of quartz and feldspars under various light conditions. The residual levels and bleaching rates of quartz and feldspars may determine the suitability of dating wind blown sands from archaeological sites in the Orkney Islands using OSL dating techniques. The results from the residual and bleaching experiments are presented in the next chapter followed by the results of the SAR protocol used to determine the ages of the archaeological samples in Chapter 5.

Chapter 4 – Analysis 1 – Modern Beach Residuals, Bleaching Experiments and the Psi Ratio

4.1 Introduction

This chapter presents and discusses the results firstly of experiments undertaken to further an understanding of the bleaching process and, secondly, presents a new method to identify partially bleached sediments. Bleaching is an essential stage in OSL dating and assessing the extent to which samples are bleached upon deposition remains one of the principle challenges to the method. The aim of measuring the luminescence signal of modern beach sands is to establish whether these deposits are indeed well-bleached. The laboratory bleaching experiments aim to measure the rate and extent of bleaching under controlled artificial daylight conditions and also to examine the spectral dependence on the bleaching rate. Field bleaching experiments provide a practical examination of bleaching rates in the Orkney Islands. The shape of the OSL decay curve is known to change with increasing exposure time and it is proposed that the shapes of natural and regenerated decay curves from quartz and from associated feldspars in the sands can be used to identify partially bleached sediments. This new method was investigated with F1 feldspar, archaeological sands and modern beach sands used in the bleaching experiments and subsequently applied to the archaeological samples.

4.2 Results of modern beach sand residual levels

Grab samples and adhesive packing tape samples were collected from the surface of beaches throughout the study area using the methods previously described in Chapter 3, Section 3.21 to determine the residual levels of possible environmental source materials. The measurements undertaken on the modern beach samples have not only provided information on the residual levels but also sample sensitivity (Section 4.3) and ease of bleaching and both sets of results have allowed a comparison to be made between the samples and the various stimulation methods used.

4.2.1 Grab sample residual levels

All of the beach samples contain both quartz and feldspars and indicate sensitivity to the TL, blue OSL and IRSL techniques. Figure 4.1 shows the residual ratio I(natural) /I(5 Gy) plotted against the number of observations for the three techniques. TL results from the Outer Hebrides and Orkney show a high residual signal (i.e. from light-insensitive traps), implying residual doses of between 20 and 100 Gy, although the Outer Hebrides samples tend to have slightly lower values. Blue residuals are much lower (2-50 Gy) but there is a clear distinction between Orkney and the much lower residuals of the Outer Hebrides. The IRSL results show a small residual signal (0.2-0.7 Gy) for both sample sets, but the Orkney and Outer Hebrides samples remain distinct from each other.

4.2.2 Adhesive packing tape residual levels

The majority of the adhesive packing tape samples were sensitive to IR, post-IR blue and blue stimulation indicating that they contained both feldspar and quartz grains. Figure 4.2 shows the residual ratios I(natural) / I(0.5 Gy) for the three stimulation methods used. Some of the samples have low residual ratios (i.e. less than 0.05) for all three stimulation methods indicating that they are well-bleached, but the majority of samples have different residual levels for the three stimulation methods used.

The IRSL results indicate that most (90%) of the samples analysed have IR residual ratios less than about 0.05 Gy. The natural response of two samples (SUTL 560 and 576) was greater than the response to the subsequent 0.5 Gy dose (Table 4.1) indicating that these samples still contain a luminescence signal of approximately 0.7 and 0.9 Gy respectively.

Although 86% of the samples showed residual levels of less than 0.05 Gy for stimulation by post-IR blue OSL indicating that the samples are well-bleached, neither of the samples with high IR residuals (SUTL 560 and 675) had high post-IR blue residuals. This suggests that for these samples, identified in Figure 4.2, the grains stimulated by post-IR blue OSL (i.e. quartz) are better bleached than the IR stimulated grains (i.e. feldspar) of these samples. The opposite appears to be true for samples SUTL 569 and 914 (Figure 4.2) which have high post-IR blue residuals but relatively low IR residuals. However, the counts for the natural signal and the response to a 0.5 Gy dose for sample SUTL 569 are both below zero, resulting in a positive residual ratio close to 1 (Table 4.1).

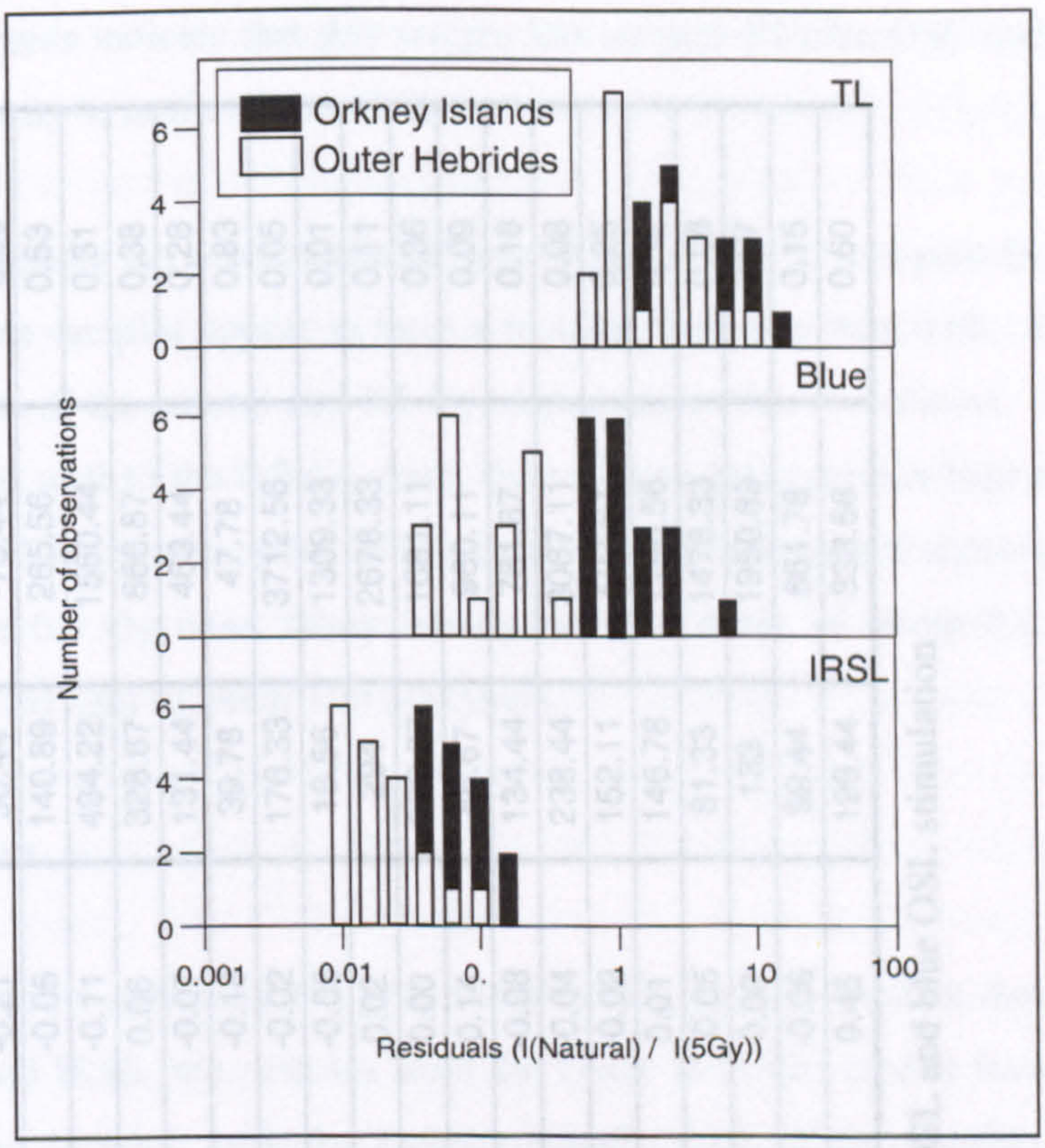

Figure 4.1 – Comparison of modern beach residuals from the Outer Hebrides and Orkney Islands using TL, blue OSL and IRSL (after Sommerville *et al.* 2001)

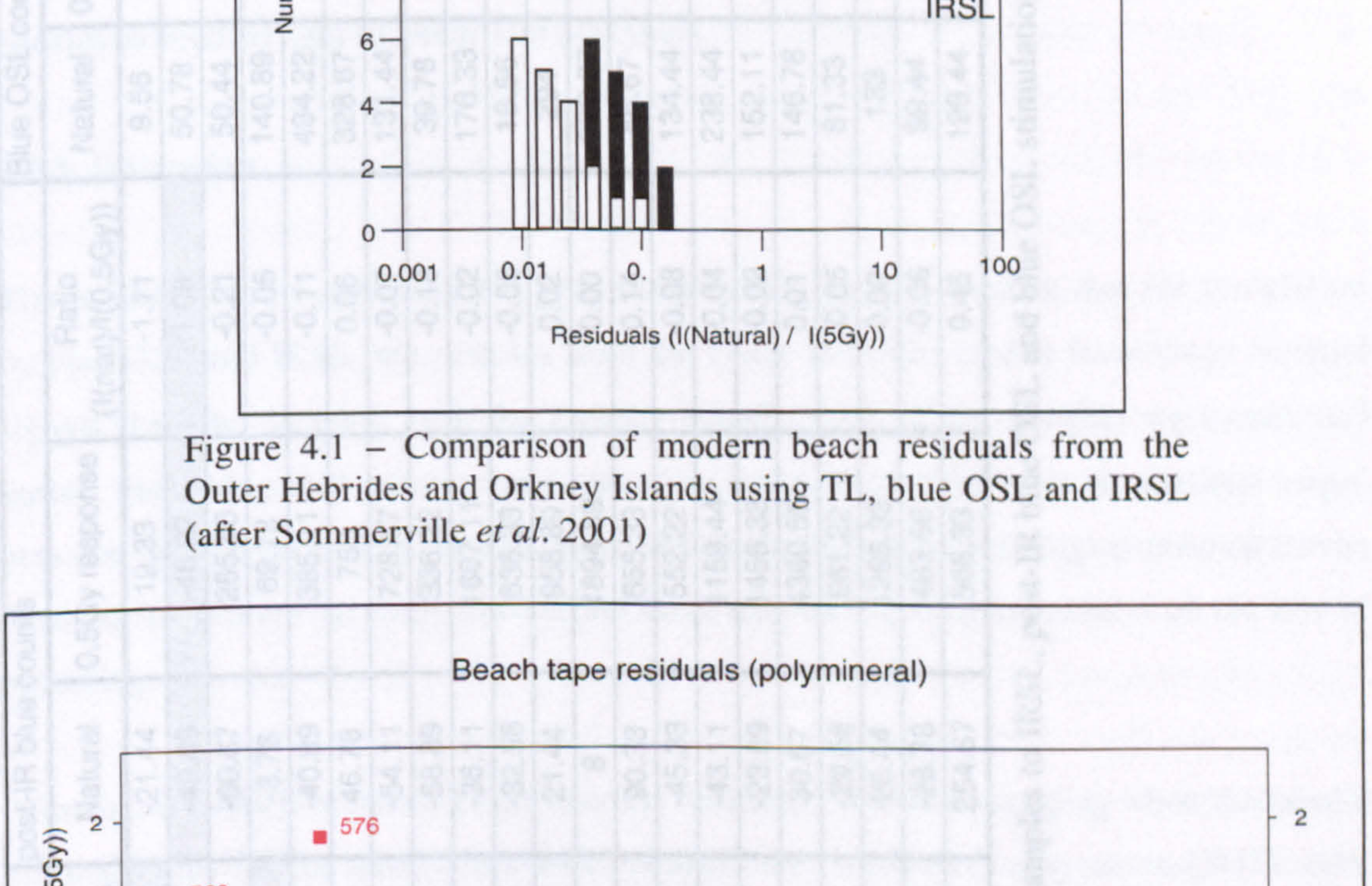

Figure 4.2 – Comparison of adhesive packing tape residuals from a selection of beaches in the Orkney Islands using IRSL, post-IR blue OSL and blue OSL.

	IRSL counts			post-IR blue counts			Blue OSL counts		
Sample	Natural	0.5Gy response	Ratio (I(nat)/I(0.5Gy))	Natural	0.5Gy response	Ratio (I(nat)/I(0.5Gy))	Natural	0.5Gy response	Ratio (I(nat)/I(0.5Gy))
560	105.78	75.22	1.41	-21.44	19.33	-1.11	9.56	48.67	0.20
569	-12.89	226.44	-0.06	-49.89	-46.22	1.08	50.78	-70.78	-0.72
570	22.22	1478.56	0.02	-60.67	285.56	-0.21	50.44	-73.44	-0.69
576	33.56	18.11	1.85	-3.78	69.78	-0.05	140.89	265.56	0.53
577	-2.22	361.56	-0.01	-40.89	385.11	-0.11	484.22	1560.44	0.31
579	105.78	3621.44	0.03	46.78	753	0.06	328.67	866.87	0.38
588	103.11	2274.56	0.05	-54.11	728.67	-0.07	131.44	463.44	0.28
630	21	363.89	0.06	-58.89	336.22	-0.18	39.78	47.78	0.83
634	84.33	3222.78	0.03	-36.11	1607.11	-0.02	176.33	3712.56	0.05
641	56.78	823.89	0.07	-32.56	636.33	-0.05	18.56	1309.33	0.01
904	57.11	2390.11	0.02	21.44	958.89	0.02	294	2678.33	0.11
905	124.44	4787.44	0.03	8	1894.89	0.00	609.67	1681.11	0.36
906	23	1000.56	0.02	90.33	655.33	0.14	86.67	980.11	0.09
907	33.33	698.33	0.05	-45.33	552.22	-0.08	134.44	761.67	0.18
908	25.89	3379.11	0.01	-43.11	1159.44	-0.04	238.44	3067.11	0.08
909	34.22	2133.33	0.02	-23.89	1456.33	-0.02	152.11	597.67	0.25
910	50.67	3104	0.02	30.67	4380.56	0.01	146.78	1190.56	0.12
911	-10.56	816.11	-0.01	-29.56	561.22	-0.05	81.33	1478.33	0.06
912	2.22	1802.22	0.00	26.44	1266.33	0.02	133	1950.89	0.07
913	22.22	725.67	0.03	-28.78	483.56	-0.06	99.44	661.78	0.15
914	18.44	365.33	0.05	254.67	566.33	0.45	199.44	333.56	0.60

Table 4.1 – Response of adhesive packing tape samples to IRSL, post-IR blue OSL and blue OSL stimulation

The negative counts indicate that this sample has no post-IR blue OSL residual signal and very low sensitivity to artificial irradiation.

The blue OSL results are more scattered than those of the IR and post-IR blue, and only about 45% of the samples appear to have a residual ratio less than 0.05. Table 4.1 shows the signal counts of the natural and 0.5 Gy responses to blue stimulation. Although many samples respond well to the 0.5 Gy dose, the residual ratios remain high due to the large natural signals. Despite this, none of these samples have a natural signal greater than the response of the 0.5 Gy dose, many having residual doses of about 0.1-0.3 Gy, which equates to residual ages of about 100-300 years.

4.2.3 Discussion

The residual level results from the grab samples (Figure 4.1) indicate that for stimulation by blue OSL and IRSL, the samples from the Outer Hebrides tend to have lower residual signals than the samples from the Orkney Islands. All of the samples were collected during the spring and summer and therefore, with little difference in daylight length between the two areas, it is surprising that the Orkney samples have higher residual levels. Reasons for this are currently unclear but there may be a geological control on the rate of bleaching.

Although the adhesive packing tape residual results are more encouraging when the sample residual ratios for the three stimulation methods are considered, only seven (SUTL 634, 641, 904, 906, 908, 911, 912) of the twenty-one samples analysed have residual levels less than about 0.05 Gy for all three methods (Figure 4.2). This indicates that both the quartz and feldspar grains from these samples are well-bleached. Many of the other samples have low residual levels when stimulated by IRSL and post-IR blue OSL, however 55% still have a significant blue OSL residual signal. The grab samples also showed higher residual levels when stimulated by blue OSL, but in all cases the associated packing tape samples had lower residuals indicating that surface samples are better bleached. The aliquots used in these experiments were polymineral and therefore higher residual levels may be expected because both the quartz and feldspar signals are measured when stimulated by blue OSL. As pointed out in previous chapters, quartz is thought to bleach faster than feldspar and therefore the large residual signal observed using blue OSL may be from the feldspar grains, but the IRSL results from the experiments indicate that the feldspar grains

have low residual levels. This suggests that quartz grains have higher residual signals, and implies that in this study area quartz bleaches at a slower rate than feldspar, possibly due to mineralogy or due to variable light conditions. Experiments were undertaken in the laboratory and field to examine the rate of bleaching in quartz and feldspars under variable light conditions and the results of these bleaching experiments are discussed in Section 4.4.

Although the amount of bleaching a sample has received prior to burial is important for all samples to ensure that the age is not overestimated, for young samples it is especially important. If the sample has not been properly bleached the latent signal still remaining in the sample prior to burial may contribute significantly to the natural signal. The palaeodoses of the archaeological samples analysed vary between about 0.1 and 7 Gy, but about half have a palaeodose less than 1 Gy and therefore if these samples are partially bleached (i.e. contain a latent residual signal prior to burial) the ages may be significantly overestimated.

Despite the modern beach sands having residual levels of less than 0.5 Gy when stimulated by blue OSL and less for IRSL, it must be questioned whether these levels should be taken into consideration when dating archaeological samples from this area. The packing tape results indicate that the surface is better bleached than grab samples taken from the top centimetre of sand. This is perhaps expected since the surface grains are more likely to be mobilised than deeper layers and additional bleaching will take place while the grains are lying on the surface of the beach prior to burial. However, not all grab samples from modern beaches in the study area have significant residual levels and this indicates that some samples may have been exposed for a sufficient length of time. For other samples, longer exposure periods may be necessary to ensure that they are fully bleached and this may be related to different mineralogy. The potential residual OSL signal within archaeological sand layers may, therefore, vary depending on the provenance of the sediment (influenced by the direction of the wind at the time of transportation and deposition). Identifying sediment provenance and hence the potential residual signal of samples in a study area whose coastline is dominated by long sandy beaches and backed by extensive dune systems is problematic. If residual levels of modern beach sands are considered when dating archaeological samples this could potentially over- or under-estimate the true OSL age of some samples. Despite this, the recognition of residual signals in modern beach sediments does flag the possibility that some archaeological samples may only have been partially bleached prior to burial. Rather than take the

residual levels into consideration, it may be more appropriate to identify partially bleached samples and deal with them accordingly. A potential new method to identify partially bleached sediments is presented and discussed in Section 4.5.

4.3 Sensitivity of modern beach sands

The residual ratios of the samples were calculated using a 5 Gy dose administered to the grab sample discs and a 0.5 Gy dose to the adhesive packing tape sample discs. The response to the administered doses allows the sensitivity of the samples to be analysed in order to determine the possibilities of dating young samples from these areas.

4.3.1 Sensitivity of grab samples

Figure 4.3 shows the sensitivity distribution in photons/Gy derived from the observed response to a 5 Gy dose. The results indicate that for each technique the Outer Hebrides samples are more sensitive than those from Orkney and this supports the suggestion made in Section 4.23 that the rate of bleaching and the response to radiation is largely controlled by the local bedrock geology. The highest sensitivities of the Outer Hebrides samples are similar for the three techniques, however the range of sensitivities increases, with TL having the narrowest range and IRSL the greatest. The Orkney samples have lower sensitivities, with similar sensitivity ranges to the Outer Hebrides. Although all of the samples show sufficient TL sensitivity to permit quantification of archaeological doses, the residuals remain a significant obstacle to accurate dating. The majority of OSL and IRSL sensitivities appear to be adequate for recording doses in the study area, but some of the samples lack sufficient sensitivity for high precision.

4.3.2 Sensitivity of adhesive packing tape samples

The grab samples described above have allowed the regional sensitivity of samples to be compared, but distinct sensitivity differences also occur within regions. The adhesive packing tape samples analysed are all from the Orkney Islands and after the natural signal was measured each sample was given a 0.5 Gy dose prior to further IRSL, post-IR blue OSL and blue OSL measurements.

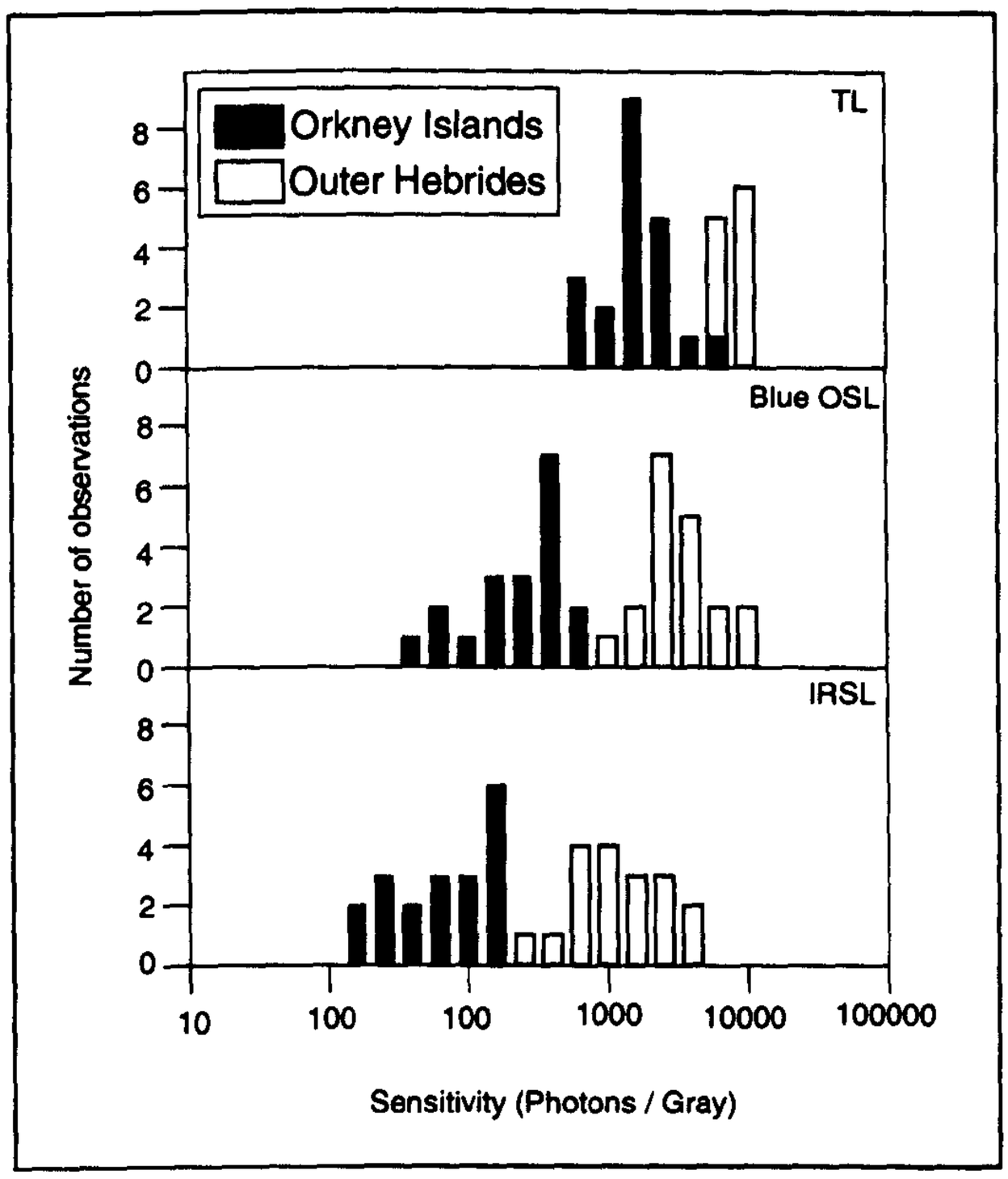

Figure 4.3 – Comparison of luminescence sensitivities from modern beaches in the Outer Hebrides and Orkney Islands using TL, blue OSL and IRSL (after Sommerville *et al.* 2001). When the discs are plotted individually the results are similar.

Although the majority of the samples show a relatively good response to the 0.5 Gy dose for all three methods of stimulation, several samples (SUTL 560, 569, 576 and 630, Figure 4.4) show little or no response and therefore dating these sands is problematic. The samples from Sanday show the lowest sensitivity to artificial irradiation (Figure 4.4).

Sample SUTL 569 shows no response to post-IR blue OSL and blue OSL and SUTL 570 has no response to blue OSL stimulation. Despite this, samples SUTL 577 and 579 from Sanday are highly sensitive to the irradiation with SUTL 577 showing a particularly good response to blue OSL. Elsewhere the range in sensitivity within individual islands and between the individual stimulation methods is apparent. The variable response to IR, post-IR blue and blue stimulation is clearly shown by the samples from Eday (Figure 4.4), which represent all the beaches on the island.

4.3.3 Discussion

The results from the grab samples indicate that although the quartz and feldspar within these samples are sensitive to artificial irradiation, the degree of sensitivity varies not only between the Outer Hebrides and the Orkney Islands (possibly due to geological variations) but also within each area. This is confirmed by the results from the adhesive packing tape samples that were all collected from beaches in the Orkney Islands. The sensitivity of these samples varies depending on the stimulation method being used which indicates that the quartz and feldspar from the various sites behave differently when artificially irradiated. This is expected due to the different luminescence properties of the minerals, but it is surprising how the sensitivity of the quartz and feldspar grains varies between beaches on each individual island (Figure 4.4). This is unlikely to be wholly due to local geological variations, since the bedrock of the Orkney Islands is dominated by Middle Old Red Sandstone. It suggests that the sand collected from the modern beaches has a variety of sources in addition to local bedrock, possibly some of which now lie offshore in the form of glacigenic deposits. This is discussed further in Chapter 5 with regard to potentially identifying the sediment provenance of the Tofts Ness samples by comparing the sensitivity of the archaeological samples with that of the modern beach samples.

The development of an automatic reader in the late 1990s using blue LEDs to measure the luminescence signal of quartz, indicates that the luminescence properties of quartz are

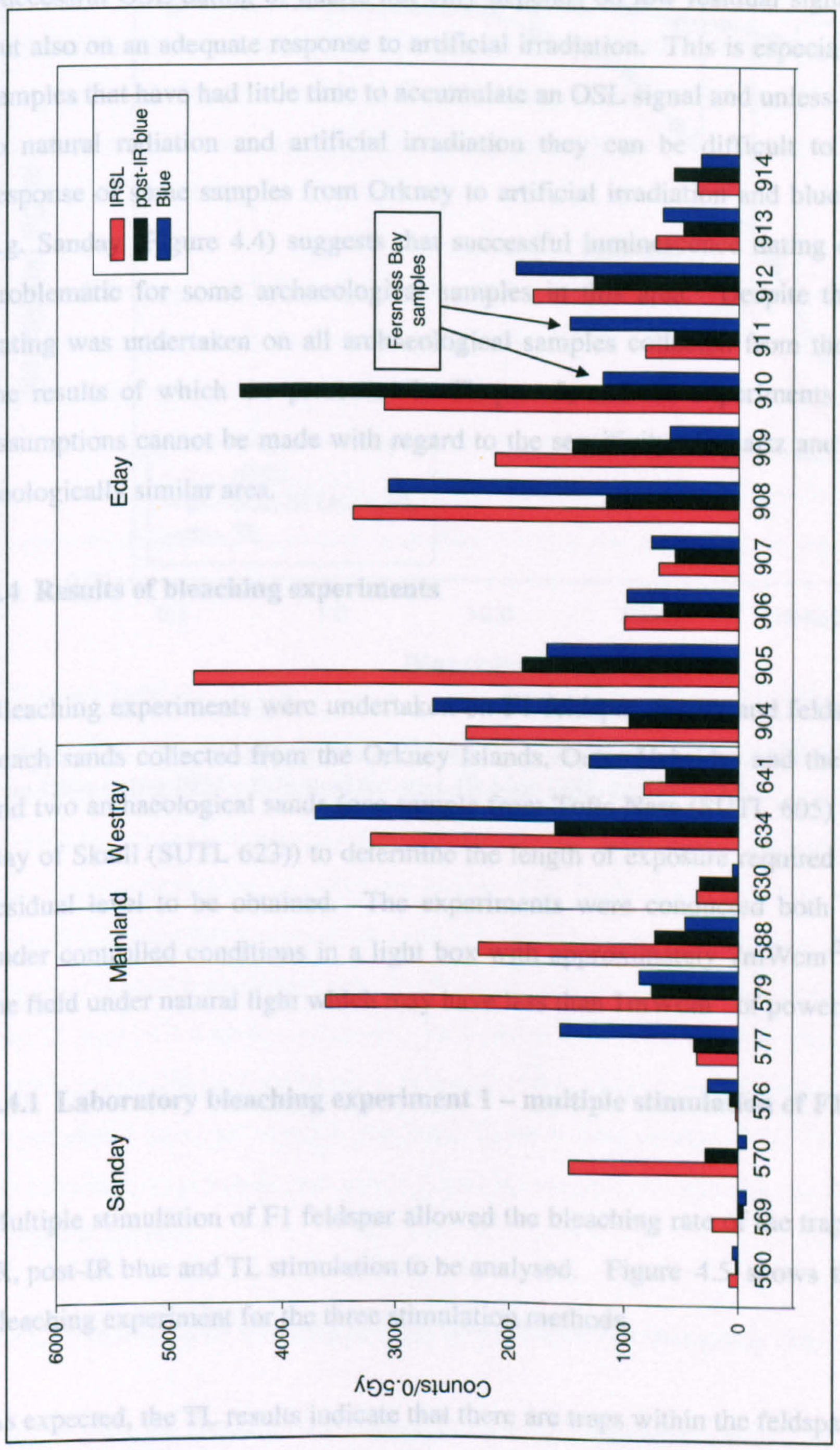

Figure 4.4 – Comparison of luminescence sensitivities from adhesive packing tape samples from the Orkney Islands using IRSL, post-IR blue OSL and blue OSL

currently thought to be more useful than feldspars for OSL dating of unheated sediments. Successful OSL dating of quartz not only depends on low residual signals prior to burial but also on an adequate response to artificial irradiation. This is especially true for young samples that have had little time to accumulate an OSL signal and unless they respond well to natural radiation and artificial irradiation they can be difficult to date. The poor response of some samples from Orkney to artificial irradiation and blue LED stimulation e.g. Sanday (Figure 4.4) suggests that successful luminescence dating of quartz may be problematic for some archaeological samples in this area. Despite these results, OSL dating was undertaken on all archaeological samples collected from the Orkney Islands, the results of which are presented in Chapter 5, and the experiments have shown that assumptions cannot be made with regard to the sensitivity of quartz and feldspar within a geologically similar area.

4.4 Results of bleaching experiments

Bleaching experiments were undertaken on F1 feldspar, quartz and feldspar from modern beach sands collected from the Orkney Islands, Outer Hebrides and the Shetland Islands and two archaeological sands (one sample from Tofts Ness (SUTL 605) and another from Bay of Skaill (SUTL 623)) to determine the length of exposure required for an acceptable residual level to be obtained. The experiments were conducted both in the laboratory under controlled conditions in a light box with approximately 7mWcm^{-2} of power and in the field under natural light which may have less than 1mWcm^{-2} of power.

4.4.1 Laboratory bleaching experiment 1 – multiple stimulation of F1 feldspar

Multiple stimulation of F1 feldspar allowed the bleaching rate of the traps associated with IR, post-IR blue and TL stimulation to be analysed. Figure 4.5 shows the results of the bleaching experiment for the three stimulation methods.

As expected, the TL results indicate that there are traps within the feldspar crystal structure which are not readily emptied by exposure to light. There is little change in the signal until the sample has been exposed to light for approximately 2.5 minutes and after 2 hours 40 minutes exposure, approximately 40% of the TL signal remains.

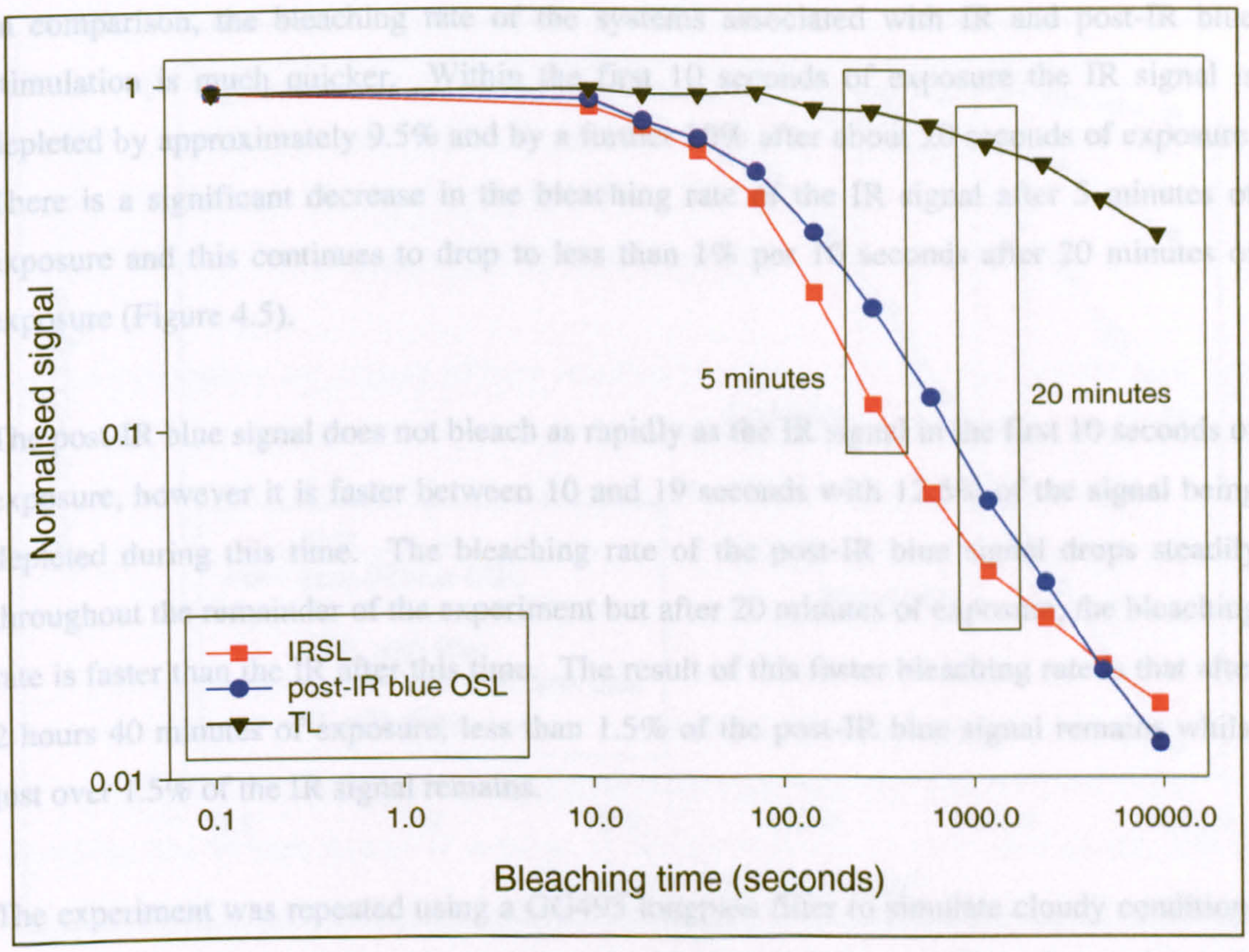

Figure 4.5 – The bleaching rate of F1 feldspar after exposure to artificial daylight with no filter using IRSL, followed by post-IR blue OSL and then TL.

In comparison, the bleaching rate of the systems associated with IR and post-IR blue stimulation is much quicker. Within the first 10 seconds of exposure the IR signal is depleted by approximately 9.5% and by a further 10% after about 20 seconds of exposure. There is a significant decrease in the bleaching rate of the IR signal after 5 minutes of exposure and this continues to drop to less than 1% per 10 seconds after 20 minutes of exposure (Figure 4.5).

The post-IR blue signal does not bleach as rapidly as the IR signal in the first 10 seconds of exposure, however it is faster between 10 and 19 seconds with 12.5% of the signal being depleted during this time. The bleaching rate of the post-IR blue signal drops steadily throughout the remainder of the experiment but after 20 minutes of exposure, the bleaching rate is faster than the IR after this time. The result of this faster bleaching rate is that after 2 hours 40 minutes of exposure, less than 1.5% of the post-IR blue signal remains whilst just over 1.5% of the IR signal remains.

The experiment was repeated using a GG495 longpass filter to simulate cloudy conditions in the laboratory and the results are shown with those of the non-filtered experiment in Figure 4.6. The bleaching rates of the traps associated with IR, post-IR blue and TL stimulation are greatly reduced due to the presence of the filter which prevents shorter blue and violet wavelengths reaching the grains. The initial bleaching rate of the IR signal is about 3.5% and after 5 minutes of exposure the bleaching rate is below 1% per 10 seconds. Despite the slower bleaching rate, the IR signal is reduced to approximately 5% of its value after 2 hours 40 minutes exposure. In contrast the initial post-IR blue bleaching rate is slightly above 1% and continues to decrease throughout the experiment leaving 11% of the signal after 2 hours 40 minutes exposure. There is little change in the TL signal throughout the bleaching experiment and after 2 hours 40 minutes of exposure, approximately 80% of the signal remains.

4.4.1.1 Summary of F1 feldspar multiple stimulation bleaching experiment

The F1 feldspar multiple stimulation bleaching experiment clearly shows how the traps associated with the various stimulation methods are bleached in artificial daylight. The TL measurements were undertaken after the IR and post-IR blue measurements and therefore it may be expected that the majority of light sensitive traps were emptied during the previous stimulation measurements. There is, however, some bleaching of the TL signal

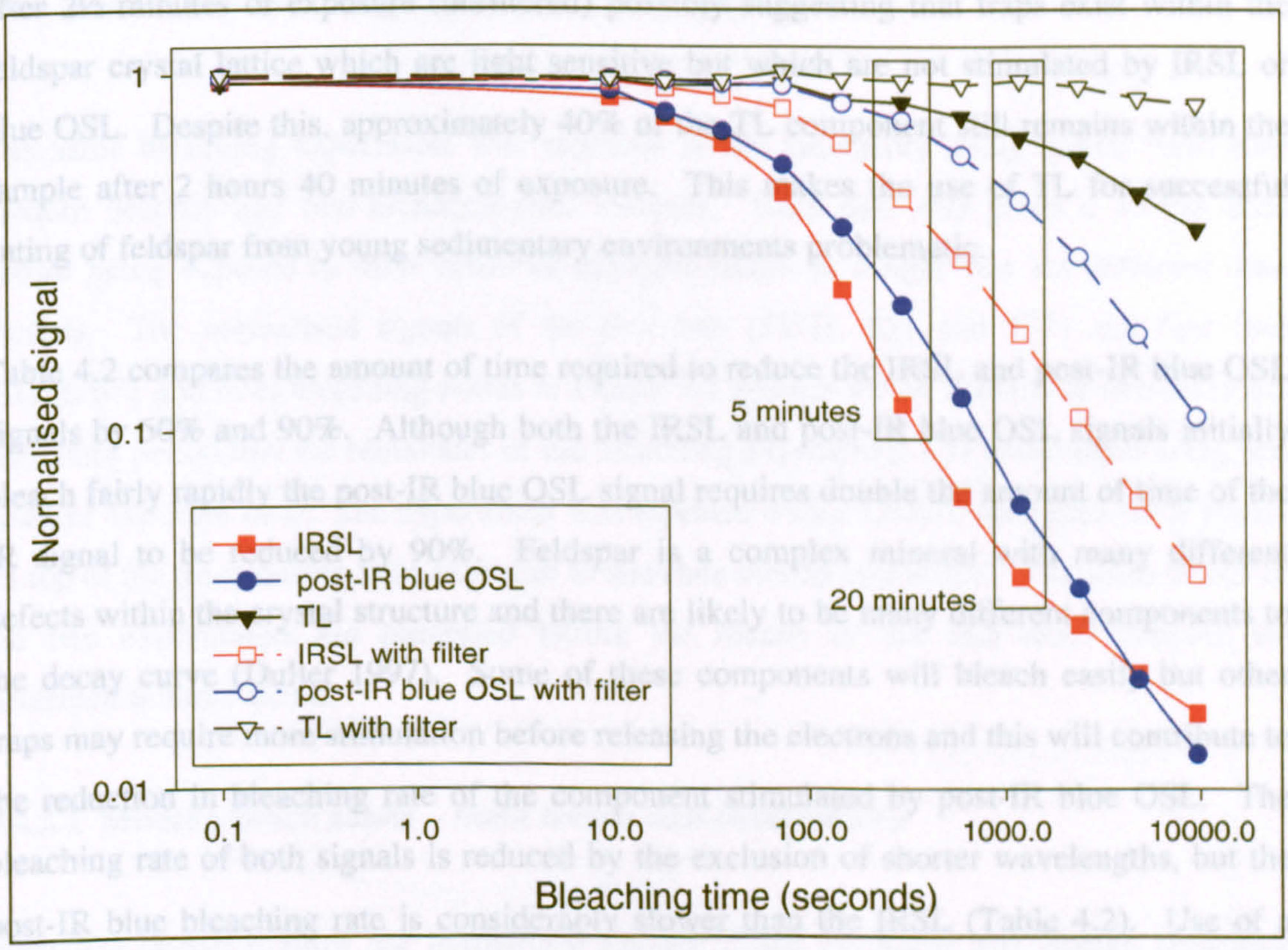

Figure 4.6 – The bleaching rate of F1 feldspar after exposure to artificial light without and with a Schott GG495 longpass filter (90% transmission at wavelengths > 540nm and 50% cut off at 495 nm) using IRSL, followed by post-IR blue OSL and then TL.

after 2½ minutes of exposure (unfiltered) possibly suggesting that traps exist within the feldspar crystal lattice which are light sensitive but which are not stimulated by IRSL or blue OSL. Despite this, approximately 40% of the TL component still remains within the sample after 2 hours 40 minutes of exposure. This makes the use of TL for successful dating of feldspar from young sedimentary environments problematic.

Table 4.2 compares the amount of time required to reduce the IRSL and post-IR blue OSL signals by 50% and 90%. Although both the IRSL and post-IR blue OSL signals initially bleach fairly rapidly the post-IR blue OSL signal requires double the amount of time of the IR signal to be reduced by 90%. Feldspar is a complex mineral with many different defects within the crystal structure and there are likely to be many different components to the decay curve (Duller 1997). Some of these components will bleach easily but other traps may require more stimulation before releasing the electrons and this will contribute to the reduction in bleaching rate of the component stimulated by post-IR blue OSL. The bleaching rate of both signals is reduced by the exclusion of shorter wavelengths, but the post-IR blue bleaching rate is considerably slower than the IRSL (Table 4.2). Use of a GG495 longpass filter effectively blocks the shorter ultraviolet and blue wavelengths that bleach traps stimulated by the post-IR blue OSL, leaving traps stimulated by the longer IR wavelengths to be bleached.

	IRSL	**Post-IR blue OSL**
No filter		
50% bleaching takes	50 seconds	100 seconds
90% bleaching takes	400 seconds	800 seconds
GG495 Filter		
50% bleaching takes	300 seconds	1000 seconds
90% bleaching takes	2500 seconds	10000 seconds

Table 4.2 – The approximate exposure time required to reduce the F1 feldspar signal by 50% and 90%, without and with a Schott GG495 longpass filter.

4.4.2 Laboratory bleaching experiment 2 – Quartz

The same bleaching experiment was repeated in the laboratory using quartz from four modern beaches and two archaeological samples. Each disc was given a 15 Gy dose before being exposed to 40W artificial daylight lamps in a light box for different time periods. The normalised signals of the first two (SUTL 521 and 577) and first four (SUTL 671 and 678) bleaching points in Figure 4.7 and 4.8 are an average of two discs per bleaching period and the remainder of the bleaching experiment was undertaken using one disc per exposure time. The experiment was repeated with a GG495 long pass filter placed on top of the discs during light exposure to simulate cloudy conditions. The main trends of the two experiments are presented before the results of the individual samples are described in more detail.

4.4.2.1 Modern beach sands - main trends and observations

Figures 4.7a and b show the normalised signals of the unfiltered and filtered bleaching experiments plotted against bleaching time. The unfiltered results indicate a rapid bleaching rate within the first 10 seconds of exposure with between 53% and 66% of the non-exposed signal remaining after this time. Twenty minutes of exposure are, however, generally required for minimum signal levels to be reached.

Introduction of the filter effectively reduces the bleaching rate and the scatter observed in the unfiltered data. Two of the samples show a slight increase in the signal after 10 seconds of exposure suggesting that the signals have not been bleached, whereas the other two samples show a decrease in the non-exposed signal by up to 20%. Despite the reduction in the bleaching rate caused by the addition of the filter, similar residual levels are obtained as those observed in the non-filtered experiment, but the filtered samples need exposure times of at least 2 hours 40 minutes, instead of 20 minutes, before these levels are reached.

4.4.2.1.1 SUTL 521

Within the first 10 seconds of exposure to artificial light, the non-filtered blue OSL signal is depleted to approximately 60% of the non-exposed signal and after 20 seconds about

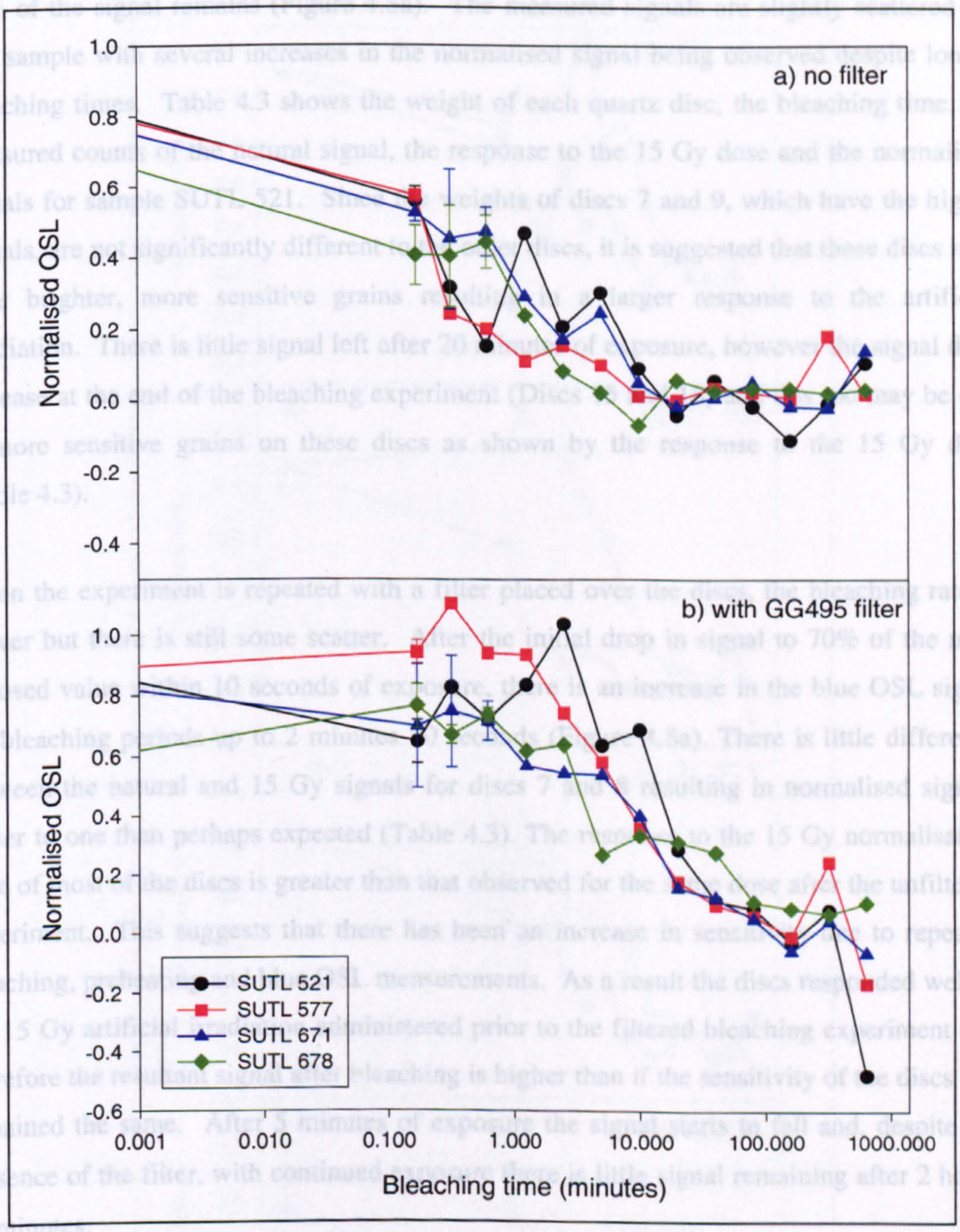

Figure 4.7 – The bleaching rate of quartz from modern beach sands in the laboratory using artificial light and blue OSL: a) without filter and b) with a Schott GG495 filter (90% transmission at wavelengths >540 nm and 50% cut-off at 495 nm). Negative values are due to low OSL signals.

35% of the signal remains (Figure 4.8a). The measured signals are slightly scattered for this sample with several increases in the normalised signal being observed despite longer bleaching times. Table 4.3 shows the weight of each quartz disc, the bleaching time, the measured counts of the natural signal, the response to the 15 Gy dose and the normalised signals for sample SUTL 521. Since the weights of discs 7 and 9, which have the higher signals, are not significantly different to the other discs, it is suggested that these discs may have brighter, more sensitive grains resulting in a larger response to the artificial irradiation. There is little signal left after 20 minutes of exposure, however the signal does increase at the end of the bleaching experiment (Discs 15 and 16) and this too may be due to more sensitive grains on these discs as shown by the response to the 15 Gy dose (Table 4.3).

When the experiment is repeated with a filter placed over the discs, the bleaching rate is slower but there is still some scatter. After the initial drop in signal to 70% of the non-exposed value within 10 seconds of exposure, there is an increase in the blue OSL signal for bleaching periods up to 2 minutes 30 seconds (Figure 4.8a). There is little difference between the natural and 15 Gy signals for discs 7 and 8 resulting in normalised signals closer to one than perhaps expected (Table 4.3). The response to the 15 Gy normalisation dose of most of the discs is greater than that observed for the same dose after the unfiltered experiment. This suggests that there has been an increase in sensitivity due to repeated bleaching, preheating and blue OSL measurements. As a result the discs responded well to the 15 Gy artificial irradiation administered prior to the filtered bleaching experiment and therefore the resultant signal after bleaching is higher than if the sensitivity of the discs had remained the same. After 5 minutes of exposure the signal starts to fall and, despite the presence of the filter, with continued exposure there is little signal remaining after 2 hours 40 minutes.

4.4.2.1.2 SUTL 577

Approximately 65% of the blue OSL signal remains after 10 seconds of exposure to artificial light, however the bleaching rate increases between 10 and 20 seconds with only about 25% of the signal remaining after 20 seconds exposure (Figure 4.8b). The bleaching rate decreases to 2.5% per 10 seconds and less with longer exposure times and after 20 minutes of exposure the lowest signal is measured. Although there is some scatter for the

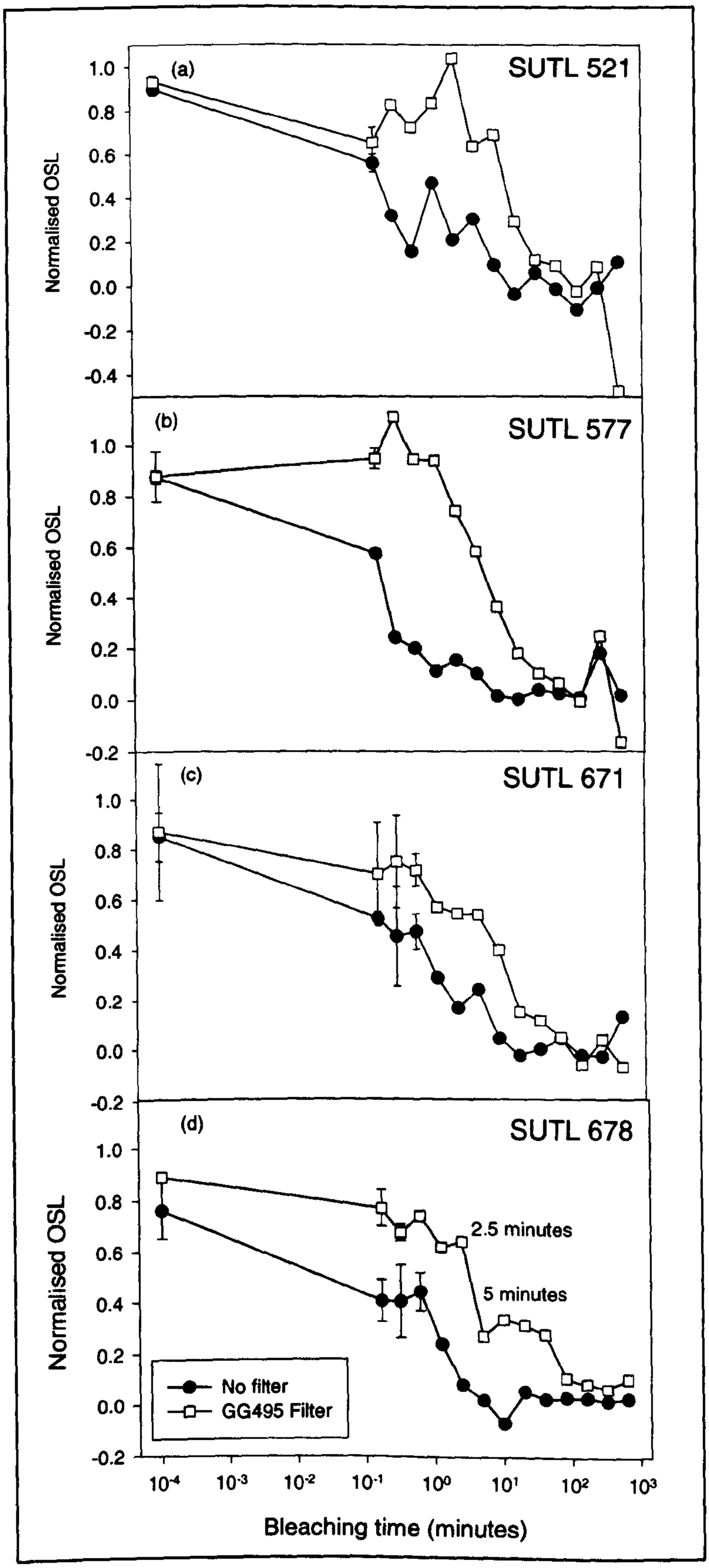

Figure 4.8a-d – The bleaching rate of the individual quartz modern beach samples in the laboratory using artificial light and blue OSL without and with a Schott GG495 filter (90% transmission at wavelengths >540 nm and 50% cut-off at 495 nm).

			Unfiltered			GG495 Filtered		
Disc	Bleaching time	Weight (mg)	Natural signal	15Gy signal	Normalised signal	Natural signal	15Gy signal	Normalised signal
1	0 secs.	4.8	628.67	715.89	0.88	777.67	818.56	0.95
2	0 secs.	4.7	3069.78	3357.44	0.91	4148.00	4576.78	0.91
3	10 secs.	5.3	7340.11	13829.33	0.53	11826.89	16869.22	0.70
4	10 secs.	5.8	1581.67	2691.56	0.59	3722.33	6197.89	0.60
5	19 secs.	5.3	949.33	2994	0.32	3123.22	3778.56	0.83
6	37 secs.	4.7	148.11	964.78	0.15	675.89	938.22	0.72
7	1 min. 15 secs.	4.6	701.78	1500	0.47	1579.78	1895.00	0.83
8	2 mins. 30 secs.	3.9	80.22	388.11	0.21	416.00	400.67	1.04
9	5 mins.	5	338.44	1121.33	0.3	928.11	1461.33	0.64
10	10 mins.	5.6	54.11	598.44	0.09	487.33	709.11	0.69
11	20 mins.	4.2	-23.11	571.11	-0.04	200.00	696.00	0.29
12	40 mins.	4.8	40.56	729.78	0.06	122.11	1074.78	0.11
13	1 hr. 20 mins.	5.8	-10.22	659.56	-0.02	61.11	700.67	0.09
14	2 hrs. 40 mins.	4.8	-47.33	427.89	-0.11	-9.22	334.89	-0.03
15	5 hrs. 20 mins.	5.5	-17.11	1744.11	-0.01	175.33	2135.56	0.08
16	10 hrs. 40 mins.	4.4	106.89	1017.67	0.11	-242.10	507.30	-0.48

Table 4.3 – Results of laboratory bleaching experiment using quartz from SUTL 521 and blue OSL

longer exposure times, the signal measured after 5 hours 20 minutes is larger than expected.

When the experiment is repeated using a filter, there is little scatter in the data (Figure 4.8b). Although the signal does increase over the first few bleaching periods, this could indicate that no bleaching is occurring during the first couple of minutes of exposure. The signal does start to drop after 2 minutes 30 seconds of bleaching to approximately 85% of the non-exposed signal and continues to drop reaching a minimum after exposure of 2 hours 40 minutes. As with the non-filtered experiment, the signal increases after 5 hours 20 minutes of exposure suggesting that hard to bleach traps may be involved. The electrons in these traps may become accessible to blue OSL during preheating by thermal transfer into light-sensitive traps, resulting in the higher signals observed for both the unfiltered and filtered experiments or it may be a measurement error.

4.4.2.1.3 SUTL 671

Within the first 10 seconds of exposure to artificial light, the blue OSL signal depletes rapidly to approximately 60% of the non-exposed signal and after 20 seconds this has been reduced to about 50% (Figure 4.8c). The bleaching rate continues to decrease as the exposure time increases and 20 minutes of exposure are required for the lowest signal to be measured.

When a filter is placed over the discs to simulate cloudy conditions, 20% of the non-exposed signal is depleted after 10 seconds of exposure. The discs require up to 10 minutes exposure with the filter before half of the signal has been bleached, but after 10 hours 40 minutes of exposure very little signal remains.

4.4.2.1.4 SUTL 678

The initial bleaching rate of this sample is the fastest of all the samples tested with approximately 55% of the signal remaining after the sample has been bleached for 10 seconds with artificial light (Figure 4.8d). The sample continues to bleach quickly and after 10 minutes of exposure the lowest signal is measured.

When the experiment is repeated and a filter is placed over the discs, the bleaching rate is much slower with 87% of the non-exposed signal remaining after 10 seconds of exposure. There is an increase in the bleaching rate between 2 minutes 30 seconds and 5 minutes (Figure 4.8d) to 5.5% per 10 seconds, compared to 0.54% per 10 seconds for the same time interval during the unfiltered bleaching. Nevertheless, approximately 10% of the non-exposed signal still remains after 10 hours 40 minutes of exposure.

4.4.2.1.5 Summary of modern beach sand laboratory quartz bleaching experiment

The bleaching experiments undertaken in the laboratory on the modern beach sands have provided information on the rate of bleaching when the full visible spectrum, provided by artificial daylight sources, is available and how these rates change when a filter blocking the shorter wavelengths is introduced. Table 4.4 shows the length of time required to reduce the quartz OSL signal by 50% and 90%. The values are based on an approximate average of the four beach sands measured. Up to 30 seconds of exposure is required to reduce the signal by 50% and 300 seconds are required for the signal to be depleted by 90%. This reflects the rate of decay of the fast/medium and slow components. The GG495 longpass filter effectively reduces the bleaching rate with several samples showing little change in the unexposed signal level over the first couple of minutes. The signal is depleted by 50% after 300 seconds of exposure (5 minutes) and approximately 6000 seconds (1.66 hours) are required to reduce the signal by 90% (Table 4.4). Despite the presence of the filter, 3 of the 4 samples appear to be fully bleached after at least 2 hours 40 minutes of exposure.

	No filter	GG495 Filter
50% bleaching takes	30 seconds	300 seconds
90% bleaching takes	300 seconds	6000 seconds

Table 4.4 – Length of time required to reduce the quartz luminescence signal by 50% and 90%. Values based on approximate average of the four beach sands measured. Schott GG495 longpass filter has 90% transmission at wavelengths >540 nm and 50% cut-off at 495 nm.

Although the experiments were undertaken in controlled laboratory conditions, the normalised unfiltered data is quite scattered and less scatter is observed in the filtered data. The cause of the scatter is likely due to the presence of brighter, more sensitive grains on

some of the discs possibly enhanced by the increased sensitivity of most discs due to repeated irradiation, preheating and OSL measurement.

4.4.2.2 Archaeological samples laboratory bleaching experiments

The laboratory bleaching experiments were repeated with two samples from archaeological sites to compare the bleaching rate of these sands with the modern beach sands presented above. The discs used in this experiment were those dispensed to determine the palaeodose of each sample. The first two data points are an average of two discs per bleaching time and the remainder of the experiment was undertaken using one disc per exposure time.

4.4.2.2.1 SUTL 605

This sample was collected from Tofts Ness, Sanday in July 1999 and represents the sandy buried soil in Test Pit 3 described in Section 3.31, Chapter 3. The quartz responds well to artificial irradiation indicating good sensitivity and when exposed to artificial light the signal bleaches quickly (Figure 4.9a). Within 10 seconds of exposure, the blue OSL signal has rapidly depleted to 65% of the non-exposed signal and after 5 minutes of exposure this has been reduced to 1% of the initial signal. When the experiment is repeated with a Schott GG495 filter placed over the discs during exposure, the bleaching rate is much slower (Figure 4.9a). After 10 seconds of exposure, 99% of the non-exposed signal remains and after 5 minutes this has been reduced to about 65%. Low signal levels (~1%) are obtained after the discs are bleached for 2 hours 40 minutes in the light box.

4.4.2.2.2 SUTL 623

This sample was collected in July 1999 at the Bay of Skaill, Mainland Orkney, close to Skara Brae and is described in more detail in Section 3.6, Chapter 3. Although this sample is not as sensitive as SUTL 605 above, the quartz responded sufficiently to the artificial irradiation for the bleaching experiment to be successful. The results of the experiment with and without a filter are shown in Figure 4.9b. After 10 seconds of exposure to the artificial light, the signal has decreased to approximately 75% of the non-exposed signal, but it bleaches rapidly over the next couple of minutes and after 2 minutes 30 seconds 5%

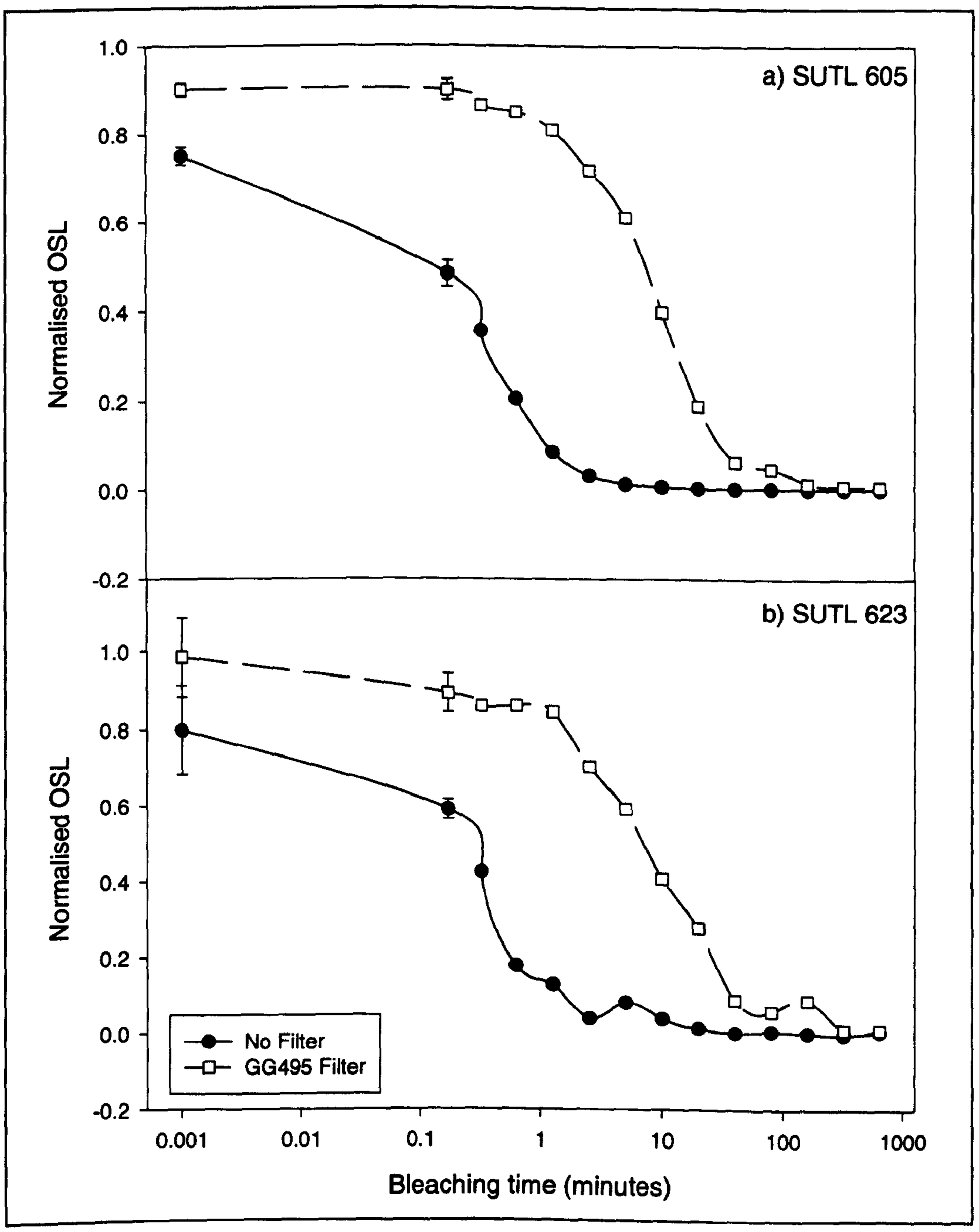

Figure 4.9a and b – Bleaching rate of archaeological samples in the laboratory using artificial light and blue OSL without and with a GG495 longpass filter (90% transmission at wavelengths >540 nm and 50% cut-off at 495 nm).

of the initial signal remains. There is an increase in signal after 5 minutes of exposure due to the test dose signal of this disc being much lower than the other discs in the run, however after 40 minutes of exposure, the signal is less than 1% of the non-exposed signal.

As with most other samples analysed, when a Schott GG495 longpass filter is placed on top of the discs during artificial light exposure, the bleaching rate is much slower. After 10 seconds of exposure, 90% of the non-exposed signal remains and approximately 40% of the signal remains after 5 minutes. This sample appears to bleach at a faster rate compared to SUTL 605 when the filter is administered, however this slows down rapidly after 20 minutes exposure and 5 hours 20 minutes of exposure are required before the lowest signal (~1%) is measured.

4.4.2.2.3 Summary of archaeological samples laboratory quartz bleaching experiment

Both samples show an initial rapid decrease in the blue OSL signal when the discs are exposed to artificial light in the laboratory and after about 10 seconds 50% of the signal has been depleted (Table 4.5). With longer exposure times the bleaching rate decreases however only 10% of the non-exposed signal remains after 60 seconds of exposure. When the experiment is repeated using a filter to simulate cloudy conditions, the bleaching rate of both samples is initially quite slow and 600 seconds of exposure are required to reduce the luminescence signal by 50%. Approximately 3000 seconds (50 minutes) of exposure reduces the signal to 90% (Table 4.5) and both signals are reduced to ~1% of the original signal after 5 hours 20 minutes (SUTL 623) and 2 hours 40 minutes (SUTL 605).

	No filter	GG495 Filter
50% bleaching takes	10 seconds	600 seconds
90% bleaching takes	60 seconds	3000 seconds

Table 4.5 – The amount of time required to reduce the quartz archaeological samples to 50% and 90% of the initial signal without and with a Schott GG495 longpass filter.

4.4.2.2.4 Comparison of F1 feldspar and quartz bleaching rates

The current literature infers that under optimal conditions i.e. with a full light spectrum, the luminescence signal of quartz will bleach more rapidly than feldspar, one of the reasons that quartz is more commonly used in OSL dating of unheated sediments. Table 4.6 and Figure 4.10 show the results from the laboratory bleaching experiments of the F1 feldspar and quartz using blue LEDs for stimulation. The graph shows that the initial bleaching rate of F1 feldspar is much slower than the quartz when the aliquots are exposed to the full light spectrum in the light box. F1 feldspar requires up to 100 seconds of exposure to reduce the luminescence signal by 50% compared to the 10-30 seconds required for quartz (Table 4.6).

	F1 feldspar	Modern beach quartz	Archaeological quartz
No filter			
50% bleaching takes	100 seconds	30 seconds	10 seconds
90% bleaching takes	800 seconds	300 seconds	60 seconds
GG495 Filter			
50% bleaching takes	1000 seconds	300 seconds	60 seconds
90% bleaching takes	10000 seconds	6000 seconds	3000 seconds

Table 4.6 – Comparison of the laboratory bleaching rates of F1 feldspar, modern beach quartz and archaeological quartz stimulated by blue OSL without and with a Schott GG495 longpass filter (90% transmission at wavelengths >540 nm and 50% cut-off at 495 nm.

When a GG495 filter is placed over the aliquots during the subsequent bleaching experiment, all of the samples bleach at a slower rate but the modern beach samples still bleach slightly faster than the F1 feldspar (Figure 4.10b, Table 4.6). This might be taken to suggest that either the modern beach quartz may be contaminated with IR sensitive minerals which are rapidly bleached even when a filter blocks the short wavelengths, or some traps within these samples are stimulated by longer wavelengths (and so related to the secondary emission peak of quartz at 610 nm which is not affected by the filter). It could be suggested that the reduction in bleaching rate of all samples after the filter is introduced is due to a drop in the power intensity of the artificial light source rather than the blocking of shorter wavelengths by the filter. A Molectron PR200 pyroelectric radiometer with a spectral wavelength range of 0.1-500 nm and 100% peak transmission

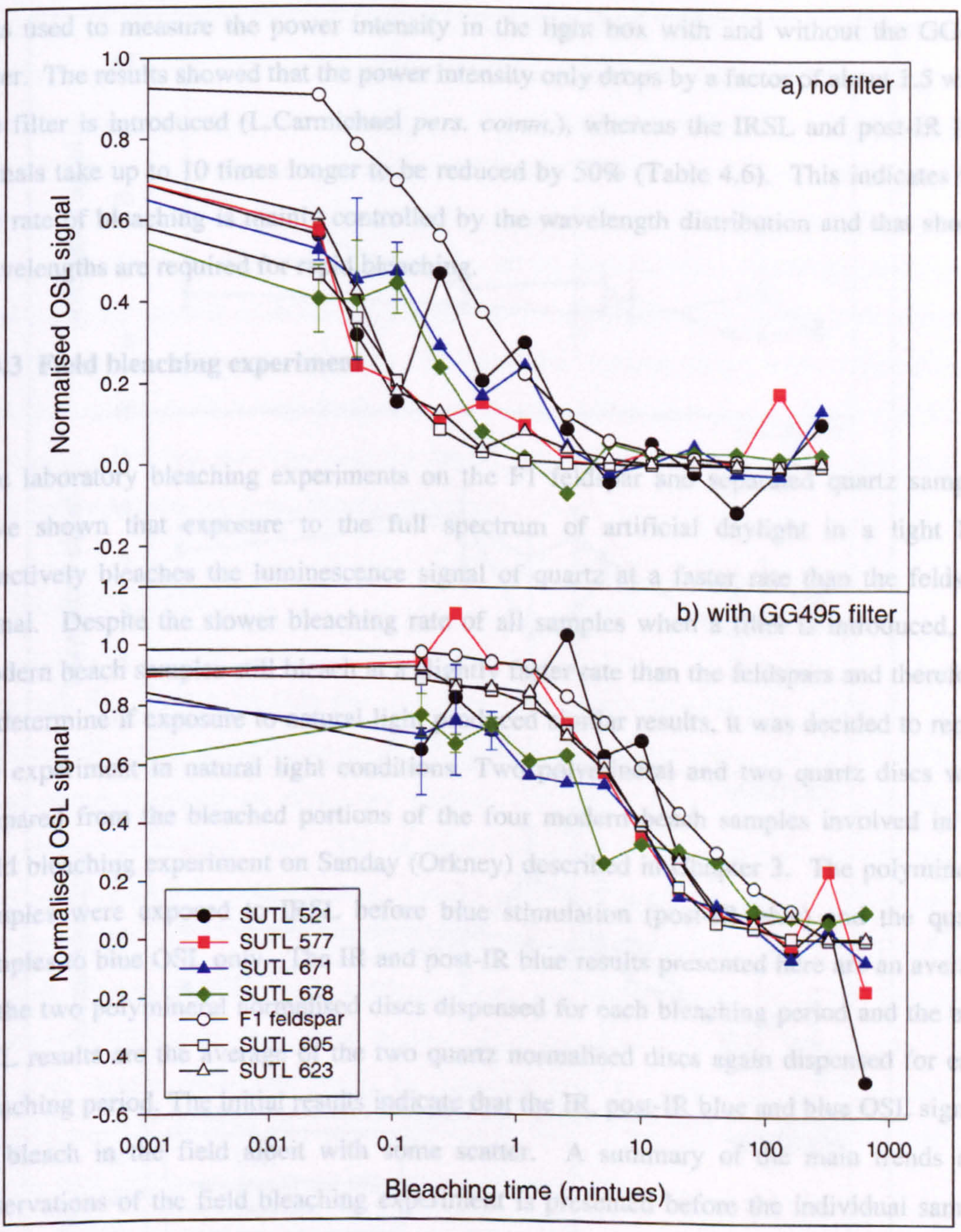

Figure 4.10 – Comparison of bleaching rates of modern beach quartz, F1 feldspar and archaeological sands: a) without filter and b) with a Schott GG495 longpass filter.

was used to measure the power intensity in the light box with and without the GG495 filter. The results showed that the power intensity only drops by a factor of about 1.5 when the filter is introduced (L.Carmichael *pers. comm.*), whereas the IRSL and post-IR blue signals take up to 10 times longer to be reduced by 50% (Table 4.6). This indicates that the rate of bleaching is mainly controlled by the wavelength distribution and that shorter wavelengths are required for rapid bleaching.

4.4.3 Field bleaching experiment

The laboratory bleaching experiments on the F1 feldspar and separated quartz samples have shown that exposure to the full spectrum of artificial daylight in a light box effectively bleaches the luminescence signal of quartz at a faster rate than the feldspar signal. Despite the slower bleaching rate of all samples when a filter is introduced, the modern beach samples still bleach at a slightly faster rate than the feldspars and therefore, to determine if exposure to natural light produced similar results, it was decided to repeat the experiment in natural light conditions. Two polymineral and two quartz discs were prepared from the bleached portions of the four modern beach samples involved in the field bleaching experiment on Sanday (Orkney) described in Chapter 3. The polymineral samples were exposed to IRSL before blue stimulation (post-IR blue) and the quartz samples to blue OSL only. The IR and post-IR blue results presented here are an average of the two polymineral normalised discs dispensed for each bleaching period and the blue OSL results are the average of the two quartz normalised discs again dispensed for each bleaching period. The initial results indicate that the IR, post-IR blue and blue OSL signals do bleach in the field albeit with some scatter. A summary of the main trends and observations of the field bleaching experiment is presented before the individual sample results are discussed in more detail.

4.4.3.1 Main trends and observations

Despite the scatter in the bleaching curves shown in Figure 4.11a-d, the majority of the samples show a fairly rapid decrease in the IR, post-IR blue and blue OSL signals after exposure to Orcadian light for 1-5 minutes, but exposure times of between 12 hours and 4 days are required for minimum signal levels to be reached. There is a general decrease in the bleaching rate of each sample with exposure time, however the rate of bleaching varies

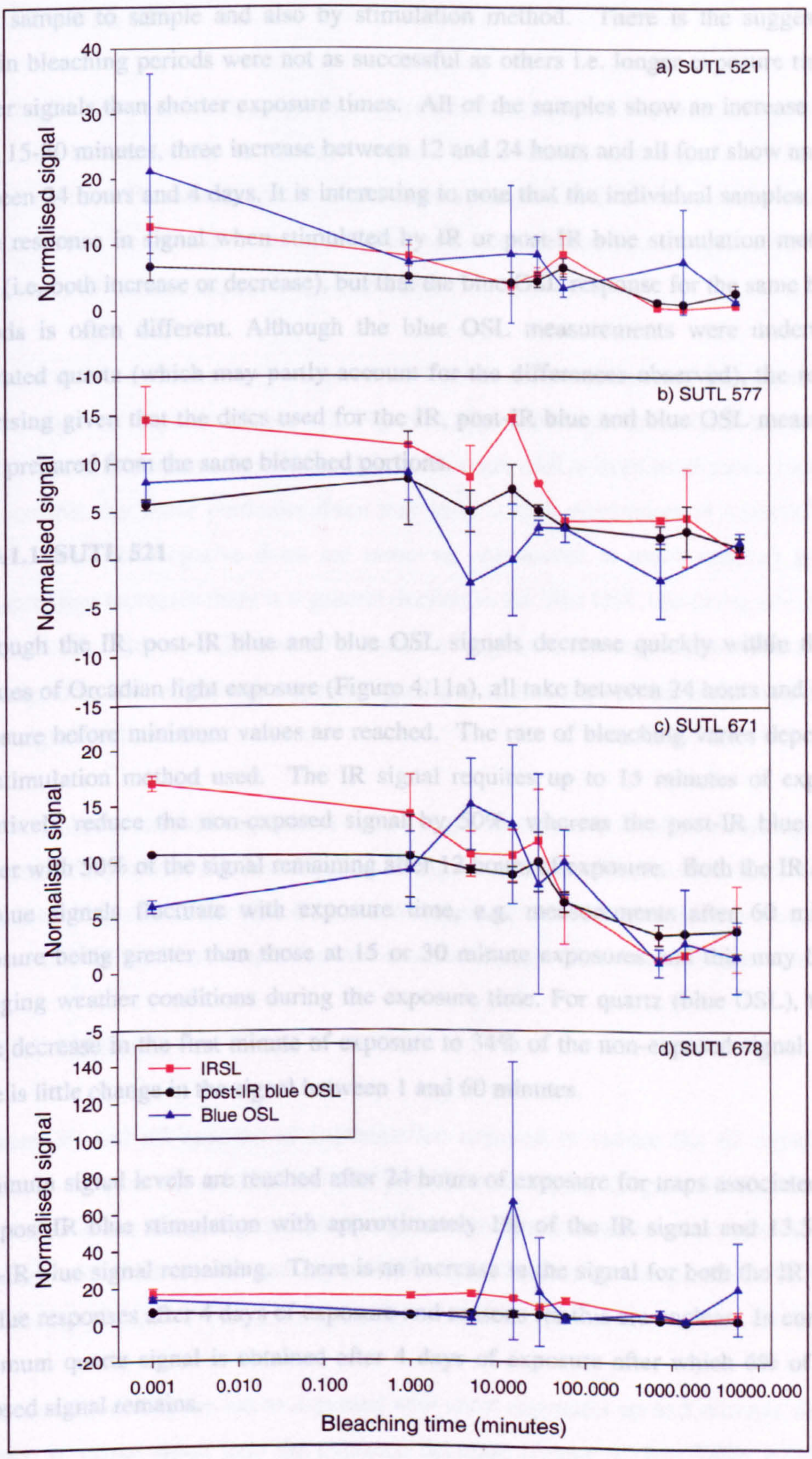

Figure 4.11a-d – The bleaching rate of polymineral modern beach sands in Orcadian light using IRSL, post-IR blue OSL and Blue OSL

from sample to sample and also by stimulation method. There is the suggestion that certain bleaching periods were not as successful as others i.e. longer exposure times have higher signals than shorter exposure times. All of the samples show an increase in signal from 15-30 minutes, three increase between 12 and 24 hours and all four show an increase between 24 hours and 4 days. It is interesting to note that the individual samples show the same response in signal when stimulated by IR or post-IR blue stimulation methods are used (i.e. both increase or decrease), but that the blue OSL response for the same bleaching periods is often different. Although the blue OSL measurements were undertaken on separated quartz (which may partly account for the differences observed), the results are surprising given that the discs used for the IR, post-IR blue and blue OSL measurements were prepared from the same bleached portions.

4.4.3.1.1 SUTL 521

Although the IR, post-IR blue and blue OSL signals decrease quickly within the first 5 minutes of Orcadian light exposure (Figure 4.11a), all take between 24 hours and 4 days of exposure before minimum values are reached. The rate of bleaching varies depending on the stimulation method used. The IR signal requires up to 15 minutes of exposure to effectively reduce the non-exposed signal by 50%, whereas the post-IR blue signal is slower with 50% of the signal remaining after 12 hours of exposure. Both the IR and post-IR blue signals fluctuate with exposure time, e.g. measurements after 60 minutes of exposure being greater than those at 15 or 30 minute exposures and this may be due to changing weather conditions during the exposure time. For quartz (blue OSL), there is a large decrease in the first minute of exposure to 34% of the non-exposed signal, however there is little change in the signal between 1 and 60 minutes.

Minimum signal levels are reached after 24 hours of exposure for traps associated with IR and post-IR blue stimulation with approximately 1% of the IR signal and 13.5% of the post-IR blue signal remaining. There is an increase in the signal for both the IR and post-IR blue responses after 4 days of exposure and reasons for this are unclear. In contrast, the minimum quartz signal is obtained after 4 days of exposure after which 6% of the non-exposed signal remains.

4.4.3.1.2 SUTL 577

Both the IR and post-IR blue signals require about 30 minutes exposure to be reduced by 50%, but both take up to 4 days exposure for the lowest signals to be reached (Figure 4.11b). The bleaching rate of the traps associated with IR stimulation continues to be faster than the post-IR blue stimulation and after an hour's exposure, 28% and 60% respectively of the non-exposed signal remains.

The blue OSL results are very scattered with some of the normalised discs giving a very low or negative response (Table 4.7, Figure 4.12). Although unlikely to be due to poor sensitivity (as this sample has shown that it responds well to beta irradiation (Figure 4.4)), it is possible that these particular discs may have a high percentage of insensitive quartz grains. Once the negative discs are removed, the scatter is much reduced and as the exposure time increases there is a general decline in the blue OSL bleaching rate and signal (Figure 4.12). Between 30 and 60 minutes of exposure are required to reduce the blue OSL signal to 50% of the non-exposed signal and after 4 days of exposure more than 10% of the signal still remains.

Each stimulation method requires at least 4 days of exposure for the lowest signals to be recorded. Only 4% of the non-exposed IR signal remains after this time and, despite the faster bleaching rate of the blue OSL when compared with the post-IR blue bleaching rate, both contain 24% of their respective non-exposed signals after 4 days of exposure.

4.4.3.1.3 SUTL 671

Between 30 and 60 minutes of exposure are required to reduce the IR signal to 50% compared to over 60 minutes for the post-IR blue signal (Figure 4.11c). Despite the differences in the bleaching rates, both signals reach their lowest values after 12 hours of exposure with 7.5% of the non-exposed IR signal remaining compared to 35.5% of the post-IR blue signal.

The blue OSL results are not as expected with short exposures up to 5 minutes showing an increase in signal rather than the expected decrease (Figure 4.11c). Table 4.8 shows the weight of each quartz disc, the bleaching time, the measured counts of the natural signal (i.e. counts measured after the bleaching), the response to the 0.5 Gy dose and the

Disc	Bleaching time	Bleached signal (counts)	0.5Gy signal (counts)	Normalised signal	Average	Error
1	0 mins	1786.44	176.78	10.11	8.05	2.05
2	0 mins	1261.44	208.78	6.04		
3	1 min	1484.44	240.56	6.17	9.1	2.9
4	1 min	3372.56	280.11	12.04		
5	15 mins	240.11	-23.56	-10.19	5.39	0
6	15 mins	183.33	34.00	5.39		
7	30 mins	278.67	-48.22	-5.78	5.86	0
8	30 mins	431.33	73.56	5.86		
9	60 mins	652.44	243.78	2.68	3.4	0.7
10	60 mins	1022.33	247.56	4.13		
11	12 hrs	705.44	149.22	4.73	3.3	1.4
12	12 hrs	212.67	111.56	1.91		
13	24 hrs	1350.89	745.22	1.81	1.81	0
14	24 hrs	204.00	-33.56	-6.08		
15	4 days	1245.00	1308.22	0.95	1.85	0.95
16	4 days	737.89	261.67	2.82		

Table 4.7 – Results of field bleaching experiment using quartz from SUTL 577 and blue OSL

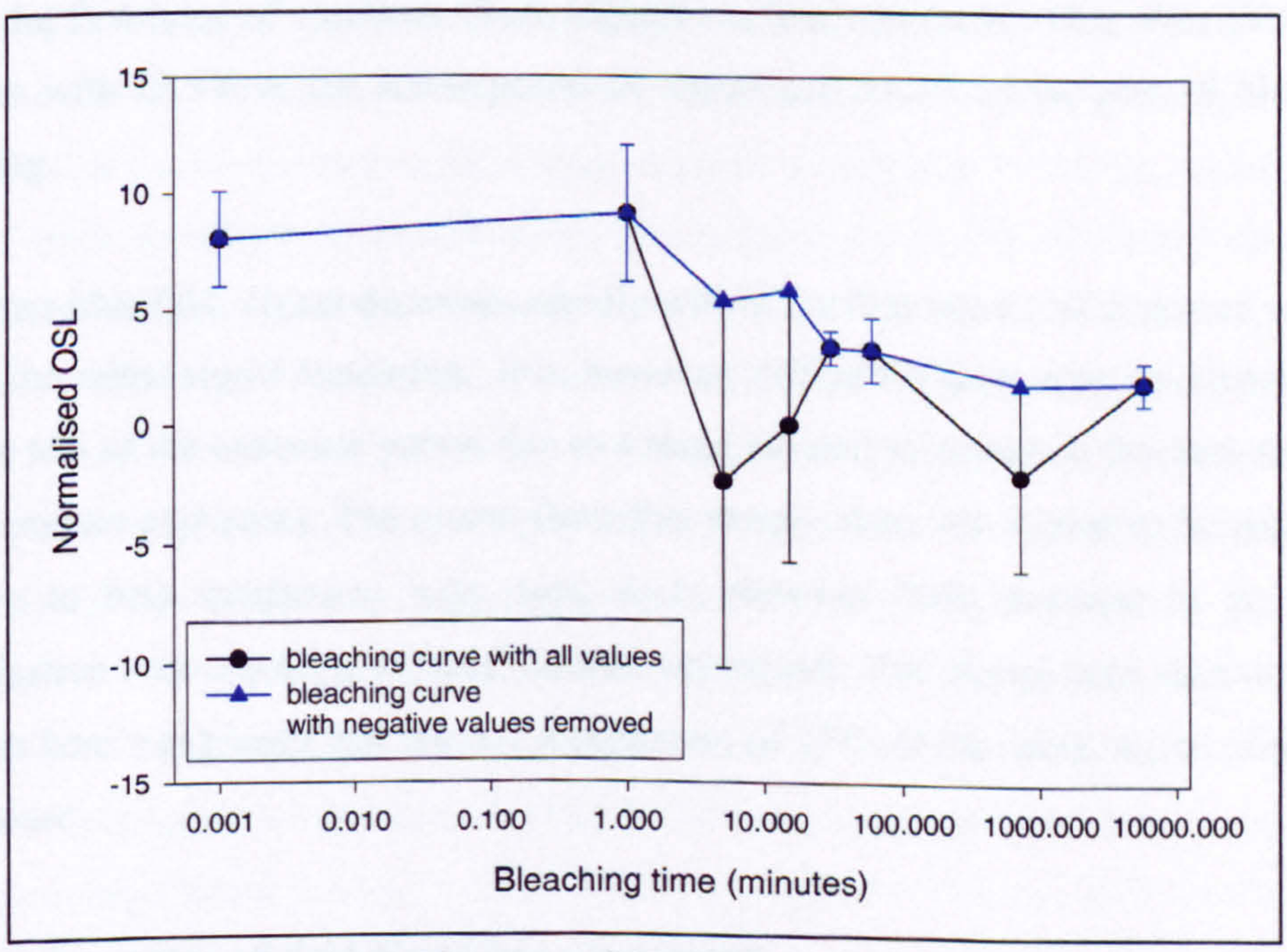

Figure 4.12 – The bleaching rate of SUTL 577 with and without the negative values removed.

Disc	Bleaching time	Weight (mg)	Natural signal	0.5Gy signal	Normalised signal
1	0 minutes	5.3	362.33	56.56	6.41
2	0 minutes	4.2	562.00	100.11	5.61
3	1 minute	5.4	473.11	68.00	6.96
4	1 minute	4.7	224.44	19.22	11.68
5	5 minutes	2.9	195.11	15.89	12.28
6	5 minutes	3.5	375.67	20.78	18.08
7	15 minutes	3.3	9276.00	502.11	18.47
8	15 minutes	4.3	50294.67	5961.22	8.44
9	30 minutes	6.1	326.00	21.67	15.05
10	30 minutes	2.9	492.89	441.89	1.12
11	60 minutes	2.3	176.89	22.00	8.04
12	60 minutes	4.0	1908.00	157.78	12.09
13	12 hours	5.0	55.67	223.89	0.25
14	12 hours	3.3	89.67	43.67	2.05
15	24 hours	3.4	2053.22	325.00	6.32
16	24 hours	3.6	38.44	-81.89	-0.47
17	4 days	3.4	154.56	39.78	3.89
18	4 days	3.0	36.22	-54.67	-0.66

Table 4.8 – Results of field bleaching experiment using quartz from SUTL 671 and blue OSL

normalised signals. Although there is some scatter between the discs, which may be due to variations in the quantity of sediment on each disc, there is no obvious pattern between heavier discs and larger signals. The sediment used on discs 7 and 8 was bleached for 15 minutes and the high natural signals are thought to be the result of poor bleaching during this period as this is observed in all samples. Discs 12 and 15 also show high natural signals, which may also be due to poor bleaching, but the other discs in each bleaching period have low signals and therefore discs 12 and 15 may contain brighter, more sensitive quartz grains. After 15 minutes of exposure, there is a general decrease in the signal with increasing exposure time and the lowest signals are recorded after 12 hours of exposure with 19% of the initial signal remaining.

4.4.3.1.4 SUTL 678

There is a clear distinction between the IR and post-IR blue signals for the first 60 minutes of exposure (Figure 4.11d) possibly due to variable sensitivity but despite this, the depletion rate of the luminescence signal stimulated by IR and post-IR blue OSL is similar during the first hour of exposure. Both signals reach a minimum value after 24 hours of exposure with 15.5% of the non-exposed IR signal and 33.5% of the post-IR blue signal remaining.

The quartz blue OSL signal decreases rapidly within the first minute of exposure with only 29% of the initial signal remaining. It is, however, difficult to determine the bleaching rate over the rest of the exposure period due to a large amount of scatter in the data after 5, 15 and 30 minute exposures. The quartz from this sample does not appear to be particularly sensitive to beta irradiation, with some discs showing little response to the 0.5 Gy normalisation dose resulting in large normalised signals. The signal does start to stabilise after one hour's exposure and reaches a minimum of 17% of the initial signal after 4 days of exposure.

4.4.3.1.5 Summary of field bleaching experiment

The field bleaching experiments show that the latent signal induced in the modern sands prior to the field experiments by the Hotspot irradiator at the Veterinary School is bleached by exposure to Orcadian light. Although the rate at which the signal is bleached varies from sample to sample (an expected result due to the different lithologies of the sediment),

there are also significant differences in the rate at which the feldspar and quartz signals are bleached. In all cases the initial IR signal bleaches faster than the post-IR blue signal, but the initial bleaching rate of the quartz blue OSL signals of samples SUTL 521 and 678 is much faster, with up to 80% of the signal depleted within the first minute of exposure. The scatter in the bleaching data for all of the samples may be partly due to changing weather conditions during the experiment, which altered the wavelength spectrum and light intensity reaching the grains. Based on the lowest signals recorded for each sample and each stimulation method, the samples contain residual signals of between 1% and 35.5% (0.15-5 Gy) of the non-exposed signal after 12 hours to 4 days of exposure. These residual levels and the relatively slow bleaching rates measured in natural conditions raise concerns for accurate optically stimulated luminescence dating of unheated sediments: full bleaching cannot be assumed prior to burial.

4.4.4 Summary and discussion of bleaching experiments

The bleaching experiments undertaken on the F1 feldspar, modern beach sands and archaeological samples have provided an insight into the bleaching characteristics of traps associated with IR, blue OSL or TL stimulation and they have indicated that light intensity is a major control on the rate of bleaching. Despite a reduction in the TL signal from F1 feldspar with increasing exposure time, the residual level after 2 hours 40 minutes bleaching in a light box is unacceptable (~40%). In conjunction with these results, the high TL residual levels from the modern beach sands discussed in Section 4.2.1 confirm that TL is unsuitable for dating young sediments in this study area. These results help explain the initial success of TL dating studies using much older archaeological samples: a large residual level will not significantly affect the luminescence age of the sample. Mejdahl (1985) did present a method to determine the extent of environmental bleaching of sediments based on TL, but the introduction of optically stimulated methods to determine the palaeodose of sediments has resulted in virtual cessation of the use of TL for sediment dating studies.

The IR and the post-IR blue signals from the F1 feldspar suggest that different traps within the crystal structure, stimulated by IR or blue wavelengths, bleach at different rates. This is confirmed by the modern beach sand analysis where not only does the stimulation wavelength affect the rate of bleaching but the mineralogy of the sand also has an effect. The four modern beach samples used in the bleaching experiments are from different

beaches throughout the Orkney Islands, Shetland Islands and the Outer Hebrides. The results indicate that although the sample from Orkney (SUTL 577) initially bleaches the most rapidly, it is the sample from the Outer Hebrides (SUTL 521), which has the lowest residual level after 4 days of exposure.

Although the fast component of the modern beach samples does bleach quickly when exposed to Orcadian light, all the samples still had a significant residual level after 4 days of exposure. In the laboratory light box, most of the signal is bleached within 20 minutes if the samples are exposed to the full spectrum. When a filter is introduced to block the shorter wavelengths which are more effective at bleaching, the samples take over 2½ hours for minimum levels to be reached: still relatively rapid when compared to the results from the field bleaching experiment. This is partly explained by the higher power intensity in the light box of about 7mWcm^{-2} compared to about 1mWcm^{-2} in natural conditions. Bleaching experiments were also undertaken on two archaeological samples in the laboratory. Both samples bleach very rapidly and are reduced to ~5% of the non-exposed signal within several minutes of exposure. Although similar residual levels are obtained when a filter is introduced, between 3 and 6 hours (SUTL 623 and 605 respectively) of exposure in the light box are required to reach these minimum levels.

The assumptions that wind blown sands are well-bleached prior to burial and that the latent signal is rapidly bleached, are both central to successful luminescence dating. Despite the knowledge that the modern beach sands and archaeological sands analysed in the laboratory are well bleached within several hours, the bleaching rates and residual levels identified in the field experiment will be of concern in instances when the exposure duration is significantly less than a few hours.

In the field, the environmental conditions at the time of transportation and deposition will influence how quickly the sands are bleached. The sand will undoubtedly be eroded, transported and deposited many times before finally being buried and each time the sand is exposed more of the latent signal will be removed. The sand in the field bleaching experiment was exposed for a set period of time and did not go through the cycle of erosion, transportation and deposition and this is perhaps reflected in a significant latent signal remaining after 4 days of exposure. Despite this, the field experiment indicates that it takes longer to reduce the latent signal when irradiated sand is exposed to natural light intensities. The weather during the experiment was predominantly cloudy and this will

also have affected the rate of bleaching. It was previously discussed in Chapter 2 that the wavelengths reaching the Earth's surface in sunlight and cloudy conditions varies considerably. For successful bleaching of quartz, exposure to UV and blue/green wavelengths is required, but in cloudy conditions these wavelengths are effectively blocked, preventing rapid bleaching of the quartz luminescence signal. For the modern beach sands in the field bleaching experiment, the feldspar residuals are less than the quartz confirming that the clouds have effectively blocked the UV wavelengths. This implies that, in the Orkney Islands, quartz does not bleach as rapidly as feldspar in cloudy conditions and therefore longer exposure times are required to reduce the residual signal prior to burial. Ideally a similar bleaching experiment could be conducted in bright sunlight conditions to determine if the optical bleaching rate in the field is as efficient as that observed in the laboratory. Although the sand layer within each petri dish used in the field bleaching experiment was relatively thin, the sand was not moved during the experiment and therefore it is possible that some of the grains were not fully exposed to the light. Periodically mixing the sand within the petri dishes during the experiment to allow all of the grains to be exposed may reduce the latent signal more rapidly.

The length of time required to bleach the samples in the laboratory and field raises the question as to whether the sand bleaches rapidly enough to be sure that the archaeological samples are well bleached during a natural event prior to burial. The results from the bleaching experiments suggest that if the sand is blowing in very bright sunshine and it has been through several cycles of erosion and bleaching, then there is a high likelihood that the samples are well bleached. However, large movements of sand are also more likely to occur during storm events that may coincide with low light levels e.g. in winter. If the sand deposits found within archaeological sites were deposited during large storm events, the lack of light may have prevented the sand from being rapidly bleached and therefore it is likely that these sand deposits are partially bleached. Researchers should be aware of this when dating wind blown sands from archaeological sites in high latitude areas where storm frequency increases during the winter and the length of daylight is relatively short.

4.5 Partial bleaching analysis and the psi (ψ) ratio

4.5.1 Introduction

As discussed above, a fundamental requirement of optically stimulated luminescence dating is the premise that the sediment being dated was well-bleached during transportation and deposition prior to burial. Aeolian sediments are generally thought to be well bleached because they are assumed to be exposed to extended periods of sunlight during transportation. There are, however, several studies which suggest that sediments which are expected to be well-bleached may in fact only be partially bleached (Clarke 1996; Roberts *et al.* 1998, Clarke *et al.* 2001; Sanderson *et al.* 2001; Sommerville *et al.* 2001). The bleaching experiments undertaken in Orkney and in the laboratory indicate that lengthy periods of exposure to sunlight or artificial daylight are required before minimum OSL residuals are acquired. The amount of sunlight a sample receives can vary depending on latitude, time of year, the amount of cloud cover, time of day and the sample height above sea level and even if samples are collected from the same area, there will be sample to sample variation. The bleaching experiments undertaken in Orkney for this research confirms this variation in bleaching rates even when all of the samples are exposed to the same environmental conditions and light intensities. There is also a considerable difference in the residual levels of samples collected from modern beaches in the Orkney Islands and Outer Hebrides (Section 4.2.1) and although it is not known how long these sands were exposed to daylight prior to collection, there appears to be a mineralogical control on the rate of bleaching.

The rate of bleaching is perhaps one of the most important issues in OSL dating, especially in high latitude areas such as the Orkney Islands where the length of daylight during the winter months is restricted to between six and nine hours per day. The movement of large quantities of sand will occur more often in winter months when storms tend to be more frequent and it may be expected that sand moved during the winter months in these high latitude areas may not be fully bleached on deposition and burial. Yet OSL dating of sand deposits from archaeological sites has great potential as a dating technique in the Orkney Islands due to the lack of organic material available for radiocarbon dating. Therefore, it is important to identify samples that might be partially bleached in order to ensure accurate dating within these sites.

Several methods have been proposed to determine the level of bleaching within sediment samples. The shine plateau test introduced by Huntley *et al.* (1985) used the plot of palaeodose versus stimulation time to determine if a sample was well-bleached at deposition. They suggested that a plateau indicated that the sample was well bleached; but a rise in the equivalent dose (D_e) with stimulation time, such as that shown in Figure 4.13, was an indication of partial bleaching. However, determining the extent of bleaching prior to burial using the shine plateau method is more complicated than previously thought (Bailey 2000). The shine plateau of a quartz sample known to be well bleached showed an increase in D_e with stimulation time (Bailey 2000) and Stokes (1994) presented a flat plateau from a quartz sample that was intentionally partially bleached. Bailey (2000) suggests that the rise in D_e observed by Huntley *et al.* (1985) may result from phototransferred thermoluminesence from the 110°C TL trap during stimulation or differences in the response of the individual OSL signal components to artificial irradiation.

Clarke (1996) proposed that partially bleached feldspar samples could be identified by plotting the normalised equivalent dose of each aliquot against the normalised natural intensity of the same aliquot. Normalisation of both the D_e and the natural intensity allows the results to be easily interpreted. The results presented by Clarke (1996) show that the D_e/ln plots of well bleached samples are tightly clustered with a small standard deviation from the mean, whereas the plots of partially bleached samples are scattered with a large standard deviation from the mean. From this Clarke (1996) suggests that the standard deviation from the mean equivalent dose may be used to determine the degree of bleaching. A threshold of 5 Gy was chosen for these samples so that samples with a standard deviation of less than 5 Gy are thought to be well-bleached and those greater than 5 Gy are poorly bleached (Clarke 1996). The threshold used by Clarke (1996) was chosen based on a wider set of data, but if this technique is used on different samples, the threshold will vary depending on the location and environment from which the samples are collected.

More recently Colls *et al.* (2001) have suggested the use of a t-test using Pearson's Correlation Coefficient to identify significant trends in the D_e versus OSL intensity. Comparing the result to a one-tailed Student's t-test distribution identifies if there is a statistically significant relationship. Samples that show no significant relationship are

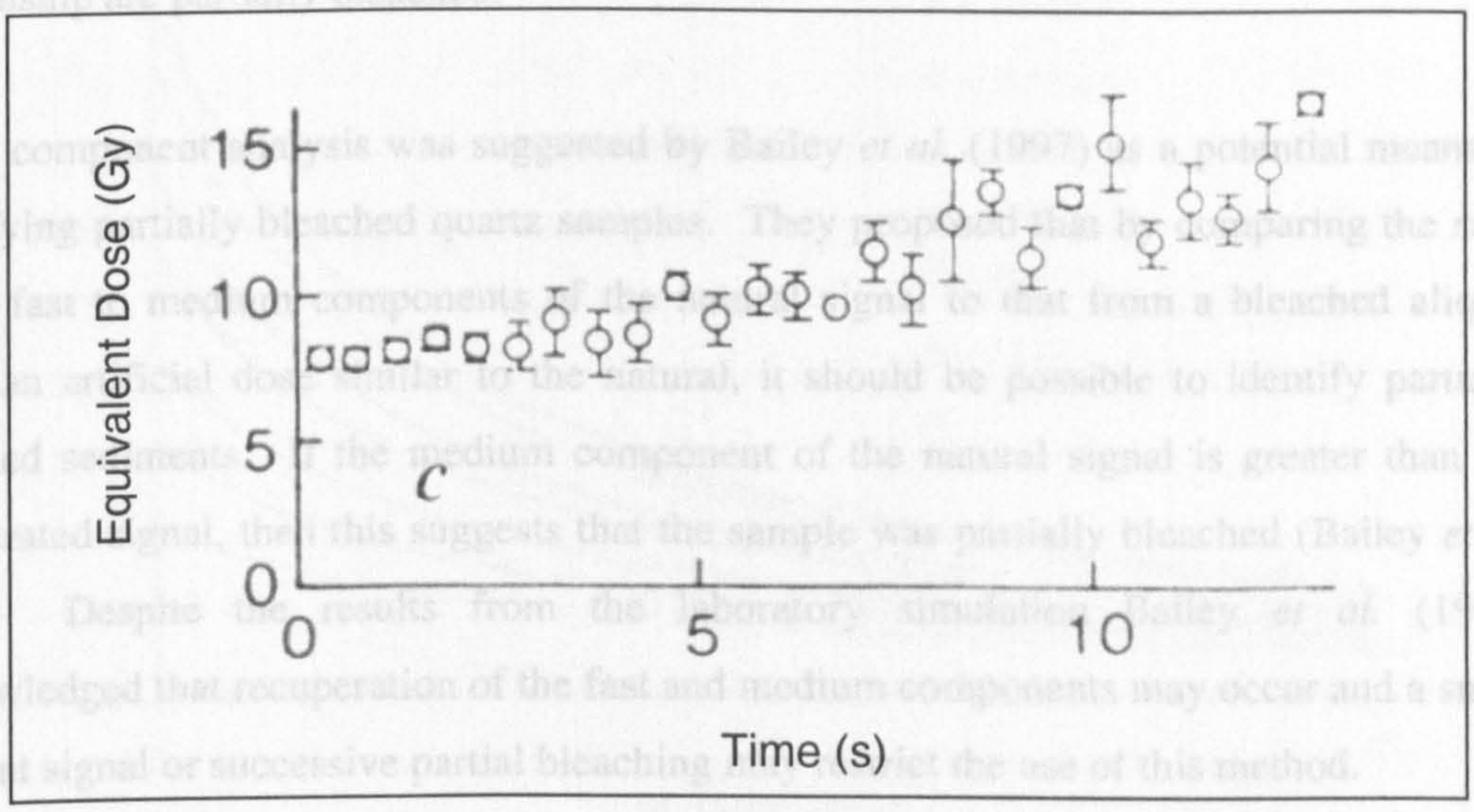

Figure 4.13 – Rise in D_e with stimulation time indicating partial bleaching for a modern beach sand (after Huntley *et al.* 1985).

thought to be uniformly bleached, whereas those that do show a statistically significant relationship are partially bleached.

Signal component analysis was suggested by Bailey *et al.* (1997) as a potential means of identifying partially bleached quartz samples. They proposed that by comparing the ratio of the fast to medium components of the natural signal to that from a bleached aliquot given an artificial dose similar to the natural, it should be possible to identify partially bleached sediments. If the medium component of the natural signal is greater than the regenerated signal, then this suggests that the sample was partially bleached (Bailey *et al.* 1997). Despite the results from the laboratory simulation Bailey *et al.* (1997) acknowledged that recuperation of the fast and medium components may occur and a small remnant signal or successive partial bleaching may restrict the use of this method.

A potential new method to identify partially bleached samples is proposed below using the shapes of the natural and regenerated feldspar decay curves to determine if a sample has been well bleached prior to burial. The method was initially applied to the F1 feldspar, archaeological sands and modern beach sands used in the bleaching experiments because they had been exposed for known periods of time and were therefore known to be partially bleached. Subsequently the method was applied to the archaeological samples.

4.5.2 Methodology

The changes in shape of the feldspar decay curve with increasing exposure to light are complex as a result of the many processes and trapping states involved, but it can be suggested that it will be similar to decay curves produced from the measurement of an aliquot that has had various doses added to it (e.g. Figure 4.14, Lang and Wagner 1997). For these reasons the terminology of 'short' (fast and medium) and 'long' associated with the various components of the quartz decay curve (Smith and Rhodes 1994) cannot be readily applied to feldspar data. Bleaching experiments by Krause *et al.* (1997) on feldspar from lake sediments in East Antarctica demonstrated that the 560 nm and 280 nm emission peaks were rapidly bleached by exposure to daylight and that a small residual remained within the 330 and 410 nm emission bands after 3 minutes of exposure. Although it cannot be assumed that the feldspar used in this experiment will behave in an identical manner, it does indicate that some traps in feldspar have a higher decay rate than others.

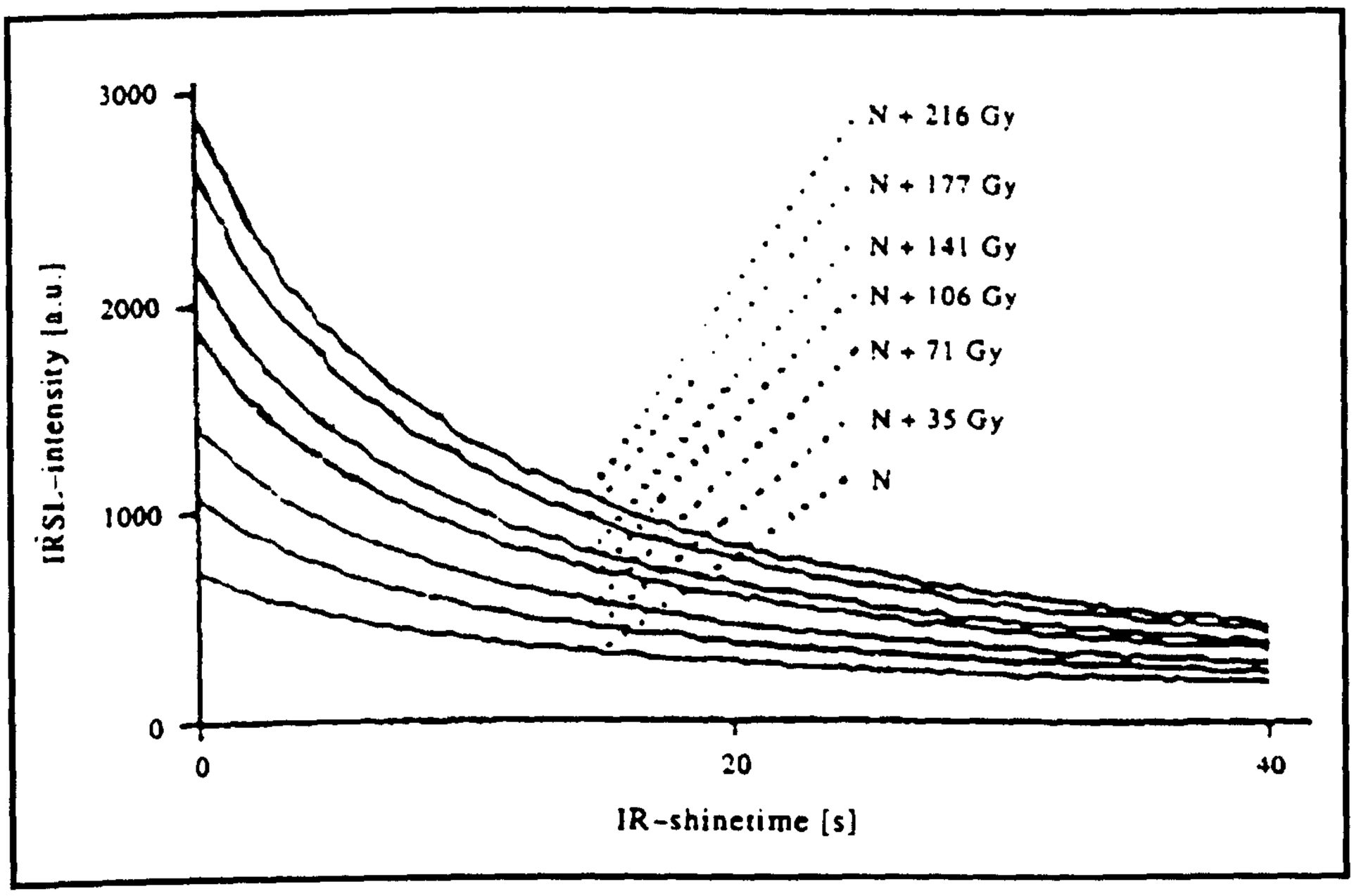

Figure 4.14 – The change in decay shape of feldspar with increasing dose (after Lang and Wagner 1997).

Figure 4.15a and b shows the decay curves obtained from the bleaching experiments undertaken on F1 feldspar using IRSL and post-IR blue stimulation. Each curve has been normalised to the 1st channel of optical stimulation and so the curves are comparable when plotted. As the bleaching time increases, the shape of the F1 feldspar decay curve becomes flatter for both IR and post-IR blue stimulation (reassuringly similar to that observed by Bailey *et al.* (1997)) due to the lower decay rate of some of the components. If the sample is only partially bleached prior to burial, the signal will be rich in these low decay rate signal components.

The contribution of signals with a low decay rate to the F1 feldspar signal stimulated by IR or post-IR blue can be determined by comparing the shape of the bleached or 'natural' decay curve to that of the unbleached or regenerated signal. Subtracting the normalised unbleached curve from the normalised natural curve isolates the amount of signal from the low decay rate components contributing to the natural signal (Figure 4.16a and b). The F1 feldspar net low decay rate results are shown in Figure 4.17a and b. As the exposure time increases, the high decay rate components are rapidly depleted and the low decay rate components become an increasingly important component in the overall OSL signal. The proportion of low decay rate traps contributing to the natural OSL signal for each curve can then be quantified by calculating the psi (ψ) ratio using:

$$\psi = \left(\frac{C}{A}\right)$$

where C is the area of the low decay rate signal (or long term component in quartz) determined by the sum of the normalised net signal after subtraction of the unbleached curve from the natural curve and A is the area of the complete natural decay curve as illustrated in Figure 4.18.

To see whether these concepts were promising as a simple means of identifying partially bleached signals from complex decay curves, the data from controlled bleaching experiments have been examined and psi ratios calculated as a function of bleaching time. When the ψ ratio of the F1 feldspar is plotted against bleaching time there is an increase in the ratio with increased bleaching time when IRSL or post-IR blue OSL is used for stimulation (Figure 4.19). An increase in the ψ ratio is expected as the proportion of the low decay rate signal contributing to the OSL signal increases. Both the IR and post-IR blue ψ ratios start to decrease at longer bleaching periods and this may be due to low signal levels and background noise creating scatter. The post-IR blue OSL ψ ratio continues to

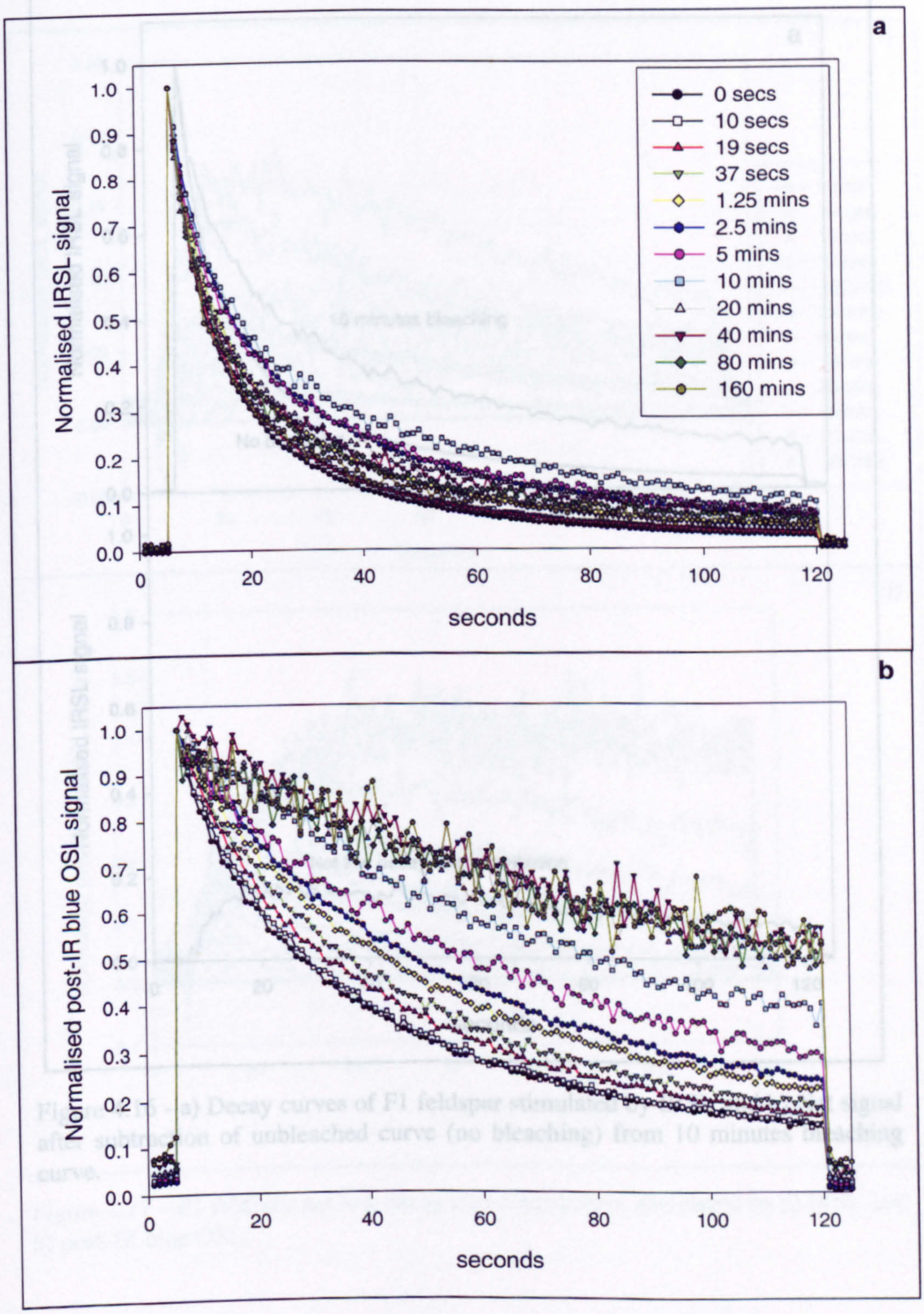

Figure 4.15 – F1 feldspar decay curves as a function of bleaching, stimulated by a) IRSL and b) post-IR blue OSL

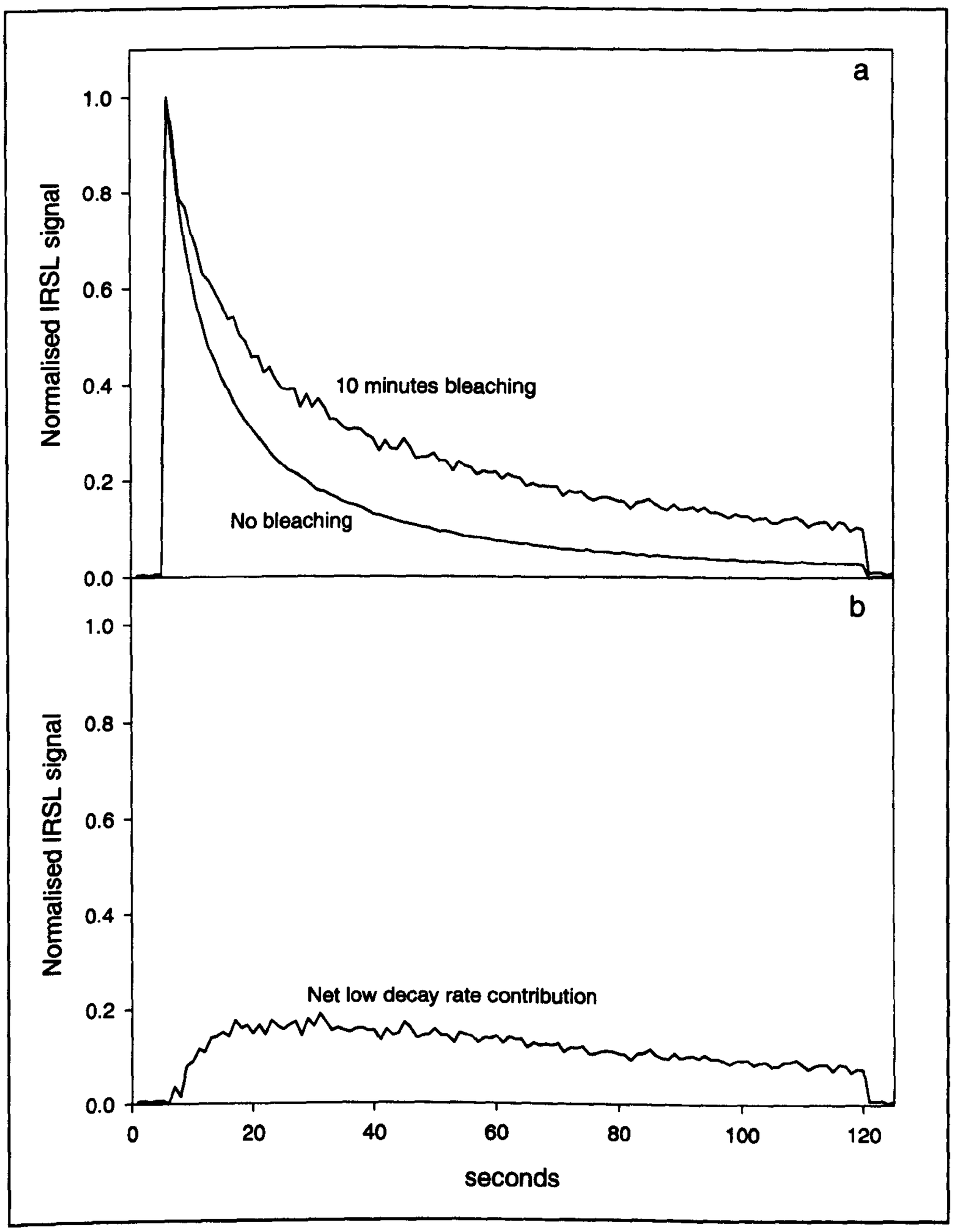

Figure 4.16 - a) Decay curves of F1 feldspar stimulated by IRSL and b) Net signal after subtraction of unbleached curve (no bleaching) from 10 minutes bleaching curve.

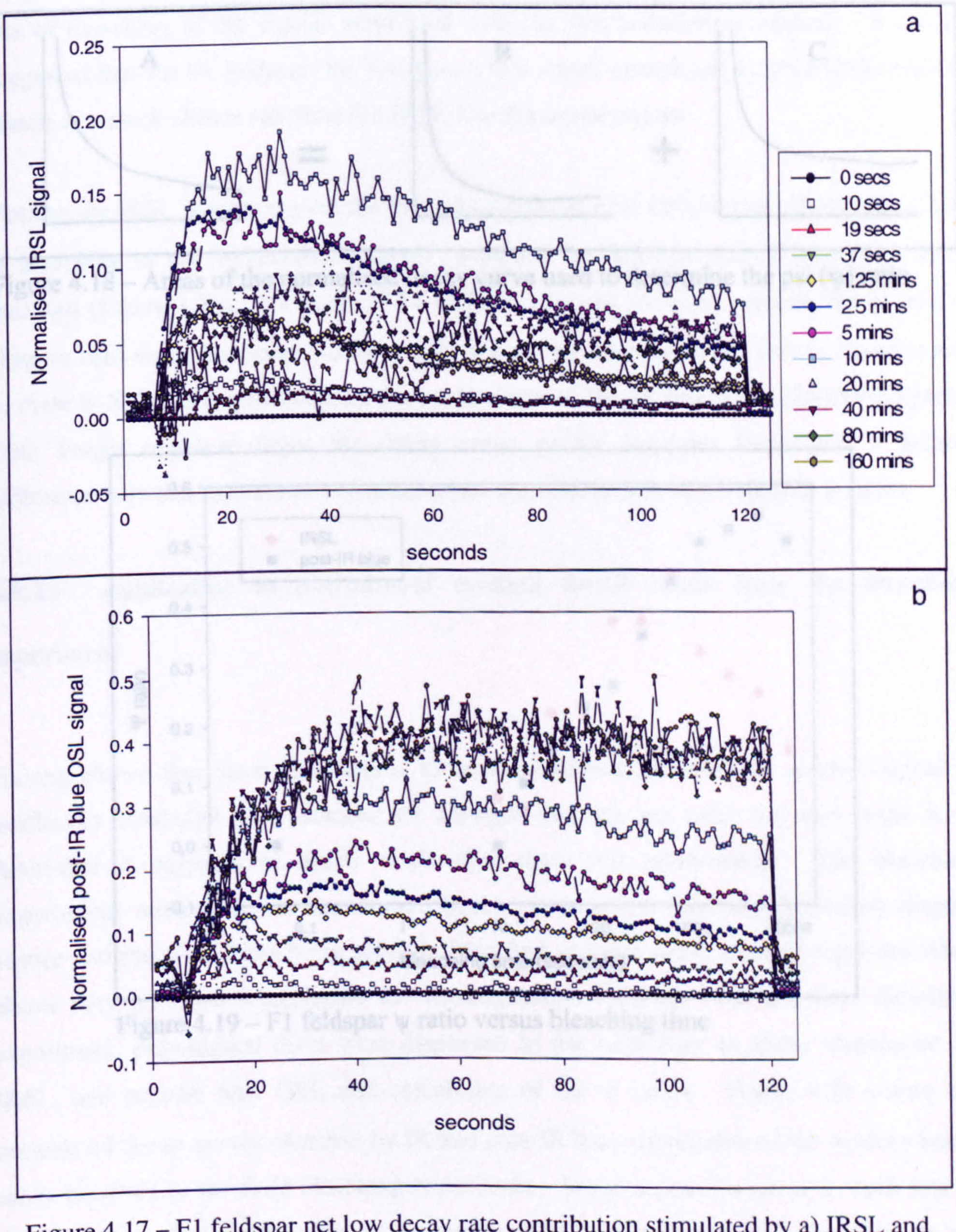

Figure 4.17 – F1 feldspar net low decay rate contribution stimulated by a) IRSL and b) post-IR blue OSL.

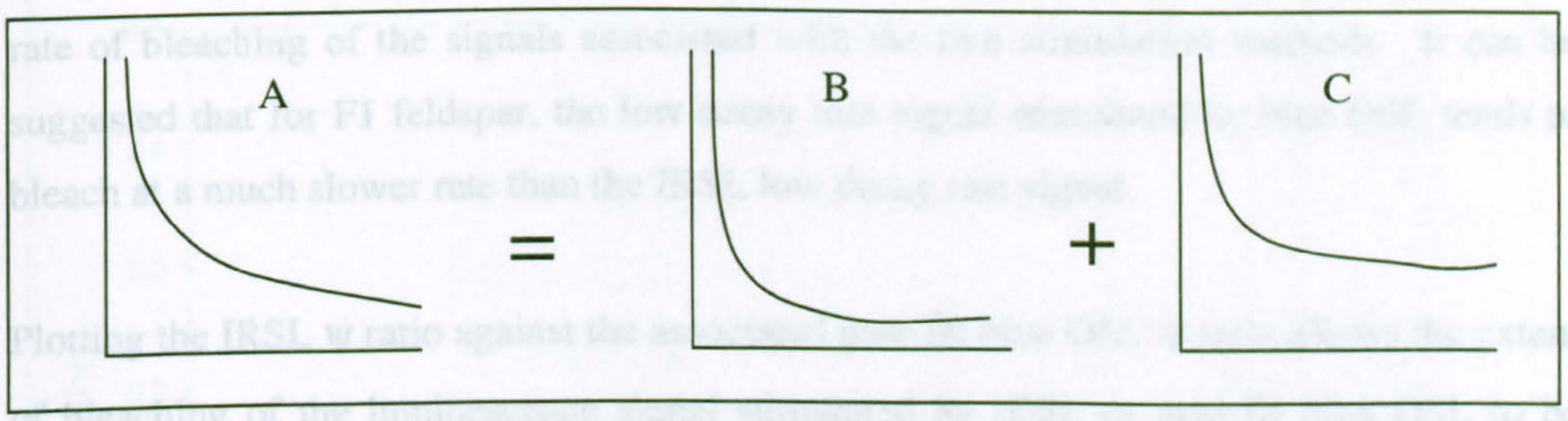

Figure 4.18 – Areas of the normalised decay curve used to determine the psi (ψ) ratio

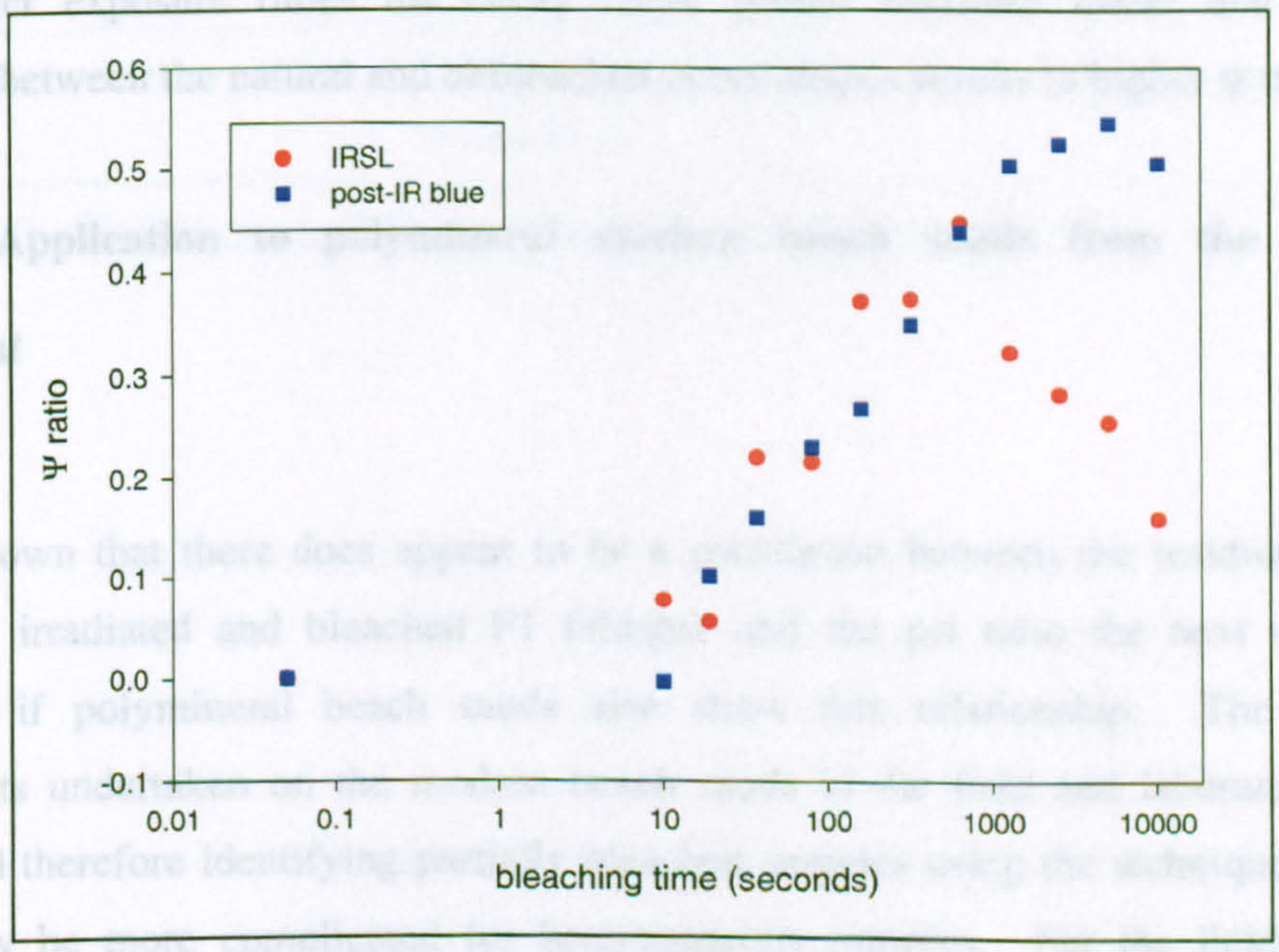

Figure 4.19 – F1 feldspar ψ ratio versus bleaching time

increase long after the IRSL ψ ratio has reached low signal levels and this may reflect the rate of bleaching of the signals associated with the two stimulation methods. It can be suggested that for F1 feldspar, the low decay rate signal stimulated by blue OSL tends to bleach at a much slower rate than the IRSL low decay rate signal.

Plotting the IRSL ψ ratio against the associated post-IR blue OSL ψ ratio allows the extent of bleaching of the luminescence signal stimulated by IRSL or post-IR blue OSL to be analysed (Figure 4.20). For discs of F1 feldspar exposed for short periods, the ψ ratio is close to zero since the decay curves are dominated by the high decay rate component and so there is little difference between the curve shape of the natural and regenerated signals. With longer exposure times the decay curve profile becomes flatter and a greater difference between the natural and unbleached curve shapes results in higher ψ ratios.

4.5.2.1 Application to polymineral modern beach sands from the bleaching experiment

Having shown that there does appear to be a correlation between the residual signal in artificially irradiated and bleached F1 feldspar and the psi ratio the next stage is to determine if polymineral beach sands also show this relationship. The bleaching experiments undertaken on the modern beach sands in the field and laboratory display scatter and therefore identifying partially bleached samples using the technique described above may be more complicated for heterogeneous samples. For the field bleaching experiment, polymineral discs were dispensed in the laboratory to allow stimulation by IRSL, and post-IR blue OSL and calculation of the ψ ratios. Figure 4.21 shows the normalised decay curves obtained by IR and post-IR blue stimulation of the modern beach sands involved in the field bleaching experiment. Some anomalies occur in both sets of decay curves. For example the decay curves of the aliquots bleached for 24 hours are flatter than the aliquots bleached for longer periods of time. This is likely to be due to the light intensity varying throughout the field bleaching experiment as a result of changing weather conditions. Apart from these the main trends are similar to the F1 feldspar, with the shape of the decay curves flattening with increased exposure time.

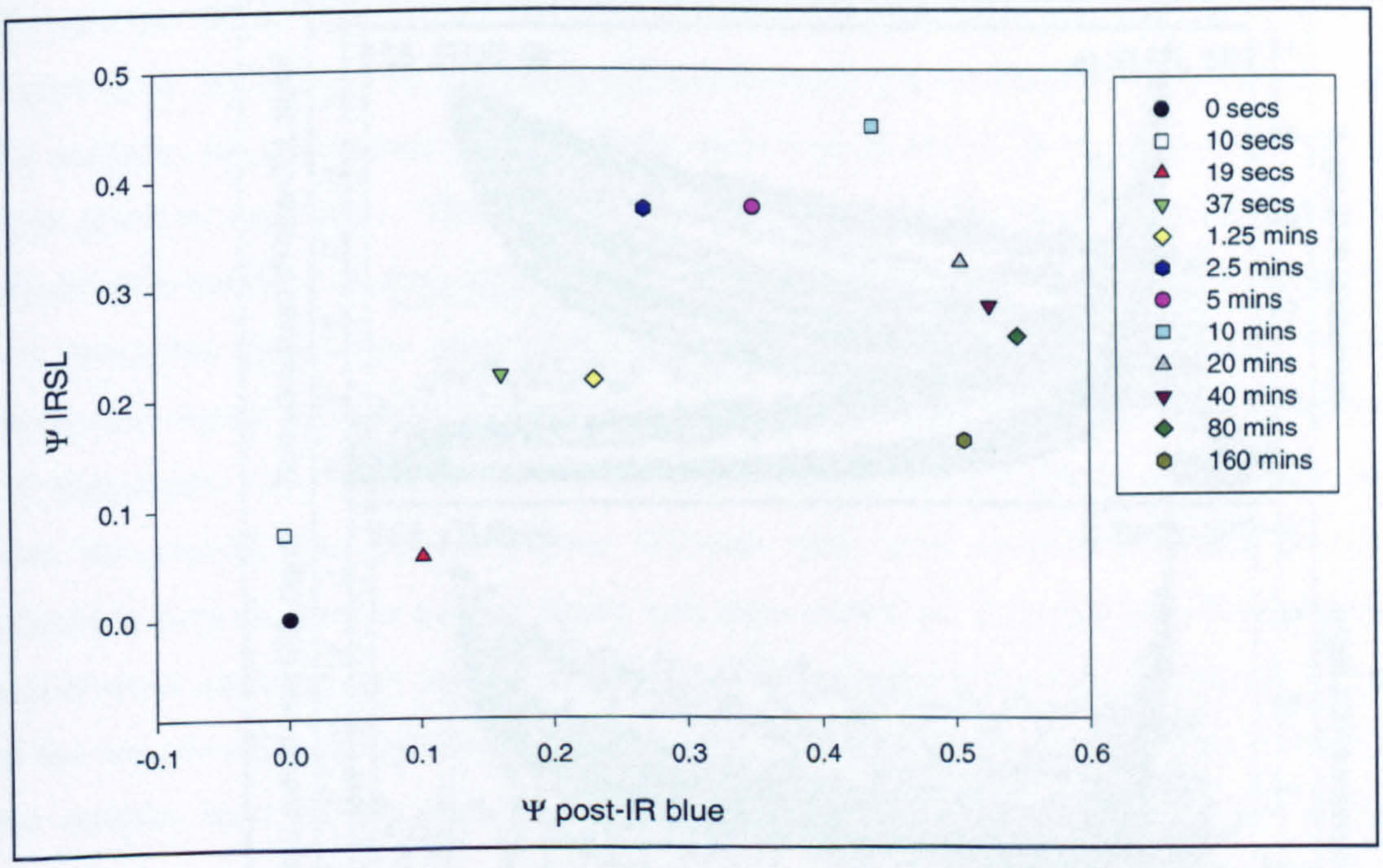

Figure 4.20 – F1 feldspar ψ IRSL ratio versus ψ post-IR blue OSL ratio

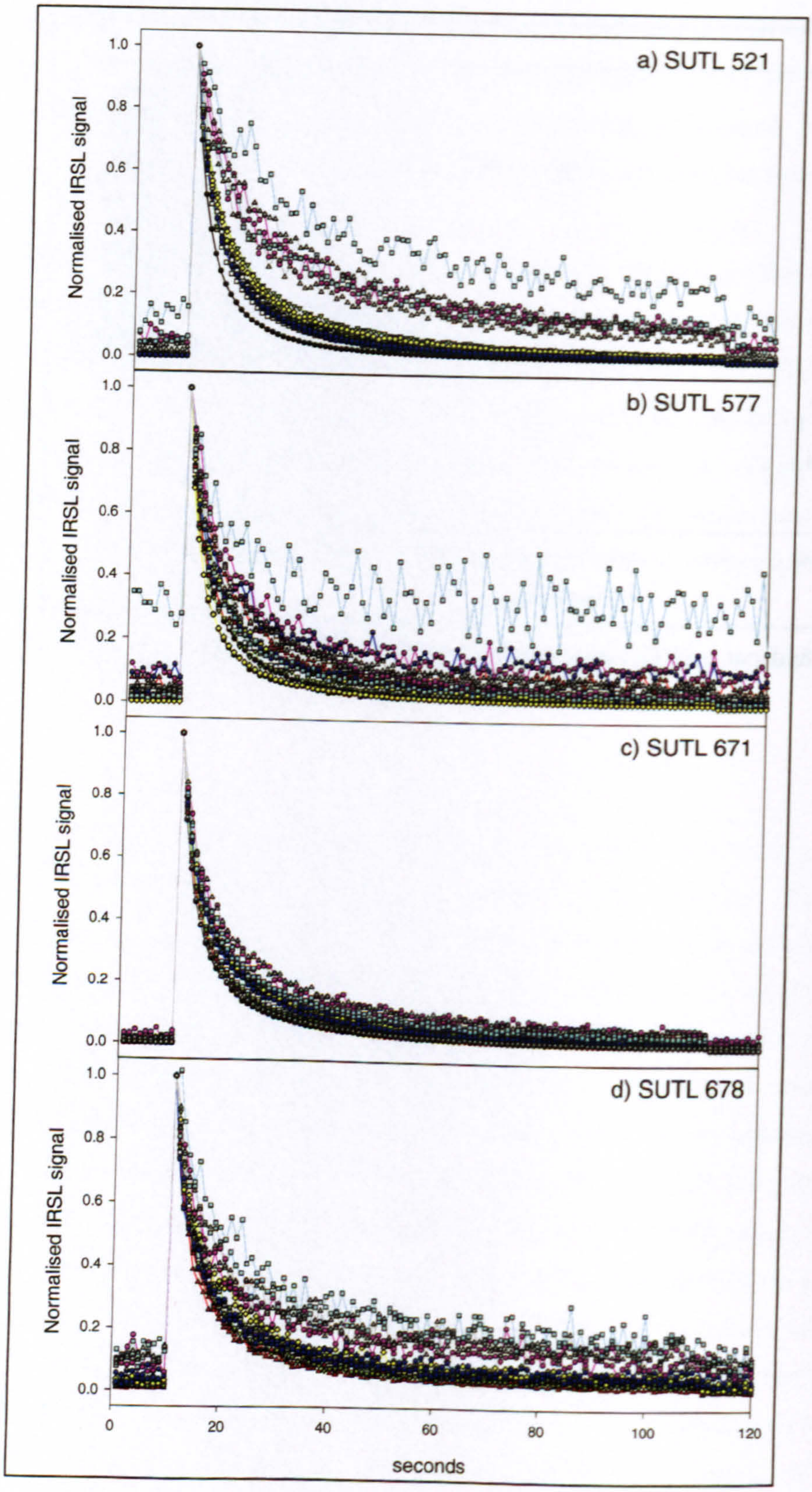
a) SUTL 521
b) SUTL 577
c) SUTL 671
d) SUTL 678
Normalised IRSL signal
1.0
0.8
0.6
0.4
0.2
0.0
0
20
40
60
80
100
120
seconds

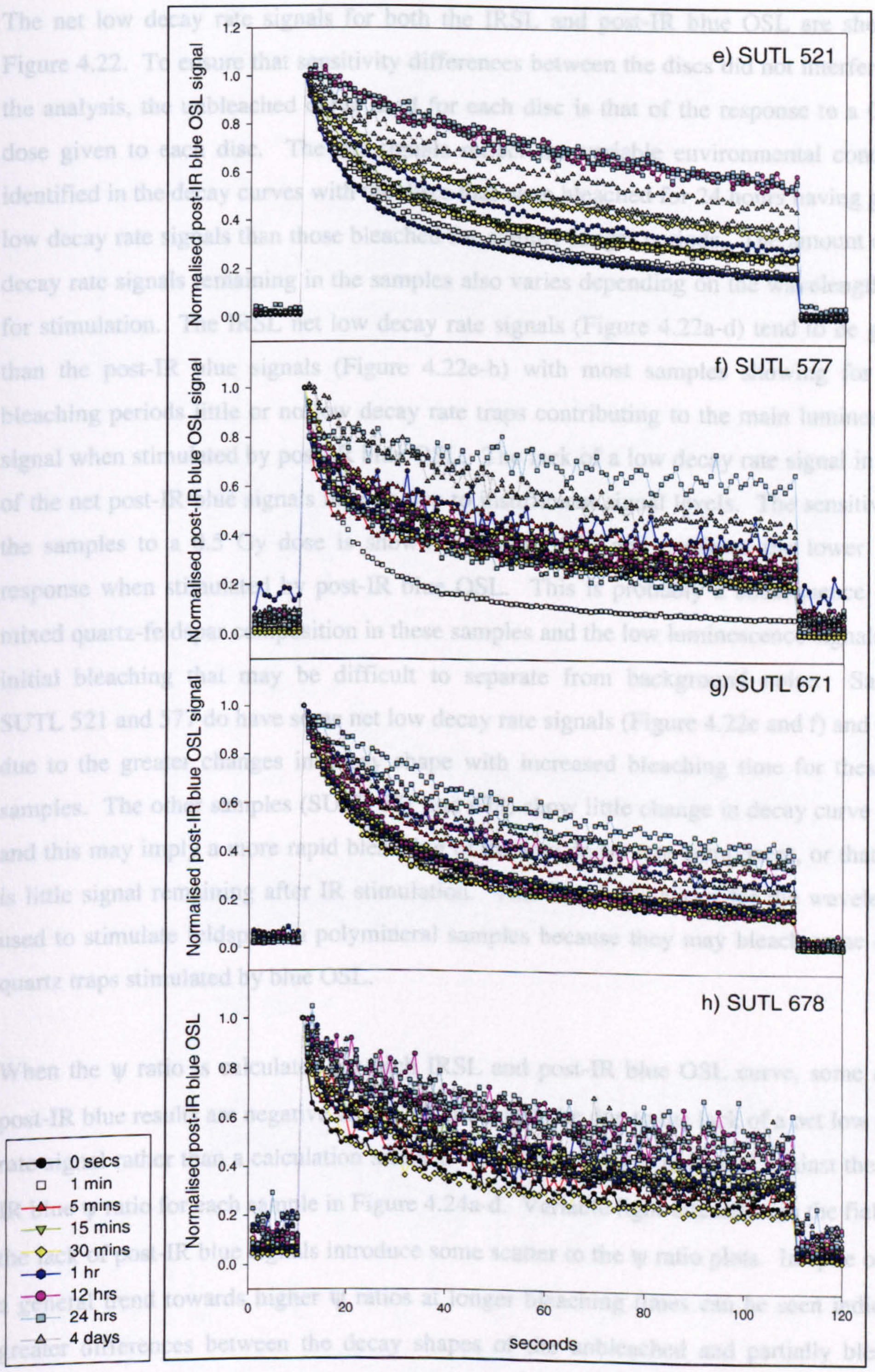

Figure 4.21 – Normalised decay curves of polymineral modern beach sand from field bleaching experiment – a-d – stimulated by IRSL and e-h – stimulated by post-IR blue OSL

The net low decay rate signals for both the IRSL and post-IR blue OSL are shown in Figure 4.22. To ensure that sensitivity differences between the discs did not interfere with the analysis, the unbleached curve used for each disc is that of the response to a 0.5 Gy dose given to each disc. The net signals reflect the variable environmental conditions identified in the decay curves with the discs that were bleached for 24 hours having greater low decay rate signals than those bleached for slightly longer periods. The amount of low decay rate signals remaining in the samples also varies depending on the wavelength used for stimulation. The IRSL net low decay rate signals (Figure 4.22a-d) tend to be greater than the post-IR blue signals (Figure 4.22e-h) with most samples showing for some bleaching periods little or no low decay rate traps contributing to the main luminescence signal when stimulated by post-IR blue OSL. The lack of a low decay rate signal in many of the net post-IR blue signals may be due to insufficient signal levels. The sensitivity of the samples to a 0.5 Gy dose is shown in Figure 4.23 and confirms the lower signal response when stimulated by post-IR blue OSL. This is probably a consequence of the mixed quartz-feldspar composition in these samples and the low luminescence signals after initial bleaching that may be difficult to separate from background noise. Samples SUTL 521 and 577 do have some net low decay rate signals (Figure 4.22e and f) and this is due to the greater changes in decay shape with increased bleaching time for these two samples. The other samples (SUTL 671 and 678) show little change in decay curve shape and this may imply a more rapid bleaching of the low decay rate component, or that there is little signal remaining after IR stimulation. This has implications for the wavelengths used to stimulate feldspars in polymineral samples because they may bleach some of the quartz traps stimulated by blue OSL.

When the ψ ratio is calculated for each IRSL and post-IR blue OSL curve, some of the post-IR blue results are negative and this is thought to be due to the lack of a net low decay rate signal rather than a calculation artefact. The IRSL ψ ratio is plotted against the post-IR blue ψ ratio for each sample in Figure 4.24a-d. Variable light intensities in the field and the lack of post-IR blue signals introduce some scatter to the ψ ratio plots. In spite of this, a general trend towards higher ψ ratios at longer bleaching times can be seen indicating greater differences between the decay shapes of the unbleached and partially bleached aliquots. This observation confirms that the psi ratio concept appears to be applicable to mixed mineralogy samples and natural bleaching intensities and that it may therefore be useful in assessing real samples. The technique can potentially be utilised in two ways.

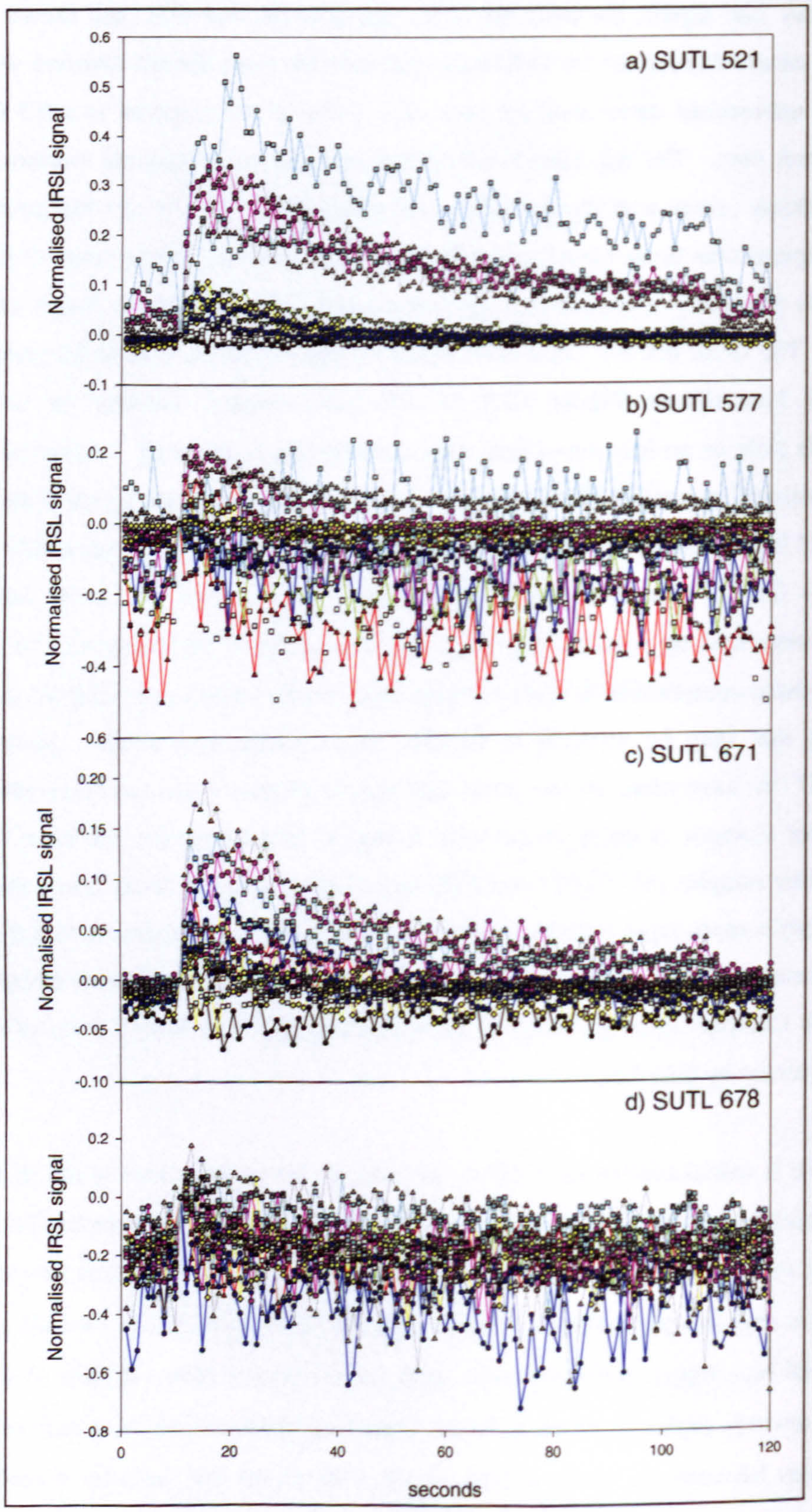
a) SUTL 521
b) SUTL 577
c) SUTL 671
d) SUTL 678
Normalised IRSL signal
seconds
0
20
40
60
80
100
120

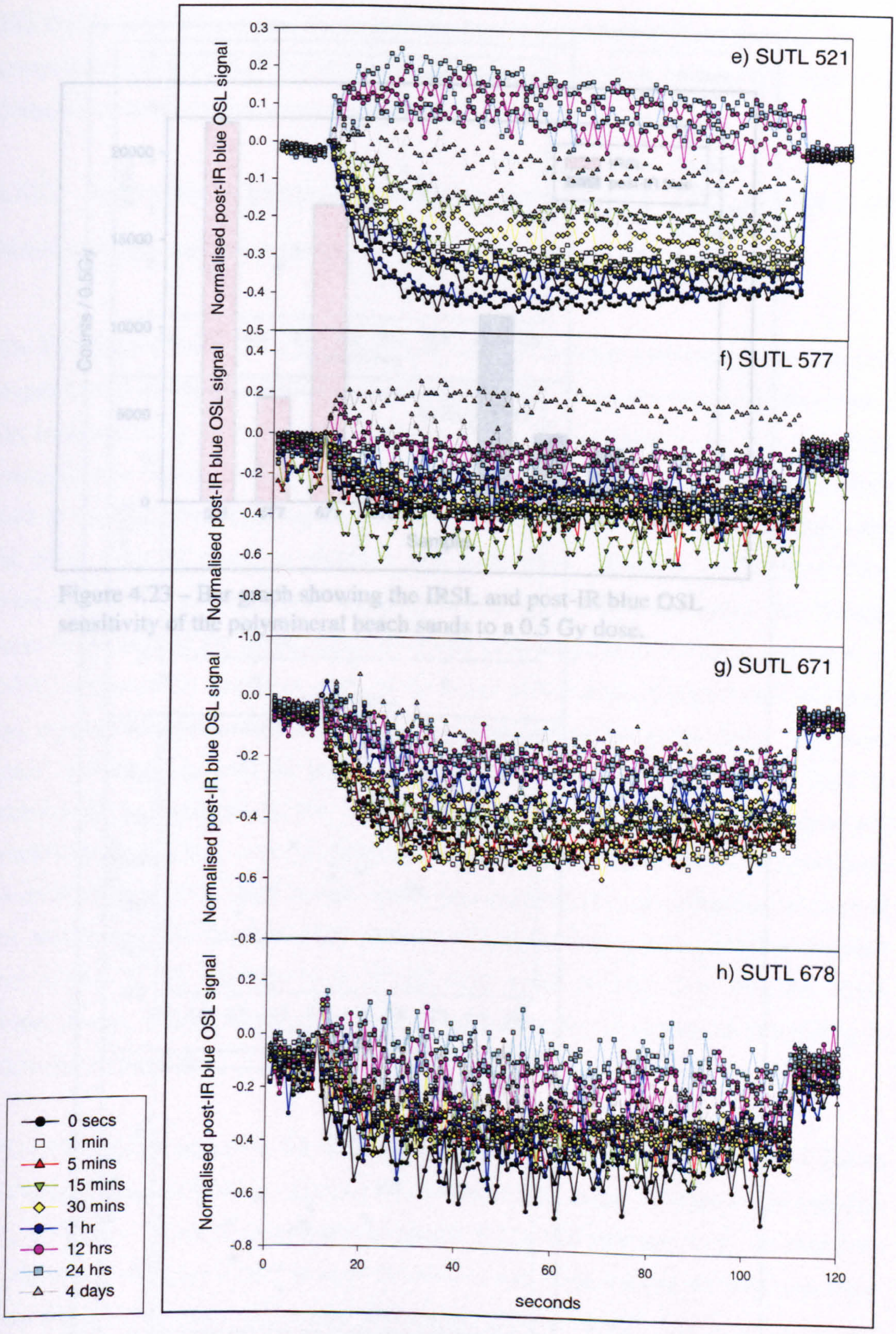

Figure 4.22 – Net low decay rate signals of polymineral beach sand from field bleaching experiment – a-d – stimulated by IRSL and e-h – stimulated by post-IR blue OSL

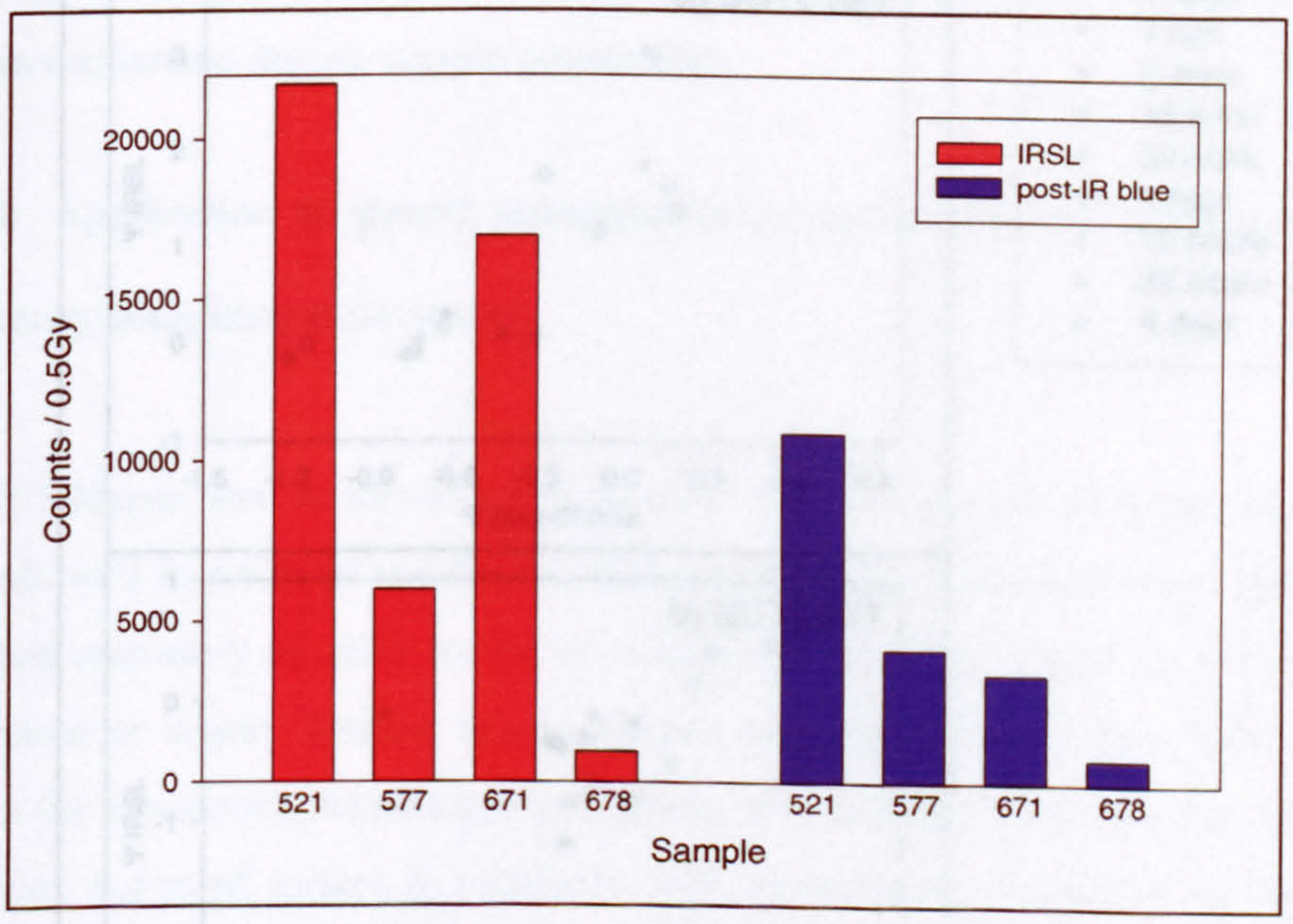

Figure 4.23 – Bar graph showing the IRSL and post-IR blue OSL sensitivity of the polymineral beach sands to a 0.5 Gy dose.

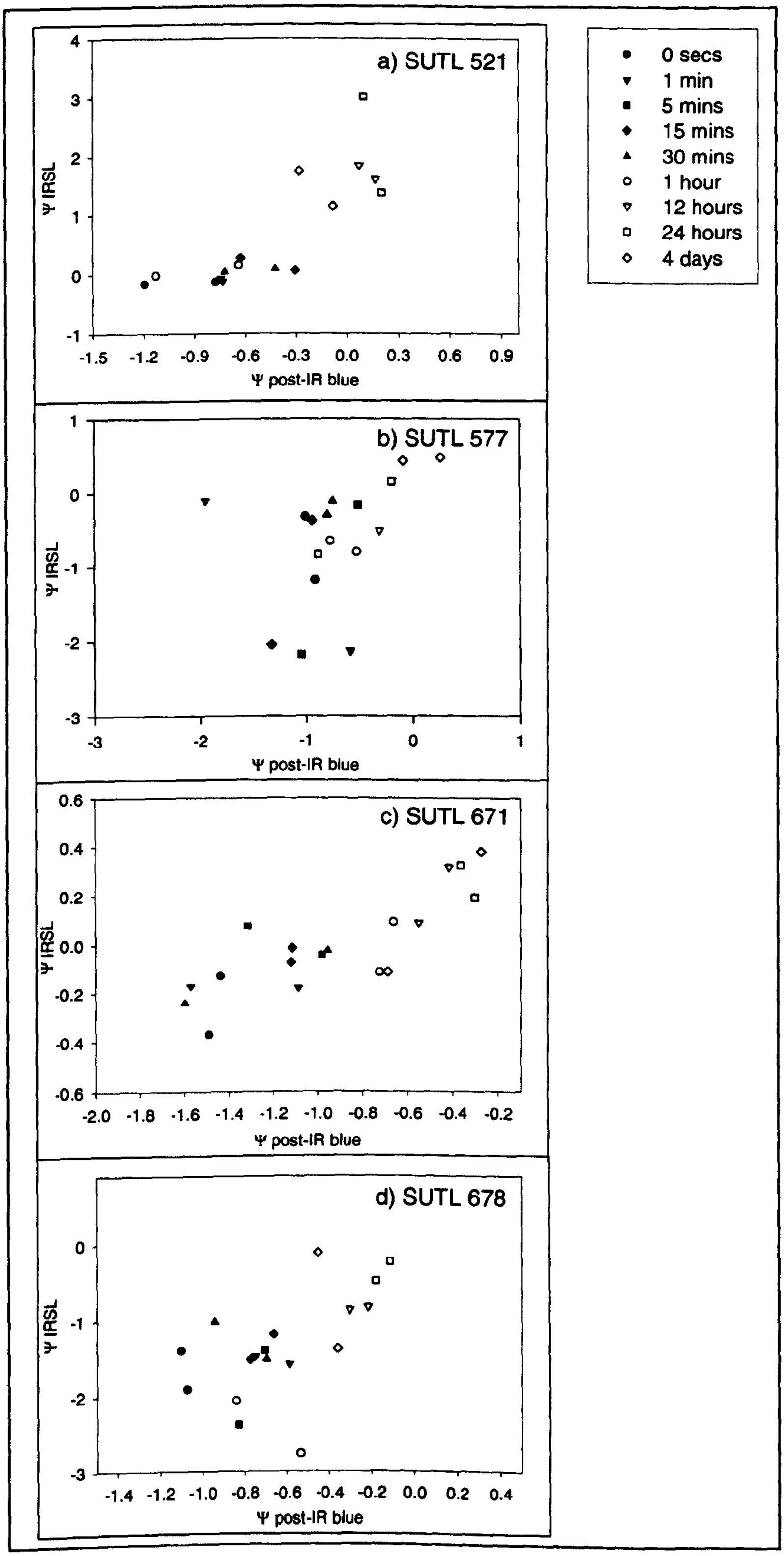

Figure 4.24 – Polymineral beach sand from the field bleaching experiment ψ IRSL ratio versus ψ post-IR blue OSL ratio

The first is to try it on quartz; however there may be a problem with the fast and medium components being too fast and the second is to use the psi ratio technique on associated feldspars separated during sample preparation.

4.5.2.2 Application to quartz separated from archaeological sands and used in the laboratory bleaching experiment

The F1 feldspar used in the experiments and analysis above is a homogenous sample that responds well to artificial irradiation, however there are numerous traps in feldspar and it has been necessary to refer to the unbleached part of the signal as the low decay rate component or signal. Testing this technique using quartz from the archaeological sands used in the laboratory bleaching experiments, also homogenous, was also attempted since the decay curve of quartz is relatively well understood. Research on the decay form characteristics of the quartz OSL signal by Bailey *et al.* (1997) has shown that changes occur in the shape of the quartz decay curve with increasing exposure to light. Bailey *et al.* (1997) attributed the change in shape of the decay curves to the different rates of charge loss associated with the short and long term components of the quartz signal. The terms 'short' and 'long' are used for quartz in this section to describe the 'easy' and 'hard' to bleach traps, or 'fast/medium' and 'slow' components associated with the OSL signal and follows the terminology used by Smith and Rhodes (1994). Due to sensitivity variations between aliquots of the same sample, rather than compare the unbleached decay curve of one aliquot with the bleached decay curve of others, the unbleached curve used for each disc is that of the response to a 15 Gy dose given to each disc after the initial measurements. Again both signals were normalised to the 1st channel of stimulation to allow easy comparison.

The quartz OSL decay curves for the archaeological samples SUTL 605 and 623 are shown in Figure 4.25a and b and as expected the curves become flatter in shape as the exposure time increases. There is some scatter in sample SUTL 623 reflected in the net long term signal shown in Figure 4.25d. Despite this there is still an increase in the long term signal contributing to the main OSL signal with longer exposure times. The ψ ratios for each sample are plotted against bleaching time in Figure 4.26a and b and the results are similar to the F1 feldspar results described above. Discs with low ψ ratios were exposed for short periods of time and are dominated by the short term component. Both samples show a

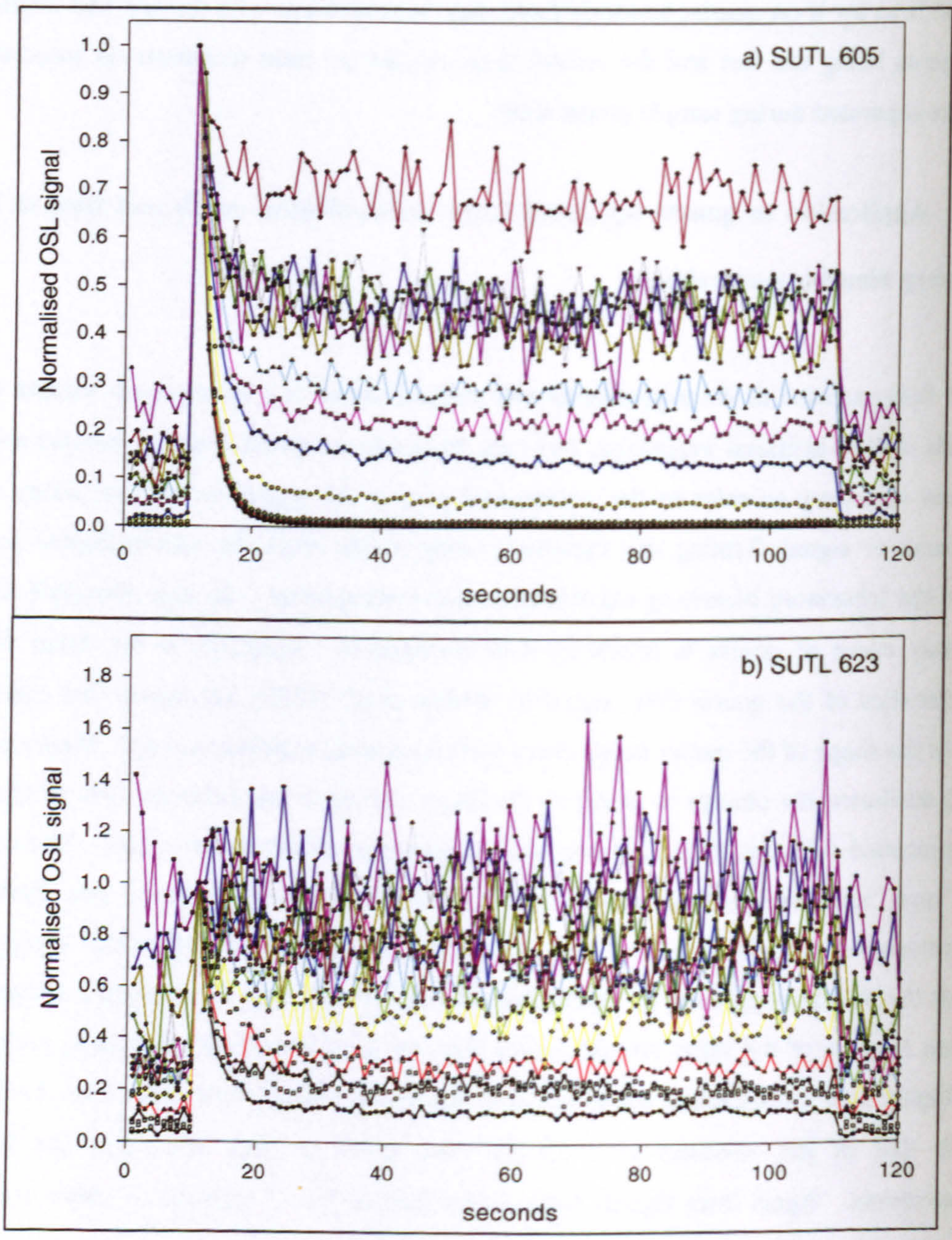
a) SUTL 605
Normalised OSL signal
1.0
0.9
0.8
0.7
0.6
0.5
0.4
0.3
0.2
0.1
0.0
0
20
40
60
80
100
120
seconds
b) SUTL 623
Normalised OSL signal
1.8
1.6
1.4
1.2
1.0
0.8
0.6
0.4
0.2
0.0
0
20
40
60
80
100
120
seconds

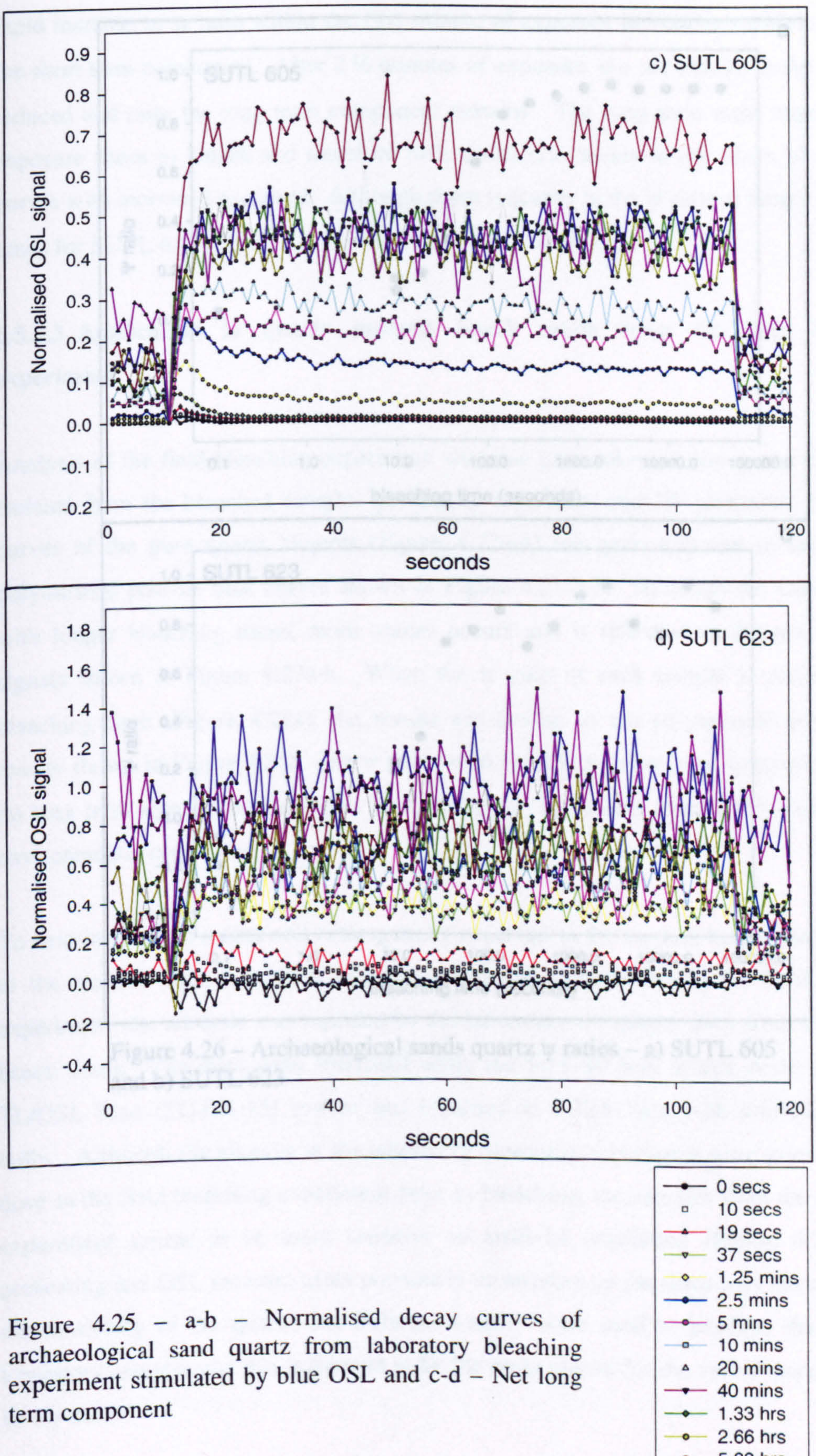

Figure 4.25 – a-b – Normalised decay curves of archaeological sand quartz from laboratory bleaching experiment stimulated by blue OSL and c-d – Net long term component

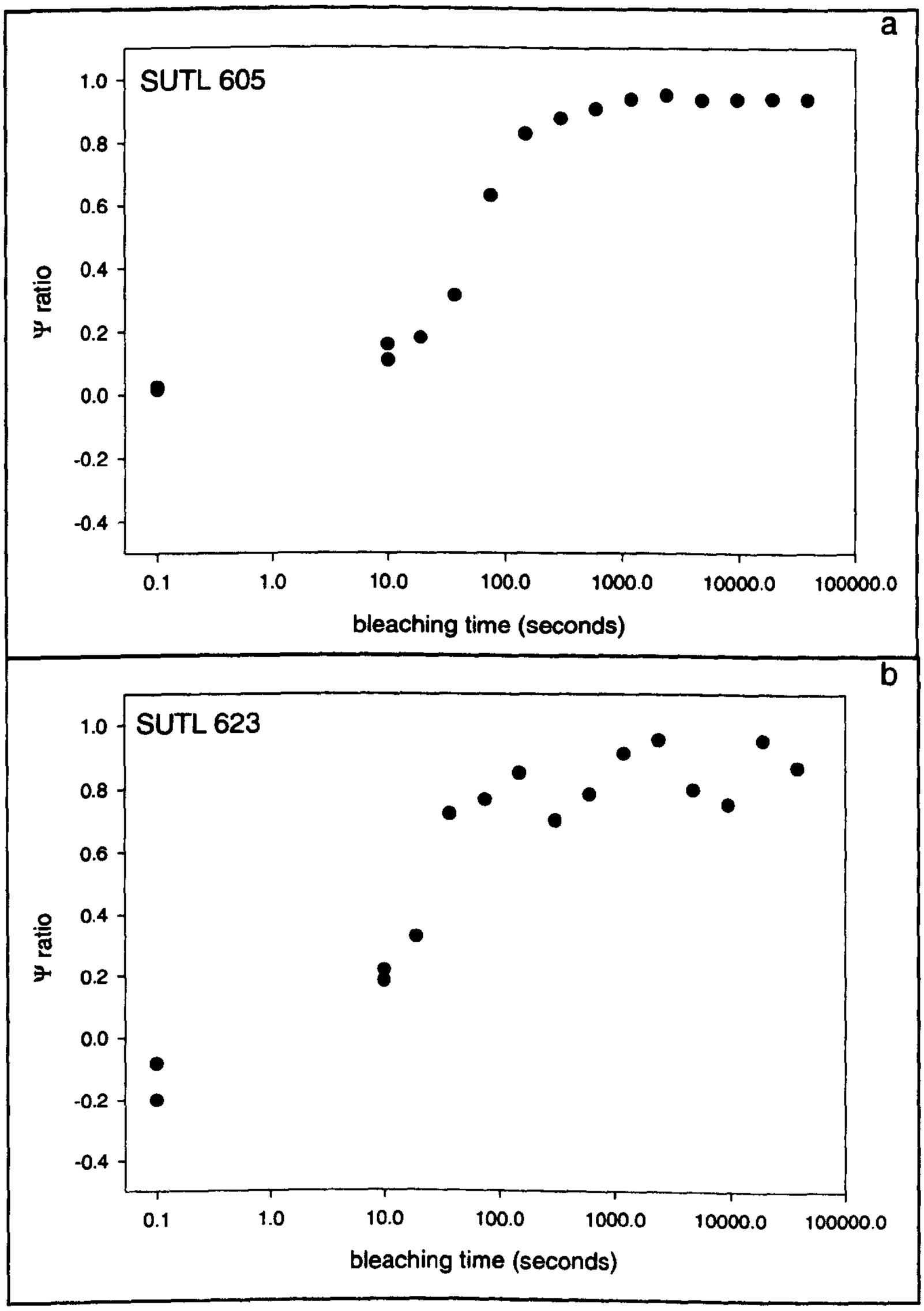

Figure 4.26 – Archaeological sands quartz ψ ratios – a) SUTL 605 and b) SUTL 623

rapid increase in ψ ratio within the first minute of exposure indicating rapid depletion of the short term component. After 2 ½ minutes of exposure, the net change in the ψ ratio is reduced and only the long term component remains. The long term traps require longer exposure times to bleach and therefore little difference occurs in the shape of the decay curves with increased exposure. Although there is scatter in the ψ ratio at longer bleaching times for SUTL 623 (Figure 4.26b), the trend is still increasing.

4.5.2.3 Application to quartz modern beach sands from the field bleaching experiment

Analysis of the field bleaching experiment was also undertaken on the quartz component isolated from the bleached samples by density separation and HF treatment. The decay curves of the pure quartz aliquots (Figure 4.27a-d) are quite different to those of the polymineral post-IR blue curves shown in Figure 4.21 e-h. Although the curves flatten with longer bleaching times, more scatter occurs and is reflected in the net long term signals shown in Figure 4.27e-h. When the ψ ratio of each sample is plotted against bleaching time (Figure 4.28a), the results are similar to the polymineral post-IR blue results shown in Figure 4.28b. The ψ ratios tend to remain below zero suggesting little or no long term signal contributing to the OSL signal, the scatter probably due to changing environmental conditions.

To determine if the scatter and heterogeneity observed in the modern beach sands was due to the variable light intensities experienced by the samples during the field bleaching experiment, the analysis was repeated in the laboratory on quartz discs from the modern beach sands. The discs were irradiated using the Sr/Y-90 beta source in the automated TL/OSL Riso (TL-DA-15) system and bleached in a light box with artificial daylight bulbs. Although the aliquots in the laboratory bleaching experiment were given the same dose as the field bleaching experiment prior to bleaching, the samples from the laboratory experiment appear to be more sensitive to artificial irradiation (Figure 4.29). The preheating and OSL measurements previously undertaken on the discs may have increased the sensitivity of the quartz, but different sources were used to irradiate the field and laboratory samples and this is thought to be the main reason for the varied response to the 15 Gy dose.

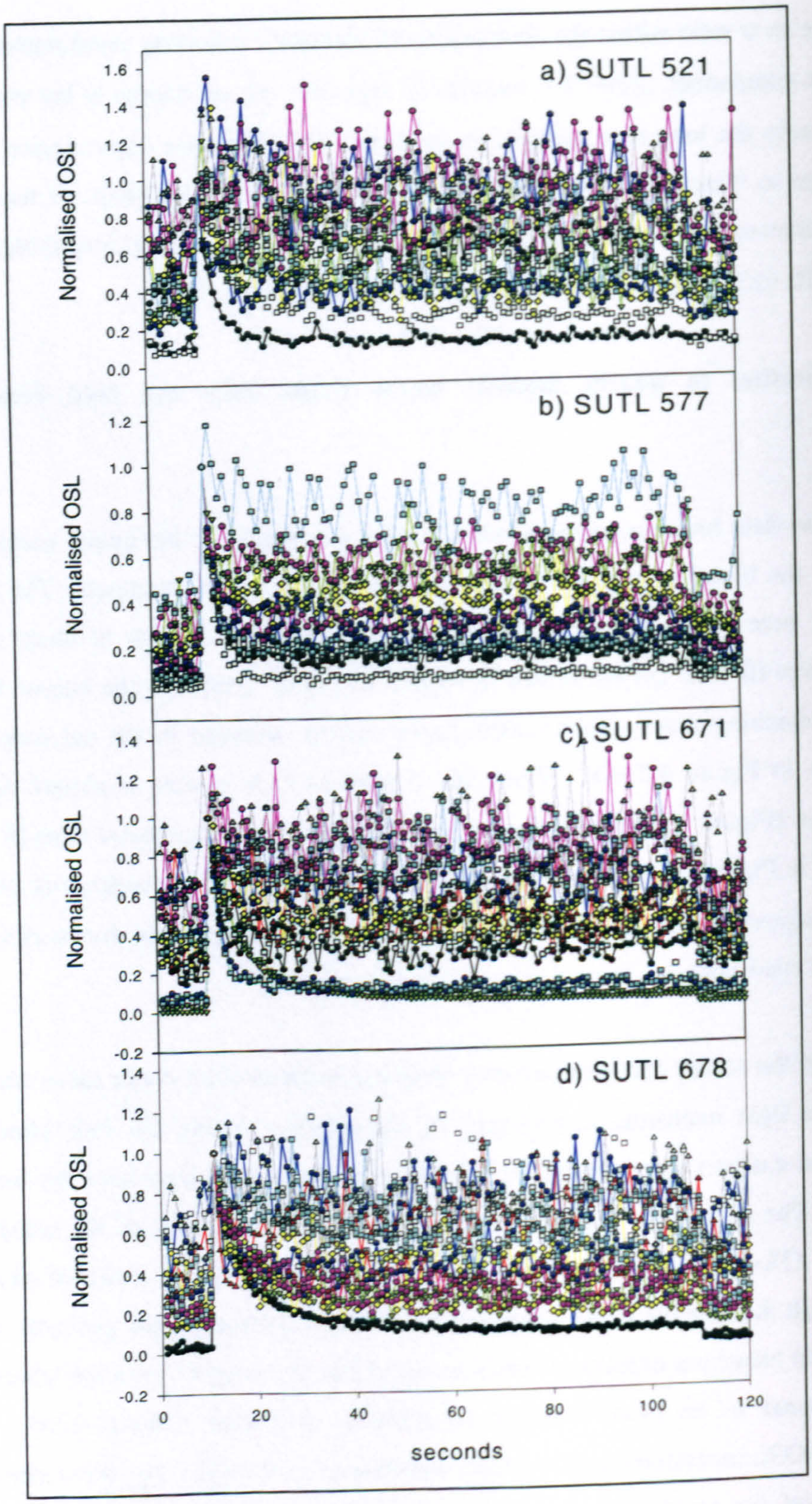
a) SUTL 521
b) SUTL 577
c) SUTL 671
d) SUTL 678
Normalised OSL
seconds
0
20
40
60
80
100
120

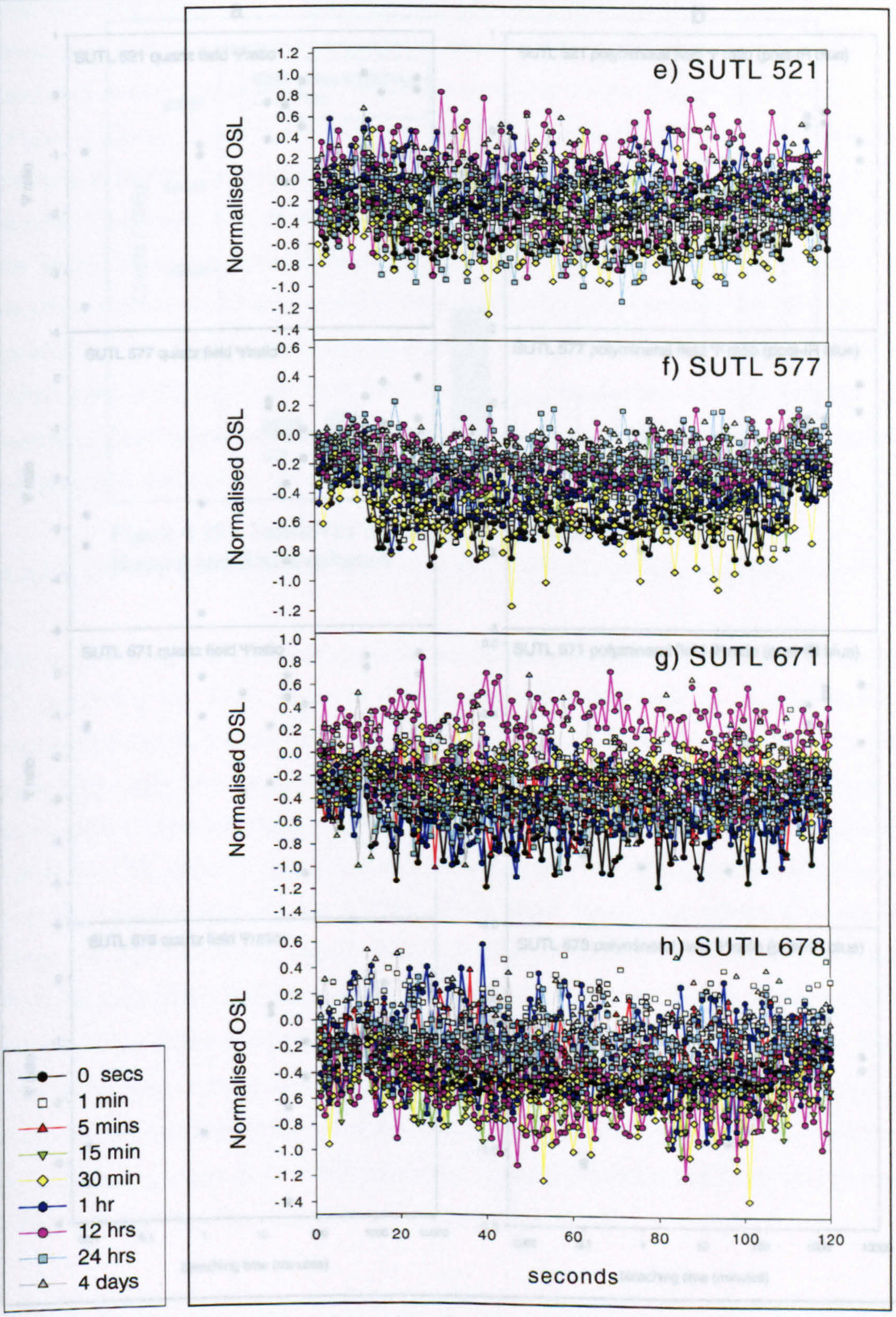

Figure 4.27 – Quartz modern beach sand from field bleaching experiment – a-d – normalised decay curves stimulated by blue OSL and e-h – the net long term component

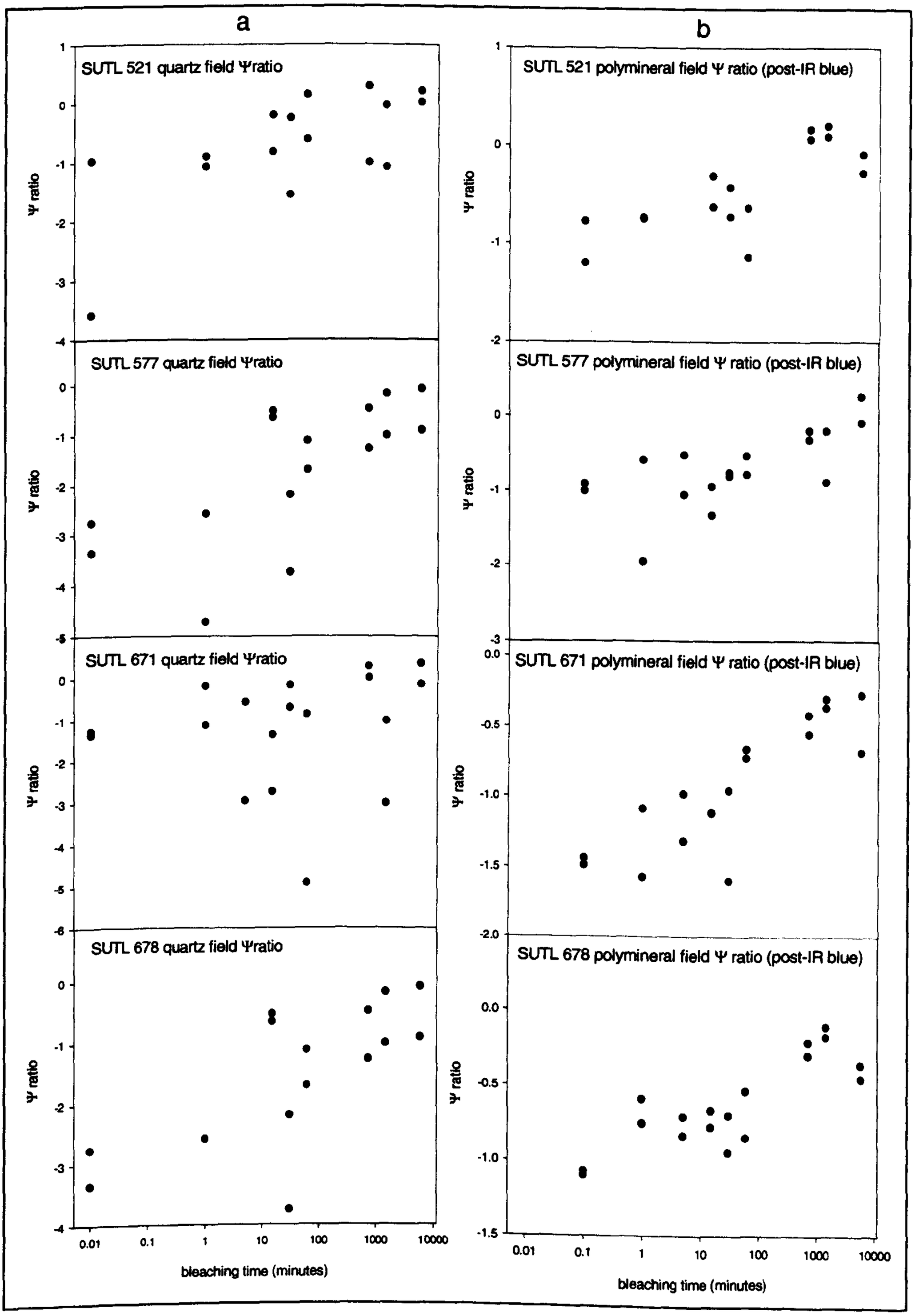

Figure 4.28 – Modern beach sand ψ ratios: a) quartz stimulated by blue OSL and b) polymineral stimulated by post-IR blue OSL

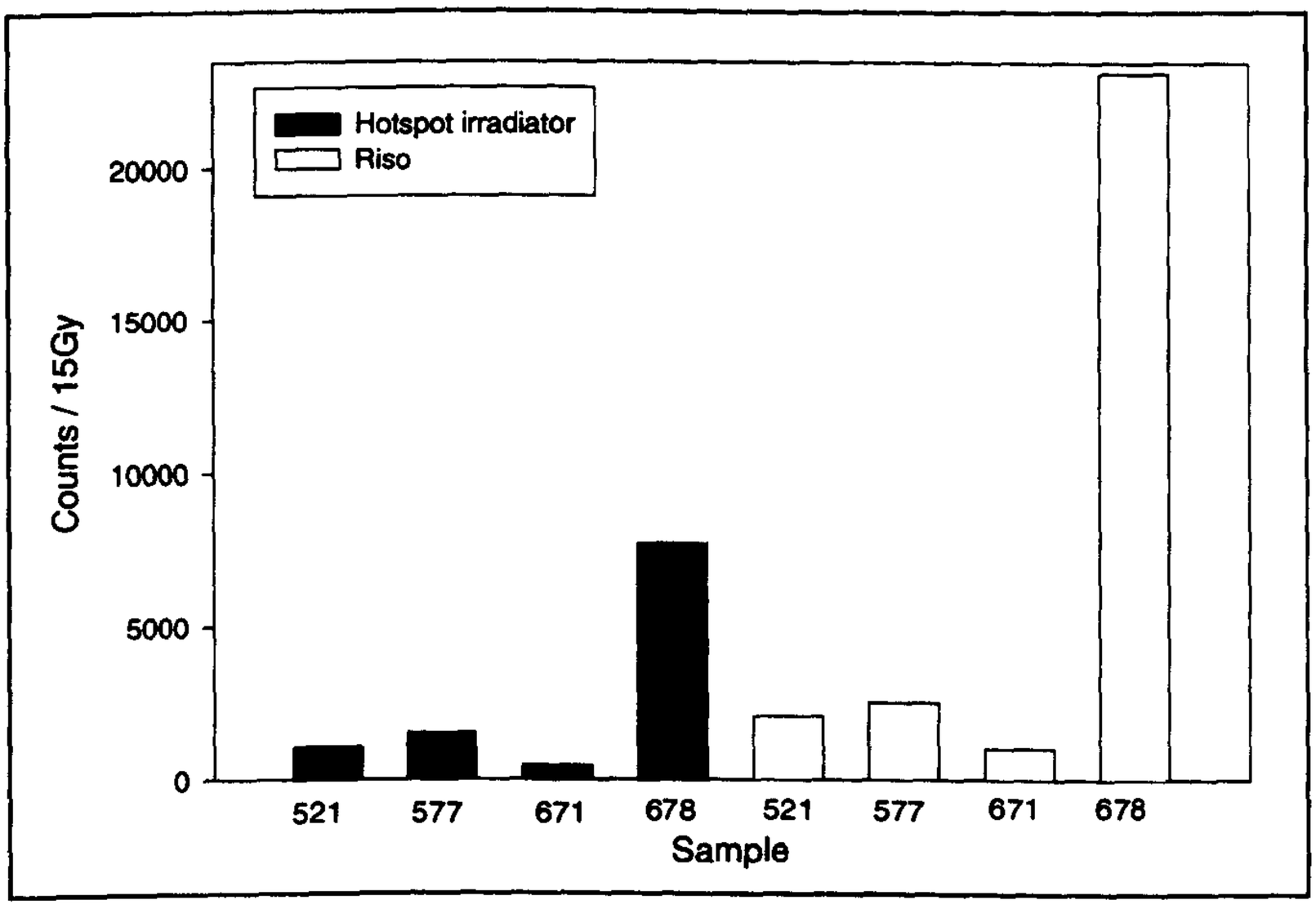

Figure 4.29 – Sensitivity of quartz from modern beach sands to the Hotspot and Riso irradiators

The bleaching times used in the laboratory bleaching experiment are much shorter than those used in the field and the greater light intensity of the artificial bulbs in the laboratory may also have contributed to the reduction in scatter in the shape of the decay curves (Figure 4.30a-d). It is suggested that the bleaching times used in the field may have been too long to register the rapid changes to the decay curve shape which occur within the first minute of exposure: a result identified from the laboratory bleaching experiment. Due to the shorter bleaching times, there is a greater difference in the decay curve shapes and therefore the amount of long term (or slow decay rate) contribution to the OSL signal is greater than that for the field bleaching experiment (Figure 4.30e-h). As a result, after the initial rapid depletion of the short term component, the ψ ratios show an increase with increased bleaching time (Figure 4.31). For three of the samples (SUTL 521, 577 and 678) the general increase in the ψ ratios are similar to the F1 feldspar experiment.

4.5.2.4 Summary of the psi (ψ) method used to identify partially bleached samples

The method described above shows that it is possible to identify partially bleached samples by comparing the decay shape of the natural signal with that of an unbleached or regenerated signal. Samples that are well-bleached prior to burial are characterised mainly by a high decay rate or short term component and have a decay shape similar to an unbleached or regenerated aliquot for that sample. If a sample is partially bleached prior to burial, the OSL signal is characterised by both high and low decay rate signals (short and long term components) and has a flatter decay curve due to contribution from the low decay rate (slow bleaching) signal. When the normalised unbleached curve is subtracted from the normalised natural curve, the remaining net signal provides an indication of the amount of low decay rate signal (long term) contributing to the natural OSL signal. The ψ ratio is the proportion of low decay rate (long term) contributing to the OSL signal and well-bleached samples should show a ψ ratio of close to zero. Samples with a greater ψ ratio suggest a greater difference between the natural and regenerated decay curve shapes, which is thought to be an indication of incomplete bleaching.

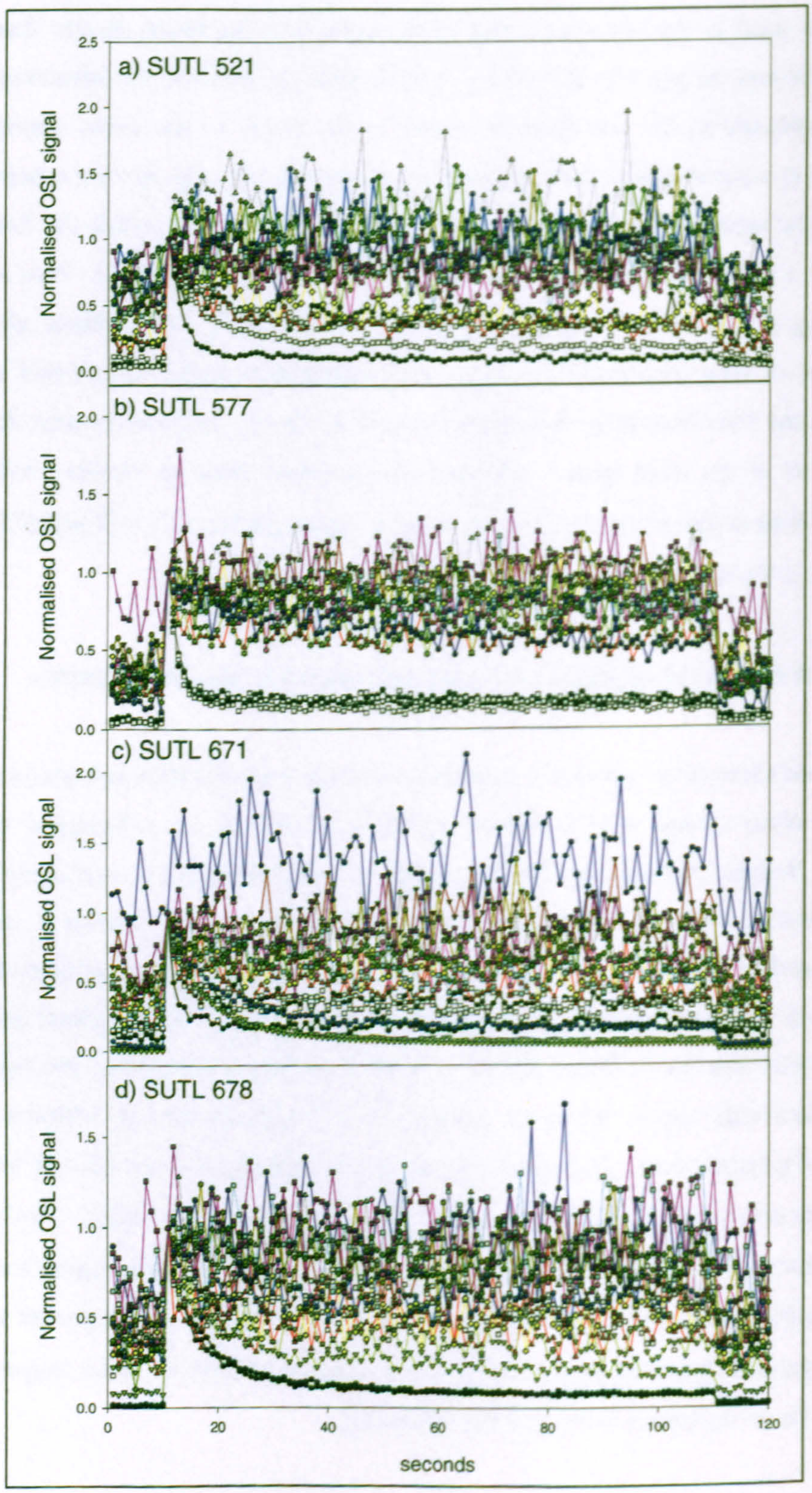
a) SUTL 521
b) SUTL 577
c) SUTL 671
d) SUTL 678
Normalised OSL signal
0.0
0.5
1.0
1.5
2.0
2.5
0
20
40
60
80
100
120
seconds

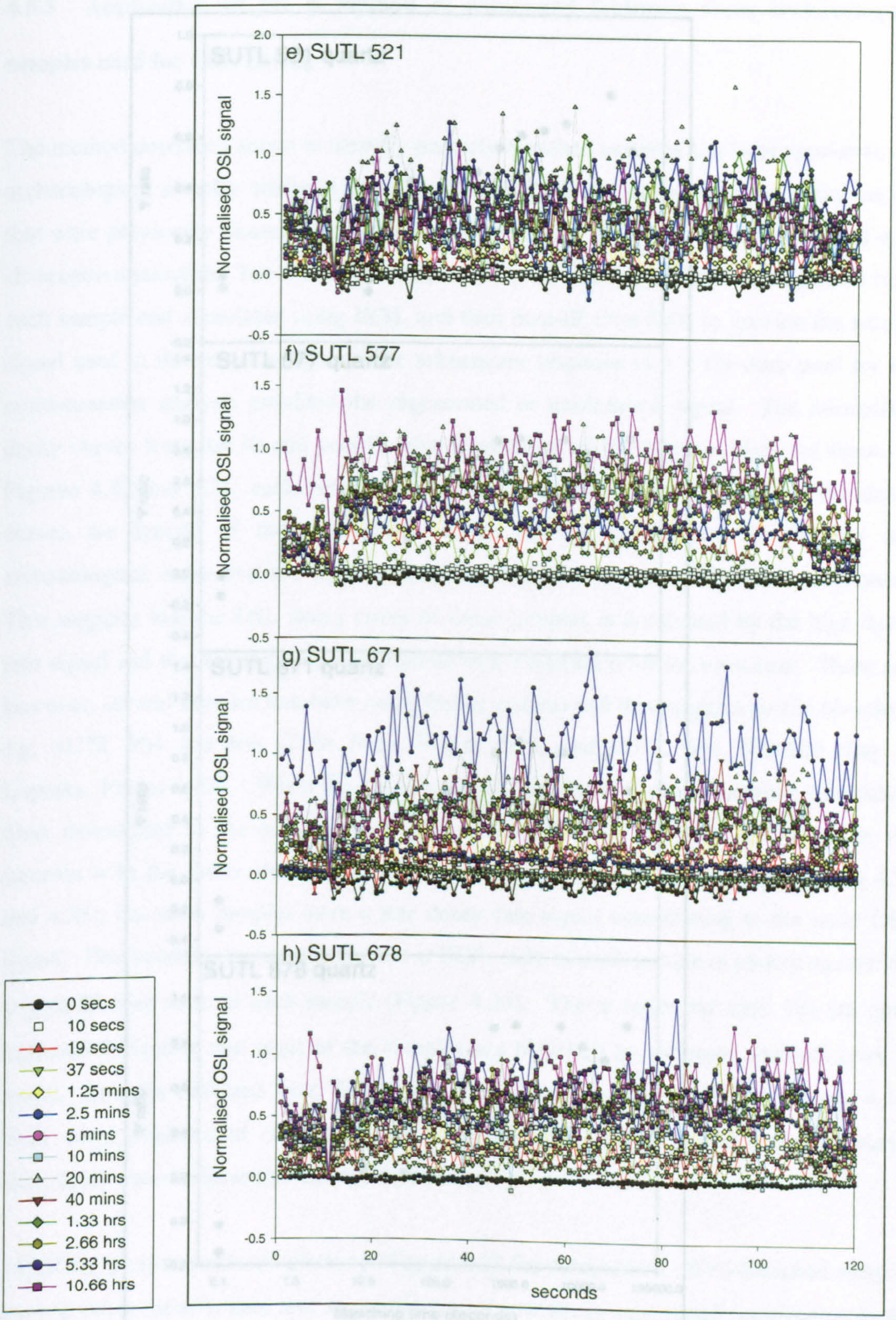

Figure 4.30 – Quartz modern beach sand bleached in the laboratory – a-d – normalised decay curves stimulated by blue OSL and e-h – the net long term contribution

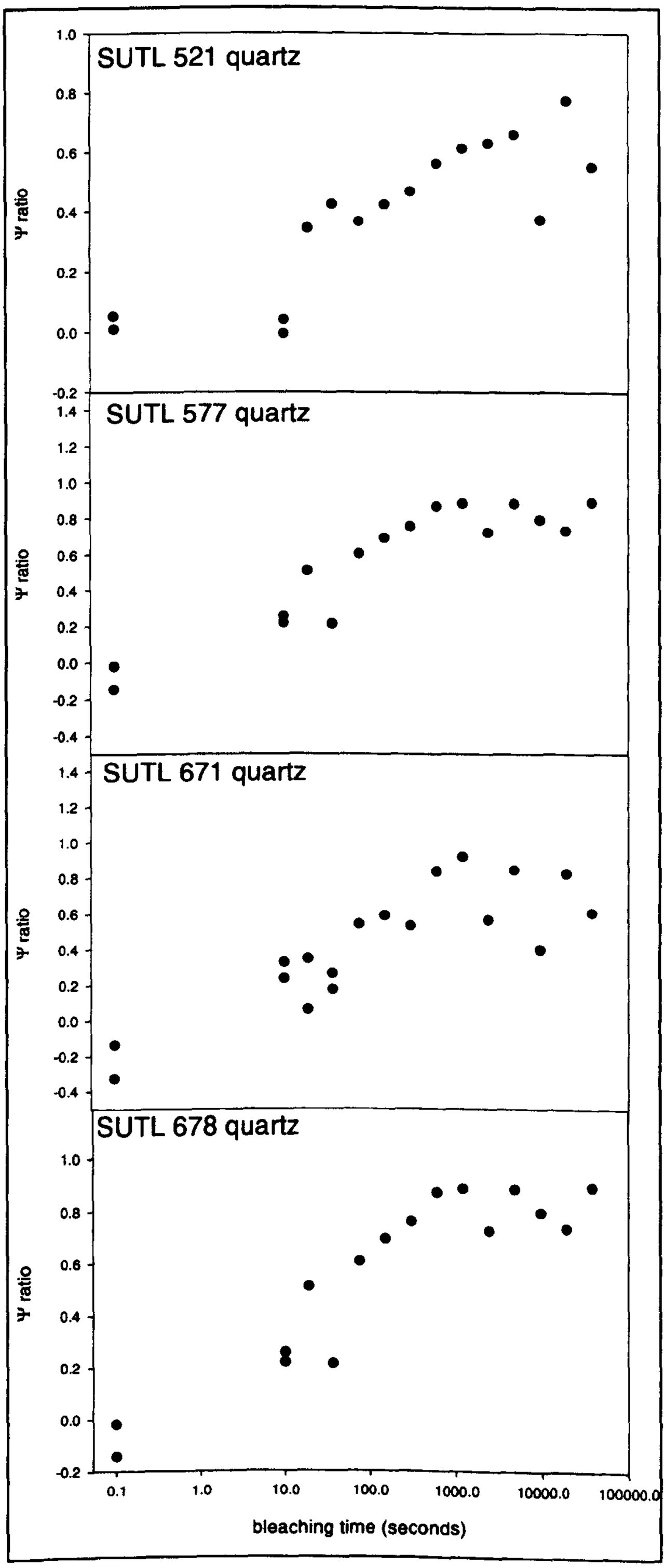

Figure 4.31 – Modern beach sand quartz ψ ratios after bleaching in the laboratory

4.5.3 Application of the ψ method to associated feldspars from archaeological samples used for OSL dating

The method described above to identify partially bleached samples has been applied to the archaeological samples analysed using the shape of the associated feldspar decay curves that were previously measured to determine if the quartz aliquots were contaminated with IR sensitive minerals. For the contamination analysis, a feldspar disc was dispensed from each sample and stimulated using IRSL and then post-IR blue OSL to provide the natural signal used in the above analysis. The subsequent response to a 1 Gy dose used for the contamination analysis provided the regenerated or unbleached signal. The normalised decay curves from the IR and post-IR blue stimulation of the feldspar discs are shown in Figures 4.32 and 4.33, each curve representing a separate sample. Many of the decay curves are typical of those described above for the unbleached F1 feldspar and archaeological sands that are dominated by the high decay rate (short term) component. This suggests that the OSL decay curve of these samples is dominated by the high decay rate signal and that the samples were indeed well bleached prior to deposition. There are, however, several samples that have much flatter profiles and this suggests partial bleaching e.g. SUTL 604 and 606 (Tofts Ness, Figure 4.32) and SUTL 884, 886-889 (Bay of Lopness, Figure 4.32). When the net low decay rate signal is plotted against stimulation time, determined by the subtraction of the unbleached curve from the natural curve, the samples with the flatter decay curves have greater net signals as expected (Figures 4.34 and 4.35), but most samples have a low decay rate signal contributing to the main OSL signal. This becomes apparent when the ψ IRSL ratio of each sample is plotted against the ψ post-IR blue ratio of each sample (Figure 4.36). The ψ ratios for each site are quite scattered indicating that most of the samples are bleached by different amounts prior to burial. Samples collected from Tofts Ness, Bay of Lopness and Quoygrew (Figure 4.36) show some evidence of clustering (dashed lines) suggesting that, within the individual sites, these samples have similar exposure histories.

All of the ψ ratio results are plotted in Figure 4.37 for comparison. Well-bleached samples have ψ ratios close to zero and as the amount of low decay rate signal contributing to the OSL signal increases, indicating partial bleaching, so does the ψ ratio. In Figure 4.37, samples in the bottom left corner of the graph with low ψ ratios are thought to be well-bleached, whereas those towards the top right have higher ψ ratios and are considered to be

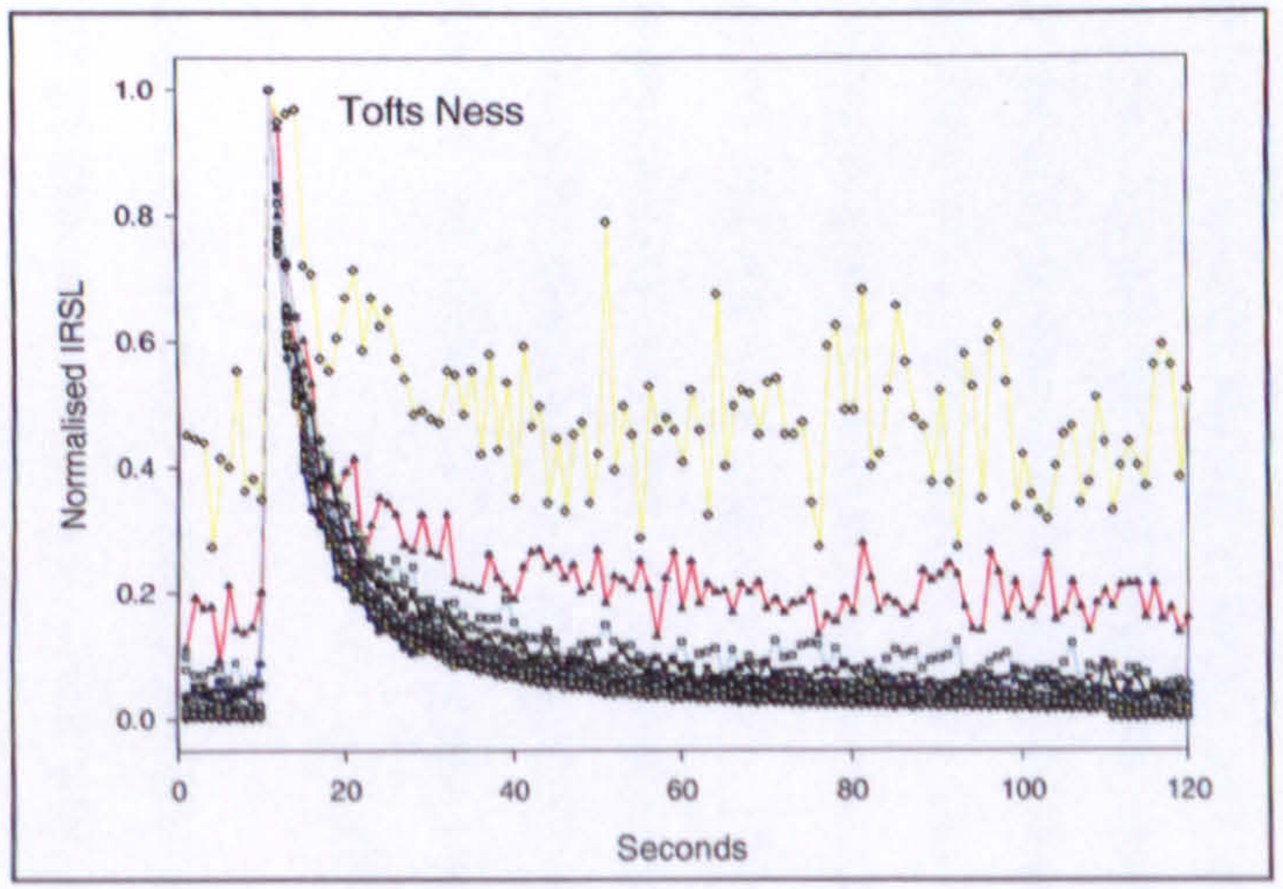
Tofts Ness
Normalised IRSL
Seconds
0.0
0.2
0.4
0.6
0.8
1.0
0
20
40
60
80
100
120

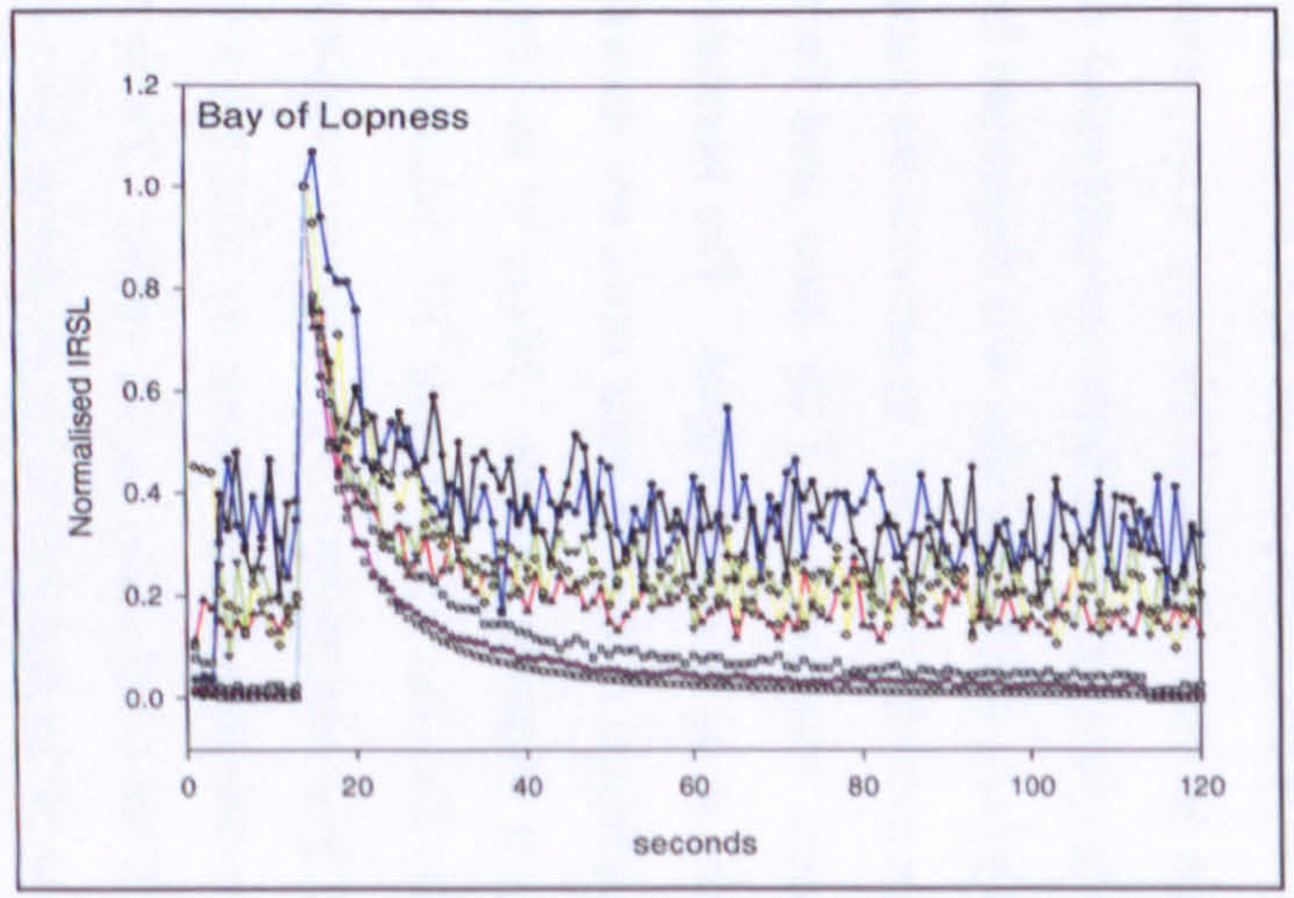
Bay of Lopness
Normalised IRSL
seconds
0.0
0.2
0.4
0.6
0.8
1.0
1.2
0
20
40
60
80
100
120

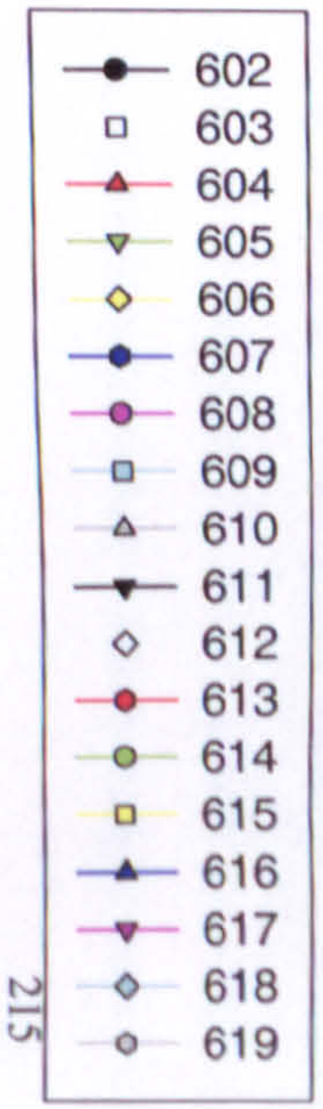
602
603
604
605
606
607
608
609
610
611
612
613
614
615
616
617
618
619

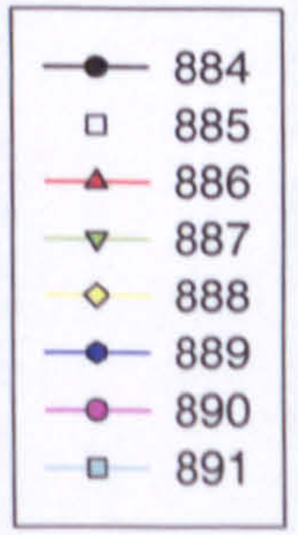
884
885
886
887
888
889
890
891

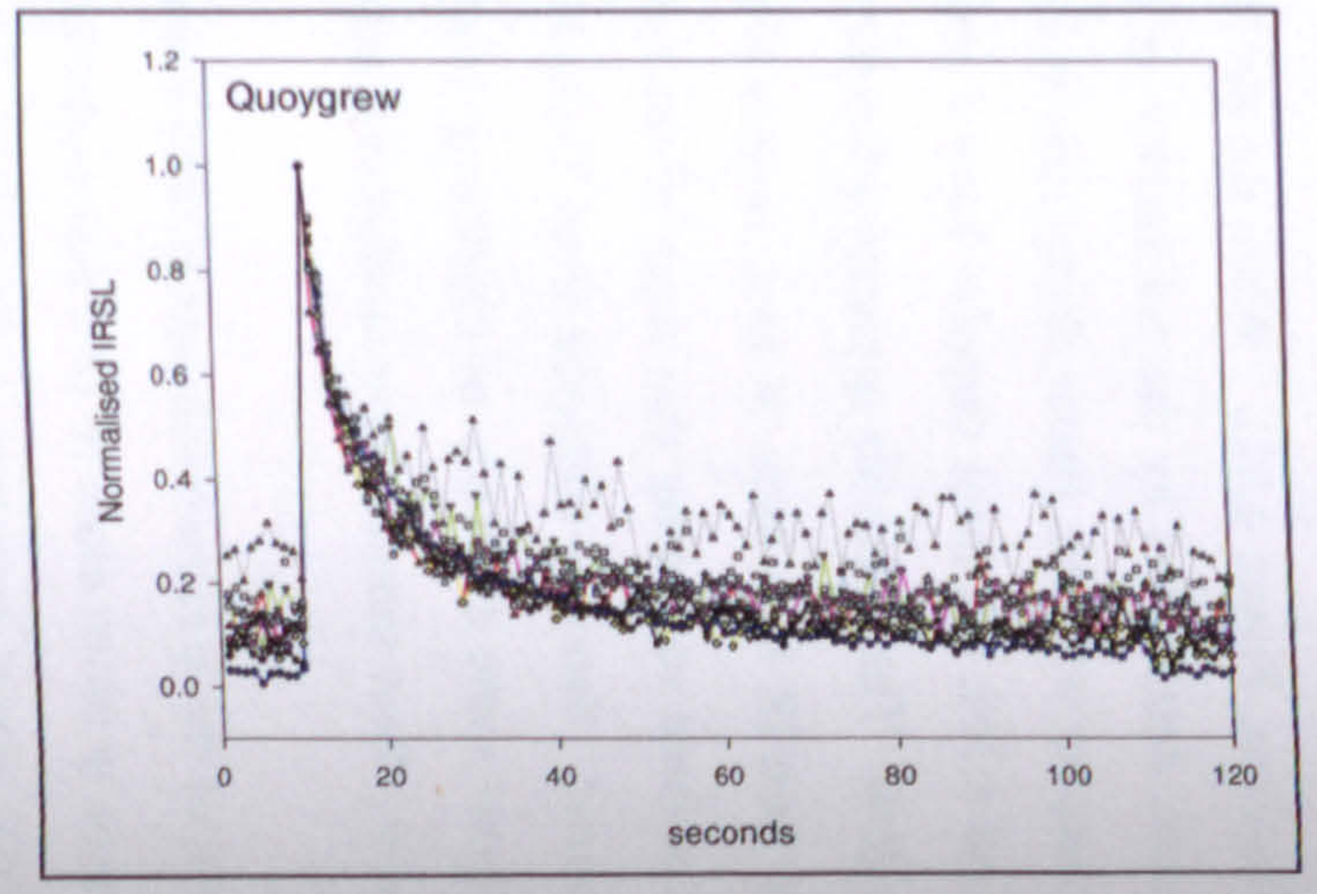
Quoygrew
Normalised IRSL
seconds
0.0
0.2
0.4
0.6
0.8
1.0
1.2
0
20
40
60
80
100
120

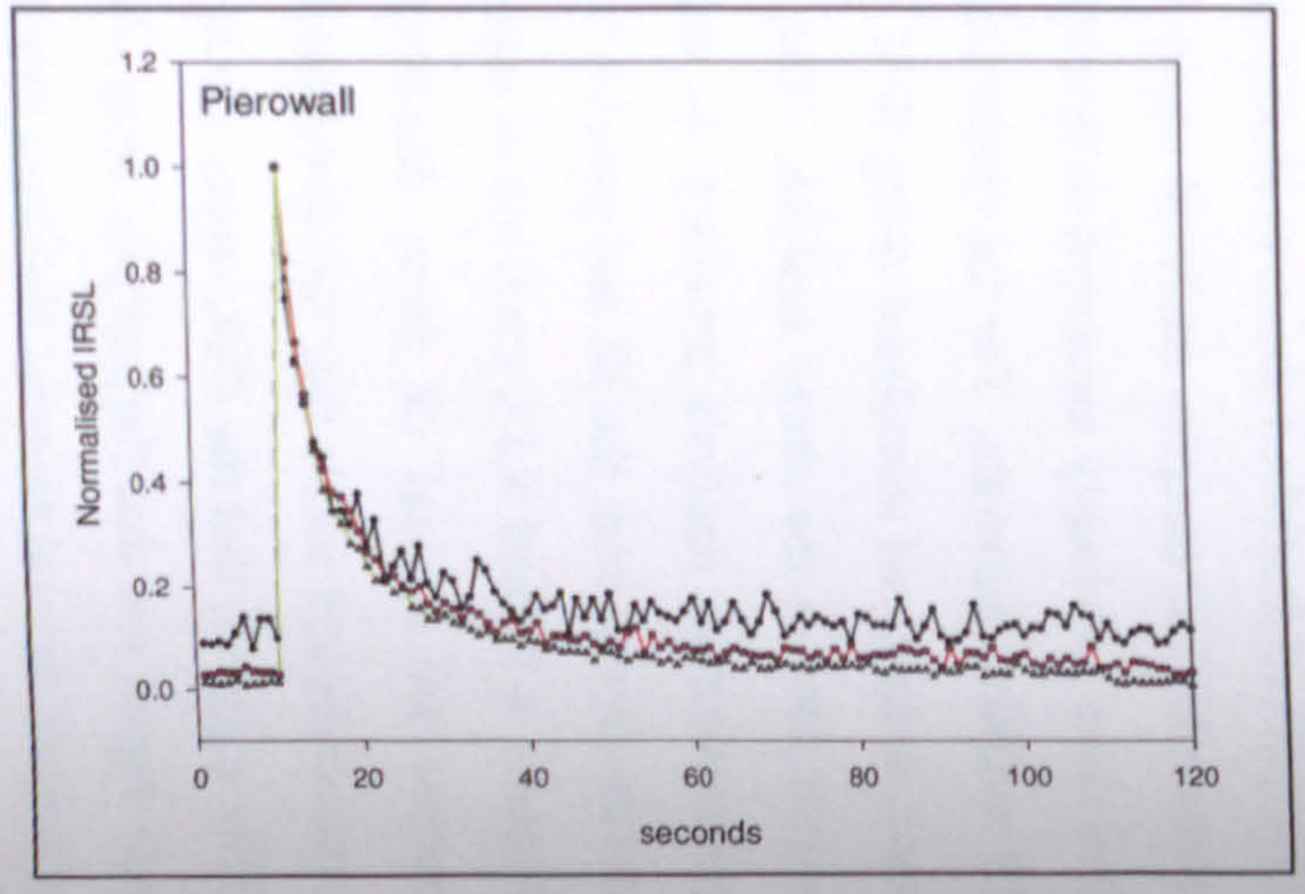
Pierowall
Normalised IRSL
seconds
0.0
0.2
0.4
0.6
0.8
1.0
1.2
0
20
40
60
80
100
120

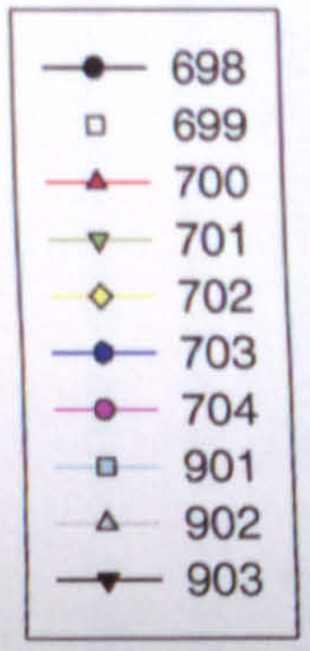
698
699
700
701
702
703
704
901
902
903

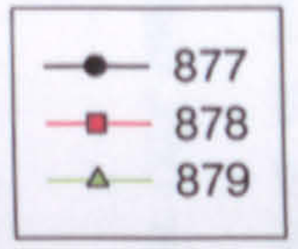
877
878
879

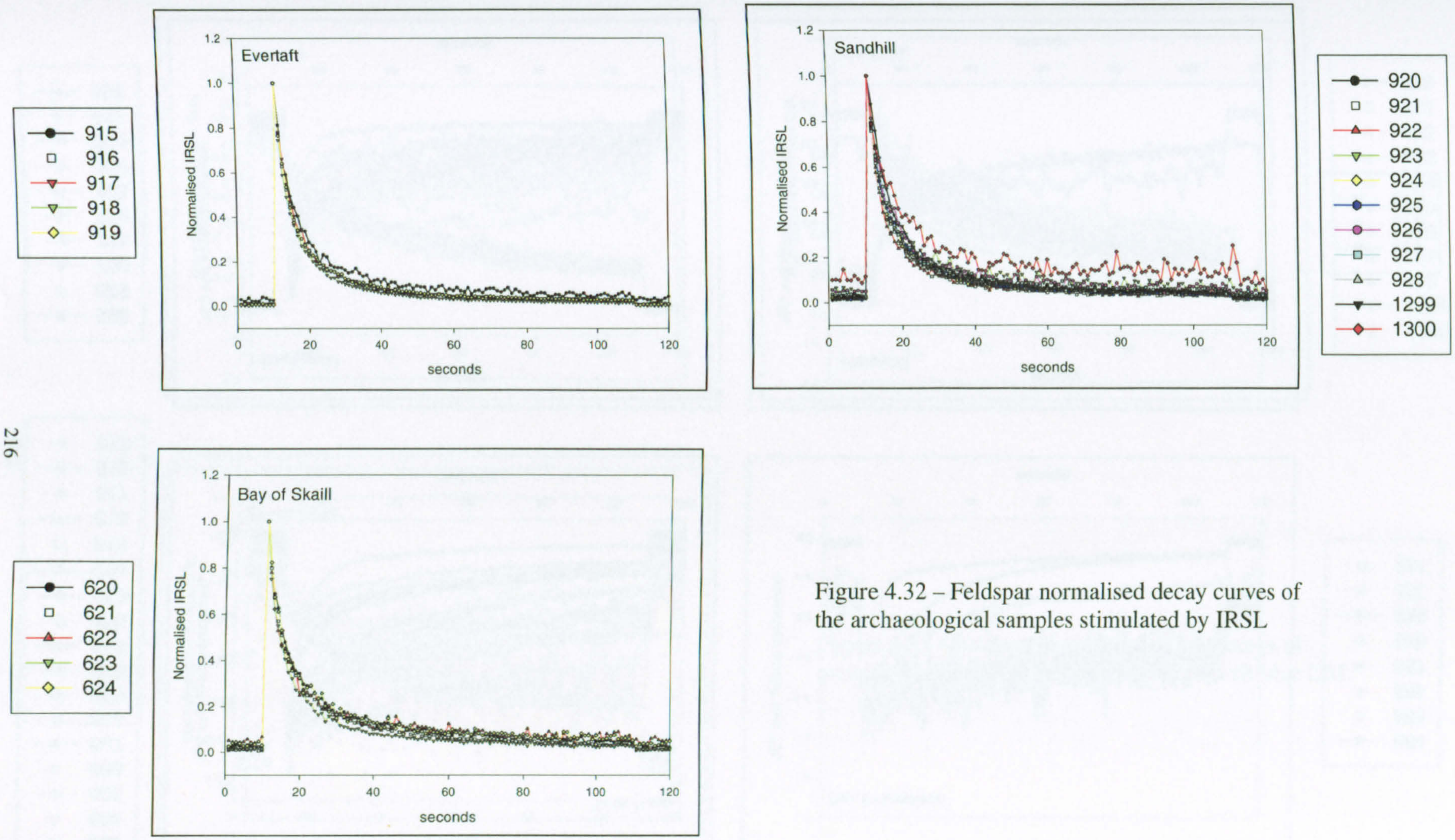

Figure 4.32 – Feldspar normalised decay curves of the archaeological samples stimulated by IRSL

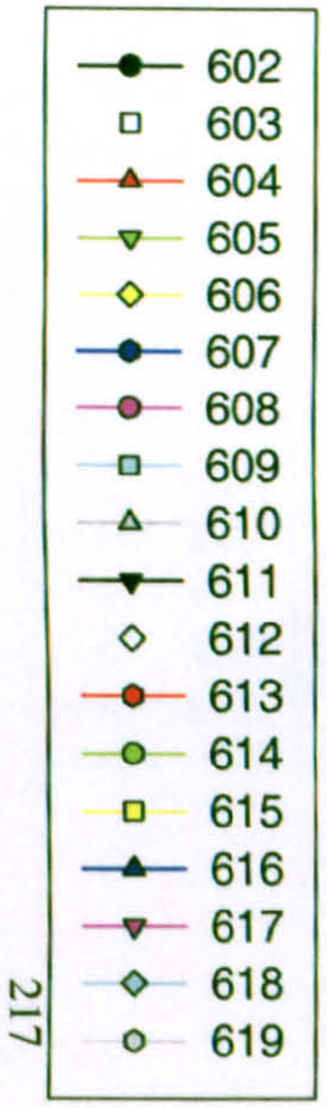
602
603
604
605
606
607
608
609
610
611
612
613
614
615
616
617
618
619

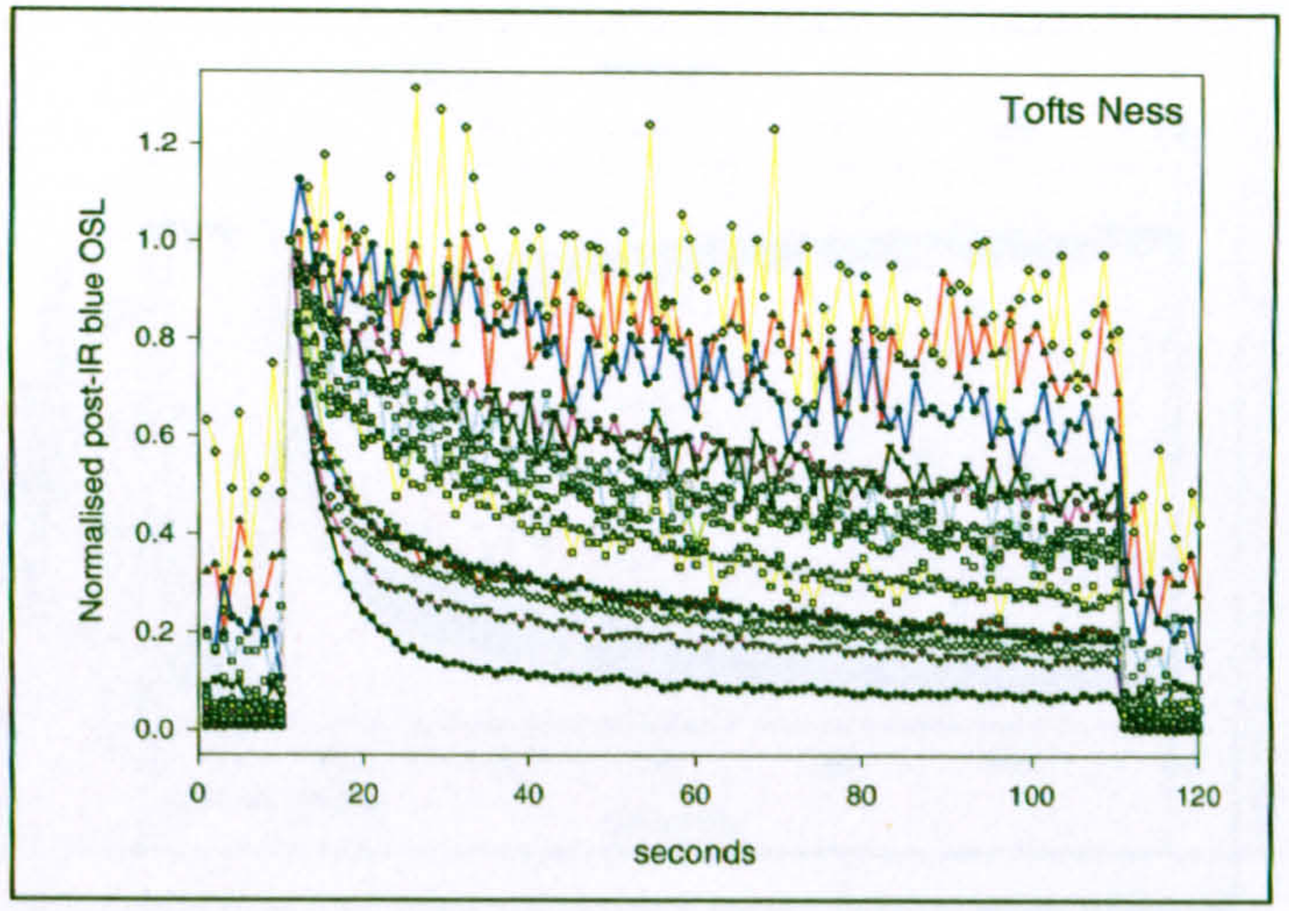
Tofts Ness
Normalised post-IR blue OSL
seconds
0.0
0.2
0.4
0.6
0.8
1.0
1.2
0
20
40
60
80
100
120

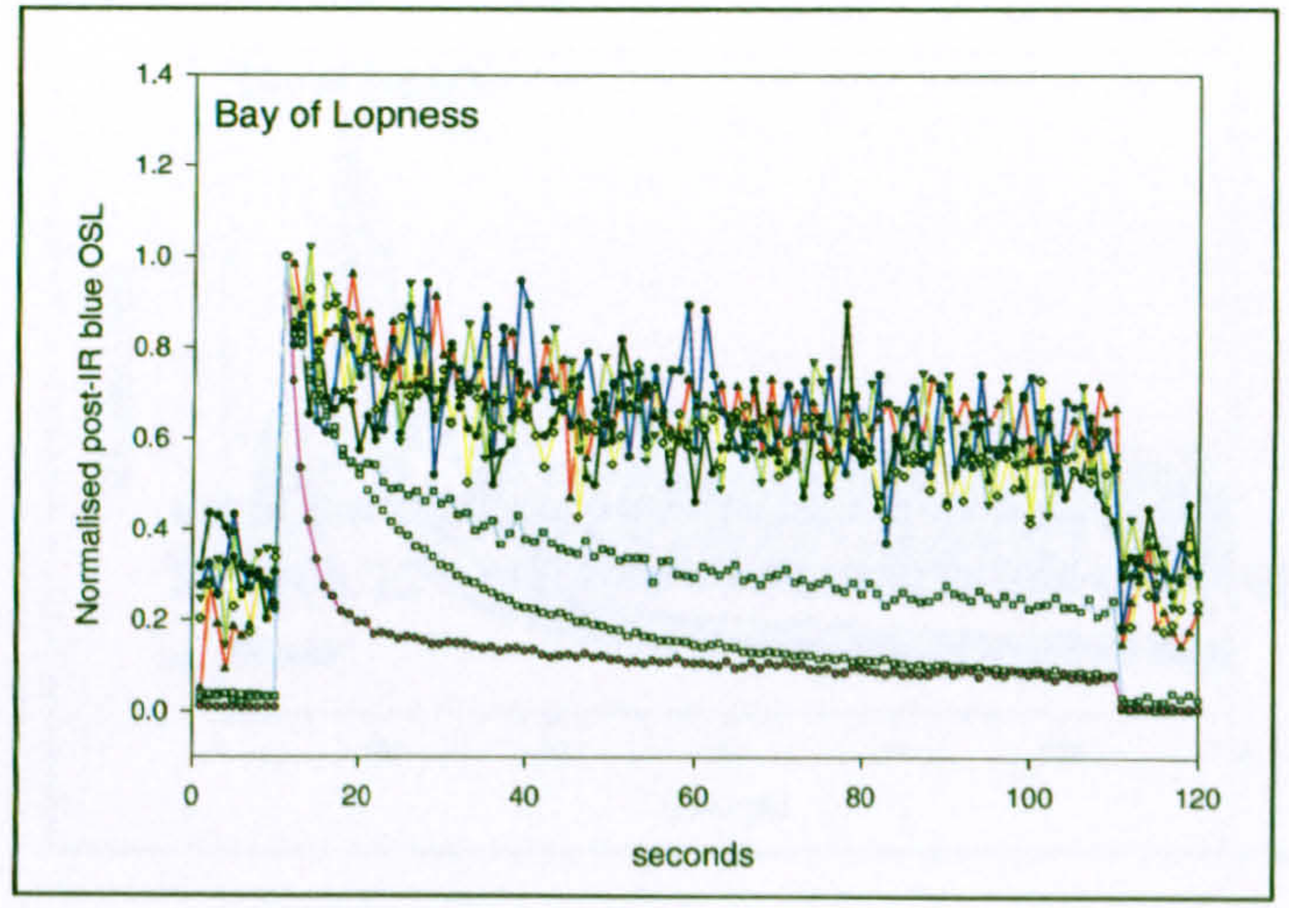
Bay of Lopness
Normalised post-IR blue OSL
seconds
0.0
0.2
0.4
0.6
0.8
1.0
1.2
1.4
0
20
40
60
80
100
120

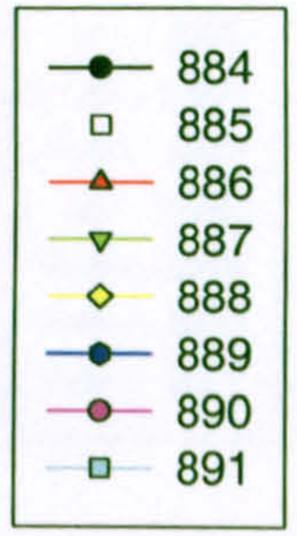
884
885
886
887
888
889
890
891

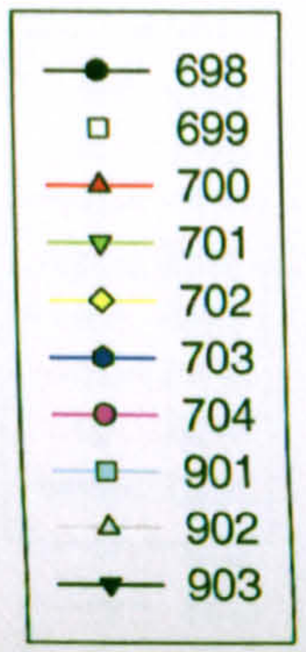
698
699
700
701
702
703
704
901
902
903

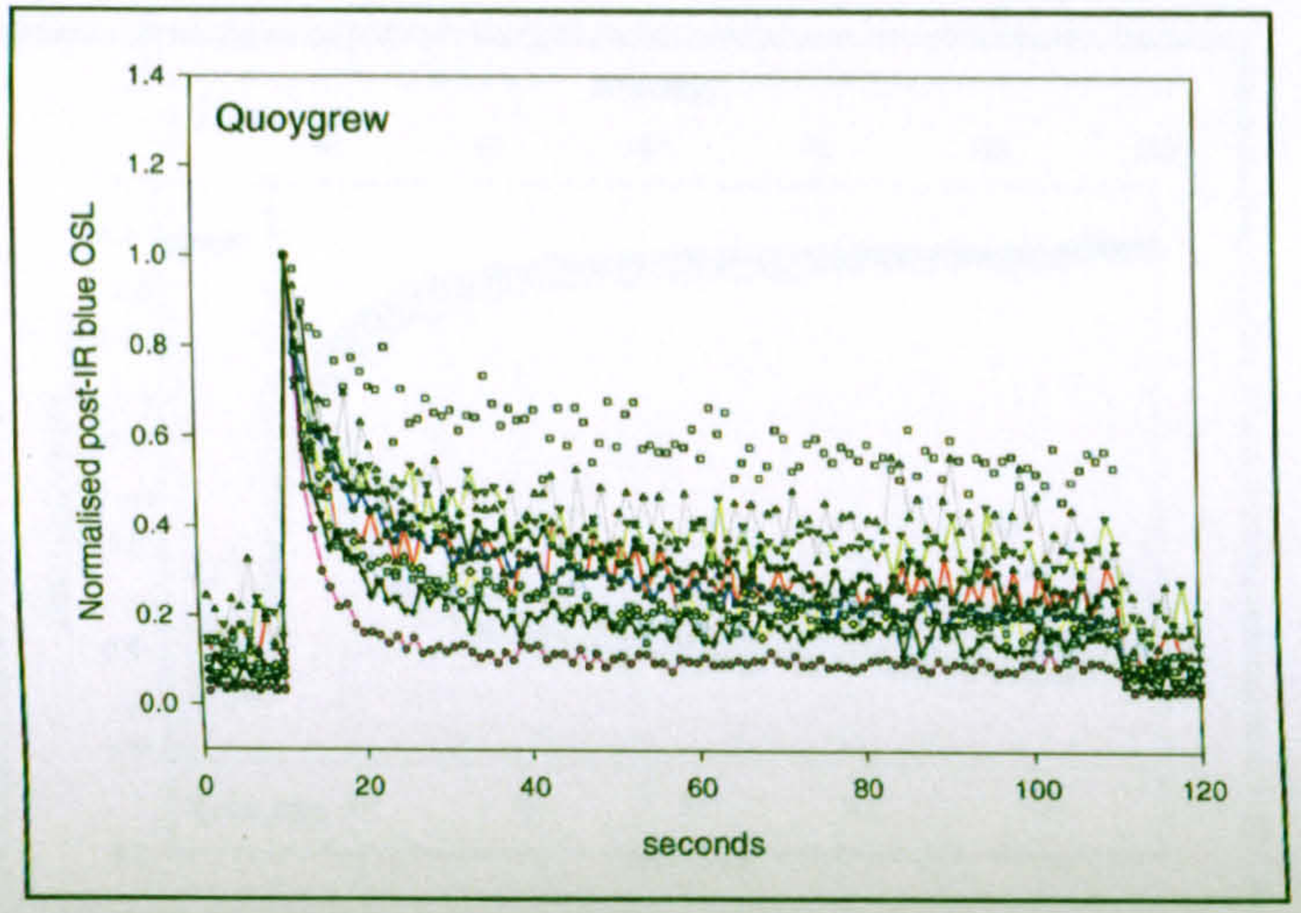
Quoygrew
Normalised post-IR blue OSL
seconds
0.0
0.2
0.4
0.6
0.8
1.0
1.2
1.4
0
20
40
60
80
100
120

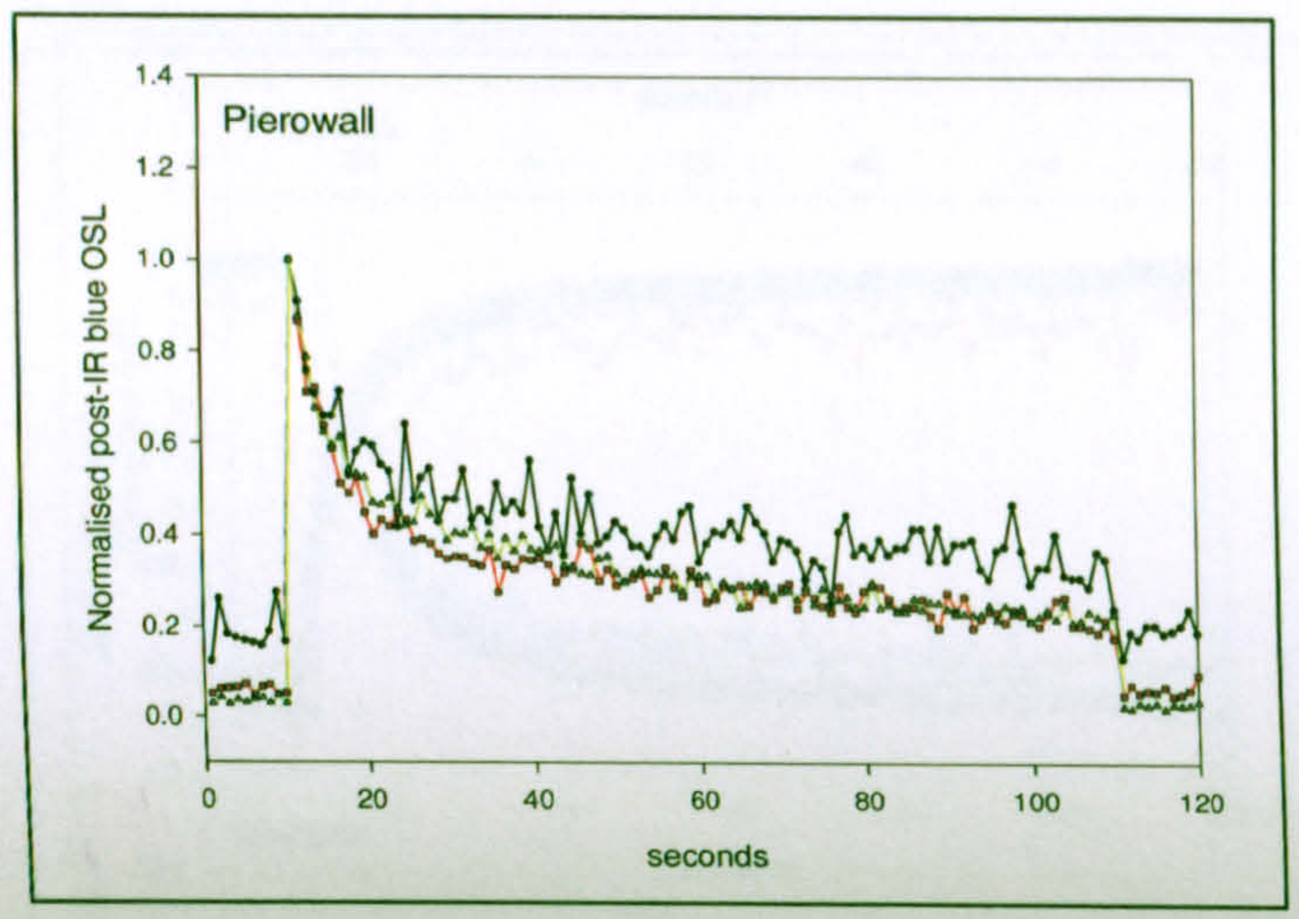
Pierowall
Normalised post-IR blue OSL
seconds
0.0
0.2
0.4
0.6
0.8
1.0
1.2
1.4
0
20
40
60
80
100
120

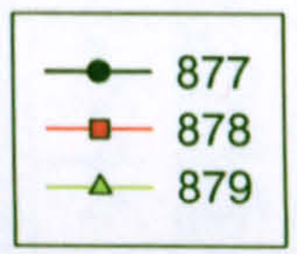
877
878
879

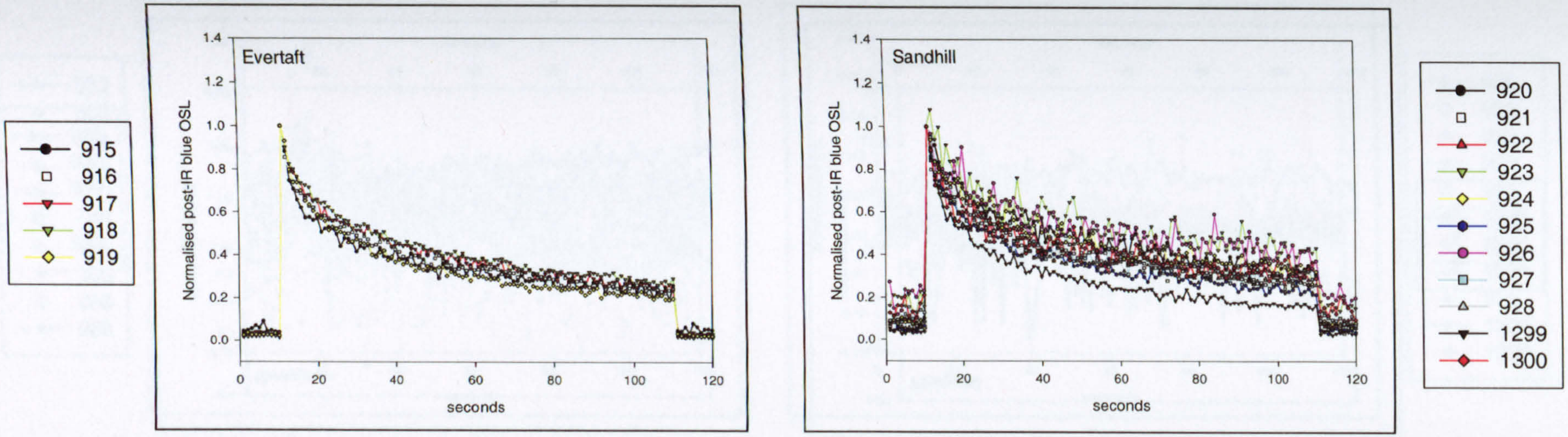

Figure 4.33 – Feldspar normalised decay curves of archaeological samples stimulated by post-IR blue OSL

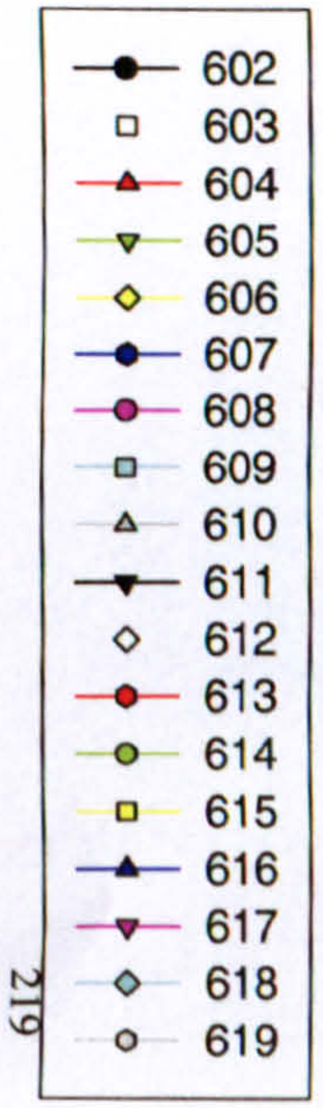
602
603
604
605
606
607
608
609
610
611
612
613
614
615
616
617
618
619

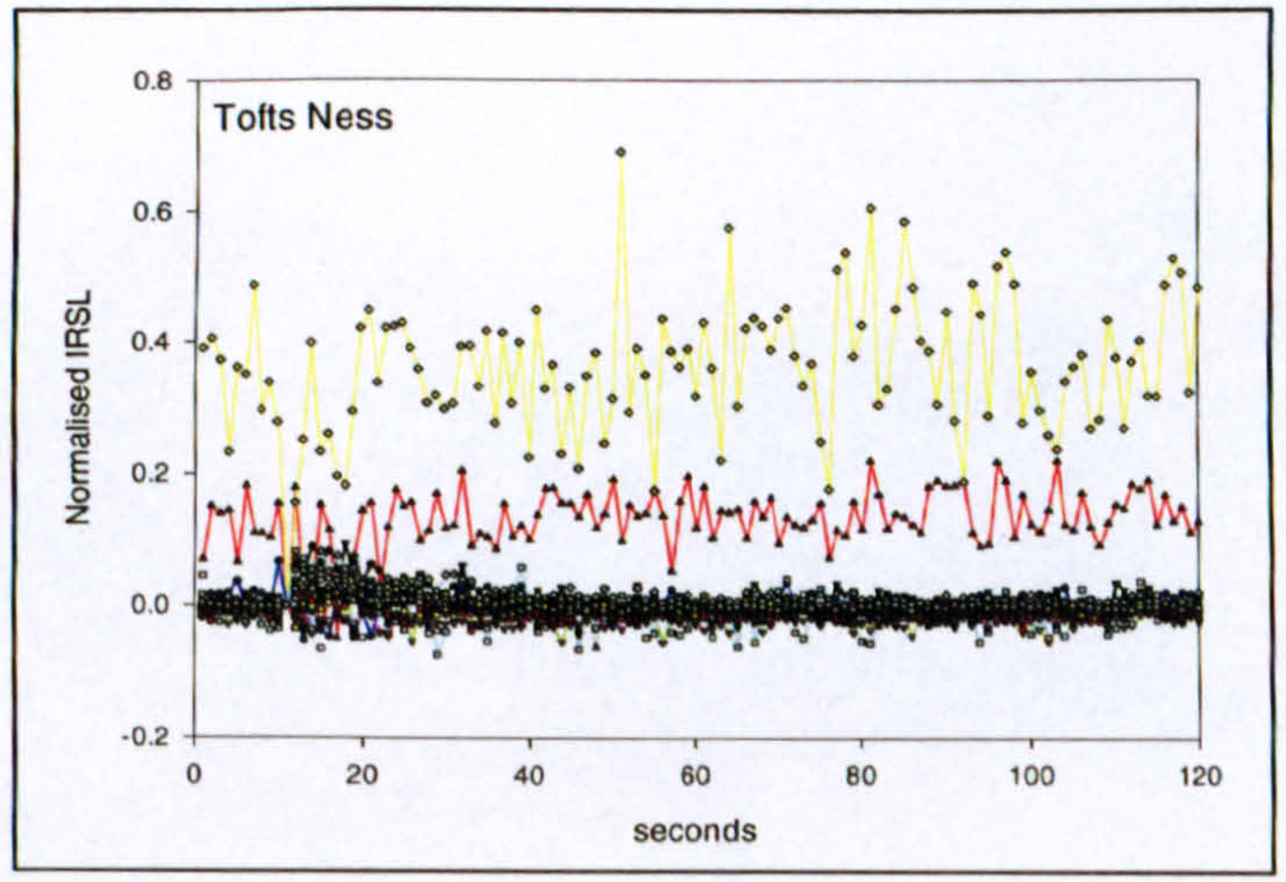
Tofts Ness
Normalised IRSL
seconds
0.8
0.6
0.4
0.2
0.0
-0.2
0
20
40
60
80
100
120

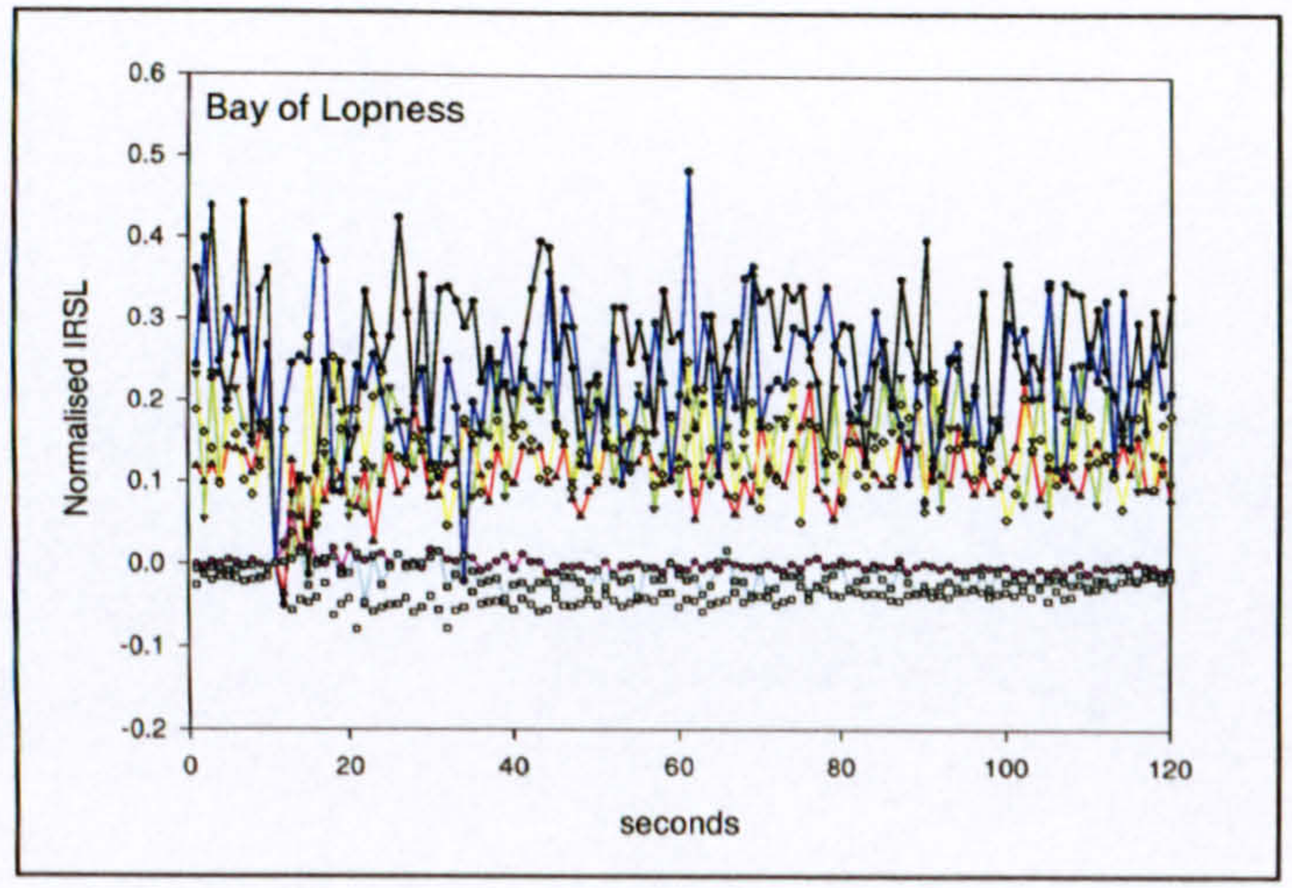
Bay of Lopness
Normalised IRSL
seconds
0.6
0.5
0.4
0.3
0.2
0.1
0.0
-0.1
-0.2
0
20
40
60
80
100
120

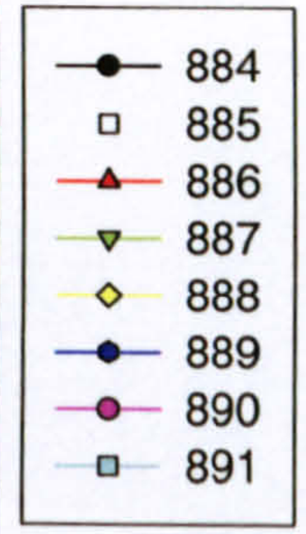
884
885
886
887
888
889
890
891

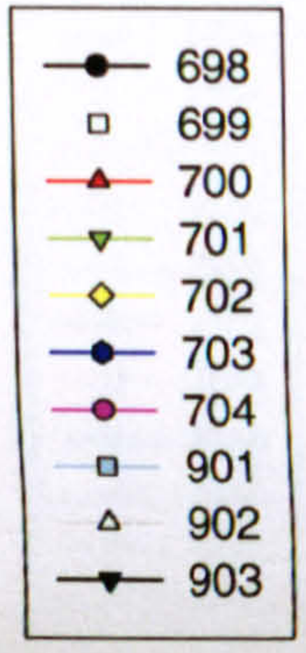
698
699
700
701
702
703
704
901
902
903

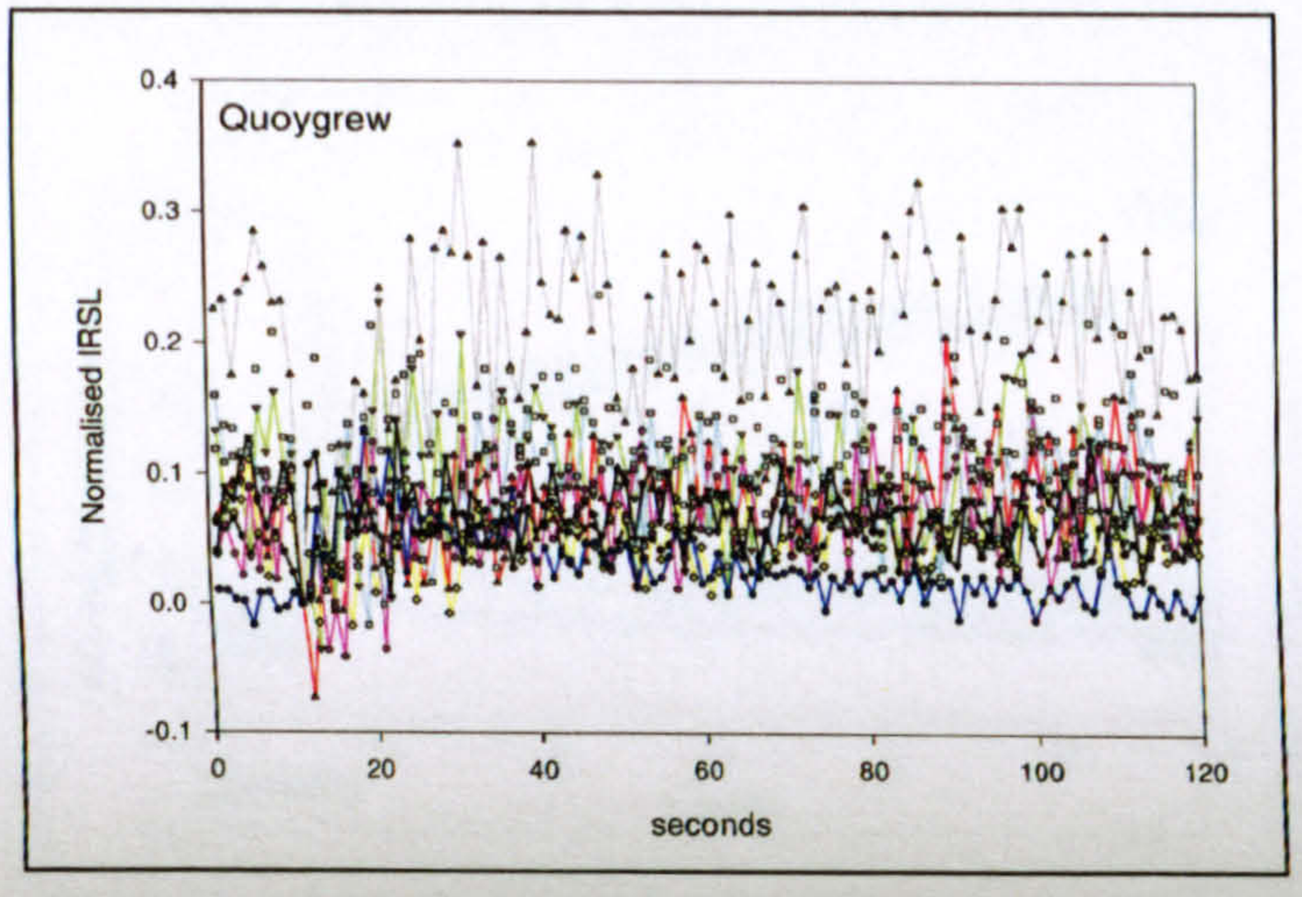
Quoygrew
Normalised IRSL
seconds
0.4
0.3
0.2
0.1
0.0
-0.1
0
20
40
60
80
100
120

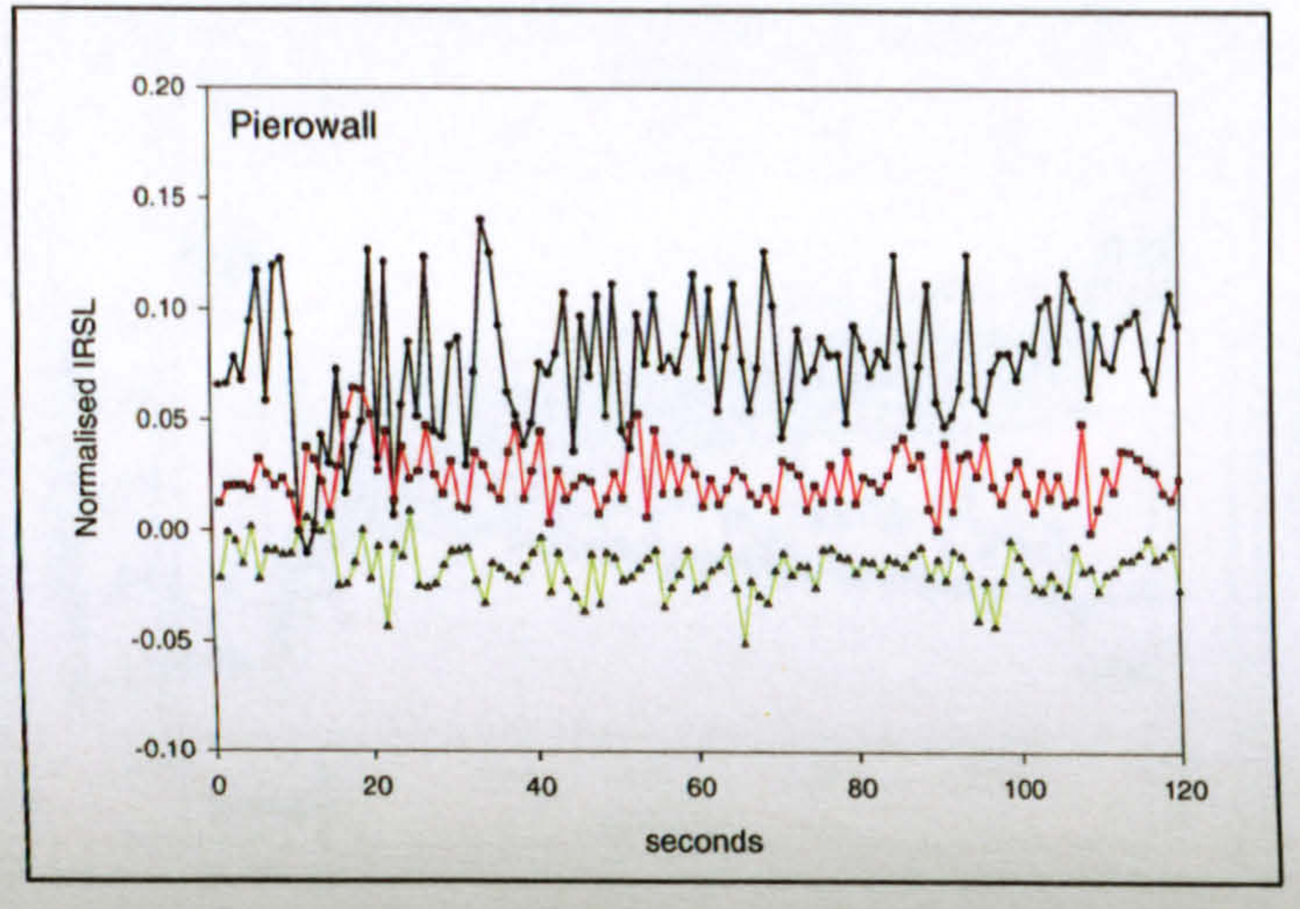
Pierowall
Normalised IRSL
seconds
0.20
0.15
0.10
0.05
0.00
-0.05
-0.10
0
20
40
60
80
100
120

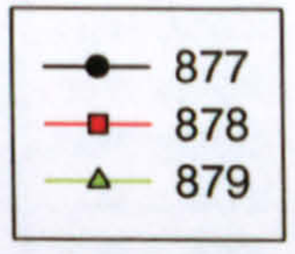
877
878
879

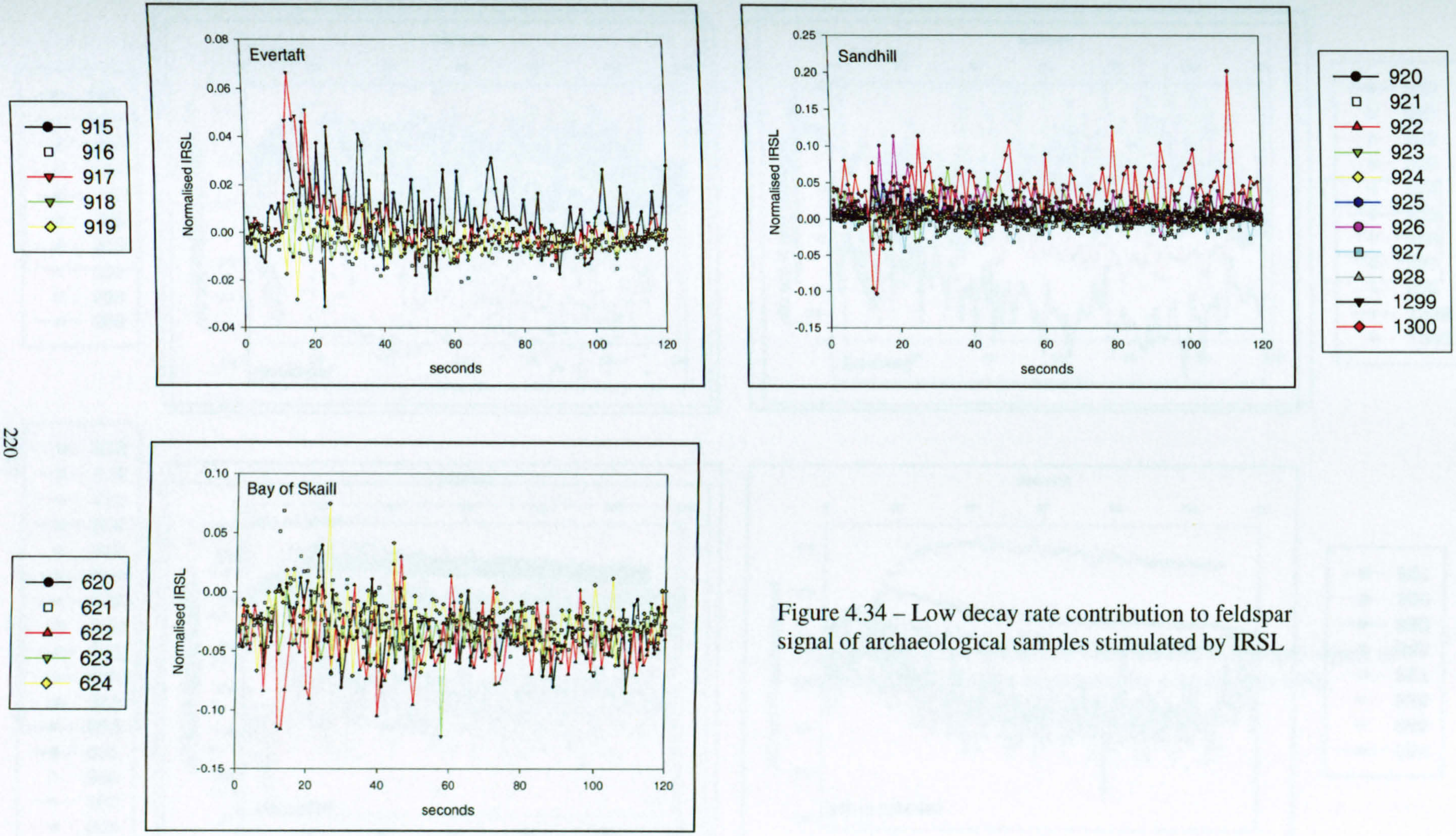

Figure 4.34 – Low decay rate contribution to feldspar signal of archaeological samples stimulated by IRSL

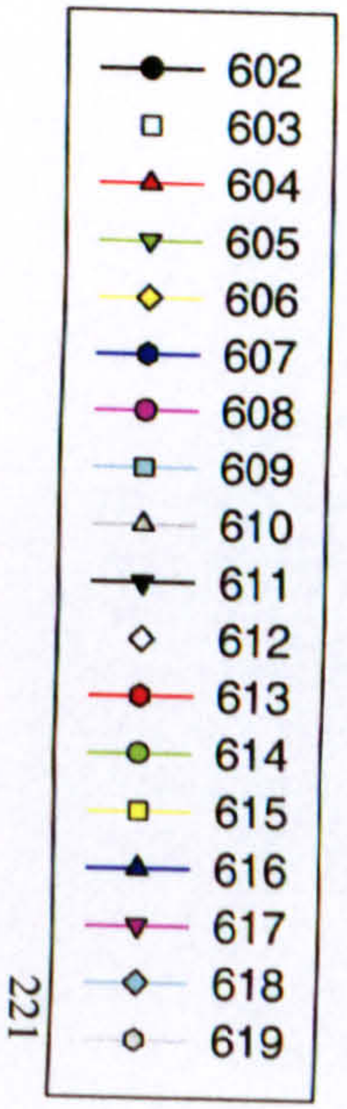
602
603
604
605
606
607
608
609
610
611
612
613
614
615
616
617
618
619

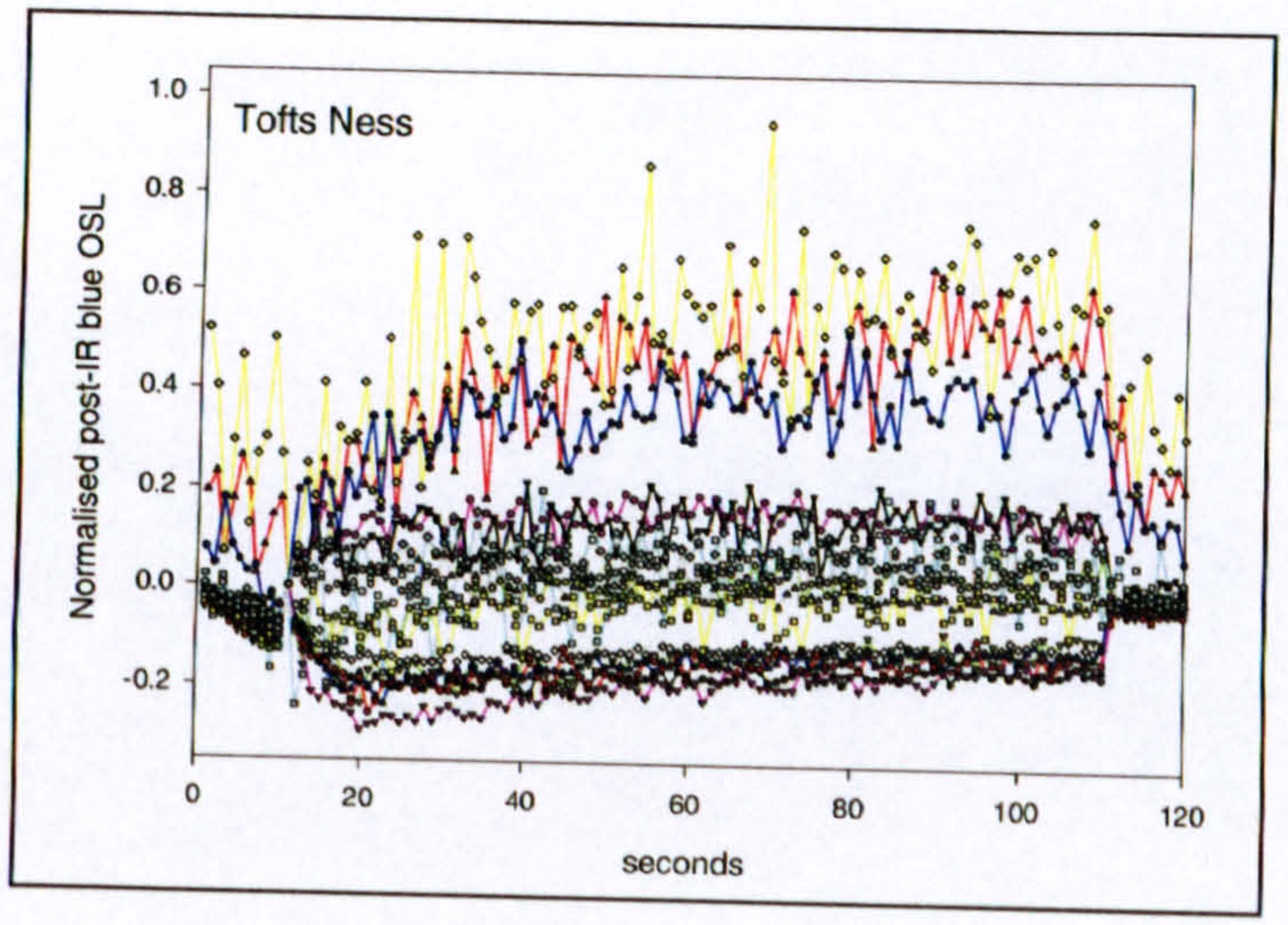
Tofts Ness
Normalised post-IR blue OSL
seconds
1.0
0.8
0.6
0.4
0.2
0.0
-0.2
0
20
40
60
80
100
120

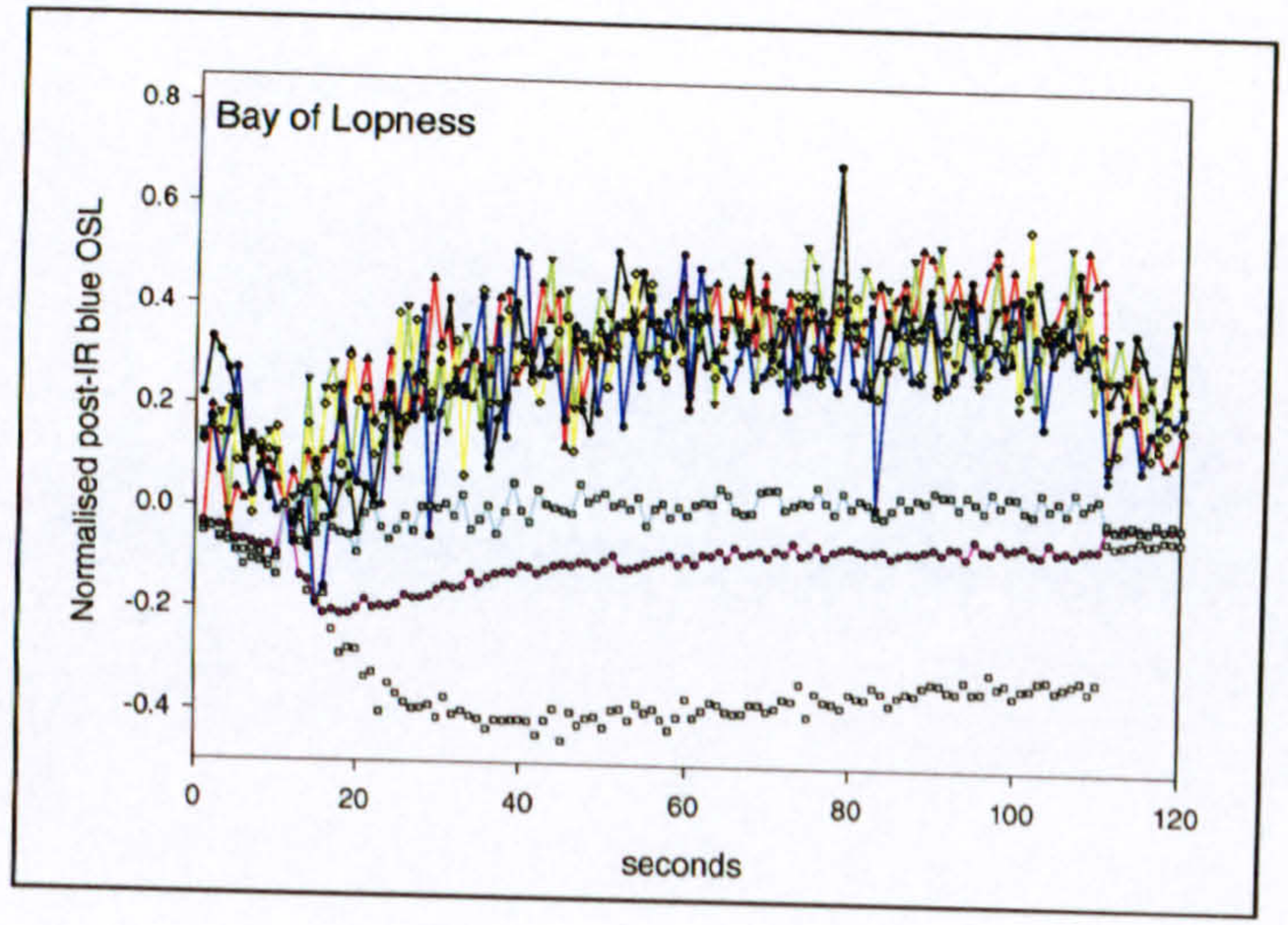
Bay of Lopness
Normalised post-IR blue OSL
seconds
0.8
0.6
0.4
0.2
0.0
-0.2
-0.4
0
20
40
60
80
100
120

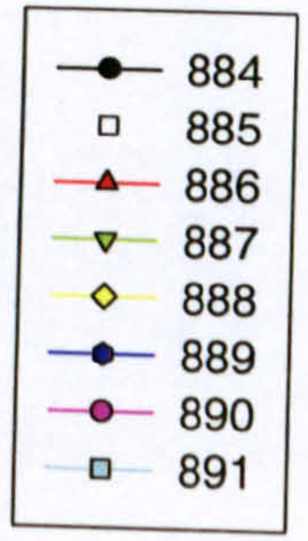
884
885
886
887
888
889
890
891

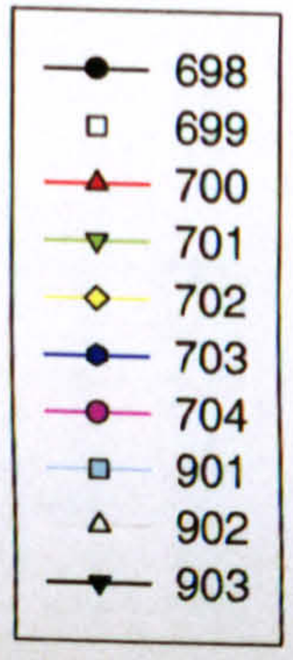
698
699
700
701
702
703
704
901
902
903

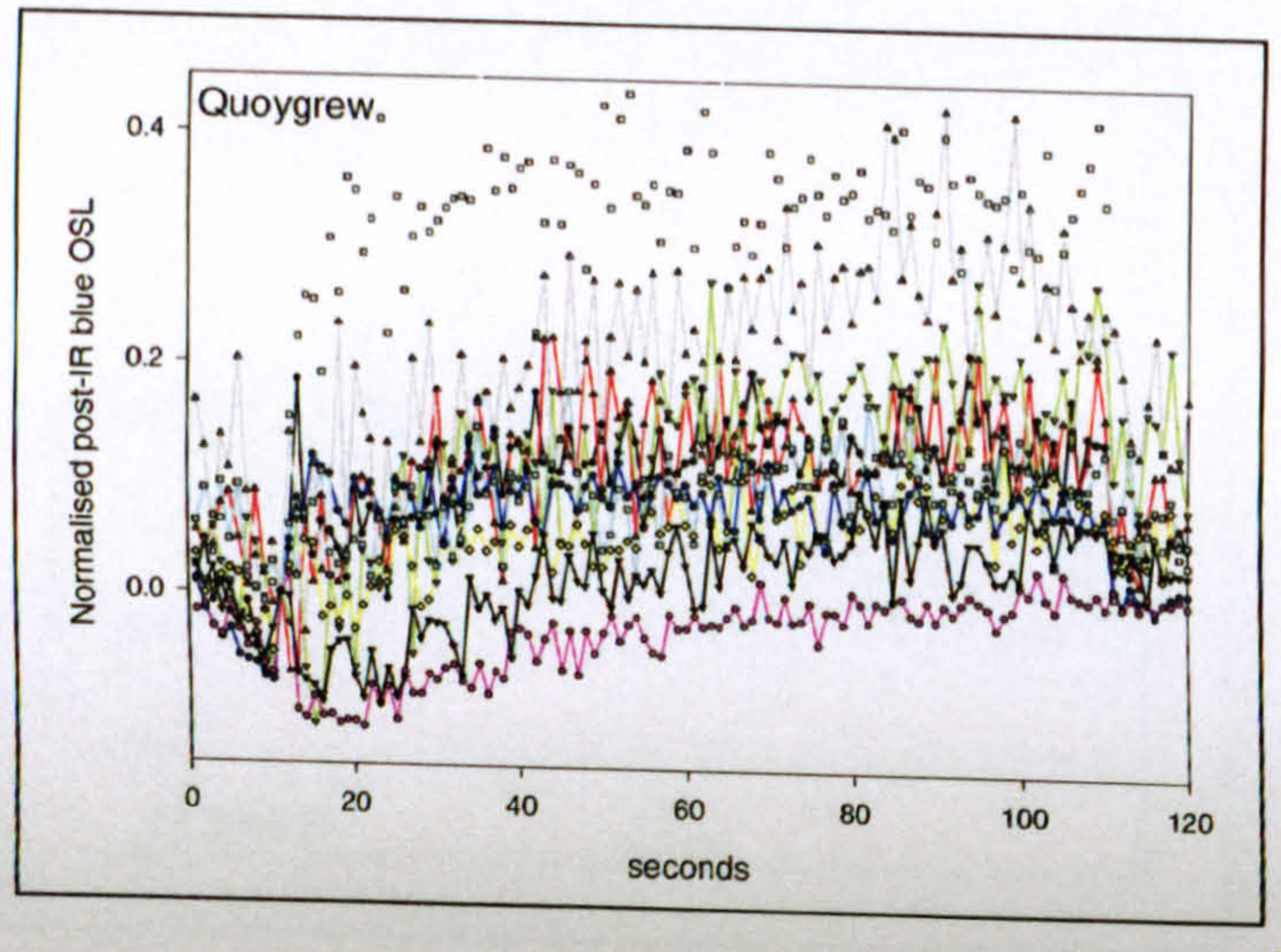
Quoygrew
Normalised post-IR blue OSL
seconds
0.4
0.2
0.0
0
20
40
60
80
100
120

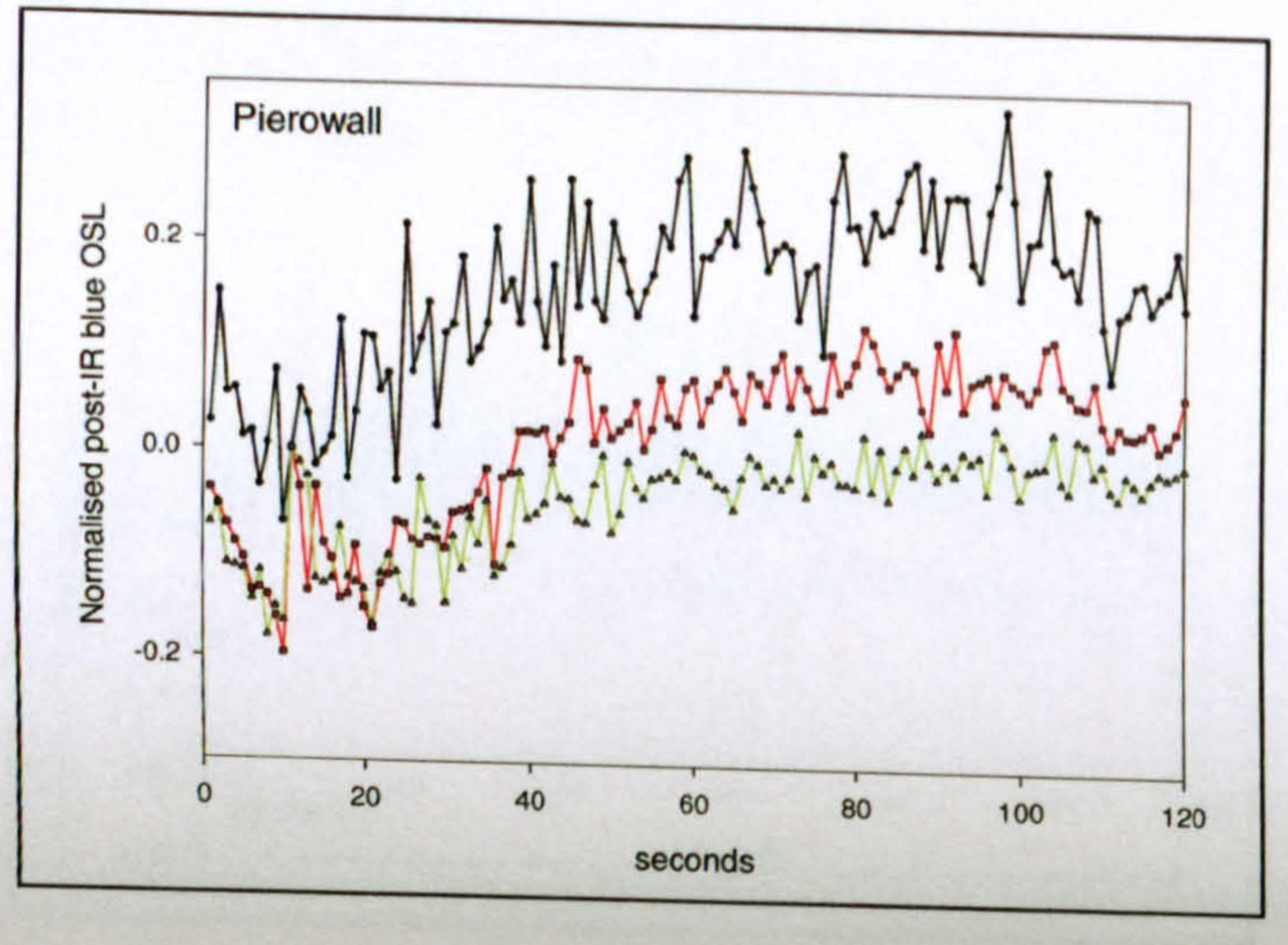
Pierowall
Normalised post-IR blue OSL
seconds
0.2
0.0
-0.2
0
20
40
60
80
100
120

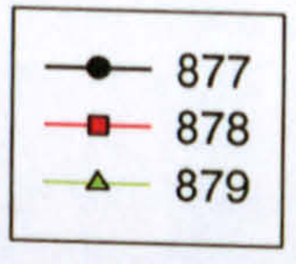
877
878
879

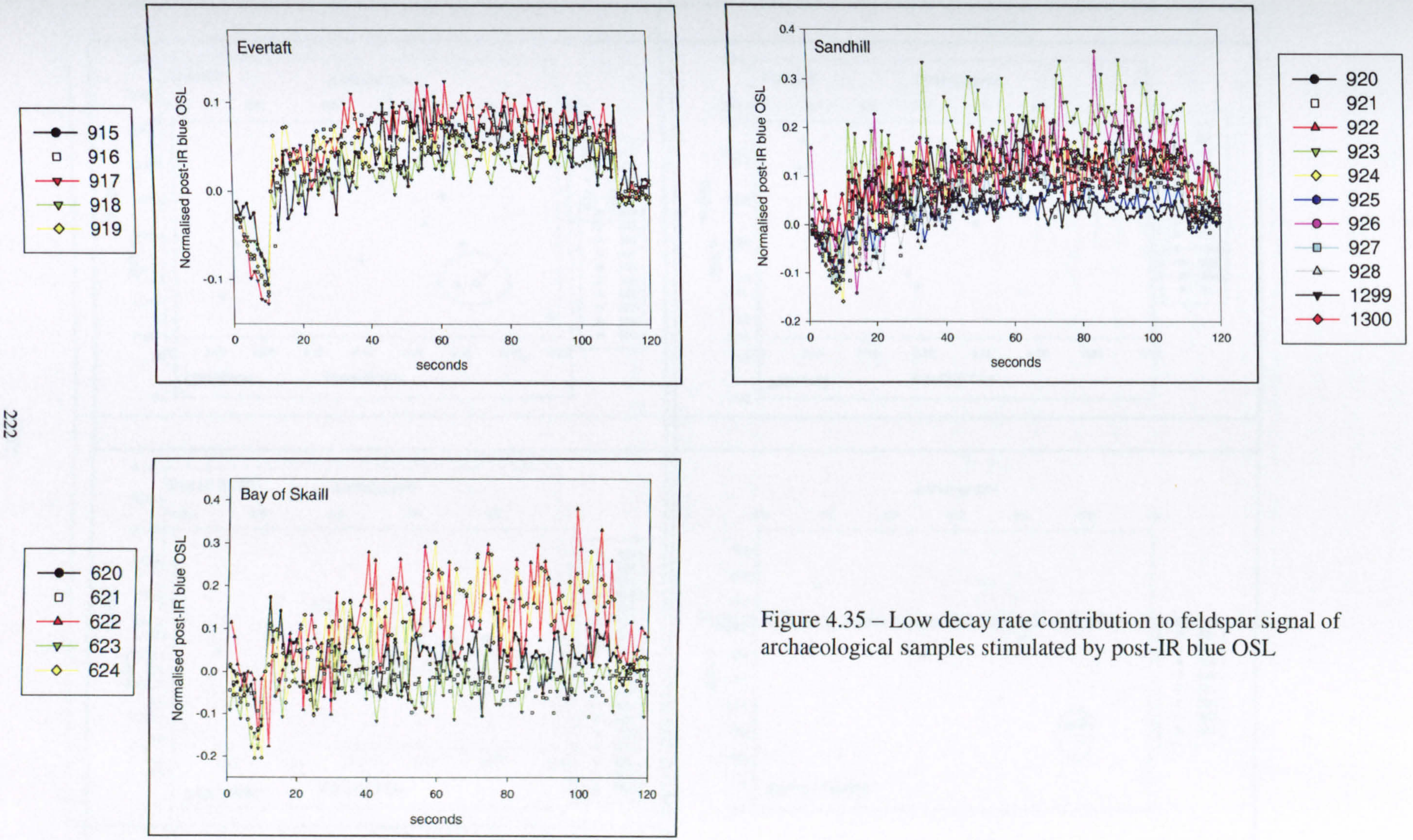

Figure 4.35 – Low decay rate contribution to feldspar signal of archaeological samples stimulated by post-IR blue OSL

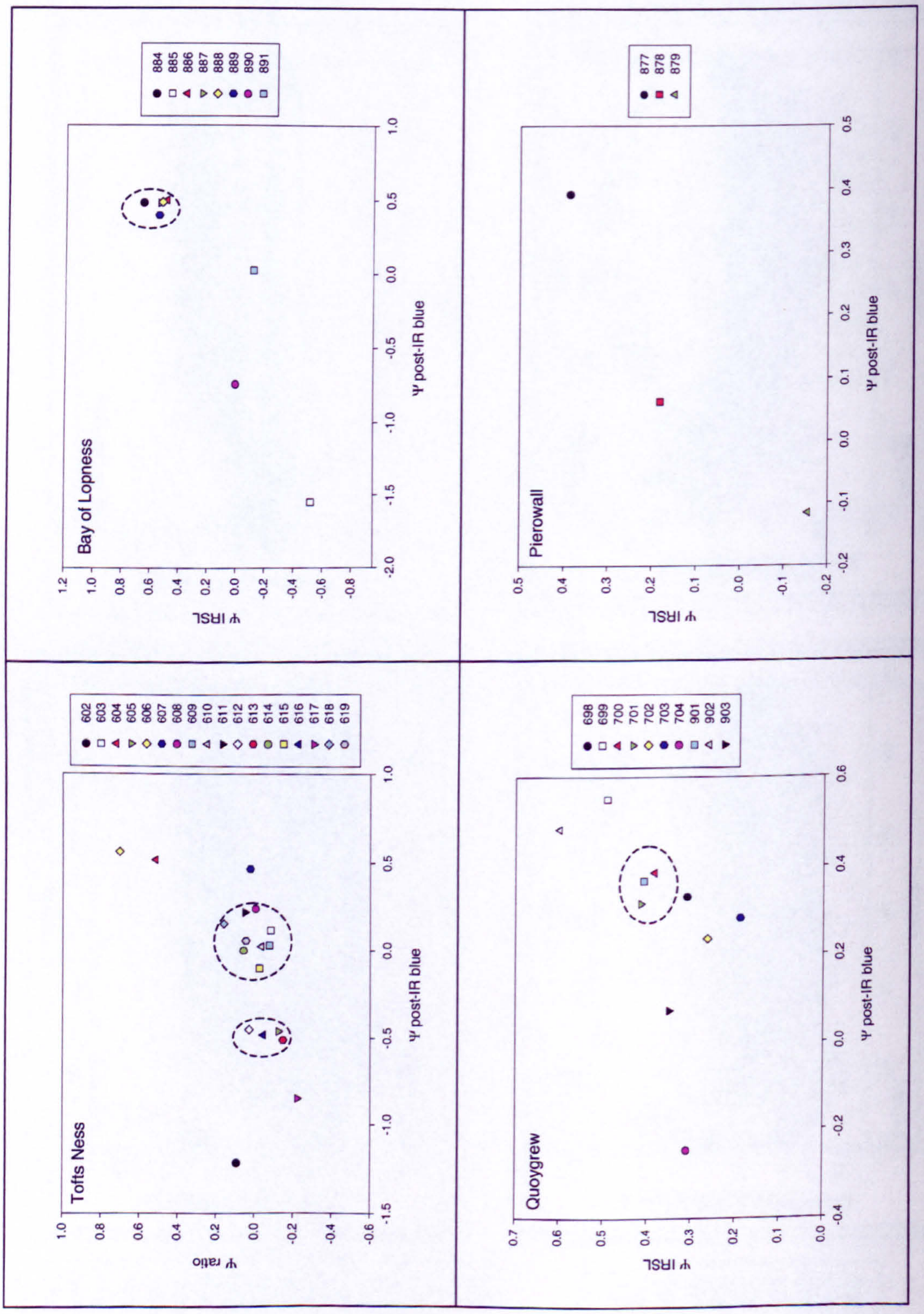
884
885
886
887
888
889
890
891
Bay of Lopness
ψ IRSL
Ψ post-IR blue
877
878
879
Pierowall
ψ IRSL
Ψ post-IR blue
602
603
604
605
606
607
608
609
610
611
612
613
614
615
616
617
618
619
Toffs Ness
ψ ratio
Ψ post-IR blue
698
699
700
701
702
703
704
901
902
903
Quoygrew
ψ IRSL
Ψ post-IR blue

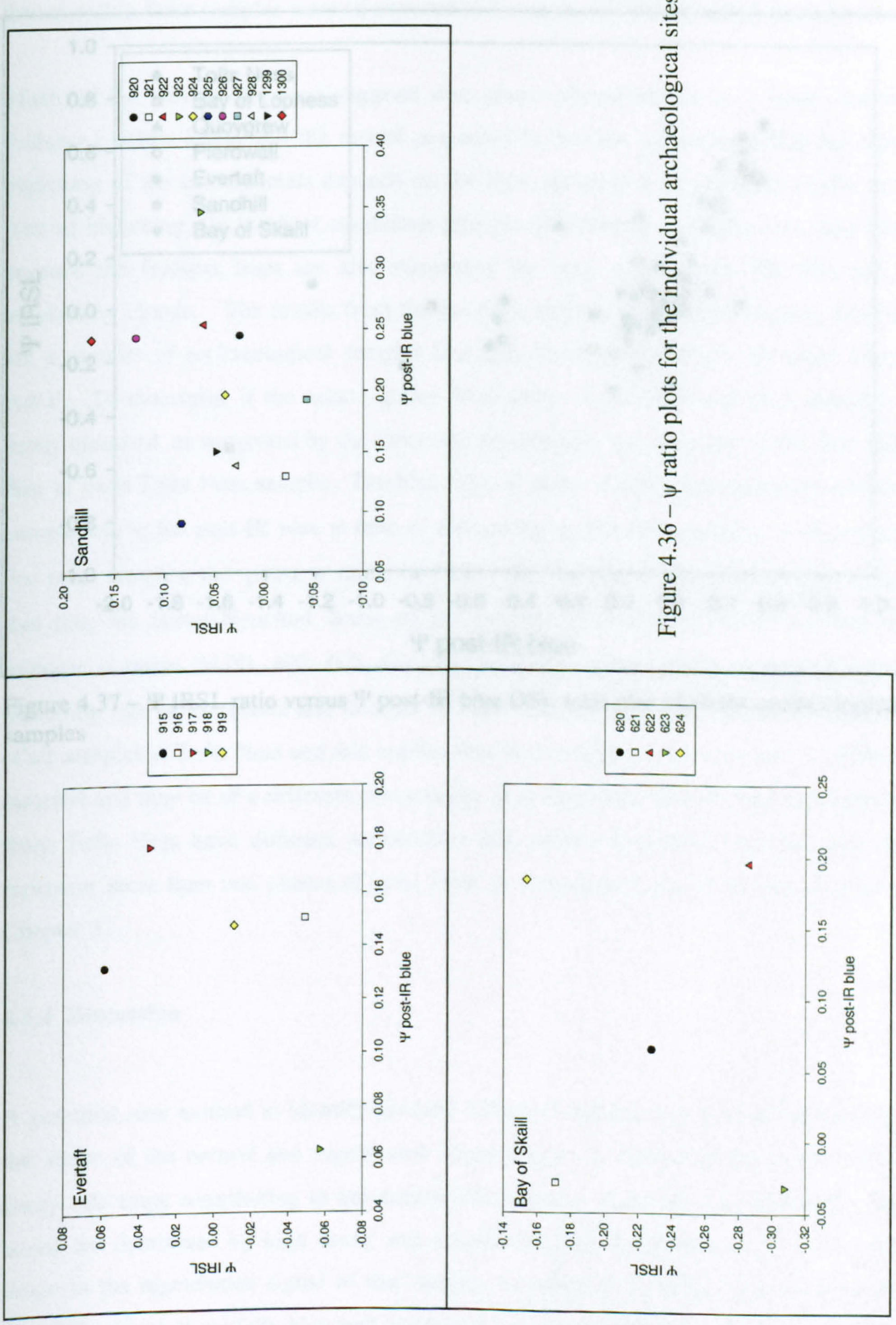

Figure 4.36 – ψ ratio plots for the individual archaeological sites

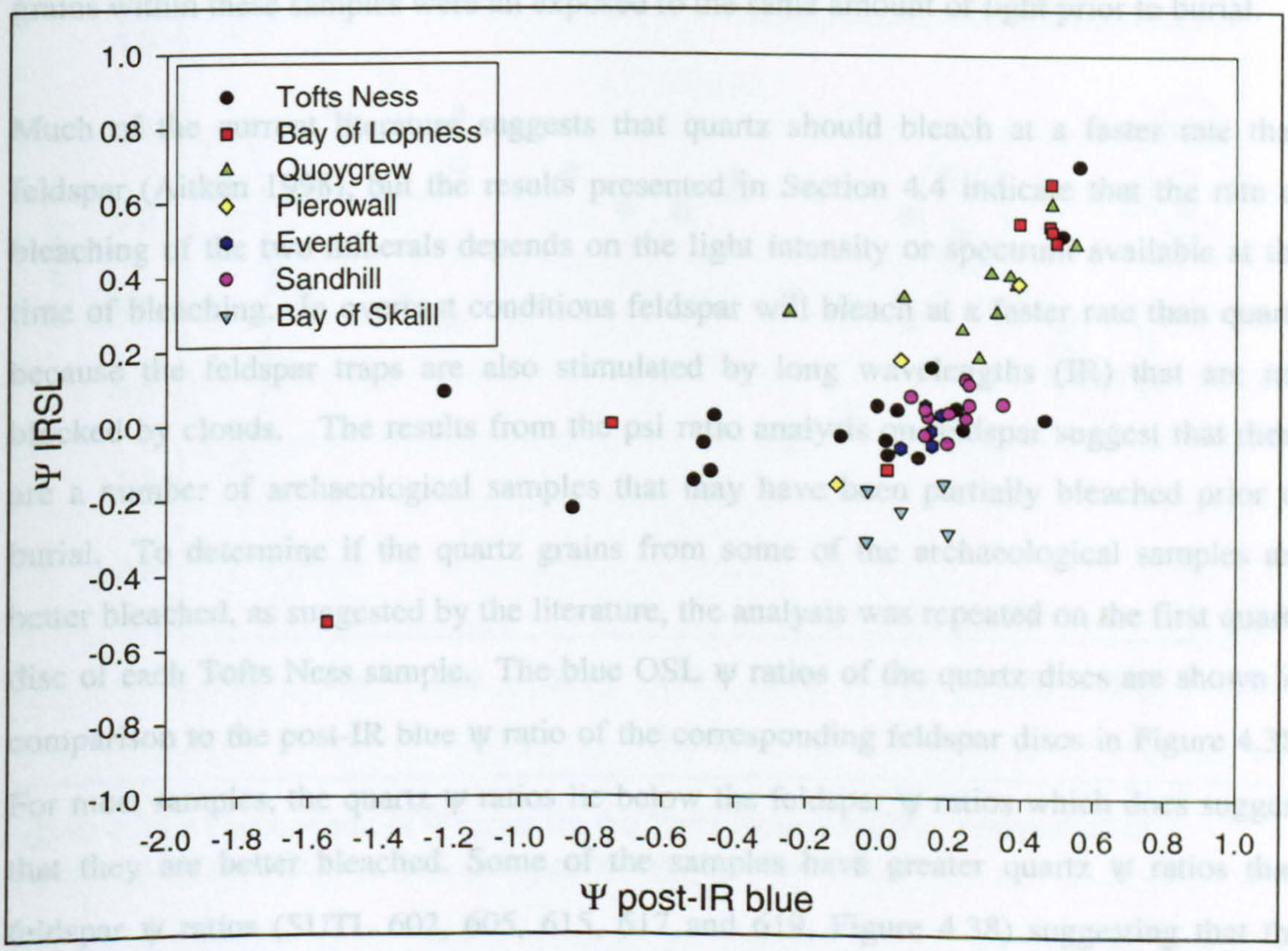

Figure 4.37 – Ψ IRSL ratio versus Ψ post-IR blue OSL ratio plot of all the archaeological samples

partially bleached. For some samples their identification as being partially bleached is surprising given that the estimated doses from the individual discs and the regenerative dose response curves are well-behaved with very little scatter. This suggests that the grains within these samples were all exposed to the same amount of light prior to burial.

Much of the current literature suggests that quartz should bleach at a faster rate than feldspar (Aitken 1998), but the results presented in Section 4.4 indicate that the rate of bleaching of the two minerals depends on the light intensity or spectrum available at the time of bleaching. In overcast conditions feldspar will bleach at a faster rate than quartz because the feldspar traps are also stimulated by long wavelengths (IR) that are not blocked by clouds. The results from the psi ratio analysis on feldspar suggest that there are a number of archaeological samples that may have been partially bleached prior to burial. To determine if the quartz grains from some of the archaeological samples are better bleached, as suggested by the literature, the analysis was repeated on the first quartz disc of each Tofts Ness sample. The blue OSL ψ ratios of the quartz discs are shown in comparison to the post-IR blue ψ ratio of the corresponding feldspar discs in Figure 4.38. For most samples, the quartz ψ ratios lie below the feldspar ψ ratios which does suggest that they are better bleached. Some of the samples have greater quartz ψ ratios than feldspar ψ ratios (SUTL 602, 605, 615, 617 and 619, Figure 4.38) suggesting that the bleaching rate of the quartz and feldspar in these samples is quite different to that of the other samples at Tofts Ness and this implies that these samples are composed of a different material and may be of a different provenance. It is suggested that because some samples from Tofts Ness have different sensitivities and various bleaching histories, they may represent more than two phases of sand blow or mixing and this is discussed further in Chapter 5.

4.5.4 Discussion

A potential new method to identify partially bleached samples has been introduced using the shape of the natural and regenerated decay curves to determine the amount of low decay rate traps contributing to the natural OSL signal. Samples well bleached prior to burial are dominated by high decay rate signals and will therefore have a similar decay shape to the regenerated signal of that sample, resulting in a psi (ψ) ratio close to zero. The OSL signal of partially bleached samples is composed of both high and low decay rate

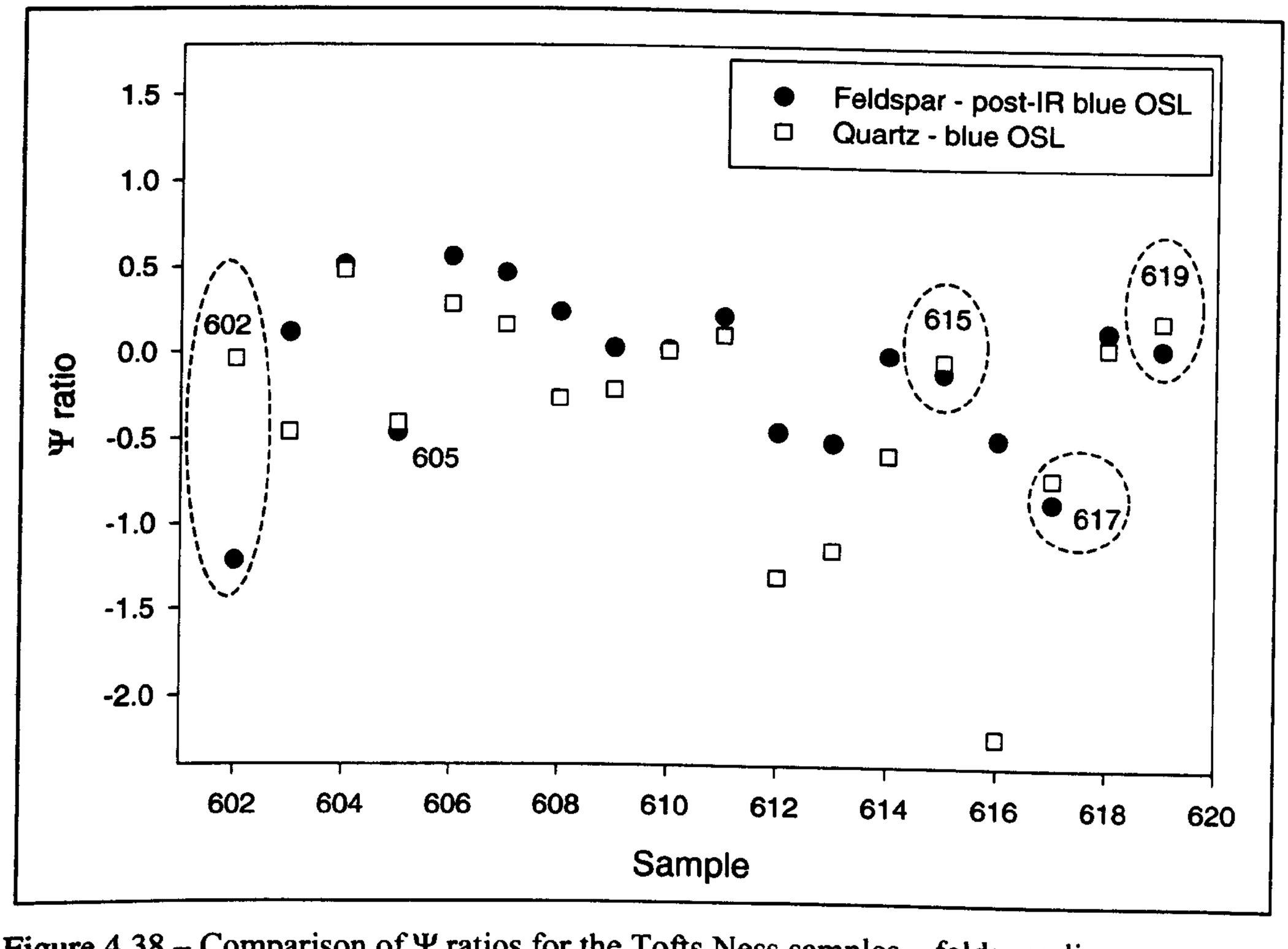

Figure 4.38 – Comparison of Ψ ratios for the Tofts Ness samples – feldspar discs stimulated by post-IR blue OSL and quartz discs by blue OSL

components and therefore the decay shape tends to be flatter as a result of the lower decay rate of some of the signal. There is a greater difference between the natural decay shape of a partially bleached sample and the regenerated signal of that sample and therefore the ψ ratio is greater.

The archaeological samples were analysed using this method and the results indicate that for most samples there appears to be a contribution to the natural luminescence signal which cannot be explained by the shape of the regenerated decay curve. Few samples have a ψ ratio close to zero and this supports the idea that sand layers deposited during storm events are more likely to be partially bleached. Many of the samples with high ψ ratios have small dating errors, for example sample SUTL 699 from Quoygrew (Figure 4.36) has a high ψ ratio but the error on the OSL age is only about 10%. The high precision suggests that the whole sample is homogenously partially bleached. If the sample was heterogeneously partially bleached i.e. some grains well bleached and others not, the ψ ratio may still be high but there would be low precision due to the range of D_e from the various aliquots. Yet not all samples that have large errors have large ψ ratios and vice versa. Some of the samples from Tofts Ness have low precision mainly as a result of poor sensitivity, yet they have low ψ ratios indicating that they were well-bleached prior to deposition and most of the natural luminescence signal appears to be from the high decay rate component.

Some of the ψ ratios from the archaeological samples and the field bleaching experiment have negative values. This is unexpected and suggests that the natural decay curve is bleaching faster than the regenerated decay curve. This is confirmed when the natural and regenerated decay curves are plotted on the same graph (e.g. SUTL 885, Figure 4.39a). The decay shape of the natural signal for both methods of stimulation is steeper than the regenerated decay curve and potential reasons for this are discussed below. When the flatter regenerated curve is subtracted from the steeper natural curve to obtain the 'C' component of the ψ ratio formula, any low decay rate component that may be contributing to the natural signal is less than that contributing to the regenerated signal. This results in negative net low decay rate signal graphs (Figure 4.39b) and negative ψ ratios as shown below for sample SUTL 885:

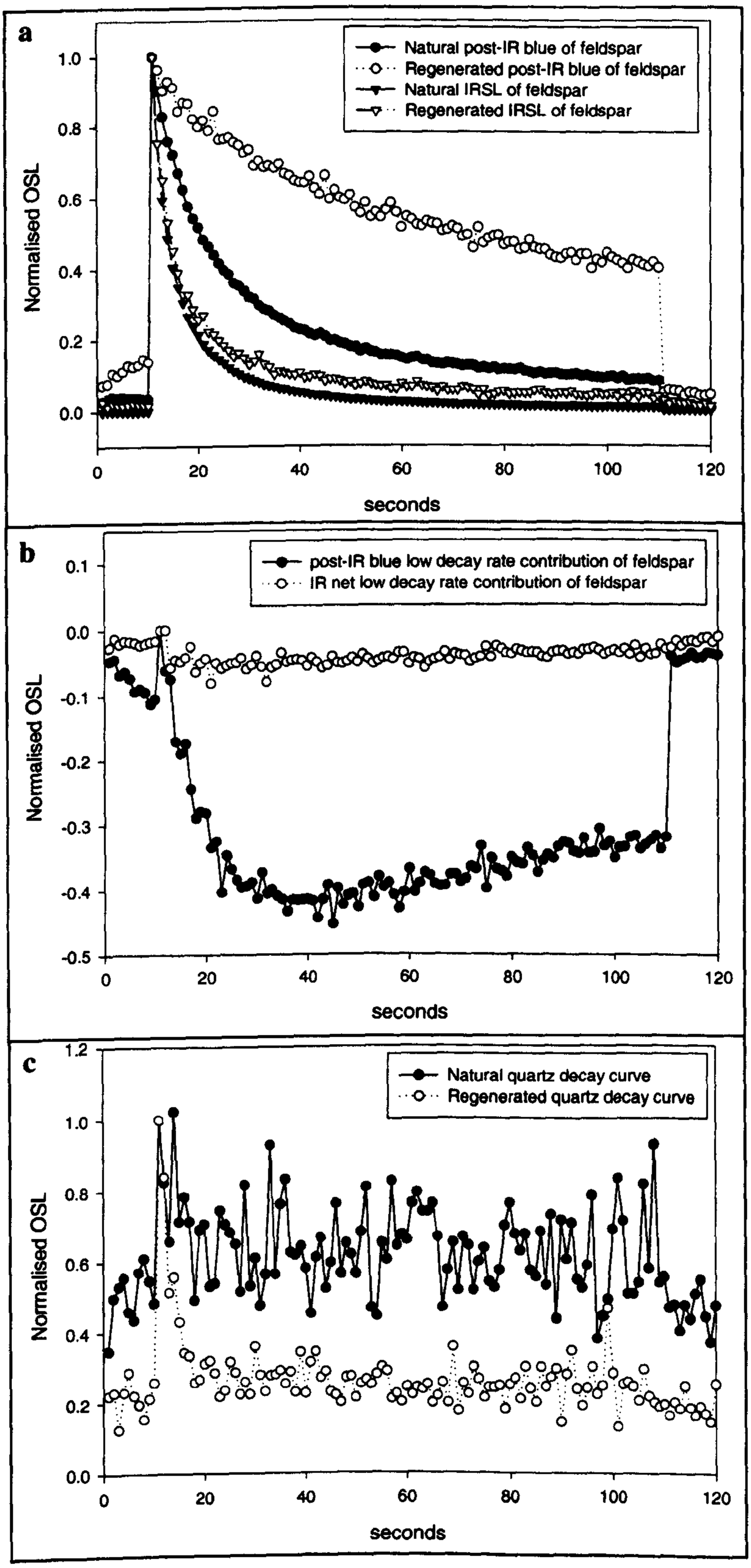

Figure 4.39 – SUTL 885 - a) Natural and regenerated decay curves of feldspar stimulated by IRSL and post-IR blue OSL; b) Net low decay rate contribution to feldspar signal stimulated by IRSL and post-IR blue OSL; c) Natural and regenerated decay curves of quartz stimulated by blue OSL.

IR ψ ratio $$\Psi = \frac{C}{A} = \frac{-4.15}{7.96} = -0.52$$

Post-IR blue ψ ratio $$\Psi = \frac{C}{A} = \frac{-35.38}{22.89} = -1.55$$

There are several reasons why the natural decay shape for these samples may be steeper than the regenerated decay curve. The first reason may be due to transfer of charge from the low decay rate component during stimulation or preheat. Each aliquot is stimulated for 100 seconds, which is longer than the 40 seconds of blue light stimulation proposed by Murray and Wintle (2000), to reduce the signal to negligible levels, although they do suggest that up to 100 seconds may be required depending on the light source. Prior to the LEDs being switched on, a 10 second background count is measured and this is repeated at the end of the stimulation. There is an abrupt change in the curves as the IR or blue LEDs are switched on and off (Figure 4.39a) and the drop to background levels at the end of the stimulation emphasises that the grains still contain a luminescence signal which has not been depleted during stimulation. During subsequent irradiation and preheating, traps contributing to the short term component will be filled and the thermally unstable traps will be emptied respectively, however the subsequent luminescence signal will be a combination of the artificial dose and the remaining low decay rate signal that was not depleted during the initial stimulation.

There is a significant difference in the post-IR blue decay shapes of sample SUTL 885 (Figure 4.39a) and, as previously suggested, the flatter decay shape suggests that the signal is mainly from the low decay rate component which has a much slower bleaching rate. The flatter decay curve of the regenerated signal is confusing given that even after the natural signal has been stimulated by IR, the post-IR blue natural signal is still relatively fast. This leads to the second possible reason for the steeper decay shapes of the natural signal; the contribution from alpha particle irradiation.

Natural radioactivity produces three types of radiation, alpha particles, beta particles and gamma rays and all penetrate sediment and grains by different amounts based on how quickly they lose their energy (Aitken 1998). Alpha particles lose their energy very rapidly and will only affect grains within about 0.03mm of the emitting nucleus and therefore external alpha particles will only penetrate the outer skin of quartz and feldspar

grains greater than about 65 μm (Aitken 1998). To obtain 'pure' quartz the grains are washed in 40% HF for 40 minutes to etch the surface of the grains and this is thought to be sufficient to remove the outside of the grains which may have been affected by an external alpha contribution (Fleming 1970; Aitken 1998). The method proposed here to identify partially bleached sediments uses the decay shape of feldspar grains and these have only been washed in 15% HF for 15 minutes to very lightly etch the surface of the grains. In luminescence dating, a beta source is commonly used for artificial irradiation because the source can be placed within the automatic reader and the sediment is deposited as a monolayer of grains onto a disc which allows full penetration of the beta particles (Aitken 1998). Gamma and alpha irradiators have also been used for administering artificial doses, however gamma irradiators are expensive and require heavy shielding and alpha irradiators are unsuitable due to the short range of alpha particles (Aitken 1998). The light etching of the feldspar grains in the sample preparation may not be sufficient to remove the alpha irradiated outer layer of the grains and therefore the natural decay curve may be a combination of both beta and alpha radiation. The regenerated dose is the result of exposure of the feldspar grains to a beta source and therefore, without the contribution from the alpha irradiation, this may change the shape of the decay curve.

To test whether this is also true for pure quartz aliquots, the natural and 1 Gy regenerated decay curves from blue stimulation of a quartz disc from sample SUTL 885 were plotted and the results are shown in Figure 4.39c. Although the IR and post-IR blue ψ ratios from the feldspar disc of this sample are both negative, the decay curves from the pure quartz disc do not behave in a similar manner to the decay curves of the feldspar disc shown in Figure 4.39a. The quartz natural decay curve is flatter than the 1 Gy curve and this suggests that the quartz fraction of this aliquot contains partially bleached grains and that the natural feldspar decay curves may be affected by alpha radiation. The analysis was repeated on a sample from Tofts Ness (SUTL 617) which is much older than sample SUTL 885 and the results are shown in Figure 4.40. Both the IR and post-IR blue ψ ratios of this sample are negative and the decay curves from the pure quartz disc also indicate that the natural decay curve is slightly steeper than the regenerated curve producing a negative ψ ratio. This suggests that the steeper decay shape of the natural curves of this sample is unlikely to be due to a contribution from alpha radiation as the outer skin of the quartz grains, which may have been irradiated by alpha particles, has effectively been removed by etching in 40% HF. Although etching in concentrated HF for 40 minutes is thought to be sufficient to remove the outer layer of quartz grains, it is possible for some

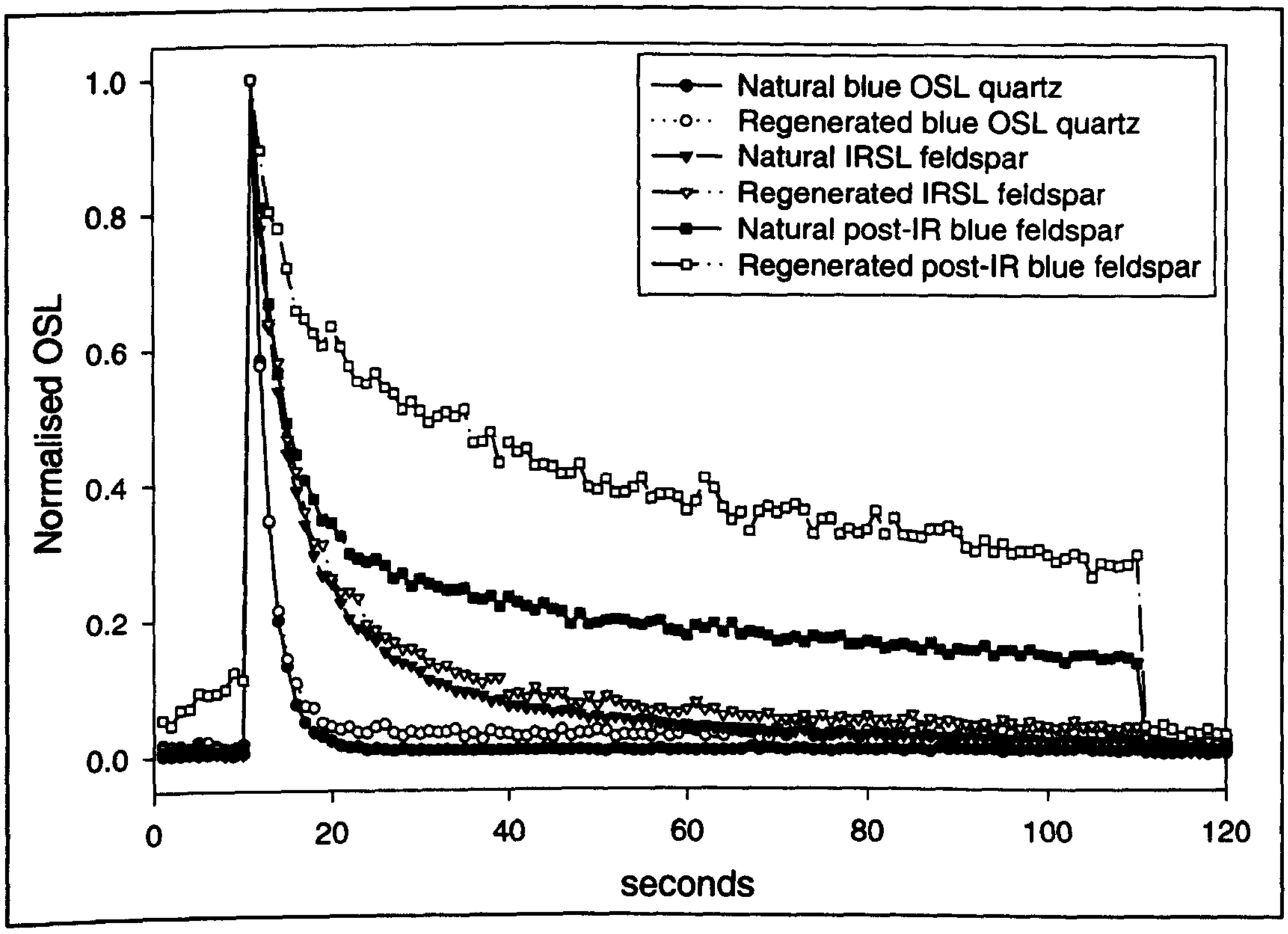

Figure 4.40 – SUTL 617 – Natural and regenerated decay curves of quartz stimulated by blue OSL and feldspar stimulated by IRSL and post-IR blue OSL

samples that this is not sufficient and longer periods may be necessary. The variable response of the quartz fraction of the samples discussed above does not confirm whether there is a significant contribution from alpha radiation in natural decay curves and this may be based on the mineralogy of the sample. Research on the decay shape of alpha irradiated quartz and feldspar grains would determine if radiation by alpha particles is different to that of beta particles and whether it contributes significantly to the luminescence signal. The results of these experiments may lead to a modification of the acid treatment currently undertaken on sediments to ensure that there is no contribution from alpha radiation to the quartz OSL signal, allowing the natural and regenerated doses generated from beta radiation alone to be comparable.

A third possible reason for the different decay shapes may be due to the variable surface texture of quartz and feldspar grains. Research on the surfaces of aeolian sand grains has shown that they are characterised by small scale features such as pits, scratches and ridges formed by mechanical abrasion, etching and precipitation of silica (Pye and Tsoar 1990; Boggs 1995). In some circumstances the precipitation of silica will infill the pits causing the grains to become smoother and rounder than they actually are (Margolis and Krinsley 1971; Nieter and Krinsley 1976). The silica precipitate may affect the amount of light penetrating the grain depending on the reflectivity or transparency of the grain and this could result in partial bleaching. The laboratory acid treatment is thought to ensure that the outer surface of the grain, including the precipitate, is removed but traps with a low decay rate may still remain filled within the grain. The low decay rate signal contributing to the natural signal may not be immediately obvious, as discussed above, but thermal transfer of electrons from deeper traps during preheating and measurement may result in the partially bleached low decay rate signal contributing to the regenerated signal. The slower bleaching rate of the low decay rate component would ensure that the shape of the regenerated decay curve would be flatter.

Another aspect of the ψ ratios is that some samples have negative IRSL ψ ratios but positive post-IR blue ψ ratios and vice versa (Figure 4.37). This suggests that whatever controls the shape of the decay curve after artificial irradiation affects only one set of traps in these samples (i.e. the traps associated with IR stimulation when the IRSL ψ ratio is negative and the traps stimulated by blue OSL when the post-IR blue ψ ratio is negative). This implies that the IRSL and blue OSL traps in feldspar grains act differently when

exposed to artificial irradiation and this suggests that they could respond differently when exposed to natural radiation.

The reasons for the flatter shape of the regenerated decay curve may be none, one, or a combination of the potential reasons outlined above and further research is needed to resolve this. Whatever the reason, the question remains as to why this occurs for some samples and not others. Of the 60 samples collected for OSL dating in the Orkney Islands, 43% have at least one ψ ratio less than zero. When these samples are compared with those that have positive ψ ratios, there is nothing to indicate that these samples should behave differently. The samples with negative ψ ratios are not any more, or less, sensitive than the positive ψ ratio samples, they have various amounts of calcium carbonate content and the OSL dates have variable precision and therefore the reason for some samples displaying negative ψ ratios currently remains unclear.

The questions raised by this new method to identify partially bleached samples need to be answered before it can be used routinely to enhance the accuracy of OSL dating. Perhaps the most important question is whether the net signal identified by the subtraction of the regenerated curve from the natural curve does indeed signify that the sample is partially bleached. Once this is determined, it may then be possible to accurately date partially bleached sediments using a correction factor. The reasons for the flatter regenerative decay curve are important in terms of how feldspar, and potentially quartz, grains react to the measurement, irradiation and preheat cycle. The issue of whether the remaining luminescence signal within the grains, after 100 seconds of stimulation, does contribute to the subsequent regenerative dose signal and hence age of the sample may depend on the analysis of the SAR results.

Aitken and Xie (1992) introduced the late light subtraction method for analysis of natural and regenerative shine down curves. This technique removes the signal that is not wanted, for example the background from the photomultiplier tube and the luminescence from the low decay rate (long term) component that was not emptied at deposition and concentrates on the signal that is rapidly and fully bleached prior to deposition. The first 10 seconds of stimulation has been chosen in the SAR analysis of the archaeological samples to represent the initial signal. A background is subtracted from the initial signal based on the average OSL signal over the remainder of the stimulation period (Figure 3.29) and this is thought to

remove any contribution from the low decay rate/long term component and background. Part of the long term component in a partially bleached sample is the residual signal and therefore subtracting an average of the remaining OSL signal will remove this residual component from the initial signal. This means that the greater the residual component to the OSL signal, the greater the amount subtracted from the initial signal. Analysing the data in this way is thought to remove any contribution from the residual signal and therefore, although some samples may be partially bleached, the OSL ages are not thought to be greatly overestimated.

Further analysis on the psi ratio has shown that the psi ratio of 53% of the samples is reduced when late light subtraction is applied. This implies that for these samples late light subtraction removes some, or all, of the residual signal (low decay rate component) contributing to the natural OSL signal. However for the remaining 47% the psi ratio increases when late light subtraction is applied. This suggests that the contribution of the low decay rate component to the OSL signal is increasing and hence there is a greater difference between the natural and regenerated decay curves after late light subtraction.

4.6 Summary of Chapter 4

This chapter has presented the results from the residual and bleaching experiments and introduced a new method to identify partially bleached samples. The residual levels from the modern beach sands confirm that TL is not a suitable technique for dating wind blown sands in this study area and despite the small residual levels observed when samples were stimulated by OSL and IRSL, these techniques remain viable for sediment dating. Modern beach sands were collected from the Outer Hebrides and the Orkney Islands for this experiment and there appears to be a geological and mineralogical control on the extent of bleaching, with samples from the Outer Hebrides having lower residuals when measured by TL, IRSL and OSL. This was confirmed in the bleaching experiments, which showed that the sample from the Outer Hebrides tended to bleach at a faster rate than the samples from the Orkney or Shetland Islands.

The bleaching experiments undertaken in the laboratory and field have shown that, in addition to mineralogy and provenance, light intensity is a major control on the rate and extent of bleaching. Rapid bleaching of both quartz and feldspar occurs when the minerals

are exposed to the full spectrum, but the rate of bleaching is severely reduced when a filter is introduced in the laboratory experiments or the samples are bleached in natural light conditions. The slow bleaching rate of quartz in the field does flag the possibility that some of the archaeological samples may be partially bleached.

The psi ratio has been introduced to identify partially bleached samples using the natural and regenerated decay curves of associated feldspars. The initial results are encouraging and suggest that with additional research, this technique may be useful in further OSL dating studies. It is unclear as to why some samples have steeper natural decay curves than regenerated decay curves, but it may be due to charge transfer, a contribution from alpha irradiation that has not been removed by the HF treatment or the variable surface texture of quartz and feldspar. Analysis of the decay curves of feldspar and quartz in this way has also raised several questions regarding how the various components respond to irradiation, bleaching and stimulation by IRSL and/or blue OSL.

Chapter 5 – Analysis 2 - OSL dating of archaeological samples

5.1 Introduction

The aim of this chapter is to present the OSL ages from the archaeological samples and to discuss these in relation to other archaeological evidence at the sites. The results of the bleaching experiments discussed in Chapter 4 indicated that samples from different areas behave differently, possibly due to mineralogical differences. However, despite the variable bleaching rates between the samples tested and also between quartz and feldspar, quartz rather than feldspar has been used to date the archaeological samples because it bleaches more rapidly than feldspar when initially exposed to light. Associated feldspars have, however, been used to check whether the samples were adequately bleached prior to burial using the psi ratio and this information can be used in the interpretation of the OSL dates.

Prior to presenting the OSL results, trends observed within the samples are discussed to gain an understanding of how the samples as a whole respond to various aspects of sample preparation and the SAR procedure. The OSL ages are then presented for each site with the SAR trends and observations being noted before interpreting the ages with regard to the stratigraphy and surrounding archaeology.

5.2 Trends and observations in the sample preparation and SAR procedure

5.2.1 Water content

Water absorbs natural radiation and therefore the water content of a sample must be taken into consideration when calculating the dose rate and age of a sample. Although the actual and saturated water contents can be measured it is difficult to determine how the water content has varied throughout the burial history of the sample. Samples that are near saturation or are very dry will have varied little, however the water content of most samples will vary depending on changes in the water table, climate and increased depth below the surface, especially from samples close to sea level. The actual water content of the samples analysed varies quite considerably with some samples having actual water contents of less than 5% (e.g. SUTL 901-903, Quoygrew, Appendix 5.1) and others are totally saturated (e.g. SUTL 1299 and 1300, Sandhill). The amount of water within the samples depends on location of the site and if the water can easily drain through the sand

layers. For example Tofts Ness lies at about 5 m above sea level and because the site now floods each year during the winter (E. Guttmann *pers.comm.*) the amount of water within the sand layers will vary quite considerably within one year. The sand layers at Tofts Ness are also interleaved with palaeosols that will prevent rapid percolation of water whereas at other sites e.g. Bay of Lopness or Quoygrew, the thick sand deposits are easily drained. It is unrealistic to determine how much radiation is absorbed by the water using either the actual or saturated water contents. Table 5.1 shows how the age of a sample will vary depending on the water content used.

Sample	Water content	Wtd. Mean D_e (Gy)	Dose Rate (mGya-1)	Age (years before AD 2000)	Date (BC/AD)
SUTL 602	Actual (21%)	4.67 ± 0.16	1.028 ± 0.066	4540 ± 330	2870–2210 BC
	Calculated (28 ± 7%)		0.986 ± 0.076	4735 ± 400	2935–2535 BC
	Saturated (35%)		0.948 ± 0.06	4900 ± 370	3270–2530 BC
SUTL 604	Actual (4%)	0.11 ± 0.03	0.42 ± 0.059	260 ± 80	AD 1660–1820
	Calculated (12 ± 8%)		0.412 ± 0.059	265 ± 80	AD 1655–1825
	Saturated (20%)		0.405 ± 0.058	270 ± 85	AD 1645–1815

Table 5.1 – Variation in sample age when various water contents are used to determine the rate

For both samples in Table 5.1 the dose rate decreases as the water content increases and therefore the age of the sample increases as the water content increases. However there is a greater range in age estimates for samples with lower precision (e.g. SUTL 602). The water content used in this analysis is the midpoint between the actual and saturated water contents (the calculated water content in Table 5.1) and therefore the error ensures that both are considered in the dose rate calculation.

5.2.2 Results of HCl treatment

The quantity of shell within the samples can provide some indication of the source of the sand within the archaeological sites. These data are obtained by weighing a small portion of each sample prior to washing in 10% HCl for 30 minutes and then re-weighing the samples after washing in de-ionised water and drying in an oven at 50°C. Figure 5.1 shows results of the HCl treatment for some of the modern beach sands collected. Between 3%

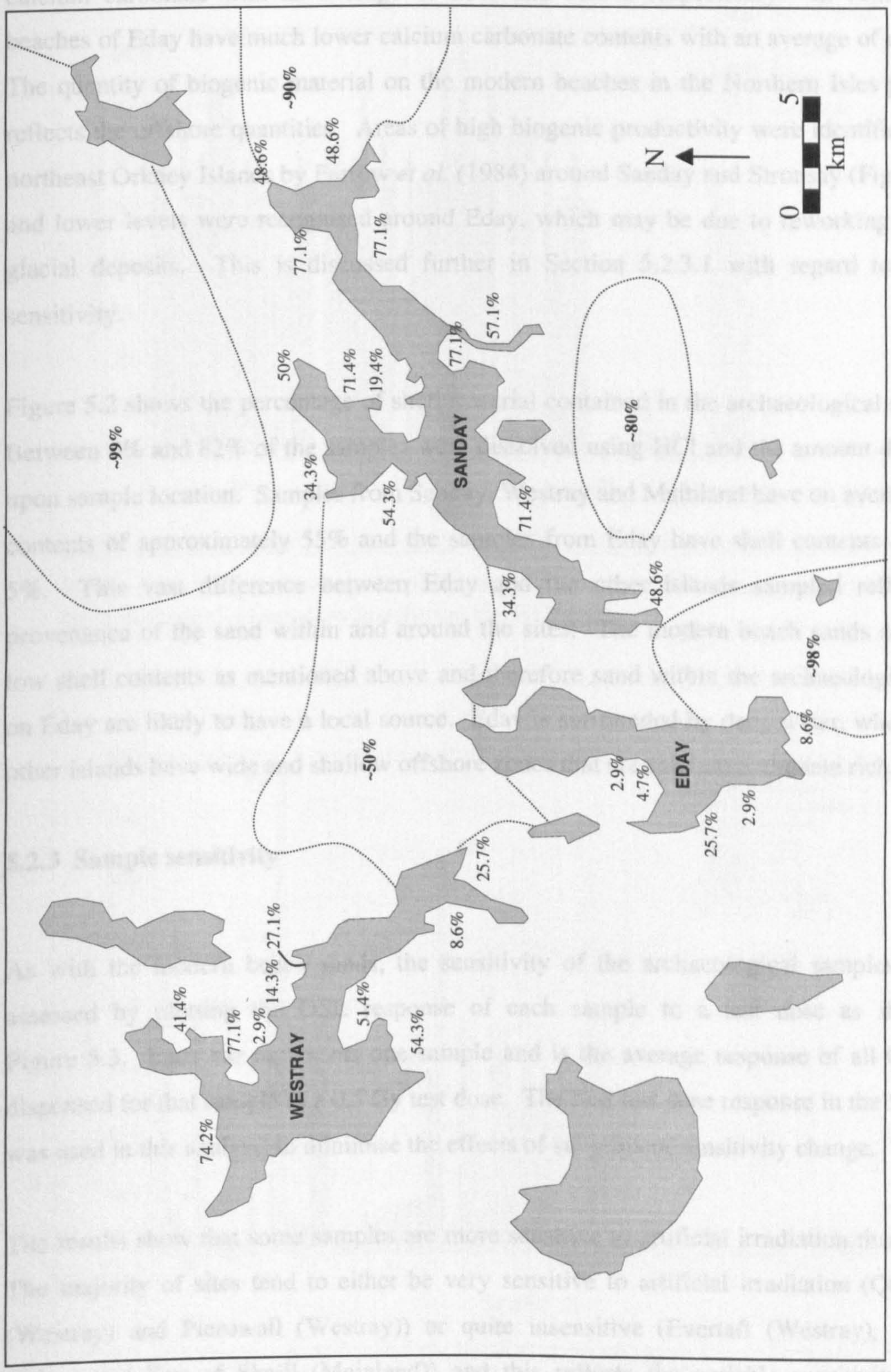

Figure 5.1 – Map of the Northern Isles of Orkney showing the percentage of calcium carbonate content on the modern beaches and in the offshore region. Offshore data from Farrow *et al.* (1984).

and 77% of the sand on the beaches of Sanday and Westray is composed of biogenic calcium carbonate with an average of 55% and 38.5% respectively. In contrast, the beaches of Eday have much lower calcium carbonate contents with an average of only 7%. The quantity of biogenic material on the modern beaches in the Northern Isles probably reflects the offshore quantities. Areas of high biogenic productivity were identified in the northeast Orkney Islands by Farrow *et al.* (1984) around Sanday and Stronsay (Figure 5.1), and lower levels were recognised around Eday, which may be due to reworking of local glacial deposits. This is discussed further in Section 5.2.3.1 with regard to sample sensitivity.

Figure 5.2 shows the percentage of shell material contained in the archaeological samples. Between 0% and 82% of the samples were dissolved using HCl and the amount depended upon sample location. Samples from Sanday, Westray and Mainland have on average shell contents of approximately 55% and the samples from Eday have shell contents of about 5%. This vast difference between Eday and the other islands sampled reflects the provenance of the sand within and around the sites. The modern beach sands also have low shell contents as mentioned above and therefore sand within the archaeological sites on Eday are likely to have a local source. Eday is surrounded by deep water, whereas the other islands have wide and shallow offshore zones that are calcium carbonate rich.

5.2.3 Sample sensitivity

As with the modern beach sands, the sensitivity of the archaeological samples can be assessed by plotting the OSL response of each sample to a test dose as shown in Figure 5.3. Each bar represents one sample and is the average response of all the discs dispensed for that sample to a 0.5 Gy test dose. The first test dose response in the SAR run was used in this analysis to minimise the effects of subsequent sensitivity change.

The results show that some samples are more sensitive to artificial irradiation than others. The majority of sites tend to either be very sensitive to artificial irradiation (Quoygrew (Westray) and Pierowall (Westray)) or quite insensitive (Evertaft (Westray), Sandhill (Eday) and Bay of Skaill (Mainland)) and this reflects the variable sensitivity of the modern beach sands previously discussed in Section 4.3 (Figures 4.3 and 4.4). The modern beaches on Eday have fairly low sensitivity and the low sensitivity of the Sandhill samples

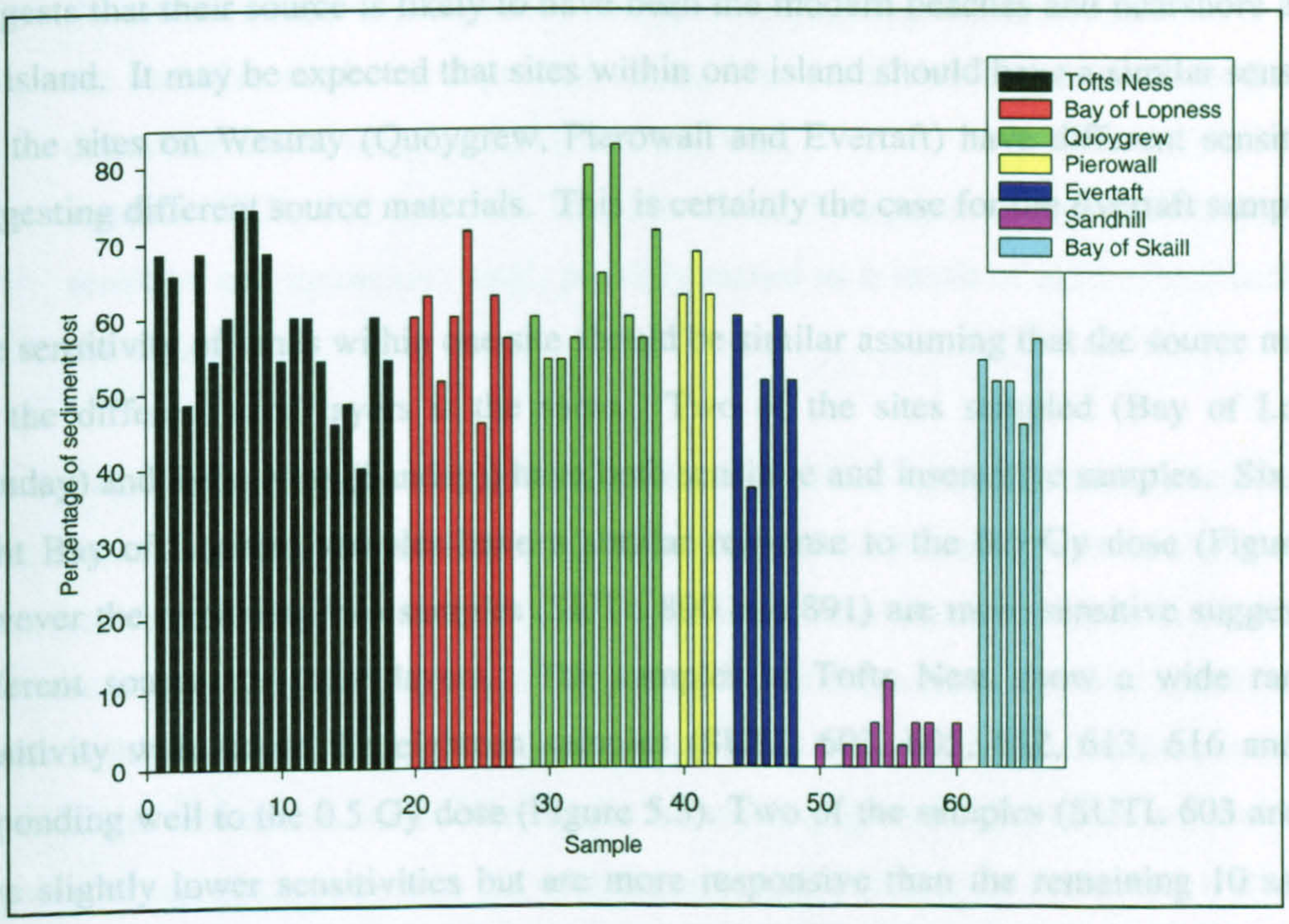

Figure 5.2 – Graph showing the percentage of calcium carbonate material within the archaeological samples lost during the HCl wash

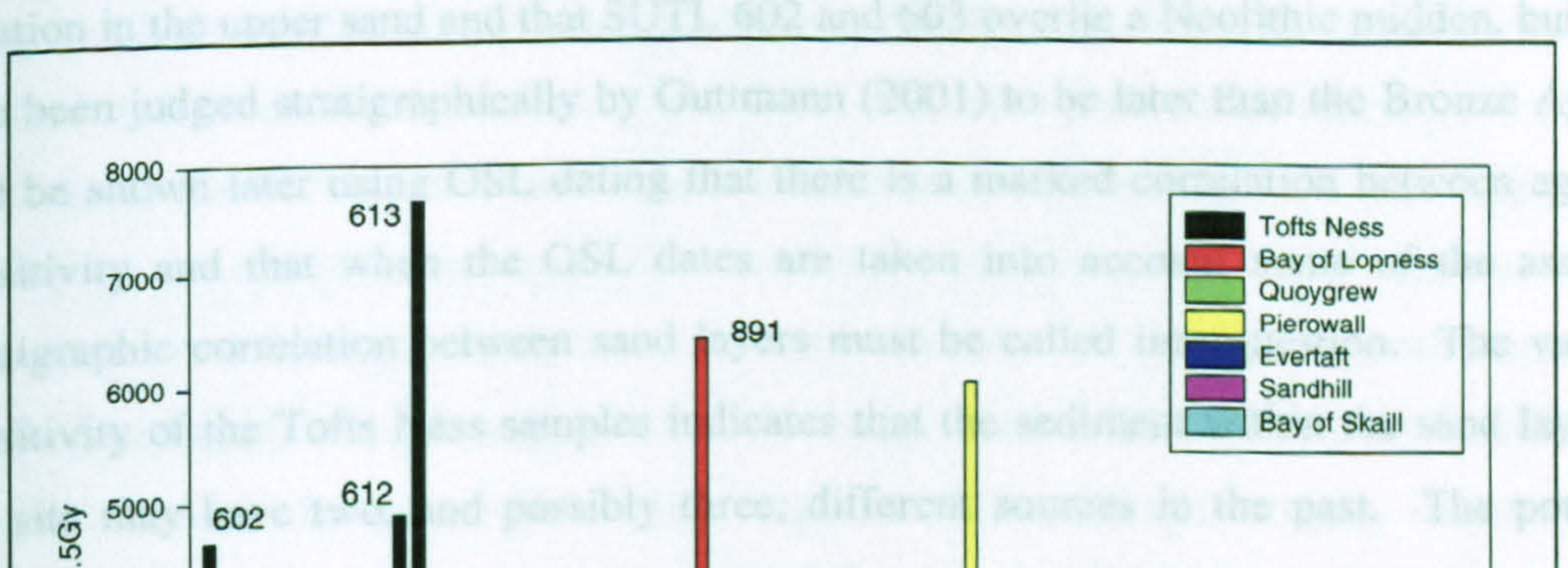

Figure 5.3 – Sensitivity of archaeological samples to a 0.5Gy dose

suggests that their source is likely to have been the modern beaches and nearshore area of the island. It may be expected that sites within one island should have a similar sensitivity but the sites on Westray (Quoygrew, Pierowall and Evertaft) have different sensitivities suggesting different source materials. This is certainly the case for the Evertaft samples.

The sensitivity of sands within one site should be similar assuming that the source material for the different sand layers is the same. Two of the sites sampled (Bay of Lopness (Sanday) and Tofts Ness (Sanday)) have both sensitive and insensitive samples. Six of the eight Bay of Lopness samples have a similar response to the 0.5 Gy dose (Figure 5.3) however the remaining two samples (SUTL 890 and 891) are more sensitive suggesting a different source for these layers. The samples at Tofts Ness show a wide range in sensitivity with six of the eighteen samples (SUTL 602, 605, 612, 613, 616 and 617) responding well to the 0.5 Gy dose (Figure 5.3). Two of the samples (SUTL 603 and 610) have slightly lower sensitivities but are more responsive than the remaining 10 samples which show poor sensitivity. Note that samples SUTL 610, 612, 613, 616, and 617 are identified as lower sands from the stratigraphy (Figure 3.7); that SUTL 605 is in a basal location in the upper sand and that SUTL 602 and 603 overlie a Neolithic midden, but have also been judged stratigraphically by Guttmann (2001) to be later than the Bronze Age. It will be shown later using OSL dating that there is a marked correlation between age and sensitivity and that when the OSL dates are taken into account some of the assumed stratigraphic correlation between sand layers must be called into question. The variable sensitivity of the Tofts Ness samples indicates that the sediment within the sand layers at the site may have two, and possibly three, different sources in the past. The potential identification of the sediment provenance of these archaeological samples using sample sensitivity is discussed further in Section 5.2.3.1 below.

It was suggested in Chapter 3 that the two sand layers identified within several test pits at Tofts Ness may have been deposited during two storm events and the high and low response of the samples to artificial irradiation may confirm this. However, Figure 5.3 shows that although the majority of higher sensitivity samples are from the lower sand layer, two of the sensitive samples, SUTL 602 and 605, were collected from the upper sand layer. There are three possible reasons for the identification of sensitive samples in the upper and lower sand layers:

(i) the sensitive sand was deposited during more than one event;

(ii) the sensitive sand was deposited during one event but there was no further sand deposition above samples SUTL 602 and 605;

(iii) samples SUTL 602 and 605, Test Pits 2 and 3 respectively, are a combination of sensitive and insensitive sand, possibly mixed as a result of agricultural activity at the site.

OSL dating of the samples will help to establish if the sand layers represent more than two storm events and this is discussed further in Section 5.3.1. It seems unlikely that there was no further significant sand deposition over the area from which samples SUTL 602 and 605 were collected, especially since other samples in these pits have low sensitivity and therefore this supports the third suggestion that some of the samples may be a mixture of sensitive and insensitive sand. The results shown in Figure 5.3 are based on the average response of the discs dispensed for each sample and therefore to determine if there is a mixture of sensitive and insensitive sand within some of the samples, the response of the 0.5 Gy dose for each disc was plotted and the results are shown in Figure 5.4. The majority of discs in the highly sensitive samples (SUTL 602, 605, 612, 613, 616 and 617) respond well to artificial irradiation and those that have poor sensitivity do not respond well. Some discs within these low sensitive samples do respond well and this suggests that mixing of the sensitive and insensitive sand may have occurred. The response of the individual discs from the highly sensitive upper samples (SUTL 602 and 605) does vary quite considerably and this suggests that the samples are a mixture of both sensitive and insensitive sand. Based on the average response of the discs, the highly sensitive sand dominates these samples. The two samples that show a moderate response to artificial irradiation (SUTL 603 and 610) confirm that mixing has occurred, probably as a result of agricultural activity.

The response of the archaeological samples to artificial irradiation has shown that OSL dating of the Evertaft (Westray), Sandhill (Eday) and Bay of Skaill (Mainland) samples is hindered by low sensitivity. Despite this, the variable sensitivity of the archaeological samples has indicated that within some of the sites there is more than one source of sand and that some mixing of the sensitive and insensitive sand has occurred, possibly due to anthropogenic activity. Future work using small aliquot equivalent dose distributions such as that presented by Olley *et al.* (1998, 1999) and Spencer *et al.* (in press) may provide such evidence.

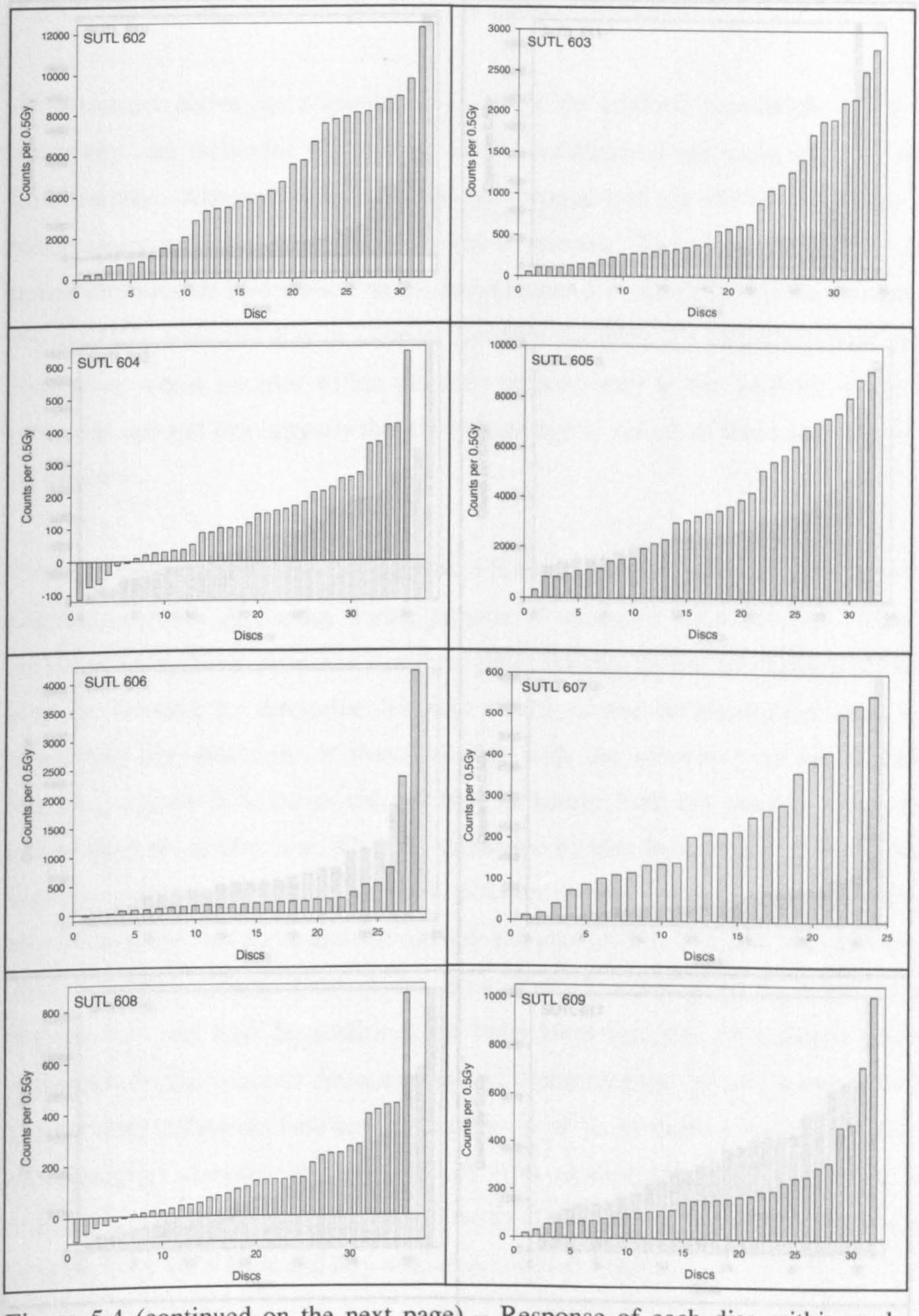

Figure 5.4 (continued on the next page) – Response of each disc within each Tofts Ness sample to a 0.5 Gy dose. The discs have not been normalised to allow the range in sensitivity of the discs per sample to be shown. Note that the y-axis scale is different for each sample reflecting the variable sensitivity between samples as well as within samples. The negative response of some discs to a 0.5 Gy dose suggests that the quartz grains on these discs do not respond well to artificial irradiation.

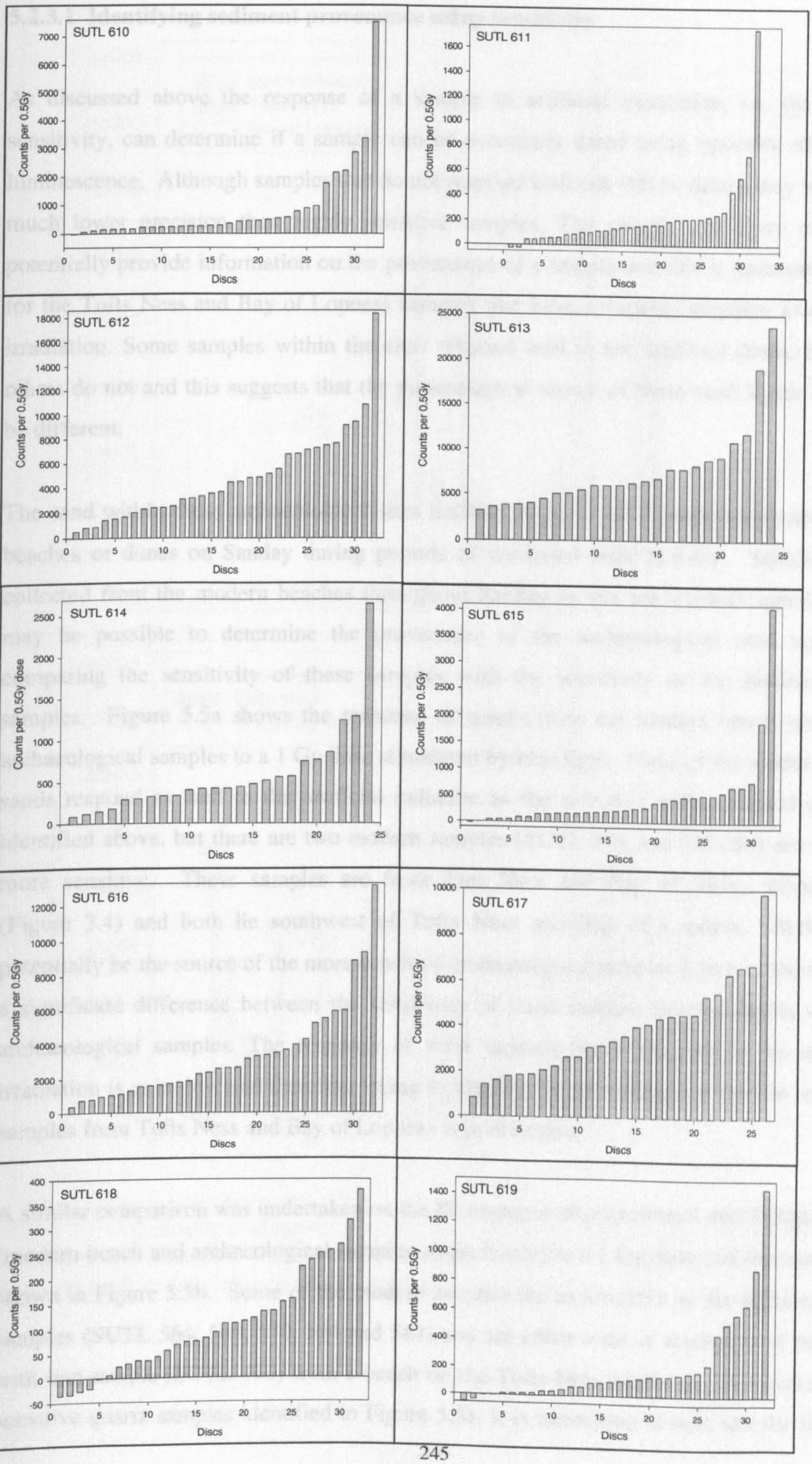
SUTL 610
Counts per 0.5Gy
Discs
SUTL 611
Counts per 0.5Gy
Discs
SUTL 612
Counts per 0.5Gy
Discs
SUTL 613
Counts per 0.5Gy
Discs
SUTL 614
Counts per 0.5Gy dose
Discs
SUTL 615
Counts per 0.5Gy
Discs
SUTL 616
Counts per 0.5Gy
Discs
SUTL 617
Counts per 0.5Gy
Discs
SUTL 618
Counts per 0.5Gy
Discs
SUTL 619
Counts per 0.5Gy
Discs

5.2.3.1 Identifying sediment provenance using sensitivity

As discussed above the response of a sample to artificial irradiation, i.e. the sample sensitivity, can determine if a sample can be accurately dated using optically stimulated luminescence. Although samples that do not respond well can still be dated, they will have much lower precision than highly sensitive samples. The sample sensitivity may also potentially provide information on the provenance of a sample and this is discussed below for the Tofts Ness and Bay of Lopness samples that have a variable response to artificial irradiation. Some samples within the sites respond well to the artificial doses, however others do not and this suggests that the mineralogical source of these sand layers is likely be different.

The sand within these archaeological sites is likely to be of local origin transported from beaches or dunes on Sanday during periods of increased wind activity. Samples were collected from the modern beaches throughout Sanday to test for residual signals and it may be possible to determine the provenance of the archaeological sand layers by comparing the sensitivity of these samples with the sensitivity of the modern beach samples. Figure 5.5a shows the response of quartz from the modern beach sands and archaeological samples to a 1 Gy dose stimulated by blue light. None of the modern beach sands respond as well to the artificial radiation as the sensitive archaeological samples identified above, but there are two modern samples (SUTL 574 and 580) that are slightly more sensitive. These samples are from Tres Ness and Bay of Stove, respectively (Figure 3.4) and both lie southwest of Tofts Ness and Bay of Lopness. Both could potentially be the source of the more sensitive archaeological samples however there is still a significant difference between the sensitivity of these modern beach samples and the archaeological samples. The response of most modern beach samples to the artificial irradiation is quite low and therefore trying to identify the provenance of the low sensitive samples from Tofts Ness and Bay of Lopness is problematic.

A similar comparison was undertaken on the IR response of polymineral and feldspar discs (modern beach and archaeological samples respectively) to a 1 Gy dose and the results are shown in Figure 5.5b. Some of the modern beaches are as sensitive as the archaeological samples (SUTL 564, 565, 570, 574 and 581) and are either west or southwest of the sites, with one sample (SUTL 570) from a beach on the Tofts Ness peninsula. For some of the sensitive quartz samples identified in Figure 5.5a, it is interesting to note that the feldspar

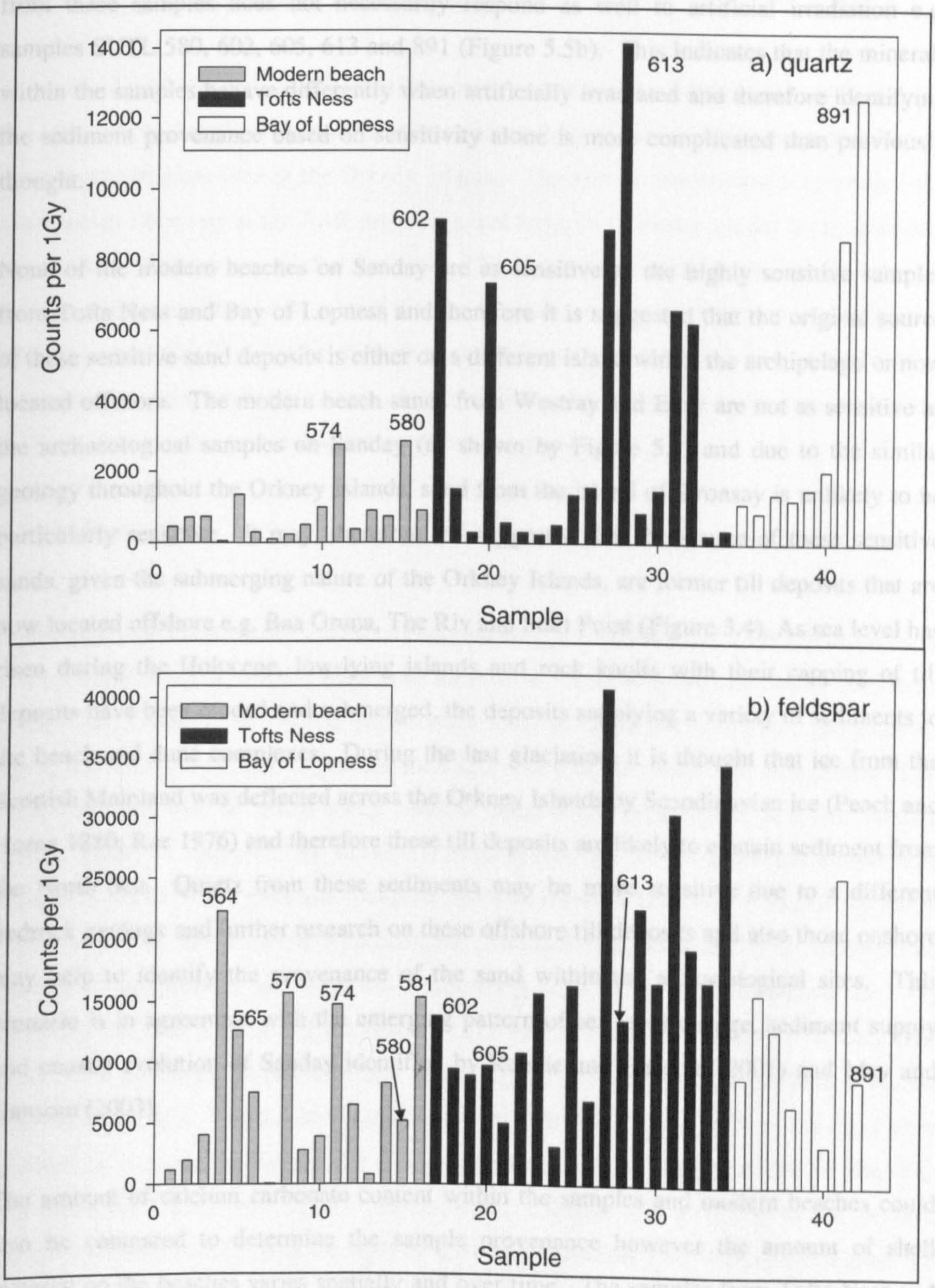

Figure 5.5 – a) Response of quartz from the Sanday modern beaches and the archaeological samples from Tofts Ness and Bay of Lopness to a 1 Gy dose and b) Response of feldspar from the modern beaches and archaeological samples to a 1 Gy dose.

from these samples does not necessarily respond as well to artificial irradiation e.g. samples SUTL 580, 602, 605, 613 and 891 (Figure 5.5b). This indicates that the minerals within the samples behave differently when artificially irradiated and therefore identifying the sediment provenance based on sensitivity alone is more complicated than previously thought.

None of the modern beaches on Sanday are as sensitive as the highly sensitive samples from Tofts Ness and Bay of Lopness and therefore it is suggested that the original source of these sensitive sand deposits is either on a different island within the archipelago or now located offshore. The modern beach sands from Westray and Eday are not as sensitive as the archaeological samples on Sanday (as shown by Figure 5.3) and due to the similar geology throughout the Orkney Islands, sand from the island of Stronsay is unlikely to be particularly sensitive. It may, therefore, be suggested that the source of these sensitive sands, given the submerging nature of the Orkney Islands, are former till deposits that are now located offshore e.g. Baa Gruna, The Riv and Start Point (Figure 3.4). As sea level has risen during the Holocene, low-lying islands and rock knolls with their capping of till deposits have been eroded and submerged, the deposits supplying a variety of sediments to the beach and dune complexes. During the last glaciation, it is thought that ice from the Scottish Mainland was deflected across the Orkney Islands by Scandinavian ice (Peach and Horne 1880; Rae 1976) and therefore these till deposits are likely to contain sediment from the North Sea. Quartz from these sediments may be more sensitive due to a different bedrock geology and further research on these offshore till deposits and also those onshore may help to identify the provenance of the sand within the archaeological sites. This scenario is in agreement with the emerging pattern of sea level change, sediment supply and coastal evolution of Sanday identified by Rennie and Hansom (2001) and May and Hansom (2003).

The amount of calcium carbonate content within the samples and modern beaches could also be compared to determine the sample provenance however the amount of shell material on the beaches varies spatially and over time. The samples from Tofts Ness and Bay of Lopness have variable amounts of shell material and in an area such as Sanday where high, but variable, levels of calcium carbonate material are common, identifying the present source beach is problematic.

5.2.4 Aspects of the modified SAR procedure

A modified SAR procedure was used here and, notwithstanding the caveats of Chapter 4, for many of the samples this procedure has successfully dated wind blown sands collected from archaeological sites in the Orkney Islands. The aim of this section is to present the main trends observed in the SAR procedure that have an influence on the acceptance and rejection of discs prior to further analysis. The first section presents the results from the preheat treatment followed by a brief discussion of the sensitivity of the samples (aimed at identifying samples that may be difficult to date due to low sensitivity). The second section discusses the main trends and results of the criteria used to accept or reject discs, before the SAR results from the archaeological samples are presented.

5.2.4.1 Preheating

Preheating each aliquot prior to OSL measurement is a necessary part of the SAR protocol to ensure that shallow unstable traps with short lifetimes are emptied and cannot contribute to the OSL signal. The preheat temperature must be sufficient to remove the unstable signal but stringent enough to prevent thermal erosion of the main OSL trap (Smith *et al.* 1986) and this can be tested using preheat temperature dependence plots (or preheat plateau plots) as suggested by Rhodes (1988). Figure 5.6 shows a preheat temperature dependence plot from each site sampled for this research and all preheat temperature dependence plots are shown in Appendix 5.2. The individual estimates of D_e represent an average of between one and eight discs depending on whether the discs passed the 1 Gy recycling test (see Section 5.2.4.3 below). For samples (SUTL 901 and 903) only four discs could be dispensed due to a lack of quartz and therefore these have been excluded from the Appendix. The Sandhill samples are very insensitive and many of the discs were rejected as a result of failing the 1 Gy recycling test or due to scatter in the data (see Sections 5.2.4.3 and 5.2.4.5 respectively). Despite the inclusion of the preheat temperature dependence plots for eight of the eleven Sandhill samples either in Figure 5.6 or Appendix 5.2, the plots are scattered due to the lack of the individual disc equivalent doses and the variable natural signals.

Although there is a great deal of scatter within each sample (as shown by the error bars on each averaged D_e (equivalent dose)), the majority of samples show no obvious decrease in D_e with increasing preheat temperature. A slight decrease in D_e is observed in samples

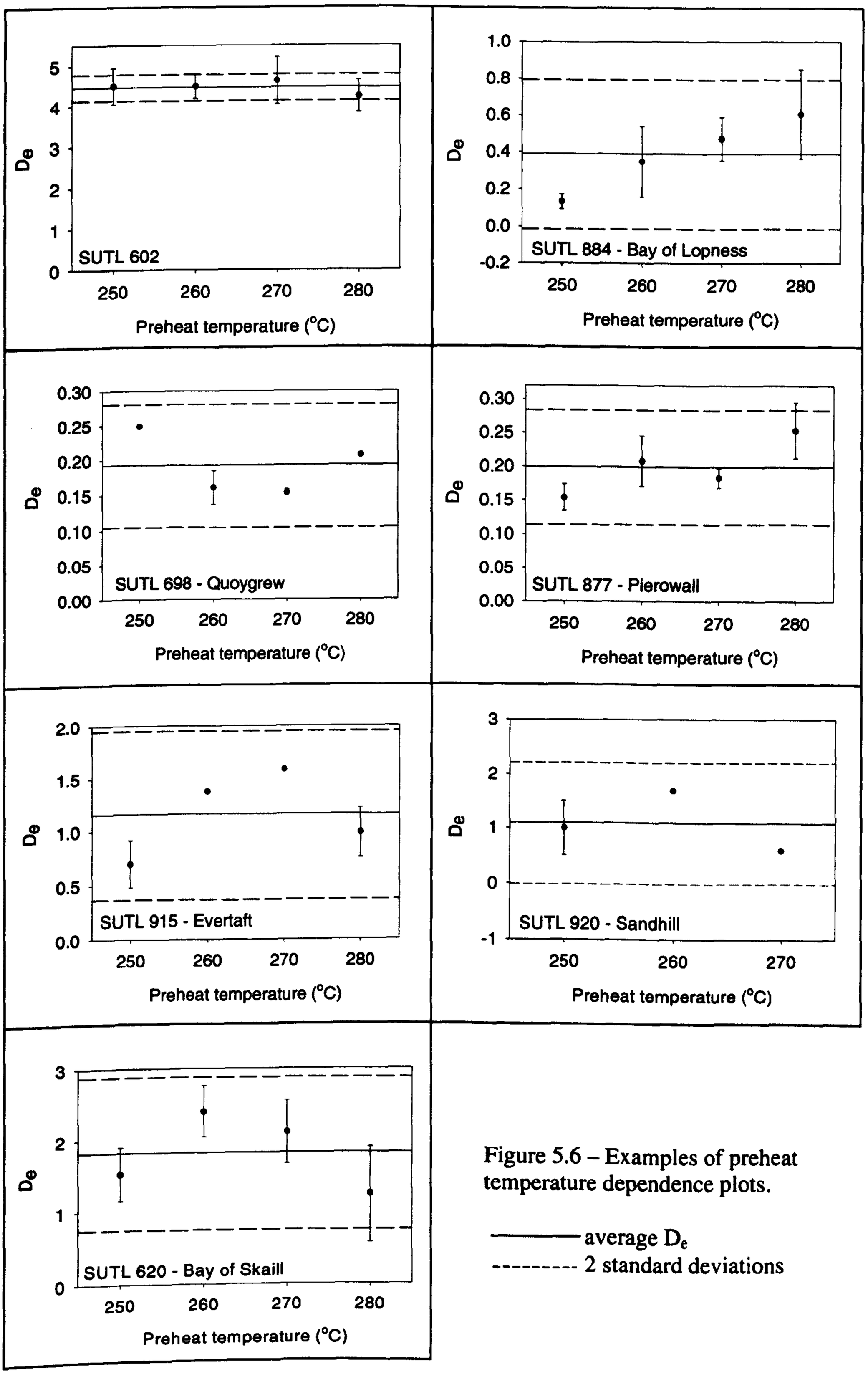

Figure 5.6 – Examples of preheat temperature dependence plots.

——— average D_e
--------- 2 standard deviations

SUTL 613, 614, 616 and 891, suggesting that there may have been some thermal erosion of the main OSL trap, but the majority of discs fall within two standard deviations of their respective mean, and therefore the observed decrease in D_e is not thought to be significant. Several samples show an increase in D_e with preheat temperature (e.g. SUTL 884) which may indicate that there is some thermal transfer during the preheat process. An alternative explanation might be that feldspar signals tend to rise with increasing preheat temperature before reaching a plateau as a result of charge transfer (Spencer 1996; Aitken 1998; Richardson 2000), however this is unlikely as the samples that show an increase in D_e with preheat temperature have no significant feldspar contamination.

The preheat temperatures used are slightly higher than that currently used by other researchers but they are within the range suggested by Murray and Wintle (2000), Banerjee *et al.* (2001) and Murray-Wallace *et al.* (2002), and the results presented here suggest that the D_e values are independent of the preheat temperature. Despite the scatter amongst the individual aliquot D_e of most samples, establishing that the D_e are independent of preheat temperature allows a weighted mean D_e to be calculated for the final age estimate.

5.2.4.2 Sensitivity changes

The OSL response of quartz is known to change in the course of a SAR run and this is thought to be due to either increased activation of luminescence centres during the preheat (Aitken 1998, Li 2002) or to a reduction in the competition for electrons by non-luminescence centres (Aitken 1998). If repeated preheating is the cause of sensitivity changes, an increase in sensitivity would be expected during the SAR run as more luminescence centres are activated (Aitken 1998). Conversely, a reducing sensitivity might result from luminescence centre depletion during successive read-out cycles, or as a result of radiation quenching. The test dose was introduced to the SAR procedure by Murray and Roberts (1998) to enable sensitivity changes to be monitored in the SAR run and to correct for these sensitivity changes by normalising the regenerative dose with the subsequent test dose. The repeated dose at the end of the SAR run checks that the normalisation has been successful and the results of the recycling ratio test are presented below in Section 5.2.4.3.

Figure 5.7 shows the percentage of samples that show an increase, decrease or scattered response to the test dose throughout the SAR run. Examples are shown in Figure 5.8 and

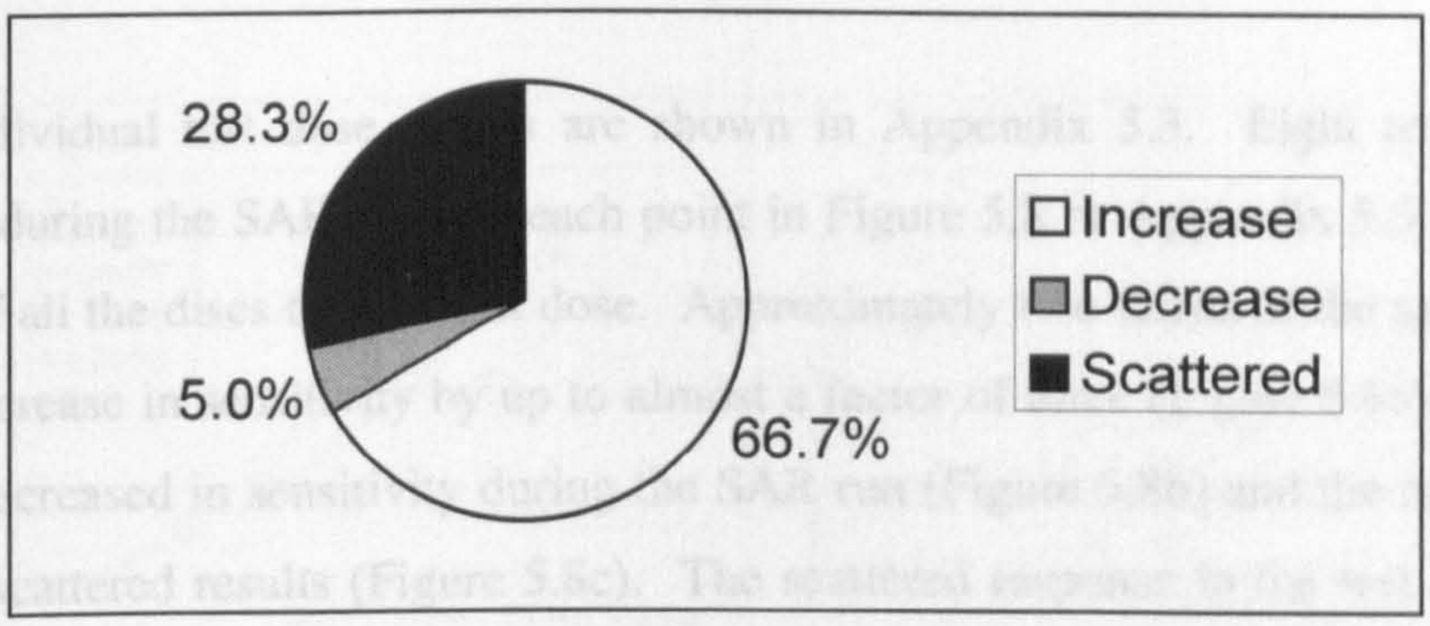

Figure 5.7 – Pie chart showing the percentage of samples that show an increase, decrease or scattered response to the test dose during the SAR run.

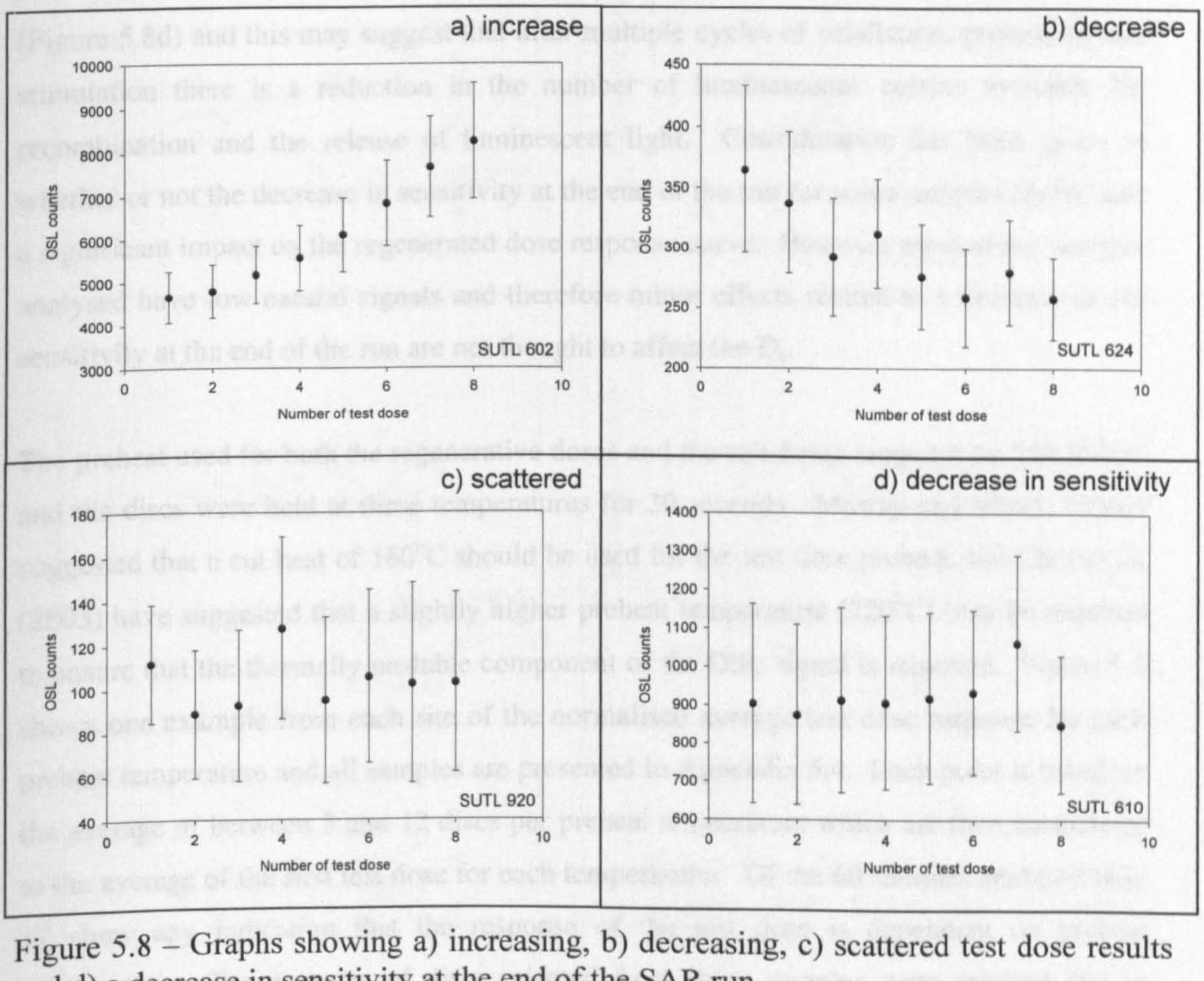

Figure 5.8 – Graphs showing a) increasing, b) decreasing, c) scattered test dose results and d) a decrease in sensitivity at the end of the SAR run

all the individual test dose results are shown in Appendix 5.3. Eight test doses were measured during the SAR run and each point in Figure 5.8 or Appendix 5.3 represents the average of all the discs to each test dose. Approximately two-thirds of the samples show a general increase in sensitivity by up to almost a factor of three (Figure 5.8a), however 5% actually decreased in sensitivity during the SAR run (Figure 5.8b) and the remaining 28% had very scattered results (Figure 5.8c). The scattered response to the test dose does not infer that the sensitivity varies during the SAR run, rather the response to the 0.5 Gy test dose is so low that the test dose cannot be accurately measured. Samples that show an increase in sensitivity tend to be those that respond well to artificial irradiation and those with scattered test dose responses are less sensitive. Twenty-five percent of the samples that increase in sensitivity show a decrease in the test dose sensitivity at the end of the run (Figure 5.8d) and this may suggest that after multiple cycles of irradiation, preheating and stimulation there is a reduction in the number of luminescence centres available for recombination and the release of luminescent light. Consideration has been given to whether or not the decrease in sensitivity at the end of the run for some samples could have a significant impact on the regenerated dose response curve. However most of the samples analysed have low natural signals and therefore minor effects related to a decrease in the sensitivity at the end of the run are not thought to affect the D_e.

The preheat used for both the regenerative doses and the test doses ranged from 250-280°C and the discs were held at these temperatures for 30 seconds. Murray and Wintle (2000) suggested that a cut heat of 160°C should be used for the test dose preheat, but Choi *et al.* (2003) have suggested that a slightly higher preheat temperature (220°C) may be required to ensure that the thermally unstable component of the OSL signal is removed. Figure 5.9 shows one example from each site of the normalised average test dose response for each preheat temperature and all samples are presented in Appendix 5.4. Each point is based on the average of between 3 and 12 discs per preheat temperature which are then normalised to the average of the first test dose for each temperature. Of the 60 samples analysed only 17 show any indication that the response of the test dose is dependent on preheat temperature. The majority of discs rejected from these samples were rejected due to recycling problems, however only 20% of discs rejected were preheated at 280°C and the majority were preheated at the lower temperature of 250°C. In addition, many of these samples do not respond well to artificial irradiation and therefore the sensitivity of the sample is perhaps more important than the temperature of the test dose preheat which appears to have little effect on sample sensitivity.

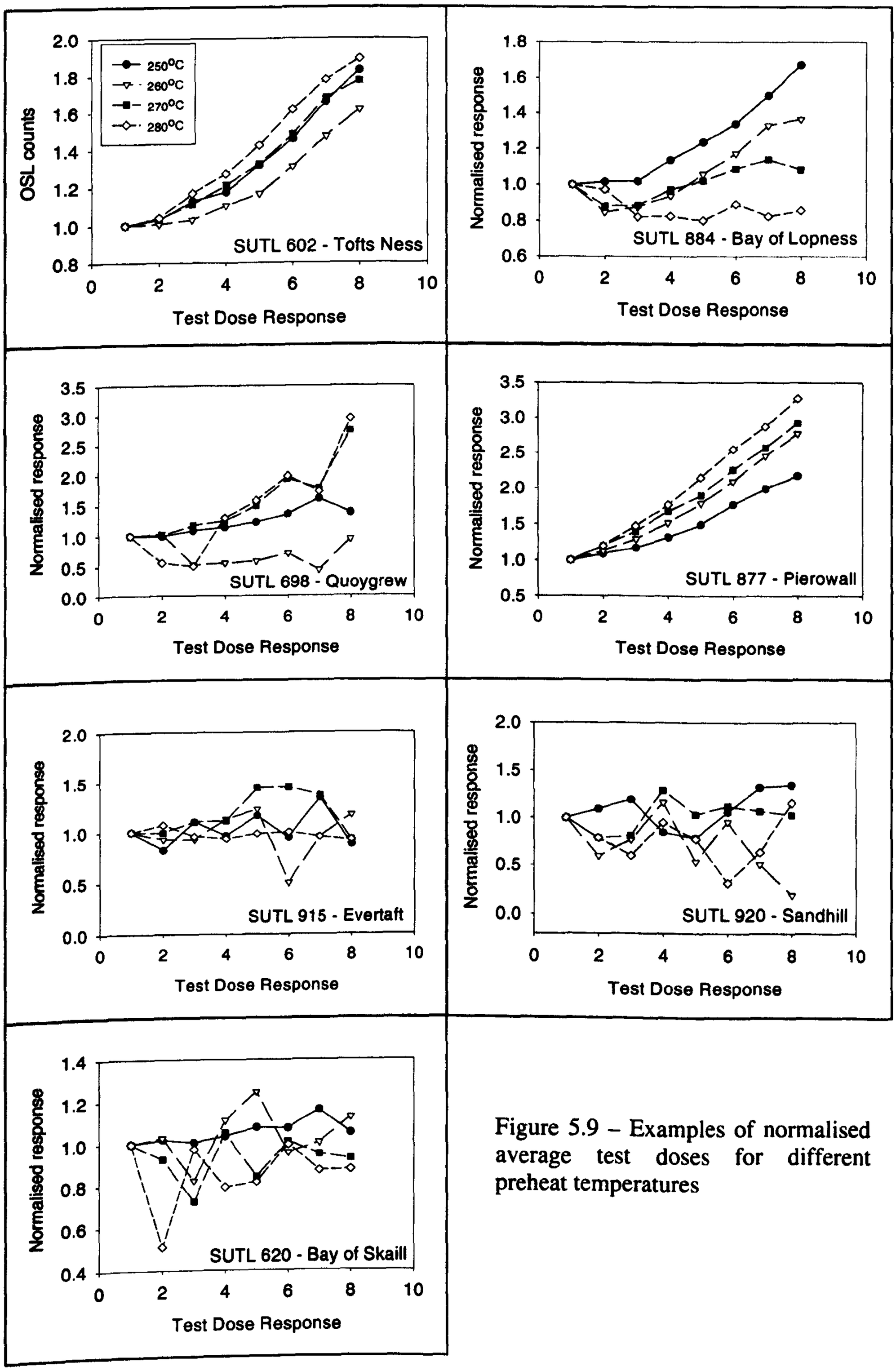

Figure 5.9 – Examples of normalised average test doses for different preheat temperatures

The results presented above indicate that not all samples experience an increase in sensitivity during the SAR run. This implies that if there are any non-activated luminescence centres within the samples, the preheat temperatures used for the regenerative and test doses do not appear to activate them. In some cases the sensitivity decreases and this may indicate destruction of luminescence centres due to the preheat regime, although this is generally associated with annealing at temperatures greater than 800°C (Li 2002).

To confirm whether the higher preheat temperatures used on the test doses increase the sensitivity of the samples unnecessarily, an experiment similar to that used to identify a suitable preheat temperature for the regenerative doses could be undertaken. Various cut-heat temperatures of between 160-280°C could be tested on aliquots of the same sample, which are run through a SAR procedure. Plotting the response of the test doses would identify if there is a significant increase in OSL sensitivity due to the test dose cut-heat temperature. Repeating the experiment using the same cut-heat temperatures but holding the aliquots at these temperatures for 30 seconds would also identify if preheating for 30 seconds influences the sample sensitivity.

5.2.4.3 1 Gy recycling ratio test

The recycling ratio test was introduced by Murray and Wintle (2000) to check that normalisation of the regenerative dose by the subsequent test dose successfully corrected for any sensitivity changes that may have occurred during the SAR run. Repeating a low regenerative dose, e.g. 1 Gy, at the end of each SAR run and normalising it with the next test dose allows a direct comparison to be made with the first 1 Gy regenerative dose. If normalisation using the test dose successfully corrects for sensitivity changes, the two points will be within 10% error of each other and the disc can be accepted for further analysis. This assumes that the aliquots are sensitive enough to allow accurate measurement of the test dose. The 'Analyst' program written by G. Duller (University of Wales, Aberystwyth) was used to determine which discs passed or failed the 1 Gy recycling ratio test. Normalisation of the regenerative doses with the subsequent test dose is successful for approximately 80% of the discs, however for the remaining 20% the test dose normalisation does not compensate for the sensitivity changes.

Figure 5.10 shows the number of discs in each sample that were rejected as a result of failing the recycling ratio test. Many of the samples which have a large number of rejected discs are those which did not respond well to the artificial irradiation and have low sensitivity. For example sample SUTL 604 has very low sensitivity as shown in Figure 5.3, and approximately 40% of the discs dispensed for that sample were rejected due to poor recycling (Figure 5.10). The samples from Sandhill follow a similar pattern and are rejected due to poor recycling and because they lack the sensitivity and precision required for accurately measuring the test doses.

5.2.4.4 Identification of IR sensitive minerals

At the end of each SAR run a 1 Gy dose was administered to each disc and subsequently measured using IR diodes. This was used in conjunction with the 1 Gy signal from two associated feldspar discs that were prepared using the 2.51-2.58 gcm^{-3} fraction from the density separation outlined in Chapter 3 and stimulated using IR and blue light. It was then possible to evaluate the proportion of quartz OSL signal on the 'quartz' aliquots using the individual values of the feldspar IR:blue OSL ratio.

Although the aim during the sample preparation procedure described in Section 3.8, Chapter 3, was to produce pure quartz grains, grains or micro-inclusions of feldspar or zircon can sometimes remain, for example due to insufficient HF etching. Feldspars and zircons are very sensitive to natural and artificial radiation and their internal dose rates tend to be higher than quartz (Aitken 1985) and therefore if the quartz is contaminated with either mineral the true age of the sample may be overestimated. For approximately 85% of the discs there was no significant contribution to the OSL signal from IR sensitive minerals but the remaining 15% were rejected from further analysis due to contamination. This is shown in more detail in Figure 5.11 where the discs have been sorted into groups based on the percentage of the OSL signal from the quartz grains on each disc. Discs with more than 10% contamination, i.e. from which less than 90% of signals could be attributed to quartz, were rejected from further analysis.

Of the 173 discs that were contaminated 69% of these were from Tofts Ness and 12% from Sandhill (Figure 5.12). The Tofts Ness results are based on two phases of sample preparation. After the first phase of sample preparation, 20% of the 260 discs showed a significant response to IR stimulation. To ensure that procedures in the sample preparation

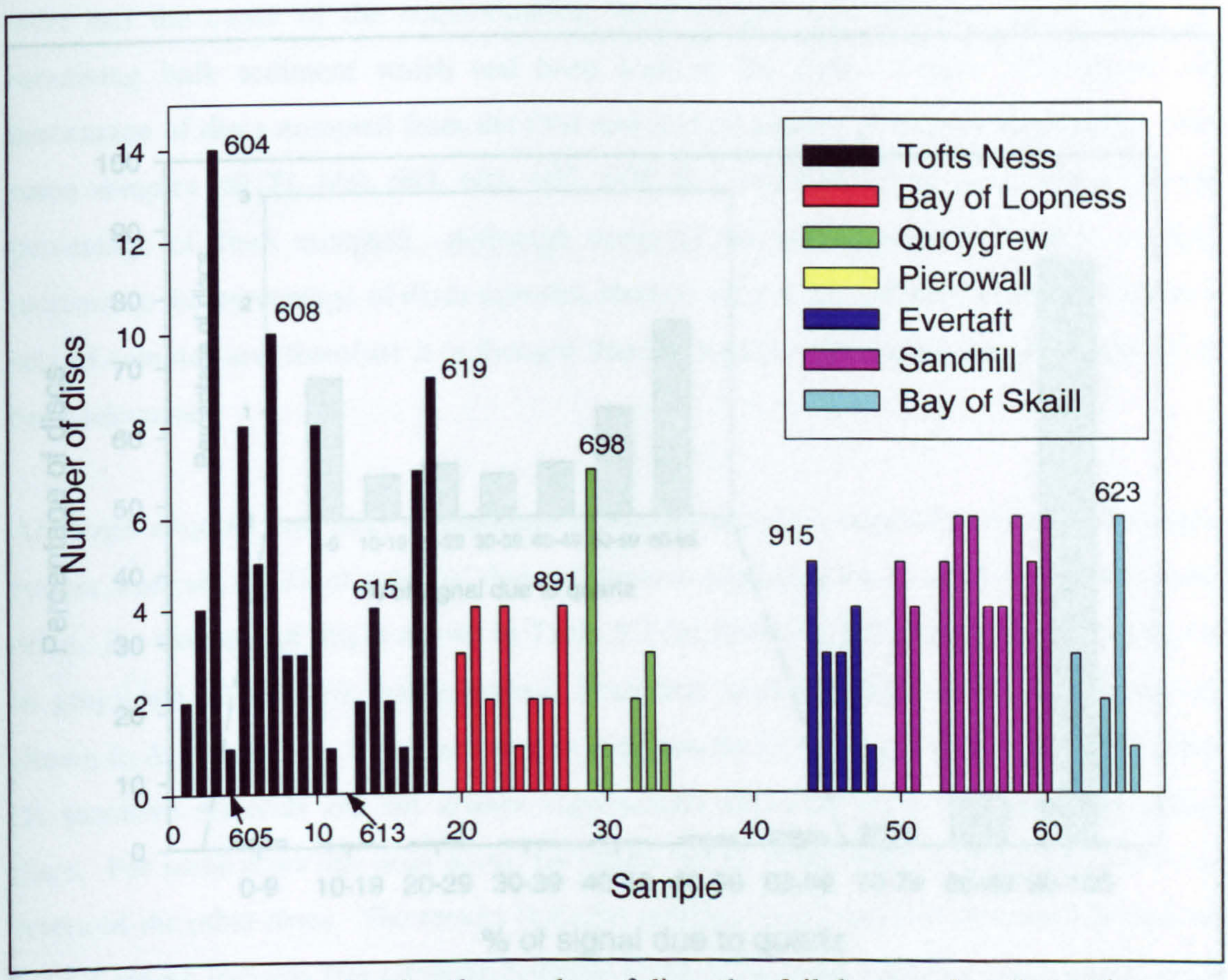

Figure 5.10 – Bar graph showing the number of discs that fail the recycle ratio test in each sample.

Figure 5.12 – Pie chart showing discs contaminated with the unexpected minerals as a percentage of all contaminated discs.

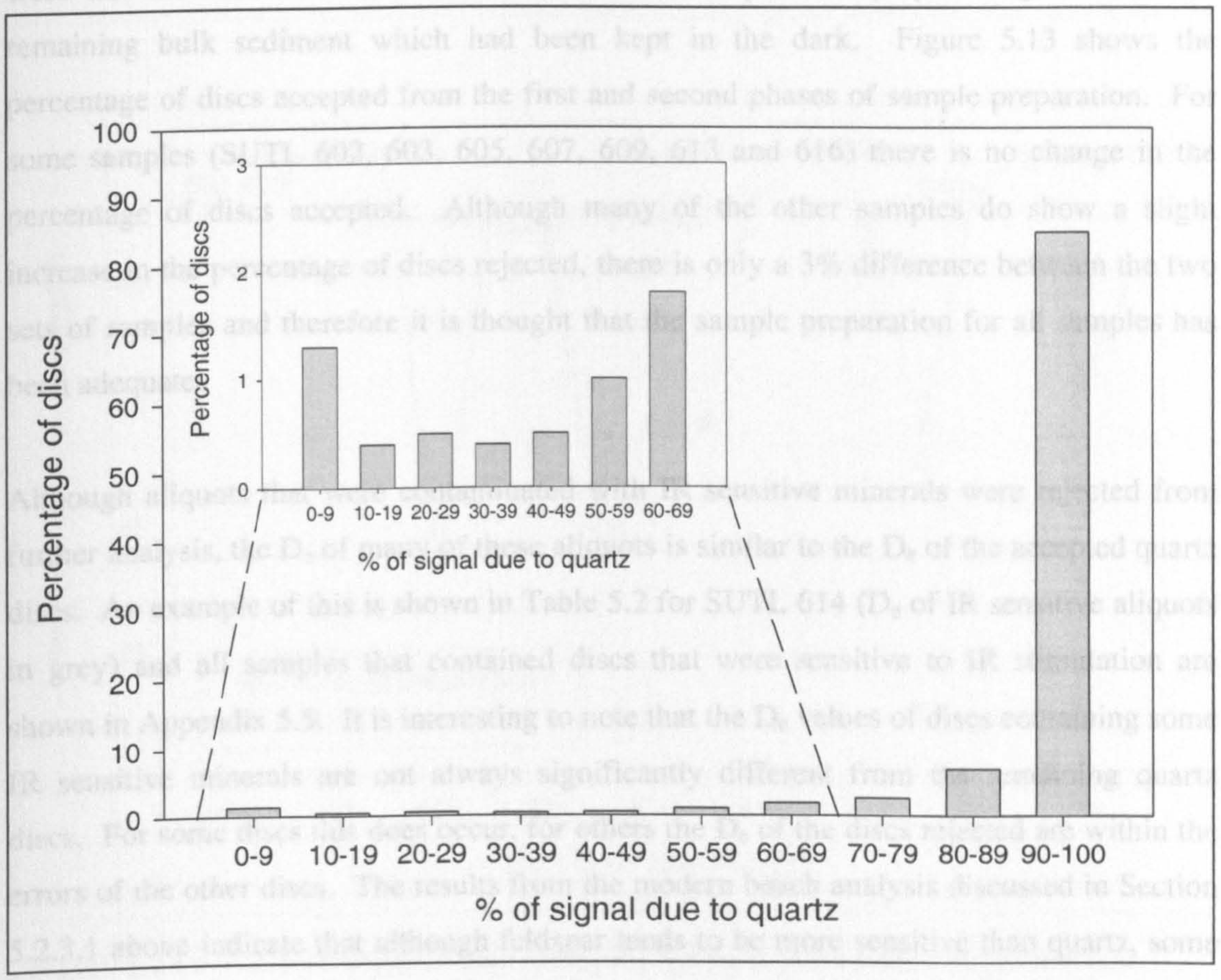

Figure 5.11 – Bar graph showing the percentage of blue OSL signal due to quartz

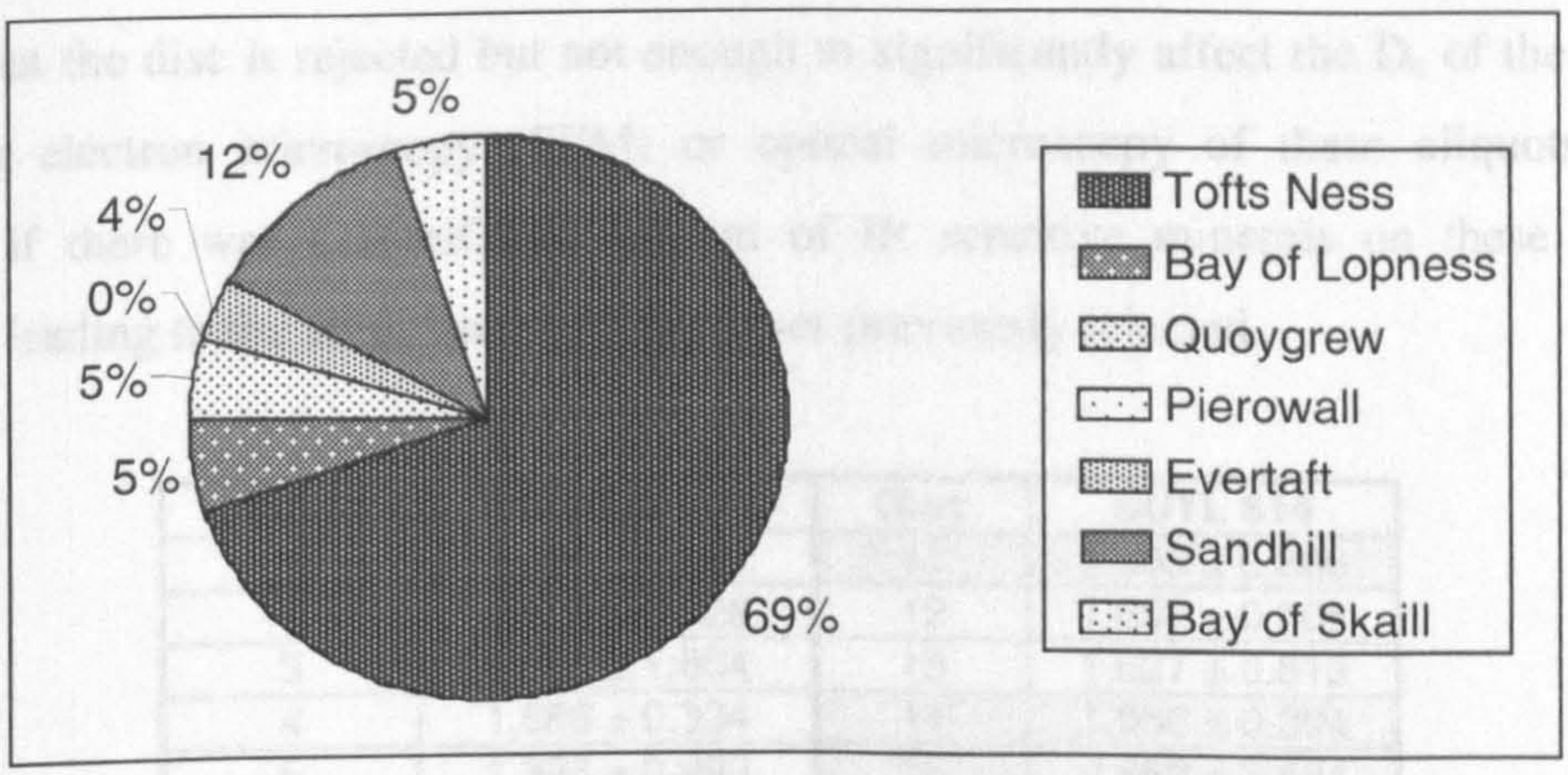

Figure 5.12 – Pie chart showing discs contaminated with IR sensitive minerals as a percentage of all contaminated discs

were not the cause of the contamination, each sample was prepared again from the remaining bulk sediment which had been kept in the dark. Figure 5.13 shows the percentage of discs accepted from the first and second phases of sample preparation. For some samples (SUTL 602, 603, 605, 607, 609, 613 and 616) there is no change in the percentage of discs accepted. Although many of the other samples do show a slight increase in the percentage of discs rejected, there is only a 3% difference between the two sets of samples and therefore it is thought that the sample preparation for all samples has been adequate.

Although aliquots that were contaminated with IR sensitive minerals were rejected from further analysis, the D_e of many of these aliquots is similar to the D_e of the accepted quartz discs. An example of this is shown in Table 5.2 for SUTL 614 (D_e of IR sensitive aliquots in grey) and all samples that contained discs that were sensitive to IR stimulation are shown in Appendix 5.5. It is interesting to note that the D_e values of discs containing some IR sensitive minerals are not always significantly different from the remaining quartz discs. For some discs this does occur, for others the D_e of the discs rejected are within the errors of the other discs. The results from the modern beach analysis discussed in Section 5.2.3.1 above indicate that although feldspar tends to be more sensitive than quartz, some of the modern beach feldspar samples do not respond well to a 1 Gy artificial dose (Figure 5.5b). This may account for some of the similar D_e values for discs contaminated by IR sensitive minerals, with the feldspar responding sufficiently to IR stimulation to ensure that the disc is rejected but not enough to significantly affect the D_e of the aliquot. Scanning electron microscopy (SEM) or optical microscopy of these aliquots would confirm if there was a significant amount of IR sensitive minerals on these aliquots possibly leading to the acceptance of some discs previously rejected.

Disc	SUTL 614	Disc	SUTL 614
1	2.796 ± 2.235	11	1.338 ± 0.286
2	2.427 ± 0.728	12	1.657 ± 0.365
3	1.801 ± 1.604	13	1.627 ± 0.813
4	1.686 ± 0.334	14	1.666 ± 0.394
5	1.324 ± 0.993	15	2.682 ± 3.584
6	1.451 ± 0.887	16	0.807 ± 0.647
7	1.517 ± 1.962	17	1.869 ± 0.318
8	1.88 ± 0.657	18	1.285 ± 0.923
9	1.421 ± 0.295	19	1.293 ± 0.536
10	1.926 ± 0.517	20	0.891 ± 0.744

Table 5.2 – The D_e of aliquots from SUTL 614. Shaded aliquots are those rejected due to contamination with IR sensitive minerals

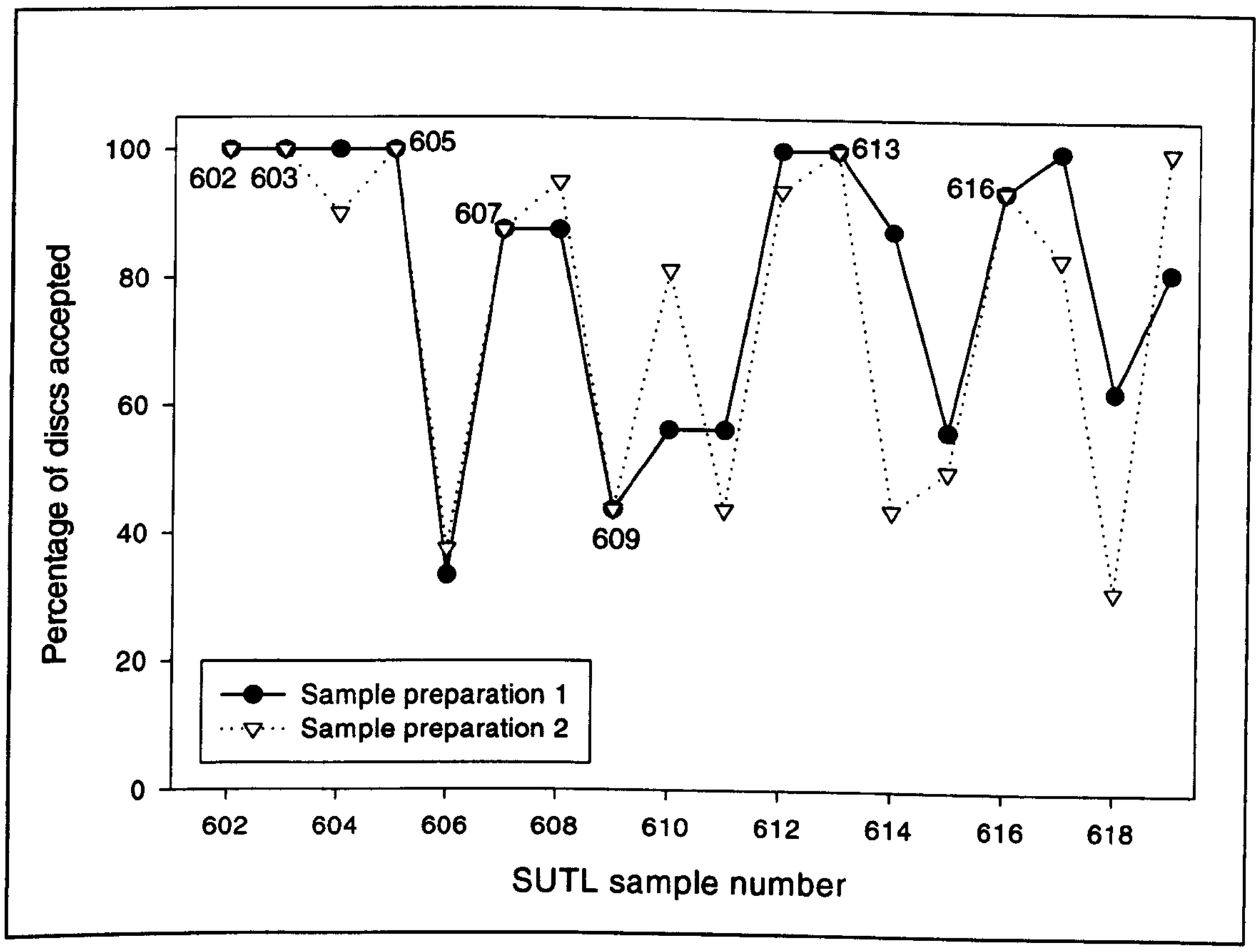

Figure 5.13 – The percentage of discs accepted for each Tofts Ness sample from the two sample preparations

5.2.4.5 Regenerative doses and dose response curves

The SAR procedure used six doses between 1 and 6 Gy to construct the regenerative dose response curves. It was suggested by Murray and Roberts (1998) that the regenerated dose should be similar to that of the natural dose and Murray and Mejdahl (1999) indicated that only one large regenerative dose is required if it is assumed that charge transfer is insignificant. To allow comparisons to be made on the performance of the SAR procedure from run to run it was decided to standardise the measurement procedure. For this reason no attempt was made to adjust the range of regenerative doses for each sample to bracket the natural doses on an individual basis. Using six doses also allowed a tight regenerative dose response curve to be constructed for each sample. The samples dated are less than 10,000 years old and therefore the luminescence signal will not be saturated. Using only one or two regenerative doses close to the natural dose level could potentially under- or over-estimate the palaeodose. Ignoring low dose responses for young samples could have a significant effect on the exponential or linear fit and resultant palaeodose of the sample.

The advantage of the regenerative technique is that the sample palaeodose is calculated by interpolation rather than extrapolation as used in the additive dose technique. For some samples analysed, extrapolation was still required because the natural OSL signals were less than 1 Gy. Despite this, the well behaved nature of many of these samples ensures that the OSL ages have high precision, however further measurements should be made for administered doses of 0, 0.25, 0.5 and 0.75 Gy to ensure that the response of these low doses is taken into consideration during the regression analysis.

For many of the samples, regenerative dose response curves such as those shown in Figure 5.14a are typical, however approximately 12% of the discs were rejected due to scattered data (Figure 5.14b) which prevented linear or exponential regression analysis of the data. The curves shown in Figure 5.14 are constructed by plotting the normalised dose response and the upper and lower errors for each dose i.e. there are three points for every dose point and this ensures that the errors are taken into consideration during the regression analysis.

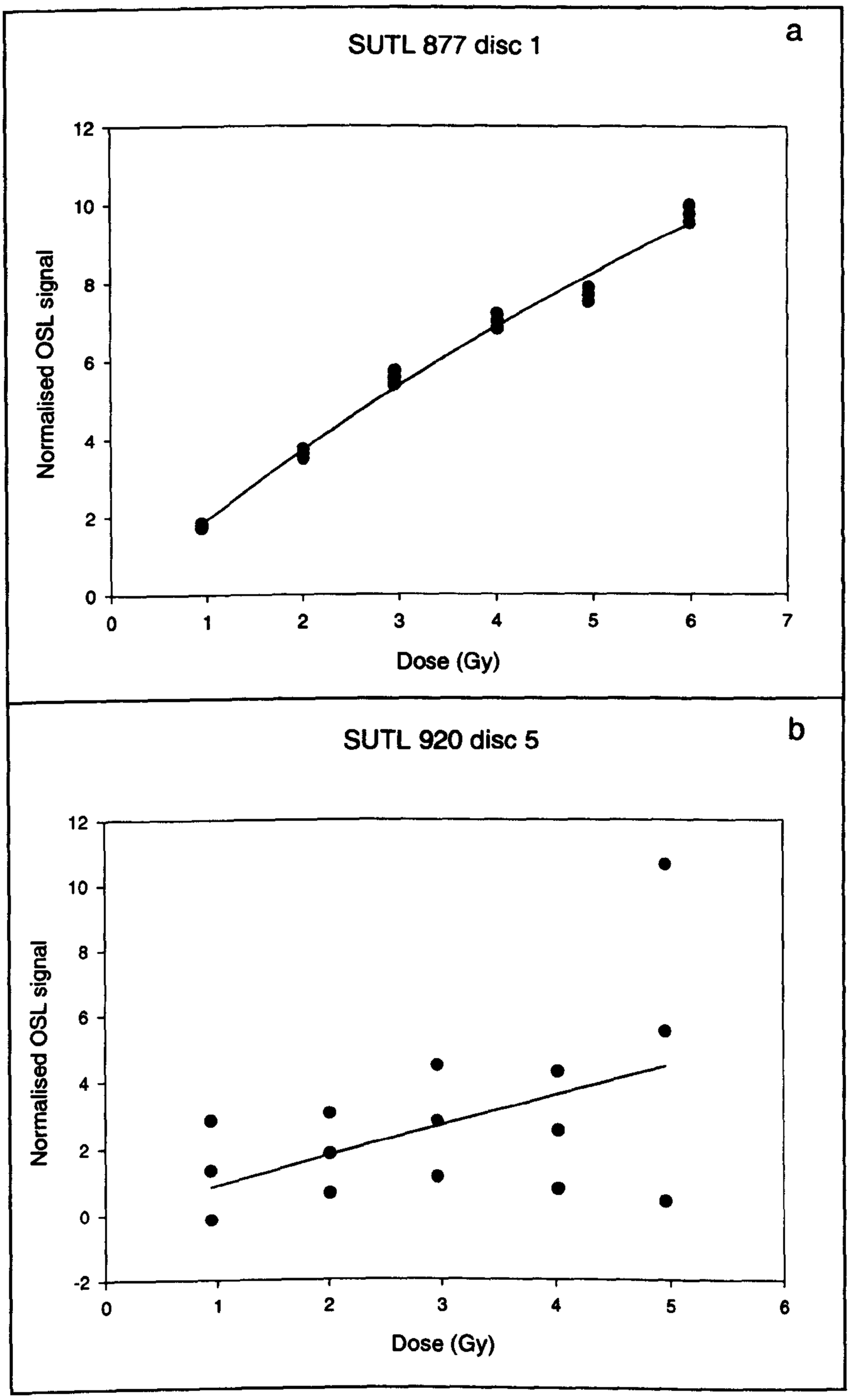

Figure 5.14 – Examples of a) well-behaved and b) scattered regenerative dose response curves

Approximately 48% of the discs rejected due to scattered data are from Tofts Ness and 37% are from Sandhill (Figure 5.15). Samples that contain a large number of discs rejected due to scattered data also tend to have a large proportion of discs rejected as a result of failing the recycling ratio test. Figure 5.16 shows the sensitivity of the Tofts Ness samples plotted against the number of discs rejected from each sample due to failing the recycling ratio test or as a result of scattered data. Samples with a large number of discs being rejected tend to be those with low sensitivity e.g. SUTL 604 and SUTL 618 (Figure 5.16) and vice versa (e.g. SUTL 613). These results show that low sensitivity restricts the number of discs accepted for further analysis and will therefore reduce the precision on the final age.

The samples with the lowest sensitivity are all from Sandhill (Eday) and therefore the OSL dates on these samples have low precision. It was suggested by Sommerville *et al.* (2001) that low sensitive samples could be more accurately dated by fitting a statistical trend through the individual sensitivity measurements and normalising the measured regenerative data to the mean sensitivity change determined for the appropriate cycle point. Figure 5.17a shows the measured test dose data for an aliquot from Sandhill and the fitted linear statistical trend. The trend is based on the assumption that the sensitivity of quartz to artificial irradiation generally increases throughout the SAR run. The regenerative data is then normalised using new test doses determined from the statistical trend and these are shown with the original normalised data in Figure 5.17b. Because a statistical trend has been used, this has removed the scatter in the test doses, and this is reflected in the trend normalised dose response curve, which is also less scattered. The technique allows samples that would normally be rejected due to low sensitivity to be dated but needs to be developed and tested to ensure that it is robust. Despite this, the precision may still be low due to limitations in the information content of the remaining signals.

5.2.4.6 Summary

Table 5.3 outlines the number of discs rejected and accepted for each sample and this is summarised in Figure 5.18. Approximately 40% of the discs dispensed for this research were rejected mainly due to contamination by IR sensitive minerals (15%) or failing the recycling ratio test (15%). The percentage of discs accepted at each site varies and this is shown in Figure 5.19. Almost 80% of the discs from Sandhill were rejected due to recycling and scattered data and this reflects the very low sensitivity of these samples. The

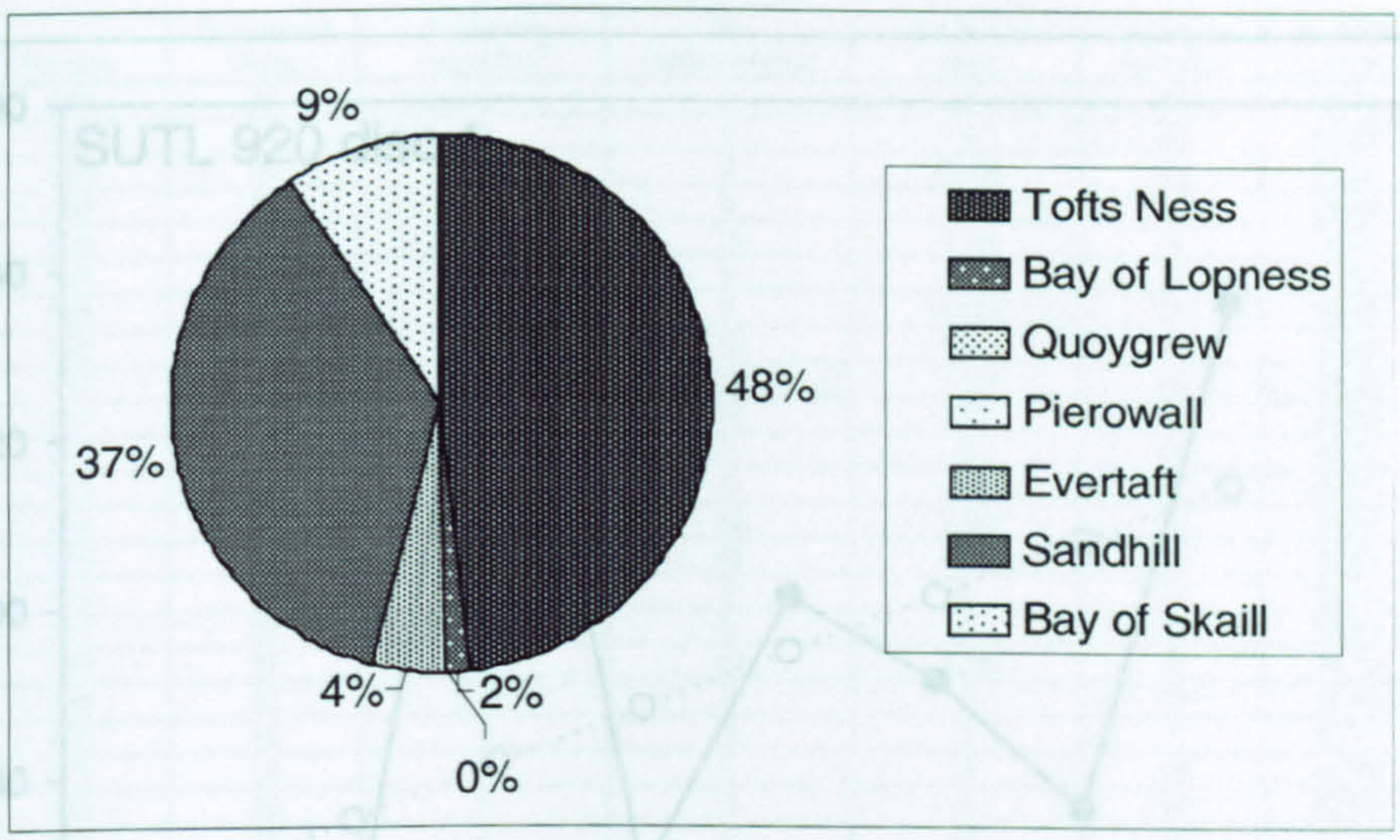

Figure 5.15 – Pie chart showing the percentage of discs with scattered data within each site

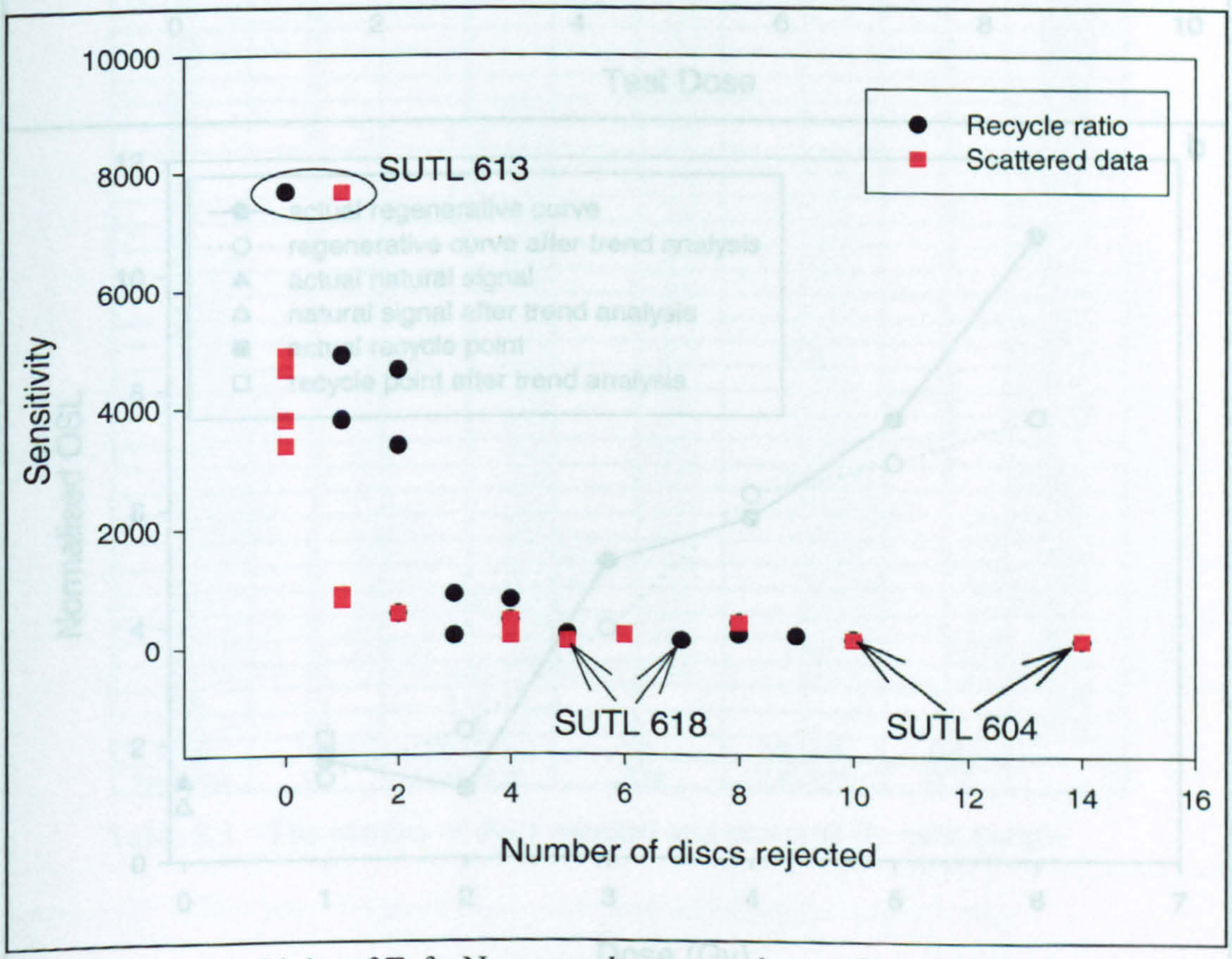

Figure 5.16 – Sensitivity of Tofts Ness samples versus the number of discs rejected either due to failing the recycle ratio test or scattered data

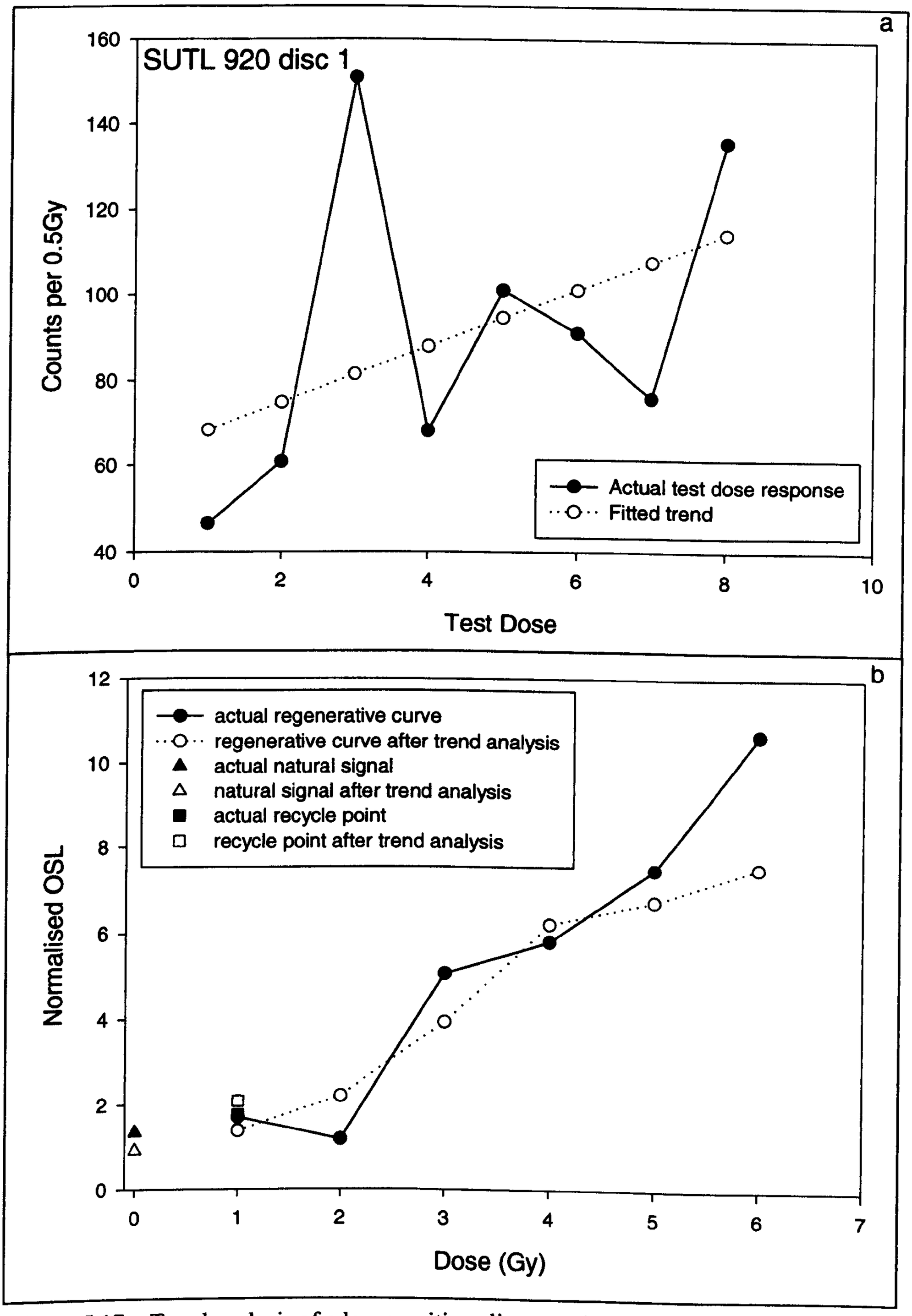

Figure 5.17 – Trend analysis of a low sensitive aliquot – a) measured test dose data and the fitted linear statistical trend and b) the actual regenerative dose response curve and the dose response curve using the new test dose data from the statistical trend.

Sample	Dispensed discs	Rejected Recycling[8]	IR contamination	Scattered data	Number Accepted	% discs accepted
602	32	2	0	0	30	93.75
603	34	4	0	1	29	85.29
604	36	14 (13)	2	10 (9)	12	33.33
605	32	1	0	0	31	96.88
606	28	8 (4)	18	8 (2)	4	14.29
607	24	5	3	4	12	50.00
608	36	10 (9)	3	14 (13)	11	30.56
609	32	3 (1)	18	4 (1)	12	37.50
610	32	3 (2)	10	1 (0)	20	62.50
611	32	8 (4)	16	6 (5)	7	21.88
612	32	1	1	0	30	93.75
613	24	0	0	1	23	95.83
614	24	2	10	2 (0)	12	50.00
615	32	4 (2)	15	4 (1)	14	43.75
616	32	2	2	0	28	87.50
617	26	1	3	0	22	84.62
618	32	7 (6)	17	5 (3)	6	18.75
619	32	9 (8)	3	6	15	46.88
620	16	3	5	1	7	43.75
621	16	0	1	4	11	68.75
622	16	2	3	1	10	62.50
623	16	6	0	3	7	43.75
624	16	1	0	2	13	81.25
698	13	7	0	0	6	46.15
699	11	1 (0)	4	0	7	63.64
700	8	0	2	0	6	75.00
701	10	2	1	0	7	70.00
702	13	3	0	0	10	76.92
703	12	1	0	0	11	91.67
704	16	0	0	0	16	100.00
877	16	0	0	0	16	100.00
878	16	0	0	0	16	100.00
879	16	0	0	0	16	100.00
884	16	3	0	0	13	81.25
885	16	4	0	0	12	75.00
886	16	2 (1)	2	1	12	75.00
887	16	4	0	0	12	75.00
888	16	1 (0)	4	1	11	68.75
889	16	2	2	0	12	75.00
890	16	2	0	0	14	87.50
891	16	4	1	0	11	68.75
901	4	0	0	0	4	100.00
902	8	0	0	0	8	100.00
903	4	0	0	0	4	100.00
915	16	5	4	2 (1)	6	37.50
916	16	3	0	1	12	75.00
917	16	3	0	1	12	75.00
918	16	4	0	0	12	75.00
919	16	1	1	2	12	75.00
920	16	5	2	7 (6)	3	18.75
921	8	4	0	4	0	0.00
922	8	0	1	5	2	25.00
923	8	5	0	1	2	25.00
924	16	6	2	6	2	12.50
925	16	6 (5)	1	6	4	25.00
926	8	4	0	2	2	25.00
927	16	4	1	4 (3)	8	50.00
928	15	6 (5)	1	6	3	20.00
1299	16	5 (2)	7	4	3	18.75
1300	16	6 (3)	5	5	3	18.75
TOTAL	1130	199 (171)	171	135 (112)	676	
Percentage	100	17.60 (15.13)	15.12	11.95 (9.91)	59.77	

Table 5.3 – The number of discs rejected and accepted for each sample

[8] It should be noted that some discs would be rejected on the basis of IR contamination ***and*** either recycling or scattered data and therefore the recycling ratio and scattered data percentages in Figure 5.18 are based on the number of discs rejected from these criteria after discs with IR contamination were removed. These numbers are shown in brackets.

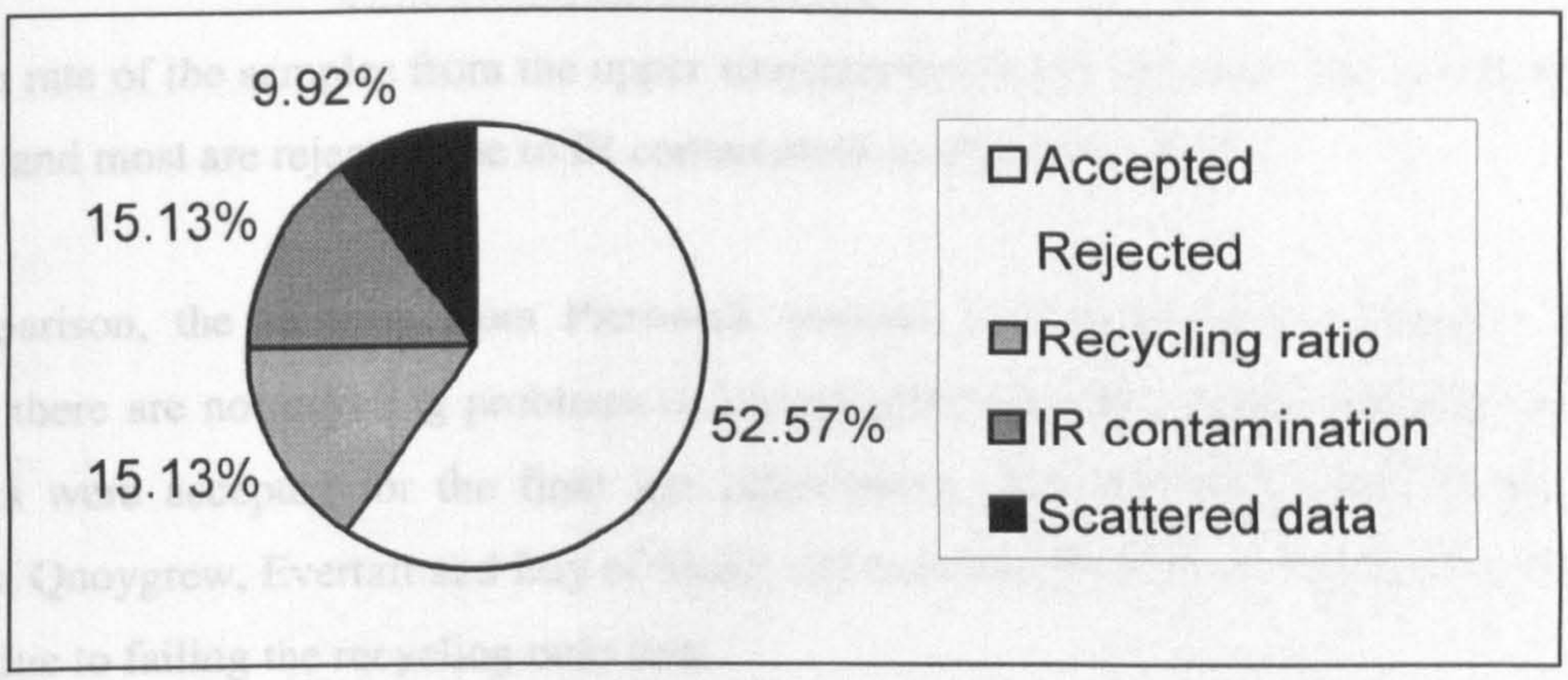

Figure 5.18 – Pie chart showing the percentage of discs accepted and rejected

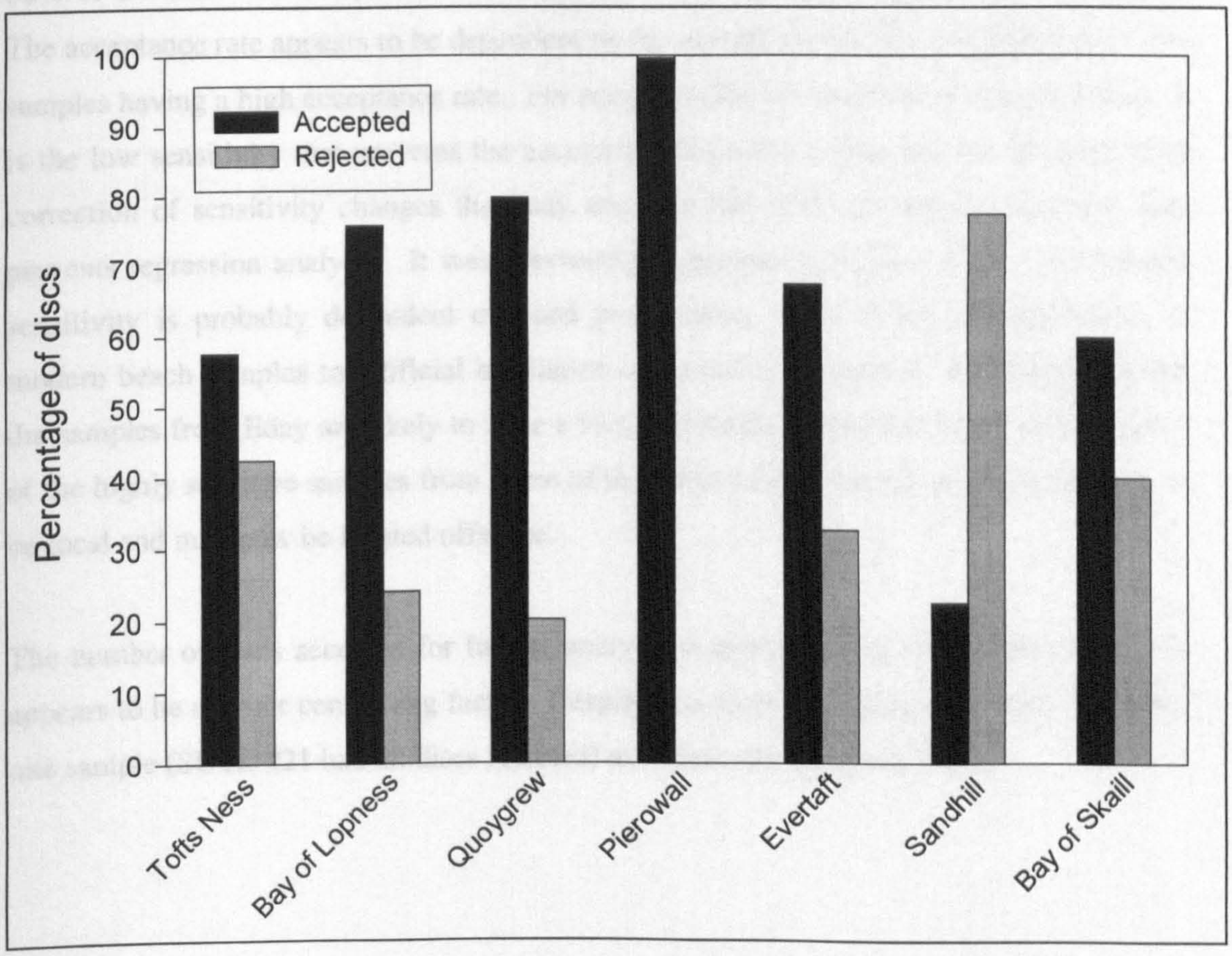

Figure 5.19 – The percentage of discs accepted and rejected at each site

rejection rate of the samples from the upper stratigraphic layers of Tofts Ness is also large (42.4%) and most are rejected due to IR contamination or low sensitivity.

In comparison, the samples from Pierowall respond well to artificial irradiation and because there are no recycling problems or contamination by IR sensitive minerals all of the discs were accepted for the final age calculations. The remaining sites of Bay of Lopness, Quoygrew, Evertaft and Bay of Skaill had between 20-40% of their discs rejected mainly due to failing the recycling ratio test.

When the samples are collated, patterns emerge in the percentage of discs accepted for each island (Figure 5.20). Only 20% of the discs from Eday are accepted whereas about 80% of the discs are accepted for Westray, 61% from Sanday and 60% from Mainland. The acceptance rate appears to be dependent on the sample sensitivity with highly sensitive samples having a high acceptance rate. For samples with low numbers of accepted discs, it is the low sensitivity that prevents the accuracy and precision required for the successful correction of sensitivity changes that may occur in the SAR run and the scattered data prevents regression analysis. It was previously suggested in Section 5.2.3.1 that sample sensitivity is probably dependent on sand provenance. Due to the low sensitivity of modern beach samples to artificial irradiation discussed in Chapter 4, it is suggested that the samples from Eday are likely to have a local (probably till) source however the source of the highly sensitive samples from some of the other archaeological sites is less likely to be local and may now be located offshore.

The number of discs accepted for further analysis is disappointing and sample sensitivity appears to be a major controlling factor. Despite this, ages have been calculated for all but one sample (SUTL 921 had all discs rejected) and these are presented below.

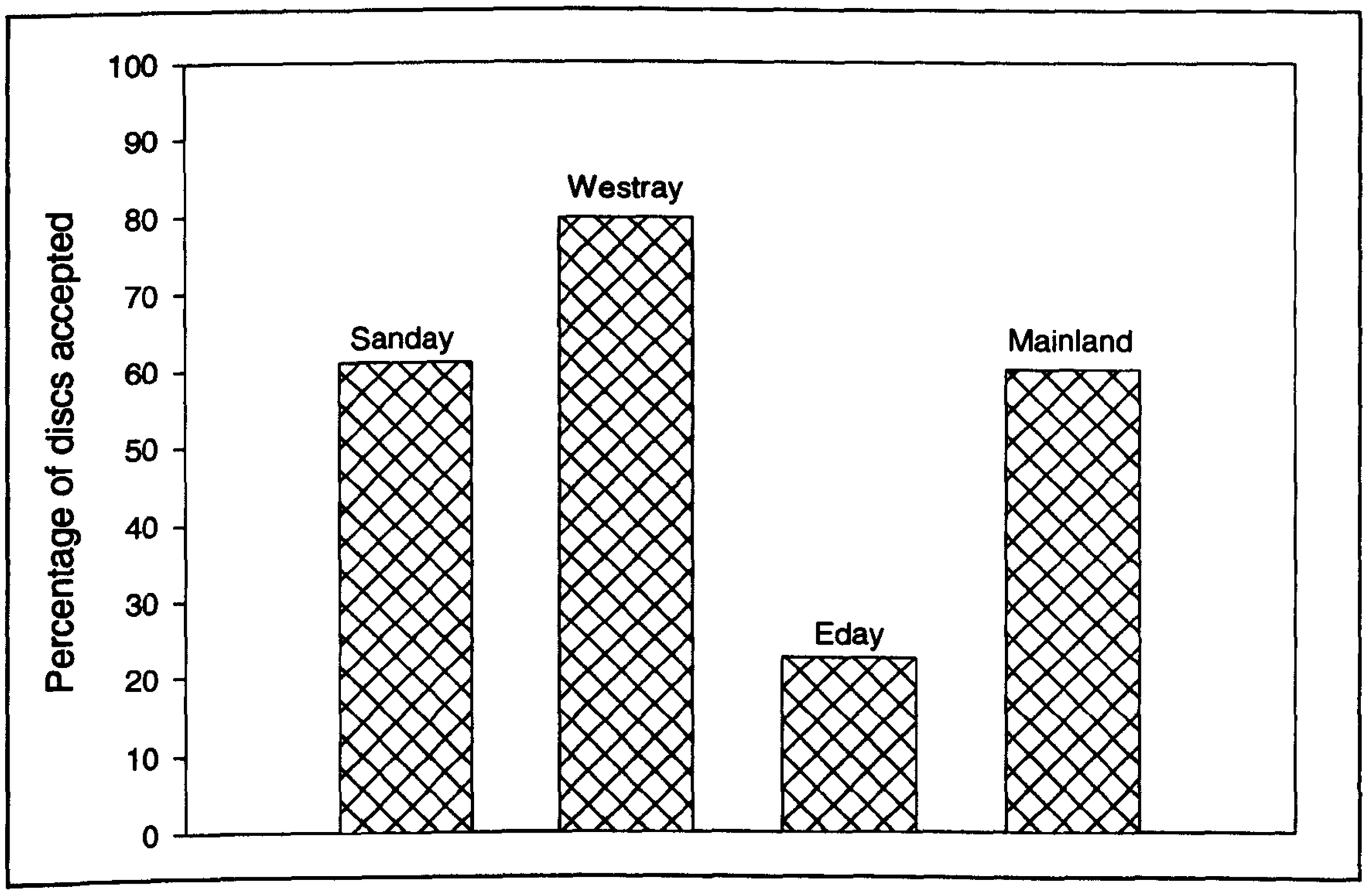

Figure 5.20 – The percentage of discs accepted from each island

5.3 Results from OSL dating of archaeological samples

As discussed above the results presented here are from those discs that passed the recycling ratio test, were not contaminated with IR sensitive minerals and regression analysis of the regenerative dose response curve was successful. The main trends within each site are discussed below in more detail before the ages of the samples are presented and how these relate to the stratigraphy and archaeology within each site.

5.3.1 Tofts Ness, Sanday

5.3.1.1 Trends within samples

The Tofts Ness samples were collected from eight test pits with one or two sand layers within each pit. All of the samples are composed of relatively coarse grained sand with a mean grain size of 250-500 μm. The water content varies between 11.5% and 63% depending on the location of the samples in the test pits, with lower samples having higher water contents. The calcium carbonate content varies little between the samples (Figure 5.2) suggesting that all of the sand layers are composed of a similar material and may therefore have come from the same source. However, as previously discussed in Section 5.2.3, when the OSL response of the samples to artificial irradiation is considered, there is a distinct difference in sensitivity between some of the samples. Most of the lower sand layer samples (SUTL 610, 612, 613, 616 and 617) respond well to the artificial irradiation, whereas those from the upper layer, except samples SUTL 602 and 605 (Figure 5.3) tend to be less sensitive. The sensitivity differences influence the dose response curves with low sensitivity samples often having a scattered response to the regenerative doses. Aliquots from these samples are rejected either for failing the recycling ratio test or the data is so scattered that regression analysis is problematic (Figure 5.21a). In comparison, the highly sensitive lower samples are well behaved and commonly produce dose response curves that display only small errors (Figure 5.21b). Only two samples (SUTL 603 and 610) are moderately sensitive to the artificial irradiation however the number of discs rejected due to recycling or contamination is also low (Table 5.3). Some of the dose response curves of these samples are very scattered whilst others have very small errors. This may be an indication that these samples are composed of a mixture of sensitive and insensitive grains.

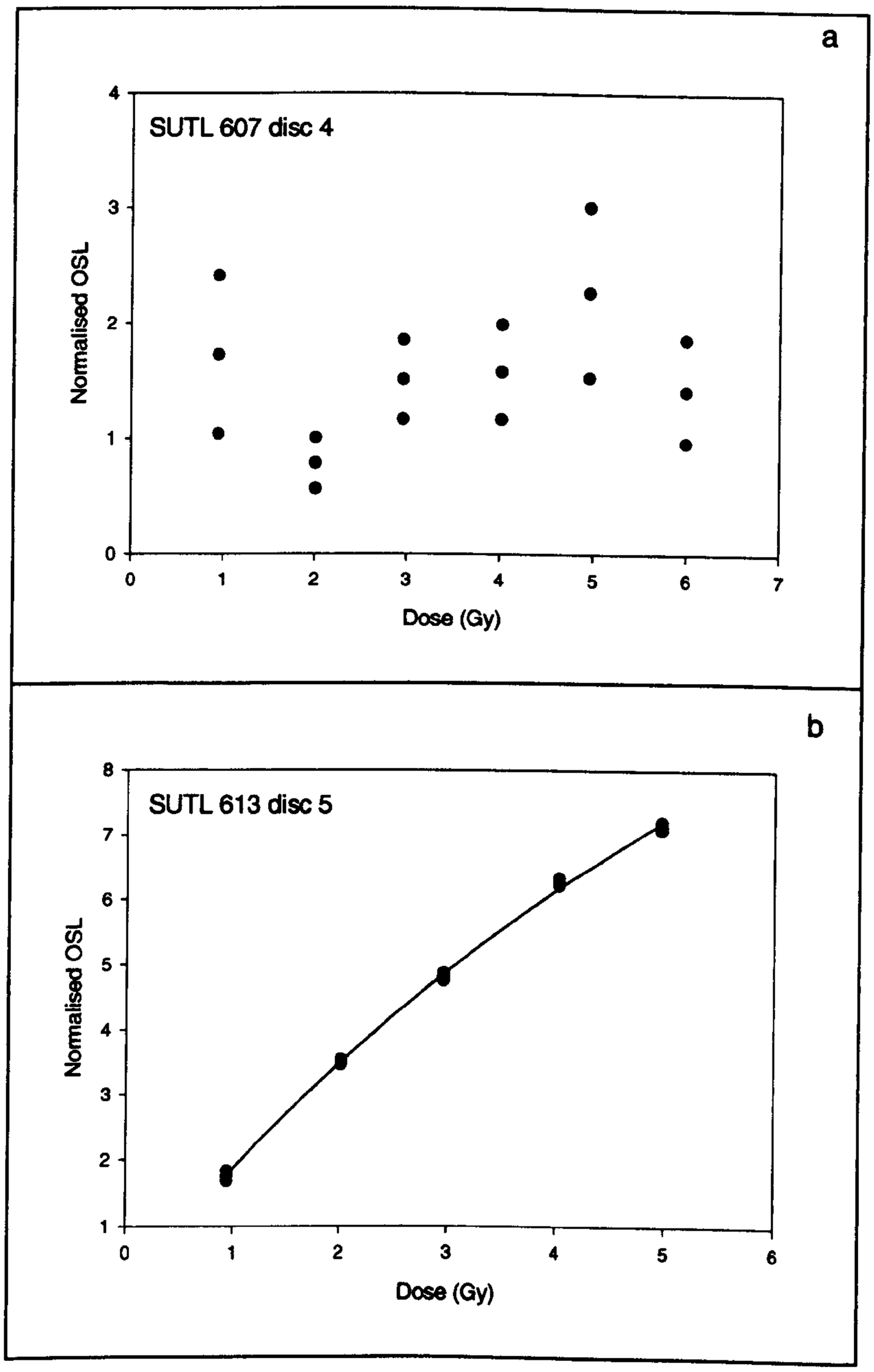

Figure 5.21 – Regenerative dose response curves from Tofts Ness; a) scattered and b) well-behaved

For some of the samples, a large number of discs were rejected because they had a significant response to IR stimulation suggesting contamination of the quartz by either feldspar grains or microinclusions within the quartz grains themselves. There is a correlation between samples that are contaminated by IR sensitive minerals and those that do not respond well to artificial irradiation (Figure 5.22), which further indicates that different sources of sand are represented at this site. These differences also broadly relate to the stratigraphic context and period of deposition.

Many of the samples from Tofts Ness were collected from thin sand layers interleaved between palaeosols (e.g. Figure 5.23). Due to different dosimetric properties, the palaeosols have a higher gamma dose rate than the sand and therefore the *in situ* gamma dose rates measured in the field are usually higher than those measured by high resolution gamma spectrometry of the sand in the laboratory (Table 5.4). To ensure that the dose rate used to determine the age of each sample is realistic, the gamma contribution from the palaeosols must be taken into consideration. As a result the dose rates of most samples from Tofts Ness are based on *in situ* field gamma dosimetry and thick source beta counting (TSBC) measured in the laboratory[9]. Lower sand layer samples SUTL 605, 616 and 617 have much higher *internal* beta and gamma dose rates than the other samples (Table 5.4) and this again suggests that these samples either have a different provenance or are a combination of sand from various sources.

5.3.1.2 OSL dates

The sample ages for each test pit are shown in Figure 5.24 and summarised in Table 5.5 with the dose rate and weighted mean equivalent dose of each sample. Samples from lower sand layers are shaded in Table 5.5 to differentiate between the two sand layers. The majority of samples appear to be in stratigraphic order within each test pit, but the samples have a wide range of ages from the Neolithic to the 19th century AD which is surprising given that only two sand layers were identified within the pits. There are, however, several samples (SUTL 604, 606 and 607) that lie close to the modern ploughed soil, and therefore the OSL dates of these samples are quite young (probably due to disturbance of the sand

[9] In some of the samples analysed, significantly different beta dose rates were produced using TSBC and high resolution gamma spectrometry, in spite of the samples being sealed for 3 weeks prior to high resolution gamma spectrometry. The differences noted may be due to either radon loss or uranium series disequilibrium at the top of the series. However for many of the samples the signal/background ratio is very low and therefore it is difficult to accurately determine if the samples are experiencing uranium series disequilibrium. Further analysis of all samples that demonstrate this effect is required in any future work and bulk samples of 100-200g (rather than the 20g used in this analysis) should be used in future measurements.

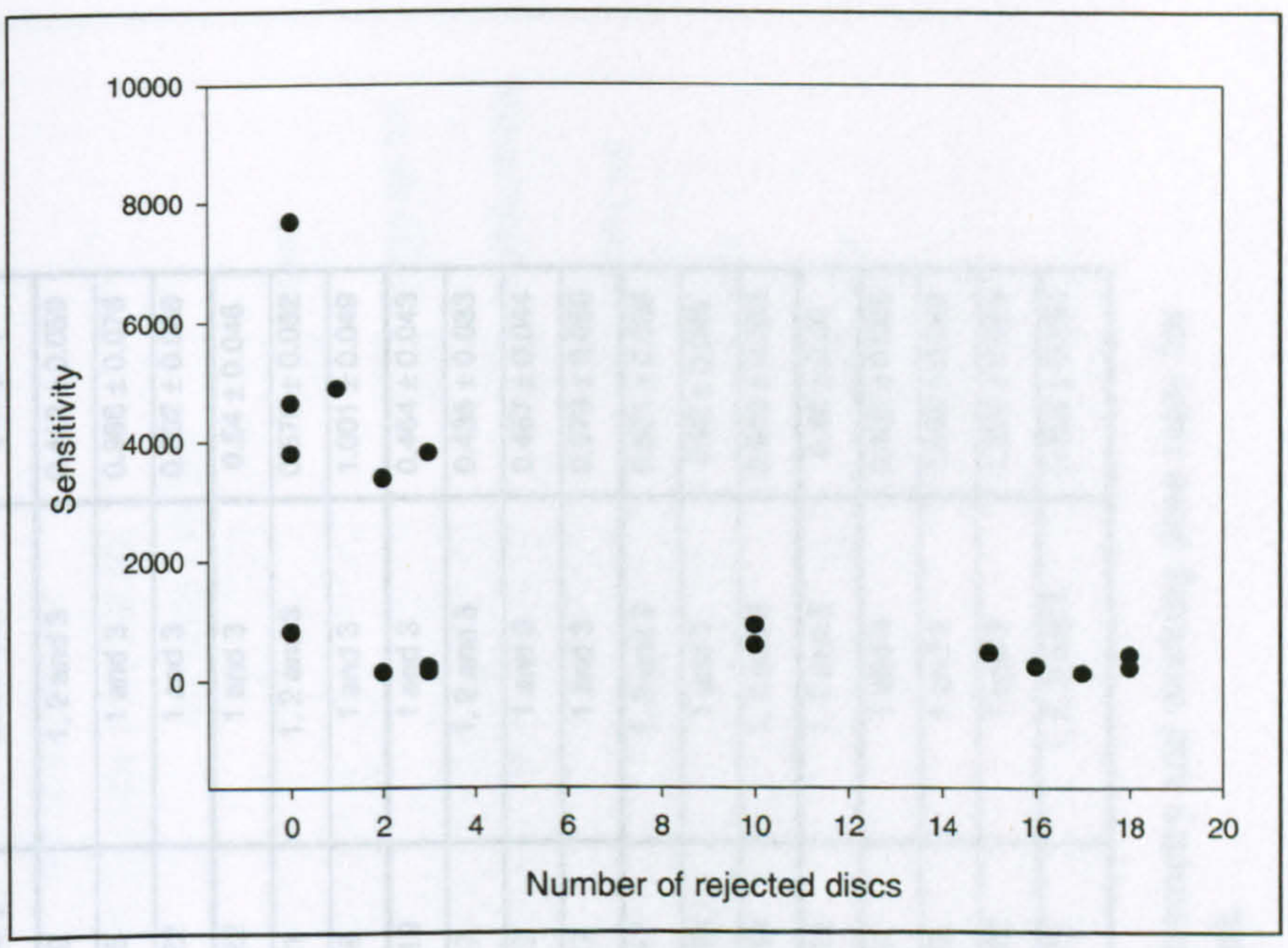

Figure 5.22 – Sensitivity of Tofts Ness samples versus the number of discs rejected due to contamination by IR sensitive minerals

Figure 5.23 – Sample collection from a thin sand layer at Tofts Ness. The palaeosols above and below the sand will have an effect on the dose rate of the sample.

Sample	Test Pit	(1) Beta dose rate using TSBC ($mGya^{-1}$)	(2) Beta dose rate using high resolution gamma ($mGya^{-1}$)	(3) Field gamma dose rate ($mGya^{-1}$)	(4) Gamma dose rate from high resolution gamma ($mGya^{-1}$)	Methods used to calculate working dose rate	Working Dose Rate ($mGya^{-1}$)
604	2	0.14 ± 0.047	0.08 ± 0.039	0.14 ± 0.05	0.03 ± 0.019	1, 2 and 3	0.412 ± 0.059
602	2	0.906 ± 0.054	0.74 ±0.046	0.19 ± 0.05	0.24 ± 0.025	1 and 3	0.986 ± 0.076
603	2	0.306 ± 0.047	0.23 ± 0.041	0.19 ± 0.05	0.048 ± 0.022	1 and 3	0.602 ± 0.068
606	3	0.149 ± 0.056	-0.335 ± 0.033	0.25 ± 0.005	-0.19 ± -0.022	1 and 3	0.54 ± 0.046
607	3	0.22 ± 0.051	0.17 ± 0.04	0.25 ± 0.005	0.05 ± 0.021	1, 2 and 3	0.578 ± 0.032
605	3	1.098 ± 0.054	0.905 ± 0.046	0.133 ± 0.005	0.27 ± 0.018	1 and 3	1.001 ± 0.049
608	4	0.21 ± 0.05	0.05 ± 0.04	0.136 ± 0.005	-0.03 ± -0.019	1 and 3	0.464 ± 0.043
609	4	0.168 ± 0.056	0.16 ± 0.039	0.136 ± 0.005	0.03 ± 0.017	1, 2 and 3	0.435 ± 0.033
611	5	0.3 ± 0.051	0.174 ± 0.039	0.062 ± 0.005	0.04 ± 0.017	1 and 3	0.457 ± 0.044
610	5	0.433 ± 0.04	0.24 ± 0.04	0.15 ± 0.05	0.04 ± 0.017	1 and 3	0.579 ± 0.059
614	6	0.184 ± 0.057	0.195 ± 0.039	0.205 ± 0.005	0.047 ± 0.017	1, 2 and 3	0.521 ± 0.033
612	6	0.504 ± 0.058	0.306 ± 0.043	0.413 ± 0.005	0.033 ± 0.018	1 and 3	0.92 ± 0.045
613	6	0.662 ± 0.064	0.583 ± 0.044	0.418 ± 0.005	0.126 ± 0.018	1, 2 and 3	0.963 ± 0.033
615	7	0.198 ± 0.05	0.22 ± 0.039	0.15 ± 0.05	0.058 ± 0.018	1, 2 and 3	0.48 ± 0.06
618	8	0.175 ± 0.053	0.188 ± 0.027	0.1 ± 0.05	0.047 ± 0.01	1 and 3	0.405 ± 0.065
616	8	1.676 ± 0.073	1.492 ± 0.056	0.45 ± 0.005	0.39 ± 0.023	1 and 3	1.546 ± 0.052
617	8	1.851 ± 0.076	1.483 ± 0.054	0.45 ± 0.005	0.398 ± 0.022	1 and 3	1.552 ± 0.053
619	9	0.189 ± 0.063	0.186 ± 0.038	0.07 ± 0.02	0.051 ± 0.015	1, 2, 3 and 4	0.366 ± 0.034

Table 5.4 – TSBC, high resolution gamma spectrometry, *in situ* field gamma spectrometry and working dose rates for Tofts Ness samples. Samples are in stratigraphic order within their respective test pit.

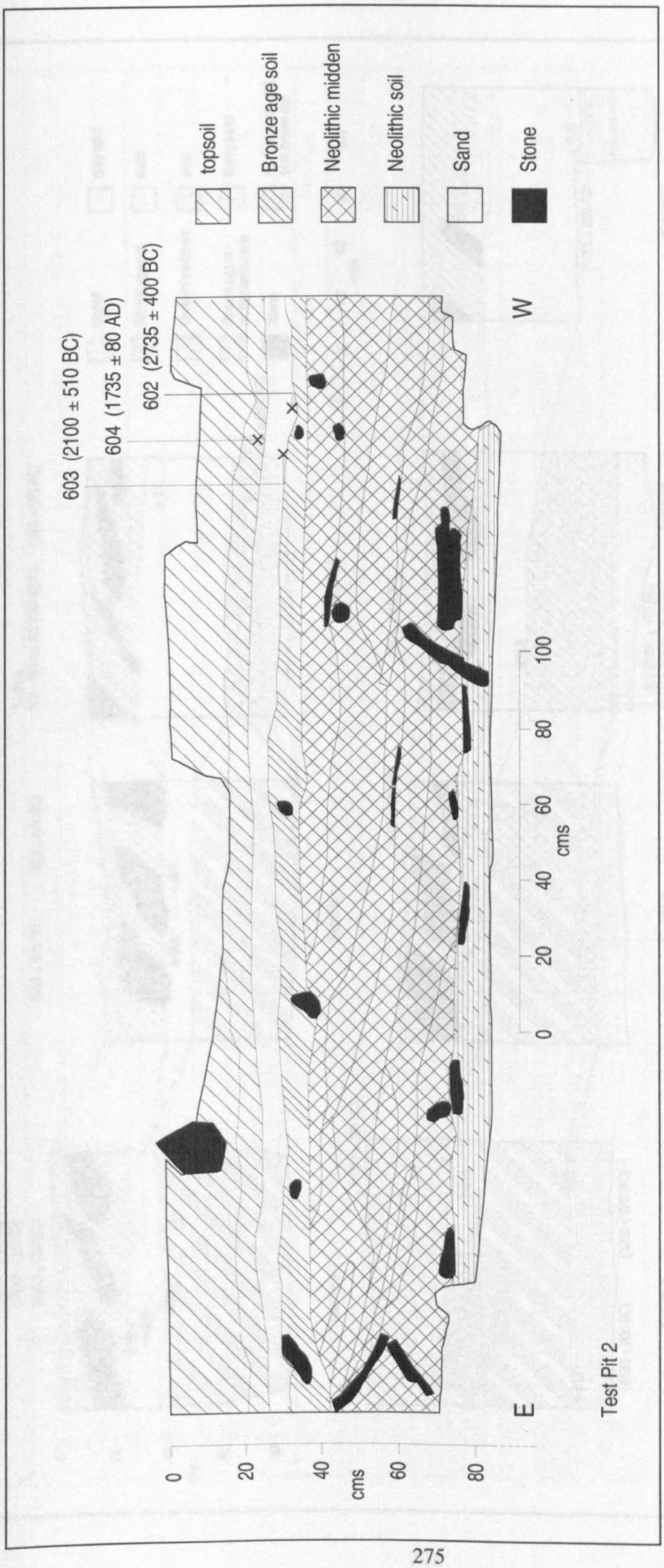

Figure 5.24 – OSL dates from Test Pit 2 at Tofts Ness, Sanday

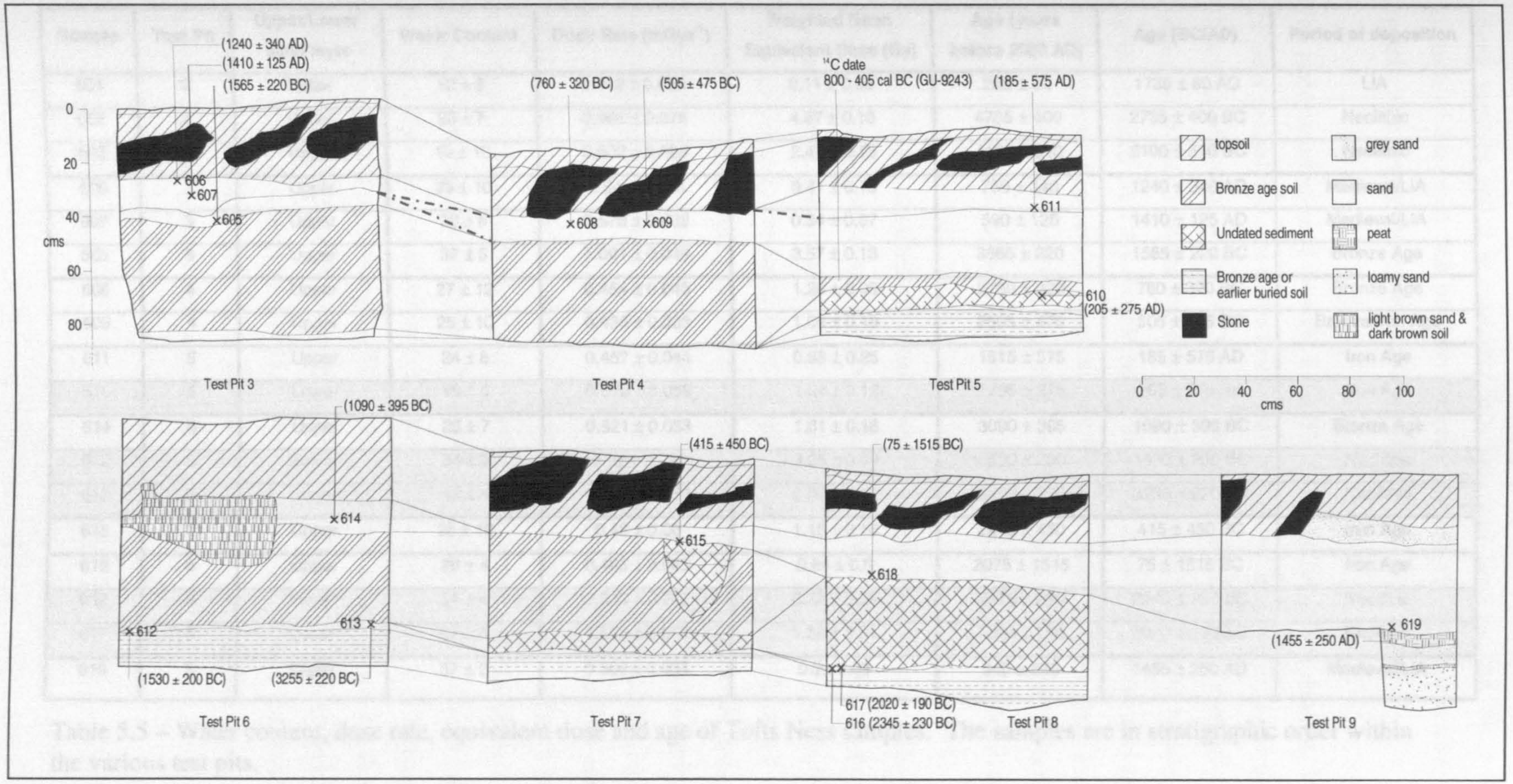

Figure 5.24 continued – OSL dates from Test Pits 3-9 at Tofts Ness, Sanday. The red dashed lines are the new stratigraphic correlations between the pits suggested by the OSL dates. Black correlation lines are used where the OSL dates are in agreement with the existing stratigraphy based on the interpretation by Guttmann (2001).

Sample	Test Pit	Upper/Lower sand layer	Water Content	Dose Rate ($mGya^{-1}$)	Weighted Mean Equivalent Dose (Gy)	Age (years before 2000 AD)	Age (BC/AD)	Period of deposition
604	2	Upper	12 ± 8	0.412 ± 0.059	0.11 ± 0.03	265 ± 80	1735 ± 80 AD	LIA
602	2	Upper	28 ± 7	0.986 ± 0.076	4.67 ± 0.16	4735 ± 400	2735 ± 400 BC	Neolithic
603	2	Upper	18 ± 10	0.602 ± 0.068	2.47 ± 0.13	4100 ± 510	2100 ± 510 BC	Neolithic
606	3	Upper	23 ± 10	0.54 ± 0.046	0.41 ± 0.18	760 ± 340	1240 ± 340 AD	Medieval/LIA
607	3	Upper	20 ± 6	0.578 ± 0.032	0.34 ± 0.07	590 ± 125	1410 ± 125 AD	Medieval/LIA
605	3	Upper	37 ± 5	1.001 ± 0.049	3.57 ± 0.13	3565 ± 220	1565 ± 220 BC	Bronze Age
608	4	Upper	27 ± 12	0.464 ± 0.043	1.28 ± 0.09	2760 ± 320	760 ± 320 BC	Bronze Age
609	4	Upper	25 ± 10	0.435 ± 0.033	1.09 ± 0.19	2505 ± 475	505 ± 475 BC	Bronze/Iron Age
611	5	Upper	24 ± 8	0.457 ± 0.044	0.83 ± 0.25	1815 ± 575	185 ± 575 AD	Iron Age
610	5	Lower	49 ± 5	0.579 ± 0.059	1.04 ± 0.12	1795 ± 275	205 ± 275 AD	Iron Age
614	6	Upper	25 ± 7	0.521 ± 0.033	1.61 ± 0.18	3090 ± 395	1090 ± 395 BC	Bronze Age
612	6	Lower	34 ± 5	0.92 ± 0.045	3.25 ± 0.09	3530 ± 200	1530 ± 200 BC	Neolithic
613	6	Lower	46 ± 4	0.963 ± 0.033	5.06 ± 0.13	5255 ± 220	3255 ± 220 BC	Neolithic
615	7	Upper	25 ± 10	0.48 ± 0.06	1.16 ± 0.16	2415 ± 450	415 ± 450 BC	Iron Age
618	8	Upper	26 ± 4	0.405 ± 0.065	0.84 ± 0.6	2075 ± 1515	75 ± 1515 BC	Iron Age
616	8	Lower	54 ± 4	1.546 ± 0.052	6.72 ± 0.28	4345 ± 230	2345 ± 230 BC	Neolithic
617	8	Lower	67 ± 5	1.552 ± 0.053	6.24 ± 0.21	4020 ± 190	2020 ± 190 BC	Neolithic
619	9	Upper	37 ± 2	0.366 ± 0.034	0.2± 0.09	545 ± 250	1455 ± 250 AD	Medieval/LIA

Table 5.5 – Water content, dose rate, equivalent dose and age of Tofts Ness samples. The samples are in stratigraphic order within the various test pits.

during ploughing). Both samples SUTL 606 and 607 have quite large errors for such young samples and it is suggested that this sand layer in Test Pit 3 (Figure 5.24) is a mixture of bleached and partially bleached grains resulting in a wide range of natural signals; again suggesting post-depositional mixing.

The upper sand layer of Test Pit 8 (SUTL 618) has been OSL dated to 75 ± 1515 BC and the poor precision is due to the low sensitivity and wide range in D_e, possibly due to partial bleaching of the six discs that were accepted for the final age estimate. The majority of discs (53%) were rejected due to contamination by IR sensitive minerals, however 28% of the discs failed the 1 Gy recycle test or scattered data which prevented regression analysis of the regenerative dose response curves. The remaining samples from the upper sand layer date to the Neolithic (SUTL 602, 603, and 605), Bronze Age (SUTL 608, 609, 614), Iron Age (SUTL 611, 615) and Little Ice Age (SUTL 619) (Table 5.5, Figure 5.24).

Four of the five samples collected from the lower sand layer at Tofts Ness date to the Neolithic/early Bronze Age (Figure 5.24, Table 5.5). This is encouraging given the range in dates from the upper sand layer, but sample SUTL 610 from Test Pit 5 is much younger than the other lower sand layer samples and has been OSL dated to the Iron Age (Table 5.5). The upper sand layer within Test Pit 5 also dates to the Iron Age yet it seems unlikely that there has been any significant mixing between the two layers. The lower sand layer is moderately sensitive to artificial irradiation and it was suggested above that this may be due to a mixture of sensitive and insensitive grains. The upper sand sample (SUTL 611) does not respond well to artificial irradiation but it has a slightly higher psi ratio than SUTL 610 below and therefore it is suggested that the upper sand layer may be partially bleached overestimating the age of the sample. A radiocarbon date of 800-405 cal BC (GU-9243) was obtained from the peat lying above SUTL 610 (Figure 5.24) and based on this result the upper sample (SUTL 611) appears to be correct but the OSL date of the lower sample (SUTL 610) is clearly problematic. There is a distinct difference in the water content of the two samples (SUTL 610, 49.5% and SUTL 611, 24.5%) and it is possible that the water within SUTL 610 has absorbed a large proportion of the natural radiation resulting in an underestimation of the OSL age.

5.3.1.3 Discussion

From archaeological evidence, the site at Tofts Ness was occupied from the Neolithic to the Iron Age with one period of temporary abandonment during the Bronze Age (Dockrill *et al.* 1994) and throughout the occupation of the site, soils were formed and developed for the growing of crops. The test pits excavated in 1999 revealed one or two sand layers interleaved between the palaeosols and they were thought to represent two depositional phases of wind blown sand that covered a substantial area. The individual OSL dates from the samples collected from the test pits are quite varied and may suggest that more than two depositional events are represented at this site (Figure 5.25). The range may, in part, be due to partial bleaching but the ψ ratios (Figure 4.36) indicate that most samples appear to have been well-bleached prior to burial supporting the idea that more than two events are represented at the site. Further evidence to suggest that there are more than two sand events is the variable sensitivity of the samples. It was noted in Section 5.3.1.1 that some of the Tofts Ness samples respond very well to artificial irradiation whereas others do not and this indicates that the sand is from at least two different sources. In Section 5.2.3.1 an attempt was made to determine the sediment provenance by comparing the sensitivity of the samples with the sensitivity of the modern beach sands. A modern beach source was not identified in the analysis and it has been suggested that the source of the very sensitive sand is likely to be till deposits that now lie offshore. This agrees with the emerging geomorphological reconstruction of the coastal evolution of Sanday proposed by May and Hansom (2003). Samples that respond well to artificial irradiation are not restricted to the upper or lower sand layer and this could be an indication that discrete sand layers were deposited at Tofts Ness from at least two different sources throughout the last 4000-5000 years.

Despite the apparent evidence for more than two depositional events, many of the samples have ages which are within error of each other and when a weighted mean is calculated for the upper and lower sand layers, two distinct periods of sand deposition are recorded (Table 5.6). In some test pits (2, 4, 6, and 8, Figure 5.24) two samples were collected from either the upper or lower sand layer and the weighted mean of these sand layers is shown in Column 4 of Table 5.6. When these dates are compared they are also within error of each other and therefore calculating a weighted mean age of the upper and lower sand layer is possible, as shown in Column 5 of Table 5.6. From these results the lower sand layer was deposited at the end of the 3rd millennium BC (2260 ± 100 BC) and this supports

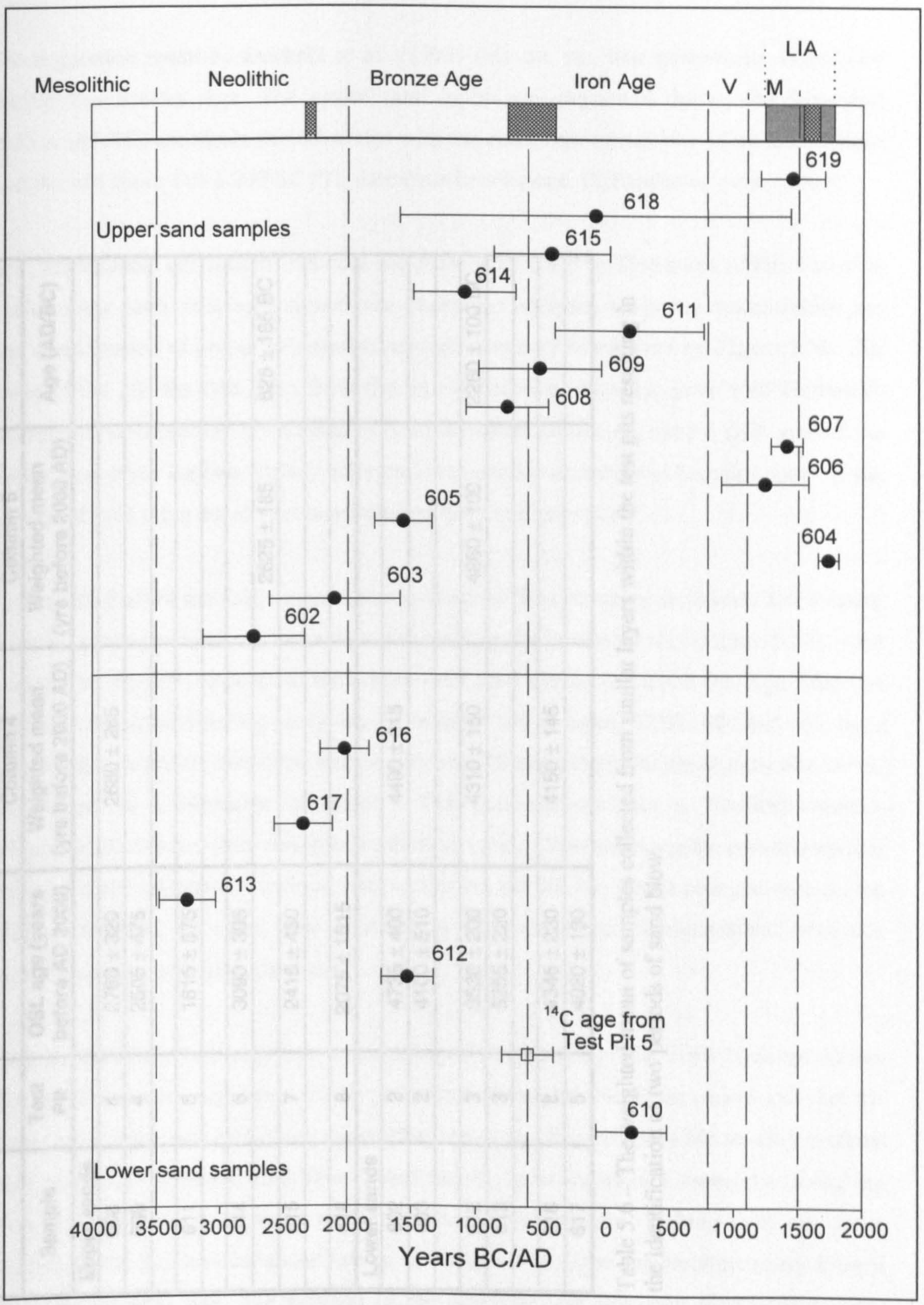

Figure 5.25 – OSL dates from Tofts Ness, radiocarbon date from Test Pit 5 and identification of periods of increased sand movement (shaded areas) using the weighted mean of the OSL dates. V = Viking M = Medieval LIA = Little Ice Age

Sample	Test Pit	OSL age (years before AD 2000)	Column 4 Weighted mean (yrs before 2000 AD)	Column 5 Weighted mean (yrs before 2000 AD)	Age (AD/BC)
Upper sands					
608	4	2760 ± 320	2680 ± 265		
609	4	2505 ± 475			
611	5	1815 ± 575			
614	6	3090 ± 395			
				2625 ± 185	625 ± 185 BC
615	7	2415 ± 450			
618	8	2075 ± 1515			
Lower sands					
602	2	4735 ± 400	4490 ± 315		
603	2	4100 ± 510			
612	3	3530 ± 200	4310 ± 150	4260 ± 100	2260 ± 100 BC
613	3	5255 ± 220			
616	8	4345 ± 230	4150 ± 145		
617	8	4020 ± 190			

Table 5.6 – The weighted mean of samples collected from similar layers within the test pits resulting in the identification of two periods of sand blow.

the suggestion made by Dockrill *et al.* (1994) that the site was temporarily abandoned during the Bronze Age. The upper sand layer was deposited during the Iron Age (625 ± 185 BC) and again this correlates with the end of the occupation of the roundhouse and the site about 410 ± 290 BC (TL date from hearthstone, D. Sanderson *pers. comm.*).

The stratigraphic correlations between the palaeosols made by Guttmann (2001) based on radiocarbon dates, thin section analysis, phosphate analysis, magnetic susceptibility and the identification of one or two sand layers are shown by black lines on Figure 5.24. For most of the pits the OSL ages from the interleaved sand deposits agree with Guttman's interpretation, especially those samples from the lower sand layer, but the OSL ages of the upper sand layer suggest slightly different stratigraphic correlations between some of the palaeosols and these are shown as red dashed lines in Figure 5.24.

In Test Pit 2 all of the OSL samples were collected from an upper sand layer that overlay what was interpreted as a Bronze Age palaeosol by Guttmann (2001) (Figure 5.24). One sample, SUTL 604, appears to have been deposited during the Little Ice Age, and was probably re-exposed during ploughing. The other two samples, SUTL 602 and 603, have been OSL dated to the Neolithic and therefore the 'Bronze Age' palaeosol must now be re-interpreted as a Neolithic palaeosol. The palaeosol overlies a Neolithic midden (Figure 5.24) and therefore this interpretation is valid. Other stratigraphic correlations that have been altered between various units within the test pits have been changed because the OSL dates have provided new information that could not be determined from the archaeology and soil analysis alone.

OSL dating of the two sand layers identified within the test pits at Tofts Ness has shown that the lower sand layer was mainly deposited during the Neolithic period and that the upper sand layer was laid down during the Iron Age. It is not possible to infer whether both periods of increased sand blow caused the site to be abandoned, especially during the Iron Age, however as a result of the increased wind activity, drifting sand may have contributed to the eventual abandonment of the site during the late Neolithic/early Bronze Age and the Iron Age. The survival of the Neolithic and Iron Age sand deposits may possibly be due to different parts of the site being used at different times allowing erosion to occur in some areas and not in others. They may also have survived as a result of rapid accumulation of soil above the sand layers aided by the addition of manure and ash by the local people (Simpson *et al.* 1998).

5.3.2 Bay of Lopness, Sanday

5.3.2.1 Trends within the samples

The samples from the Bay of Lopness were collected from a vertical dune section overlying a midden and a glacial till which protrudes at beach level (Figure 3.10). Radiocarbon dating was undertaken on marine shells and a sheep bone from the upper part of the midden and these returned ages of cal BC 200-cal AD 80 (GU-9247), cal AD 135-430 (GU-9247A) and cal AD 40-165 (GU-9248) respectively (Figure 3.10) indicating deposition during the Iron Age. A marine reservoir effect of 405 ± 40 years (Harkness 1983) was applied before calibration of the radiocarbon dates from the marine shells but it is not known whether the sheep bone was from a seaweed eating species and therefore the marine reservoir effect has not been applied to this sample. Eight samples were collected for OSL dating, seven from the vertical dune section and one from a sand lens within the midden and the majority were composed of medium grained sand. The samples contained between approximately 45%-70% shell material with an average of about 58% and the water content varied between approximately 5.5%-17.5%. The water content increased with depth in the section until the palaeosol (Figure 3.10) after which there was a slight decrease. The sand lens within the midden contained the highest water content at 17.5%.

The sensitivity of the samples to artificial irradiation does vary slightly within the section. Most of the samples are reasonably sensitive, but the two lowest samples (SUTL 890 and 891) are much more sensitive to a 0.5 Gy dose as shown in Figure 5.26. The dose response curves of the less sensitive samples are slightly scattered and although the regenerative curves of the highly sensitive samples tend to be well behaved, several discs from most samples (between 6% and 25%) are rejected due to failing the recycling ratio test. A further 7% of the discs were rejected due to contamination by IR sensitive minerals and most of the discs were from sample SUTL 888 lying directly below the palaeosol (Figure 3.10). As mentioned above for Tofts Ness, the variable sensitivity of the Bay of Lopness samples suggests that the sand within the lower sand layer and midden (SUTL 890 and 891) has a different provenance to that of the upper sand deposits. None of the modern beaches have a similar sensitivity to these lower samples and therefore it is thought that the source may now be offshore, an interpretation consistent with recent geomorphological reconstructions (May and Hansom 2003).

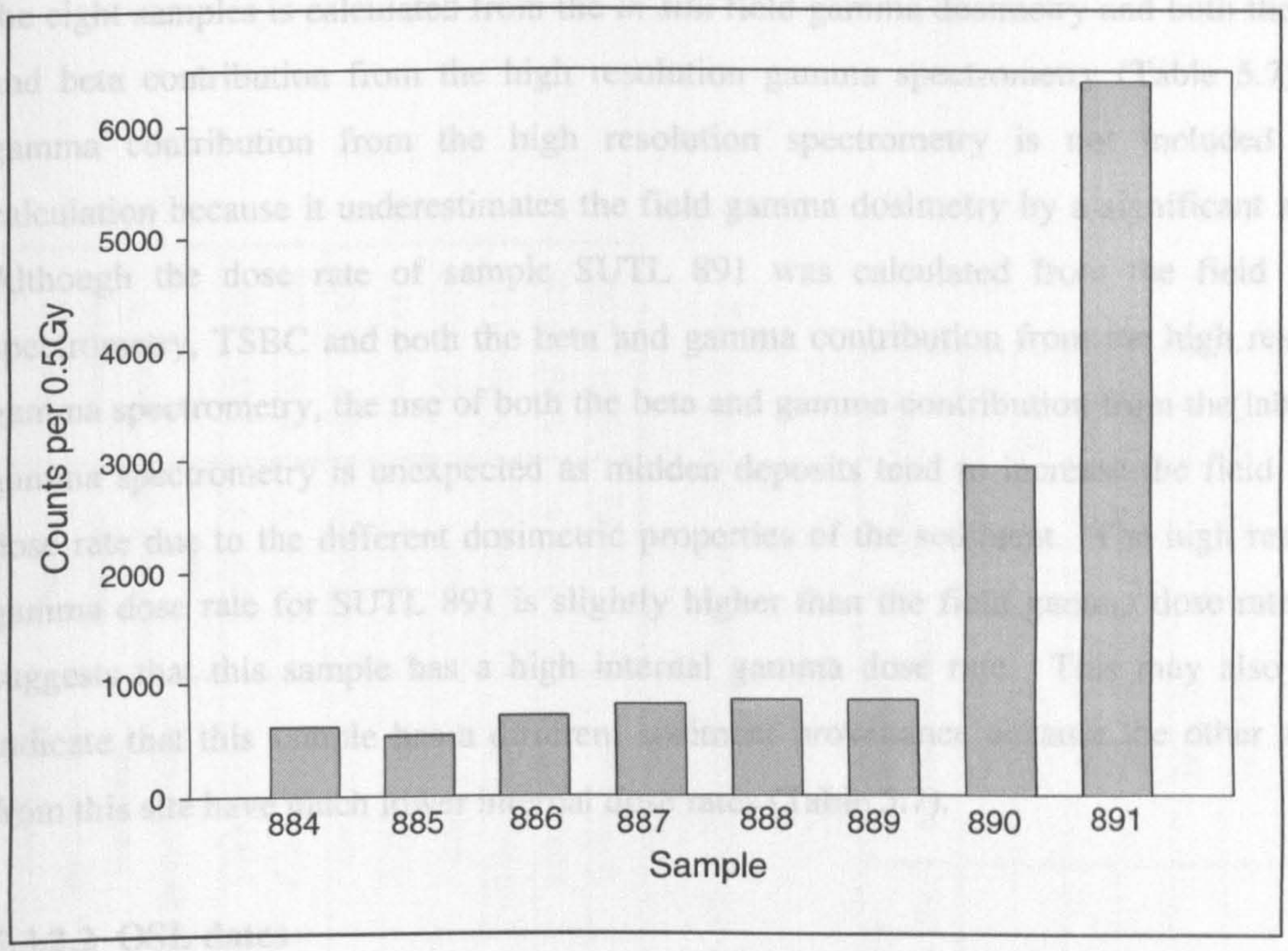

Figure 5.26 – Sensitivity of Bay of Lopness samples to a 0.5 Gy dose

The majority of sand layers are quite homogenous and therefore the dose rate for seven of the eight samples is calculated from the *in situ* field gamma dosimetry and both the TSBC and beta contribution from the high resolution gamma spectrometry (Table 5.7). The gamma contribution from the high resolution spectrometry is not included in the calculation because it underestimates the field gamma dosimetry by a significant amount. Although the dose rate of sample SUTL 891 was calculated from the field gamma spectrometry, TSBC and both the beta and gamma contribution from the high resolution gamma spectrometry, the use of both the beta and gamma contribution from the laboratory gamma spectrometry is unexpected as midden deposits tend to increase the field gamma dose rate due to the different dosimetric properties of the sediment. The high resolution gamma dose rate for SUTL 891 is slightly higher than the field gamma dose rate which suggests that this sample has a high internal gamma dose rate. This may also further indicate that this sample has a different sediment provenance because the other samples from this site have much lower internal dose rates (Table 5.7).

5.3.2.2 OSL dates

Figure 5.27 shows the OSL ages of the Bay of Lopness samples in their stratigraphic context and the details of the dose rate, estimated dose and age of each sample are summarised in Table 5.8. The samples within and directly above the midden layer (SUTL 891 and 890 respectively) were deposited during the late Bronze Age and they are about 500 years older than the upper part of the midden deposit which was radiocarbon dated to the Iron Age (Figure 5.27). The older dates for these sand deposits within and directly above the midden might be indicating that the sand was partially bleached prior to burial, however both samples have psi ratios close to zero and this is thought to indicate that the sand was adequately bleached prior to burial.

Chronologically there is a gap of over 2000 years before the next sand layer is deposited and all of the remaining samples (SUTL 884-889) are deposited within a period of approximately 200 years during the 15^{th}-17^{th} centuries AD. Sample SUTL 887, lying directly above the palaeosol (Figure 5.27), is approximately 100 years older than the underlying sample (SUTL 888) and its psi ratio suggests that it may be partially bleached. In contrast, the sample overlying SUTL 887, sample SUTL 886, is the youngest in the section and this is surprising given that it was collected from a relatively homogenous thick sand layer in the middle of the section. Although the OSL ages of these samples are not

Sample	Unit	(1) Beta dose rate using TSBC ($mGya^{-1}$)	(2) Beta dose rate using high resolution gamma ($mGya^{-1}$)	(3) Field gamma dose rate ($mGya^{-1}$)	(4) Gamma dose rate from high resolution gamma ($mGya^{-1}$)	Methods used to calculate working dose rate	Working Dose Rate ($mGya^{-1}$)
884	10	0.214 ± 0.055	0.155 ± 0.031	0.105 ± 0.025	0.057 ± 0.015	1, 2 and 3	0.431 ± 0.05
885	9	0.098 ± 0.045	0.084 ± 0.045	0.1 ± 0.02	0.017 ± 0.024	1, 2 and 3	0.353 ± 0.038
886	9	0.067 ± 0.041	0.183 ± 0.039	0.095 ± 0.015	0.069 ± 0.019	1, 2 and 3	0.371 ± 0.034
887	6	0.231 ± 0.047	0.114 ± 0.041	0.095 ± 0.015	0.02 ± 0.021	1 and 3	0.44 ± 0.047
888	5	0.202 ± 0.032	0.102 ± 0.038	0.09 ± 0.001	0.038 ± 0.018	1 and 3	0.422 ± 0.038
889	3	0.145 ± 0.054	0.198 ± 0.04	0.125 ± 0.005	0.043 ± 0.019	1, 2 and 3	0.435 ± 0.036
890	2	0.218 ± 0.048	0.273 ± 0.039	0.195 ± 0.015	0.081 ± 0.019	1, 2 and 3	0.559 ± 0.038
891	1	0.832 ± 0.05	0.748 ± 0.044	0.205 ± 0.025	0.27 ± 0.024	1, 2, 3 and 4	0.981 ± 0.048

Table 5.7 – TSBC, high resolution gamma spectrometry, *in situ* field gamma dose rate and working dose rate of Bay of Lopness samples.

Sample	Unit	Water Content	Dose Rate ($mGya^{-1}$)	Weighted Mean Equivalent Dose (Gy)	Age (years before 2000 AD)	Date (BC/AD)
884	10	30 ± 10	0.431 ± 0.05	0.21 ± 0.05	535 ± 155	1465 ± 155 AD
885	9	18 ± 15	0.353 ± 0.038	0.19 ± 0.04	540 ± 130	1460 ± 130 AD
886	9	20 ± 13	0.329 ± 0.039	0.15 ± 0.003	405 ± 90	1595 ± 90 AD
887	6	25 ± 15	0.44 ± 0.047	0.23 ± 0.03	520 ± 90	1480 ± 90 AD
888	5	20 ± 13	0.422 ± 0.038	0.18 ± 0.03	425 ± 80	1575 ± 80 AD
889	3	20 ± 13	0.435 ± 0.036	0.23 ± 0.02	530 ± 65	1470 ± 65 AD
890	2	20 ± 10	0.559 ± 0.038	1.6 ± 0.09	2865 ± 255	865 ± 255 BC
891	1	23 ± 6	0.981 ± 0.048	3.02 ± 0.08	3080 ± 170	1080 ± 170 BC

Table 5.8 – Water content, dose rate, equivalent dose and age of Bay of Lopness samples

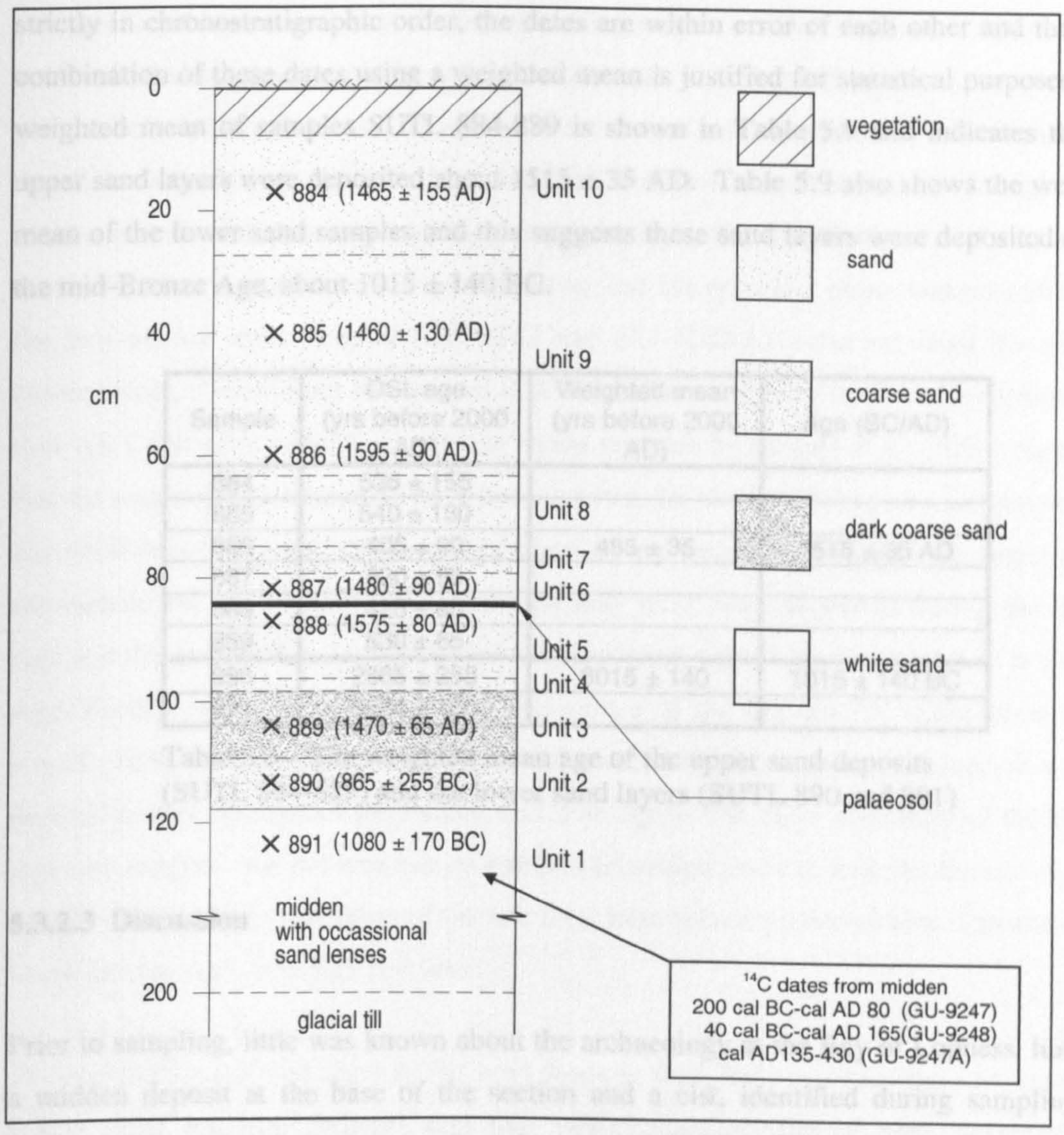

Figure 5.27 – OSL dates and radiocarbon dates from the Bay of Lopness and the upper OSL dates are within error of each other

strictly in chronostratigraphic order, the dates are within error of each other and therefore combination of these dates using a weighted mean is justified for statistical purposes. The weighted mean of samples SUTL 884-889 is shown in Table 5.9 and indicates that the upper sand layers were deposited about 1515 ± 35 AD. Table 5.9 also shows the weighted mean of the lower sand samples and this suggests these sand layers were deposited during the mid-Bronze Age, about 1015 ± 140 BC.

Sample	OSL age (yrs before 2000 AD)	Weighted mean (yrs before 2000 AD)	Age (BC/AD)
884	535 ± 155		
885	540 ± 130		
886	405 ± 90	485 ± 35	1515 ± 35 AD
887	520 ± 90		
888	425 ± 80		
889	530 ± 65		
890	2865 ± 255	3015 ± 140	1015 ± 140 BC
891	3080 ± 170		

Table 5.9 – The weighted mean age of the upper sand deposits (SUTL 884-889) and the lower sand layers (SUTL 890 and 891)

5.3.2.3 Discussion

Prior to sampling, little was known about the archaeology at the Bay of Lopness, however a midden deposit at the base of the section and a cist, identified during sampling and subsequently excavated, were radiocarbon dated to the Iron Age and Bronze Age respectively providing some constraints to the OSL ages from the overlying sand deposits. Although both the cist and midden directly overlie glacial deposits, the radiocarbon dates indicate that the cist was constructed prior to deposition of the midden and it can be suggested that before the cist was exposed by coastal erosion, the Iron Age midden extended over and buried the Bronze Age cist.

Most of the upper layers of sand deposition at this site took place during the 16th century AD in a period known as the Little Ice Age which due to historical records is known to have been cooler and windier than today's climate. The lower sand layers were expected to date to the mid/late Iron Age or later based on the radiocarbon dates from the underlying midden, but they appear to have been deposited and buried during the late Bronze Age. The older ages for these samples may be a result of partially bleached sand contaminating

younger sand layers or being deposited onto younger midden deposits. Alternatively, unbleached older sands could be redeposited on top of younger deposits if the event took place wholly within darkness. However, from the psi ratio analysis there is no indication that these samples are partially bleached and therefore the dates are not thought to be overestimated. In turn, the radiocarbon dates may be underestimated if the marine reservoir effect is not taken into consideration, but the reservoir effect was considered for the two marine shell samples (GU-9247 and GU-9247-A) collected from the midden. Nevertheless, it should not be assumed that the marine reservoir correction is constant over time (G. Cook *pers. comm.*), despite the recent research by Reimer *et al.* (2002) suggesting that the reservoir age appears to have been constant for the last 2000 years and possibly the last 6000 years. The samples for radiocarbon dating were collected from the upper part of the midden but the majority of the midden may have been deposited during the Bronze Age and the radiocarbon samples dated may represent deposition at a later date in the Iron Age. Further sampling from the base and centre of the midden for radiocarbon dating would clarify if the midden was deposited exclusively during the Iron Age or whether deposition was throughout the Bronze and Iron Ages. The close proximity of the Bronze Age cist suggests that the area has probably been settled since at least the Bronze Age and possibly earlier and other areas of the site may have been used for midden deposits dating to the Bronze Age, Iron Age and later.

The weighted mean OSL ages of the sand deposits from the Bay of Lopness are plotted in Figure 5.28 and they indicate that two well-defined periods of sand movement are represented at this site, one during the Bronze Age and the other during the Little Ice Age (LIA). Sand deposits dating to the Iron Age and Viking/Medieval period are not represented at the site, which may suggest that there was limited sand deposition at this time. This may indicate that the climate was stable during this period, but several samples from nearby Tofts Ness appear to have been deposited at this time and therefore this explanation seems unlikely. Another possible explanation is that the cist and midden would originally have been located further inland and may have been less affected by blowing sand. As sea level has risen the coastline and dunes have slowly encroached inland resulting in the exposure of the cist and midden and burial of the landscape by drifting sand. Although there may have been a significant delay between deposition of the midden and inundation by sand, there is no evidence of a weathered upper surface to the midden or development of a palaeosol. This indicates that conditions were either not

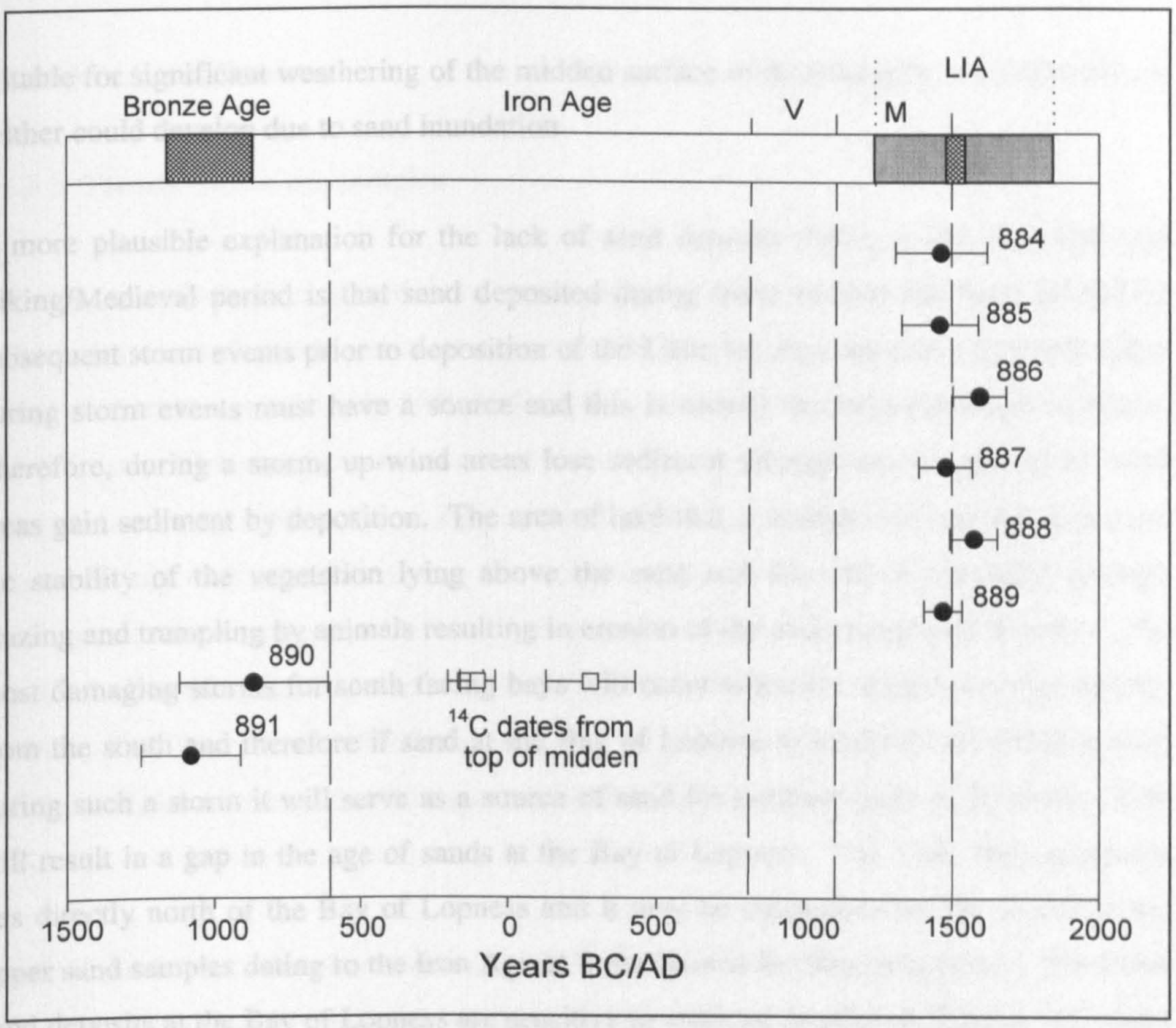

Figure 5.28 – OSL dates from the Bay of Lopness and the radiocarbon dates from the midden deposit. Two periods of increased sand movement have been identified using the weighted mean of the OSL dates and these are shown as the shaded areas in the diagram. V = Viking M = Medieval LIA = Little Ice Age

suitable for significant weathering of the midden surface or development of a palaeosol, or neither could develop due to sand inundation.

A more plausible explanation for the lack of sand deposits dating to the Iron Age and Viking/Medieval period is that sand deposited during these periods has been eroded by subsequent storm events prior to deposition of the Little Ice Age deposits. Sand deposited during storm events must have a source and this is usually the adjacent dunes or beach. Therefore, during a storm, up-wind areas lose sediment through erosion and down-wind areas gain sediment by deposition. The area of land that is eroded will vary depending on the stability of the vegetation lying above the sand and this can be damaged through grazing and trampling by animals resulting in erosion of the underlying sand deposits. The most damaging storms for south facing bays will occur when the wind is coming directly from the south and therefore if sand at the Bay of Lopness is available for transportation during such a storm it will serve as a source of sand for northern parts of the island. This will result in a gap in the age of sands at the Bay of Lopness. The Tofts Ness peninsula lies directly north of the Bay of Lopness and it may be suggested that the source of the upper sand samples dating to the Iron Age at Tofts Ness is the Bay of Lopness. The lower sand deposits at the Bay of Lopness are sensitive to artificial irradiation (Figure 5.3) which may support this hypothesis however most of the upper sand layers from Tofts Ness have low sensitivity. Therefore, it seems unlikely that the Bay of Lopness is the source of the upper sand deposits at Tofts Ness unless there has been a considerable degree of mixing with low sensitive sand.

It is therefore thought that sand deposition at the Bay of Lopness has occurred since at least the Bronze Age but due to the selective erosion of the sand dunes, possibly due to disturbance of the surface vegetation, there is no evidence for sand deposition during the Iron Age, Viking and Medieval periods. The next period of sand deposition that is recorded at this site occurred during the Little Ice Age and the thick layers of sand suggest that large quantities of sand were available for rapid deposition.

5.3.3 Quoygrew, Westray

5.3.3.1 Trends within the samples

Ten OSL samples were collected from Quoygrew, eight from sand layers in three test pits and two from a shell midden excavated during 1999 and 2000 (Figure 3.12). The samples contain between approximately 54%-82% of shell material and have a mean grain size of 250-500 μm. The water content tends to vary between the pits rather than the samples themselves. In Test Pit 7 the water content varies between 4%-9.5%, with the sample nearest the top of the section having the highest water content. This is unusual because sand tends to be very permeable however a silty loam layer containing a peat lens lies directly below this sand layer restricting the flow of water through the sand. The sand layers in Test Pits 101 and 102 have relatively low water contents of between 3.5%-5% and the samples from the midden deposit have the highest water content of approximately 17%.

Despite all of the samples from Quoygrew responding relatively well to artificial irradiation (Figure 5.29) and the regenerative dose response curves indicating that the samples are well behaved, 13% of the discs were rejected because they failed the recycling ratio test. A further 7% of the discs were rejected due to contamination by IR sensitive minerals and most of these were rejected from SUTL 699.

The dose rate of each pit tends to vary rather than the individual sample dose rates and Table 5.10 shows the TSBC, *in situ* field gamma dosimetry, high resolution gamma spectrometry and working dose rates for the 10 samples. The majority of the dose rates are calculated from the TSBC, *in situ* field gamma spectrometry and only the beta contribution from the laboratory gamma spectrometry. For many of the samples the internal gamma dose rate measured by the high resolution gamma spectrometer underestimates the field gamma dosimetry and therefore an average of the two dose rates would result in an overestimation of the sample age. The samples from the midden (SUTL 703 and 704) have a higher dose rate, almost double that of the homogenous sands in Test Pit 7 and this is due to their higher internal dose rates Table 5.10). The dose rates for the samples from Test Pits 101 and 102 (SUTL 901-903) are also quite high and this is thought to be due to the higher dosimetric properties of the palaeosols above and below the sand layers contributing to the *in situ* field gamma dose rates.

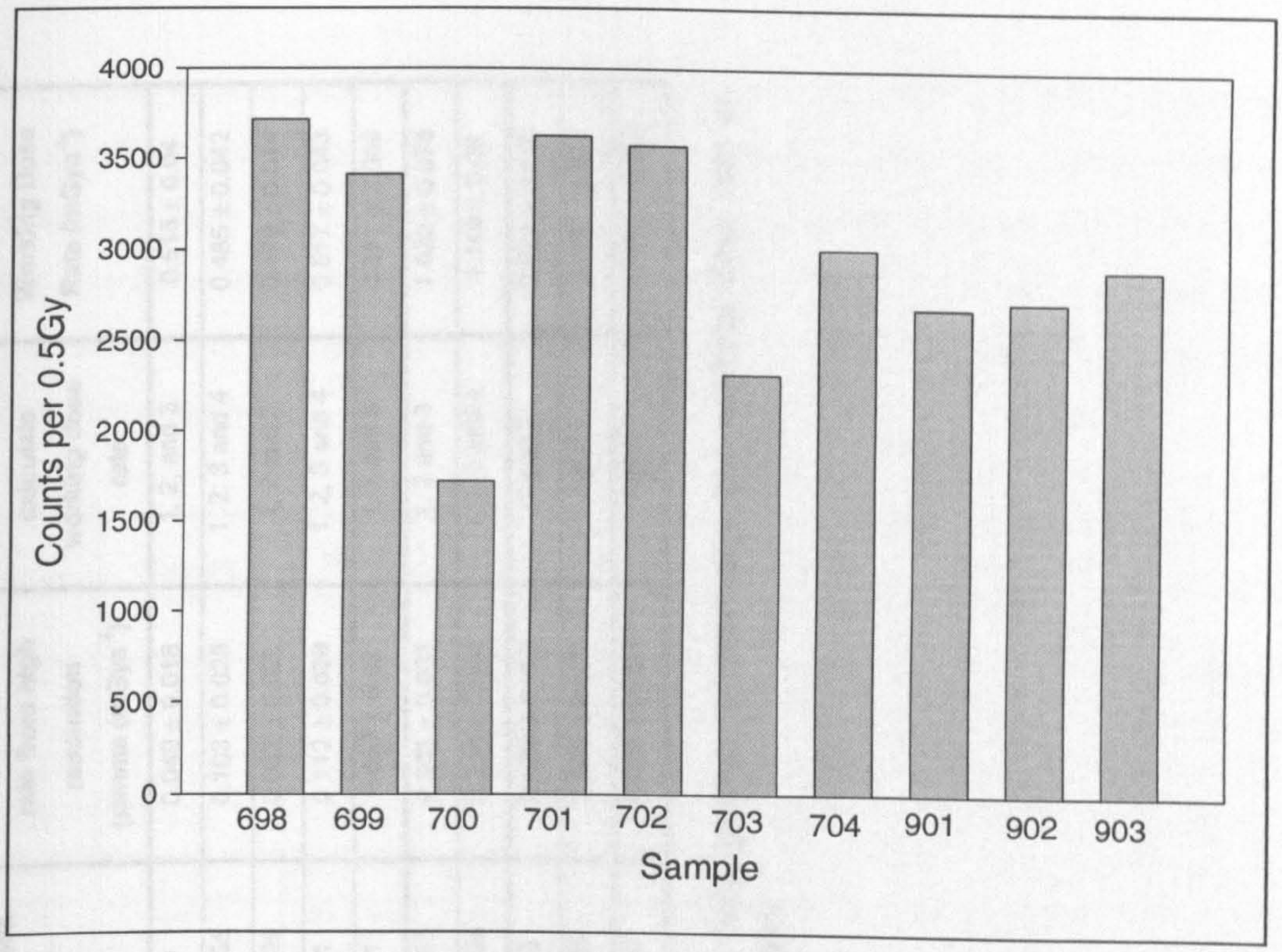

Figure 5.29 – Sensitivity of Quoygrew samples to a 0.5 Gy dose

Sample	Test Pit (unit)	(1) Beta dose rate from TSBC ($mGya^{-1}$)	(2) Beta dose rate from high resolution gamma ($mGya^{-1}$)	(3) Field gamma dose rate ($mGya^{-1}$)	(4) Gamma dose rate from high resolution gamma ($mGya^{-1}$)	Methods used to calculate working dose rate	Working Dose Rate ($mGya^{-1}$)
698	7 (11)	0.254 ± 0.049	0.246 ± 0.041	0.16 ± 0.0	0.049 ± 0.018	1, 2, and 3	0.515 ± 0.04
699	7 (7)	0.202 ± 0.061	0.285 ± 0.042	0.135 ± 0.005	0.103 ± 0.025	1, 2, 3 and 4	0.485 ± 0.042
700	7 (6)	0.296 ± 0.052	0.207 ± 0.039	0.115 ± 0.005	0.062 ± 0.021	1, 2 and 3	0.479 ± 0.044
701	7 (6)	0.279 ± 0.032	0.274 ± 0.049	0.15 ± 0.01	0.112 ± 0.028	1, 2, 3 and 4	0.517 ± 0.043
702	7 (3)	0.308 ± 0.075	0.259 ± 0.04	0.16 ± 0.01	0.067 ± 0.02	1, 2 and 3	0.551 ± 0.048
703	Area G	0.818 ± 0.071	0.713 ± 0.045	0.335 ± 0.005	0.206 ± 0.031	1, 2 and 3	1.022 ± 0.076
704	Area G	1.076 ± 0.069	0.882 ± 0.056	0.335 ± 0.005	0.318 ± 0.044	1, 2, 3 and 4	1.148 ± 0.09
902	102 (3)	0.643 ± 0.068	0.445 ± 0.044	0.31 ± 0.03	0.123 ± 0.033	1 and 3	0.921 ± 0.116
901	102 (5)	0.223 ± 0.087	0.13 ± 0.045	0.449 ± 0.05	0.036 ± 0.025	1 and 3	0.799 ± 0.087
903	101 (1)	0.419 ± 0.071	0.173 ± 0.047	0.625 ± 0.07	0.024 ± 0.024	1 and 3	1.1182 ± 0.099

Table 5.10 – TSBC, high resolution gamma spectrometry, *in situ* field gamma spectrometry and working dose rate of Quoygrew samples. Samples are in stratigraphic order within their pits.

5.3.2.2 OSL dates

The sample ages for each test pit are shown in Figures 5.30, 5.31 and 5.32 and summarised in Table 5.11 with the dose rate and weighted mean equivalent dose of each sample. All of the samples have high precision partly due to the well-behaved nature of the samples, but it may also indicate that the quartz grains within each sample were either all well-bleached prior to burial or that the grains were exposed to a similar amount of light and have the same bleaching history.

Sample	Test Pit (unit)	Water Content	Dose Rate ($mGya^{-1}$)	Weighted mean estimated dose (Gy)	Age (years before 2000 AD)	Date (BC/AD)
698	7 (11)	27 ± 17	0.515 ± 0.04	0.17 ± 0.01	330 ± 30	1670 ± 30 AD
699	7 (7)	18 ± 11	0.485 ± 0.042	0.23 ± 0.01	475 ± 45	1525 ± 45 AD
700	7 (6)	22 ± 18	0.479 ± 0.044	0.2 ± 0.02	420 ± 55	1580 ± 55 AD
701	7 (6)	20 ± 14	0.517 ± 0.043	0.26 ± 0.02	500 ± 55	1500 ± 55 AD
702	7 (3)	20 ± 14	0.551 ± 0.048	0.3 ± 0.04	545 ± 85	1455 ± 85 AD
703	Area G	31 ± 15	1.022 ± 0.076	0.51 ± 0.03	500 ± 45	1500 ± 45 AD
704	Area G	32 ± 14	1.148 ± 0.09	0.55 ± 0.04	480 ± 50	1520 ± 50 AD
902	102 (5)	30 ± 26	0.921 ± 0.116	0.09 ± 0.01	100 ± 15	1900 ± 15 AD
901	102 (3)	18 ± 14	0.8 ± 0.087	0.21 ± 0.03	260 ± 45	1740 ± 45 AD
903	101 (1)	19 ± 14	1.118 ± 0.1	0.31 ± 0.04	275 ± 45	1725 ± 45 AD

Table 5.11 – Water content, dose rate, equivalent dose and age of Quoygrew samples

Test Pit 7 had the thickest sand deposits on the site and all the samples were deposited rapidly during the late 15th–late 17th centuries AD. Apart from one sample (SUTL 699, Figure 5.30), the OSL dates are in chronostratigraphic order and the psi ratio analysis of SUTL 699 (Figure 4.36) suggests that this sample may be partially bleached and therefore the OSL age is overestimated.

The samples from Area G (SUTL 703 and 704) were deposited at the beginning of the 16th century AD (Figure 5.31) and these correlate well with sample SUTL 701 in Test Pit 7, which may indicate that there was sand deposition over a large part of the site during this time.

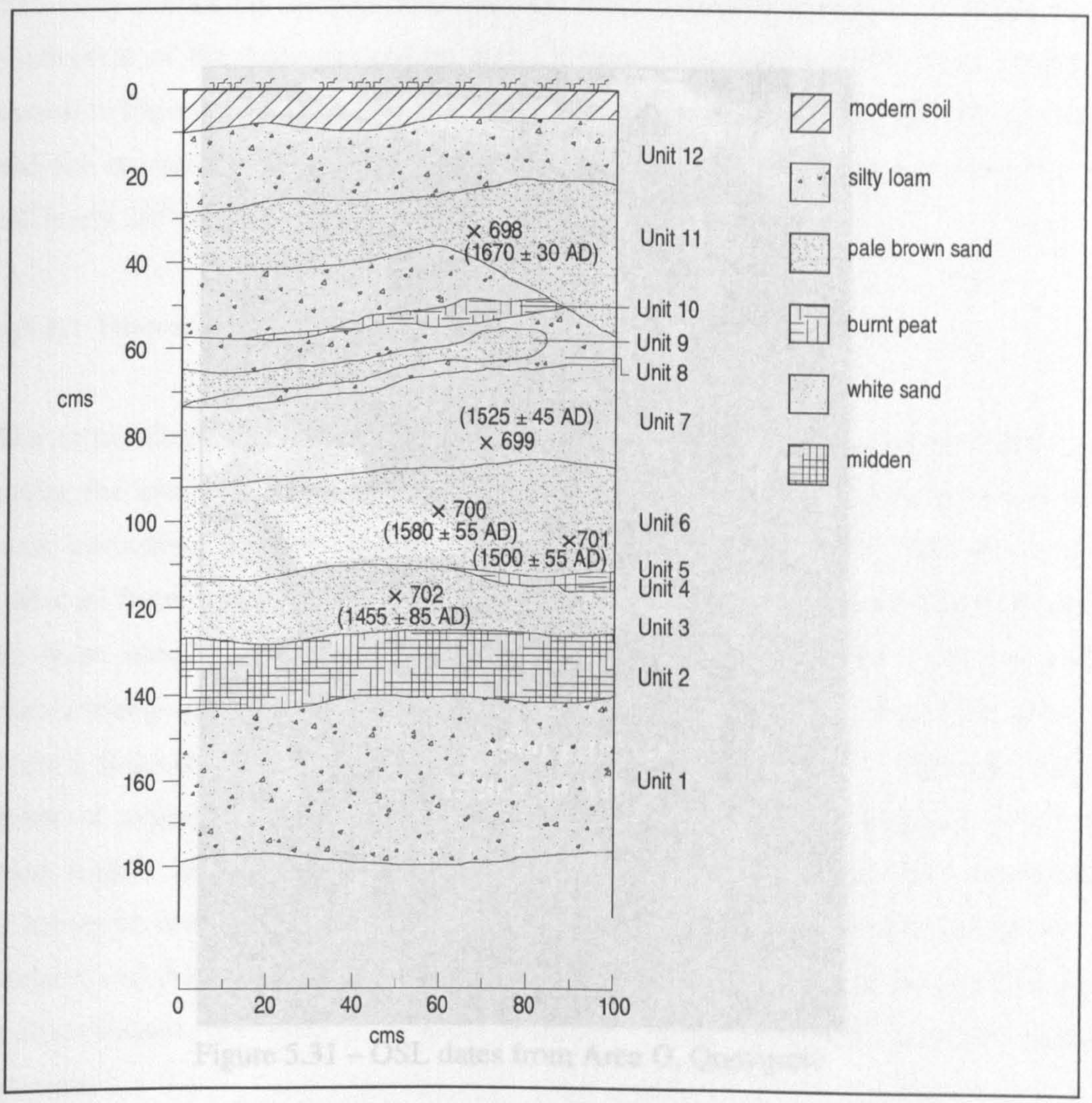

Figure 5.30 – OSL dates from Test Pit 7, Quoygrew

Figure 5.31 – OSL dates from Area G, Quoygrew

The three remaining samples from the site were collected from Test Pits 101 and 102 south-west of the main excavation area (Figure 3.12) and the OSL dates obtained are shown in Figure 5.32. Samples SUTL 901 and 903 both date to the mid 18th century AD and the remaining sample, SUTL 902, was deposited almost 100 years later in the late 19th/early 20th century AD.

5.3.2.3 Discussion

The archaeological evidence from Quoygrew indicates that the site was occupied at least during the late Viking/early Medieval period and possibly earlier. Only one pit within the main excavation was sampled for OSL dating; two samples (SUTL 703 and 704) were collected from the shell midden of Area G (Figure 3.12). A weighted mean (Table 5.12) on these samples shows that the sand was deposited about 1510 ± 30 AD and this chronostratigraphically links with a radiocarbon date of cal AD 1005-1260 (AA-3135) from a fragment of horse pelvis below the OSL sampling layer. The OSL dates do, however, suggest that the site was still occupied, or at least the midden was still being used, slightly later than previously proposed by Barrett *et al.* (2000a). These samples may however be contaminated by the infiltration of younger quartz grains through the shell midden and therefore the 15th/16th century AD dates for these samples could be slightly underestimated, but there is no clear indication of this from the D_e of the individual aliquots.

Sample	Test Pit	OSL age (yrs before 2000 AD)	Weighted mean (yrs before 2000 AD)	Weighted mean (yrs before 2000 AD)	Date (BC/AD)
703	Area G	500 ± 45	490 ± 30		
704	Area G	480 ± 50			
699	7 (Unit 7)	475 ± 45		480 ± 20	1520 ± 20 AD
700	7 (Unit 6)	420 ± 55	475 ± 30		
701	7 (Unit 6)	500 ± 55			
702	7 (Unit 3)	545 ± 85			
903	102 (Unit 3)	275 ± 45			
901	101 (Unit 1)	260 ± 45	390 ± 25		1610 ± 25 AD
698	7 (Unit 11)	330 ± 30			

Table 5.12 – Weighted mean age of samples from Area G and Test Pit 7, also from Test Pit 101, 102 and the upper sand layer of Test Pit 7.

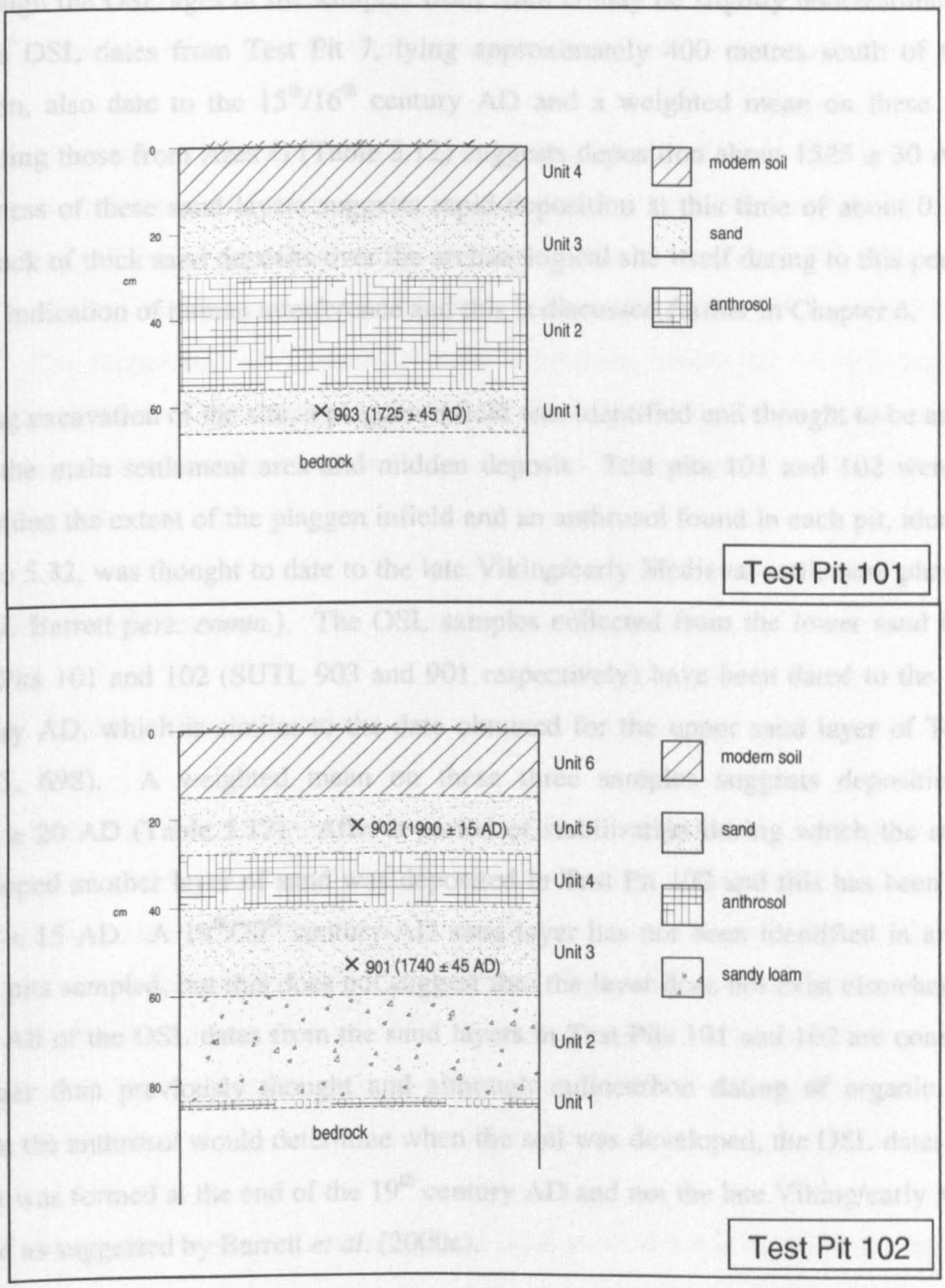

Figure 5.32 – OSL dates from Test Pits 101 and 102, Quoygrew. The OSL dates from the lower sand layers are within error of each other and are thought to have been deposited during the same storm event.

Although the OSL ages of the samples from Area G may be slightly underestimated, four of the OSL dates from Test Pit 7, lying approximately 400 metres south of the shell midden, also date to the 15th/16th century AD and a weighted mean on these samples, including those from Area G (Table 5.12) suggests deposition about 1525 ± 30 AD. The thickness of these sand layers suggests rapid deposition at this time of about 0.16cm/yr. The lack of thick sand deposits over the archaeological site itself dating to this period may be an indication of human interference and this is discussed further in Chapter 6.

During excavation of the site, a plaggen infield was identified and thought to be associated with the main settlement area and midden deposit. Test pits 101 and 102 were dug to determine the extent of the plaggen infield and an anthrosol found in each pit, identified in Figure 5.32, was thought to date to the late Viking/early Medieval settlement phase of the site (J. Barrett *pers. comm.*). The OSL samples collected from the lower sand layers of Test Pits 101 and 102 (SUTL 903 and 901 respectively) have been dated to the mid 18th century AD, which is similar to the date obtained for the upper sand layer of Test Pit 7 (SUTL 698). A weighted mean on these three samples suggests deposition about 1700 ± 20 AD (Table 5.12). After a period of stabilisation during which the anthrosol, developed another layer of sand was deposited in Test Pit 102 and this has been dated to 1900 ± 15 AD. A 19th/20th century AD sand layer has not been identified in any of the other pits sampled, but this does not suggest that the layer does not exist elsewhere on the site. All of the OSL dates from the sand layers in Test Pits 101 and 102 are considerably younger than previously thought and although radiocarbon dating of organic material within the anthrosol would determine when the soil was developed, the OSL dates indicate that it was formed at the end of the 19th century AD and not the late Viking/early Medieval period as suggested by Barrett *et al.* (2000a).

Test pits 101 and 102 are relatively close together, adjacent to the shoreline and in these circumstances it may be expected that the ages of the sand layers should be similar. As mentioned above, the upper sand layer of Test Pit 7 also has a similar age and it is approximately 150 metres inland from the other test pits. It is tempting to suggest that these sand layers in the 3 test pits were deposited during a single storm event about 1700 ± 20 AD. Quoygrew is located on the west coast of Westray and is therefore exposed to strong westerly winds generated in the North Atlantic. Historical records from Westray indicate that significant areas of land have been inundated by sand, especially areas west of

the Links of Noltland (Fereday 1990) and therefore it is reasonable to infer that the 17/18th century AD sand layers at Quoygrew were deposited during a single event.

The weighted mean OSL dates from Quoygrew have been plotted in Figure 5.33 and they indicate that all but one sand layer were deposited during the Little Ice Age. Three periods of sand movement are identified within the site on the basis of the OSL dates and these occurred during the 16th century AD, 17/18th centuries AD and the 19th century AD (Figure 5.33). The recognition of 3 phases of sand movement within the last 600 years, using optically stimulated luminescence dating, confirms that the technique can date young events and this will be discussed further with regard to the other sites sampled in Section 6.2, Chapter 6.

5.3.4 Pierowall, Westray

5.3.4.1 Trends within the samples

The samples from Pierowall were collected close to the ruined church of Lady Kirk from a test pit which contained a flagstone at the base overlain by three sand layers, the lower one of which was separated from the upper two layers by a palaeosol (Figure 3.16). Three samples were collected from the pit and all are composed of medium grained sand with a calcium carbonate content of about 65%. The water content increases with depth in the pit from about 6.5% in the upper sand layer to approximately 11.5% in the lower sand layer above the flagstone.

All of the samples respond well to artificial irradiation and this is reinforced by the well behaved regenerative dose response curves of each sample (e.g. Figure 5.34). Although the test dose responses for each disc do increase throughout the SAR run (Figure 5.35) indicating an increase in sensitivity, none of the discs were rejected due to recycling problems and therefore the test dose normalisation successfully corrects the sensitivity changes.

The samples from Pierowall all have relatively high dose rates (Table 5.13) and this reflects the higher dosimetry of the flagstone and palaeosol within the test pit. As a result the *in situ* field gamma dose rates are much higher than the gamma dose rates from the high resolution gamma spectrometry (Table 5.13) and therefore only the *in situ* field

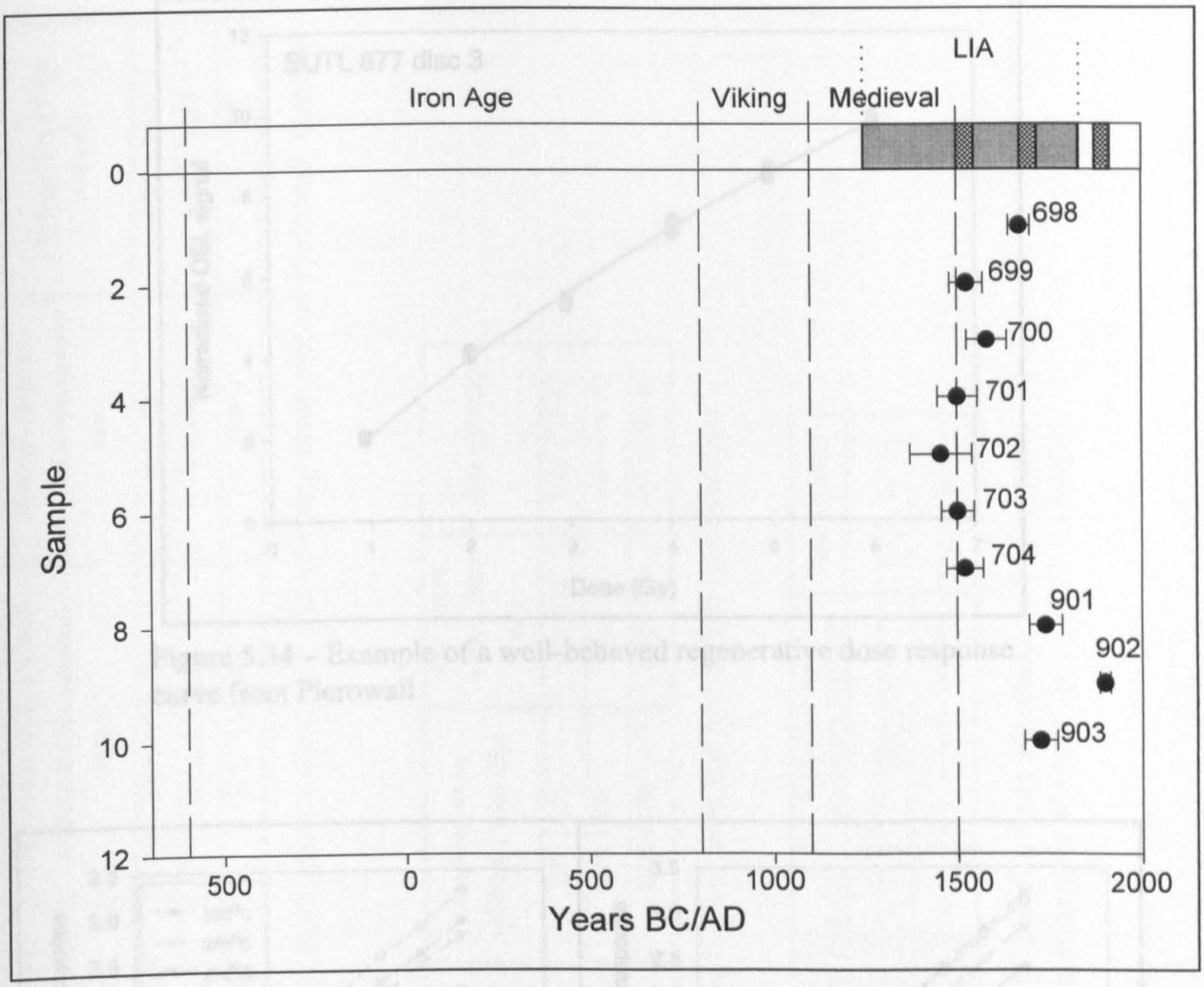

Figure 5.33 – OSL dates from Quoygrew and the identification of three periods of increased sand movement (shaded areas), two of which occurred during the Little Ice Age (LIA).

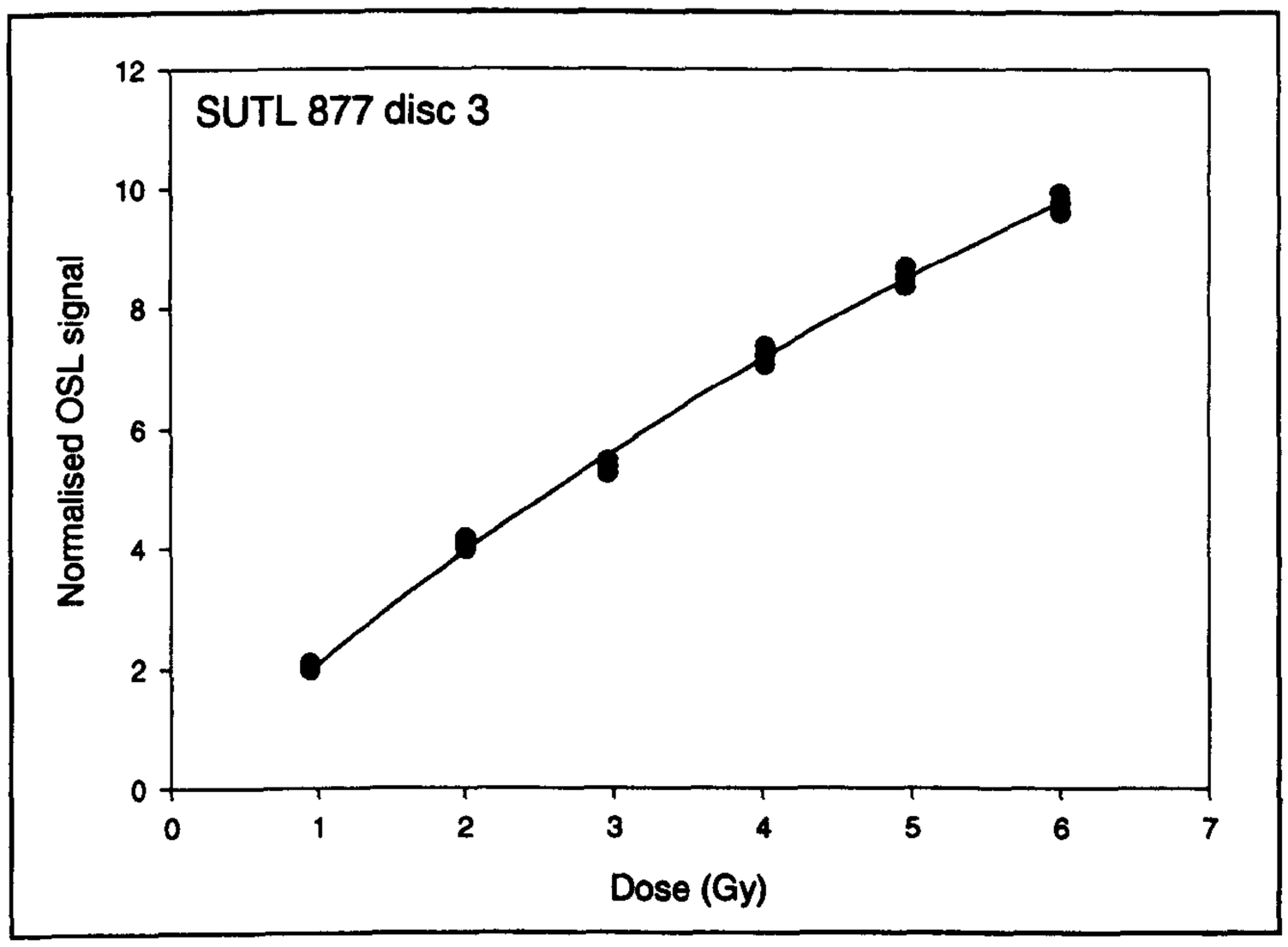

Figure 5.34 – Example of a well-behaved regenerative dose response curve from Pierowall

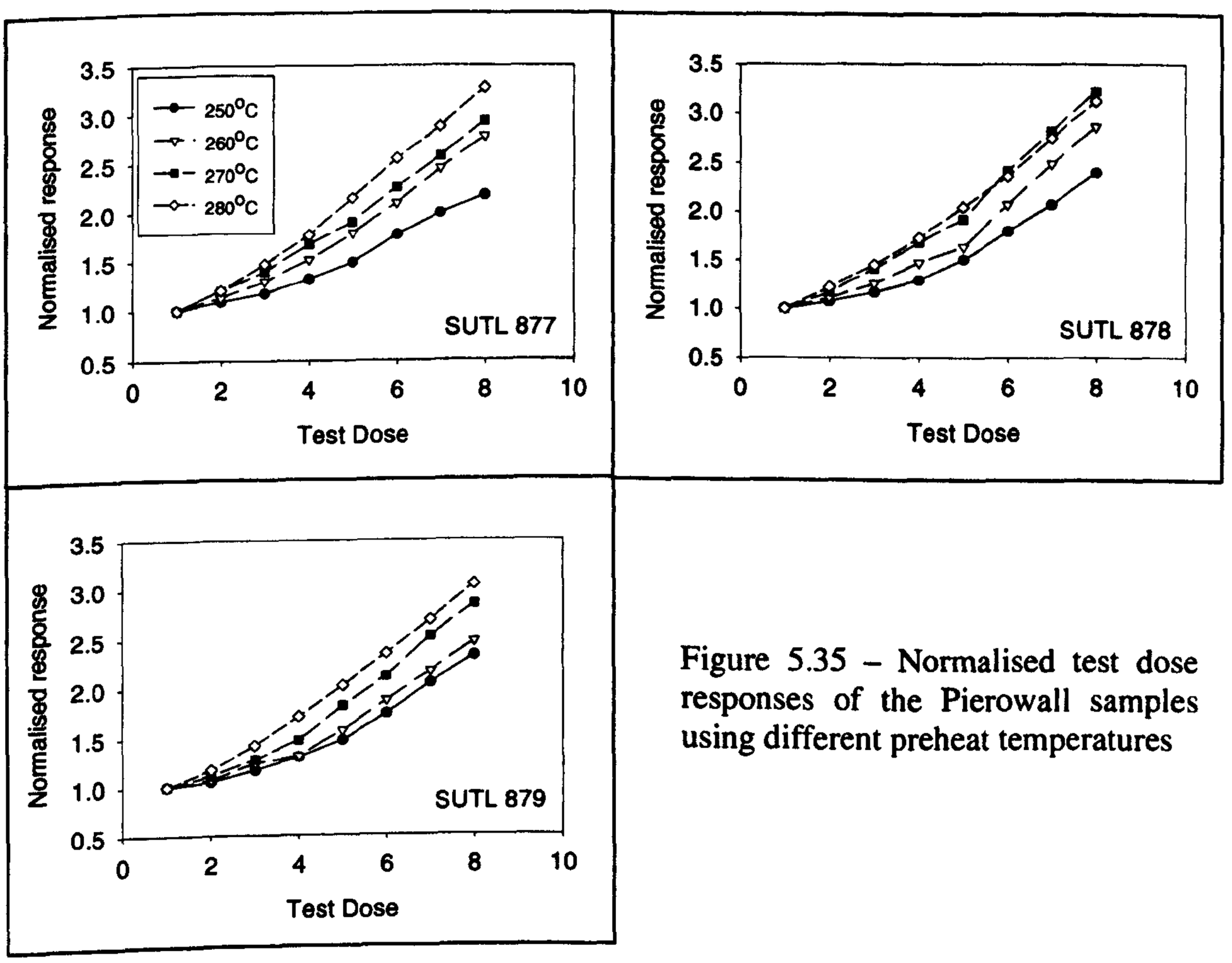

Figure 5.35 – Normalised test dose responses of the Pierowall samples using different preheat temperatures

Sample	Unit	(1) Beta dose rate from TSBC ($mGya^{-1}$)	(2) Beta dose rate from high resolution gamma ($mGya^{-1}$)	(3) Field gamma dose rate ($mGya^{-1}$)	(4) Gamma dose rate from high resolution gamma ($mGya^{-1}$)	Methods used to calculate working dose rate	Working Dose Rate ($mGya^{-1}$)
877	4	0.291 ± 0.055	0.245 ± 0.042	0.233 ± 0.024	0.073 ± 0.023	1, 2 and 3	0.621 ± 0.046
878	3	0.37 ± 0.06	0.417 ± 0.042	0.283 ± 0.03	0.138 ± 0.027	1, 2 and 3	0.749 ± 0.059
879	1	0.491 ± 0.085	0.462 ± 0.034	0.58 ± 0.062	0.167 ± 0.016	1, 2 and 3	1.089 ± 0.087

Table 5.13 – TSBC, high resolution gamma spectrometry, *in situ* field gamma dose rate and working dose rate of Pierowall samples. Samples are in stratigraphic order.

Sample	Unit	Water Content	Dose Rate ($mGya^{-1}$)	Weighted mean estimated dose (Gy)	Age (years before 2000 AD)	Date (BC/AD)
877	4	16 ± 10	0.621 ± 0.046	0.17 ± 0.01	275 ± 25	1725 ± 25 AD
878	3	22 ± 14	0.749 ± 0.059	0.46 ± 0.01	615 ± 50	1385 ± 50 AD
879	1	27 ± 16	1.089 ± 0.087	2.55 ± 0.08	2340 ± 200	340 ± 200 BC

Table 5.14 – Water content, dose rate, equivalent dose and age of Pierowall samples

Sample	Site	OSL age (yrs before 2000 AD)	Weighted mean (yrs before 2000 AD)	Date (BC/AD)
877	Pierowall	275 ± 25		
901	Quoygrew (TP102)	260 ± 45	290 ± 15	1710 ± 15 AD
903	Quoygrew (TP101)	275 ± 45		
678	Quoygrew (TP&7)	330 ± 30		

Table 5.15 – Weighted mean age of samples from Pierowall and Quoygrew suggesting sand deposition over a large area in Westray about 1710 ± 15 AD.

gamma dose rates have been used in conjunction with the TSBC and beta contribution from the high resolution spectrometry to determine the working dose rates of these samples.

5.3.4.2 OSL dates

The OSL dates for the test pit at Pierowall are shown in Figure 5.36 and summarised in Table 5.14 with the dose rate and weighted mean equivalent dose of each sample. The lower sand (SUTL 879) was deposited approximately 2300 years ago during the early Iron Age and a palaeosol separates this sand layer from the upper sand layers that were deposited and buried in the mid-late 14th century AD (SUTL 878) and the early 18th century AD (SUTL 877) as shown in Figure 5.36.

5.3.4.3 Discussion

The OSL ages from the test pit at Pierowall are in chronostratigraphic order and three periods of sand movement have been recorded in the pit as shown in Figure 5.37. Although the earliest sand movement recorded at the site occurred during the early Iron Age (SUTL 879), there may be another unidentified sand layer (or layers) below the flagstone which was not removed during sampling. There are no archaeological controls within the pit itself, but the age of the sand does correlate with a multi-period archaeological site that was excavated in Pierowall and which contained early Iron Age structures that were constructed on a layer of sand (Sharples *et al.* 1984). It is suggested that this sand layer and the sand layer in the test pit at Pierowall were deposited at a similar time.

The lower sand layer is sealed by a palaeosol and two sand layers deposited during the 14th century AD (SUTL 878) and the 18th century AD (SUTL 877) overlie the palaeosol. Despite the palaeosol separating the prehistoric and historic sand layers there is a gap of about 1200 years between the layers (a similar scenario to that recorded at the Bay of Lopness in Section 5.3.2.3). At both sites there is no record of sand deposition during the Viking/Medieval periods and as with the Bay of Lopness it is suggested that any sand that was deposited during the Viking/Medieval periods was eroded prior to deposition of the 14th century AD sand layer. The 14th century AD sample was collected from the top of the

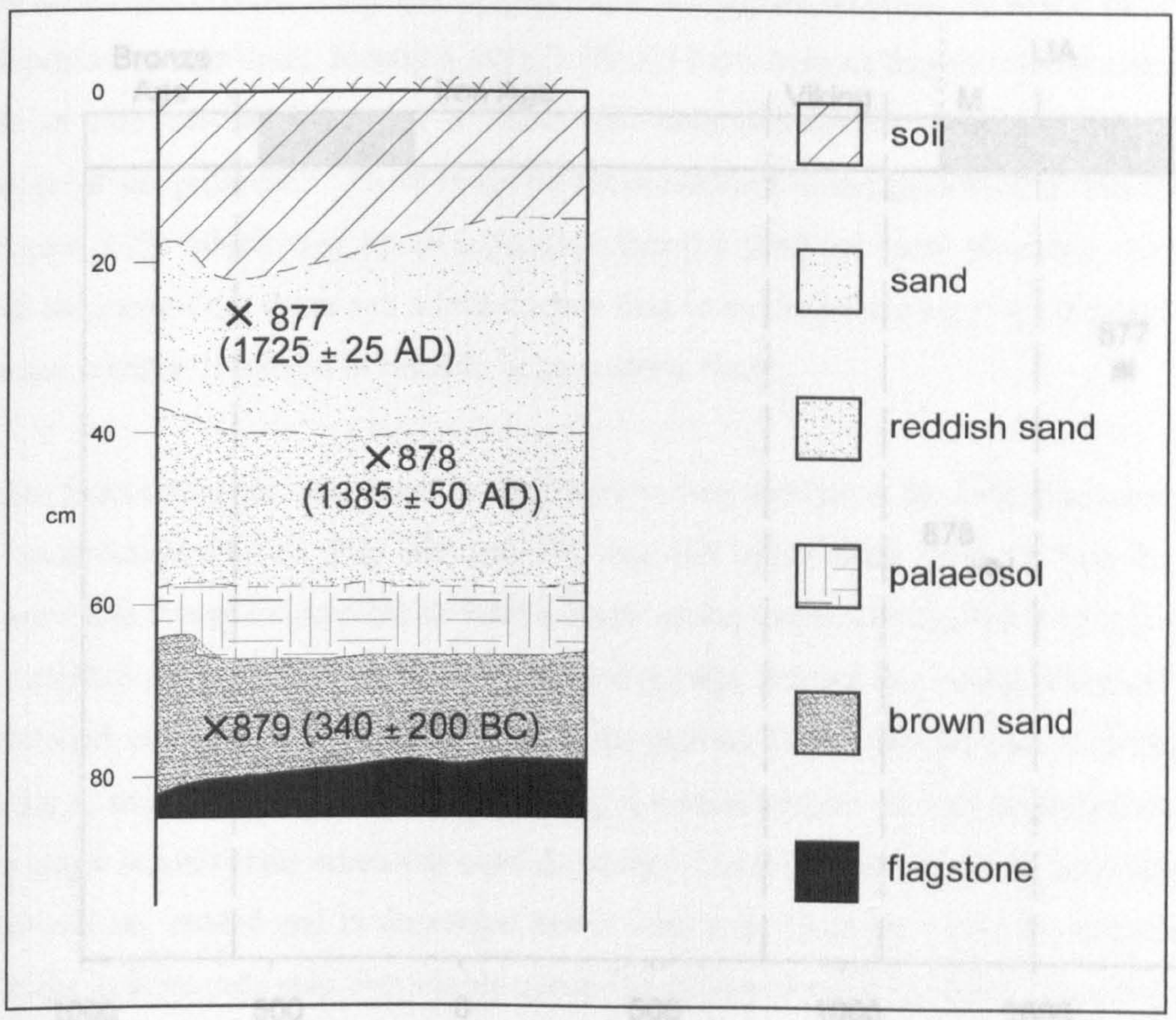

Figure 5.36 – OSL dates from the test pit at Pierowall

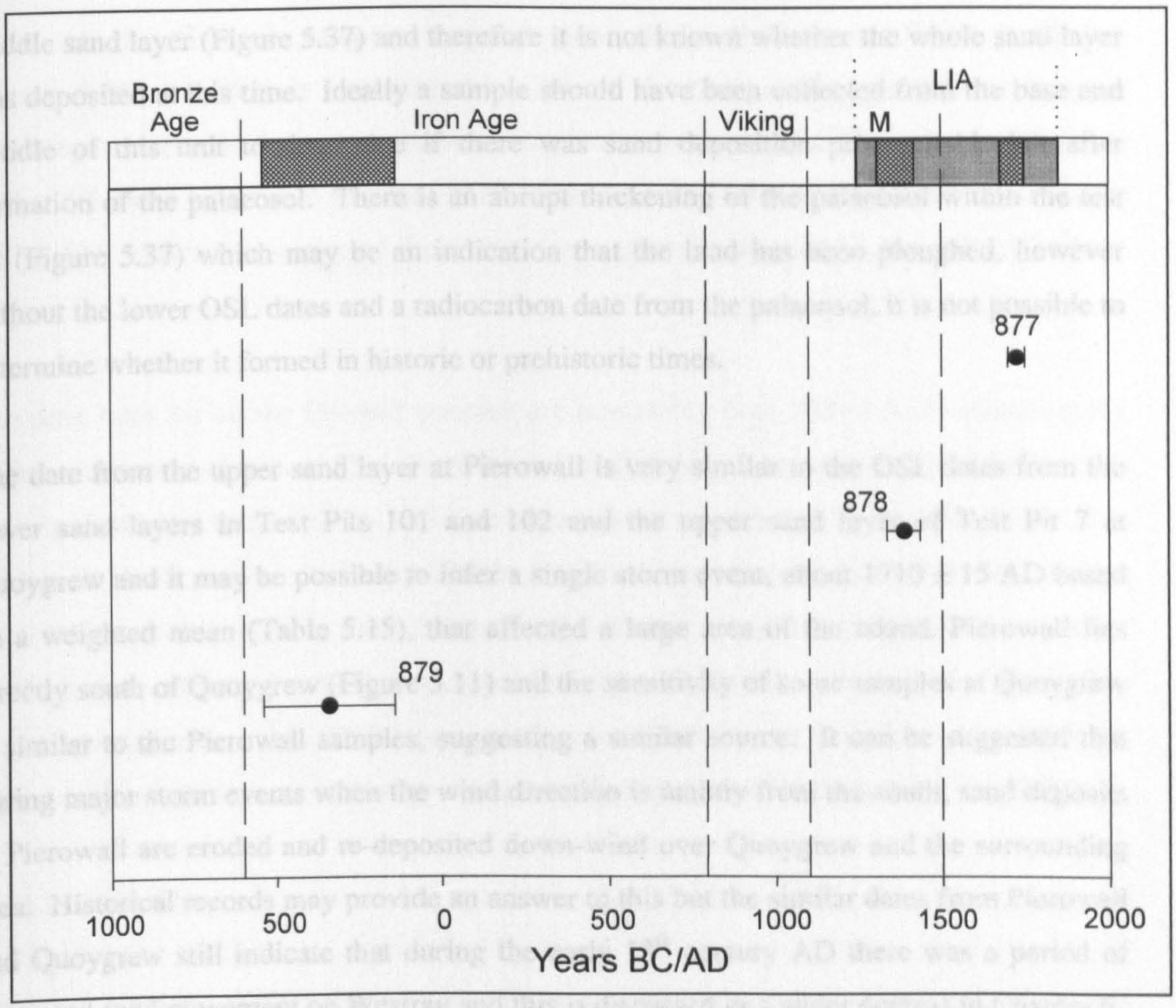

Figure 5.37 – OSL dates from Pierowall and the identification of three periods of sand movement (shaded areas). M = Medieval LIA = Little Ice Age

middle sand layer (Figure 5.37) and therefore it is not known whether the whole sand layer was deposited at this time. Ideally a sample should have been collected from the base and middle of this unit to determine if there was sand deposition prior to this but after formation of the palaeosol. There is an abrupt thickening of the palaeosol within the test pit (Figure 5.37) which may be an indication that the land has been ploughed, however without the lower OSL dates and a radiocarbon date from the palaeosol, it is not possible to determine whether it formed in historic or prehistoric times.

The date from the upper sand layer at Pierowall is very similar to the OSL dates from the lower sand layers in Test Pits 101 and 102 and the upper sand layer of Test Pit 7 at Quoygrew and it may be possible to infer a single storm event, about 1710 ± 15 AD based on a weighted mean (Table 5.15), that affected a large area of the island. Pierowall lies directly south of Quoygrew (Figure 3.11) and the sensitivity of some samples at Quoygrew is similar to the Pierowall samples, suggesting a similar source. It can be suggested that during major storm events when the wind direction is mainly from the south, sand deposits at Pierowall are eroded and re-deposited down-wind over Quoygrew and the surrounding area. Historical records may provide an answer to this but the similar dates from Pierowall and Quoygrew still indicate that during the early 18th century AD there was a period of increased sand movement on Westray and this is discussed in a wider context in Chapter 6.

5.3.5 Evertaft, Westray

5.3.5.1 Trends within the samples

Five OSL samples were collected from a currently eroding vertical cliff section at Evertaft which contains sand layers interspersed with midden deposits and a rubble horizon which protrudes from the cliff face near the top of the section (Figure 3.17). The samples are composed of medium grained sand with between 37%-60% shell material. The water content increases with depth in the section, however the midden layers may have some influence on the water content by slowing the movement of water through the section. This may be a contributing factor to the slightly higher water content of sample SUTL 917 (21%±15%) which was collected from below SUTL 916 (18%±13%) in the same sand layer (Figure 3.17).

None of the Evertaft samples respond particularly well to artificial irradiation (Figure 5.38), resulting in approximately 25% of the discs being rejected due to poor recycling or scattered data which prevents regression analysis of the regenerative data. A further 6% had a significant response to IR stimulation and 80% of these were from sample SUTL 915 which was collected from the upper sand layer close to the rubble horizon (Figure 3.17).

The dose rates for all the Evertaft samples are reasonably high (Table 5.16) reflecting the higher dosimetry of the midden deposits and walled structure. As a result the internal gamma dosimetry measured by high resolution gamma spectrometry is much lower than the *in situ* field gamma dosimetry (Table 5.16) and therefore to ensure that the gamma contribution to the working dose rate is similar to that actually received by the samples during burial, only the *in situ* field gamma dose rates were used. For the beta contribution to the working dose rates, TSBC was mainly used because the beta dose rates from the high resolution gamma spectrometry were outwith the lower error margins of the TSBC.

5.3.5.2 OSL dates

The OSL ages for the 5 samples collected from Evertaft are shown in Figure 5.39 and summarised in Table 5.17 and the dates provide *terminus post quem* and *terminus ante quem* for deposition of the midden deposits. Although the OSL dates are not strictly in chronostratigraphic order they do identify two periods of increased sand movement. The upper and middle sand layers were both deposited during the Viking Age (Figure 5.39, Table 5.17) and this is surprising given that the sand layers within this section are relatively thick and it was initially thought the site may have been temporarily abandoned on several occasions due to sand inundation. A weighted mean on these samples suggests that they were deposited about 940 ± 110 AD (Table 5.18).

Sample	Location within section	OSL age (yrs before 2000 AD)	Weighted mean (yrs before 2000 AD)	Date (BC/AD)
915	Upper sand	1080 ± 165		
916	Middle sand	1195 ± 210	1060 ± 110	940 ± 110 AD
917	Middle sand	910 ± 200		
918	Lower sand	1875 ± 195	1760 ± 165	240 ± 165 AD
919	Lowest sand	1450 ± 325		

Table 5.18 – Weighted mean ages of upper/middle sands and lower sands identifying two periods of increased sand movement.

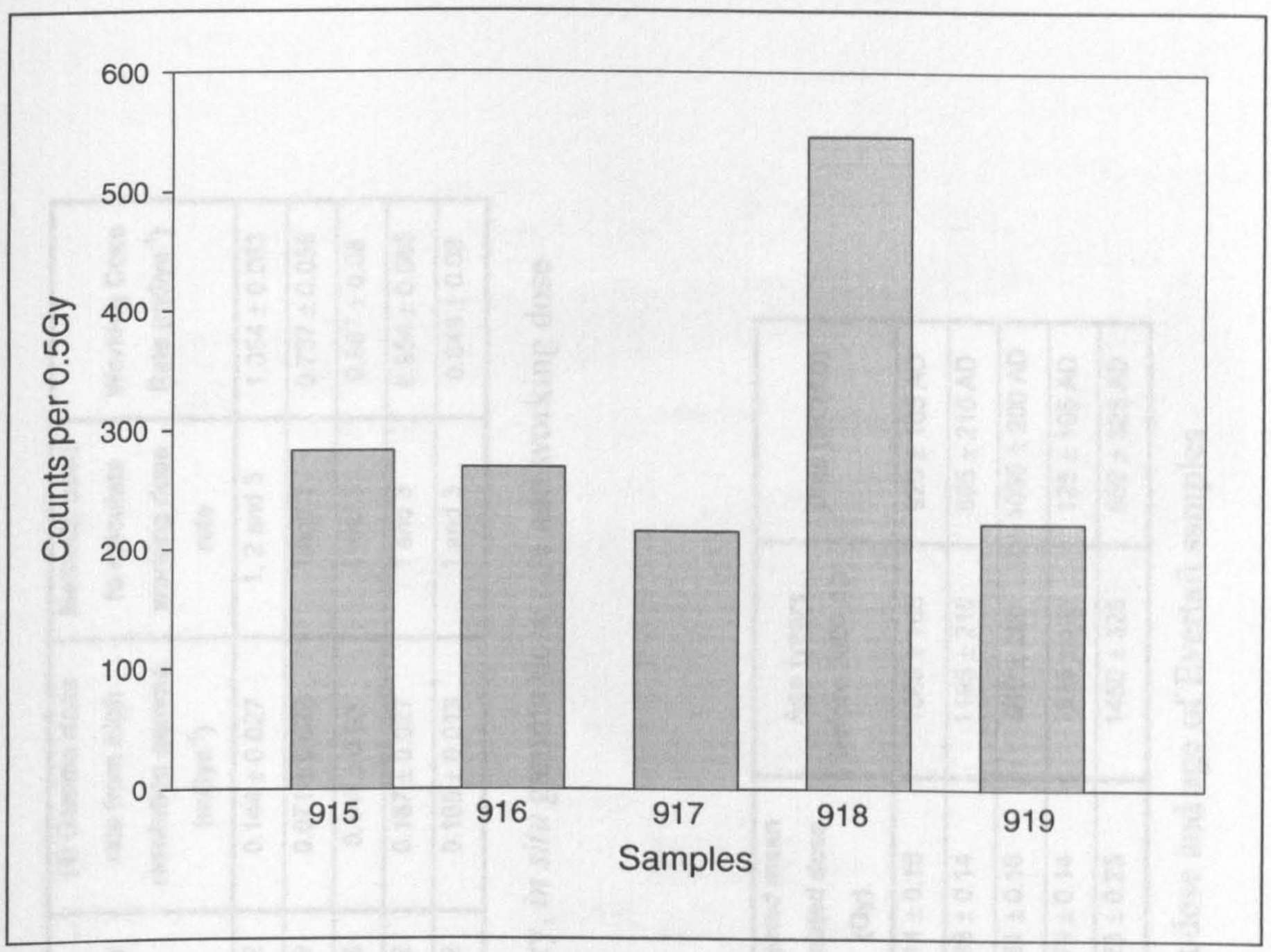

Figure 5.38 – Sensitivity of Evertaft samples to a 0.5 Gy dose

Sample	Unit	(1) Beta dose rate from TSBC ($mGya^{-1}$)	(2) Beta dose rate from high resolution gamma ($mGya^{-1}$)	(3) Field gamma dose rate ($mGya^{-1}$)	(4) Gamma dose rate from high resolution gamma ($mGya^{-1}$)	Methods used to calculate working dose rate	Working Dose Rate ($mGya^{-1}$)
915	7	0.514 ± 0.057	0.433 ± 0.041	0.528 ± 0.002	0.144 ± 0.027	1, 2 and 3	1.054 ± 0.063
916	5	0.453 ± 0.034	0.307 ± 0.043	0.215 ± 0.019	0.071 ± 0.025	1 and 3	0.737 ± 0.058
917	5	0.623 ± 0.039	0.476 ± 0.044	0.253 ± 0.028	0.148 ± 0.03	1 and 3	0.887 ± 0.08
918	3	0.622 ± 0.048	0.524 ± 0.043	0.316 ± 0.012	0.187 ± 0.027	1 and 3	0.954 ± 0.065
919	1	0.583 ± 0.077	0.411 ± 0.029	0.248 ± 0.012	0.165 ± 0.013	1 and 3	0.849 ± 0.08

Table 5.16 – TSBC, high resolution gamma spectrometry, *in situ* gamma dose rate and working dose rates of Evertaft samples

Sample	Unit	Water Content	Dose Rate ($mGya^{-1}$)	Weighted mean estimated dose (Gy)	Age (years before 2000 AD)	Date (BC/AD)
915	7	21 ± 16	1.054 ± 0.063	1.14 ± 0.16	1080 ± 165	920 ± 165 AD
916	5	18 ± 13	0.737 ± 0.058	0.88 ± 0.14	1195 ± 210	805 ± 210 AD
917	5	21 ± 15	0.887 ± 0.08	0.81 ± 0.16	910 ± 200	1090 ± 200 AD
918	3	20 ± 11	0.954 ± 0.065	1.79 ± 0.14	1875 ± 195	125 ± 195 AD
919	1	22 ± 13	0.849 ± 0.08	1.23 ± 0.25	1450 ± 325	550 ± 325 AD

Table 5.17 – Water content, dose rate, equivalent dose and age of Evertaft samples

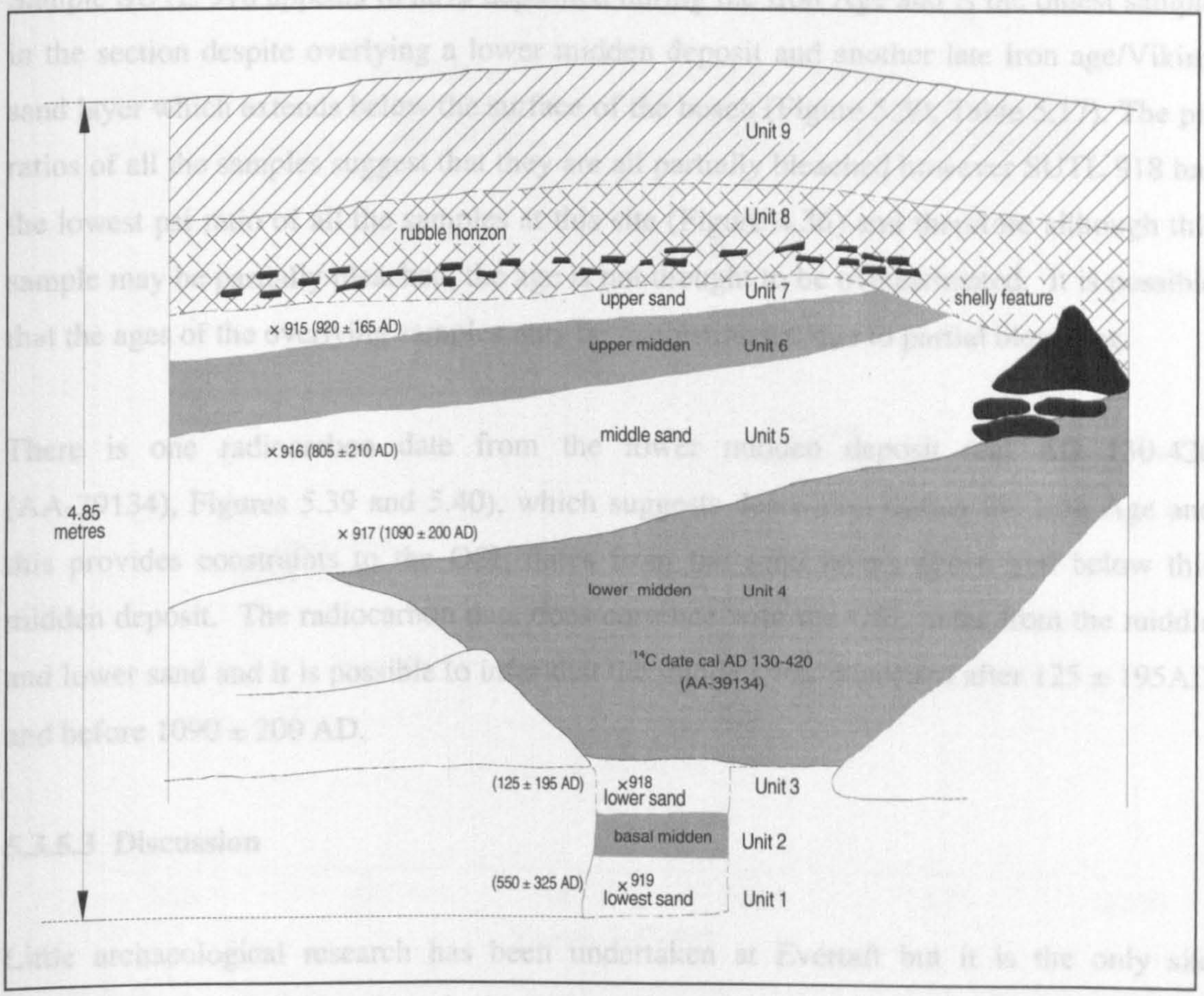

Figure 5.39 – OSL dates and radiocarbon dates from the exposed section at Evertaft. The OSL dates from the middle and upper sand date to the Viking period and those in the lower sand layers to the late Iron Age.

Sample SUTL 918 appears to have deposited during the Iron Age and is the oldest sample in the section despite overlying a lower midden deposit and another late Iron age/Viking sand layer which extends below the surface of the beach (Figure 5.39, Table 5.17). The psi ratios of all the samples suggest that they are all partially bleached however SUTL 918 has the lowest psi ratio of all the samples at this site (Figure 4.36) and therefore although this sample may be partially bleached, the age is not thought to be overestimated. It is possible that the ages of the overlying samples may be overestimated due to partial bleaching.

There is one radiocarbon date from the lower midden deposit (cal AD 130-420 (AA-39134), Figures 5.39 and 5.40), which suggests deposition during the Iron Age and this provides constraints to the OSL dates from the sand layers above and below this midden deposit. The radiocarbon date does correlate with the OSL dates from the middle and lower sand and it is possible to infer that the midden was deposited after 125 ± 195AD and before 1090 ± 200 AD.

5.3.5.3 Discussion

Little archaeological research has been undertaken at Evertaft but it is the only site sampled that has 4 midden deposits in one stratigraphic section interleaved with thick sand deposits. Initially it was thought that the sand layers were thick enough to suggest that the site may have been periodically abandoned after sand deposition, however the OSL dates from the sand layers indicate that all of the sand was deposited during the late Iron Age and Viking periods (Figure 5.40). None of the samples respond particularly well to artificial irradiation and therefore the precision on the OSL dates is quite low. As a result any evidence of abandonment is lost. Barrett *et al.* (2000a) did suggest that the upper midden may have been intentionally redeposited from lower midden elsewhere on the site to stabilise the sand and the OSL dates do support this hypothesis (Figure 5.39). Additional radiocarbon dating of the midden deposits would provide further constraints to the occupation period or periods at this site.

As mentioned above, the sensitivity of the Evertaft samples is quite low and this is even more apparent when their sensitivity is compared to the samples from Quoygrew and Pierowall (Figure 5.41). This suggests that the sand at Evertaft has a different provenance and this is surprising given that the three sites are all located relatively close together at the north end of Westray (Figure 3.11). Although the sensitivity of the modern beach sands

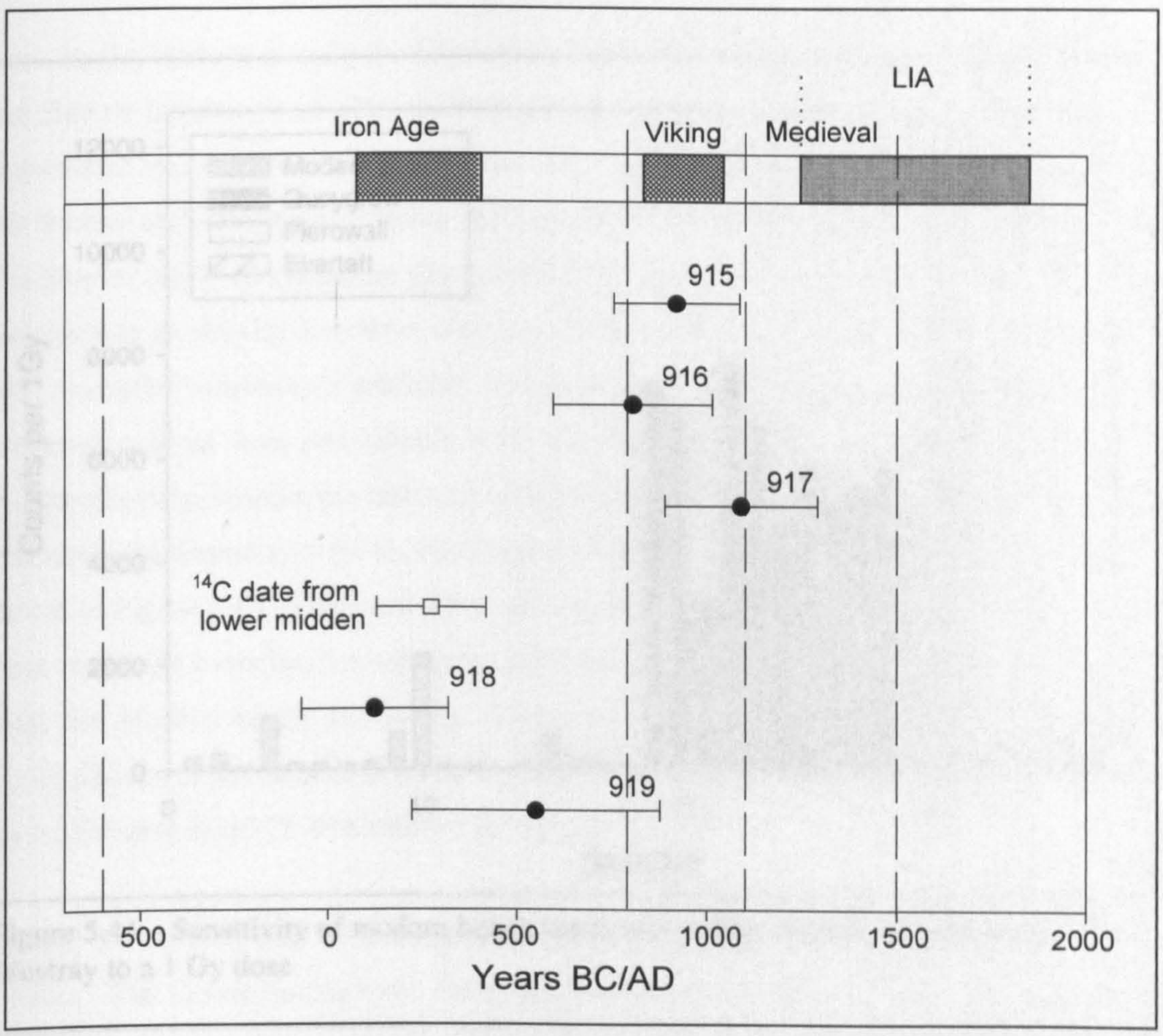

Figure 5.40 – OSL dates from Evertaft and the radiocarbon date from the lower midden from Evertaft. Two periods of increased sand blow have been identified at this site. LIA = Little Ice Age

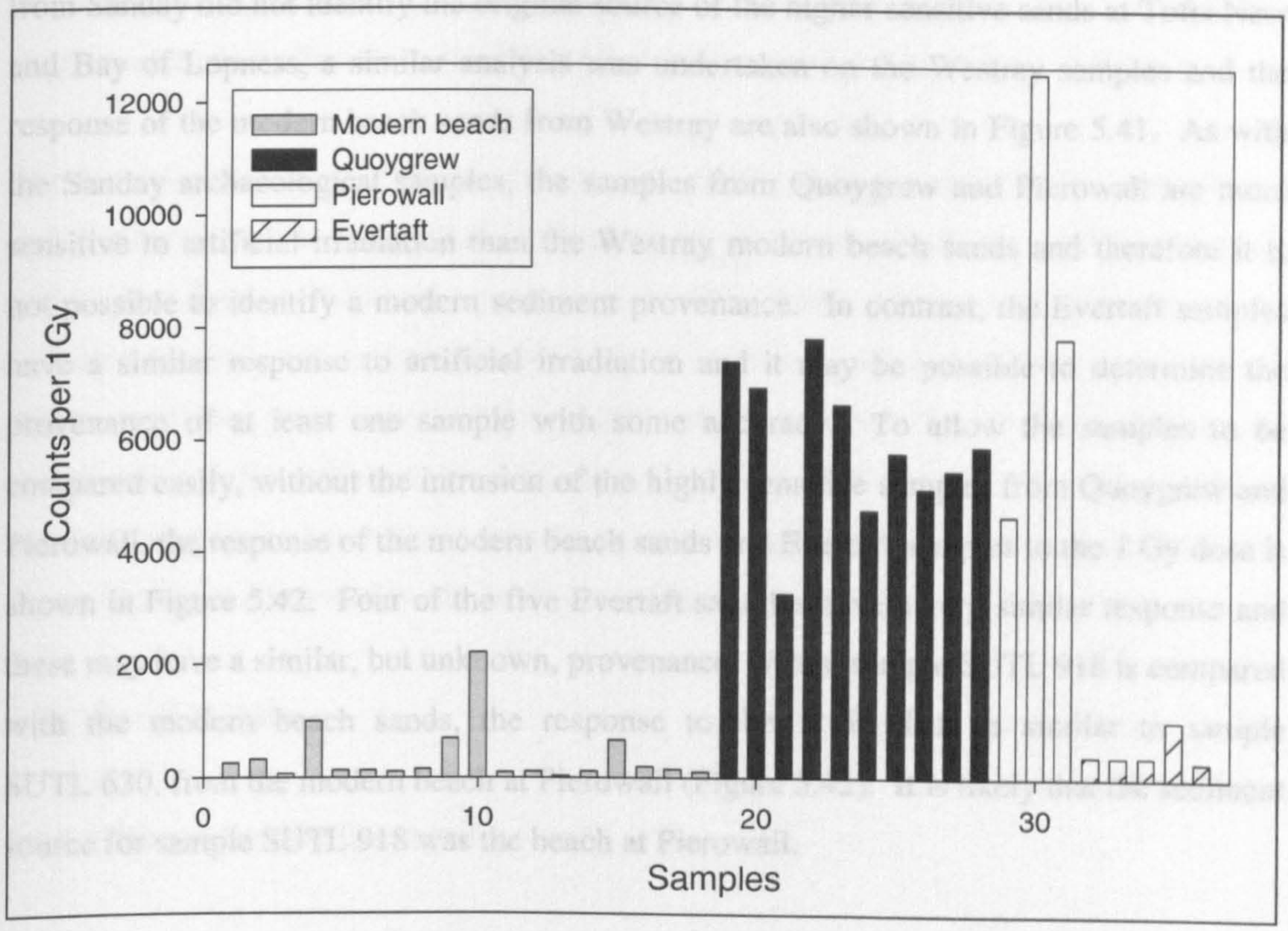

Figure 5.41 – Sensitivity of modern beach sands and archaeological samples from Westray to a 1 Gy dose

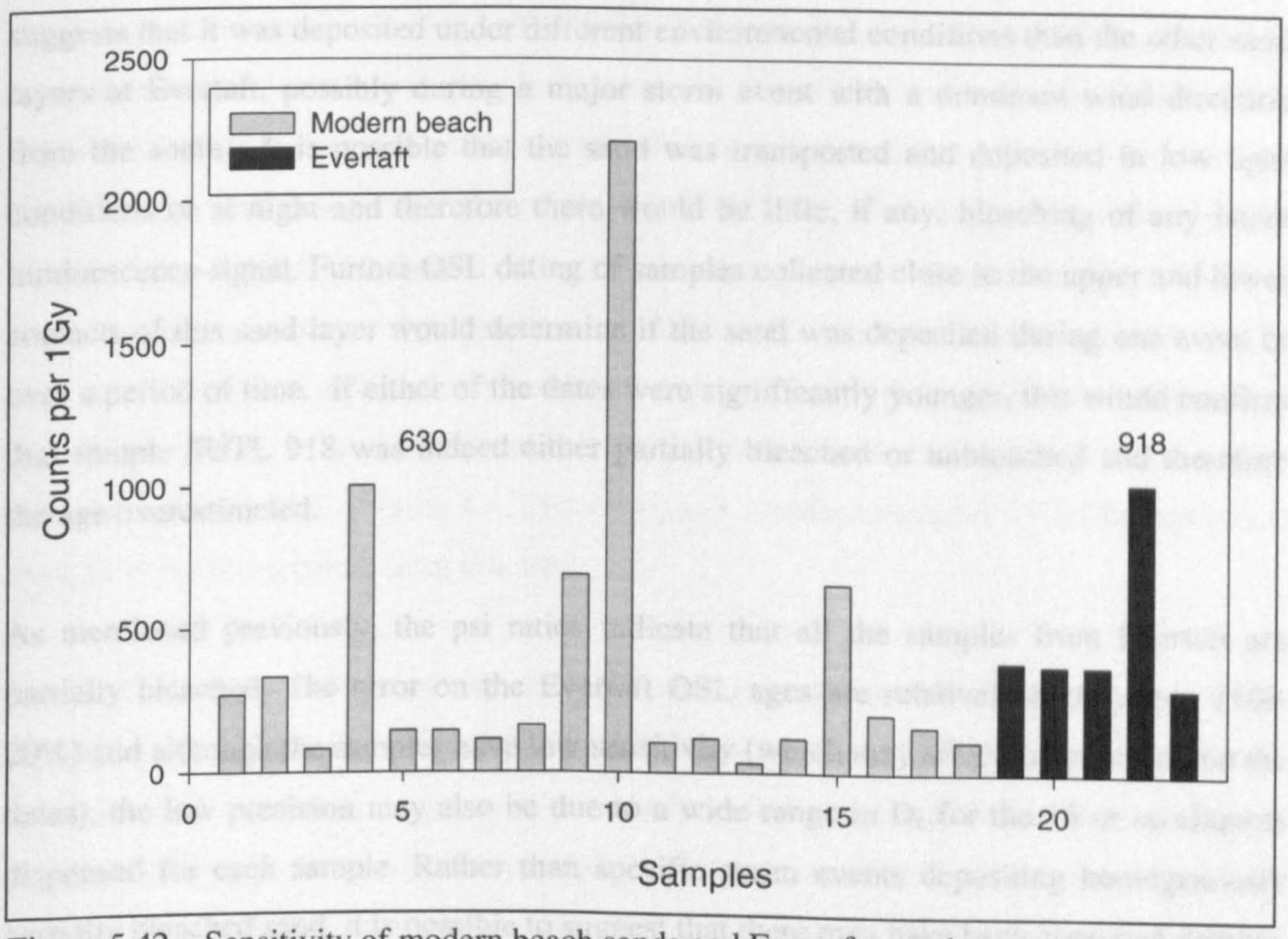

Figure 5.42 – Sensitivity of modern beach sands and Evertaft samples to a 1 Gy dose

from Sanday did not identify the original source of the higher sensitive sands at Tofts Ness and Bay of Lopness, a similar analysis was undertaken on the Westray samples and the response of the modern beach sands from Westray are also shown in Figure 5.41. As with the Sanday archaeological samples, the samples from Quoygrew and Pierowall are more sensitive to artificial irradiation than the Westray modern beach sands and therefore it is not possible to identify a modern sediment provenance. In contrast, the Evertaft samples have a similar response to artificial irradiation and it may be possible to determine the provenance of at least one sample with some accuracy. To allow the samples to be compared easily, without the intrusion of the highly sensitive samples from Quoygrew and Pierowall, the response of the modern beach sands and Evertaft samples to the 1 Gy dose is shown in Figure 5.42. Four of the five Evertaft samples have a very similar response and these may have a similar, but unknown, provenance. When sample SUTL 918 is compared with the modern beach sands, the response to the 1 Gy dose is similar to sample SUTL 630, from the modern beach at Pierowall (Figure 5.42). It is likely that the sediment source for sample SUTL 918 was the beach at Pierowall.

Sample SUTL 918 was OSL dated to the Iron Age and it is the oldest sample in the section. The anomalous age and the proposed different sediment source for this sample suggests that it was deposited under different environmental conditions than the other sand layers at Evertaft, possibly during a major storm event with a dominant wind direction from the south. It is possible that the sand was transported and deposited in low light conditions or at night and therefore there would be little, if any, bleaching of any latent luminescence signal. Further OSL dating of samples collected close to the upper and lower contacts of this sand layer would determine if the sand was deposited during one event or over a period of time. If either of the dates were significantly younger, this would confirm that sample SUTL 918 was indeed either partially bleached or unbleached and therefore the age overestimated.

As mentioned previously, the psi ratios indicate that all the samples from Evertaft are partially bleached. The error on the Evertaft OSL ages are relatively high (about 15%-20%) and although the samples have low sensitivity (which may affect the precision on the dates), the low precision may also be due to a wide range in D_e for the 16 or so aliquots dispensed for each sample. Rather than specific storm events depositing homogenously partially bleached sand, it is possible to suggest that there may have been continual drifting

of sand resulting in heterogeneous bleaching of the quartz grains. This supports the suggestion made by Barrett *et al.* (2000a) that drifting sand was a problem at this site.

The depositional history of the sand layers and midden deposits at Evertaft is complicated and further research is required. Determining the age of all the middens through radiocarbon dating would help to constrain the OSL dates. More samples should also be collected for OSL dating from the sand layers (especially from the lower sand layer) to determine if they were deposited during large storm events or by continual drifting and accumulation. Nevertheless, the OSL ages from the sand layers within the section at Evertaft indicate that the layers represent an extended period of sand movement during the first millennium AD and this will be discussed further in Section 6.2, Chapter 6.

5.3.6 Sandhill, Eday

5.3.6.1 Trends within the samples

Ten test pits were dug across Sandhill on Eday to sample sand layers interleaved between peat deposits (Figure 3.19). Nine of the test pits contained one sand layer, but the tenth pit, close to the burnt mound at Skaill (Figure 3.19), was dug slightly deeper and was found to contain two sand layers which were both sampled. The sand contained within all the pits is slightly finer than the other sites presented with a mean grain size of 125-250 μm. Calcium carbonate contents of these samples (0%-11%) reflect the low quantity of shell material found within the modern Eday beaches and suggests that the sand came from a local beach/dune source. The dominant wind direction in the Orkney Islands is from the west and to the west of Sandhill there is a large, relatively shallow, inlet called Fersness Bay (Figure 3.19). The quartz from the modern beach sand from Fersness Bay is quite insensitive to blue OSL (Figure 4.4, Chapter 4) and therefore the sand within the test pits is thought to have originated from this bay.

The actual water content of the samples varies across Sandhill and appears to be topographically controlled (Figure 5.43). Although samples SUTL 920 and 921 are close to the Burn of Mussetter, they are still relatively well-drained and have a water content of approximately 16%. Towards the top of the hill, the water content decreases to about 13% however this increases to approximately 25% for sample SUTL 924 which is sited in a small depression (Figure 5.43). From the chambered cairn, identified on Figure 3.19, the

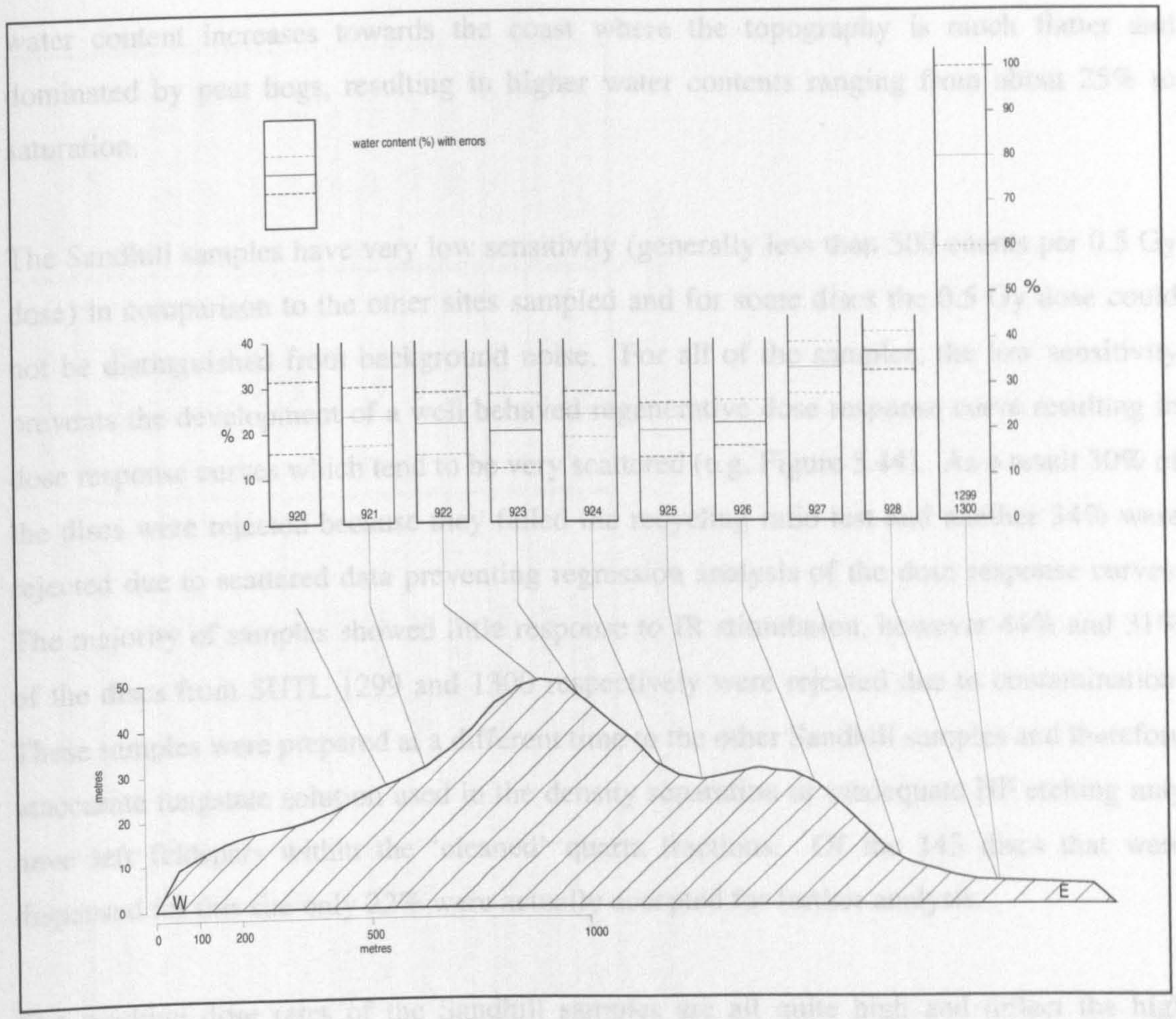

Figure 5.43 – Water content of samples from Sandhill, Eday

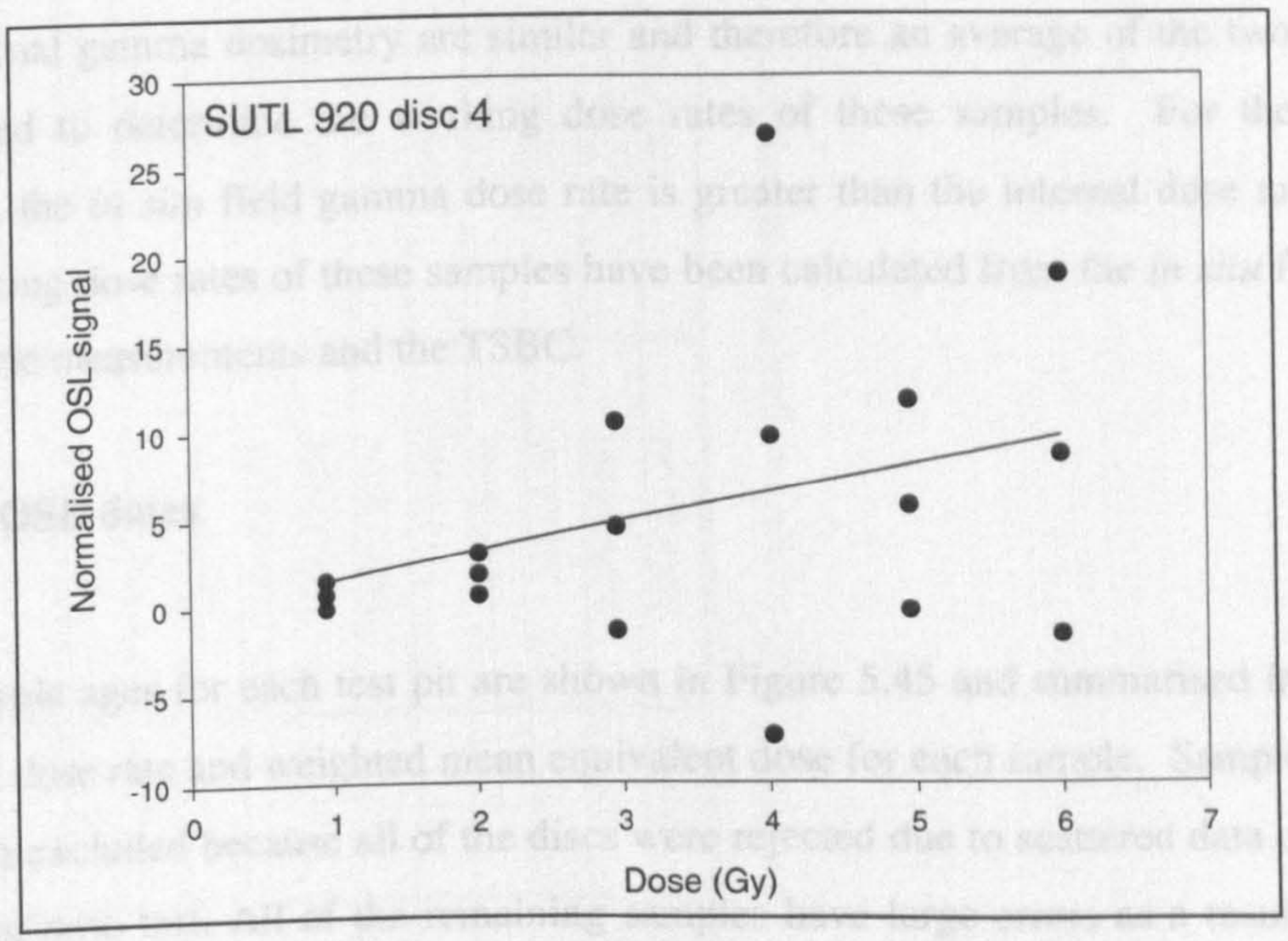

Figure 5.44 – Typical scattered regenerative dose response curve from a Sandhill aliquot

water content increases towards the coast where the topography is much flatter and dominated by peat bogs, resulting in higher water contents ranging from about 25% to saturation.

The Sandhill samples have very low sensitivity (generally less than 500 counts per 0.5 Gy dose) in comparison to the other sites sampled and for some discs the 0.5 Gy dose could not be distinguished from background noise. For all of the samples, the low sensitivity prevents the development of a well behaved regenerative dose response curve resulting in dose response curves which tend to be very scattered (e.g. Figure 5.44). As a result 30% of the discs were rejected because they failed the recycling ratio test and another 34% were rejected due to scattered data preventing regression analysis of the dose response curves. The majority of samples showed little response to IR stimulation, however 44% and 31% of the discs from SUTL 1299 and 1300 respectively were rejected due to contamination. These samples were prepared at a different time to the other Sandhill samples and therefore inaccurate tungstate solution used in the density separation or inadequate HF etching may have left feldspars within the 'cleaned' quartz fractions. Of the 143 discs that were dispensed for this site only 22% were actually accepted for further analysis.

The working dose rates of the Sandhill samples are all quite high and reflect the high internal beta dose rates measured by TSBC and high resolution gamma dosimetry (Table 5.19). For samples SUTL 920, 921, 924 and 925, the field gamma spectrometry and internal gamma dosimetry are similar and therefore an average of the two values has been used to determine the working dose rates of these samples. For the remaining samples, the *in situ* field gamma dose rate is greater than the internal dose rate therefore the working dose rates of these samples have been calculated from the *in situ* field gamma dosimetric measurements and the TSBC.

5.3.6.2 OSL dates

The sample ages for each test pit are shown in Figure 5.45 and summarised in Table 5.20 with the dose rate and weighted mean equivalent dose for each sample. Sample SUTL 921 has been excluded because all of the discs were rejected due to scattered data or failing the recycling ratio test. All of the remaining samples have large errors as a result of the low sensitivity of the sand and therefore environmental interpretation of the site based on the

Sample	Test Pit	(1) Beta dose rate from TSBC ($mGya^{-1}$)	(2) Beta dose rate from high resolution gamma ($mGya^{-1}$)	(3) Field gamma dose rate ($mGya^{-1}$)	(4) Gamma dose rate from high resolution gamma ($mGya^{-1}$)	Methods used to calculate working dose rate	Working Dose Rate ($mGya^{-1}$)
920	1	1.029 ± 0.049	0.746 ±0.047	0.174 ± 0.017	0.177 ± 0.022	1 and 3	0.982 ± 0.059
921	2	1.014 ± 0.064	0.774 ± 0.049	0.161 ± 0.012	0.158 ± 0.023	1, 3 and 4	1.061 ± 0.066
922	3	1.012 ± 0.053	0.05 ± 0.2	0.126 ± 0.011	0.022 ± 0.021	1 and 3	1.034 ± 0.066
923	4	0.956 ± 0.056	0.796 ± 0.046	0.212 ± 0.022	0.222 ± 0.024	1 and 3	1.04 ± 0.06
924	5	1.268 ± 0.059	0.047 ± 0.213	0.275 ± 0.024	0.021 ± 0.021	1 and 3	1.348 ± 0.067
925	6	1.029 ± 0.044	0.698 ± 0.048	0.144 ± 0.022	0.156 ± 0.024	1 and 3	1.085 ± 0.061
926	7	1.114 ± 0.045	0.048 ± 0.207	0.219 ± 0.009	0.021 ± 0.02	1 and 3	1.169 ± 0.038
927	8	1.226 ± 0.043	1.054 ± 0.049	0.373 ± 0.01	0.25 ± 0.02	1 and 3	1.348 ± 0.05
928	9	1.242 ± 0.07	1.075 ± 0.049	0.158 ± 0.032	0.267 ± 0.019	1 and 3	1.116 ± 0.063
1300	10	0.978 ± 0.081	0.775 ± 0.046	0.18 ± 0.02	0.114 ± 0.018	1, 2 and 3	0.81 ± 0.072
1299	10	0.934 ± 0.042	0.849 ± 0.047	0.22 ± 0.03	0.136 ± 0.02	1 and 3	0.811 ± 0.064

Table 5.19 – TSBC, high resolution gamma spectrometry, *in situ* field gamma spectrometry and working dose rates of Sandhill samples

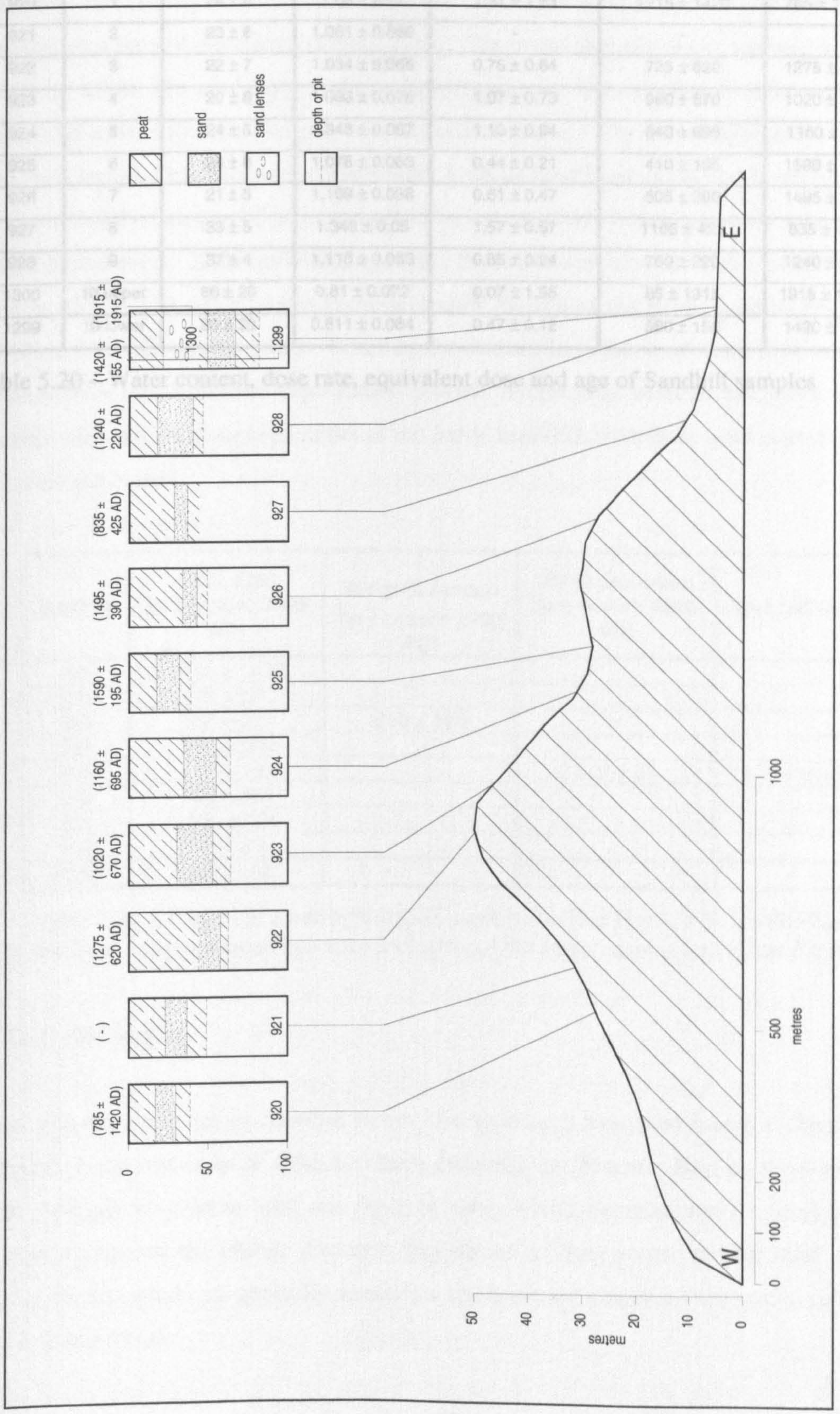

Figure 5.45 – OSL dates from Sandhill, Eday

Sample	Test Pit	Water Content	Dose Rate ($mGya^{-1}$)	Weighted mean estimated dose (Gy)	Age (years before 2000 AD)	Date (BC/AD)
920	1	24 ± 8	1.08 ± 0.07	1.31 ± 1.53	1215 ± 1420	785 ± 1420 AD
921	2	23 ± 6	1.061 ± 0.066	-	-	-
922	3	22 ± 7	1.034 ± 0.066	0.75 ± 0.64	725 ± 620	1275 ± 620 AD
923	4	20 ± 8	1.093 ± 0.075	1.07 ± 0.73	980 ± 670	1020 ± 670 AD
924	5	24 ± 5	1.348 ± 0.067	1.13 ± 0.94	840 ± 695	1160 ± 695 AD
925	6	20 ± 6	1.078 ± 0.063	0.44 ± 0.21	410 ± 195	1590 ± 195 AD
926	7	21 ± 5	1.169 ± 0.038	0.61 ± 0.47	505 ± 390	1495 ± 390 AD
927	8	33 ± 5	1.348 ± 0.05	1.57 ± 0.57	1165 ± 425	835 ± 425 AD
928	9	37 ± 4	1.116 ± 0.063	0.85 ± 0.24	760 ± 220	1240 ± 220 AD
1300	10 upper	80 ± 20	0.81 ± 0.072	0.07 ± 1.55	85 ± 1915	1915 ± 1915 AD
1299	10 lower	80 ± 20	0.811 ± 0.064	0.47 ± 0.12	580 ± 155	1420 ± 155 AD

Table 5.20 – Water content, dose rate, equivalent dose and age of Sandhill samples

OSL dates is problematic. Only Test Pit 10 was excavated to a sufficient depth to allow two sand layers to be sampled. The lower sand sample (SUTL 1299) was deposited during the early 15th century AD, but the error on the upper sand sample (SUTL 1300) is too large to suggest a date of deposition (Figure 5.45). The remaining pits were dug to a sufficient depth to allow one sand layer to be sampled and it is assumed that further sand layers would have been found if the pits were excavated further. The initial hypothesis was that the sand layer within each pit may represent a single sand blow event and it can be readily seen that all the dates and their errors could be interpreted as being consistent with a single depositional event. If the individual ages and their errors are combined the weighted mean age is 1360 ± 120 AD which is consistent with the age of the lower sand in Test Pit 10 (1420 ± 155 AD) (Table 5.21). Whether the counter hypothesis of more than one trans-island event represents the depositional process is currently unclear, but given the low sensitivities and resulting high errors of the individual OSL data there is no reason to argue for multiple events.

Sample	OSL age (yrs before 2000 AD)	Weighted mean (yrs before 2000 AD)	Weighted mean (yrs before 2000 AD)	Date (BC/AD)
920	1215 ± 1420			
922	725 ± 620			
923	980 ± 670	640 ± 120		
924	840 ± 695			
925	410 ± 195		620 ± 95	1380 ± 95 AD
926	505 ± 390			
927	1165 ± 425			
928	760 ± 220			
1299	580 ± 155			

Table 5.21 – Weighted mean age of OSL ages from Test Pits 1, 3-9, Sandhill and the final weighted mean age after inclusion of the lower sand layer in Test Pit 10.

5.3.6.3 Discussion

Test pits were dug across Sandhill to test the hypothesis that sand found at Skaill Burnt Mound on the east coast of Eday had been derived from Fersness Bay, on the west coast. Each test pit revealed at least one layer of sand, which suggests that the sand cover is continuous across the island. Fersness Bay seems a likely source for the sand deposits given that the winds are generally westerlies and there are almost no alternative sources of sand on the island.

The low sensitivity of the Sandhill samples is a major restriction on accurate OSL dating and a method has been proposed in Section 5.2.4.5 that may allow such low sensitive samples to be dated. Despite the low sensitivity, OSL dates have been calculated for 10 of the 11 samples and the weighted mean of these dates suggests that sand deposition occurred during the 14th century AD. The identification of two sand layers interleaved by peat deposits in Test Pit 10 may suggest that that at least one and possibly several storm periods are represented (Sommerville *et al.* 2003) and similar sequences of sand and peat layers have been observed in peat and at peat cutting sites elsewhere on the island (E. Popplewell, *pers. comm*). Radiocarbon samples were collected from the lower peat layers of Test Pits 2 and 5 and an upper peat layer sample was also collected from Test Pit 5. The radiocarbon dates are shown in Figure 5.46. The OSL date (1160 ± 695 AD) from the sand layer in Test Pit 5 (SUTL 924) has very low precision but it lies chronostratigraphically between the two radiocarbon dates (cal AD 135-420, GU-9240 and cal AD 1525-1950, GU-9241) and suggests that the inundation of sand effectively stopped the growth of peat possibly during the 12th century AD. Although an OSL date is unavailable for Test Pit 2 because all the discs were rejected from sample SUTL 921, the radiocarbon date of the underlying peat (cal AD 885-1030 GU-9242) is significantly different to that of Test Pit 5 (Figure 5.46), but it does suggest that the sand layer lying directly above it was also probably deposited during the 11th/12th century AD.

The OSL dates are within error of each other and with the inclusion of the lower sand layer in Test Pit 10 (Table 5.21) this suggests that they may have been deposited during one sand blow event about 1360 ± 120 AD. A similar OSL date has been obtained from the middle sand layer at Pierowall (SUTL 878, 1385 ± 50 AD), and the upper sand deposits at the Bay of Lopness also have similar dates (1475 ± 90AD) suggesting that there was substantial movement of sand in the Orkney Islands during this period. The low precision on the upper sand layer in Test Pit 10 prevents an accurate interpretation of this sand layer and although it may have been deposited during another sand blow event it may also represent sand recycled from lower layers elsewhere on the island, exposed by agriculture, grazing or peat cutting. To determine whether more than one sand blow event is recorded on the island, further test pits need to be dug to a sufficient depth to identify other sand layers constrained by peat. Collection of peat deposits from the test pits for radiocarbon dating would help to constrain the OSL dates above. If the OSL dates record multiple sand blow events, it is possible that after inundation of a large area by sand, subsequent erosion resulted in only irregular pockets of sand remaining within the landscape. The sand layer

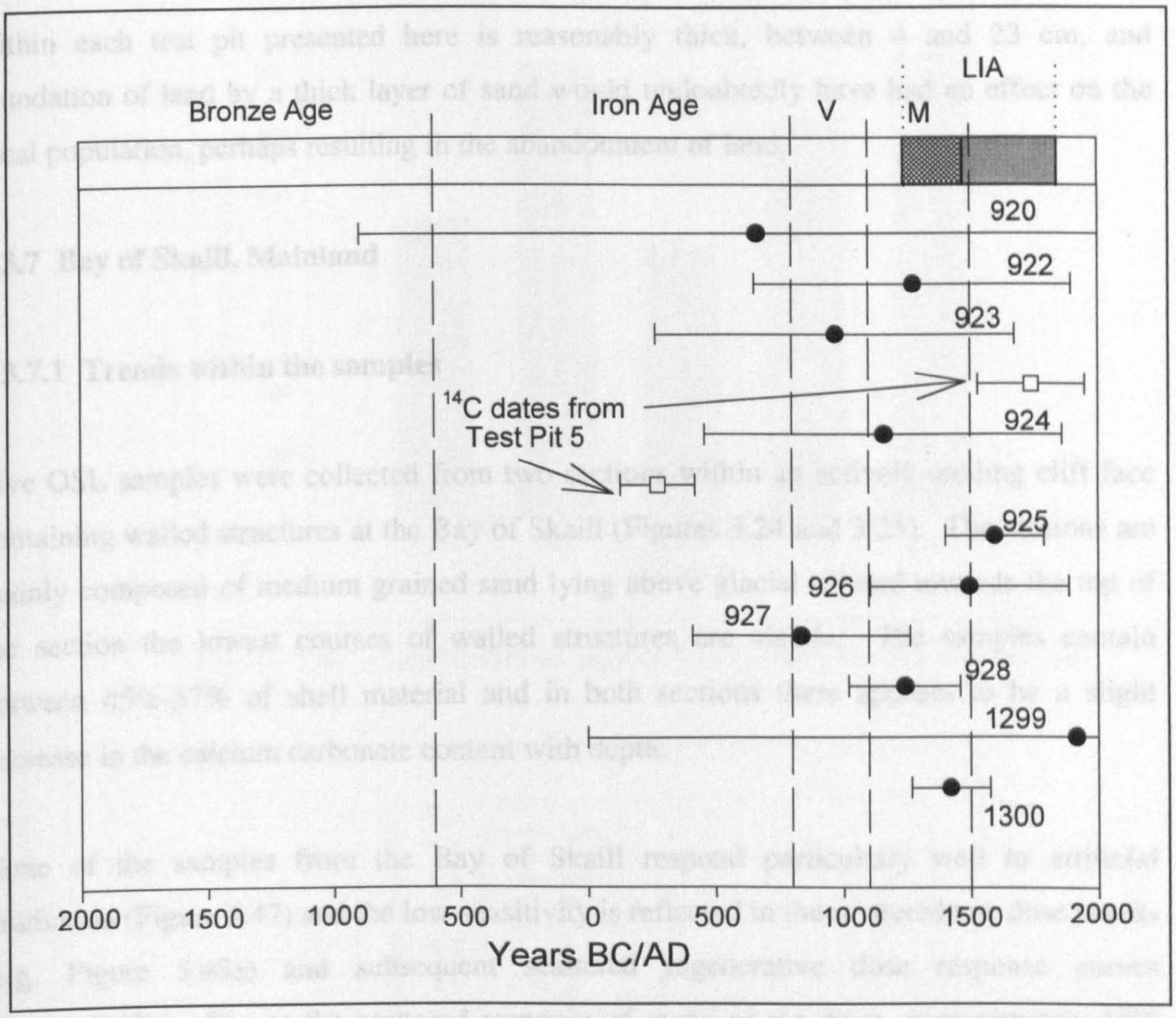

Figure 5.46 – OSL dates from Sandhill and the radiocarbon dates from Test Pit 5. The OSL dates are within error of each other allowing a weighted mean age of 1360 ± 120 AD to be calculated. V = Viking M = Medieval LIA = Little Ice Age

within each test pit presented here is reasonably thick, between 4 and 23 cm, and inundation of land by a thick layer of sand would undoubtedly have had an effect on the local population, perhaps resulting in the abandonment of land.

5.3.7 Bay of Skaill, Mainland

5.3.7.1 Trends within the samples

Five OSL samples were collected from two sections within an actively eroding cliff face containing walled structures at the Bay of Skaill (Figures 3.24 and 3.25). The sections are mainly composed of medium grained sand lying above glacial till and towards the top of the section the lowest courses of walled structures are visible. The samples contain between 45%-57% of shell material and in both sections there appears to be a slight decrease in the calcium carbonate content with depth.

None of the samples from the Bay of Skaill respond particularly well to artificial irradiation (Figure 5.47) and the low sensitivity is reflected in the scattered test dose results (e.g. Figure 5.48a) and subsequent scattered regenerative dose response curves (Figure 5.48b). Due to the scattered response of many of the discs, approximately 15% were rejected for failing the recycling ratio test and another 15% were rejected due to scattered data preventing regression analysis. A further 11% were rejected because they were contaminated by IR sensitive minerals.

The working dose rate for each sample from the Bay of Skaill is relatively high (Table 5.22) compared to other sites sampled for this research and is possibly the result of different bedrock geology. Stromness Flags dominate the bedrock geology in western Mainland whereas the Northern Isles are mainly composed of Rousay Flags and Eday Beds. All the samples have high internal beta dose rates (Table 5.22) and although the internal gamma dose rates measured by high resolution gamma spectrometry are reasonably high the *in situ* field gamma dose rates tend to be greater. As a result, the gamma contribution to the working dose rate for three of the five samples is from the *in situ* field gamma spectrometry alone.

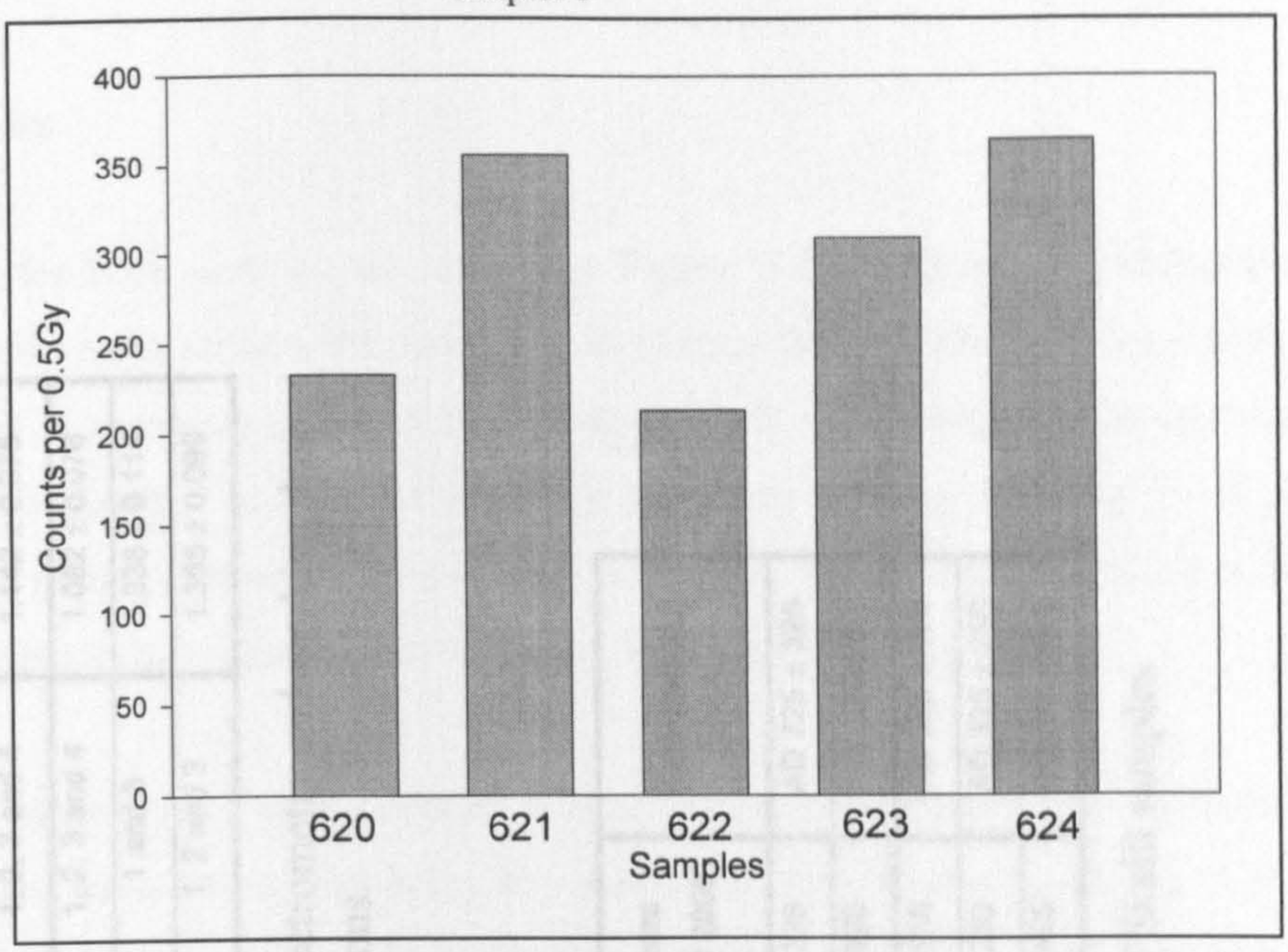

Figure 5.47 – Sensitivity of Bay of Skaill samples to a 0.5 Gy dose

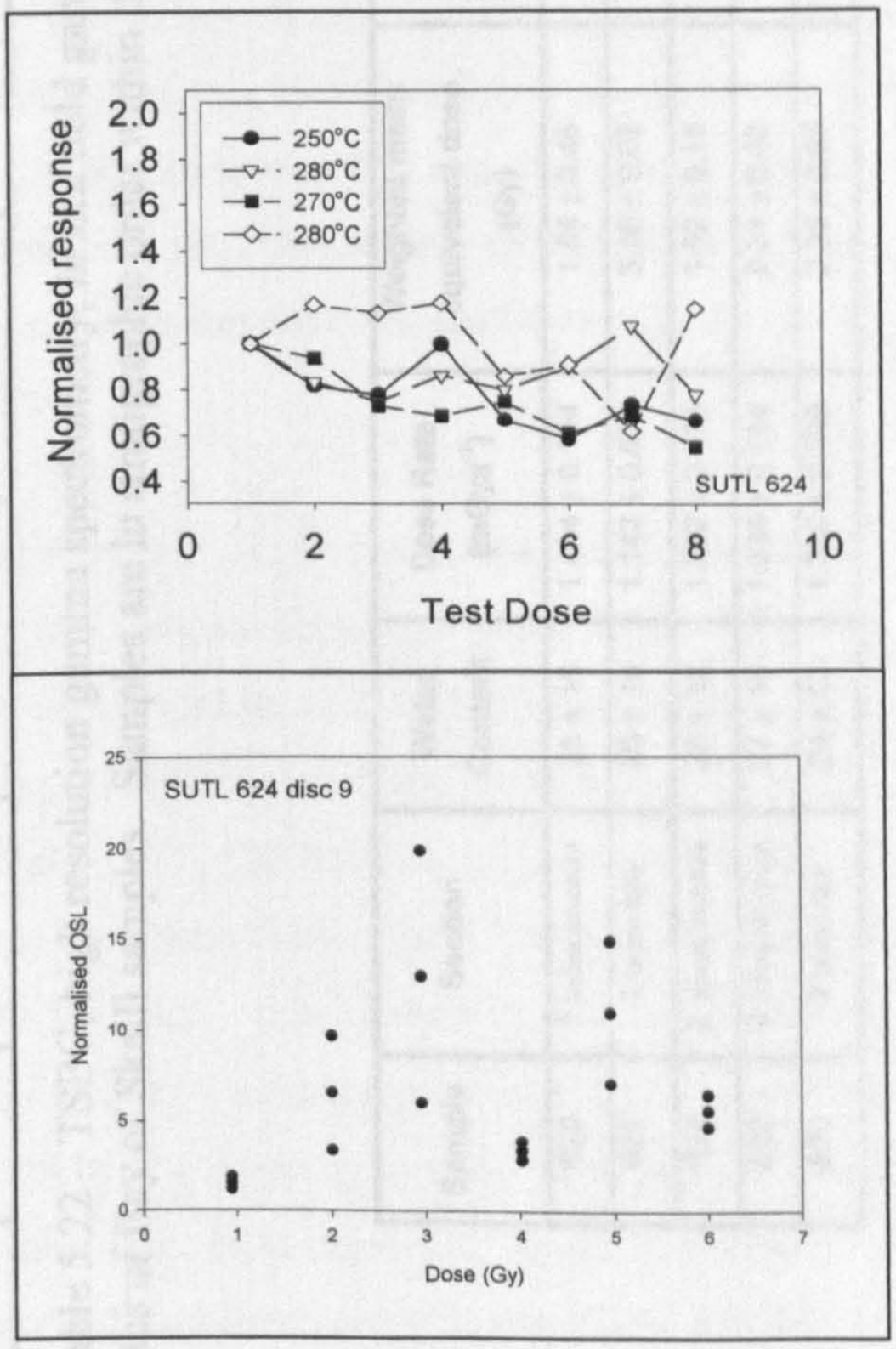

Figure 5.48 – Examples of a) scattered test dose responses and b) the subsequent scattered regenerative dose response curve for a sample from the Bay of Skaill

Sample	Section	(1) Beta dose rate from TSBC ($mGya^{-1}$)	(2) Beta dose rate from high resolution gamma ($mGya^{-1}$)	(3) Field gamma dose rate ($mGya^{-1}$)	(4) Gamma dose rate from high resolution gamma ($mGya^{-1}$)	Methods used to calculate working dose rate	Working Dose Rate ($mGya^{-1}$)
620	1	0.921 ± 0.063	0.804 ± 0.031	0.62 ± 0.01	0.33 ± 0.017	1 and 3	1.444 ± 0.104
621	1	0.866 ± 0.064	0.86 ± 0.048	0.33 ± 0.01	0.327 ± 0.037	1, 2, 3 and 4	1.142 ± 0.075
624	2	0.611 ± 0.063	0.545 ± 0.044	0.5 ± 0.01	0.187 ± 0.035	1, 2, 3 and 4	1.082 ± 0.076
622	2	1.22 ± 0.066	0.999 ± 0.047	0.41 ± 0.01	0.387 ± 0.053	1 and 3	1.338 ± 0.114
623	2	0.957 ± 0.069	0.755 ± 0.046	0.5 ± 0.01	0.285 ± 0.039	1, 2 and 3	1.355 ± 0.099

Table 5.22 – TSBC, high resolution gamma spectrometry, *in situ* field gamma spectrometry and working dose rates of Bay of Skaill samples. Samples are in stratigraphic order within the sections.

Sample	Section	Water Content	Dose Rate ($mGya^{-1}$)	Weighted mean equivalent dose (Gy)	Age (years before AD 2000)	Date (BC/AD)
620	1 below structure	25 ± 15	1.444 ± 0.104	1.84 ± 0.45	1275 ± 325	AD 725 ± 325
621	1 below 620	20 ± 10	1.142 ± 0.075	3.16 ± 0.68	2765 ± 620	765 ± 620 BC
624	2 above structure	26 ± 18	1.082 ± 0.076	1.52 ± 0.18	1405 ± 195	AD 595 ± 195
622	2 below structure	27 ± 15	1.338 ± 0.114	2.24 ± 0.32	1675 ± 280	AD 325 ± 280
623	2 below 622	24 ± 13	1.355 ± 0.099	2.25 ± 0.65	1660 ± 495	AD 340 ± 495

Table 5.23 – Water content, dose rate, equivalent dose and age of Bay of Skaill samples

5.3.7.2 OSL dates

The OSL dates for both sections are shown in Figure 5.49a and b and summarised in Table 5.23. Within each section the dates are in chronostratigraphic order but there has been a great deal of slumping and erosion at both sections. The samples from underneath the structures are thought to be unaffected by slumping as they were collected from cleaned vertical sections, however the OSL age on the upper sample (SUTL 624) of Section 2 lying above the walled structure cannot be as confidently accepted.

The purpose of dating these sand deposits was to provide a *terminus post quem* for the construction of the walled structures lying above the thick sand deposits. Rather than date when the sand was deposited, it was hypothesised that the sands lying below the structures may have been exposed prior to laying the lowest course of stones. As a result, the OSL date of the sand lying below the stones should provide a date for construction. Sample SUTL 620 in Section 1 (Figure 5.49a) lies close to the contact with the overlying structure and the OSL date suggests that the sand was last exposed to light some time during the 8th century AD. The OSL date from the other sample (SUTL 622) that lies directly below the walled structure in Section 2 indicates that this sand was exposed slightly earlier in the late Iron Age (4th century AD).

If the sand lying directly below the walled structures was anthropogenically bleached, then the OSL dates of the lower sand samples should be much older. Sample SUTL 621 lies approximately 35 cm below SUTL 620 in Section 1 (Figure 5.49a) and was deposited at some point in the 8th century BC during the late Bronze Age or early Iron Age. In Section 2 (Figure 5.49b) sample SUTL 623 lies only 15 cm below SUTL 622 and the OSL date suggests that it may have been deposited in the 4th century AD (AD 340 ± 495). As a result of the large error on this date, this sample is not significantly older than the overlying sample. This may be due to anthropogenic mixing of bleached and unbleached sediment or due to the infiltration of younger grains that were possibly bleached during the anthropogenic activity, into the older sand deposits. There is a greater vertical distance between the samples in Section 1 and therefore it is suggested that the lowest sample in this section (SUTL 621) remained buried and unexposed whilst the structure above was constructed.

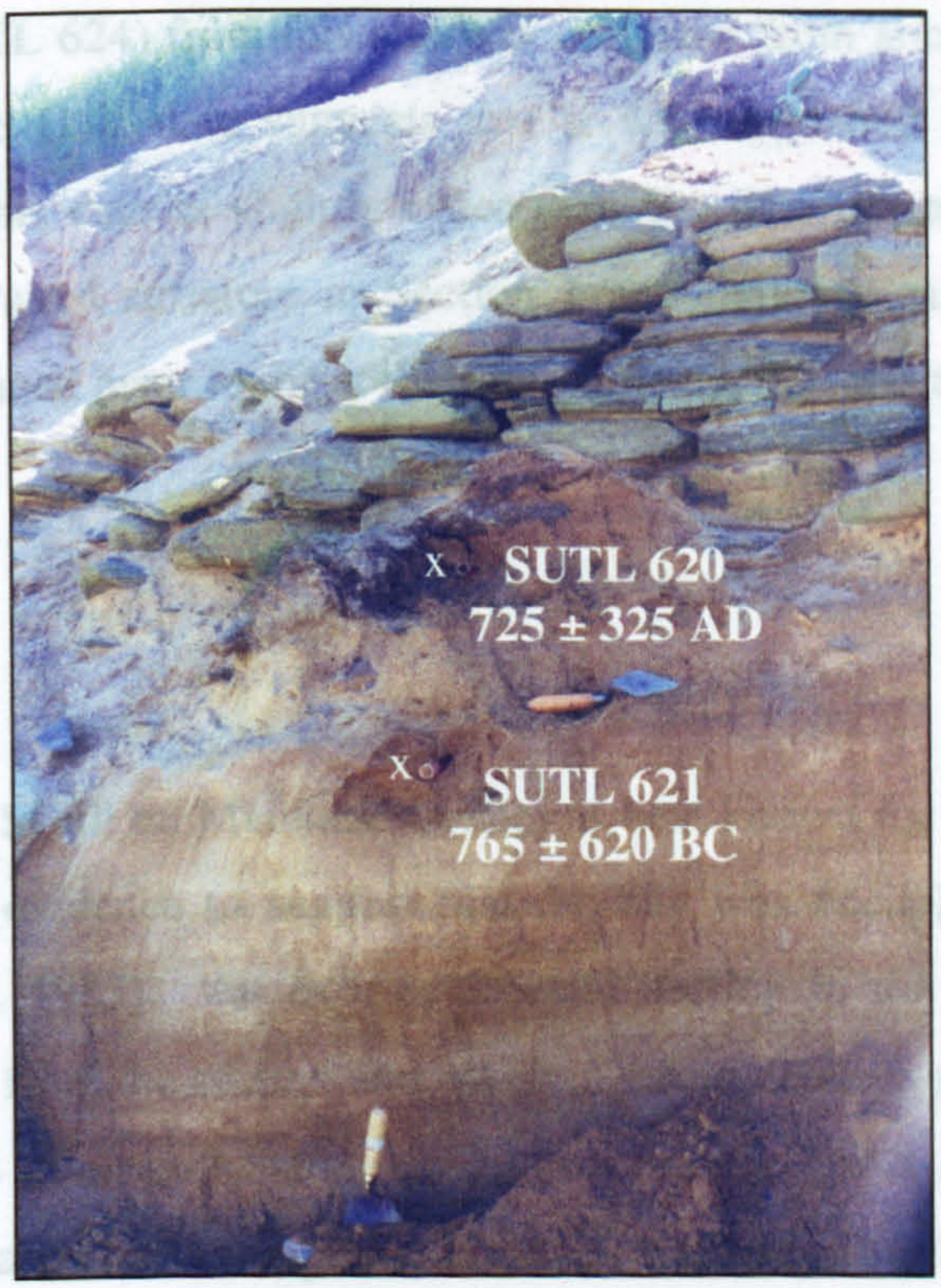

Figure 5.49a –OSL dates from Section 1, Bay of Skaill

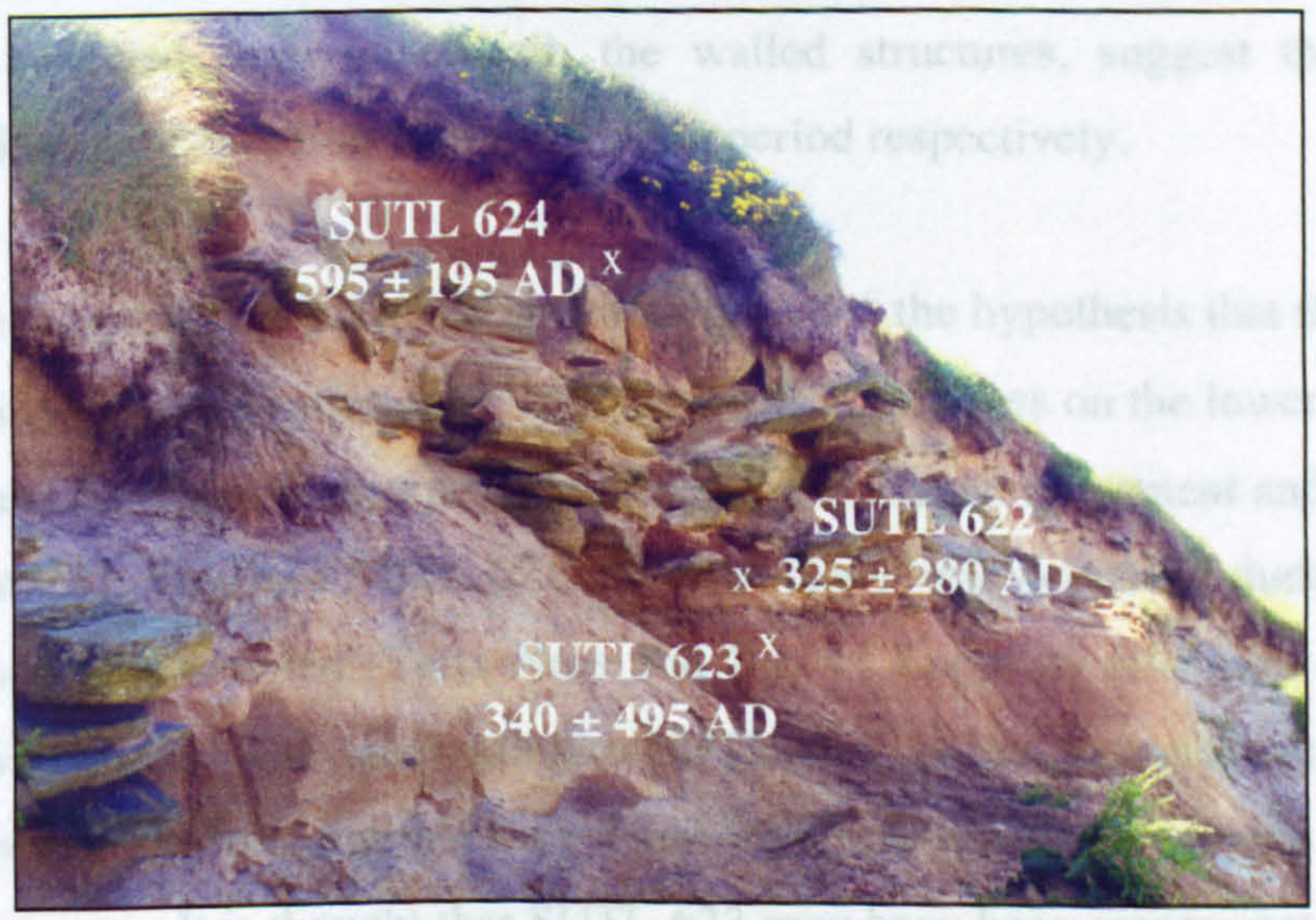

Figure 5.49b – OSL dates from Section 2, Bay of Skaill

The last sample (SUTL 624) from this site was collected from above the walled structure in Section 2 and the OSL date suggests that it was deposited and buried during the 6th century AD. This date is slightly older than the date of sample SUTL 620 lying directly below the walled structure in Section 1 and may indicate that the structure in Section 2 was abandoned prior to, or at the same time as, the structure in Section 1 started to be constructed.

5.3.7.3 Discussion

Although the Bay of Skaill on Mainland Orkney is best known for the Neolithic village of Skara Brae, there is evidence to suggest that the bay was occupied up until the Viking period (Morris *et al.* 1985). An exposed coastal section in the bay containing walled structures protruding from the section and overlying sand deposits provided an opportunity to try and determine if optically stimulated luminescence could assist the dating of the structures. This is based on the hypothesis that as a result of anthropogenic activity, the sand immediately below the structures was bleached prior to construction and that the latent luminescence signal started to accumulate after the sand was sealed by further sand deposits or the lowest course of stones. The OSL ages of the sand deposits from both sections are shown in Figure 5.50 and the dates of samples SUTL 622 (Section 2) and 620 (Section 1) collected from underneath the walled structures, suggest that they were constructed during the late Iron Age and Viking period respectively.

Although the samples were collected specifically to test the hypothesis that the sands lying under the structures were anthropogenically reset, the OSL ages on the lower sand samples (SUTL 621 and 623) should also provide information on sand movement and deposition in the bay. The OSL age from SUTL 621 indicates that it was deposited during the Bronze Age and other sites sampled (Tofts Ness and Bay of Lopness) also have sand deposits dating to this period. The other sample, SUTL 623, is not thought to represent sand movement in the late Iron Age because it has a similar age to the sample lying directly below the structure. It is thought that SUTL 623 may have been contaminated by younger quartz grains through anthropogenic activity and therefore additional sampling from lower in the section is required to provide information on the movement and deposition of wind blown sands at this site.

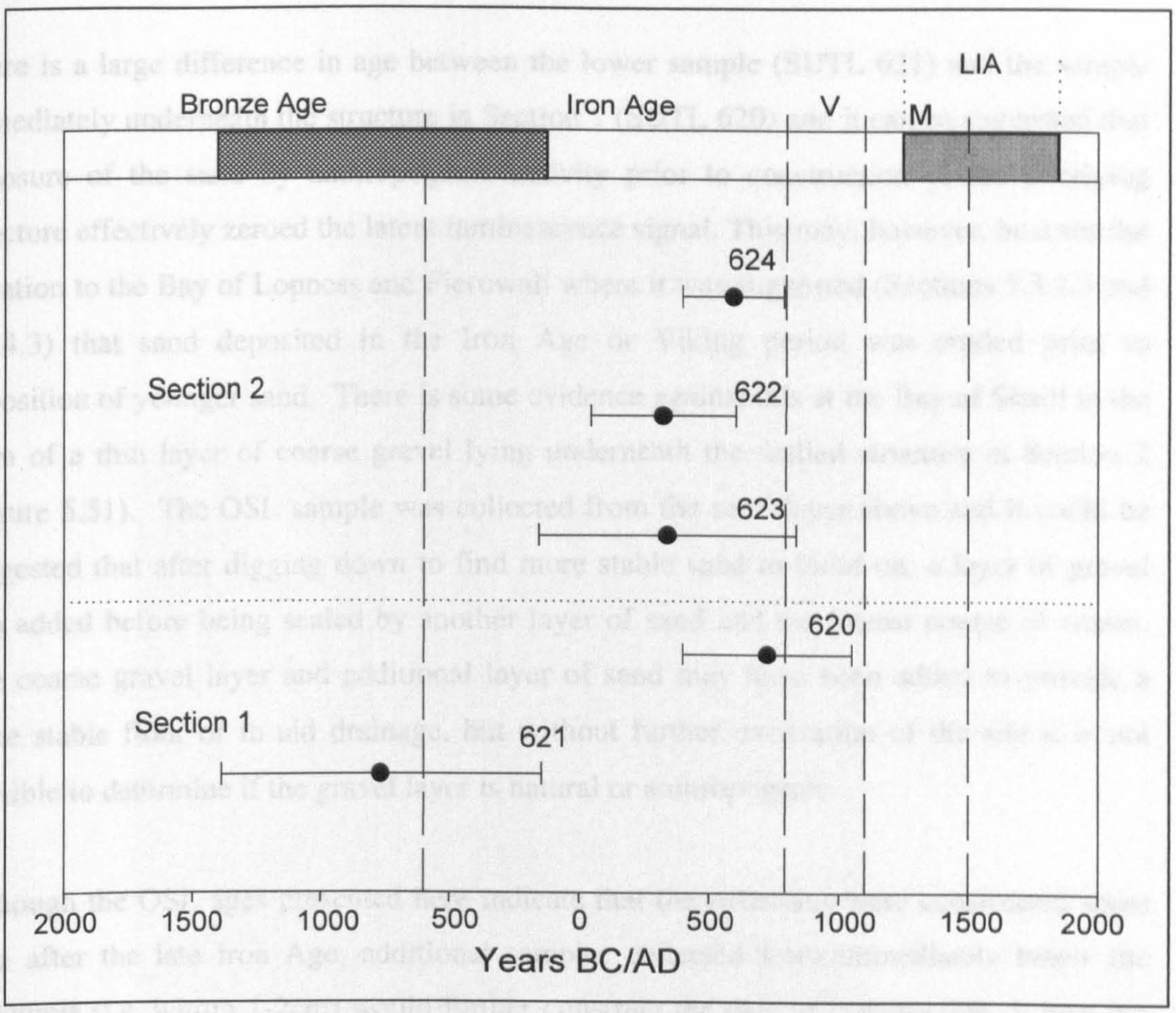

Figure 5.50 – OSL dates from the Bay of Skaill and the identification of one period of sand movement. V = Viking M = Medieval LIA = Little Ice Age

There is a large difference in age between the lower sample (SUTL 621) and the sample immediately underneath the structure in Section 1 (SUTL 620) and it can be suggested that exposure of the sand by anthropogenic activity prior to construction of the overlying structure effectively zeroed the latent luminescence signal. This may, however, be a similar situation to the Bay of Lopness and Pierowall where it was suggested (Sections 5.3.2.3 and 5.3.4.3) that sand deposited in the Iron Age or Viking period was eroded prior to deposition of younger sand. There is some evidence against this at the Bay of Skaill in the form of a thin layer of coarse gravel lying underneath the walled structure in Section 2 (Figure 5.51). The OSL sample was collected from the sand layer above and it could be suggested that after digging down to find more stable sand to build on, a layer of gravel was added before being sealed by another layer of sand and the lowest course of stones. The coarse gravel layer and additional layer of sand may have been added to provide a more stable floor or to aid drainage, but without further excavation of the site it is not possible to determine if the gravel layer is natural or anthropogenic.

Although the OSL ages presented here indicate that the structures were constructed some time after the late Iron Age, additional samples collected from immediately below the structures (i.e. within 1-2cm) would further constrain the date of construction. It may not be possible to determine if the sand was anthropogenically or naturally reset as both processes have a similar result, nevertheless sampling at close intervals throughout both sections would provide more information on the rate of sand deposition. Morris *et al.* (1985) and James (1999) have discussed other archaeological structures in the section and the radiocarbon date from the burial cist does provide some constraint to the age of the surrounding structures. Section 2 lies close to the cist excavated by H. James in 1996 and although the walled structure in the section lies on a similar stratigraphic level, the OSL date suggests that it was constructed prior to the burial. Further OSL sampling around the cist would provide further constraints on sand deposition and perhaps confirm whether sand is anthropogenically reset prior to construction of structures in the area. If confirmed this opens up many opportunities to accurately date archaeological sites in sandy areas that have little organic material available for radiocarbon dating.

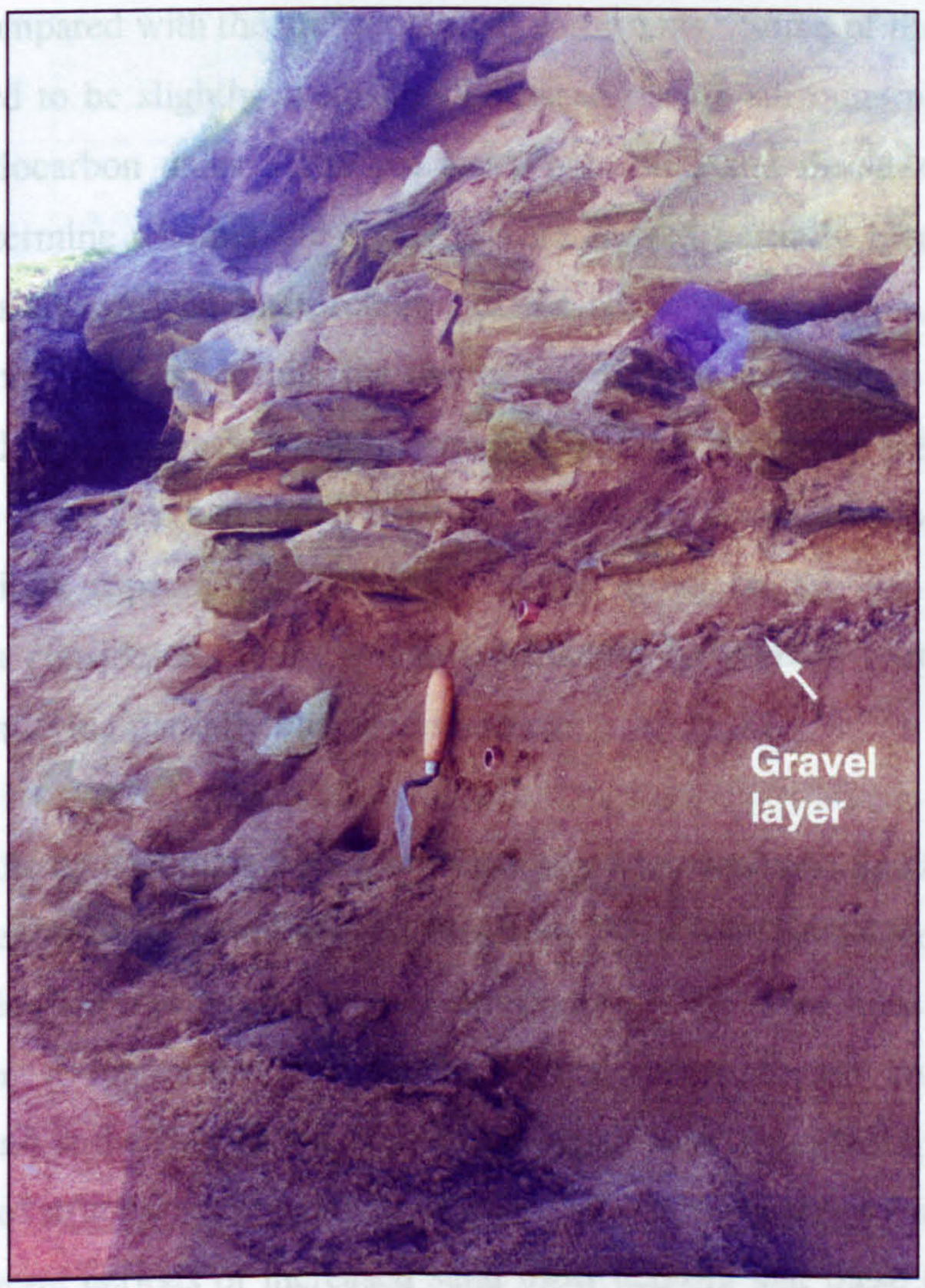

Figure 5.51 – Gravel layer underneath the walled structure in Section 2 at the Bay of Skaill that may have been emplaced to provide a stable floor or aid drainage

5.4 Summary of OSL dates from the archaeological sites

The previous sections have presented the OSL ages for the various sites and discussed how these have compared with the archaeological constraints. Some of the OSL ages presented are considered to be slightly overestimated based on the surrounding archaeology and/or available radiocarbon dates. The psi ratio, presented and discussed in Chapter 4, has helped to determine whether these samples are indeed partially bleached and this has in some circumstances aided interpretation of the sites. Nevertheless, the identification of erroneously old samples, despite the use of late light subtraction in the SAR analysis, is worrying and it is suggested that in some cases the late light subtraction may not be removing the entire residual signal from the main OSL signal. Further research on the psi ratio is required, especially with regard to the effect on the psi ratio after late light subtraction is considered, before it can confidently be used in routine OSL dating as a means of identifying partially bleached samples.

For some of the archaeological sites sampled, e.g. Pierowall and Sandhill, little was known about the sites prior to sampling and therefore the results presented here have provided new archaeological and environmental information. At other sites the OSL dates have confirmed or re-interpreted the archaeological interpretation (e.g. Tofts Ness and Quoygrew) and at the Bay of Skaill, the OSL dates have provided *terminus post quem* for construction of structures overlying sand deposits. The OSL dates from each site have also identified several periods of increased sand blow activity and these have been collated in Figure 5.52 for an intra- and inter-island comparison to be made. Shaded areas in Figure 5.52 identify the periods of increased sand movement and these are mainly based on the weighted mean ages recognised within the individual sites discussed previously.

Tofts Ness and Bay of Lopness are both on the island of Sanday and the younger samples in both sites were deposited about the late 15th/early 16th century AD during the Little Ice Age. A further two periods of sand blow was identified from the remaining samples at Tofts Ness and these were deposited during the Neolithic and the late Bronze/early Iron Age. Two of the Bay of Lopness samples were deposited during the Bronze Age but there is no indication of sand movement at this site during the Iron Age or Viking period. It is suggested that any sand that was deposited during these periods was eroded prior to deposition of the Little Ice Age deposits.

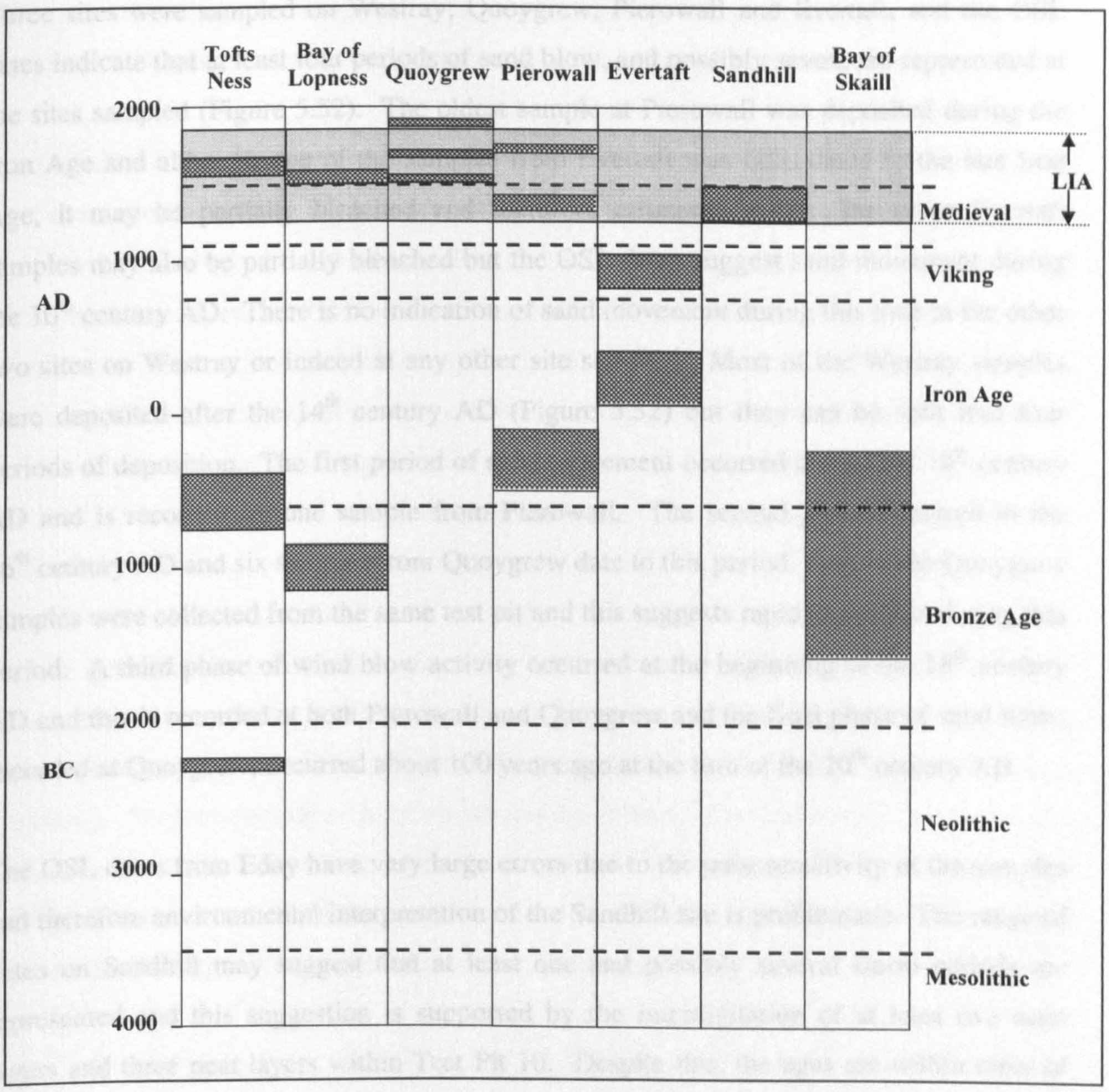

Figure 5.52 – The periods of sand movement identified using the weighted mean OSL age from the various sites where possible.

Three sites were sampled on Westray; Quoygrew, Pierowall and Evertaft, and the OSL dates indicate that at least four periods of sand blow, and possibly seven, are represented at the sites sampled (Figure 5.52). The oldest sample at Pierowall was deposited during the Iron Age and although one of the samples from Evertaft was OSL dated to the late Iron Age, it may be partially bleached and therefore erroneously old. The other Evertaft samples may also be partially bleached but the OSL dates suggest sand movement during the 10th century AD. There is no indication of sand movement during this time at the other two sites on Westray or indeed at any other site sampled. Most of the Westray samples were deposited after the 14th century AD (Figure 5.52) but they can be split into four periods of deposition. The first period of sand movement occurred during the 14th century AD and is recorded by one sample from Pierowall. The second phase occurred in the 16th century AD and six samples from Quoygrew date to this period. Four of the Quoygrew samples were collected from the same test pit and this suggests rapid deposition during this period. A third phase of wind blow activity occurred at the beginning of the 18th century AD and this is recorded at both Pierowall and Quoygrew and the final phase of sand blow, recorded at Quoygrew, occurred about 100 years ago at the turn of the 20th century AD.

The OSL dates from Eday have very large errors due to the poor sensitivity of the samples and therefore environmental interpretation of the Sandhill site is problematic. The range of dates on Sandhill may suggest that at least one and possibly several storm periods are represented and this suggestion is supported by the interdigitation of at least two sand layers and three peat layers within Test Pit 10. Despite this, the ages are within error of each other and the weighted mean age suggests sand deposition about 1360 ± 120 AD. This is in agreement with the lower sand layer in Test Pit 10 and the upper sand layer in this test pit may represent the re-deposition of sand eroded from other sand deposits on the island. The absence of any pit without sand suggests that the sand cover is continuous from west to east, but at present the data are not yet sufficient to ascertain whether multiple events have occurred.

The final site at the Bay of Skaill has been dated not to infer periods of sand movement but to determine if construction of walled structures lying above the thick sand deposits effectively zeroed the sand immediately underneath the stones. Nevertheless, one sample (SUTL 621) from this site is represented on Figure 5.52 as it is thought that it does represent sand deposition during the Bronze Age. The other OSL dates indicate that the

structures in the two sections were not constructed at the same time and it has been suggested that as one building was abandoned, construction may have started on the other.

If all of the OSL dates from the Orkney Islands are considered, six phases of increased sand movement can be identified: the Neolithic, the Bronze Age, two periods in the Iron Age, the 10th century AD and the 14th-late 19th centuries AD, which is also known as the Little Ice Age. There is little correlation between the periods of sand blow on the various islands apart from sand deposited during the Little Ice Age. Although this may imply that the timing of sand movement and deposition varied between the islands it is more likely that the gaps in the chronostratigraphy at the various sites represent periods of erosion and this will vary spatially and temporally depending on the stability of the various dune systems.

This chapter has presented the results from OSL dating of sand deposits collected from archaeological sites in the Orkney Islands and it has shown that OSL dating is a viable dating technique in this area, despite the problems with low sensitivity and partial bleaching. Various periods of sand movement have been identified within the prehistoric and historic periods in the Orkney Islands and these will be discussed in more detail in the following chapter with regard to periods of sand blow identified in other areas of northern Europe and the impact of such periods on the local population.

Chapter 6 – Wind blow events in Orkney and the wider context

6.1 Introduction

The previous chapter presented and discussed the results from OSL dating of wind blown sands collected from archaeological sites in the Orkney Islands and despite the low sensitivity of some samples, ages were calculated for all but one sample. Using the OSL dates from these samples it has been possible to identify periods of increased sand movement in the Holocene in the Orkney Islands. OSL dating has also been used in conjunction with other dating methods to identify periods of climatic instability in other areas of north-west Europe and the aim of this chapter is to interrelate these periods of instability in the wider environmental context. It also aims to examine how these periods of increased windiness may have affected the local island populations.

6.2 Identifying periods of increased windiness in history and prehistory

The strength of the wind in a low pressure system is linked to the pressure gradient that exists between high and low-pressure systems that develop in the Atlantic. The displacement of these systems controls the amount of cyclonic activity that occurs in northern Europe (Lamb 1985). Displacement of high and low-pressure systems is known to have varied during the Holocene and this may be linked either to changes in the energy levels of the general circulation or to the expansion or reduction of the polar ice cap (Lamb 1988). An expansion in the polar ice cap creates higher pressure over the Arctic and forces cooler air to lower latitudes increasing the pressure gradient and hence affecting the strength of the wind in the low pressure systems (Lamb 1985). More recent research has related storminess to the North Atlantic Oscillation (NAO); an index used to identify climate variability in the North Atlantic (Dawson *et al.* 2001). The NAO index was developed by Hurrell (1995) and Appenzeller *et al.* (1998) and is based on the difference in air pressure between the Azores high and the Icelandic low. When there is a strong Azores high and a deep Icelandic low the NAO is strongly positive and this has been shown to correspond to periods of time with increased storminess in the North Atlantic (Dawson *et al.* 2001). There is good agreement between the NAO index and records of gale day frequency in Edinburgh and therefore Dawson *et al.* (2001) suggest that periods of increased storminess around the Scottish coastline correspond to periods when the NAO is

positive. Appenzeller *et al.* (1998) reconstructed the NAO index from about AD 1650 (Figure 6.1) and the various periods of strongly positive NAO, and hence increased storminess, are highlighted e.g. 1690's, 1720's, 1760's, 1810-1840 and 1910. The NAO index is defined as the difference in sea level pressure at Lisbon, Portugal and Stykkisholmúr, Iceland and therefore it is likely that similar periods of climatic stability and instability are recognised throughout northern Europe and possibly southern Europe. The periods of increased sand movement, and hence increased windiness, recognised in the Orkney Islands identified and discussed in Chapter 5 are shown in Figure 6.2, and this diagram also includes several sites in Ireland, Denmark and other parts of Scotland to try and identify similar periods of instability within north-west Europe. It has been observed that for many of the unstable periods identified in the Orkney Islands similar periods are recognised in north-west Europe. These are discussed below in more detail.

6.2.1 The Mesolithic and Neolithic periods

None of the sites sampled for OSL dating in the Northern Isles of Orkney record significant sand movement during the Mesolithic but Vega Leinert *et al.* (2000) identified Mesolithic sand movement at the Bay of Skaill, Mainland Orkney, based on radiocarbon dates from intertidal peat deposits, and evidence of Mesolithic sand movement has been found in other areas of north-west Europe (e.g. the Southern Isles of the Outer Herbides, NW and SW Ireland and the west coast of Denmark, Figure 6.2). The apparent lack of sand movement in the Mesolithic in the Northern Isles may suggest that any beach/dune systems that did exist were stable. Alternatively, since sea level was much lower during the Mesolithic than at present (Figure 6.3) it is more likely that any sand movement that did occur during this period did not extend substantially inland (or uphill) and has more limited preservation potential.

At deglaciation (approximately 14,000 radiocarbon years ago in Orkney), much of the Orkney Island archipelago would have been one island due to the low sea level (~ 100 metres below present sea level). Sea level rose rapidly over the period 12000-5000 years and progressively flooded the low-lying land creating individual till-covered islands separated by channels. Current research by A. Rennie (University of Glasgow) on the shoreline response to changes in sediment supply and sea level on a submerging coastline has indicated that by about 7000 years ago the island of Sanday was probably a small archipelago (Rennie and Hansom 2001). However, as sea level continued to rise, gravels

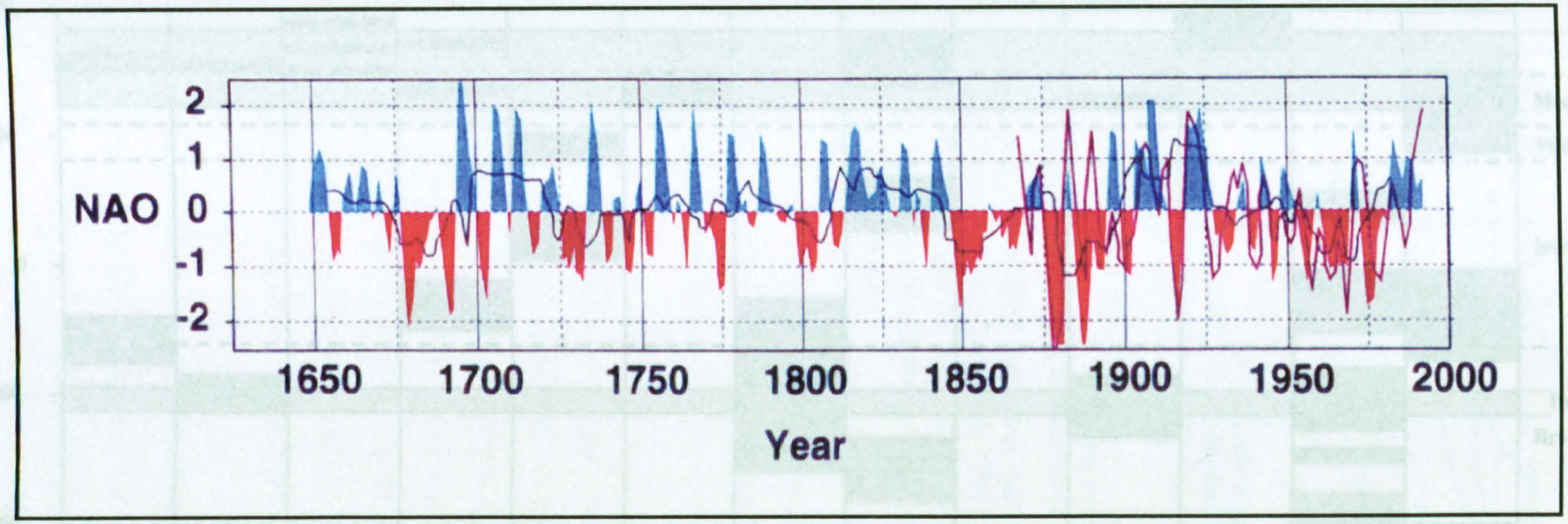

Figure 6.1 – The pattern of change in the North Atlantic Oscillation Index (NAO) from 1650 AD to present (after Appenzeller *et al.* 1998). A positive NAO index is an indication of a greater pressure gradient between the Azores high and the Icelandic low and this results in stormier conditions. Several periods of increased storm activity can be identified e.g. 1690's, 1720's, 1760's, 1810-1840 and 1910 AD. The black line running through the data is a running mean for the dataset and the purple trend line from c.1865 is the pattern of NAO changes as calculated using historical air pressure data.

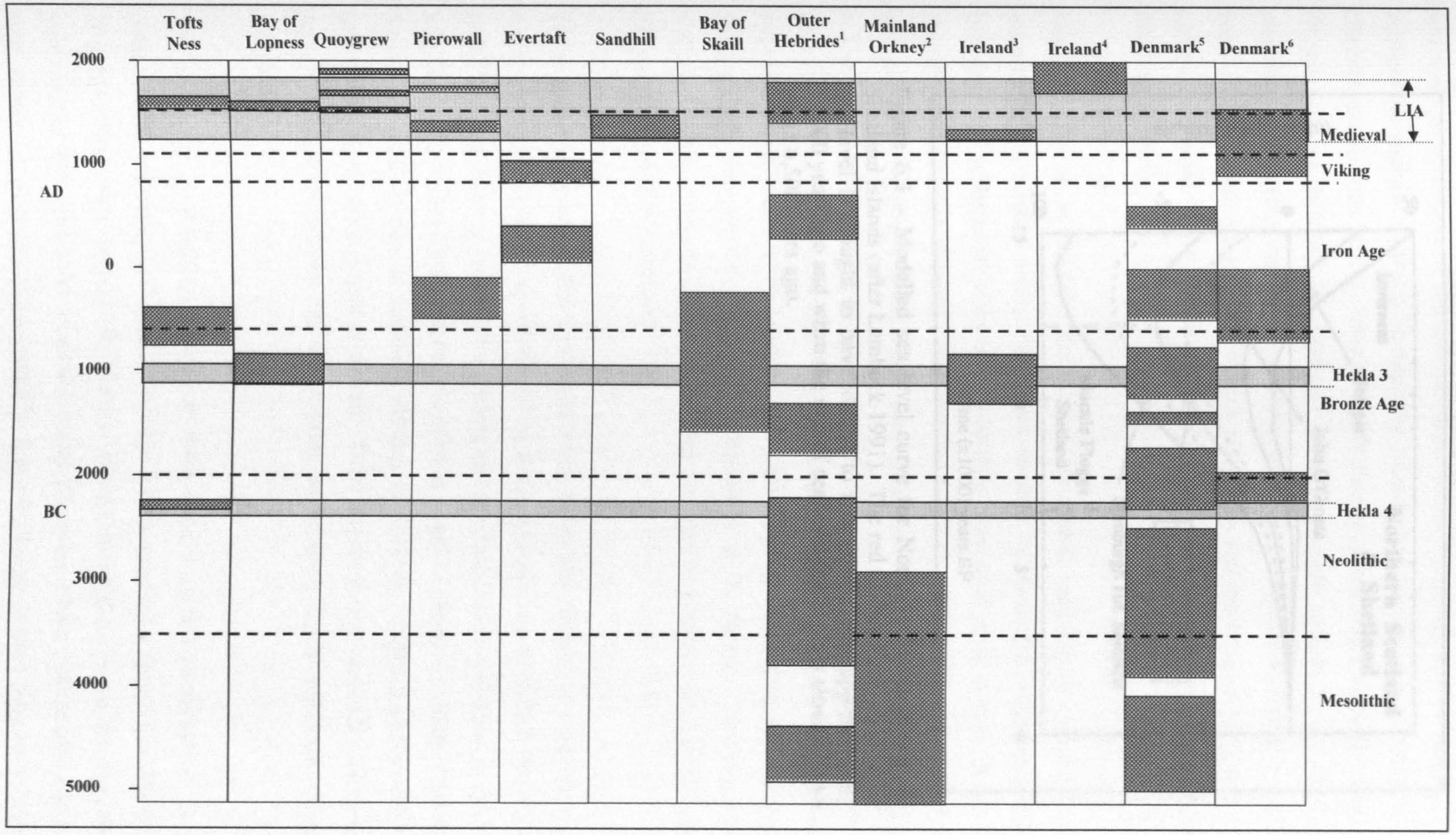

Figure 6.2 – Periods of increased sand movement (shaded areas) identified in the Orkney Islands and north-west Europe.

1) Gilbertson *et al.* 1999; 2) Leinert *et al.* 2000; 3) Wilson and Braley 1997; 4) Wintle *et al.* 1998; 5) Clemmensen *et al.* 2001a; 5) Clemmensen *et al.* 2001b

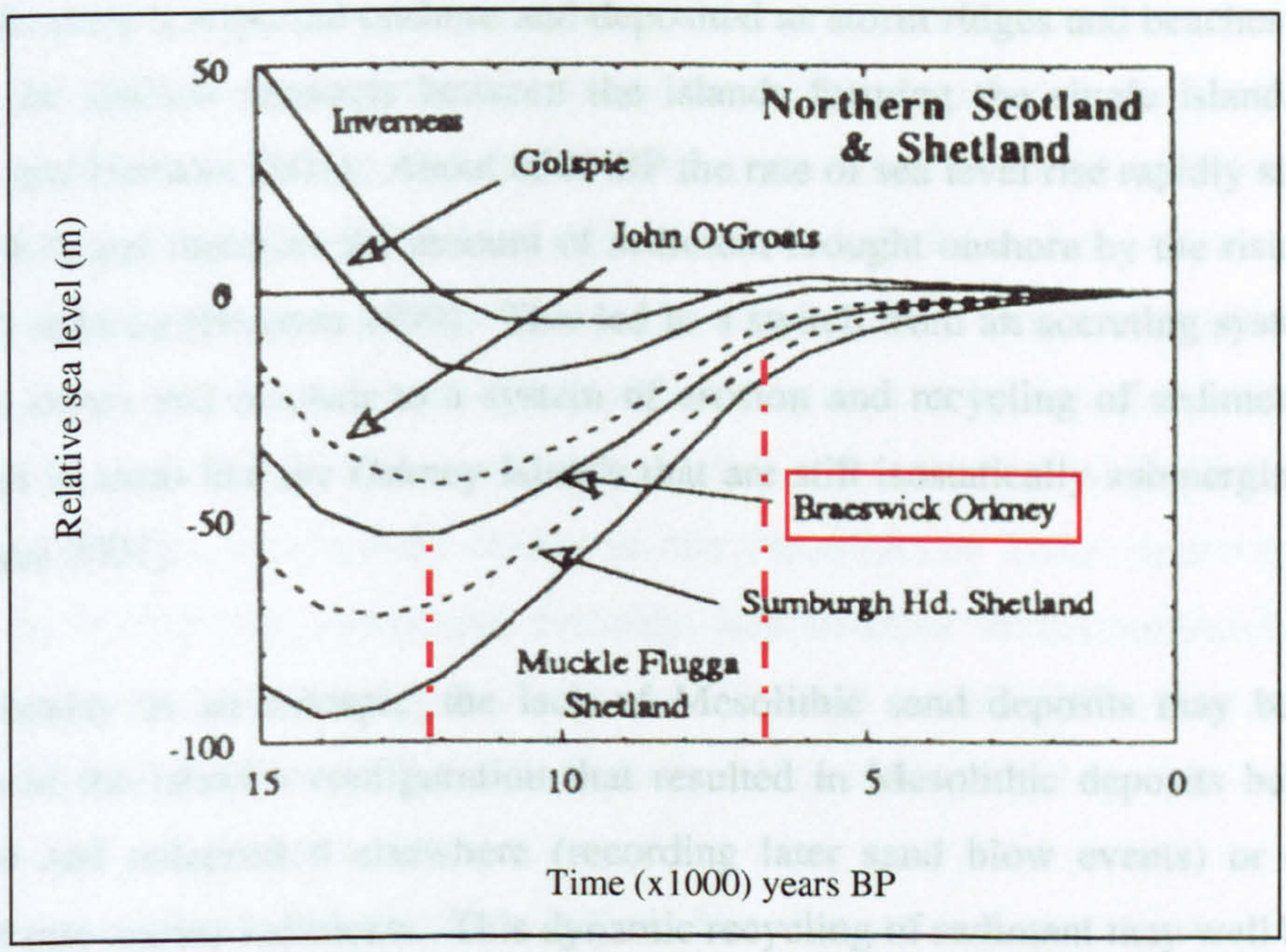

Figure 6.3 – Modelled sea level curve for Northern Scotland and the Shetland Islands (after Lambeck 1991). The red dashed lines show when sea level is thought to have started to rise in this area approximately 12,000 years ago and when the rate of sea level rise rapidly slowed down about 6,500 years ago.

and sands were transported onshore and deposited as storm ridges and beaches that slowly infilled the shallow channels between the islands forming the single island of Sanday (Rennie and Hansom 2001). About 6500 BP the rate of sea level rise rapidly slowed down (Figure 6.3) and therefore the amount of sediment brought onshore by the rising sea level was also reduced (Hansom 1999). This led to a switch from an accreting system forming beaches, dunes and machair to a system of erosion and recycling of sediment, which is enhanced in areas like the Orkney Islands that are still isostatically submerging (Hansom and Angus 2001).

Using Sanday as an example, the lack of Mesolithic sand deposits may be related to changes in the island's configuration that resulted in Mesolithic deposits being eroded, bleached and redeposited elsewhere (recording later sand blow events) or eroded and recycled into marine sediments. This dynamic recycling of sediment may well be expected on such a low-lying sand-filled island, such as Sanday, that is continually submerging. At any one date rapid sand deposition down-wind (e.g. Tofts Ness) is supplied by erosion of beaches and dunes up-wind (e.g. Bay of Lopness). Thus the potential for recording an event affecting both sites is greater down-wind than up-wind since the sediments have been eroded from the latter to produce deposition at the former. For example, under dominant southerly storms Iron Age sand deposits may be absent at the Bay of Lopness but appear down-wind at Tofts Ness.

There is currently no evidence to suggest that Eday was formed in a similar manner to Sanday since it is higher and surrounded by deep channels. Nevertheless, the coastlines of both Eday and Westray are actively eroding and any Mesolithic sand deposits that did exist are likely to have been removed and recycled in a similar fashion to those of Sanday. The Mesolithic sand deposits identified in the Bay of Skaill by Vega Leinert *et al.* (2000) are intertidal and are being eroded at present. Their preservation is due to the sheltered nature of the bay, which protects the beach from large storm waves generated in the North Atlantic.

The Neolithic is generally thought to have been a period characterised by warmer temperatures and drier conditions favourable for the growth of crops in northern latitudes (Ritchie 1995), but in most of NW Europe, climatic oscillations in the Neolithic have been recorded by fluctuations in woodland cover (Tipping 1994). Although anthropogenic deforestation may, in part, be responsible, it is not thought to have been on a large enough

scale to significantly reduce woodland cover without the assistance of a climate component (Barclay 1998). Neolithic sand movements have been recorded in the Northern Isles of Orkney at Tofts Ness (Sanday) and also in other parts of Northern Europe, e.g. the Southern Isles of the Outer Hebrides (Gilbertson *et al.* 1999) and the Vejers dunefield on the west coast of Denmark (Clemmensen *et al.* 2001a). From the sites sampled so far there appears to be no other evidence for sand movement at this time in the Northern Isles (Figure 6.2) (although other unsampled sites may contain such deposits). The identification of sand deposits dating to the Neolithic at Tofts Ness suggests early occupation during this period and, possibly, improvement of the surrounding land for agriculture using ash and organic material (Dockrill *et al.* 1994) that enhanced the preservation potential of Neolithic wind blown sands on the site.

OSL dating of the wind blown sands at Tofts Ness has reinterpreted the age of a palaeosol lying directly below wind blown sands in Test Pit 2. The palaeosol was previously interpreted as dating to the Bronze Age by Guttmann (2001) because it stratigraphically overlies Neolithic midden deposits, however the OSL dates from the overlying sand layer date to the Neolithic and therefore the 'Bronze Age' palaeosol should now be reinterpreted as a Neolithic palaeosol.

The age of the sand layer in Test Pit 2 is similar to other samples at Tofts Ness allowing a weighted mean OSL age to be calculated providing a depositional date of 2260 ± 100 BC. This period is regarded as the late Neolithic and environmental evidence suggests that there was a deterioration in climate at this time. This deterioration is recorded by the decline of Scots Pine (*Pinus sylvestris*) in Northern Scotland at approximately 2000 BC (Gear and Huntley 1991; Blackford *et al.* 1992). Northern Scotland is beyond the northern limit of Scots pine today but sub-fossil tree stumps and pine pollen have been identified in peat deposits in Sutherland and Caithness, indicating that pine trees did grow in these marginal areas. Blackford *et al.* (1992) proposed that the decline in pine pollen may have been related to the acidic volcanic ash fallout from the Hekla 4 eruption in Iceland (~2350-2250 BC, Pilcher *et al.* 1996), or to a volcanically induced deterioration in climate. Recent volcanic activity indicates that eruptions do have an influence on climate, resulting in cooler temperatures and wetter conditions (Baillie 1989, Birks 1994; Grattan *et al.* 1999). The date of the Hekla 4 eruption (~2350-2250 BC) correlates well with the period of increased sand movement identified at Tofts Ness (2260 ± 100 BC) (Figure 6.2), which likely led to, or contributed to, the temporary abandonment of the site. Although there is

no direct evidence of Hekla 4 tephra in the Northern Isles of Orkney, tephra from Hekla 4 has been identified nearby on Hoy (Dugmore *et al.* 1995) and in other parts of the United Kingdom (Dugmore *et al.* 1995; Pilcher and Hall 1996; Pilcher *et al.* 1996). Climate was probably already deteriorating in the late Neolithic but it seems likely that there was a further deterioration in climate after the Hekla 4 eruption that may have resulted in increased marginalisation of land and the temporary or permanent abandonment of sites such as Tofts Ness. Another site in the Orkney Islands that may have been abandoned as a result of further climatic deterioration and increased storm activity after the Hekla 4 eruption is the Neolithic village of Skara Brae on Mainland Orkney. Radiocarbon dates from animal bones collected from the final phase of occupation suggest abandonment of the site about 2450 cal BC (Clarke 1976a). The village is thought to have been temporarily abandoned due to sand inundation in an earlier occupation phase, however it is currently not clear how much time elapsed between the two phases of occupation (Clarke 1976a). OSL dating of these deposits may provide the answer to this. It seems likely that Hekla 4 exacerbated a late Neolithic climate deterioration which affected Orkney and other parts of Scotland and north-west Europe.

6.2.2 The Bronze Age

Although the climate had started to deteriorate in the late Neolithic, into the start of the Bronze Age, agriculture and woodland cover remained relatively extensive. However, a deterioration in climate in the Bronze Age resulted in the spread and growth of peat and heather moorland at the expense of agriculture and woodland cover (Davidson and Jones 1985; Tipping 1994; Edwards and Whittington 1997; Barrett 1999). This deterioration in climate was likely to have been accompanied by an increase in storm activity as discussed previously. Two of the sites sampled in Orkney record sand movement during the Bronze Age; Bay of Lopness and Bay of Skaill (Figure 6.2) and similar periods of climatic instability are recorded from the Uists in the Outer Hebrides (Gilbertson *et al.* 1999), in north-west Ireland (Wilson and Braley 1997) and at the Vejers dunefield in western Denmark (Clemmensen 2001a) (Figure 6.2).

Two of the Bay of Lopness samples date to this period and a weighted mean OSL age was calculated providing a date of 1015 ± 140 BC for sand deposition. This is very similar to the age of the Hekla 3 eruption, which is thought to have erupted sometime between 1160-920 BC (Eiríksson *et al.* 2000) during the late Bronze Age (Figure 6.2). Evidence for

the Hekla 3 eruption in north-west Europe is limited but Burgess (1989) suggested that it is represented in an apparent gap in the late Bronze Age settlement history of northern Scotland and increased growth rings in a speleothem in north-west Scotland have been dated to 1135 ± 130 BC by Baker *et al.* (1995). Other evidence for a period of climatic instability in the late Bronze Age linked to Hekla 3 has come from Irish oak tree ring evidence which suggests that climate deteriorated for about 20 years after the eruption (Baillie 1989). In north-west Europe a period of increased sand movement dating to the this period has been identified in north-west Ireland and the Vejers dunefield in Denmark (Figure 6.2). The late Bronze Age sand deposits at the Bay of Lopness may be related to the subsequent climatic deterioration after the Hekla 3 eruption. Bronze Age sand deposits were also identified at the Bay of Skaill, however the OSL date has low precision and suggests deposition in the late Bronze Age (765 ± 620 BC). Further sampling for OSL dating below this deposit may identify the Hekla 3 event.

The impact of climate deterioration on the local community of Sanday is not known from the site at the Bay of Lopness since there is no archaeology lying directly above the coastal section that was sampled. The lack of archaeology may indicate that that site was abandoned after deposition of the midden however since a farm exists today on top of a settlement mound only 250 metres from the section, it can be suggested that the site has been settled, perhaps continuously, since at least the Bronze Age. It seems likely that in the same way as occurred after Hekla 4, the Hekla 3 eruption led to enhanced marginalisation of agriculture and destabilisation of sandy areas leading to greater susceptibility to wind blow events.

6.2.3 The Iron Age

Climate continued to deteriorate in the late Bronze/early Iron Age. This further reduced the amount of available land for agriculture and is thought to be one of the reasons for the development of brochs in northern Scotland (Armit 1990). Evidence for a cooler and wetter climate is recorded in peat bogs in north-west Scotland and throughout the United Kingdom based on the identification of recurrence surfaces (Turner 1981; Anderson 1998). These surfaces mark the point at which there was rejuvenation of the bog due to an increase in the amount of water available (Blackford 1993; Anderson 1998). Further evidence for the expansion of peat and heathland comes from sites throughout western and northern Scotland (e.g. Lewis and the Orkney Islands) where prehistoric field systems and

ard marks have been discovered underneath blanket peat deposits (Lamb 1984; Bohncke 1988; Ritchie 1995; Whittington and Edwards 1997).

Evidence for deteriorating environmental conditions during the Iron Age are also recorded by shifts of settlement. On North Uist in the Outer Hebrides early prehistoric settlements were located in eastern and central locations but in the Iron Age these inland locations had been abandoned in favour of coastal sites (Figure 6.4a-c). Subsequent movement showed settlement gravitating towards the sandier west coast (Armit 1998). The remains of early settlements in eastern and central areas of the Uists indicate that these areas were once suitable for settlement but a deterioration of climate and expansion of peat may have contributed to their abandonment. The sandy machair plain and associated resources on the west coast would have been an attractive alternative (Armit 1998).

Four of the seven sites sampled here (Tofts Ness, Pierowall, Evertaft and Bay of Skaill, Figure 6.2) in the Orkney Islands record increased sand movement during the Iron Age and these sites are located on three of the four islands sampled (Sanday, Westray and Mainland). Although sand movement of this age was not recorded at Bay of Lopness or Quoygrew this should not imply that the sites were not affected and it was suggested in Chapter 5 that the absence of such deposits at the Bay of Lopness is likely to be due to erosion of sand and redeposition elsewhere dating to this period, possibly under erosional southerly wind events. The recognition of increased wind activity throughout the Orkney archipelago lends support to the archaeological and environmental evidence for a cooler and wetter period in the Iron Age, a period of climatic instability clearly recorded at both the Vejers and Lodbjerg dune systems on the Danish west coast (Figure 6.2, Clemmensen *et al.* 2001a and b). Late Iron Age sand movement has also been recorded in the Southern Isles of the Outer Hebrides (Figure 6.2) (Gilbertson *et al.* 1999) and the onset of sand deposition at Low Hauxley, Northumberland also occurred at this time (Sommerville *et al.* forthcoming).

The upper sand layers at Tofts Ness were OSL dated to the early Iron Age and a weighted mean suggests deposition approximately 625 ± 185 BC and this correlates with the abandonment of the site about 410 ± 290 BC. The similar dates suggest that it is possible that the site was abandoned due to drifting sand/sand inundation. However, there is little indication from the other sites sampled how the movement of sand during this period affected the local population. The OSL dates from Evertaft indicate occupation in the Late

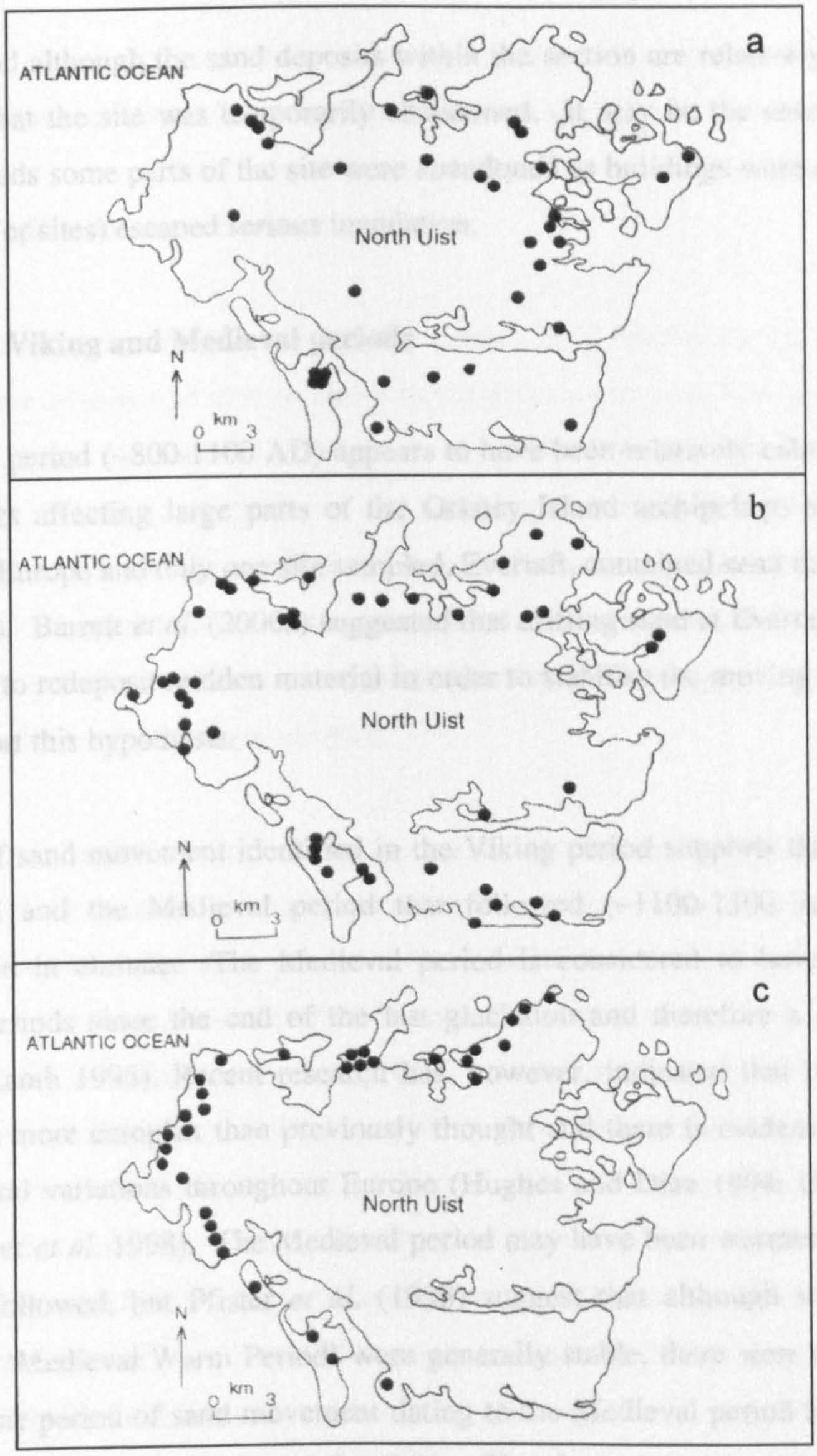

Figure 6.4 – The movement of people from the central and eastern areas of North Uist to the west coast: a) distribution of causewayed and walled islets; b) distribution of atlantic roundhouses; c) distribution of post-Medieval settlement (after Armit 1998).

Iron Age and although the sand deposits within the section are relatively thick there is no indication that the site was temporarily abandoned. It may be the case that during such stormy periods some parts of the site were abandoned as buildings were engulfed, whereas other parts (or sites) escaped serious inundation.

6.2.4 The Viking and Medieval periods

The Viking period (~800-1100 AD) appears to have been relatively calm in terms of large storm events affecting large parts of the Orkney Island archipelago and other areas of north-west Europe and only one site sampled, Evertaft, contained sand dating to this period (Figure 6.2). Barrett *et al.* (2000a) suggested that drifting sand at Evertaft caused the local inhabitants to redeposit midden material in order to stabilise the moving sand and the OSL dates support this hypothesis.

The lack of sand movement identified in the Viking period supports the view that during this period and the Medieval period that followed (~1100-1500 AD) there was an amelioration in climate. The Medieval period is considered to have been one of the warmest periods since the end of the last glaciation and therefore a period of climatic stability (Lamb 1995). Recent research has, however, indicated that climate during this period was more complex than previously thought and there is evidence of both regional and temporal variations throughout Europe (Hughes and Diaz 1994; Ogilvie and Farmer 1997; Pfister *et al.* 1998). The Medieval period may have been warmer than the Little Ice Age that followed, but Pfister *et al.* (1998) suggest that although winter temperatures during the 'Medieval Warm Period' were generally stable, there were colder and warmer phases. One period of sand movement dating to the Medieval period is recognised in the Orkney Islands at Pierowall and Sandhill. The dates from the middle sand layer in Pierowall and the 10 test pits on Sandhill are very similar and they provide a weighted mean OSL date of 1385 ± 45 AD. Sand movement at this time is also recorded in north west Ireland by Wilson and Braley (1997) and at the Lodbjerg dunes in Denmark by Clemmensen *et al.* (2001b) (Figure 6.2). Despite the identification of increased sand movement during the Medieval period at two sites in Orkney, lending support to the current thoughts on fluctuations in climate patterns during this period, most of the sites sampled do not record such a period of sand movement. This may imply that the majority of dune systems were stable and there was little erosion and redeposition, however it is

possible that deterioration of the climate during the subsequent Little Ice Age, and its attendant erosion, may have erased earlier records of sand deposition.

6.2.5 The Little Ice Age

The Little Ice Age is clearly represented at almost all of the sites sampled for OSL dating in the Orkney Islands and also in many locations in north-west Europe e.g. the Southern Isles of the Outer Hebrides (Gilbertson *et al.* 1999), NW and SW Ireland (Wilson and Braley 1997; Wintle *et al.* 1998), at the Lodbjerg dunefield in Denmark (Clemmensen 2001b) (Figure 6.2) and in north-east England (Wilson *et al.* 2001; Sommerville *et al.* forthcoming). Sand deposition during this period is not recorded at Evertaft or the Bay of Skaill however both sites are actively eroding and Little Ice Age deposits may be located further inland from the sections sampled.

All of the OSL samples from the Orkney Islands that date to the Little Ice Age are shown in Figure 6.5 and three distinct periods of sand movement can be identified. A weighted mean of the dates within each group has been calculated to identify if any specific storm events occurred at that time. The first period of increased sand movement in the Northern Isles of Orkney occurred approximately 1500 ± 15 AD and although no specific storms are recorded by Lamb (1991) or Hickey (1997) this period of increased sand movement coincides with the Rental Records of Sinclair (AD 1492) which noted areas of land abandoned due to drifting sand in Sanday. One such area that may have been abandoned due to drifting sand is at the Bay of Lopness where thick deposits of wind blown sand were laid down about 1515 ± 35 AD. This period of sand movement may be linked to another eruption of Hekla in 1510 AD, evidence of which has been identified elsewhere in the British Isles (Dugmore *et al.* 1996), but this eruption is thought to be much smaller than Hekla 3 and 4 and therefore it may not have had such a large environmental impact. Other evidence for increased sand movement is recorded in the rental records for Scatness, southern Shetland, where between 1550 and 1590 AD, farmers petitioned for reduced rent due to the loss of land through sand blow (A. Dawson *pers. comm.*).

The second period of sand movement identified in the Orkney Islands occurred approximately 1710 ± 15 AD and Hickey (1997) recorded sand movement and coastal flooding at Culbin and Findhorn, respectively, at this time. The village of Culbin and 16 farms were buried in sand in AD 1694 and as a result of the disaster, an Act was passed in

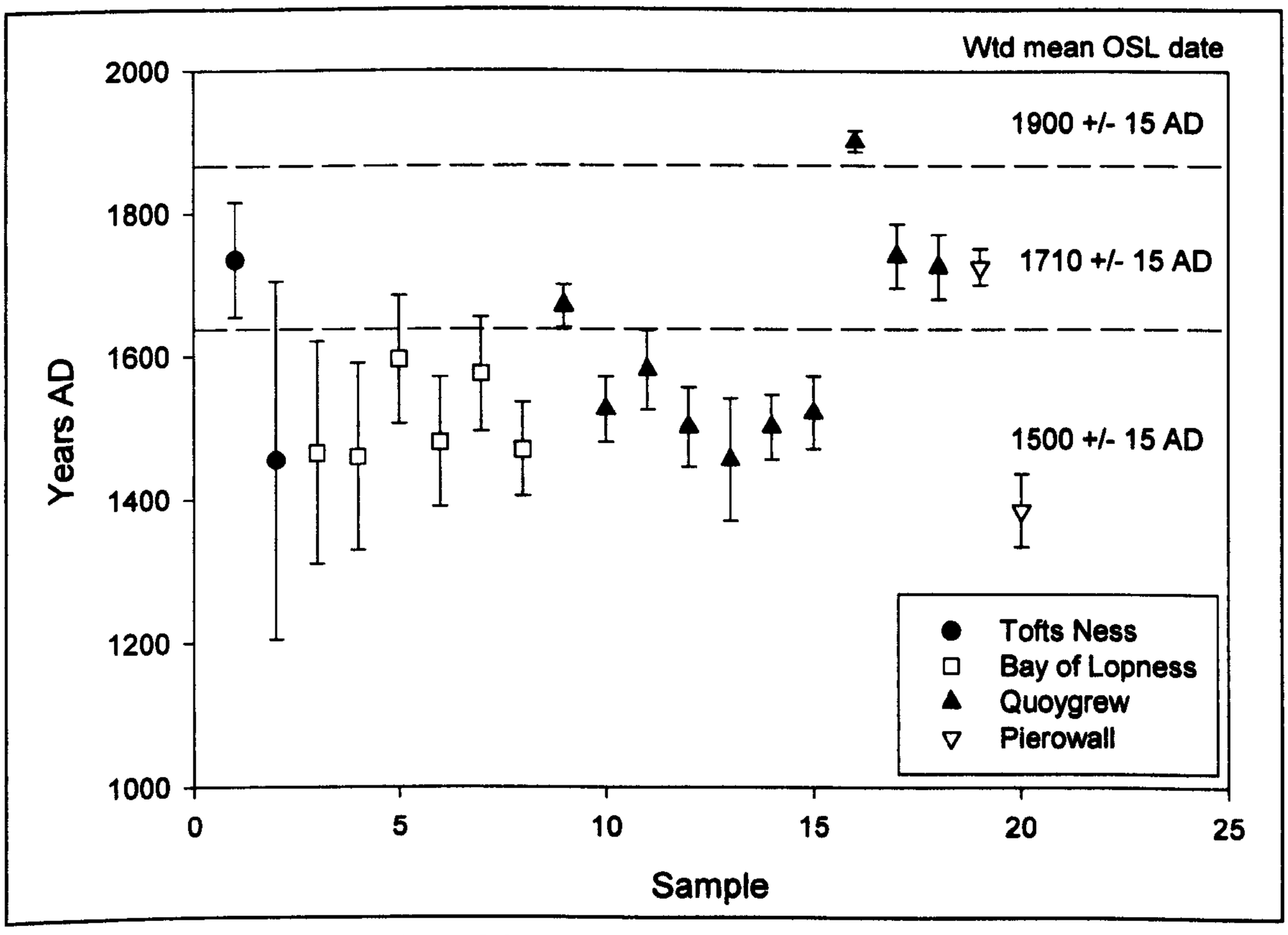

Figure 6.5 – The identification of three periods of sand movement within the Little Ice Age from the OSL dates

the Scottish Parliament the following year preventing the removal of marram grass from sand dunes (Willis 1986). Lamb (1991) also records a storm in AD 1697 that buried the site of Udal on North Uist (Outer Hebrides). Historical records from the Outer Hebrides note that during this storm the very fertile land on south-east Pabbay was overwhelmed by sand leading to the abandonment of farms in the area (Crawford 1967; May and Hansom 2003). The 17th century AD also saw the onset of rapid sand deposition and wind blow at the Loch of Strathbeg and the coastal village of Rattray in Aberdeenshire, a process that was complete by 1720 AD and led to the closure of the harbour inlet and the abandonment of the settlement of Rattray (Willis 1986; May and Hansom 2003). Further evidence for increased sand blow in the mid 18th century AD comes from Forvie, also in Aberdeenshire, where the proprietor of the estate felt it was necessary to reduce the tenant farmers rent due to sand damage (Willis 1986).

The final period of sand movement in the Little Ice Age, or just after, recorded in the Orkney Islands by OSL dating, is represented by sample SUTL 902 from Quoygrew and this was deposited about 1900 ± 15 AD (Figure 6.5). Both Lamb (1991) and Hickey (1997) have identified several storm events in the late 19th/early 20th century that may have deposited the sand layer from which this sample was collected. The NAO index, discussed in Section 6.2, is positive in the early 20th century AD (Figure 6.1) and this supports the identification of increased storminess and sand blow at this time.

Quoygrew is the only site sampled that is known to have been settled during the Viking/early Medieval period onwards and therefore the potential impact of sand deposits on the local inhabitants will be discussed in more detail. The weighted mean OSL dates from the midden (Area G) and Test Pit 7 indicate that there was sand deposition about 1520 ± 20 AD, however it is not thought to have been extensive or severe enough to cause abandonment of the site. This is perhaps surprising given that the sand deposits in Test Pit 7 were rapidly deposited suggesting extensive sand movement at this time. The midden deposits at Quoygrew contain a distinct lower layer dominated by mammal bones and a well-defined upper layer that was sampled for OSL dating and is dominated by marine shells. The radiocarbon date from the midden of cal AD 1005-1260 is from the interface between the two layers and one of the questions Barrett *et al.* (2000a) raise is why there was intensification in the use of marine resources at this time. They suggest that the increase may be due to changes in economic activity or that disposal of shell material was moved to this area. Although the OSL samples from Area G date to the early 16th century

AD there may be a correlation between increased sand movement at the start of the Little Ice Age (about AD 1250, Grove 1988) and the increase in use of marine resources at this time. This implies that although the increase in sand movement did not cause the site to be abandoned, some areas of agricultural land may have been abandoned due to drifting sand resulting in a switch to, or the intensification in the use of, marine resources. Although sand deposits were not found over the archaeological site, drifting sand was probably a problem within the settlement itself.

The site of Quoygrew was originally referred to as Nether Trenabie, however today the farm of Trenabie is located on top of a hill overlooking the archaeological site. Barrett *et al.* (2000a) suggested that Quoygrew may have been the original location for the settlement and they proposed that it moved to its current location in the mid 18th century AD. This is based on details provided by Fereday (1990) who discussed the lives of the Balfour family in Orkney between AD 1747 and 1799. William Balfour was a supporter of the Jacobites and in AD 1746, after he refused to give himself up, his house at Trenaby (Trenabie) was burnt to the ground (Fereday 1990). Eight years later (AD 1754) he was able to build a two-storey house at Trenaby (Fereday 1990), and although details are not given as to where the new house was constructed it is likely to have been moved to the top of the hill at this time. The NAO index was strongly positive in the 1750's (Figure 6.1) and sand layers within Test Pits 101 and 102 also date to the mid 18th century AD, suggesting that the new house was built on top of the nearby hill to avoid the sand drifts. The improved plaggen land around Quoygrew appears to have still been in use at the end of the 18th century AD as shown by the development of an anthrosol above the mid 18th century AD wind blown sand deposits in Test Pit 101 and 102. Although the anthrosol has not been radiocarbon dated the OSL date from the upper sand layer in Test Pit 102 provides a *terminus post quem* in the late 19th century AD. The OSL dates from Quoygrew indicate that there was a great deal of sand movement in the area during the Little Ice Age. Initially the inundation of sand may have been slow and thus had little effect on the residents, however drifting sand was a problem elsewhere on Westray (e.g. land ruined by blowing sand at Gill Farm, Fereday 1990), and may have affected Quoygrew.

There are undoubtedly many sites that were inundated by sand during the Little Ice Age but the continued build-up of the land at Quoygrew has ensured that these deposits have been preserved in a similar fashion to the Neolithic sand deposits at Tofts Ness. The identification of three periods of sand movement within the Little Ice Age in the Orkney

Islands shows that OSL dating can accurately date young wind blown sands that are sufficiently sensitive to artificial irradiation. It also supports the view of Grove (1988) that climatic fluctuations occurred within the Little Ice Age and that some periods deviated more from the longer-term climatic norms than others.

6.3 Summary of Chapter 6

Several periods of increased wind activity have been identified in the Orkney Islands by OSL dating of wind blown sands from archaeological sites, these periods of climatic instability also being recorded in coastal sites in north-west Europe and other environmental records derived from tree rings and peat bogs. Phases of increased sand blow that have been identified occurred in the Neolithic, the Bronze Age, two periods in the Iron Age, the Viking/Medieval period and the Little Ice Age (Figure 6.2). At least two and possibly three periods of increased sand blow in the Orkney Islands correlate with various eruptions of Hekla: 2350-2250 BC (Hekla 4), 1160-920 BC (Hekla 3) and possibly 1510 AD. A deterioration in climate is thought to accompany large volcanic eruptions and it has been suggested that Tofts Ness and possibly Skara Brae, may have been abandoned at the time of the Hekla 4 eruption. This is not to say that the sites were abandoned directly as a result of the Hekla eruption but that at a time when climate was already deteriorating, the eruption may have contributed to the climatic instability. It is thought that this is the first time that a possible correlation has been recognised between increased sand movement and the deterioration in climate in the Orkney Islands and the Hekla 4 and 3 eruptions in Iceland.

The recent development of the NAO index has shown that climate during the last 400 years and specifically the Little Ice Age has fluctuated and this is supported by the OSL dates from most sites sampled in the Orkney Islands. The impact of drifting sand or sand inundation on the local population can only be inferred and although one or two large storm events may be recorded in the sites sampled, the majority of samples suggest that drifting sand was perhaps more of a concern to the local inhabitants and that ultimately this may have led to the abandonment of land.

Chapter 7 – Conclusions

The main aims of this project are to use OSL to successfully date wind blown sands from archaeological sites in Northern Scotland and in doing so to identify periods of increased sand movement in the Holocene in the Orkney Islands. In order to accept the dates with confidence experiments were undertaken on modern beach sands to establish the extent and rate of bleaching of quartz and feldspar in controlled and natural conditions using modern beach sands collected from the Orkney Islands and Outer Hebrides. The following conclusions can be drawn reflecting the aims of the work outlined above and in Chapter 1.

- OSL has proved to be a reliable and robust technique that can successfully date wind blown sands from archaeological sites in the Orkney Islands. The OSL dates of the sand collected from the archaeological sites have provided accurate environmental and archaeological information that has aided the interpretation, or reinterpretation, of the individual sites sampled. In an area where the use of other dating methods is often precluded by a lack of organic material, OSL dating has proved a viable technique that can accurately date sediments either naturally transported and deposited or exposed by anthropogenic activity, in the mid- to late-Holocene.

- The OSL dating has identified six periods of increased sand movement in the Holocene in the Orkney Islands. The periods of climatic deterioration recognised in the Orkney Islands match those identified at other sites within Scotland and north-west Europe and are consistent with chronologies derived from other environmental indicators such as tree rings and peat bogs. It has been shown that the earliest sand deposits in the Orkney Islands date to the late Neolithic, a period of increased sand blow that may relate to the climatic deterioration that is thought to have occurred after the eruption of Hekla 4 and possibly resulting in the temporary, or permanent, abandonment of land or sites in Europe. Only one Orkney site sampled for OSL dating contained Neolithic deposits, however it is thought very likely that other archaeological sites in the Orkney Islands will contain such deposits. Several sites contain Bronze Age deposits (possibly related to Hekla 3) and Iron Age deposits, but others do not. The lack of such deposits at other sites sampled may indicate either that adjacent dune systems were stable and there was no deposition, or more likely, that sand movement and subsequent erosion and redeposition has erased any record of sand deposited in these time periods. For deposition to occur, erosion of some areas is

essential and so up-wind source areas may have been eroded during the Bronze and Iron Age to provide down-wind deposition at the same time period. The Viking/Medieval period is generally thought to have been a relatively stable period, however there are OSL dates from several sites which suggest that there was some sand movement in this period, supporting recent thoughts on climatic fluctuations within the 'climatic optimum' of the Medieval period. Almost all sites sampled contain Little Ice Age sand deposits and the identification of four periods of increased storm activity during this period contributes to the current knowledge of climatic fluctuations within the Little Ice Age. The impact of sand movement and deposition on the local communities can only be inferred. The OSL dates suggest that although large storm events are relatively frequent, drifting sand from lesser events was a common problem in the Northern Isles of Orkney. The former led to the immediate abandonment of land, but the latter may have contributed to increased marginality and slower abandonment.

- In order to have confidence in the above OSL dates and wider correlations several methodological issues have been addressed in the OSL techniques. These are bulleted below.

- The modified SAR procedure has successfully dated wind blown sands from archaeological sites in the Orkney Islands despite the low sensitivity of some samples. There appears to be no thermal erosion of the main OSL signal using preheat temperatures of between 240-280°C and the test dose normalisation successfully corrects for sensitivity changes in 80% of the discs dispensed. The test dose preheat used is different to that currently used elsewhere and although it does not appear to significantly increase quartz sensitivity in these samples, further research on samples from different geological areas is needed to determine if there is any such influence.

- The SAR results have shown that sample sensitivity can be a major limiting factor for accurate OSL dating of wind blown sands and it should not be assumed that samples from the same geological area have the same sensitivity. Based on the assumption that quartz sensitivity increases throughout the SAR run, it is proposed here that fitting a linear statistical trend through the test dose data may reduce some of the scatter observed in the regenerative dose response curves of low sensitive samples. This will allow an exponential or linear line to be fitted through the corrected regenerative data and an age calculated for the aliquot, however precision may still be low due to variations in the natural signals or

partial bleaching. Further research is required to determine if this is a feasible solution for dating low sensitive samples.

- It is suggested here that the variable response of samples from the same site to artificial irradiation indicates that the sand layers from which the samples were collected have a different provenance. Comparing the sensitivity of the archaeological samples with the response of modern beach sands to artificial irradiation may identify a source for the archaeological samples. None of the modern beaches on Sanday responded as well to artificial irradiation as the archaeological samples and therefore it was not possible to accurately determine a modern source for the highly sensitive samples, for example at Tofts Ness and Bay of Lopness. A similar analysis was undertaken on the samples from Westray but the source of only one sample from Evertaft was potentially identified. Since the sediment provenance of the archaeological samples is not from the local modern beaches, the original terrestrial source either no longer exists (it has been eroded away) or it now lies offshore due to the continual submergence and erosion of the shoreline. The latter scenario is most likely given the Holocene evolution of the Orkney coastline.

- Modern beach sands from the study area do have slight residual OSL signals and these may be significant when attempting to date young samples from the area. A comparison with samples from the Outer Hebrides has shown that these beaches have lower residual levels than the beaches in the Orkney Islands. It is suggested that in addition to the length of exposure and the light intensity, there may be a geological control on the rate and extent of bleaching. In addition to geological variations there is also a mineralogical control with quartz from both the Outer Hebrides and Orkney Islands having a greater residual signal than feldspars. Rapid bleaching of the quartz OSL signal requires exposure not only to visible wavelengths but also to UV wavelengths and therefore if clouds block the shorter wavelengths this will reduce the bleaching rate of quartz. Not all quartz samples from modern beaches have significant residual levels and thus the amount of potential residual signal contributing to the natural OSL signal of an archaeological sample will vary depending on the sediment provenance of the sand being dated.

- The bleaching experiments undertaken both in the laboratory and in the field have shown that light intensity is a major control on the rate and extent of bleaching prior to burial. Sand exposed to natural daylight in the Orkney Islands had a significant OSL signal remaining after 4 days of exposure. The residual OSL signal of sand eroded,

transported and deposited several times prior to burial is likely to be low in comparison to sand that has been deposited during large storm events when light levels are low. The intensity of light that the sand is exposed to prior to burial is especially important when dating sand layers from archaeological sites in high latitude areas, where the length of daylight during the winter months is restricted to a few hours and there is an increase in the frequency of storms.

- A potential new method to identify partially bleached samples, the psi (ψ) ratio, has been proposed using the shape of the natural and regenerated decay curves of feldspar to determine the contribution from the unbleached or residual component in the natural OSL signal. Questions still remain as to why the natural curve of some samples is steeper than the regenerated curve resulting in negative psi (ψ) ratios. However, although several reasons have been proposed, further research is required before this method can be confidently used in routine OSL dating.

Areas of future research

This study has identified several possibilities for future research and these are summarised as follows:

- OSL dating of sand deposits from the Orkney Islands has aided the interpretation of the archaeological sites sampled and provided information for climatic reconstruction that can be applied across north-west Europe. However, there is a lack of luminescence studies spanning the Holocene and OSL has the potential to date a much wider range of archaeological and non-archaeological sites.

- The identification of the original sediment source of the highly sensitive samples needs to be resolved and it has been suggested that the source may be former till deposits that now lie offshore. Till does outcrop at a few terrestrial sites in the Northern Isles of Orkney, e.g. Bay of Lopness, and analysis of these till deposits should help to identify the sediment provenance of the highly sensitive samples. Cross-linking the OSL work with ongoing sediment budget and sea level change research in Orkney is likely to be a profitable area of future research.

- Fully bleached samples lie at the core of accurate OSL dating and this study has shown that light intensity is a major controlling factor on the rate of bleaching of both quartz and feldspar. There was a considerable residual signal after 4 days of exposure to Orcadian light however it is not known how quickly these same samples would bleach under optimal conditions and experiments now need to be undertaken to determine this. Further bleaching experiments in the field and laboratory for various lengths of time, with variable light intensities and with separated minerals will enhance our understanding of the bleaching process.

- It has become apparent that in addition to the environmental control on the rate and extent of bleaching, i.e. light intensity, there appears to be a geological control as shown by the comparison between the Orkney Islands and Outer Hebrides residual levels and the bleaching experiments. Comparing these results with similar residual and bleaching experiments on samples collected from modern beaches on the Shetland Islands and/or mainland Scotland, which have different bedrock lithologies, would confirm is there is a geological control.

- The psi ratio has been introduced as a potential new method to identify partially bleached samples. Late light subtraction was not considered in the initial psi ratio analysis and this method should be applied to determine if it effectively removes any residual signal that is still contained within the grains. For some samples the decay shapes of the quartz and feldspar grains behave differently when exposed to artificial irradiation and this raises further questions regarding the bleaching rate and geological background of the various minerals. These questions need to be resolved, possibly be comparing the decay curves of samples from a variety of areas with different bedrock geology, before the technique can be used in routine OSL dating.

References

Aitken, M.J. (1974) *Physics and archaeology*. Clarendon Press, Oxford.

Aitken, M.J. (1985) *Thermoluminescence Dating*. Academic Press, London.

Aitken, M.J. (1989) Luminescence dating: a guide for non-specialists. *Archaeometry*, 31, 2, 147-159.

Aitken, M.J. (1990) *Science-based dating in archaeology*. Longman, New York.

Aitken, M.J. (1998) *An Introduction to Optical Dating: The dating of Quaternary sediments by the use of Photon-Stimulated Luminescence*. Oxford Science Publications, Oxford.

Aitken, M.J., Tite, M.S. and Reid, J. (1963) Thermoluminescent dating: progress report. *Archaeometry*, 6, 65-75.

Aitken, M.J. and Smith, B.W. (1988) Optical dating: recuperation after bleaching. *Quaternary Science Reviews*, 7, 387-393.

Aitken, M.J. and Xie, J. (1992) Optical dating using infrared diodes: young samples. *Quaternary Science Reviews*, 11, 147-152.

Anderson, D.E. (1998) A reconstruction of Holocene climatic changes from peat bogs in north-west Scotland. *Boreas*, 27, 208-224.

Angus, S. and Elliott, M.M. (1992) Erosion in Scottish machair with particular reference to the Outer Hebrides. In, *Coastal Dunes: geomorphology, ecology and management for conservation*. Edited by R.W.G Carter, T.G.F. Curtis and M.J. Sheehy-Skeffington, Balkema, Rotterdam, p93-112.

Anthony, I., Houston, I. and Sanderson, D.C.W. (1999/2000) *An investigation of bleaching of luminescence from quartz and feldspars under laboratory safelights*. Internal report, Scottish Universities Research and Reactor Centre.

Anthony, I., Sanderson, D., Housley, R., Downes, J. and Robertson, J. (2000) Eday burnt mounds, Orkney (Eday parish), archaeological works. *Discovery and Excavation in Scotland*, 2000, 63.

Anthony, I.M.C., Sanderson, D.C.W., Cook, G.T., Abernethy, D. and Housley, R.A. (2001) Dating a burnt mound from Kilmartin, Argyll, Scotland. *Quaternary Science Reviews*, 20, 5-9, 921-926.

Appenzeller, C., Stocker, T.F. and Anklin, N. (1998) North Atlantic Oscillation dynamics recorded in Greenland ice cores. *Science*, 282, 446-449.

Armit, I. (1990) Epilogue: The Atlantic Scottish Iron Age. In, *Beyond the Brochs*. Edited by I. Armit, Edinburgh University Press, Edinburgh, p194-210.

Armit, I. (1992) *The Later Prehistory of the Western Isles of Scotland.* BAR, British Series 221.

Armit, I. (1997) *Celtic Scotland.* Historic Scotland.

Armit, I. (1998) Human responses to marginality. In, *Life on the Edge: Human Settlement and Marginality.* Edited by C.M. Mills and G. Coles, Oxbow Monograph 100, Oxford, p31-38.

Armit, I. and Ralston, I.B.M. (1997) The Iron Age. In, *Scotland: Environment and Archaeology, 8000BC-AD1000.* Edited by K.J. Edwards and I.B.M. Ralston, John Wiley and Sons, Chichester, p169-193.

Ashmore, P.J. (1996) *Neolithic and Bronze Age Scotland.* B.T.Batsford Ltd, London.

Ashmore, P.J. (1999) Dating the ring of stones and chambered cairn at Calanais. *Antiquity*, 73, 128-130.

Baden-Powell, D.F.W. (1938) On the glacial and interglacial marine beds of Northern Lewis. *Geological Magazine*, 75, 395-409.

Baden-Powell, D.F.W. and Elton, C. (1937) On the relationship between a raised beach deposit and an Iron Age midden on the Island of Lewis. *Proceedings of the Society of Antiquaries of Scotland*, 71, 347-365.

Bailey, R.M. (2000) The interpretation of quartz optically stimulated luminescence equivalent dose versus time plots. *Radiation Measurements*, 32, 129-140.

Bailey, R.M., Smith, B.W. and Rhodes, E.J. (1997) Partial bleaching and the decay form characteristics of quartz OSL. *Radiation Measurements*, 27, 2, 123-136.

Baker, A., Smart, P.L., Barnes, W.L., Edwards, R.L. and Farrant, A. (1995) The Hekla 3 volcanic eruption recorded in a Scottish speleothem? *The Holocene*, 5, 3, 336-342.

Ballantyne, C.K. and Dawson, A.G. (1997) Geomorphology and Landscape Change. In, *Scotland: Environment and Archaeology, 8000 BC- AD 1000.* Edited by K.J. Edwards and I.B.M. Ralston. John Wiley and Sons Ltd, p23-44.

Baillie, M.G.L. (1982) *Tree-Ring Dating and Archaeology.* Croom Helm, London.

Baillie, M.G.L. (1989) Hekla 3: how big was it? *Endeavour*, New Series, 13, 2, 78-81.

Banerjee, D. and Bøtter-Jensen, L. and Murray, A.S. (2000) Retrospective dosimetry: estimation of the dose to quartz using the single-aliquot regenerative-dose protocol. *Applied Radiation and Isotopes*, 52, 831-844.

Banerjee, D., Murray, A.S., Bøtter-Jensen, L. and Lang, A. (2001) Equivalent dose estimation using a single aliquot of polymineral fine grains. *Radiation Measurements*, 33, 73-94.

Barclay, G.J. (1998) *Farmers, Temples and Tombs: Scotland in the Neolithic and Early Bronze Age*. Canongate Books, Edinburgh.

Barfield, L. and Hodder, M. (1987) Burnt mounds as saunas, and the prehistory of bathing. *Antiquity*, 61, 370-379.

Barne, J.H., Robson, C.F., Kaznowska, S.S., Doody, J.P., Davidson, N.C. and Buck, A.L. (1997) *Coasts and seas of the United Kingdom: Region 2 Orkney*. Joint Nature Conservation Committee.

Barrett, J.C. (1999) Rethinking the Bronze Age environment. *Quaternary Proceedings*, 7, 493-500.

Barrett, J., Simpson, I. and Davis, T. (1997) Quoygrew-Nether Trenabie. *Discovery and Excavation in Scotland*, 1997, p61.

Barrett, J., James, H. and O'Connor, T. (2000a) *Excavations at Quoygrew, Westray, Orkney: Interim Report 2000*. Unpublished report, Department of Archaeology, University of York.

Barrett, J., Beukens, R., Simpson, I., Ashmore, P., Poaps, S. and Huntley, J. (2000b) What was the Viking Age and When did it Happen? A view from Orkney. *Norwegian Archaeological Review*, 33, 1, 1-39.

Barry, R.G. and Chorley, R.J. (1971) *Atmosphere, Weather and Climate*. Methuen and Co. Ltd., London.

Bell, W.T. and Zimmerman, D.W. (1978) The effect of HF acid etching on the morphology of quartz inclusions for thermoluminescence dating. *Archaeometry*, 20, 1, 63-65.

Berger, G.W. (1988) Dating Quaternary events by luminescence. *Geological Society of America*, Special Paper 227, 13-50.

Berger, G.W. and Huntley, D.J. (1982) Thermoluminescence dating of terrigenous sediments. *PACT*, 6, 495-504.

Berry, R.J. (1985) *The Natural History of Orkney*. Collins, London.

Birks, H.J.B. (1994) Did Icelandic volcanic eruptions influence the post-glacial vegetational history of the British Isles. *Trends in Ecology and Evolution*, 9, 312-314.

Blackford, J. (1993) Peat bogs as sources of proxy climatic data: past approaches and future research. In, *Climate Change and Human Impact on the Landscape*. Edited by F.M. Chambers, Chapman and Hall, London, p47-56.

Blackford, J.J., Edwards, K.J., Dugmore, A.J., Cook, G.T. and Buckland, P.C. (1992) Icelandic volcanic ash and the mid-Holocene Scots pine (Pinus sylvestris) pollen decline in northern Scotland. *The Holocene*, 2, 3, 260-265.

Bluszcz, A. (2001) Simultaneous OSL and TL dating of sediments. *Quaternary Science Reviews*, 20, 761-766.

Boggs, S. (1995) *Principles of Sedimentology and Stratigraphy*. Prentice Hall, New Jersey.

Bohncke, S.J.P. (1988) Vegetation and habitation history of the Callanish area, Isle of Lewis, Scotland. In, *Cultural Landscape: Past, Present and Future*. Edited by H.H. Birks, H.J.B. Birks, P.E. Kaland and D. Moe, Cambridge University Press, Cambridge, p445-461.

Bothner, M.H. and Johnson, N.M. (1969) Natural thermoluminescent dosimetry in Late Pleistocene pelagic sediments. *Journal of Geophysical Research*, 74, 22, 5331-5338.

Bøtter-Jensen, L. (1997) Luminescence techniques: instrumentation and methods. *Radiation Measurements*, 27, 5/6, 749-768.

Bøtter-Jensen, L. and Duller, G.A.T. (1992) A new system for measuring optically stimulated luminescence from quartz samples. *Nuclear Tracks and Radiation Measurements*, 20, 4, 549-553.

Bøtter-Jensen, L., Duller, G.A.T. and Poolton, N.R.J. (1994) Excitation and emission spectrometry of stimulated luminescence from quartz and feldspars. *Radiation Measurements*, 23, 2/3, 613-616.

Bøtter-Jensen, L., Duller, G.A.T., Murray, A.S. and Banerjee, D. (1999a) Blue light emitting diodes for optical stimulation of quartz in retrospective dosimetry and dating. *Radiation Protection Dosimetry*, 84, 1-4, 335-340.

Bøtter-Jensen, L., Mejdahl, V. and Murray, A.S. (1999b) New light on OSL. *Quaternary Geochronology*, 18, 303-309.

Bøtter-Jensen, L., Bulur, E., Duller, G.A.T. and Murray, A.S. (2000) Advances in luminescence instrument systems. *Radiation Measurements*, 32, 523-528.

Boyle, R. (1664) *Experiments and considerations upon colours with observations on a diamond that shines in the dark.* Henry Herringham, London.

Briggs, D. (1977) *Sediments*. Butterworths, London.

Burcham, W.E. (1973) *Nuclear physics: an introduction*. Longman, London.

Burgess, C. (1989) Volcanoes, catastrophe and the global crisis of the late second millennium BC. *Current Archaeology*, 10, 325-329.

Campbell, E.N., Housley, R.A. and Taylor, M. (in press) Charred food residues from Hebridean Iron Age pottery: analysis and dating. In, *Atlantic Connections and Adaptations: economies, environments and subsistence in lands bordering the North Atlantic*. Edited by R.A Housley and G. Coles, Oxbow Books, Oxford.

Carr, S.J., Haflidason, H. and Sejrup, H.P. (2000) Micromorphological evidence supporting Late Weichselian glaciation of the Northern North Sea. *Boreas*, 29, 315-328.

Caseldine, C.J. and Whittington, G. (1975) Appendix 2. Pollen analysis from the Stones of Stenness, Orkney. *Proceedings of the Society of Antiquaries of Scotland*, 107, 37-40.

Childe, V.G. (1931) *Skara Brae: A Pictish village in Orkney*. Kegan Paul, Trench, Trubner and Co Ltd., London.

Childe, V.G. (1954) Maes Howe. *Proceedings of the Society of Antiquaries of Scotland*, **88**, 155-172.

Childe, V.G. and Paterson, J.W. (1929) Provisional report on the excavations at Skara Brae, and on finds from the 1927 and 1928 campaigns. *Proceedings of the Society of Antiquaries of Scotland*, 63, 225-280.

Choi, J.H., Murray, A.S., Jain, M., Cheong, C.S. and Chang, H.W. (2003) Luminescence dating of well-sorted marine terrace sediments on the southeastern coast of Korea. *Quaternary Science Reviews*, 22, 2-4, 407-421.

Church, M. (1998) *Archaeological evaluation of two subterranean, drystone dwellings exposed by coastal erosion at Galson, Isle of Lewis; November 1997 and August 1998.* Unpublished internal report, Report no. 407, Centre for Field Archaeology, University of Edinburgh.

Clark, R.J. (1992) *Photostimulated Luminescence as an Archaeological Dating Tool.* Unpublished Ph.D. thesis, University of Glasgow.

Clark, R.J. and Sanderson, D.C.W. (1994) Photostimulated luminescence excitation spectroscopy of feldspars and micas. *Radiation Measurements*, 23, 2/3, 641-646.

Clark, R.J., Bailiff, I.K. and Tooley, M.J. (1997) A preliminary study of time-resolved luminescence in some feldspars. *Radiation Measurements*, 27, 2, 211-220.

Clarke, D.V. (1976a) *The Neolithic Village at Skara Brae, Orkney: 1972-73 Excavations: an interim report*. Department of the Environment, H.M.S.O., Edinburgh.

Clarke, D.V. (1976b) Excavations at Skara Brae a summary account. In, *Settlement and Economy in the Third and Second Millennia BC.* Edited by C. Burgess and R. Miket, British Archaeological Reports 33, p233-250.

Clarke, D.V., Hope, R. and Wickham-Jones, C. (1978) The Links of Noltland. *Current Archaeology*, 6, 44-46.

Clarke, M.L. (1996) IRSL dating of sands: bleaching characteristics at deposition inferred from the use of single aliquots. *Radiation Measurements*, 26, 4, 611-620.

Clarke, M.L. and Rendell, H.M. (1997) Infra-red stimulated luminescence spectra of alkali feldspars. *Radiation Measurements*, 27, 2, 221-236.

Clarke, M.L. and Rendell, H.M. (2000) The development of a methodology for luminescence dating of Holocene sediments at the land-ocean interface. In, *Holocene Land-Ocean Interaction and Environmental Change around the North Sea.* Edited by I. Shennan and J. Andrews, Geological Society, Special Publications 166, London, 69-86.

Clarke, M.L., Rendell, H.M., Hoare, P.G., Godby, S.P. and Stevenson, C.R. (2001) The timing of coversand deposition in northwest Norfolk, UK: a cautionary tale. *Quaternary Science Reviews*, 20, 705-713.

Clemmensen, L.B., Andreasen, F., Heinemeier, J. and Murray, A. (2001a) A Holocene coastal aeolian system, Vejers, Denmark: landscape evolution and sequence stratigraphy. *Terra Nova*, 13, 129-134.

Clemmensen, L.B., Pye, K., Murray, A. and Heinemeiers, J. (2001b) Sedimentology, stratigraphy and landscape evolution of a Holocene coastal dune system, Lodbjerg, NW Jutland, Denmark. *Sedimentology*, 48, 3-27.

Colls, A.E., Stokes, S., Blum, M.D. and Straffin, E. (2001) Age limits on the Late Quaternary evolution of the upper Loire River. *Quaternary Science Reviews*, 20, 743-750.

Crawford, I.A. (1967) Hebridean settlement at Siabaidh, Berneray, Harris. *Post Medieval Archaeology*, 1, 84-89.

Crawford, I. and Switsur, R. (1977) Sandscaping and C14: the Udal, N. Uist. *Antiquity*, 51, 124-136.

Critchfield, H.J. (1983) *General Climatology*. Prentice-Hall Inc., New Jersey.

Dalland, M. (1992a) Scar: a Viking boat burial. *Current Archaeology*, 11, 475-477.

Dalland, M. (1992b) Scar (Cross and Burness parish): Viking boat grave. *Discovery and Excavation in Scotland*, 1993, p81-82.

Daniels, F., Boyd, C.A. and Saunders, D.F. (1953) Thermoluminescence as a research tool. *Science*, 117, 343-349.

Daniell, W. (1821) *A voyage around Great Britain*. Longman, Hurst, Rees and Brown, London.

Davidson, D.A. and Jones, R.L. (1985) The Environment of Orkney. In, *The Prehistory of Orkney*. Edited by C. Renfrew, Edinburgh University Press, p10-35.

Dawson, A.G., Smith, D.E. and Dawson, S. (2001) *Potential impacts of climate change on sea levels around Scotland*. Research Survey and Monitoring Report No. 178, Scottish Natural Heritage.

Dickson, C. (2000) The decline of woodland in Orkney: Early Neolithic to Late Iron Age. In, *People as an Agent of Environmental Change*. Edited by R.A. Nicholson and T.P. O'Connor, Oxbow Books, Oxford, p37-44.

Dickson, C. and Dickson, J. (2000) *Plants and People in Ancient Scotland*, Tempus, Stroud.

Dickson, J.H. (1992) North American driftwood, especially *Picea* (spruce), from archaeological sites in the Hebrides and Northern Isles of Scotland. *Review of Palaeobotany and Palynology*, 73, 49-56.

Dockrill, S.J., Bond, J.M., Milles, A., Simpson, I. and Ambers, J. (1994) Tofts Ness, Sanday, Orkney. An integrated study of a buried Orcadian landscape. In, *Whither Environmental Archaeology*. Edited by R. Luff and P. Rowley-Conwy, Oxbow Monograph 38, p115-132.

Dreimanis, A., Hütt, G., Raukas, A. and Whippey, P.W. (1978) Dating methods of Pleistocene deposits and their problems: 1. Thermoluminescence dating. Geoscience Canada, 5, 55-60.

Dugmore, A.J., Larsen, G. and Newton, A.J. (1995) Seven tephra isochrones in Scotland. *The Holocene*, 5, 3, 257-266.

Dugmore, A.J., Newton, A.J., Edwards, K.J., Larsen, G., Blackford, J.J. and Cook, G.T. (1996) Long-distance marker horizons from small-scale eruptions: British tephra deposits from the AD 1510 eruption of Hekla, Iceland. *Journal of Quaternary Science*, 11, 6, 511-516.

Duller, G.A.T. (1991) Equivalent dose determination using single aliquots. *Nuclear Tracks and Radiation Measurements*, 18, 4, 371-378.

Duller, G.A.T. (1994) Luminescence dating of poorly bleached sediments from Scotland. *Quaternary Science Reviews*, 13, 5-7, 521-524.

Duller, G.A.T. (1997) Behavioural studies of stimulated luminescence from feldspars. *Radiation Measurements*, 27, 5/6, 663-694.

Duller, G.A.T., Wintle, A.G. and Hall, A.M. (1995) Luminescence dating and its application to key Pre-Late Devensian sites in Scotland. *Quaternary Science Reviews*, 14, 5, 495-519.

Duller, G.A.T., Bøtter-Jensen, L. and Mejdahl, V. (1999) An automated iterative procedure for determining palaeodoses using the SARA method. *Quaternary Geochronology*, 18, 293-301.

Duller, G.A.T., Bøtter-Jensen, L. and Murray, A.S. (2000) Optical dating of single sand-sized grains of quartz: sources of variability. *Radiation Measurements*, 32, 453-457.

Edlin, H.L. (1976) The Culbin Sands. *Environment and Man (Reclamation)*, 4, 1-31.

Edwards, A.J.H. (1924) Report on the excavation of an earth-house at Galson, Borve, Lewis. *Proceedings of the Society of Antiquaries of Scotland*, 58, 185-203.

Edwards, K.J. (1996) A Mesolithic of the Western and Northern Isles of Scotland? Evidence from Pollen and Charcoal. In, *The Early Prehistory of Scotland.* Edited by T. Pollard and A. Morrison, Edinburgh University Press, Edinburgh, p23-38.

Edwards, K.J. and Whittington, G. (1997) Vegetation Change. In, *Scotland: Environment and Archaeology, 8000BC-AD1000.* Edited by K.J. Edwards and I.B.M. Ralston, John Wiley and Sons, Chichester, p63-82.

Eiríksson, J., Knudsen, K.L., Haflidason, H. and Heinemeier, J. (2000) Chronology of late Holocene climatic events in the northern North Atlantic based on AMS 14C dates and tephra markers from the volcano Hekla, Iceland. *Journal of Quaternary Science*, 15, 6, 573-580.

Farrow, G.E., Allen, N.H and Akpan, E.B. (1984) Bioclastic carbonate sedimentation on a high-latitude, tide-dominated shelf: northeast Orkney Islands, Scotland. *Journal of Sedimentary Petrology*, 54, 2, 373-393.

Fereday, R.P. (1990) *The Orkney Balfours 1747-99*. Tempvs Reparatvm

Fleming, S.J. (1966) Study of thermoluminescence of crystalline extracts from pottery. *Archaeometry*, 9, 170-173.

Fleming, S.J. (1970) Thermoluminescent dating: refinement of the quartz inclusion method. *Archaeometry*, 12, 2, 133-145.

Fleming, S.J. (1973) The pre-dose technique: a new thermoluminescent dating method. *Archaeometry*, 15, 1, 13-30.

Fleming, S.J. (1979) *Thermoluminescence techniques in archaeology*. Clarendon Press, Oxford.

Flett, J.S. (1920) The submarine contours around the Orkneys. *Transactions of the Edinburgh Geological Society*, 11, 42-49.

Flinn, D. (1978) The glaciation of the Outer Hebrides. *Geological Journal*, 13, 2, 195-199.

Fojut, N. (1993) *The Brochs of Gurness and Midhowe*. Historic Scotland. HMSO, Edinburgh.

Fojut, N., Pringle, D. and Walker, B. (1994) *The ancient monuments of the Western Isles*. Historic Scotland, HMSO, Edinburgh.

Fraser, D. (1983) *Land and Society in Neolithic Orkney*. BAR, British Series 117, Oxford.

Galloway, R.B. (1992) Towards the use of green light emitting diodes for the optically stimulated luminescence dating of quartz and feldspar. *Measurement Science and Technology*, 3, 330-335.

Galloway, R.B., Hong, D.G. and Napier, H.J. (1997) A substantially improved green-light-emitting diode system for luminescence stimulation. *Measurement Science and Technology*, 8, 267-271.

Gear, A.J. and Huntley, B. (1991) Rapid changes in the range limits of Scots Pine 4000 years ago. *Science*, 251, 544-547.

Geikie, J. (1873) On the glacial phenomena of the Long Island or Outer Hebrides. First Paper. *Proceedings of the Geological Society*, 29, 532-545.

Geikie, J. (1878) On the glacial phenomena of the Long Island or Outer Hebrides. Second Paper. *Quarterly Journal of the Geological Society*, 34, 819-867.

Gilbertson, D.D., Schwenninger, J.-L, Kemp, R.A. and Rhodes, E.J. (1999) Sand-drift and soil formation along an exposed North Atlantic coastline: 14,000 years of diverse geomorphological, climatic and human impacts. *Journal of Archaeological Science*, 26, 439-469.

Godfrey-Smith, D.I. (1994) Thermal effects in the optically stimulated luminescence of quartz and mixed feldspars from sediments. *Journal of Physics D Applied Physics*, 27, 1737-1746.

Godfrey-Smith, D.I., Huntley, D.J. and Chen, W.-H. (1988) Optical dating studies of quartz and feldspar sediment extracts. *Quaternary Science Reviews*, 7, 373-380.

Graham-Campbell, J. and Batey, C.E. (1998) *Vikings in Scotland: an archaeological survey*. Edinburgh University Press, Edinburgh.

Grattan, J., Gilbertson, D. and Charman,. D. (1999) Modelling the impact of Icelandic volcanic eruptions upon the prehistoric societies and environment of northern and western Britain. In, *Volcanoes in the Quaternary*. Edited by C.R. Firth and W.J. McGuire, Geological Society Special Publications 161, London, p109-124.

Greig, S. (1940) *Viking Antiquities in Great Britain and Ireland, Part 2: Viking Antiquities in Scotland.* Edited by H. Shetelig, Aschehoug, Oslo.

Grogler, N., Houtermans, F.G. and Stauffer, H. (1960) Ueber die Datierung von Keramik und Ziegel durch Thermolumineszenz. *Helvetica Physica Acta*, 33, 595-596.

Grove, J.M. (1988) *The Little Ice Age*. Routledge, London.

Guérin, G. and Valladas, G. (1980) Thermoluminescence dating of volcanic plagioclases. *Nature*, 286, 697-699.

Guttmann, E.B. (2001) *Continuity and change in arable land management in the Northern Isles: Evidence from anthropogenic soils*. University of Stirling, unpublished thesis.

Hall, A.M. (1996) An introduction to the Prehistory of Orkney. In, *Quaternary of Orkney – Field Guide*. Edited by A.M. Hall, Quaternary Research Association, London, p30-36.

Hall, A.M. and Bent, A.J.A. (1990) The limits of the last British ice sheet in Northern Scotland and the adjacent shelf. *Quaternary Newsletter*, 61, 2-12.

Hall, A.M., Duller, G., Jarvis, J. and Wintle, A.G. (1995) Middle Devensian ice-proximal gravels at Howe-of-Byth, Grampian Region. *Scottish Journal of Geology*, 31, 61-64.

Hall, A.M., Gordon, J.E., Whittington, G., Duller, G.A.T. and Heijnis, H. (2002) Sedimentology, palaeoecology and geochronology of Marine Isotope Stage 5 deposits on the Shetland Islands, Scotland. *Journal of Quaternary Science*, 17, 1, 51-67.

Hansom, J.D. (1999) The coastal geomorphology of Scotland: understanding sediment budgets for effective coastal management. In, *Scotland's Living Coastline*. Edited by Baxter, J.M., Duncan, K., Atkins, K. and Lees, S.M., HMSO, Edinburgh, p34-44.

Hansom, J.D. (2001) Coastal sensitivity to environmental change: a view from the beach. *Catena*, 42, 291-305.

Hansom, J.D. and Angus, S. (2001) Tir a' machair (Land of the Machair): Sediment supply and climate change scenarios for the future of the Outer Hebrides machair. In, *Earth Science and the Natural Heritage*. Edited by J.E. Gordon and K.F. Lees, The Stationery Office, Edinburgh, p68-81.

Harkness, D.D. (1983) The extent of natural ^{14}C deficiency in the coastal environment of the United Kingdom. In, *^{14}C and Archaeology*, Groningen August 1981, p351-364.

Hedges, J.W. (1986) From the First Inhabitants to the Viking Settlement. In, *The People of Orkney*, edited by R.J. Berry and H.N. Firth, The Orkney Press, Kirkwall, p20-53.

Hickey, K.R. (1997) *Documentary record of coastal storms in Scotland, 1500-1991 AD.* Unpublished Ph.D. thesis, University of Coventry.

Hughes, M.K. and Diaz, H.F. (1994) Was there a 'Medieval Warm Period', and if so, where and when? *Climatic Change*, 109-142.

Huntley, D.J. and Johnson, H.P. (1976) Thermoluminescence as a potential means of dating siliceous ocean sediments. *Canadian Journal of Earth Sciences*, 13, 593-596.

Huntley, D.J., Godfrey-Smith, D.I. and Thewalt, M.L.W. (1985) Optical dating of sediments. *Nature*, 313, 105-107.

Hurrell, J.W. (1995) Decadal trends in the North Atlantic Oscillation: regional temperature and precipitation. *Nature*, 269, 676-679.

Hütt, G., Jaek, I. and Tchonka, J. (1988) Optical dating: K-feldspars optical response stimulation spectra. *Quaternary Science Reviews*, 7, 381-385.

Huxtable, J. and Jacobi, R.M. (1982) Thermoluminescence dating of burned flints from a British Mesolithic site: Longmoor Inclosure, East Hampshire. *Archaeometry*, 24, 2, 164-169.

Hydrographic Office (1899) *Tidal Streams: Coast of Scotland.* Admirality, London.

Jain, M. and Singhvi, A.K. (2001) Limits to depletion of blue-green light stimulated luminescence in feldspars: implications for quartz dating. *Radiation Measurements*, 33, 883-892.

James, H. (1999) Excavations of a medieval cemetery at Skaill House, and a cist in the Bay of Skaill, Sandwick, Orkney. *Proceedings of the Society of Antiquaries of Scotland*, 129, 743-777.

Jansen, J.H.F. (1976) Late Pleistocene and Holocene history of the northern North Sea, based on acoustic reflection records. *Netherlands Journal of Sea Research*, 10, 1, 1-43.

Jehu, T.J. and Craig, R.M. (1933) Geology of the Outer Hebrides. *Transactions of the Royal Society of Edinburgh*, 57, 3, 839-873.

Johnson, N.M. and Blanchard, R.L. (1967) Radiation dosimetry from the natural thermoluminescence of fossil shells. *The American Mineralogist*, 52, 1297-1310.

Jungner, H. and Bøtter-Jensen, L. (1994) Study of sensitivity change of OSL signals from quartz and feldspars as a function of preheat temperature. *Radiation Measurements*, 23, 2/3, 621-624.

Klein, C. (2002) *The 22nd edition of the manual of mineral science. John Wiley and Sons, Inc, New York.*

Kolstrup, E. and Mejdahl, V. (1986) Three frost wedge casts from Jutland (Denmark) and TL dating of their infill. *Boreas*, 15, 311-321.

Krause, W.E., Krbetschek, M.R. and Stolz, W. (1997) Dating of Quaternary lake sediments from the Schirmacher Oasis (East Antarctica) by infra-red stimulated luminescence (IRSL) detected at the wavelength of 560 nm. *Quaternary Science Reviews*, 16, 387-392.

Krbetschek, M.R., Götze, J., Dietrich, A. and Trautmann, T. (1997) Spectral information from minerals relevant for luminescence dating. *Radiation Measurements*, 27, 5/6, 695-748.

Lamb, H.H. (1977) *Climate Present, Past and Future volume 2, Climatic history and the future*. Methuen and Co. Ltd., London.

Lamb, H.H. (1985) The Little Ice Age period and the great storms within it. In, *The Climatic Scene*. Edited by M.J. Tooley and G.M. Sheail, George Allen and Unwin, London, p104-131.

Lamb, H.H. (1988) *Weather, climate and human affairs: a book of essays and other papers*. Routledge, London.

Lamb, H. (1991) *Historic storms of the North Sea, British Isles and Northwest Europe*. Cambridge University Press, Cambridge.

Lamb, H.H. (1995) *Climate, History and the Modern World*. Routledge, London.

Lamb, R.G. (1983) *Papa Westray and Westray (with adjacent small islands), Orkney Islands area: an archaeological survey*. Royal Commission on the Ancient and Historical Monuments of Scotland, Edinburgh.

Lamb, R.G. (1984) *Eday and Stronsay (with adjacent small islands), Orkney Islands area: an archaeological survey*. Royal Commission on the Ancient and Historical Monuments of Scotland, Edinburgh.

Lambeck, K. (1991) Glacial rebound and sea level change in the British Isles. *Terra Nova*, 3, 379-389.

Lamothe, M., Balescu, S. and Auclair, M. (1994) Natural IRSL intensities and apparent luminescence ages of single feldspar grains extracted from partially bleached sediments. *Radiation Measurements*, 23, 2/3, 555-561.

Lang, A. and Miuscov, V.F. (1967) Dislocations and fault surfaces in synthetic quartz. *Acta Crystallographica*, 12, 2377-2483.

Lang, A. and Wagner, G.A. (1997) Infrared stimulated luminescence dating of Holocene colluvial sediments using the 410 nm emission. *Quaternary Science Reviews*, 16, 393-396.

LeMarche, V.C. (1974) Palaeoclimatic inferences from long tree-ring records. *Science*, 183, 4129, 1043-1048.

Li, S, -H. (2002) Luminescence sensitivity changes of quartz by bleaching, annealing and UV exposure. *Radiation Effects and Defects in Solids*, 157, 357-364.

Li, S.-H. and Yin, G.-M. (2001) Luminescence dating of young volcanic activity in China. *Quaternary Science Reviews*, 20, 5-9, 865-868.

Lowe, J.J. and Walker, M.J.C. (1984) *Reconstructing Quaternary Environments*. Longman, Harlow.

Macdonald, C. (1982) *Lewis: The story of an Island*. Acair LTD.

Margolis, S.V. and Krinsley, D.H. (1971) Submicroscopic frosting on eolian and subaqueous quartz sand grains. *Geological Society of America Bulletin*, 82, 3395-3406.

Marwick, H. (1931/32) Notes on Viking burials in Orkney. *Proceedings of the Orkney Antiquarian Society*, 10, 27-29.

Mather, A.S., Smith, J.S. and Ritchie, W. (1974) *Beaches of Orkney*. Department of Geography, University of Aberdeen.

May, V.J. and Hansom, J.D. (2003) *Coastal geomorphology of Great Britain*. GCR Series. Joint Nature Conservation Committee, Peterborough.

McCoy, D.G., Prescott, J.R and Nation, R.J. (2000) Some aspects of single-grain luminescence dating. *Radiation Measurements*, 32, 859-864.

McDougall, D.J. (1968) *Thermoluminescence of Geological Materials*. Academic Press, New York.

McFee, S.W.S. and Tite, M.S. (1994) Investigations into the thermoluminescence properties of single quartz grains using an imaging photon detector. *Radiation Measurements*, 23, 355-360.

McKeever, S.W.S. (1985) *Thermoluminescence of solids*. Cambridge University Press, Cambridge.

Mejdahl, V. (1983) Feldspar inclusion dating of ceramics and burnt stones. *PACT*, 9, 351-364.

Mejdahl, V. (1985) Thermoluminescence dating of partially bleached sediments. *Nuclear Tracks and Radiation Measurements*, 10, 4-6, 711-715.

Mejdahl, V. (1988) The plateau method for dating partially bleached sediments by thermoluminescence. *Quaternary Science Reviews*, 7, 347-348.

Mejdahl, V. and Winther-Nielsen, M. (1982) TL dating based on feldspar inclusions, *PACT*, 6, 426-437.

Mejdahl, V. and Wintle, A.G. (1984) Thermoluminescence applied to age determination in archaeology and geology. In, *Thermoluminescence and Thermoluminescent Dosimetry, volume III.* Edited by Y.S. Horowitz, CRC Press Inc, Florida, p133-190.

Mejdahl, V. and Bøtter-Jensen, L. (1994) Luminescence dating of archaeological materials using a new technique based on single aliquot measurements. *Quaternary Geochronology*, 13, 551-554.

Mejdahl, V. and Christiansen, H.H. (1994) Procedures used for luminescence dating of sediments. *Quaternary Geochronology*, 13, 403-406.

Mercier, N., Valladas, H. and Valladas, G. (1995) Flint thermoluminescence dates from the CFR Laboratory at GIF: contributions to the study of the chronology of the Middle Palaeolithic. *Quaternary Science Reviews*, 14, 351-364.

Miller, D.H. (1981*) Energy at the surface of the Earth.* Academic Press, New York.

Moore, H. and Wilson, G. (2000) Links of Noltland, Westray, Orkney (Westray Parish), prehistoric settlement, burial. *Discovery and Excavation in Scotland*, 2000, 69.

Morris, C. (1979) Brough of Birsay (Birsay and Harray parish) building remains. *Discovery and Excavation in Scotland*, 1979, p21-22.

Morris, C. (1982) Skaill (Sandwick parish), survey. *Discovery and Excavation in Scotland*, 1982, 17.

Morris, C.D. (1989) *The Birsay Bay Project volume 1.* University of Durham, Department of Archaeology, Monograph Series no. 1.

Morris, C. (1991) The Viking and Early Settlement Archaeological Research Project. *Current Archaeology*, 11, 298-302.

Morris, C.D. (1993) The Birsay Bay Project: A Resume. In, *The Viking Age in Caithness, Orkney and the North Atlantic.* Edited by C.E. Batey, J. Jesch and C.D. Morris, Edinburgh University Press, Edinburgh, p285-307.

Morris, C.D. (1996) *The Birsay Bay Project volume 2.* University of Durham, Department of Archaeology, Monograph Series no. 2.

Morris, C.D., Emery, N., Owen, O.A., Rains, M.J. and Watt, H.M. (1985) Skaill, Sandwick, Orkney: Preliminary investigations of a mound-site near Skara Brae. *Glasgow Archaeological Journal*, 12, 82-92.

Morris, C.D. and Emery, N. (1986) The chapel and enclosure on the Brough of Deerness, Orkney: survey and excavations, 1975-1977. *Proceedings of the Society of Antiquaries of Scotland*, 116, 301-374.

Morrison, A. (1967) Harris Estate Papers, 1724-1754. *Transactions of the Gaelic Society of Inverness*, 45, 33-97.

Murray, A.S. (1996) Incomplete stimulation of luminescence in young quartz sediments and its effect on the regenerated signal. *Radiation Measurements*, 26, 1, 221-231.

Murray, A.S., Olley, J.M. and Caitcheon, G.G. (1995) Measurement of equivalent doses in quartz from contemporary water-lain sediments using optically stimulated luminescence. *Quaternary Science Reviews*, 14, 365-371.

Murray, A.S., Roberts, R.G. and Wintle, A.G. (1997) Equivalent dose measurement using a single aliquot of quartz. *Radiation Measurements*, 27, 2, 171-184.

Murray, A.S. and Roberts, R.G. (1998) Measurement of the equivalent dose in quartz using a regenerative-dose single-aliquot protocol. *Radiation Measurements*, 29, 5, 503-515.

Murray, A.S. and Wintle, A.G. (1998) Factors controlling the shape of the OSL decay curve in quartz. *Radiation Measurements*, 29, 1, 65-79.

Murray, A.S. and Mejdahl, V. (1999) Comparison of regenerative-dose single-aliquot and multiple-aliquot (SARA) protocols using heated quartz from archaeological sites. *Quaternary Geochronology*, 18, 223-229.

Murray, A.S. and Wintle, A.G. (2000) Luminescence dating of quartz using an improved single-aliquot regenerative-dose protocol. *Radiation Measurements*, 32, 57-73.

Murray, A.S. and Clemmensen, L.B. (2001) Luminescence dating of Holocene aeolian sand movement, Thy, Denmark. *Quaternary Science Reviews*, 20, 751-754.

Murray-Wallace, C.V., Banerjee, D., Bourman, R.P., Olley, J.M. and Brooke, B.P. (2002) Optically stimulated luminescence dating of Holocene relict foredunes, Guichen Bay, South Australia. *Quaternary Science Reviews*, 21, 1077-1086.

Mykura, W. (1976) *British Regional Geology. Orkney and Shetland.* Natural Environment Research Council, Edinburgh.

Mykura, W. (1991) Old Red Sandstone. In, *Geology of Scotland*, edited by G.Y. Craig, Geological Society, Bath, p297-344.

Nature Conservancy Council (1978) *Orkney – Localities of Geological and Geomorphological Importance.* Geology and Physiography Section, Nature Conservancy Council, Newbury.

Neighbour, T. and Church, M. (2001) *The eroding settlement and Iron Age cemetery at Galson, Isle of Lewis. Erosion face recording and geophysical survey.* Unpublished internal report, Report no. 625, Centre for Field Archaeology, University of Edinburgh.

New Stat. Acc. (1845) *The New Statistical Account of Scotland, 1845.*

Nieter, W.M. and Krinsley, D.H. (1976) The production and recognition of aeolian features on sand grains by silt abrasion. *Sedimentology*, 23, 713-720.

NMRS No. HY74NE 1 CANMORE database. The Royal Commission on the Ancient and Historical Monuments of Scotland.

O'Hare, G. and Sweeney, J. (1986) *The Atmospheric System.* Oliver and Boyd, Edinburgh.

Ogilvie, A. and Farmer, G. (1997) Documenting the Medieval climate. In, *Climates of the British Isles: present, past and future.* Edited by M. Hulme and E. Barrow, Routledge, London, p112-133.

Olley, J., Caitcheon, G. and Murray, A. (1998) The distribution of apparent dose as determined by optically stimulated luminescence in small aliquots of fluvial quartz: *implications for dating young sediments. Quaternary Science Reviews*, 17, 1033-1040.

Olley, J.M., Caitcheon, G.G. and Roberts, R.G. (1999) The origin of dose distributions in fluvial sediments, and the prospect of dating single grains from fluvial deposits using optically stimulated luminescence. *Radiation Measurements*, 30, 207-217.

Owen, O.A. (1993) Tuquoy, Westray, Orkney. A challenge for the future? In, *The Viking Age in Caithness, Orkney and the North Atlantic.* Edited by C.E. Batey, J. Jesch and C.D. Morris, Edinburgh University Press, Edinburgh, p318-339.

Owen, O. and Dalland, M. (1999) *Scar: a Viking boat burial on Sanday, Orkney.* Tuckwell, East Linton.

Peach, B.N. and Horne, J. (1880) The Glaciation of the Orkney Islands. *Quarterly Journal of the Geological Society of London*, 36, 648-663.

Peacock, J.D. (1981) Quaternary Research Association Excursion Guide – Lewis and Harris. *Quaternary Newsletter*, 35, 45-54.

Peacock, J.D. (1984) *Quaternary geology of the Outer Hebrides.* British Geological Survey Report, volume 16, no.2.

Peterkin, A. (1820) *Rentals of the ancient earldom and bishoprick of Orkney; with some other explanatory and relative documents.* Edinburgh.

Pettijohn, F.J., Potter, P.E. and Siever, R. (1987) *Sand and Sandstone.* Springer-Verlag.

Pfister, C., Luterbacher, J., Schwarz-Zanetti, G. and Wegmann, M. (1998) Winter air temperature variations in western Europe during the Early and High Middle Ages (AD 750-1300). *The Holocene*, 8, 5, 535-552.

Pilcher, J.R. and Hall, V.A. (1996) Tephrochronological studies in northern England. *The Holocene*, 6, 1, 100-105.

Pilcher, J.R., Hall, V.A. and McCormac, F.G. (1996) An outline of tephrochronology for the Holocene of the north of Ireland. *Journal of Quaternary Science*, 11, 6, 485-494.

Poolton, N.R.J. and Bailiff, I.K. (1989) The use of LEDs as an excitation source for photoluminescence dating of sediments. *Ancient TL*, 7, 1, 18-20.

Prasad, S. and Gupta, S.K. (1999) Luminescence dating of a 54m long core from Nal region, western India – implications. *Quaternary Science Reviews*, 18, 1495-1505.

Prescott, J.R. (1983) Thermoluminescence dating of sand dunes at Roonka, South Australia. *PACT*, 9, 505-512.

Prescott, J.R. and Stephan, L.G. (1982) The contribution of cosmic radiation to the environmental dose for thermoluminescent dating: Latitude, altitude and depth dependences. *PACT*, 6, 17-25.

Pye, K. and Tsoar, H. (1990) Aeolian sand and sand dunes. Unwin Hyman, London.

Rae, D.A. (1976) *Aspects of glaciation in Orkney.* University of Liverpool unpublished PhD thesis.

RCAHMS (1946) *Twelfth report with an inventory of the ancient monuments of Orkney and Shetland.* Royal Commission on the Ancient and Historical Monuments of Scotland., Edinburgh.

Reimer, P.J., McCormac, F.G., Moore, J., McCormick, F. and Murray, E.V. (2002) Marine radiocarbon reservoir corrections for the mid- to late Holocene in the eastern subpolar North Atlantic. *The Holocene*, 12, 2, 123-135.

Rendell, H.M. (1985) The precision of water content estimates in the thermoluminescence dating of loess from Northern Pakistan. *Nuclear Tracks and Radiation Measurements*, 10, 4-6, 763-768.

Rendell, H.M., Gamble, I.J.A. and Towsend, P.D. (1983) Thermoluminescence dating of loess from the Potwar Plateau, northern Pakistan. *PACT*, 9, 555-562.

Rennie, A.F. and Hansom, J.D. (2001) *Shoreline response to changes in sediment supply and sea level on a submerging coast, Sanday, Orkney.* Research Report to Scottish Natural Heritage, Edinburgh.

Rhodes, E.J. (1988) Methodological considerations in the optical dating of quartz. *Quaternary Science Reviews*, 7, 395-400.

Richards, C. (1994) Skaill Bay – Late Neolithic butchery site. *Discovery and Excavation Scotland*, 1994, p92.

Richards, C. (1996) Henges and Water. *Journal of Material Culture*, 1, 3, 313-336.

Richardson, C.A. (2000) Preheat-induced signal enhancement in the infrared stimulated luminescence of young and bleached sediment samples. *Radiation Measurements*, 32, 541-547.

Richardson, C.A. (2001) Residual luminescence signals in modern coastal sediments. *Quaternary Science Reviews*, 20, 887-892.

Richardson, J.S. (1948) *The Broch of Gurness: Aikerness, West Mainland, Orkney.* H.M.S.O., Edinburgh.

Rink, W.J. (1999) Quartz luminescence as a light-sensitive indicator of sediment transport in coastal processes. *Journal of Coastal Research*, 15, 1, 148-154.

Ritchie, A. (1971) Birsay, Buckquoy. *Discovery and Excavation in Scotland*, 1971, 55.

Ritchie, A. (1983) Birsay around AD 800. *Orkney Heritage*, 2, 46-66.

Ritchie, A. (1985b) *Exploring Scotland's Heritage: Orkney and Shetland.* Royal Commission on the Ancient and Historic Monuments of Scotland, Edinburgh.

Ritchie, A. (1993) *Viking Scotland.* Historic Scotland, B.T. Batsford Ltd, London.

Ritchie, A. (1995) *Prehistoric Orkney*. Historic Scotland.

Ritchie, A. (1996) *Orkney*. Royal Commission on the Ancient and Historic Monuments of Scotland, Edinburgh.

Ritchie, A. and Ritchie, G. (1995) *The ancient monuments of Orkney*. Historic Scotland, HMSO, Edinburgh.

Ritchie, G. and Harman, M. (1985) *Exploring Scotland's Heritage: Argyll and the Western Isles*. Royal Commission on the Ancient and Historic Monuments of Scotland, Edinburgh.

Ritchie, J.N.G. (1975) The Stones of Stenness, Orkney. *Proceedings of the Society of Antiquaries of Scotland*, 107, 1-60.

Ritchie, W. (1985a) Inter-tidal and sub-tidal organic deposits and sea level changes in the Uists, Outer Hebrides. *Scottish Journal of Geology*, 21, 2, 161-176.

Ritchie, W. (1993) Borve. In, *Quaternary of Scotland.* Edited by J.E. Gordon and D.E. Sutherland, Chapman and Hall, London, p429-431.

Ritchie, W. and Mather, A. (1970) *The Beaches of Lewis and Harris: a survey of the beach, dune and machair areas of Lewis and Harris.* Department of Geography, University of Aberdeen.

Roberts, H.M. and Wintle, A.G. (2001) Equivalent dose determinations for polymineralic fine-grains using the SAR protocol: application to a Holocene sequence of the Chinese Loess Plateau. *Quaternary Science Reviews*, 20, 859-863.

Roberts, R., Bird, M., Olley, J., Galbraith, R., Lawson, E., Laslett, G., Yoshida, H., Jones, R., Fullager, R., Jacobsen, G. and Hua, Q. (1998) Optical and radiocarbon dating at Jinmium rock shelter in northern Australia. *Nature*, 393, 358-362.

Roberts, R.G. (1997) Luminescence dating in archaeology: from origins to optical. *Radiation Measurements*, 27, 5/6, 819-892.

Roberts, R.G., Spooner, N.A. and Questiaux, D.G. (1994) Palaeodose underestimates caused by extended-duration preheats in the optical dating of quartz. *Radiation Measurements*, 23, 2/3, 647-653.

Robertson, J. and Downes, J. (2000) *Stenchme Lop Ness: Rescue excavation of a cist at Lop Ness, Sanday, Orkney.* Unpublished Data Structure report, Orkney Archaeological Trust.

Robertson, J., Anthony, I., Sanderson, D., Downes, J. and Housley, R. (2000) *Characterisation and Dating of Burnt Mounds from Orkney and Shetland: Eday Burnt Mounds.* Historic Scotland Report.

Robin, G. de Q. (1977) Ice cores and climatic change. *Philosophical Transactions of the Royal Society of London B*, 280, 143-168.

Sanderson, D.C.W. (1988) Thick Source Beta Counting (TSBC): a rapid method for measuring beta dose-rates. *Nuclear Tracks and Radiation Measurements*, 14, 1/2, 203-207.

Sanderson, D.C.W. (1990) Luminescence detection of irradiated foods. In, *Food Irradiation and the Chemist.* Edited by D.E. Johnston and M.H. Stevenson, p25-56.

Sanderson, D.C.W. (1991) Photostimulated luminescence (PSL): a new approach to identifying irradiated foods. In, *Potential New Methods of Detection of Irradiated Food.* Edited by J.J. Raffi and J.-J. Belliardo, Commission of the European Communities, p159-167.

Sanderson, D.C.W., Carmichael, L.A., Clark, P.A. and Clark, R.J. (1992) *Development of luminescence tests to identify irradiated food. Final report: Project N1701.* Scottish Universities Research and Reactor Centre.

Sanderson, D.C.W. and Clark, R.J. (1994) Pulsed photostimulated luminescence of alkali feldspars. *Radiation Measurements*, 23, 2/3, 633-639.

Sanderson, D.C.W., Carmichael, L., Ni Riain, S., Naylor, J. and Spencer, J.Q. (1994) Luminescence studies to identify irradiated food. *Food Science and Technology*, 8, 2, 93-96.

Sanderson, D.C.W., Carmichael, L. and Naylor, J.D. (1996) Recent advances in thermoluminescence and photostimulated luminescence detection methods for irradiated foods. In, *Detection Methods for Irradiated Foods: Current status.* Edited by C.H. McMurray, E.M. Stewart, R. Gray and J. Pearce, The Royal Society of Chemistry, p124-138.

Sanderson, D.C.W., Bishop, P., Houston, I. and Boonsener, M. (2001) Luminescence characterisation of quartz-rich cover sands from NE Thailand. *Quaternary Science Reviews*, 20, 893-900.

Schei, L.K. and Moberg, G. (1985) *The Orkney Story.* B.T. Batsford Ltd., London.

Schwenninger, J.-L. (1996) *The evolution of coastal sand dunes in the Southern Isles of the Outer Hebrides of Scotland.* Unpublished Ph.D. Dissertation, University of London.

Sejrup, H.P., Haflidason, H., Aarseth, I., King, E., Forsberg, C.F., Long, D. and Rokoengen, K. (1994) Late Weichselian glaciation history of the northern North Sea. *Boreas*, 23, 1-13.

Sejrup, H.P., Larsen, E., Landvik, J., King, E.L., Haflidason, H. and Nesje, A. (2000) Quaternary glaciations in southern Fennoscandia: evidence from southwestern Norway and the northern North Sea region. *Quaternary Science Reviews*, 19, 667-685.

Sharples, N.M, Barlow, A., Birkett, D.A., Clarke, A., Clarke, A.S., MacCormick, F., Stenhouse, M.J., Swinney, G., Wickham-Jones, C.R. and Yarrington, C.H. (1984) Excavations at Pierowall Quarry, Westray, Orkney. *Proceedings of the Antiquaries of Scotland*, 114, 75-125.

Shepherd, A. (1996) Skara Brae. In, *Quaternary of Orkney – Field Guide*. Edited by A.M. Hall, Quaternary Research Association, London, p97-111.

Shepherd, I.A.G. and Tuckwell, A.N. (1979) Traces of beaker-period cultivation at Rosinish, Benbecula. *Proceedings of the Society of Antiquaries of Scotland*, 108, 108-113.

Short, M.A. and Huntley, D.J. (1992) Infrared stimulation of quartz. *Ancient TL*, 10, 2, 19-21.

Simpson, B. (1998) *Skaill Bay*. Report No. 619, GUARD, University of Glasgow.

Simpson, I.A. (1998) Early land management at Tofts Ness, Sanday, Orkney: the evidence of thin section micromorphology. In, *Life on the Edge, Human Settlement and Marginality*. Edited by C.M. Mills and G. Coles, Oxbow Monograph, Oxford, p91-98.

Simpson, I.A. and Dockrill, S.J. (1996) Early cultivated soils at Tofts Ness, Sanday, Orkney. In, *The Quaternary of Orkney Field Guide*. Edited by A.M. Hall, Quaternary Research Association, London, p130-144.

Simpson, I.A., Dockrill, S.J., Bull, I.D. and Evershed, R.P. (1998) Early anthropogenic soil formation at Tofts Ness, Sanday, Orkney. *Journal of Archaeological Science*, 25, 729-746.

Sinclair, H. (1492) *Mss, Rental*, Orkney Archives, D2/7

Singarayer, J.S., Bailey, R.M. and Rhodes, E.J. (2000) Potential of the slow component of quartz OSL age determination of sedimentary samples. *Radiation Measurements*, 32, 873-880.

Singarayer, J.S. and Bailey, R.M. (in press) Further investigations of the quartz optically stimulated luminescence components using linear modulation. *Radiation Measurements*.

Singhvi, A.K., Sharma, Y.P. and Agrawal, D.P. (1982) Thermoluminescence dating of sand dunes in Rajasthan, India. *Nature*, 295, 313-315.

Sissons, J.B. (1967) *The evolution of Scotland's scenery*. Oliver and Boyd, Edinburgh.

Smith, B.W. and Rhodes, E.J. (1994) Charge movements in quartz and their relevance to optical dating. *Radiation Measurements*, 23, 2/3, 329-333.

Smith, B.W., Aitken, M.J., Rhodes, E.J., Robinson, P.D. and Geldard, D.M. (1986) Optical dating: Methodological Aspects. *Radiation Protection Dosimetry*, 17, 229-233.

Smith, B.W., Rhodes, E.J., Stokes, S., Spooner, N.A. and Aitken, M.J. (1990) Optical dating of sediments: initial quartz results from Oxford. *Archaeometry*, 32, 1, 19-31.

Smith, D.E. (1997) Sea-level change in Scotland during the Devensian and Holocene. In, *Reflections on the Ice Age in Scotland.* Edited by J.E. Gordon, Scottish Association of Geography Teachers, Linlithgow and Scottish Natural Heritage, Edinburgh, p136-151.

Sommerville, A.A., Sanderson, D.C.W., Hansom, J.D. and Housley, R.A. (2001) Luminescence dating of aeolian sands from archaeological sites in Northern Britain: a preliminary study. *Quaternary Science Reviews*, 20, 5-9, 913-919.

Sommerville, A.A., Hansom, J.D., Sanderson, D.C.W. and Housley, R.A. (2003) Optically stimulated luminescence dating of large storm events in Northern Scotland. *Quaternary Science Reviews*, 22, 10-13, 1085-1092.

Sommerville, A.A., Sanderson, D.C.W., Hansom, J.D., Housley, R.A. and Bonsall, C. (forthcoming) Quartz SAR-OSL dates and the onset of dune formation at Low Hauxley, near Amble, Northumberland, England.

Spencer, J.Q. (1996) *The development of luminescence methods to measure thermal exposure in lithic and ceramic materials.* Unpublished Ph.D. thesis, University of Glasgow.

Spencer, J.Q., Sanderson, D.C.W., Deckers, K. and Sommerville, A.A. (in press) Assessing mixed dose distributions in young sediments identified using small aliquots and a simple two-step SAR procedure: the F-statistic as a diagnostic tool. *Radiation Measurements.*

Spooner, N.A. (1994) On the optical dating signal from quartz. *Radiation Measurements*, 23, 2/3, 593-600.

Spooner, N.A., Prescott, J.R. and Hutton, J.T. (1988) The effect of illumination wavelength on the bleaching of the thermoluminescence (TL) of quartz. *Quaternary Science Reviews*, 7, 325-329.

Spooner, N.A. and Questiaux, D.G. (1989) Optical dating – Achnheim beyond the Eemian using green and infra-red stimulation. *Synopses from a workshop on long and short range limits in luminescence dating.* Occasional publication 9, Research Laboratory for Archaeology and the History of Art, Oxford University, p97-103.

Steers, J.A. (1937) The Culbin Sands and Burghead Bay. *Geographical Journal*, 90, 498-528.

Steers, J.A. (1973) *The Coastline of Scotland.* Cambridge University Press.

Stevenson, R. (1818) Observations upon the Alveus or general bed of the German Ocean and British Channel. *Memoirs of the Wernerian Natural History Society*, 2, (1811-1816), 464-490.

Stokes, S. (1992) Optical dating of young (modern) sediments using quartz: results from a selection of depositional environments. *Quaternary Science Reviews*, 11, 153-159.

Stokes, S. (1994) The timing of OSL sensitivity changes in a natural quartz. *Radiation Measurements*, 23, 2/3, 601-605.

Stoneham, D. (1991) Authenticity Testing. In, *Scientific Dating Methods*. Edited by H.Y. Göksu, M. Oberhofer and D. Regulla. Kluwer Academic Publishers, p175-192.

Stoneham, D. and Stokes, S. (1991) An investigation of the relationship of the 110°C TL peak and optically stimulated luminescence in sedimentary quartz. *Nuclear Tracks and Radiation Measurements*, 18, 1/2, 119-123.

Sutherland, D.G. (1984) The Quaternary deposits and landforms of Scotland and the neighbouring shelves: a review. *Quaternary Science Reviews*, 3, 157-254.

Sutherland, D.G. and Gordon, J.E. (1993) The Orkney Islands. In, *The Quaternary of Scotland*. Edited by J.E. Gordon and D.G. Sutherland, Chapman and Hall, London, p70-82.

Sutherland, D.G. and Walker, M.J.C. (1984) A late Devensian ice-free area and possible interglacial site on the Isle of Lewis, Scotland. *Nature*, 309, 701-703.

Thomson, W.P.L. (1984) Fifteenth Century Depression in Orkney: the Evidence of Lord Henry Sinclair's Rentals. In, *Essays in Shetland History*. Edited by B.E. Crawford, The Shetland Times, Lerwick.

Thompson, F. (1999) *Lewis and Harris*. Pevensey Island Guides, David and Charles, Hong Kong.

Thorsteinsson, A. (1968) The Viking burial place at Pierowall, Westray, Orkney. In, *The Fifth Viking Congress*. Edited by B. Niclasen, Føroya Fróoskaparfelag, Tórsharn, p150-173.

Tindall, J. (1981) *Scottish Island Hopping – A Handbook for the Independent Traveller*. Sphere Books Ltd.

Tipping, R. (1994) The form and fate of Scotland's woodlands. *Proceedings of the Society of Antiquaries of Scotland*, 124, 1-54.

Tite, M.S. (1966) Thermoluminescent dating of ancient ceramics: a reassessment. *Archaeometry*, 9, 155-169.

Tite, M.S. and Waine, J. (1962) Thermoluminescence dating: a re-appraisal. *Archaeometry*, 5, 53-79.

Traill, W. (1868) On submarine forests and other remains of indigenous wood in Orkney. *Transactions of the Botanical Society of Edinburgh*, 9, 146-154.

Turner, J. (1981) The Iron Age. In, *The Environment in British Prehistory*. Edited by I.G. Simmons and M.J. Tooley, Duckworth, London, p250-281.

Twidell, J. and Weir, T. (1986) *Renewable Energy Resources*. Spon, London.

Vega Leinert, A.C. de la, Keen, D.H., Jones, R.L., Wells, J.M. and Smith, D.E. (2000) Mid-Holocene environmental changes in the Bay of Skaill, Mainland Orkney, Scotland: an integrated geomorphological, sedimentological and stratigraphical study. *Journal of Quaternary Science*, 15, 5, 509-528.

Von Weymarn, J.A. (1979) A new concept of glaciation in Lewis and Harris, Outer Hebrides. *Proceedings of the Royal Society of Edinburgh*, 77B, 97-105.

Walton, K. (1956) Rattray: a study in coastal evolution. *Scottish Geographical Magazine*, 72, 2, 85-97.

Watt, W.G.T. (1888) Notice of discovery of a stone cist with an Iron Age internment at Skaill Bay. *Proceedings of the Society of Antiquaries of Scotland*, 22, 283-285.

Whittington, G. and Edwards, K.J. (1997) Climate Change. In, *Scotland: Environment and Archaeology, 8000 BC – AD 1000.* Edited by K.J. Edwards and I.B.M. Ralston, John Wiley and Sons, Chichester, p11-22.

Whittow, J. (1992) *Geology and Scenery in Britain.* Chapman and Hall, London.

Wickham-Jones, C.R. (1994) *Scotland's First Settlers.* B.T. Batsford Ltd for Historic Scotland.

Willis, D.P. (1986) *Sand and Silence – Lost villages of the North.* Centre for Scottish Studies, University of Aberdeen,

Wilson, G.V., Edwards, W., Knox, J., Jones, R.C.B. and Stephens, J.V. (1935) *The geology of the Orkneys.* Memoir of the Geological Survey of Scotland.

Wilson, G.V. and Knox, J. (1936) The Geology of the Orkney and Shetland Islands. *Proceedings of the Geological Association*, 47, 270-282.

Wilson, P. and Braley, S.M. (1997) Development and age structure of Holocene coastal sand dunes at Horn Head, near Dunfanaghy, Co Donegal, Ireland. *The Holocene*, 7, 2, 187-197.

Wilson, P., Orford, J.D., Knight, J., Braley, S.M. and Wintle, A.G. (2001) Late-Holocene (post-4000 years BP) coastal dune development in Northumberland, northeast England. *The Holocene*, 11, 2, 215-229.

Wintle, A.G. (1973) Anomalous fading of thermoluminescence in mineral samples. *Nature*, 245, 143-144.

Wintle, A.G. (1991) Luminescence Dating. In, *Quaternary Dating Methods – A User's Guide.* Edited by P.L. Smart and P.D. Frances, Quaternary Research Association, Technical Guide 4, 108-127.

Wintle, A.G. (1997) Luminescence dating: laboratory procedures and protocols. *Radiation Measurements*, 27, 5/6, 769-817.

Wintle, A.G. and Huntley, D.J. (1979) Thermoluminescence dating of deep-sea sediment core. *Nature*, 279, 710-712.

Wintle, A.G. and Huntley, D.J. (1980) Thermoluminescence dating of ocean sediments. *Canadian Journal of Earth Sciences*, 17, 348-360.

Wintle, A.G. and Huntley, D.J. (1982) Thermoluminescence dating of sediments. *Quaternary Science Reviews*, 1, 31-53.

Wintle, A.G. and Murray, A.S. (1997) The relationship between quartz thermoluminescence, photo-transferred thermoluminescence, and optically stimulated luminescence. *Radiation Measurements*, 27, 4, 611-624.

Wintle, A.G. and Murray, A.S. (1998) Towards the development of a preheat procedure for OSL dating of quartz. *Radiation Measurements*, 29, 1, 81-94.

Wintle, A.G., Clarke, M.L., Musson, F.M., Orford, J.D. and Devoy, R.J.N. (1998) Luminescence dating of recent dunes on Inch Spit, Dingle Bay, southwest Ireland. *The Holocene*, 8, 3, 331-339.

Zimmerman, D.W. (1967) Thermoluminescence from fine grains from ancient pottery. *Archaeometry*, 10, 26-28.

Zimmerman, D.W. (1971) Thermoluminescent dating using fine grains from pottery. *Archaeometry*, 13, 1, 29-52.

Appendix 5.1 – Actual, saturated and calculated water content of all samples

		Water content (%)					Water content (%)		
Site	Sample	Actual	Saturated	Calculated	Site	Sample	Actual	Saturated	Calculated
Tofts Ness	602	21.4	35.8	28 +/- 7	Quoygrew	702	6.15	34.29	20 +/- 14
	603	11.4	28.8	18 +/- 10		703	16.91	47.4	31 +/- 15
	604	4.37	20	12 +/- 8		704	17.64	45.95	32 +/- 14
	605	38.3	42.7	37 +/- 5		901	4.46	32.94	30 +/- 26
	606	11.8	33.3	23 +/- 10		902	3.81	55.58	18 +/- 14
	607	14	26.3	20 +/- 6		903	4.96	33.1	19 +/- 14
	608	14.2	40.9	27 +/- 12	Pierowall	877	6.4	27.01	16 +/- 10
	609	14.6	34.5	25 +/- 10		878	7.93	35.05	22 +/- 14
	610	49.4	no data	49 +/- 5		879	11.33	42.72	27 +/- 16
	611	15.4	32.8	24 +/- 8	Evertaft	915	5.38	37.77	21 +/- 16
	612	35.9	38.2	34 +/- 5		916	5.52	31.62	18 +/- 13
	613	43.1	50.1	46 +/- 4		917	7.46	35.24	21 +/- 15
	614	19	32.1	25 +/- 7		918	9.69	31.46	20 +/- 11
	615	15.5	35.5	25 +/- 10		919	10.4	35.32	22 +/- 13
	616	50.5	58.5	54 +/- 4	Sandhill	920	15.94	32.48	24 +/- 8
	617	63.1	71.8	67 +/- 5		921	17.42	28.94	23 +/- 6
	618	22.9	31.1	26 +/- 4		922	16.18	28.76	22 +/- 7
	619	36.7	38.5	37 +/- 2		923	12.54	28.64	20 +/- 8
Bay of	884	no data	44.69	30 +/- 10		924	24.31	no data	24 +/- 5
Lopness	885	5.7	33.4	18 +/- 15		925	15.51	26.77	20 +/- 6
	886	6.76	33.55	20 +/- 13		926	25.88	26.18	21 +/- 5
	887	9.43	39.7	25 +/- 15		927	33.67	no data	33 +/- 5
	888	7.58	33.13	20 +/- 13		928	34.55	40.88	37 +/- 4
	889	6.78	32.84	20 +/- 13		1299	100	100	80 +/- 20
	890	7.62	30.96	20 +/- 10		1300	100	100	80 +/- 20
	891	17.5	29.92	23 +/- 6	Bay of	620	9.17	40.42	25 +/- 15
Quoygrew	698	9.6	44.1	27 +/- 17	Skaill	621	10.4	29.19	20 +/- 10
	699	7.73	29.91	18 +/- 11		622	12.23	41.82	27 +/- 15
	700	3.97	40.07	22 +/- 18		623	11.76	37.33	24 +/- 13
	701	6.51	34.11	20 +/- 14		624	7.02	43.55	26 +/- 18

Appendix 5.2 – Preheat temperature dependence plots

TOFTS NESS

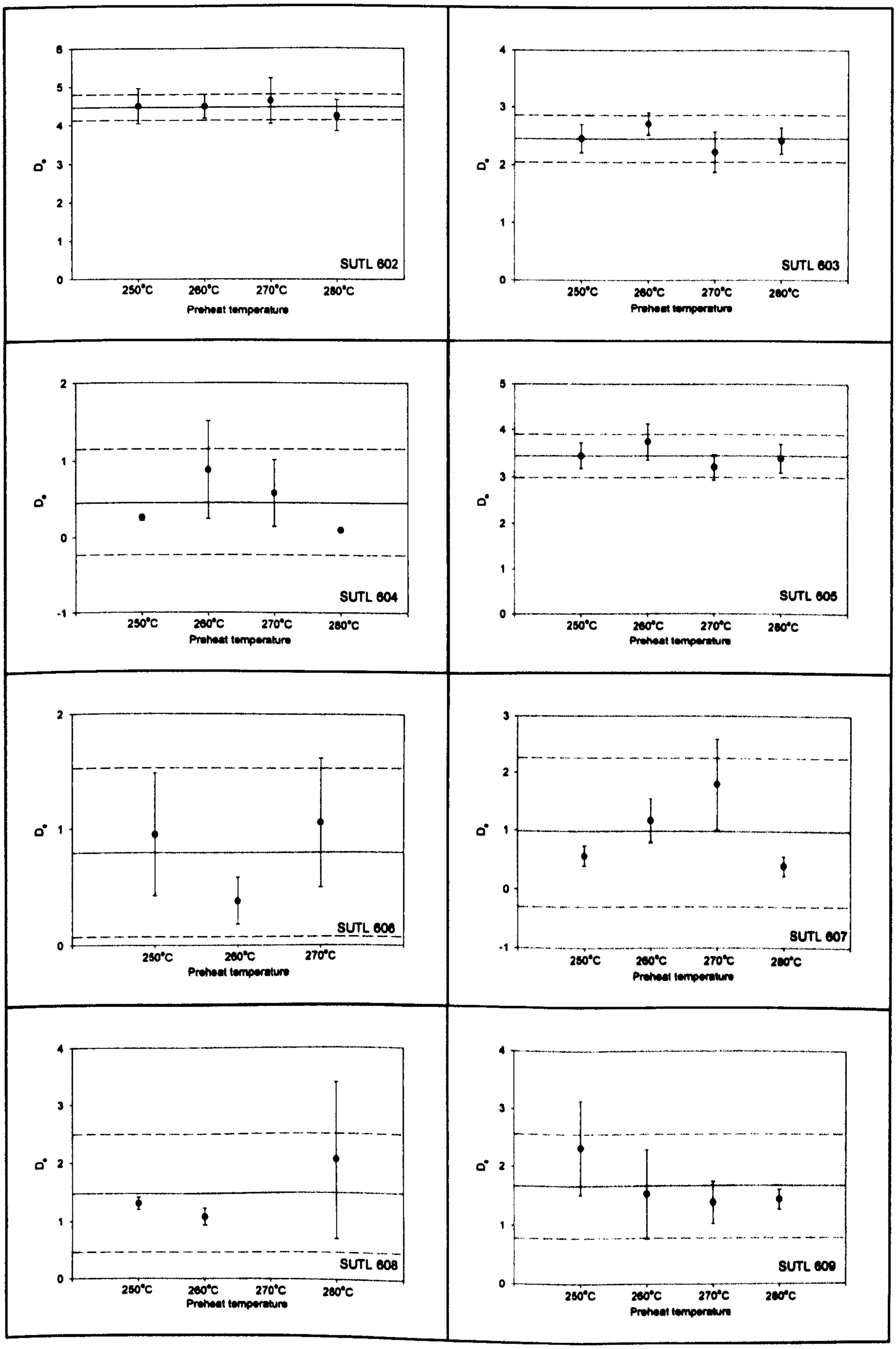

Appendix 5.2

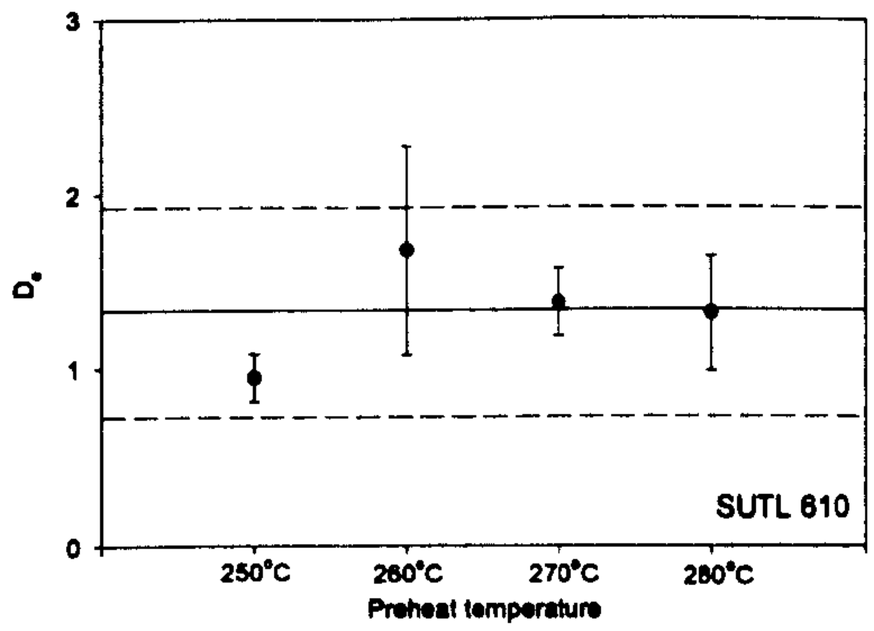
3
2
1
0
D_o
SUTL 610
250°C
260°C
270°C
280°C
Preheat temperature

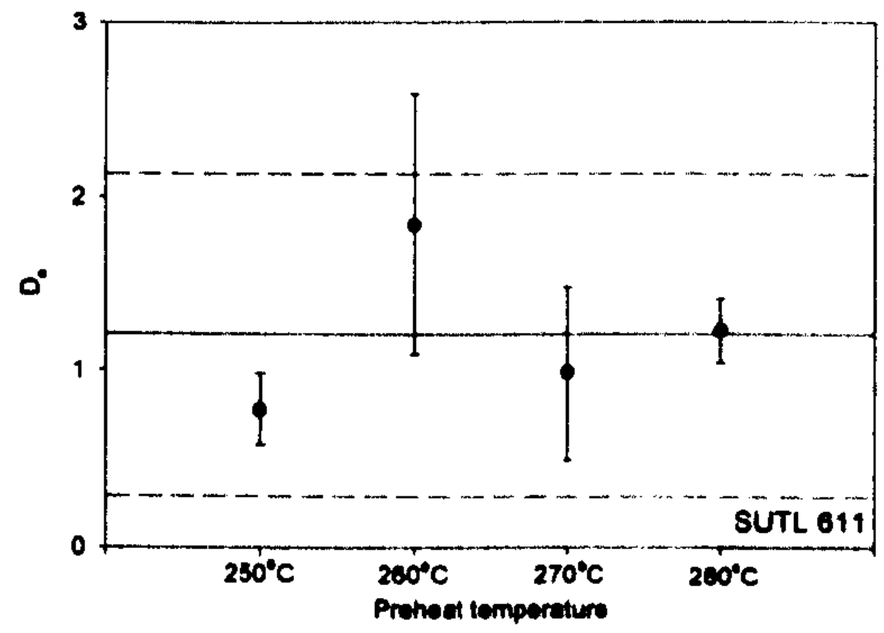
3
2
1
0
D_o
SUTL 611
250°C
260°C
270°C
280°C
Preheat temperature

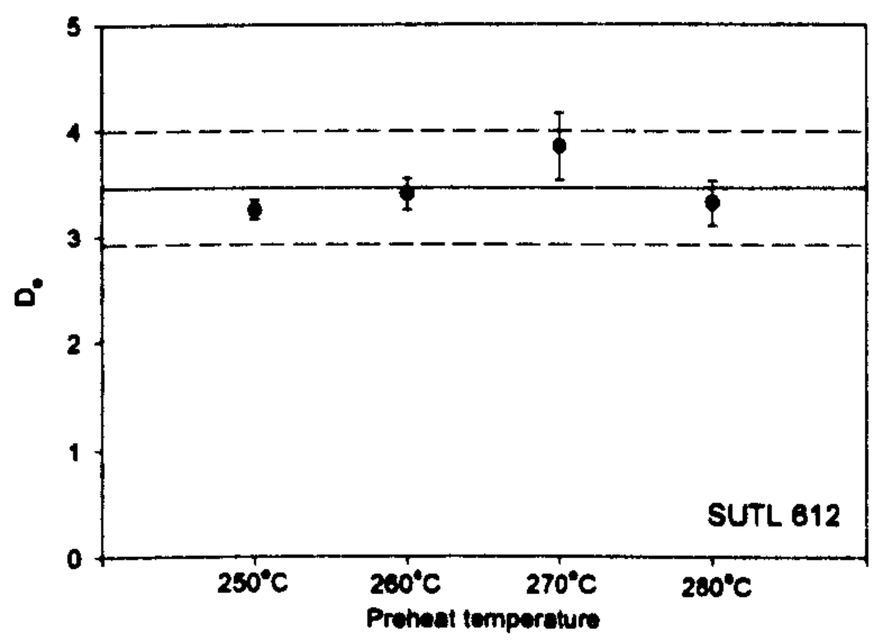
5
4
3
2
1
0
D_o
SUTL 612
250°C
260°C
270°C
280°C
Preheat temperature

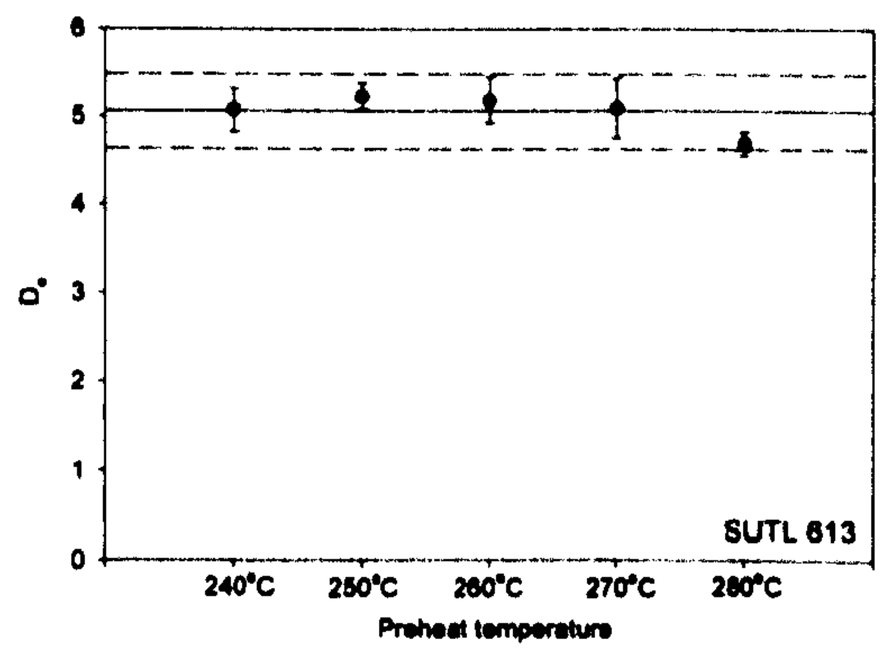
6
5
4
3
2
1
0
D_o
SUTL 613
240°C
250°C
260°C
270°C
280°C
Preheat temperature

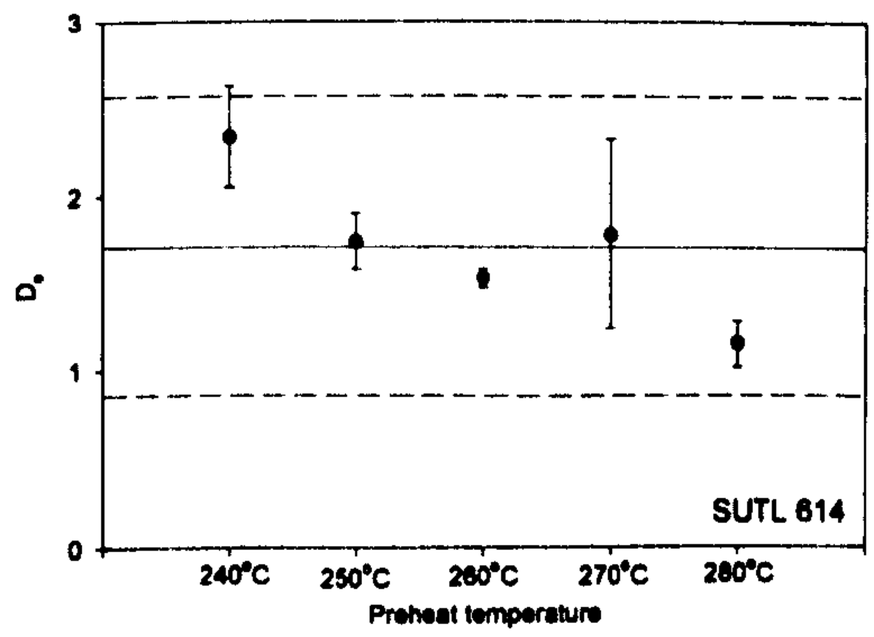
3
2
1
0
D_o
SUTL 614
240°C
250°C
260°C
270°C
280°C
Preheat temperature

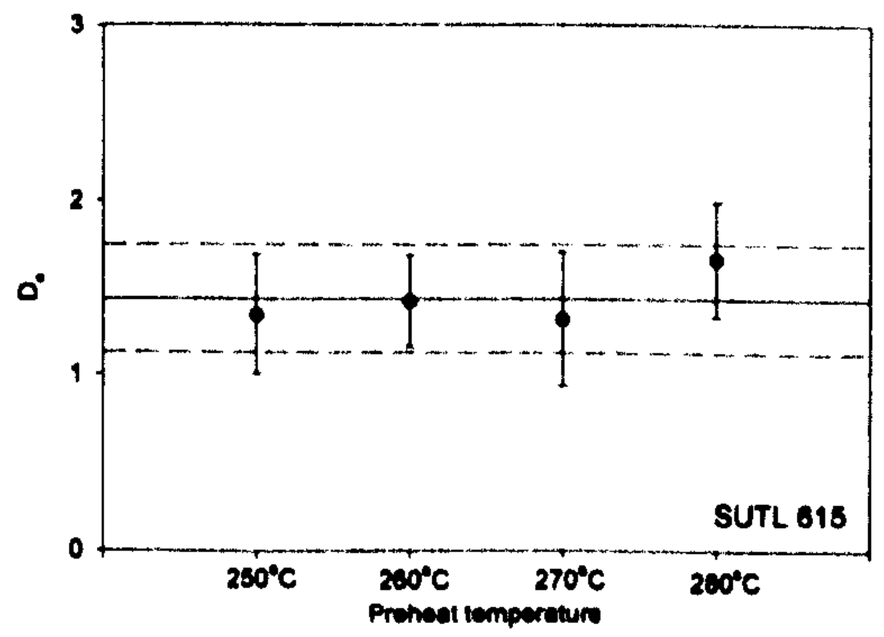
3
2
1
0
D_o
SUTL 615
250°C
260°C
270°C
280°C
Preheat temperature

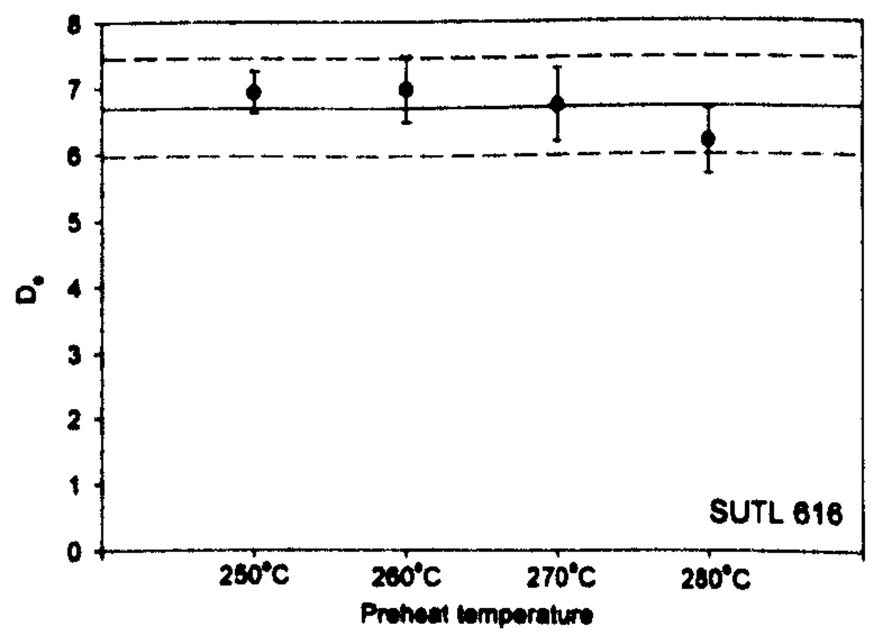
8
7
6
5
4
3
2
1
0
D_o
SUTL 616
250°C
260°C
270°C
280°C
Preheat temperature

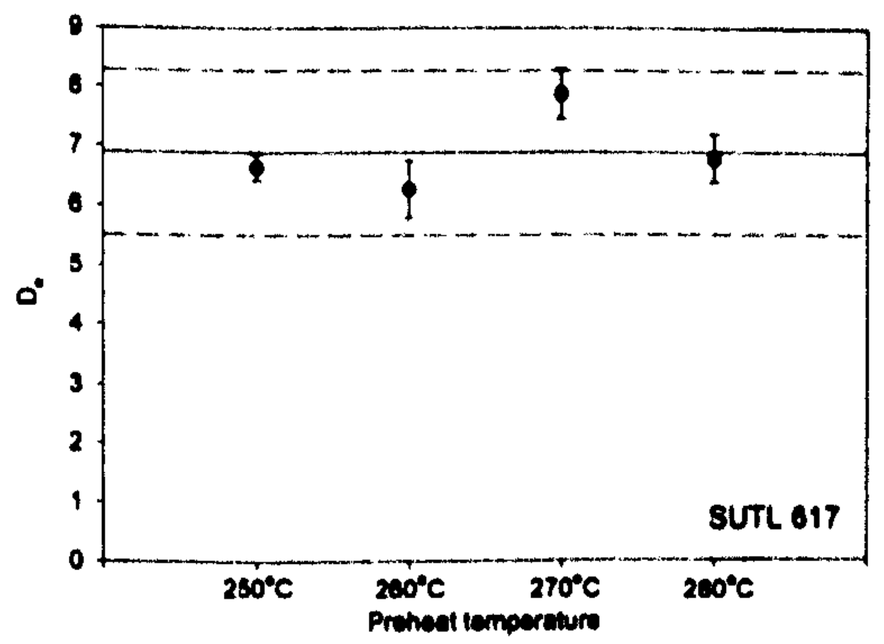
9
8
7
6
5
4
3
2
1
0
D_o
SUTL 617
250°C
260°C
270°C
280°C
Preheat temperature

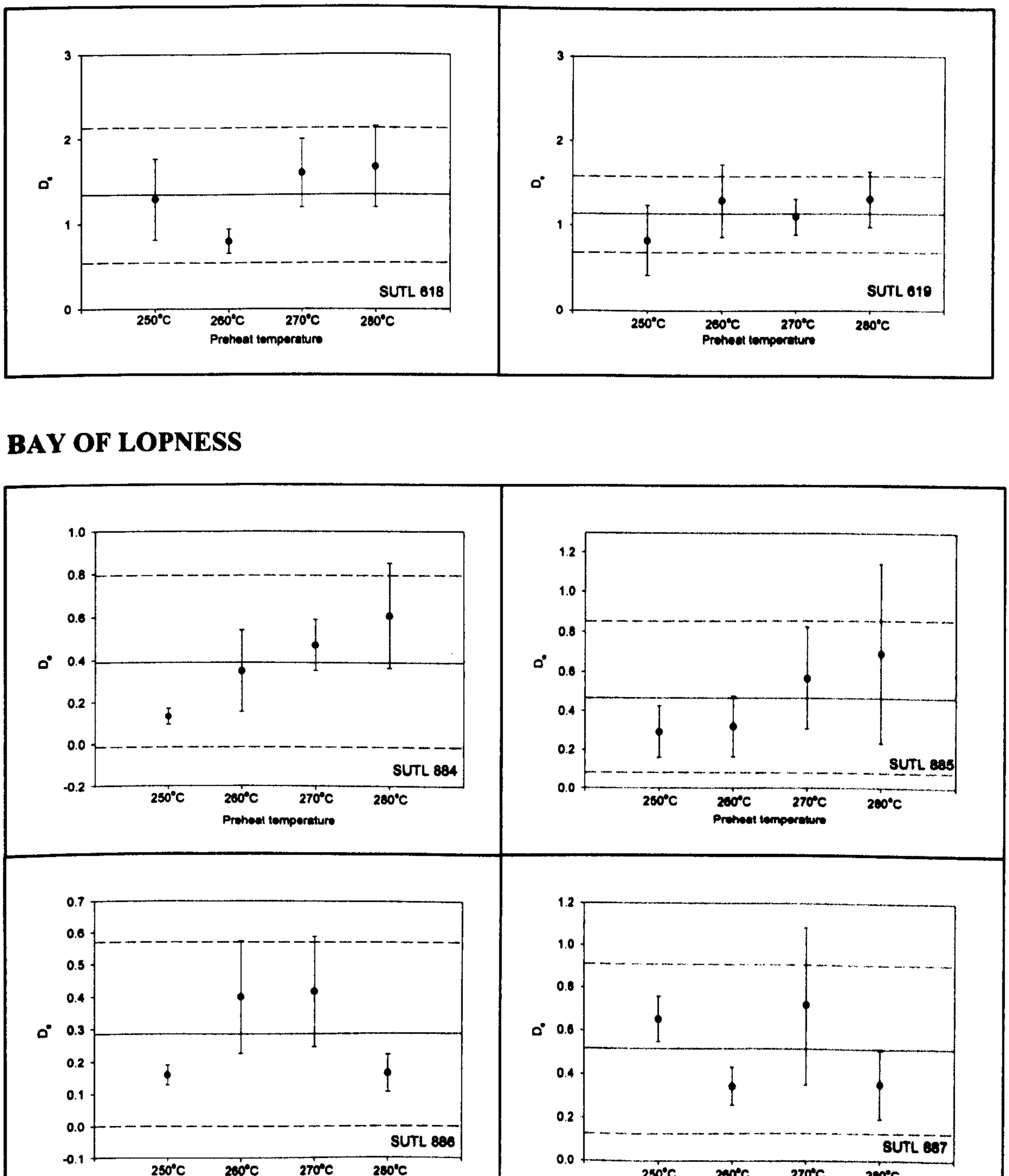
BAY OF LOPNESS
SUTL 618
SUTL 619
SUTL 884
SUTL 885
SUTL 886
SUTL 887
SUTL 888
SUTL 889
D°
Preheat temperature
250°C
260°C
270°C
280°C

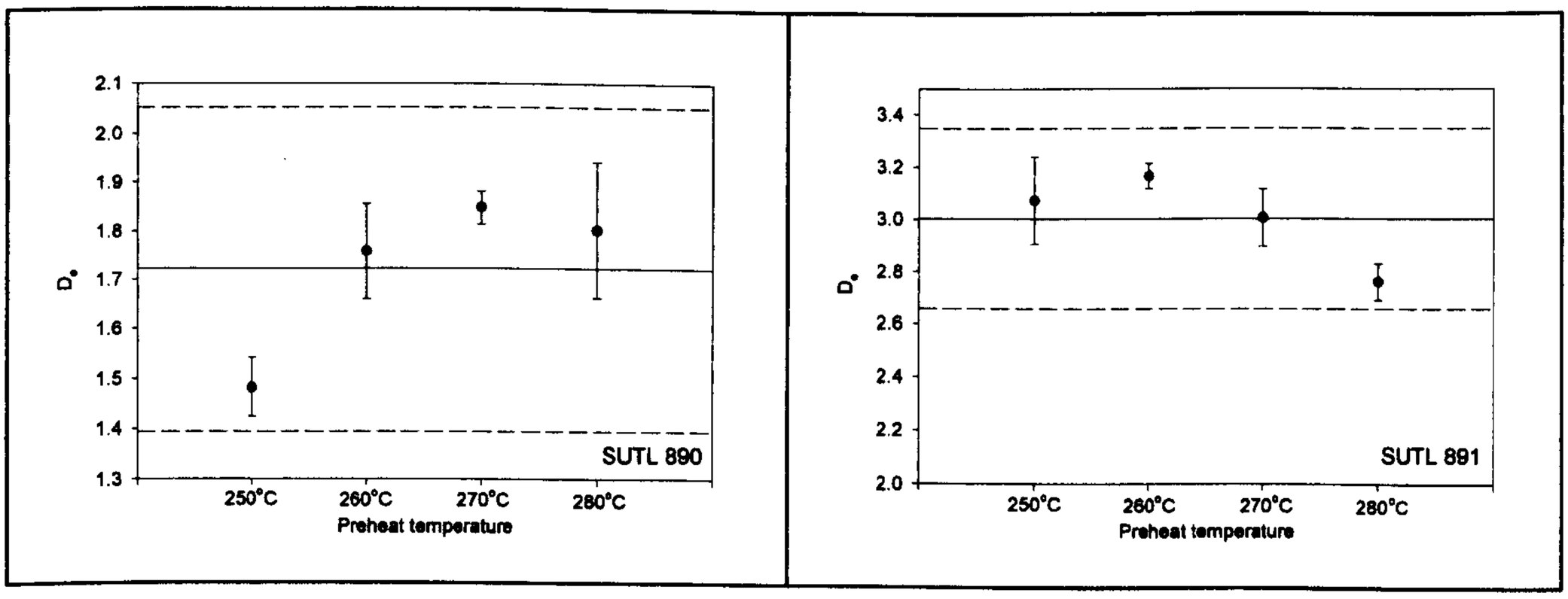
2.1
2.0
1.9
1.8
1.7
1.6
1.5
1.4
1.3
D•
SUTL 890
250°C
260°C
270°C
280°C
Preheat temperature

3.4
3.2
3.0
2.8
2.6
2.4
2.2
2.0
D•
SUTL 891
250°C
260°C
270°C
280°C
Preheat temperature

QUOYGREW

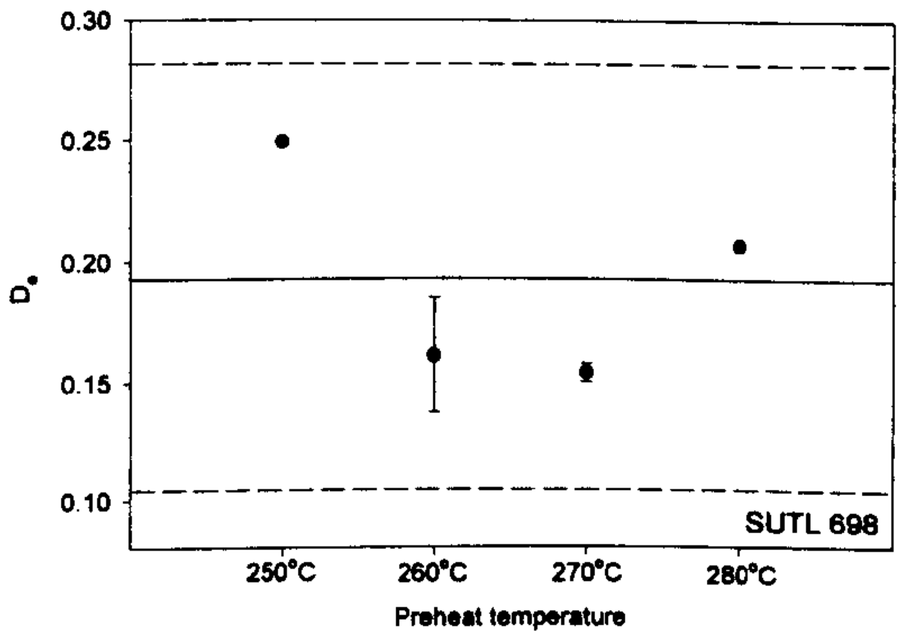
0.30
0.25
0.20
0.15
0.10
D•
SUTL 698
250°C
260°C
270°C
280°C
Preheat temperature

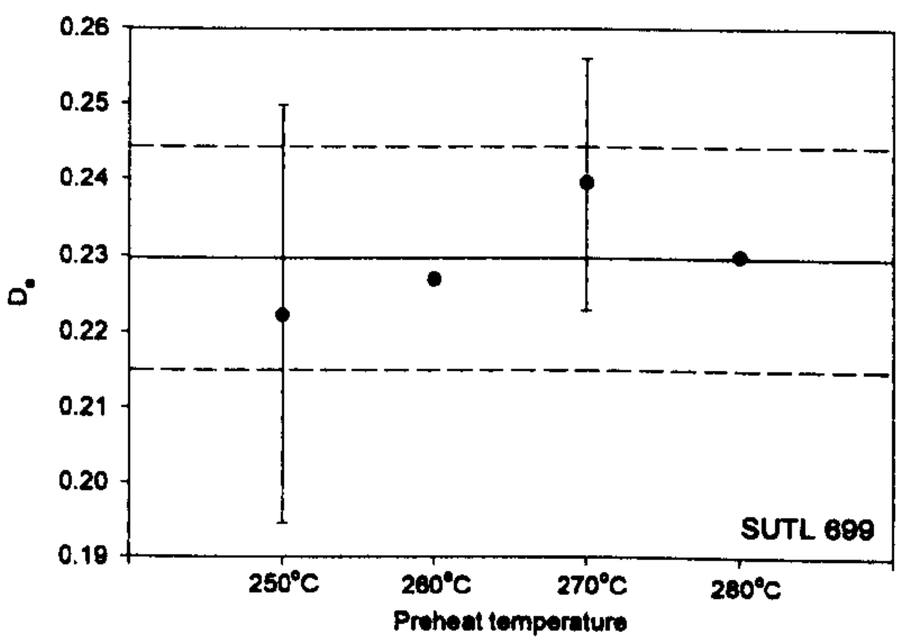
0.26
0.25
0.24
0.23
0.22
0.21
0.20
0.19
D•
SUTL 699
250°C
260°C
270°C
280°C
Preheat temperature

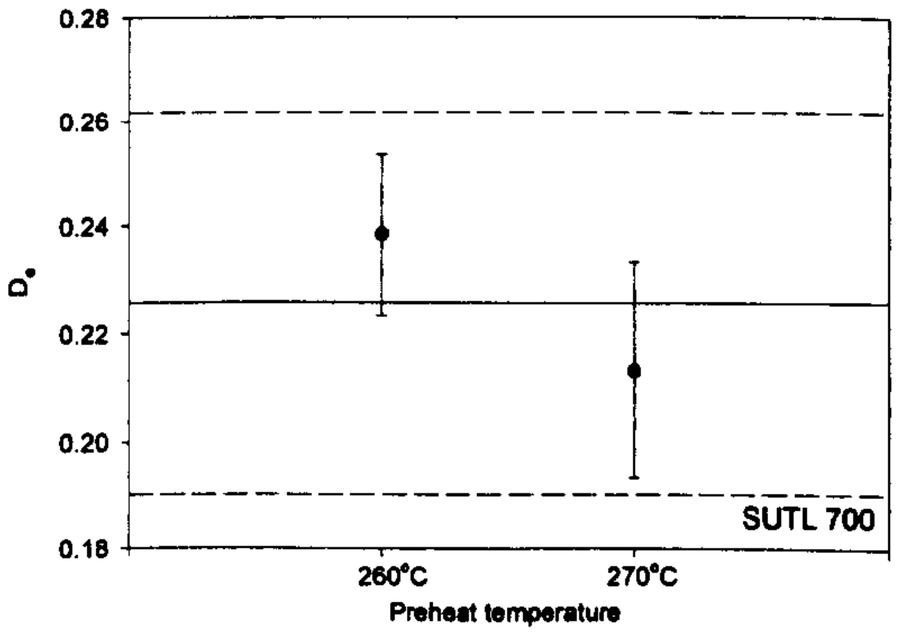
0.28
0.26
0.24
0.22
0.20
0.18
D•
SUTL 700
260°C
270°C
Preheat temperature

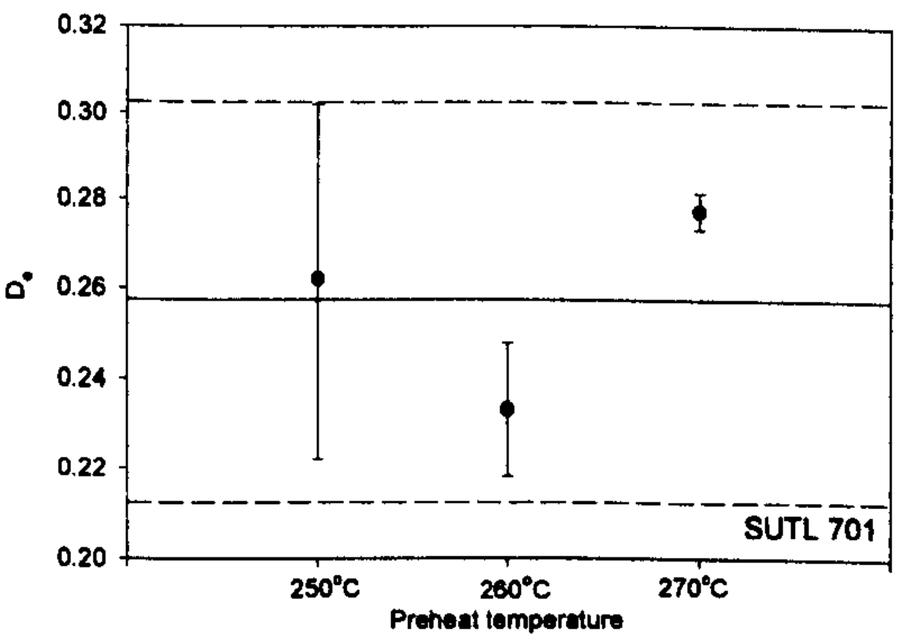
0.32
0.30
0.28
0.26
0.24
0.22
0.20
D•
SUTL 701
250°C
260°C
270°C
Preheat temperature

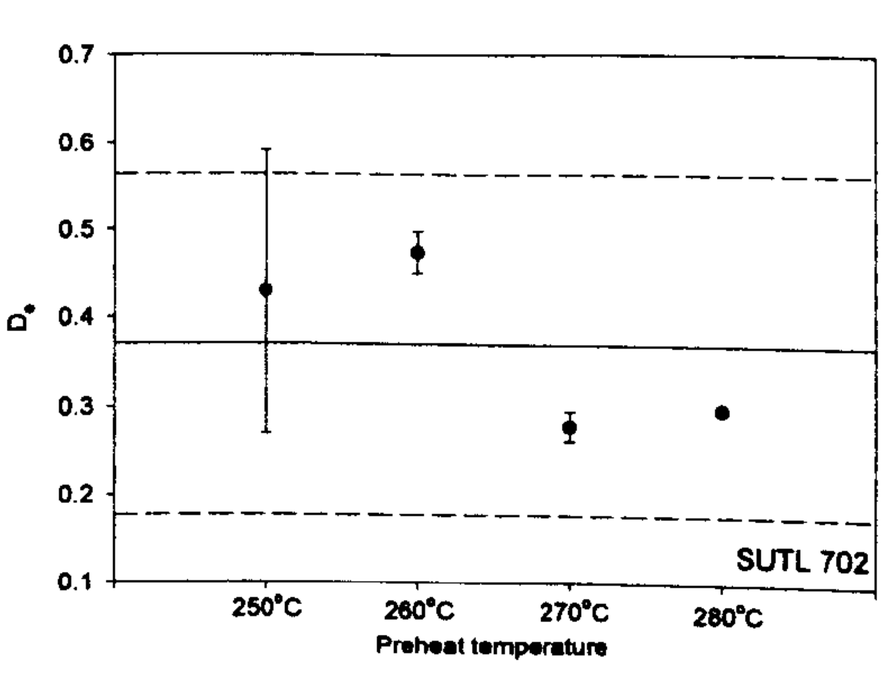
0.7
0.6
0.5
0.4
0.3
0.2
0.1
D•
SUTL 702
250°C
260°C
270°C
280°C
Preheat temperature

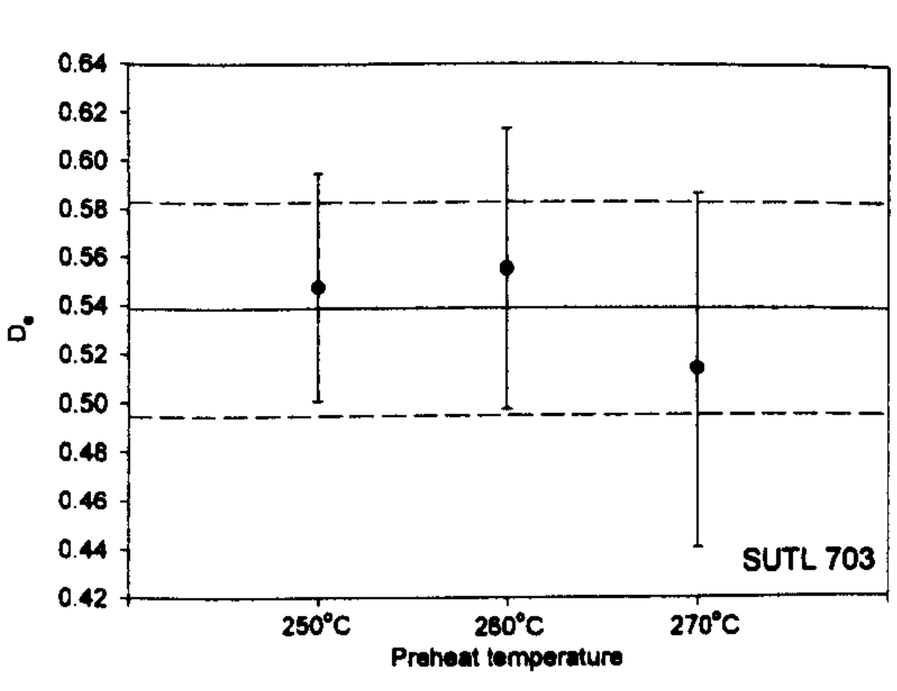
0.64
0.62
0.60
0.58
0.56
0.54
0.52
0.50
0.48
0.46
0.44
0.42
D•
SUTL 703
250°C
260°C
270°C
Preheat temperature

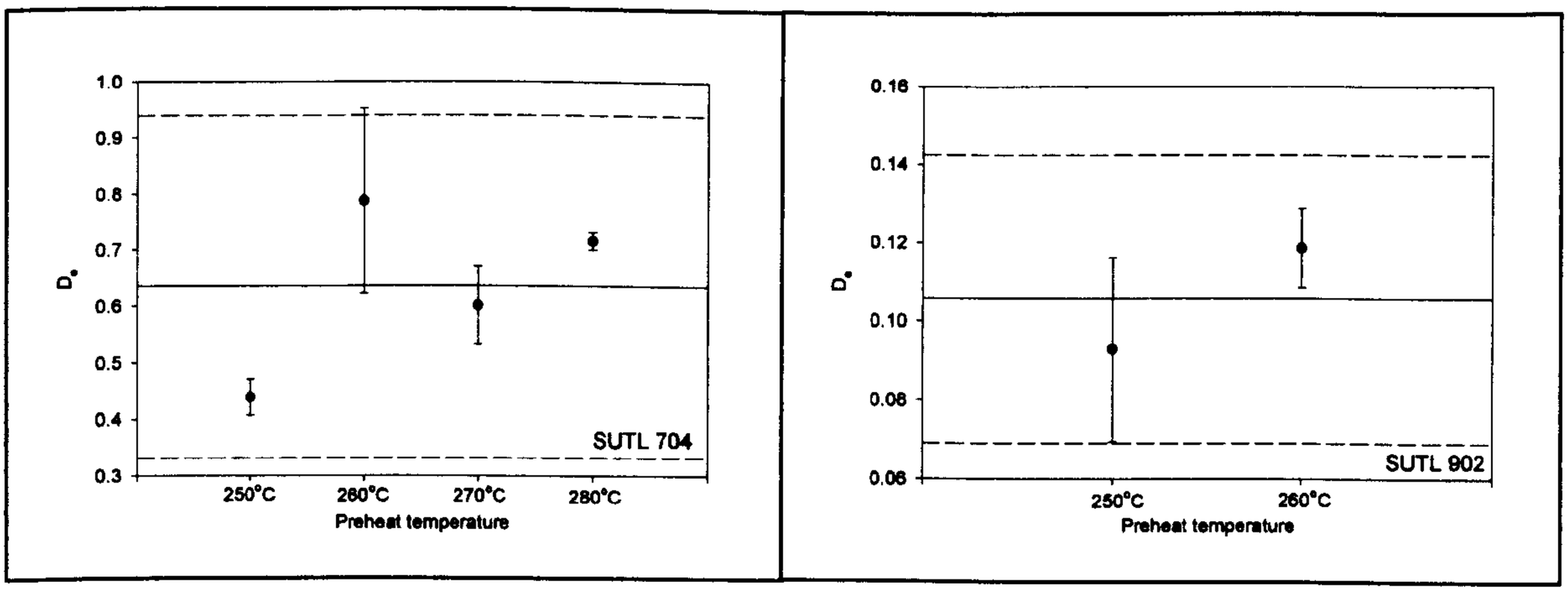
1.0
0.9
0.8
0.7
0.6
0.5
0.4
0.3
D*
SUTL 704
250°C
260°C
270°C
280°C
Preheat temperature
0.16
0.14
0.12
0.10
0.08
0.06
D*
SUTL 902
250°C
260°C
Preheat temperature

PIEROWALL

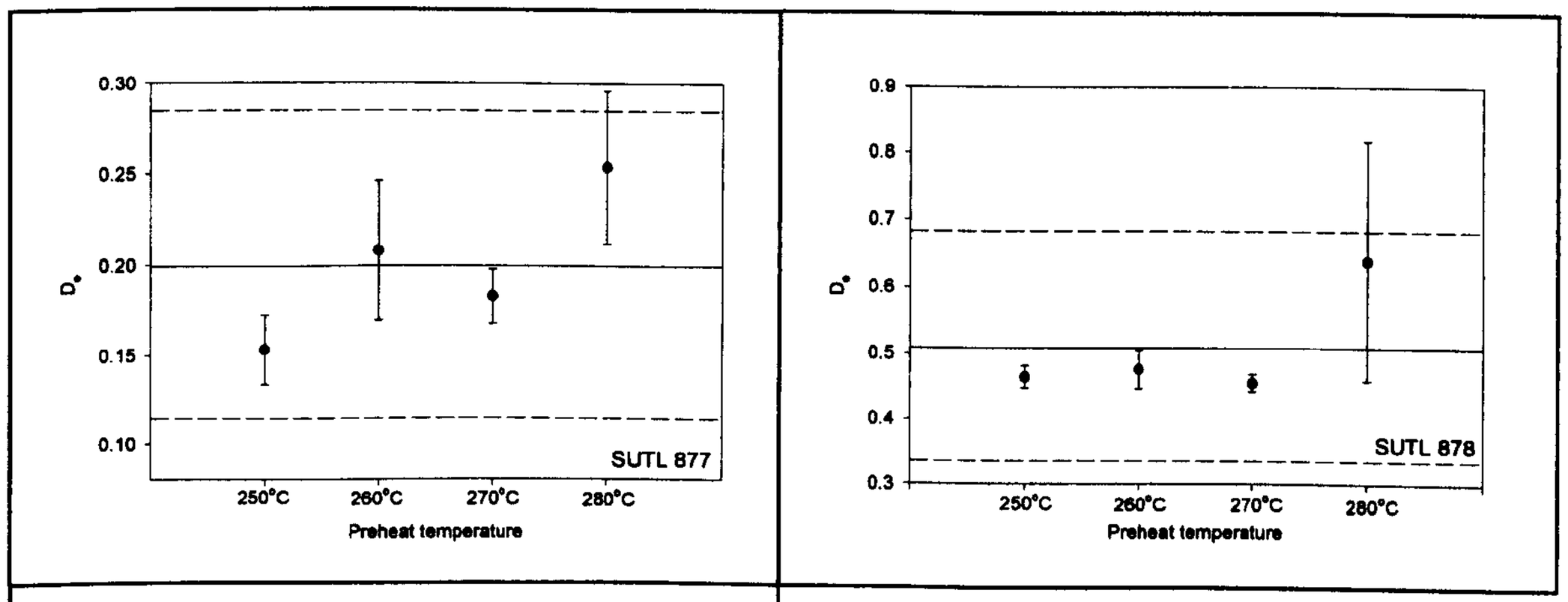
0.30
0.25
0.20
0.15
0.10
D*
SUTL 877
250°C
260°C
270°C
280°C
Preheat temperature
0.9
0.8
0.7
0.6
0.5
0.4
0.3
D*
SUTL 878
250°C
260°C
270°C
280°C
Preheat temperature

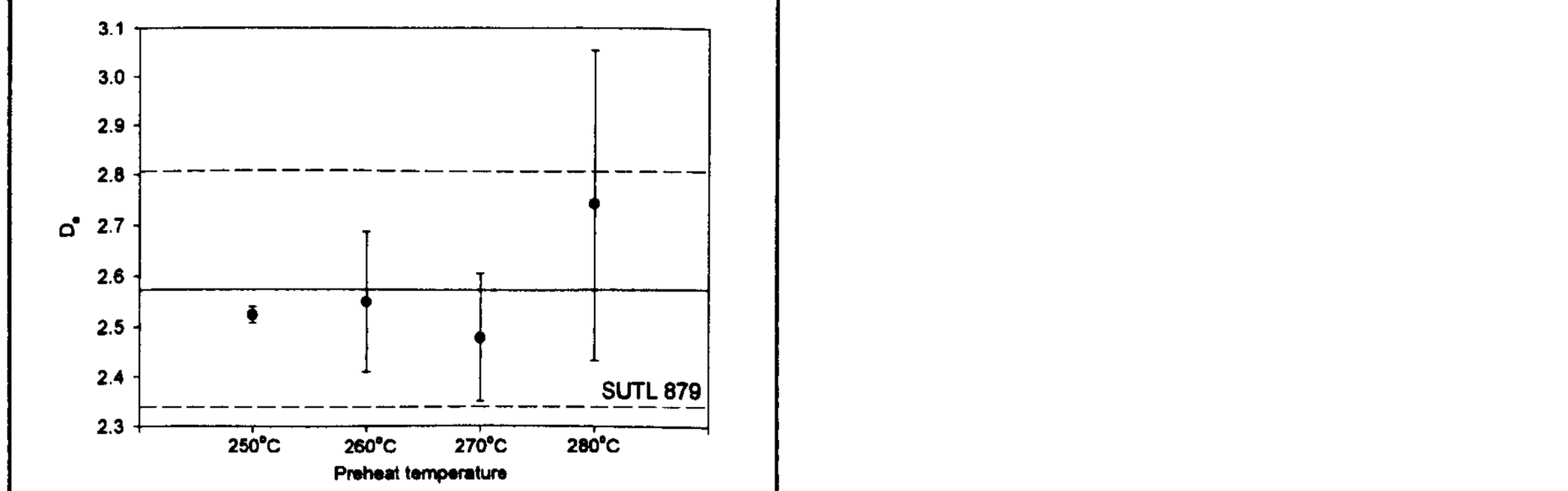
3.1
3.0
2.9
2.8
2.7
2.6
2.5
2.4
2.3
D*
SUTL 879
250°C
260°C
270°C
280°C
Preheat temperature

EVERTAFT

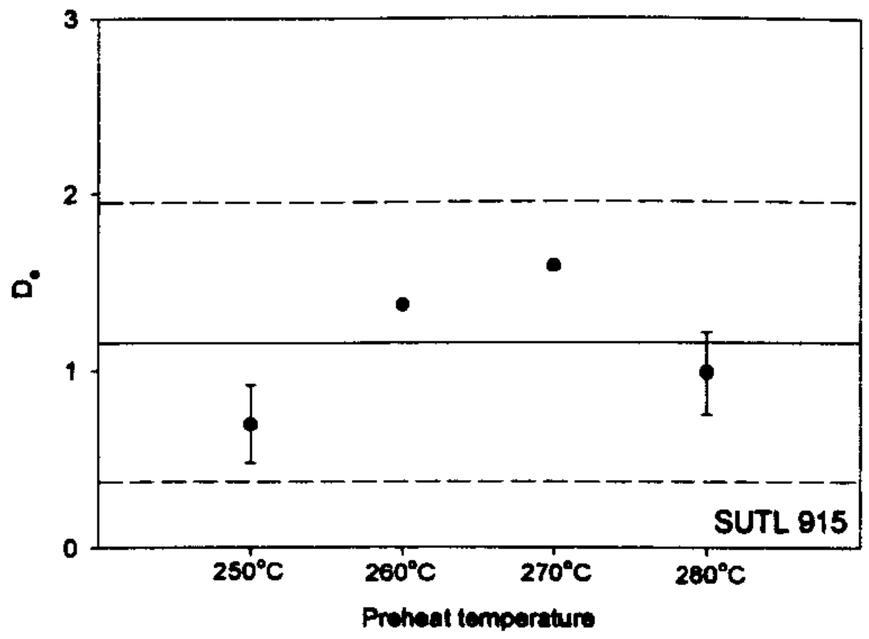
3
2
1
0
D*
SUTL 915
250°C
260°C
270°C
280°C
Preheat temperature

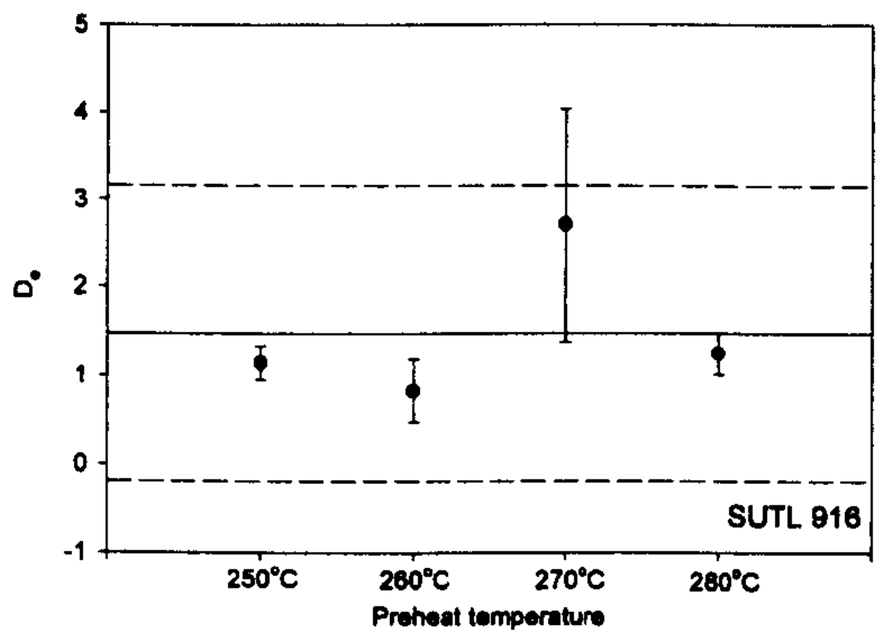
5
4
3
2
1
0
-1
D*
SUTL 916
250°C
260°C
270°C
280°C
Preheat temperature

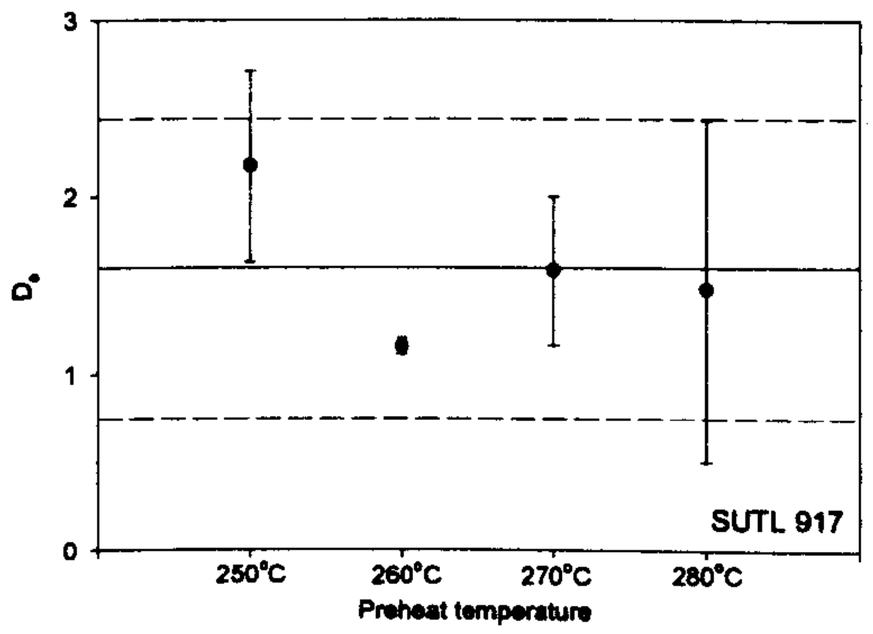
3
2
1
0
D*
SUTL 917
250°C
260°C
270°C
280°C
Preheat temperature

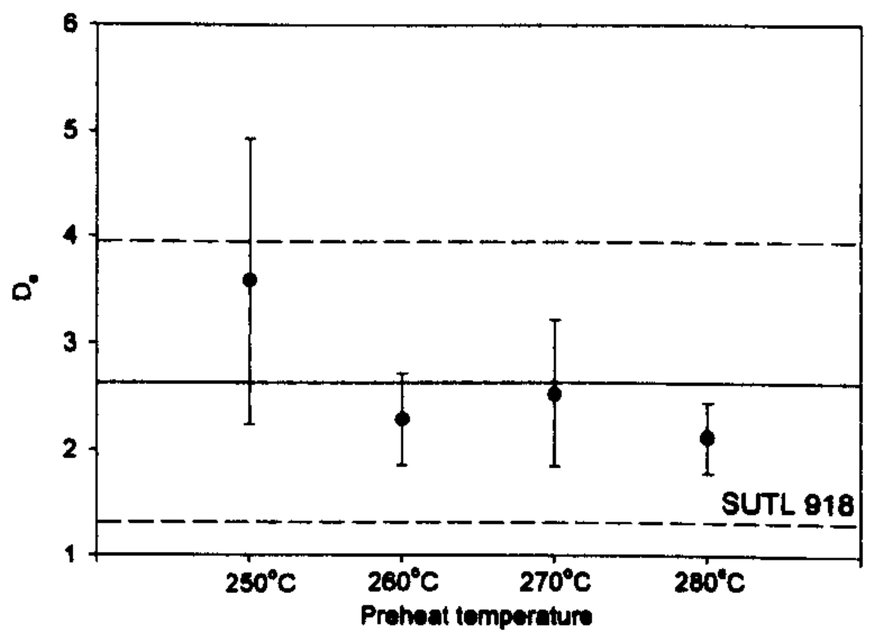
6
5
4
3
2
1
D*
SUTL 918
250°C
260°C
270°C
280°C
Preheat temperature

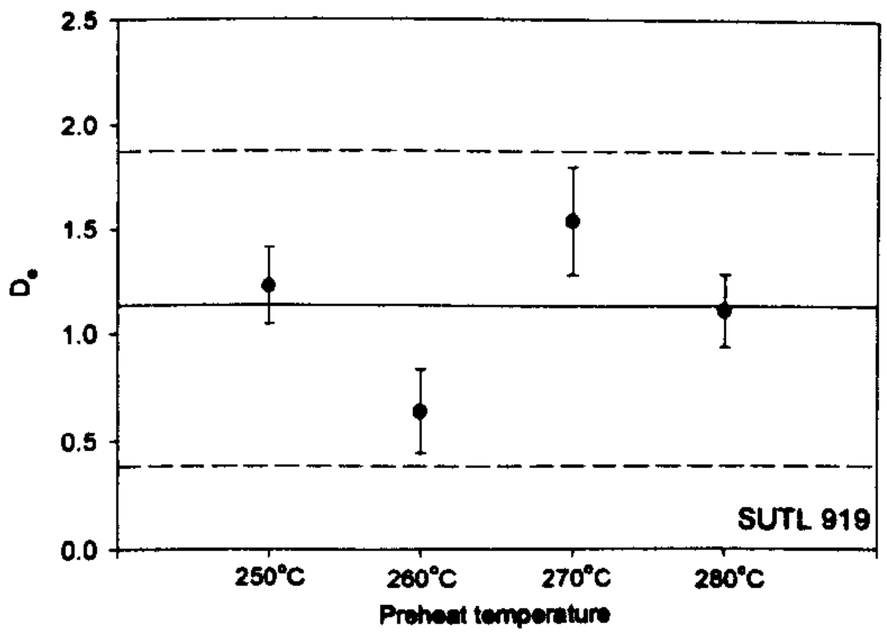
2.5
2.0
1.5
1.0
0.5
0.0
D*
SUTL 919
250°C
260°C
270°C
280°C
Preheat temperature

SANDHILL

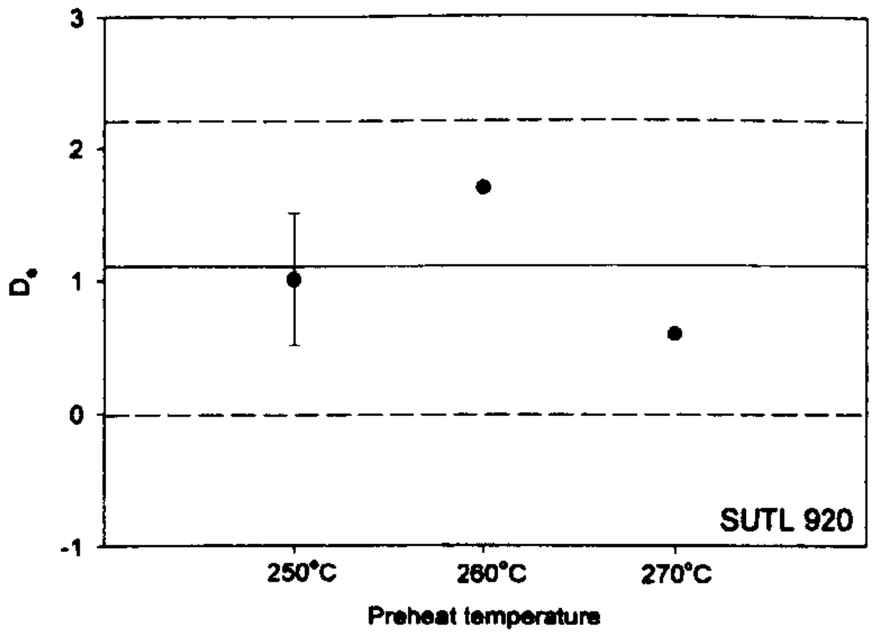
3
2
1
0
-1
D*
SUTL 920
250°C
260°C
270°C
Preheat temperature

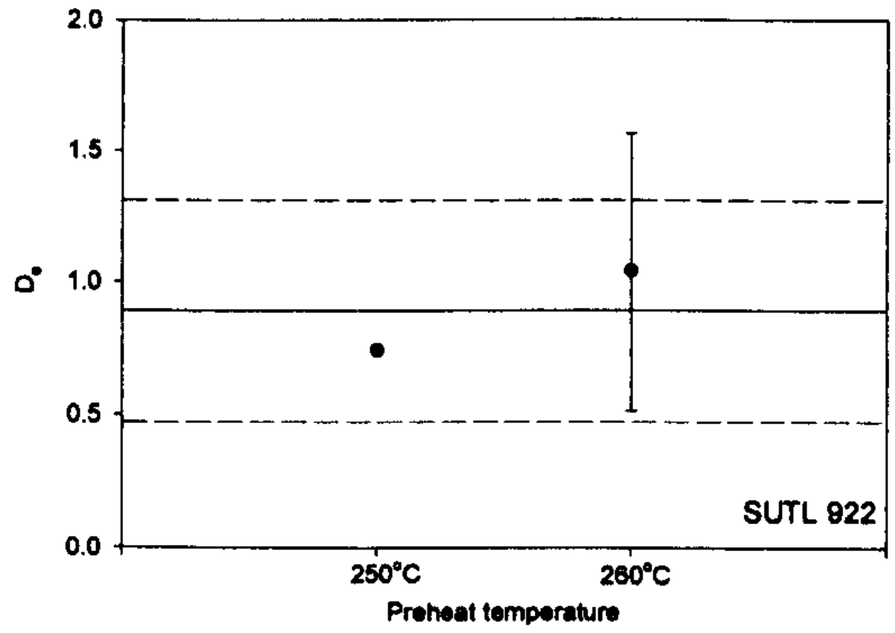
2.0
1.5
1.0
0.5
0.0
D*
SUTL 922
250°C
260°C
Preheat temperature

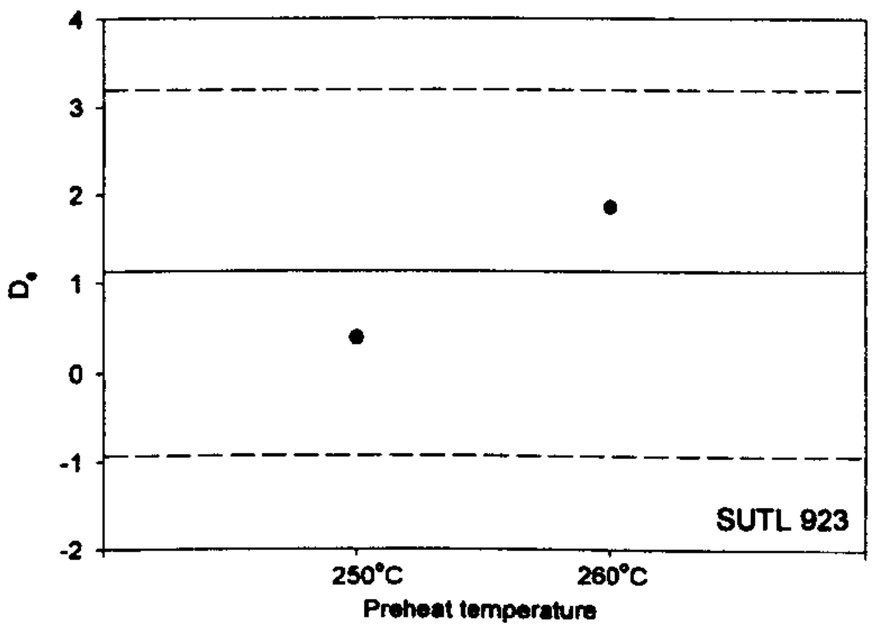
4
3
2
1
0
-1
-2
D*
SUTL 923
250°C
260°C
Preheat temperature

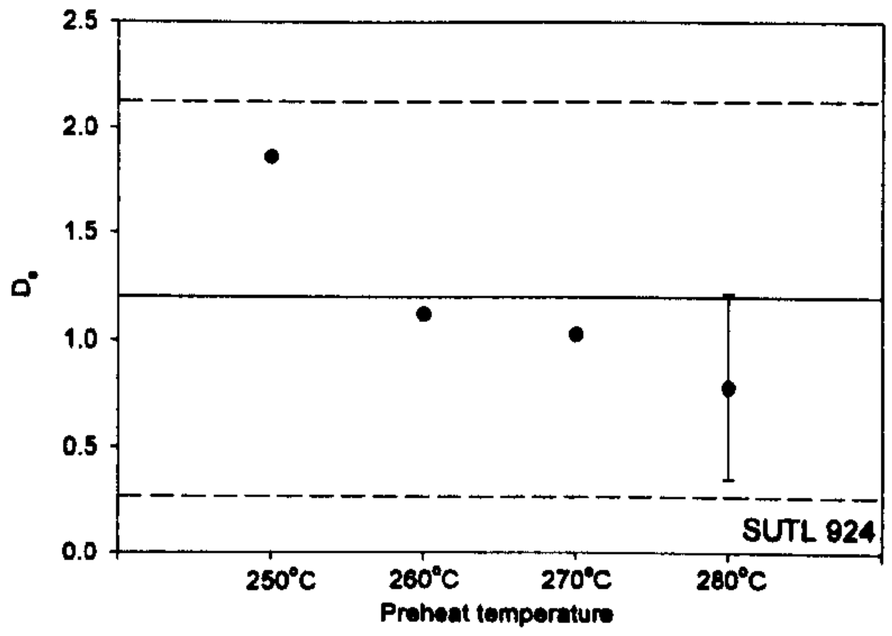
2.5
2.0
1.5
1.0
0.5
0.0
D*
SUTL 924
250°C
260°C
270°C
280°C
Preheat temperature

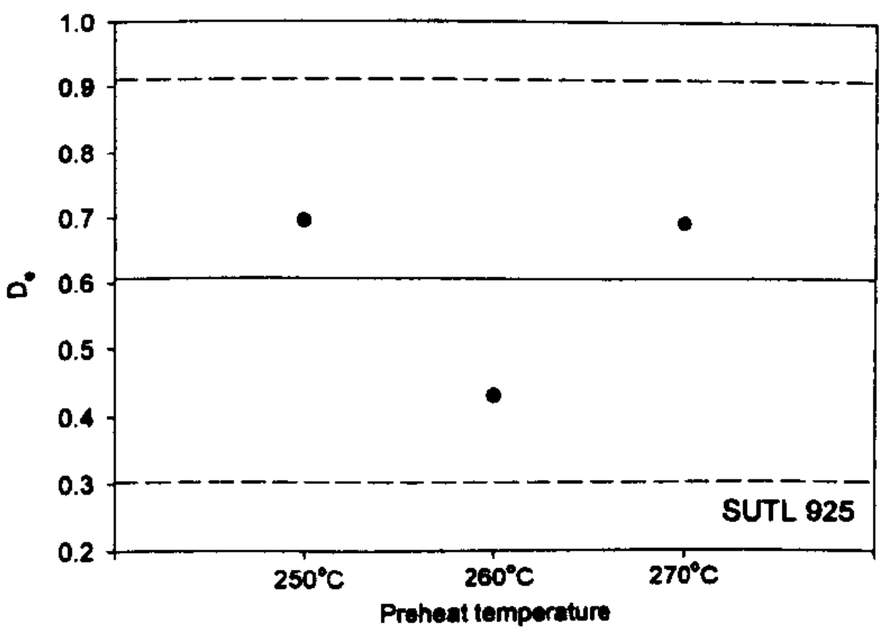
1.0
0.9
0.8
0.7
0.6
0.5
0.4
0.3
0.2
D*
SUTL 925
250°C
260°C
270°C
Preheat temperature

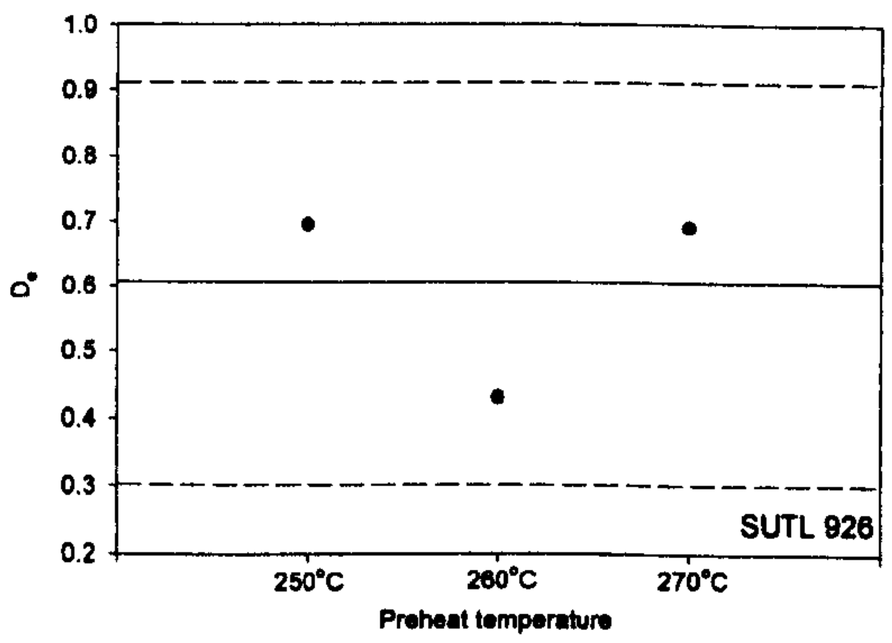
1.0
0.9
0.8
0.7
0.6
0.5
0.4
0.3
0.2
D*
SUTL 926
250°C
260°C
270°C
Preheat temperature

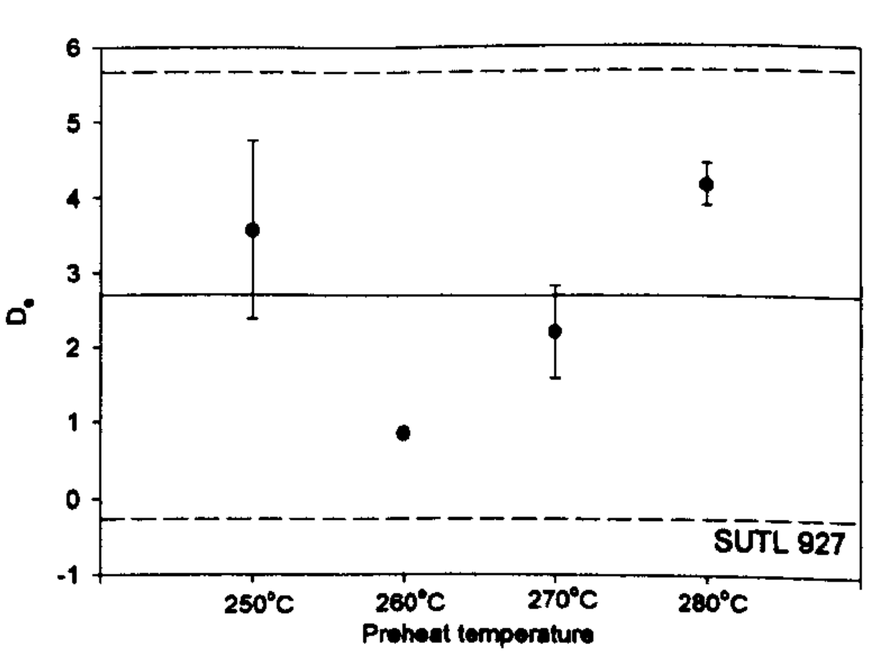
6
5
4
3
2
1
0
-1
D*
SUTL 927
250°C
260°C
270°C
280°C
Preheat temperature

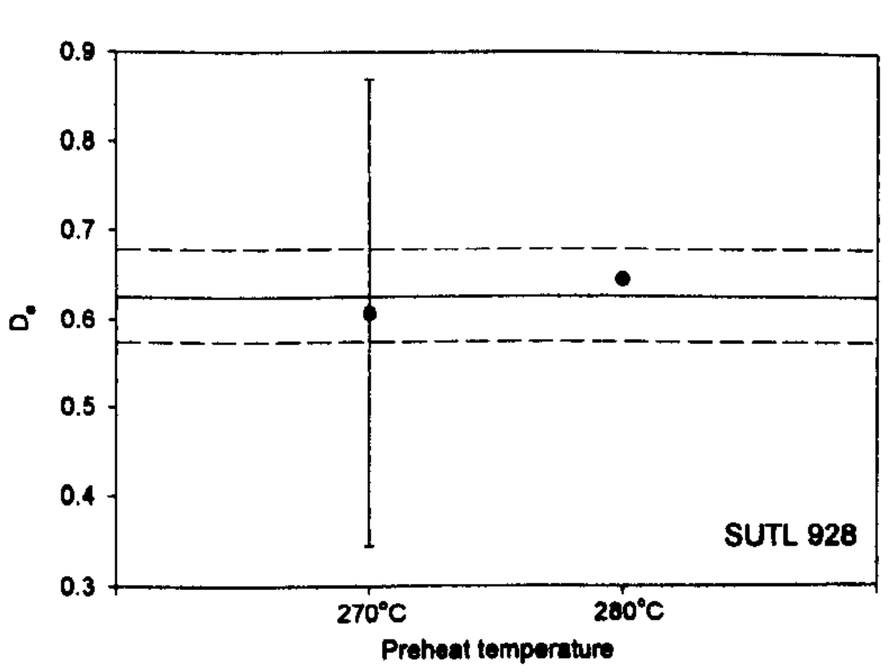
0.9
0.8
0.7
0.6
0.5
0.4
0.3
D*
SUTL 928
270°C
280°C
Preheat temperature

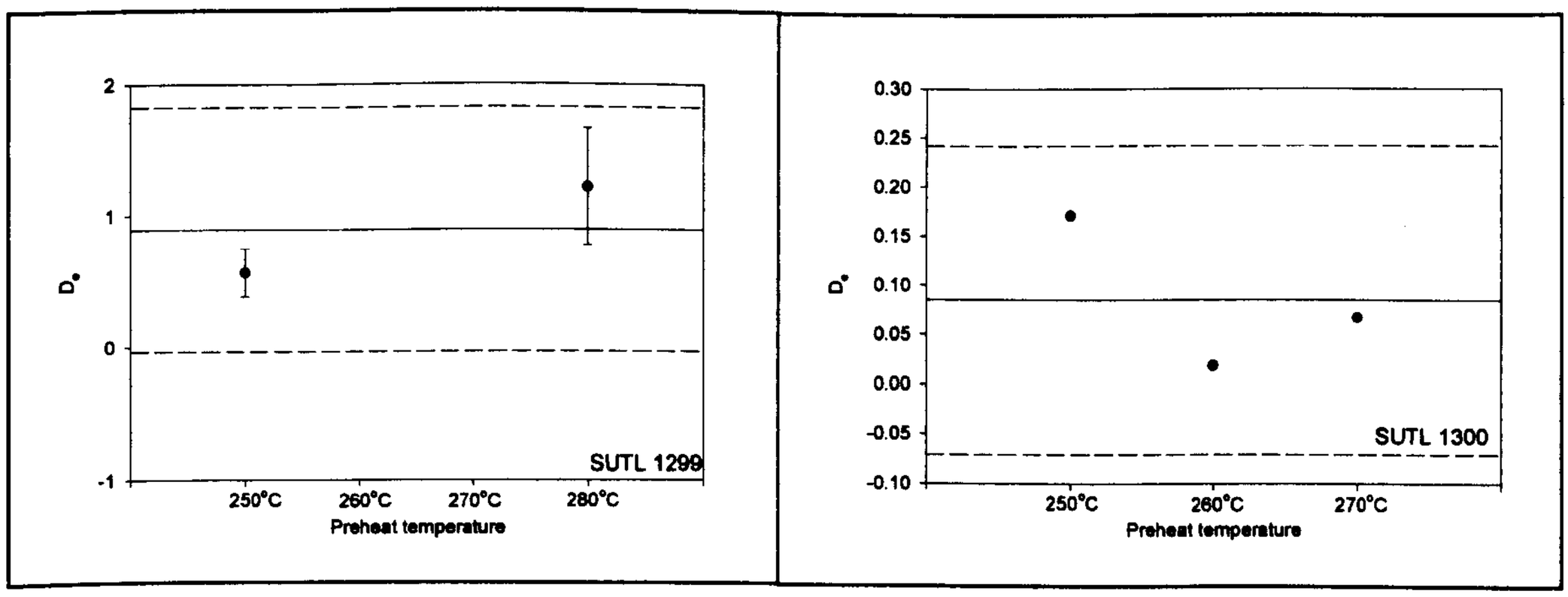

BAY OF SKAILL

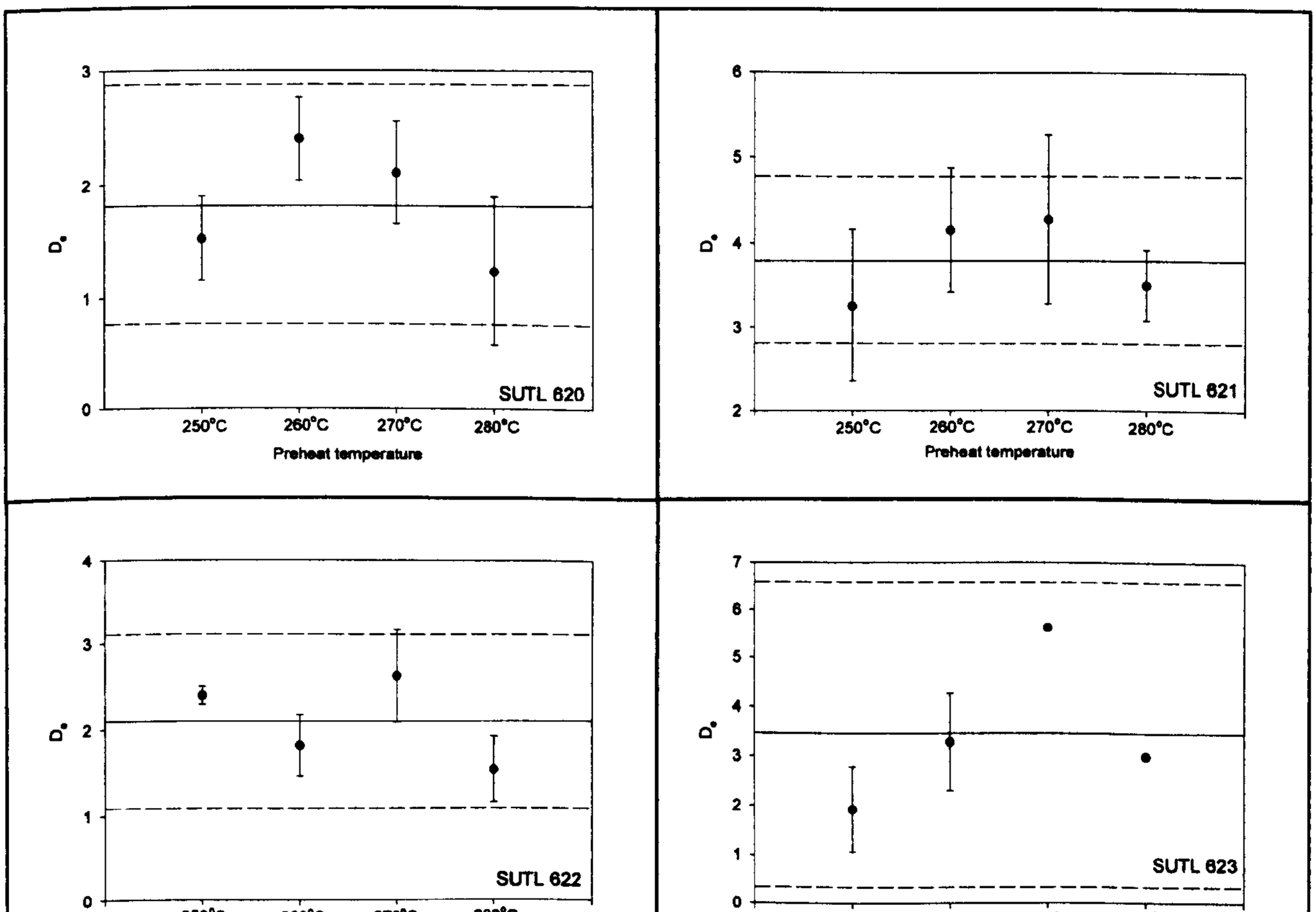

Appendix 5.3 – Mean and standard error of test dose response of all discs for each sample

TOFTS NESS

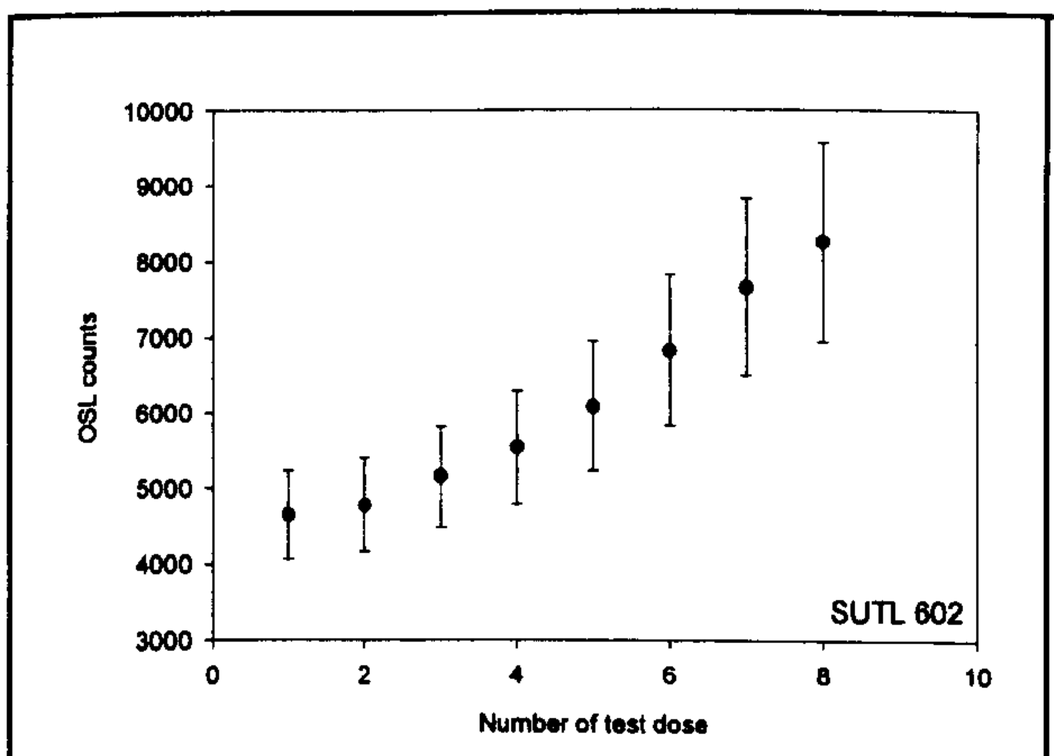

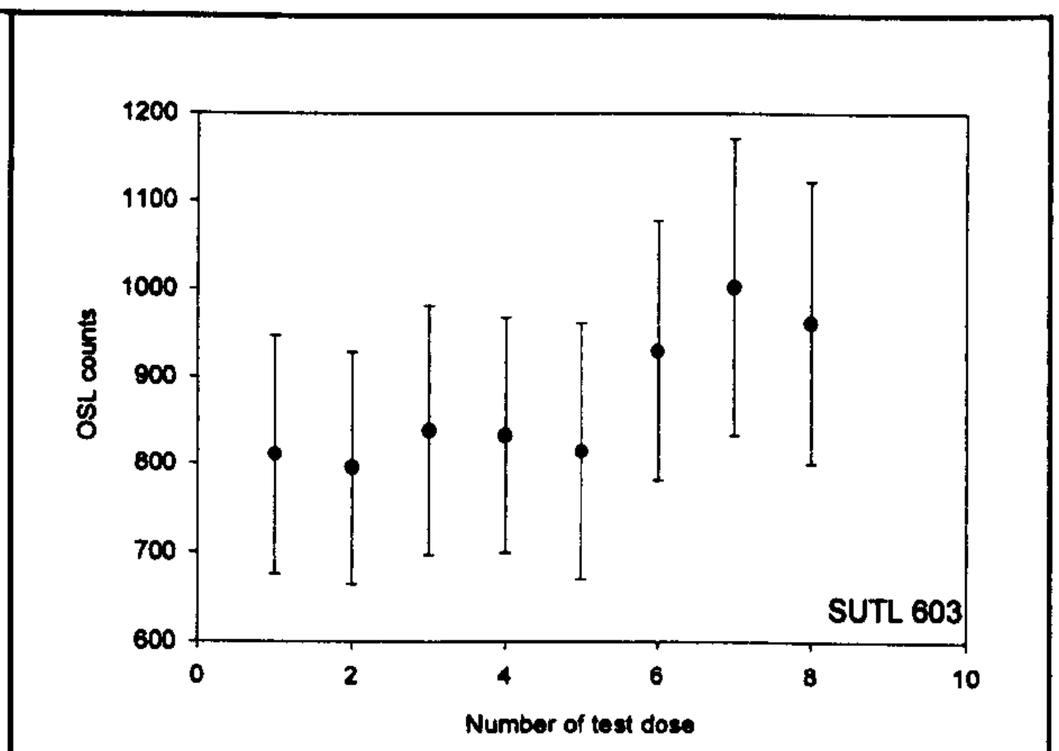

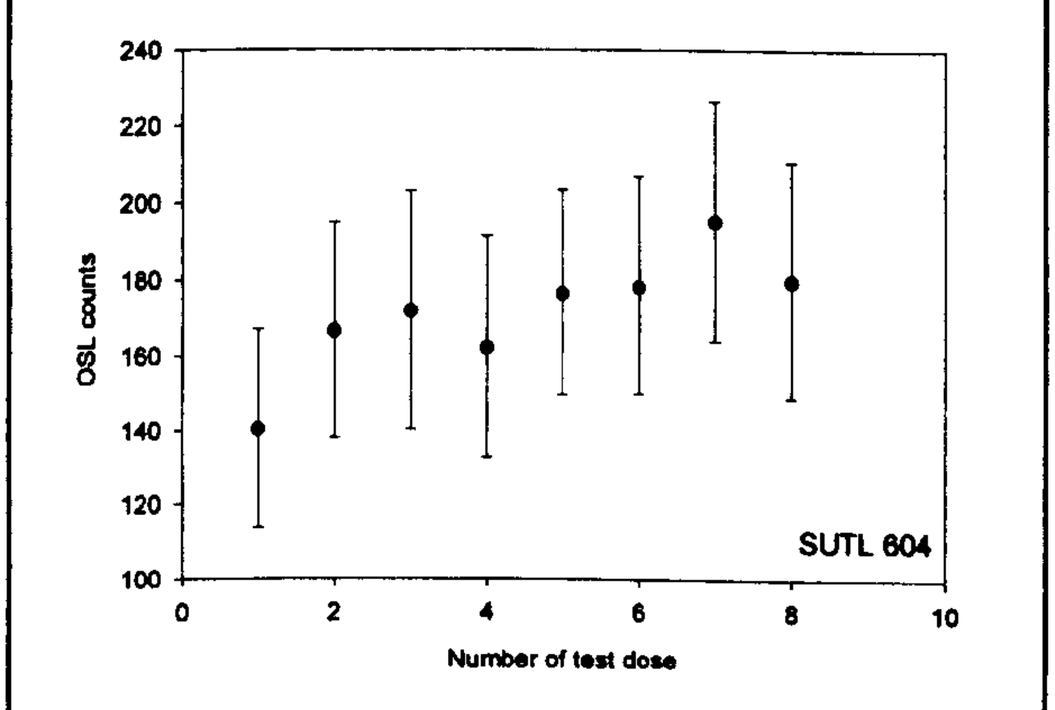

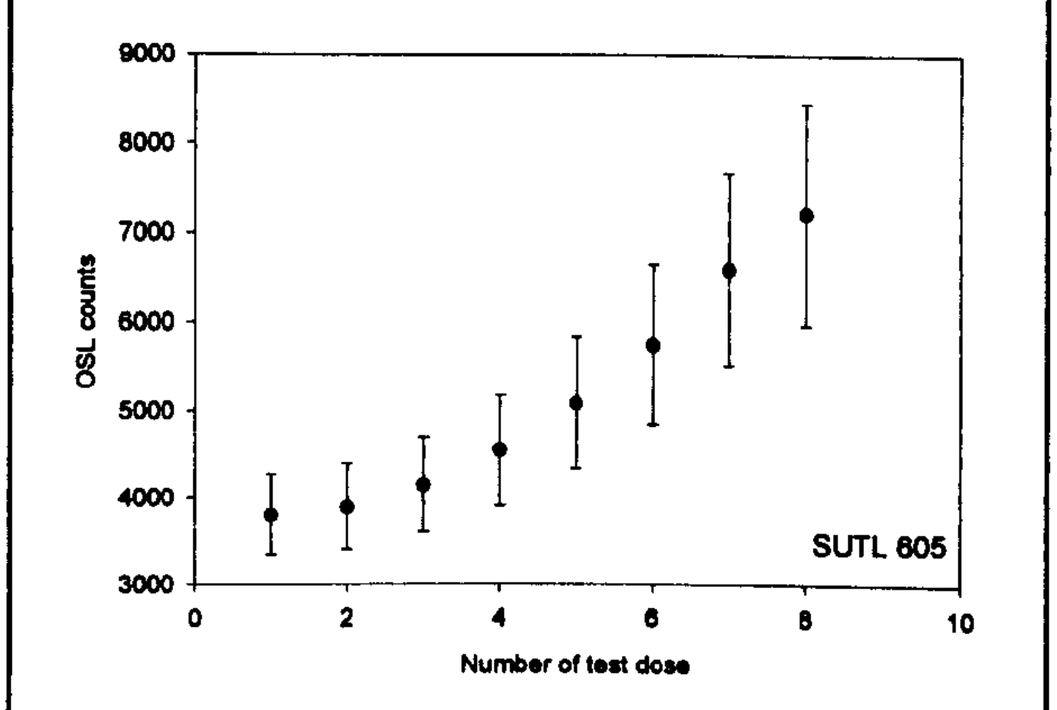

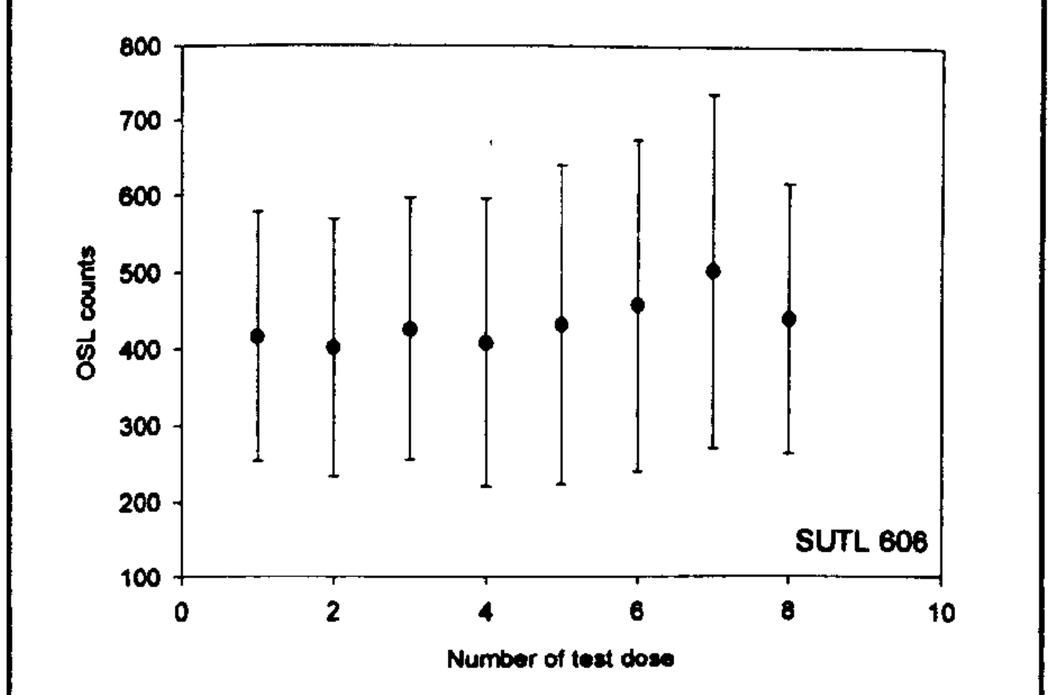

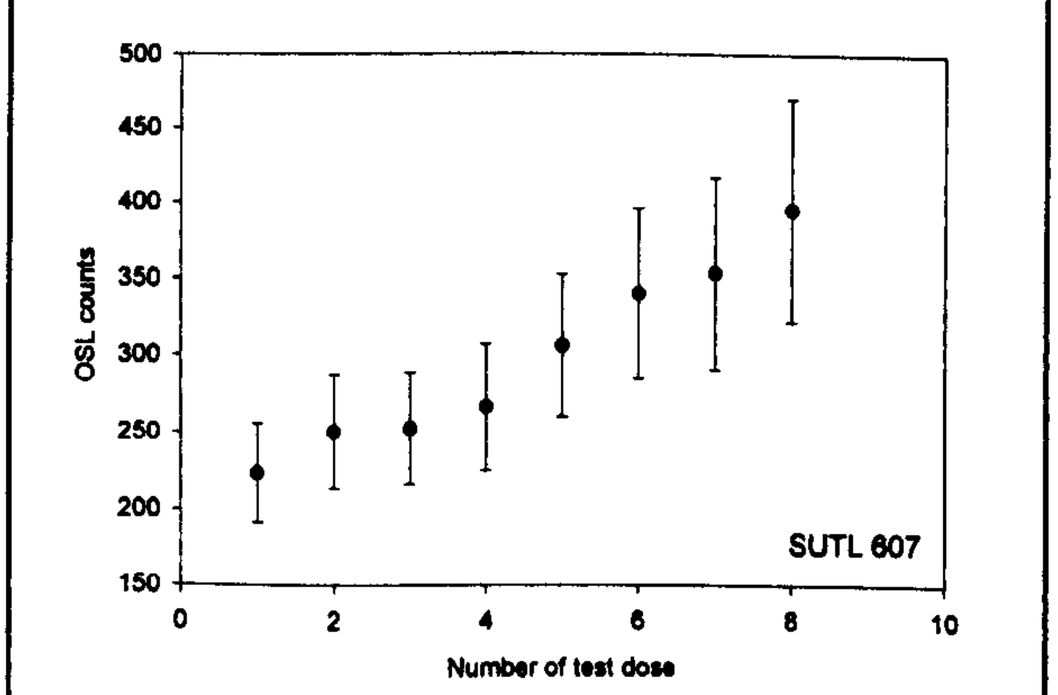

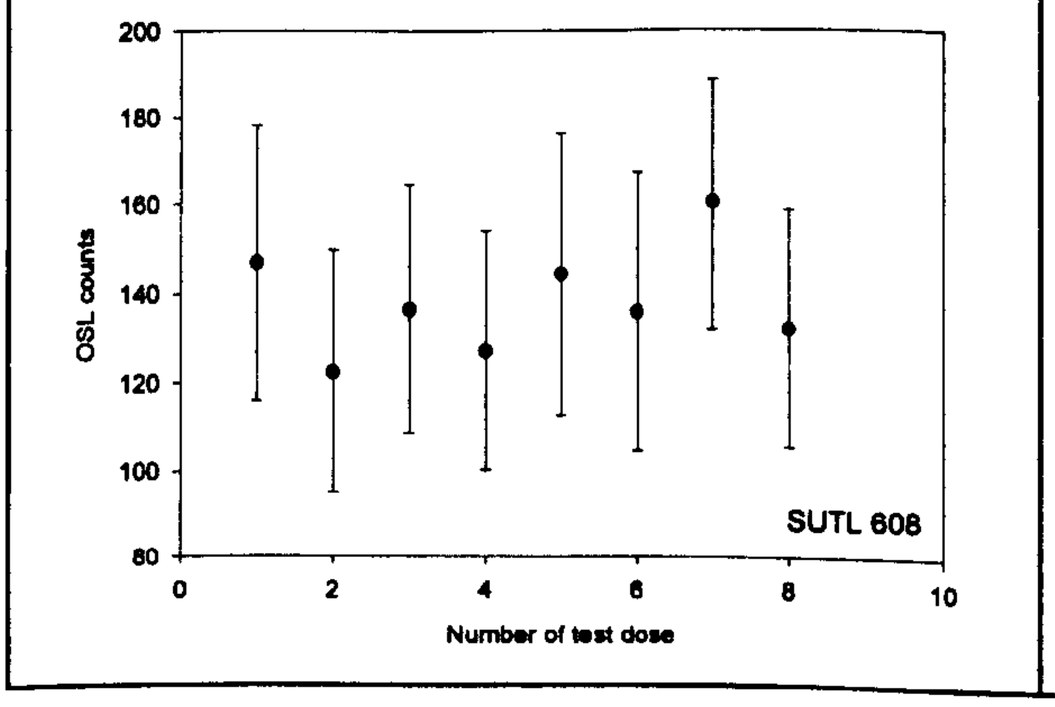

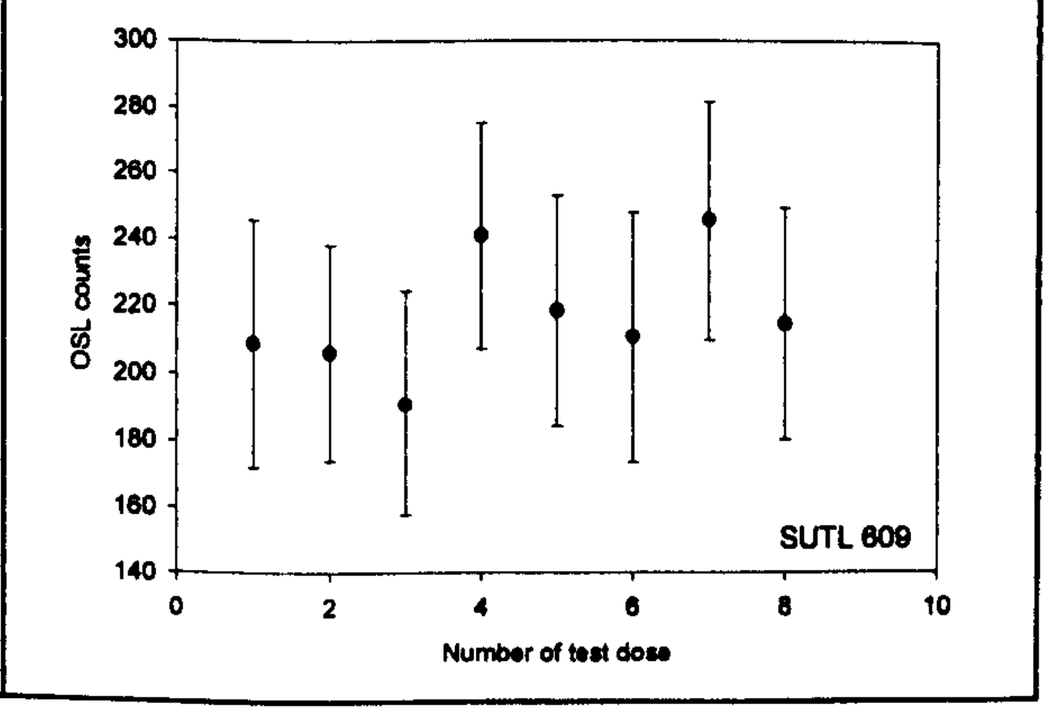

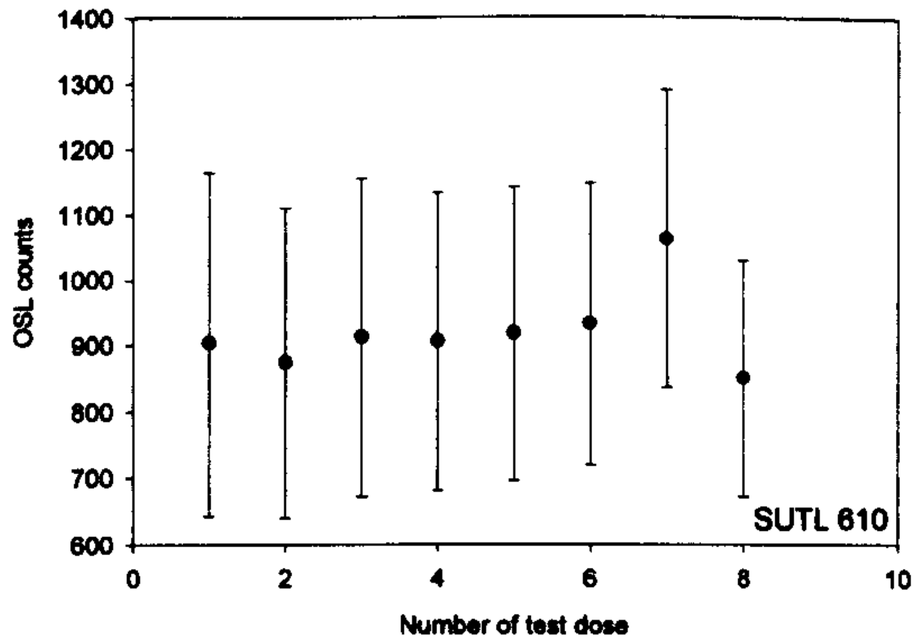
OSL counts
Number of test dose
SUTL 610

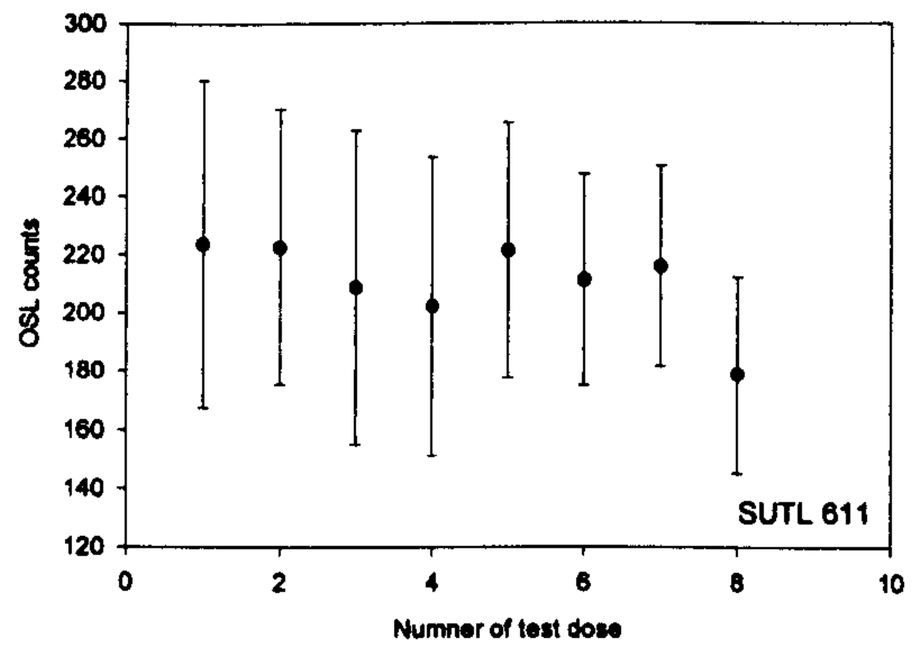
OSL counts
Numner of test dose
SUTL 611

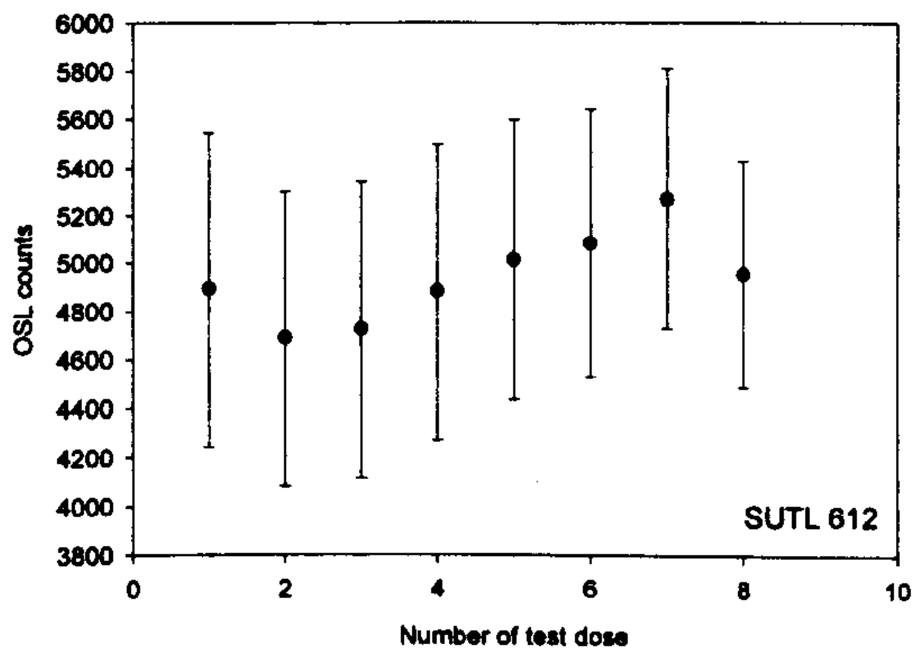
OSL counts
Number of test dose
SUTL 612

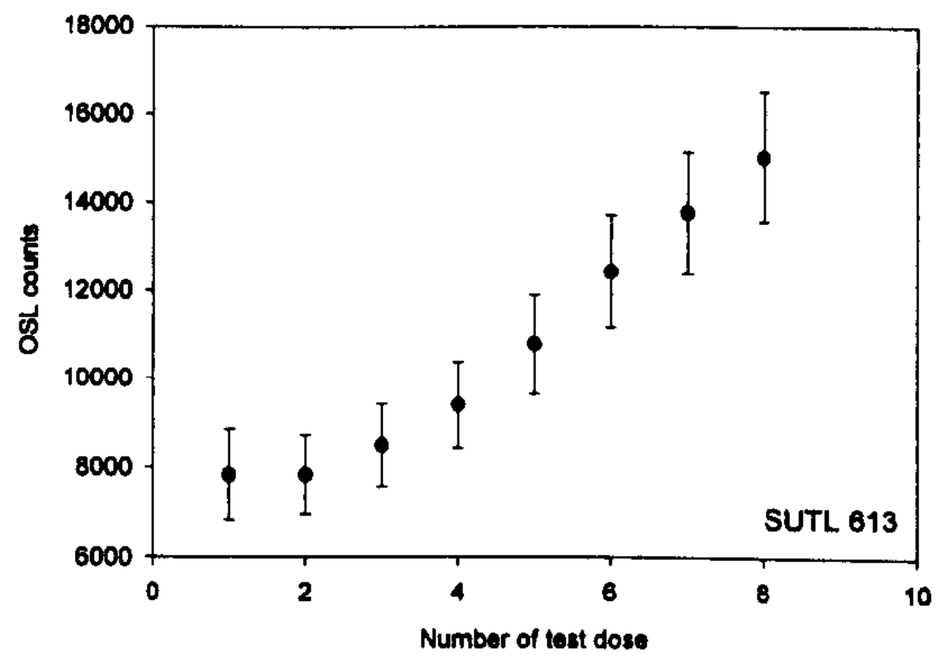
OSL counts
Number of test dose
SUTL 613

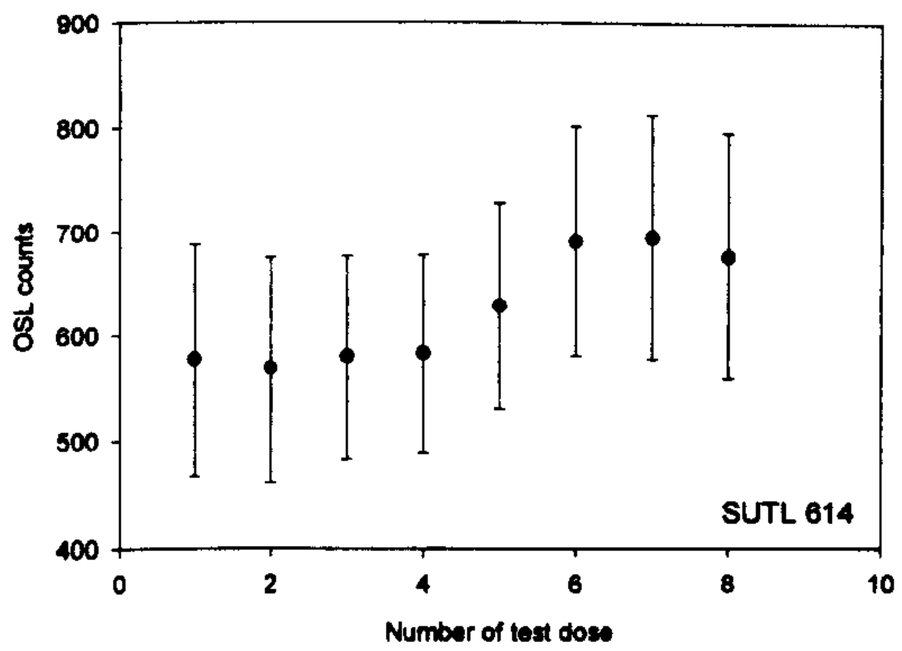
OSL counts
Number of test dose
SUTL 614

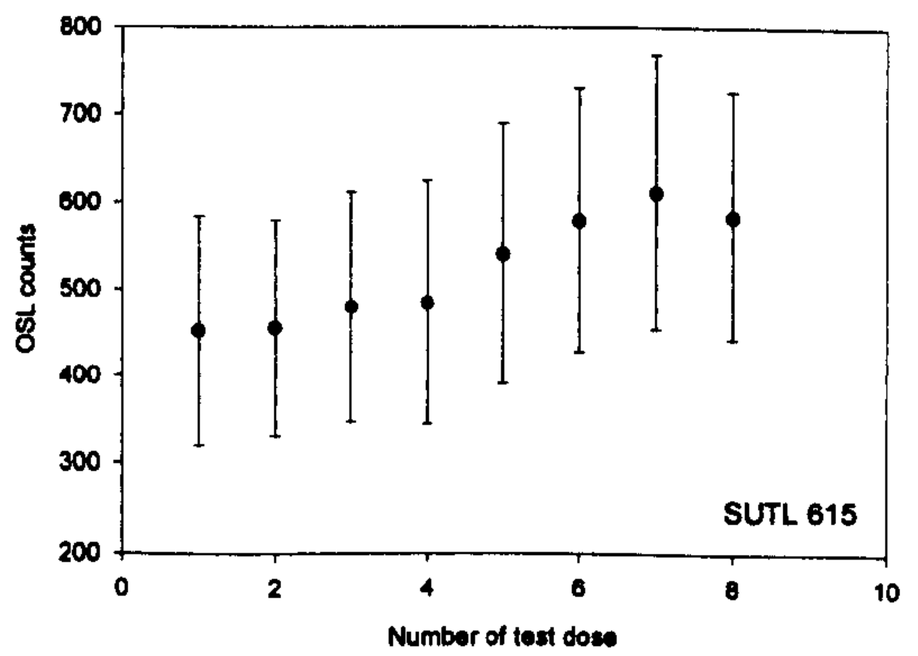
OSL counts
Number of test dose
SUTL 615

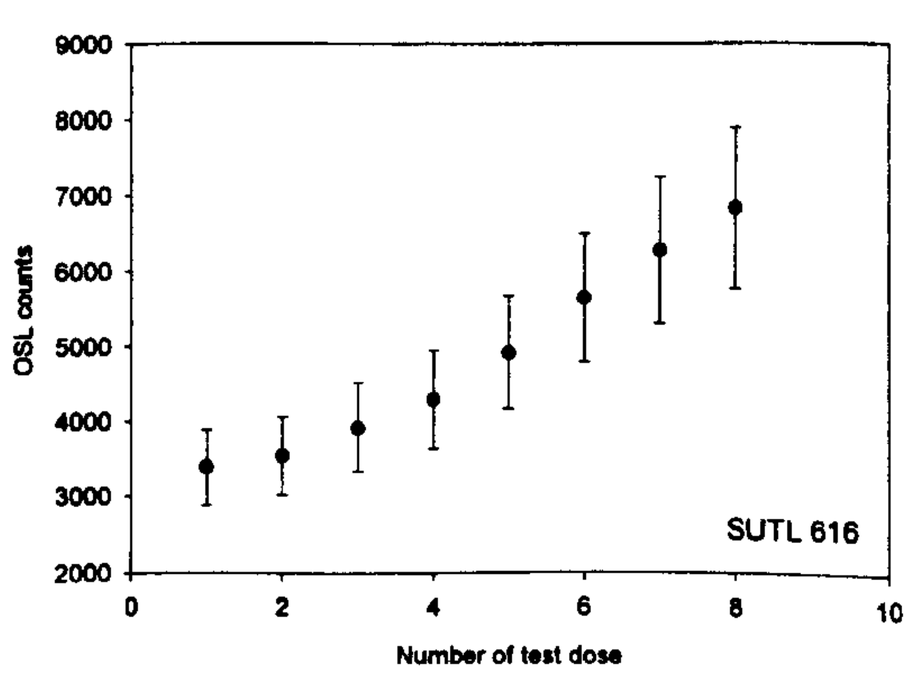
OSL counts
Number of test dose
SUTL 616

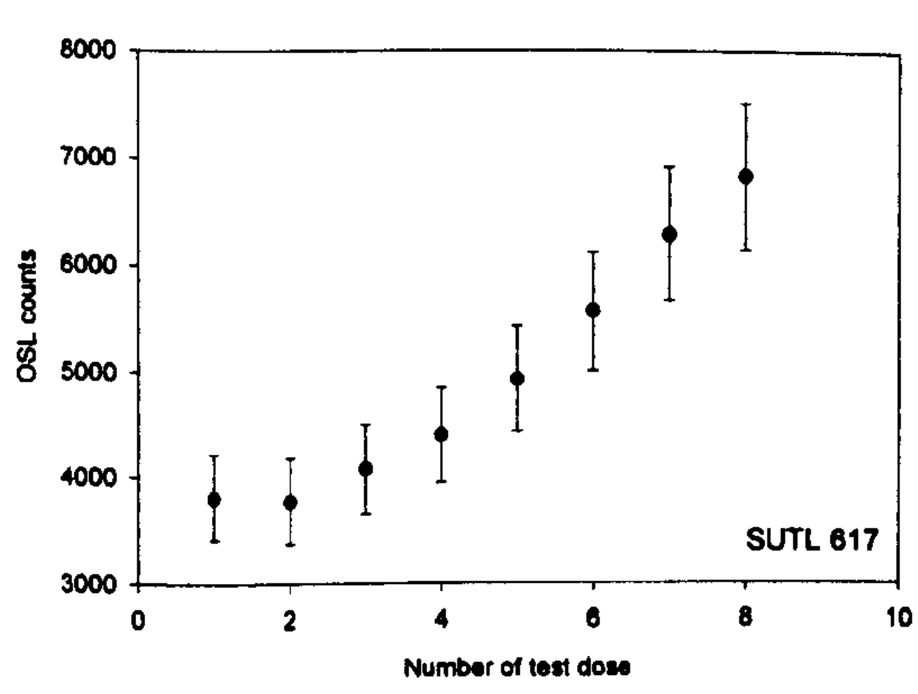
OSL counts
Number of test dose
SUTL 617

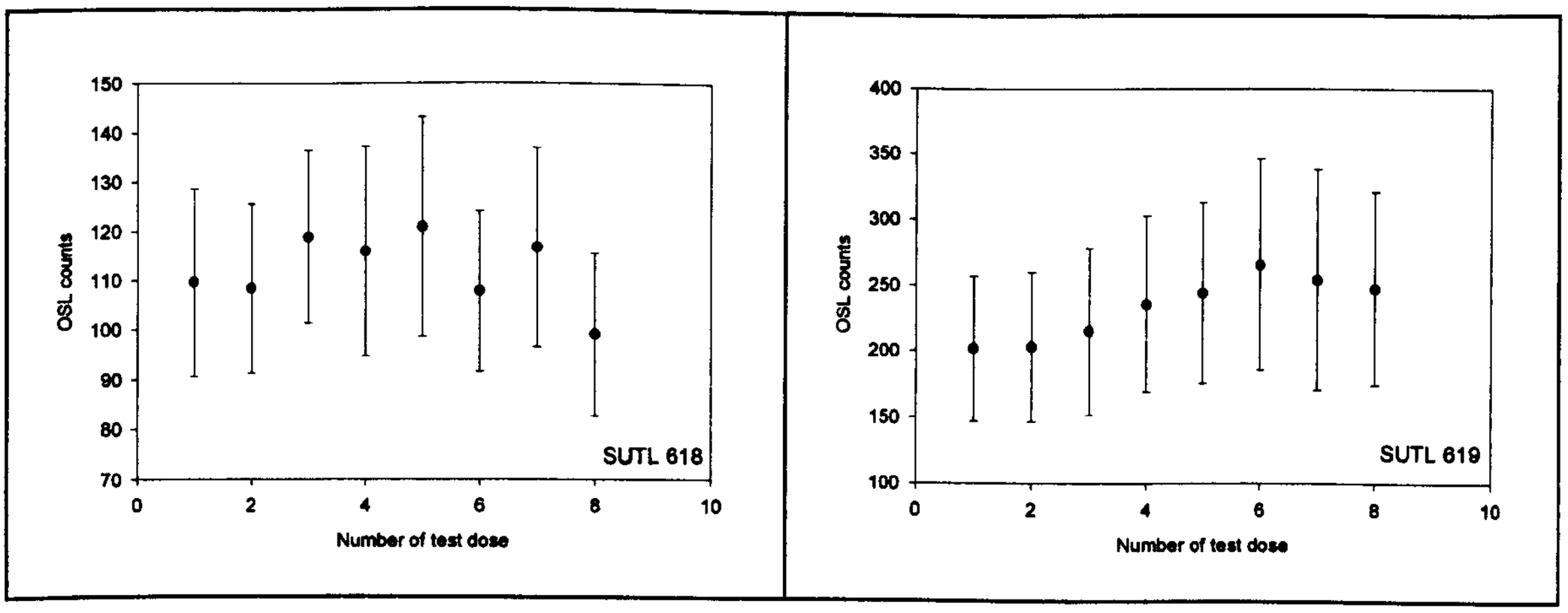

BAY OF LOPNESS

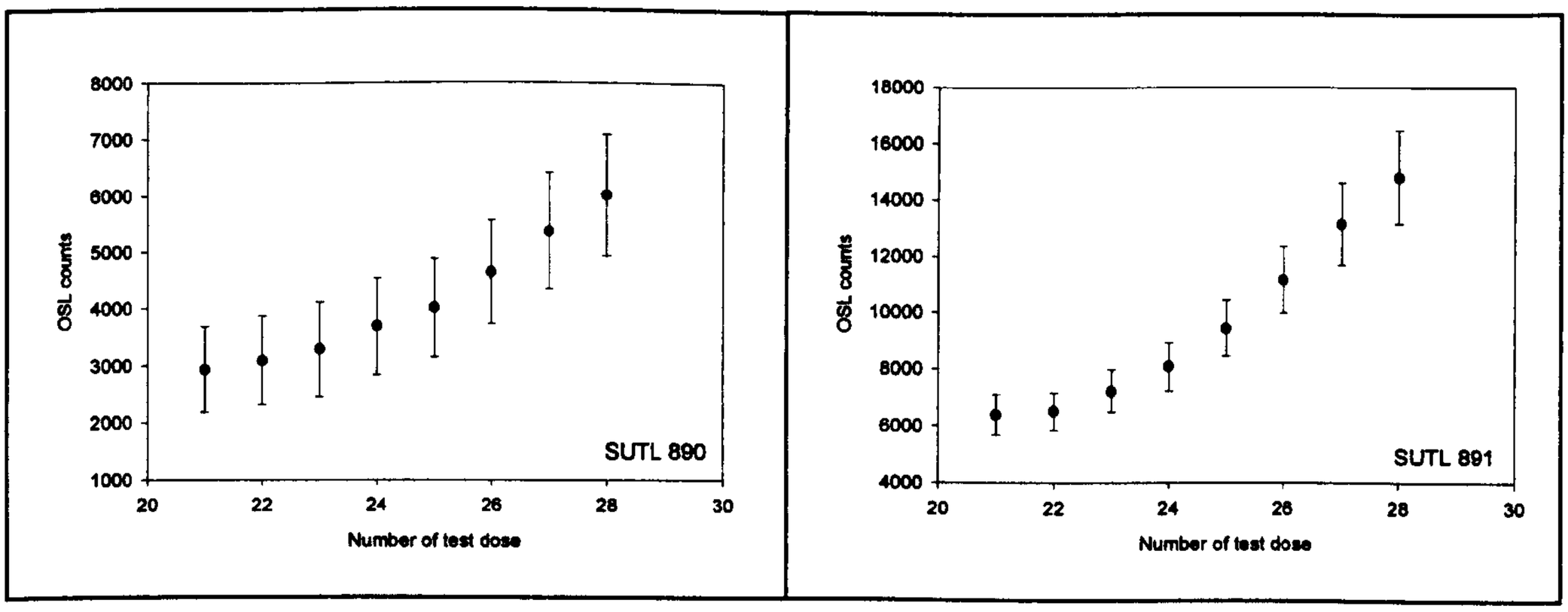
8000
7000
6000
5000
4000
3000
2000
1000
OSL counts
20
22
24
26
28
30
Number of test dose
SUTL 890
18000
16000
14000
12000
10000
8000
6000
4000
OSL counts
20
22
24
26
28
30
Number of test dose
SUTL 891

QUOYGREW

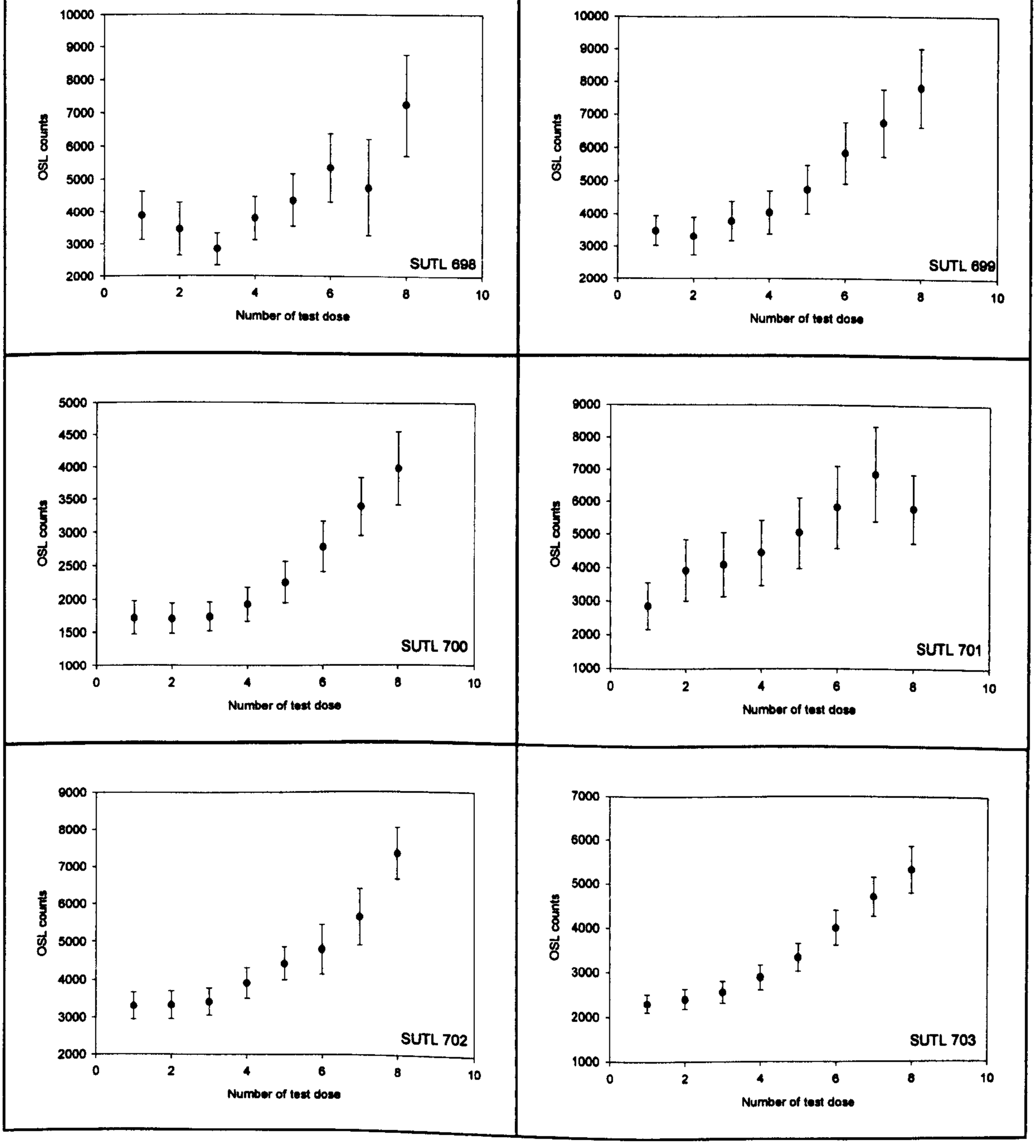
10000
9000
8000
7000
6000
5000
4000
3000
2000
OSL counts
0
2
4
6
8
10
Number of test dose
SUTL 698
10000
9000
8000
7000
6000
5000
4000
3000
2000
OSL counts
0
2
4
6
8
10
Number of test dose
SUTL 699
5000
4500
4000
3500
3000
2500
2000
1500
1000
OSL counts
0
2
4
6
8
10
Number of test dose
SUTL 700
9000
8000
7000
6000
5000
4000
3000
2000
1000
OSL counts
0
2
4
6
8
10
Number of test dose
SUTL 701
9000
8000
7000
6000
5000
4000
3000
2000
OSL counts
0
2
4
6
8
10
Number of test dose
SUTL 702
7000
6000
5000
4000
3000
2000
1000
OSL counts
0
2
4
6
8
10
Number of test dose
SUTL 703

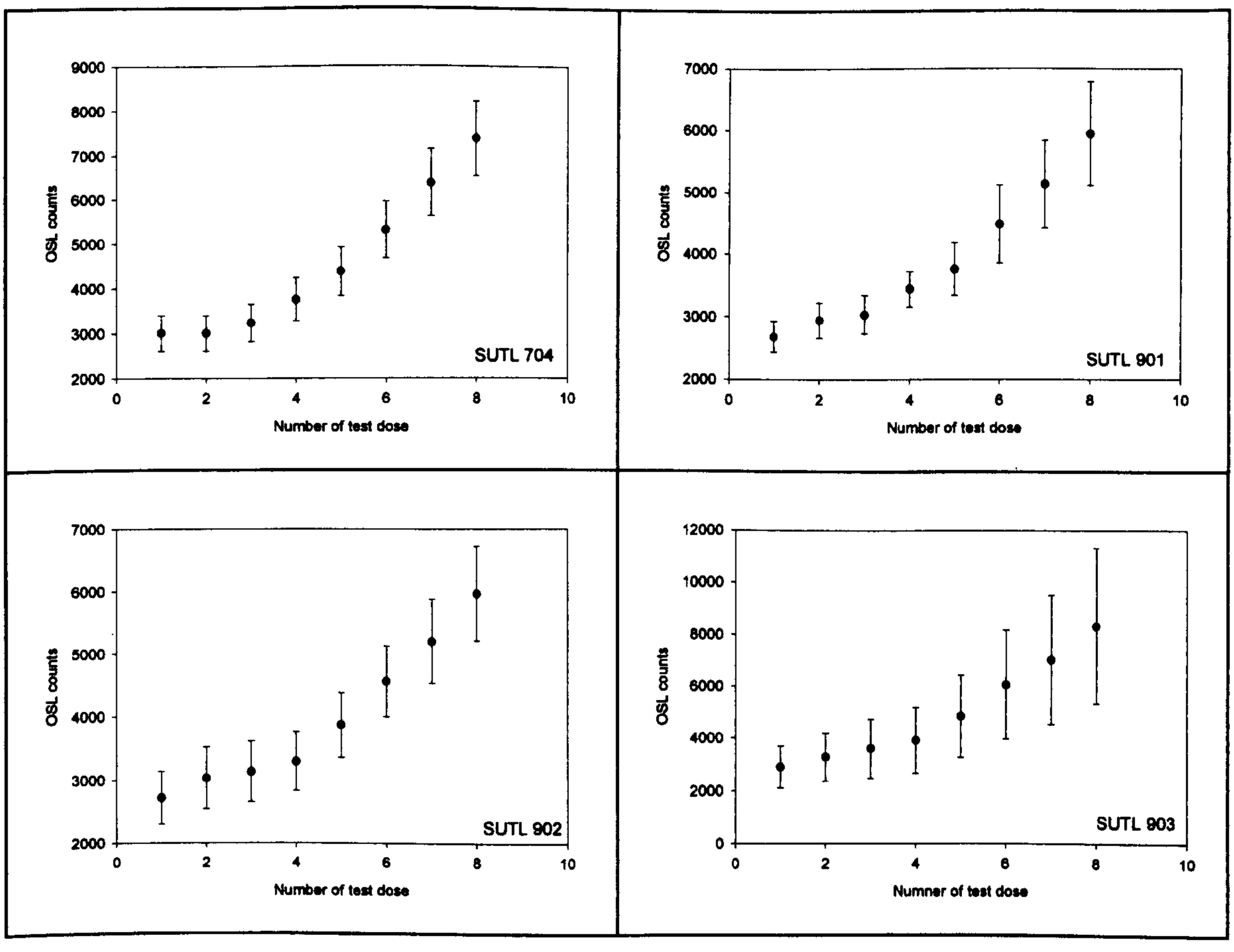
OSL counts
Number of test dose
SUTL 704
SUTL 901
SUTL 902
SUTL 903
Numner of test dose

PIEROWALL

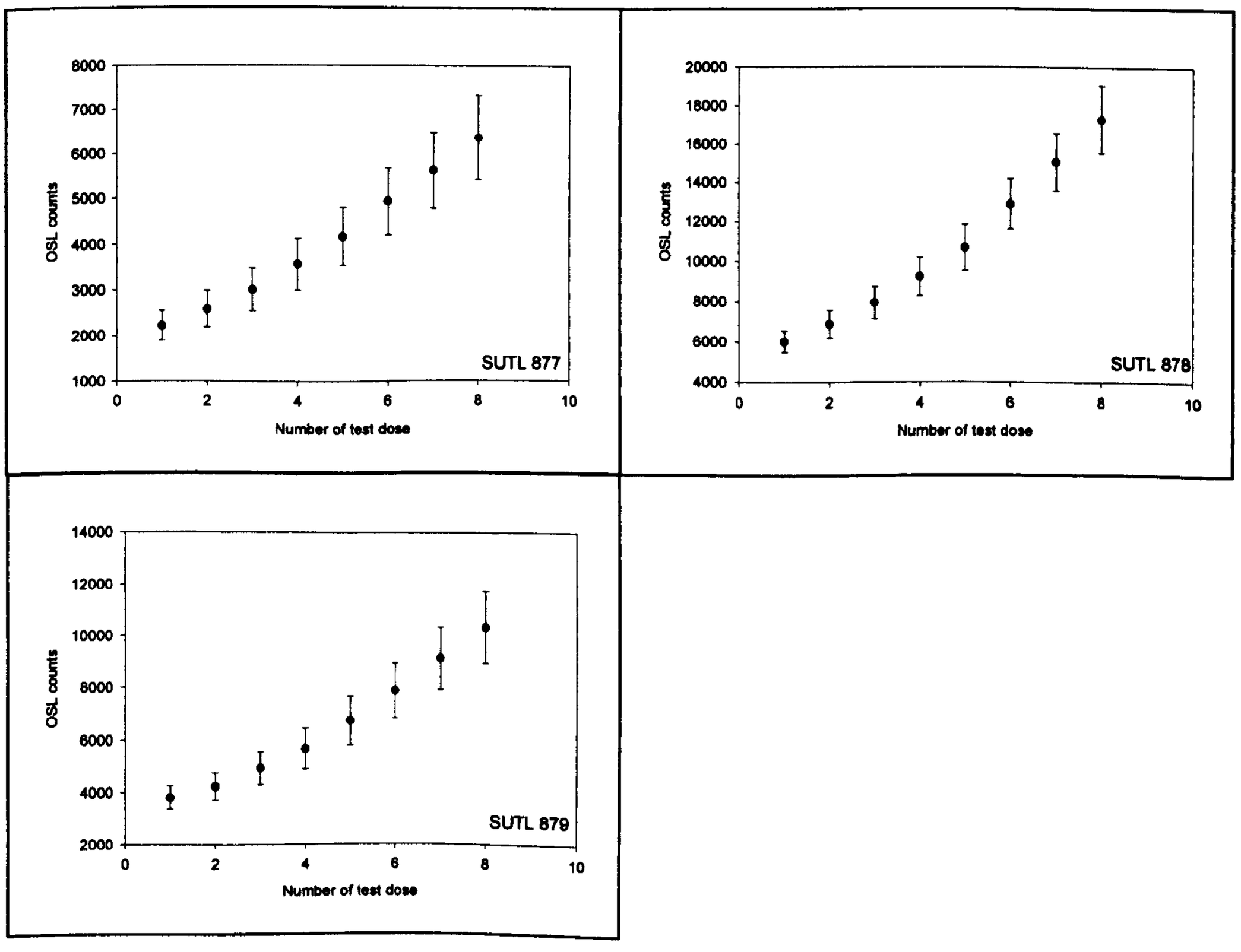
OSL counts
Number of test dose
SUTL 877
SUTL 878
SUTL 879

EVERTAFT

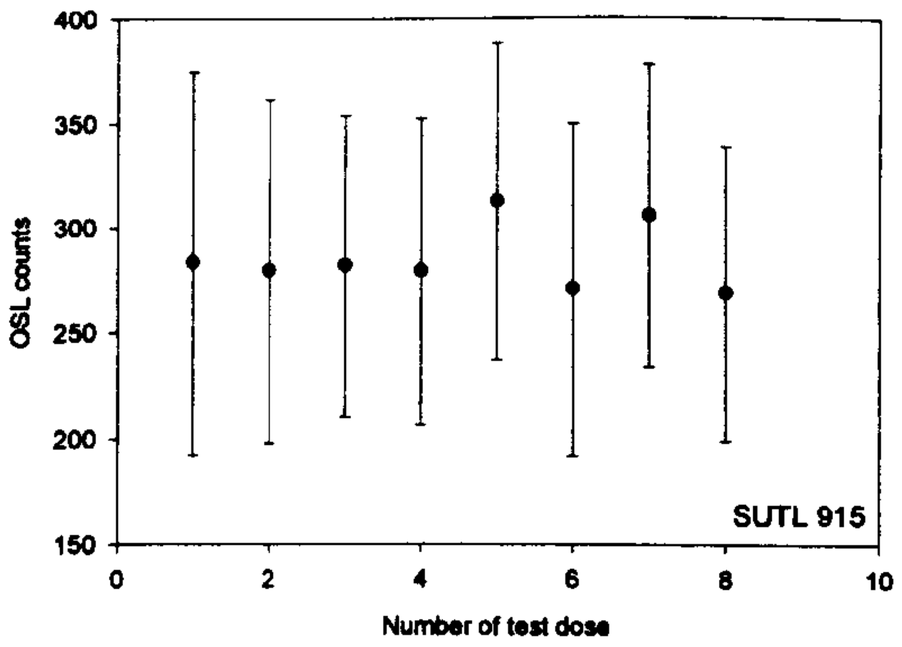
OSL counts
Number of test dose
SUTL 915

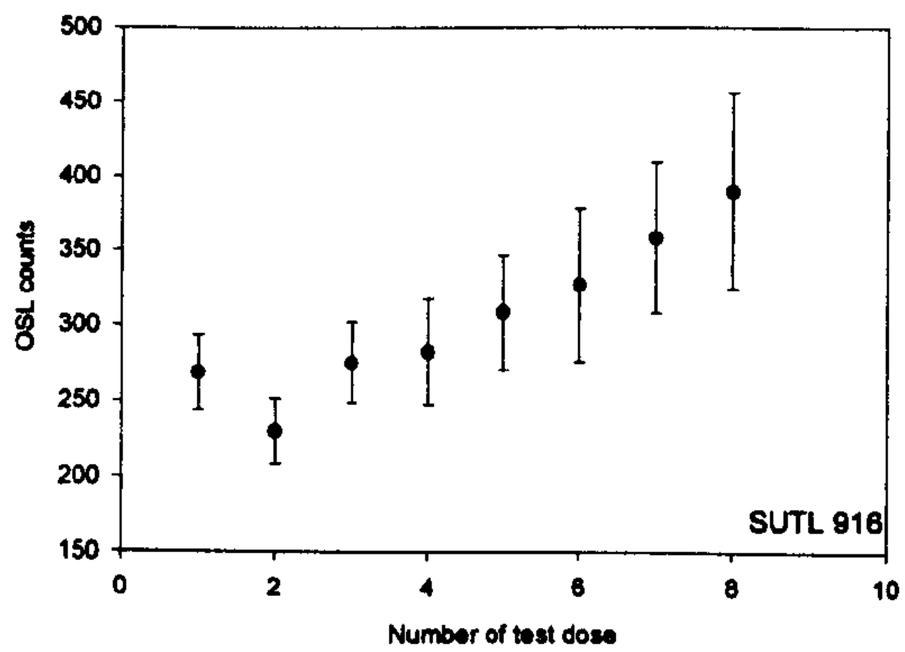
OSL counts
Number of test dose
SUTL 916

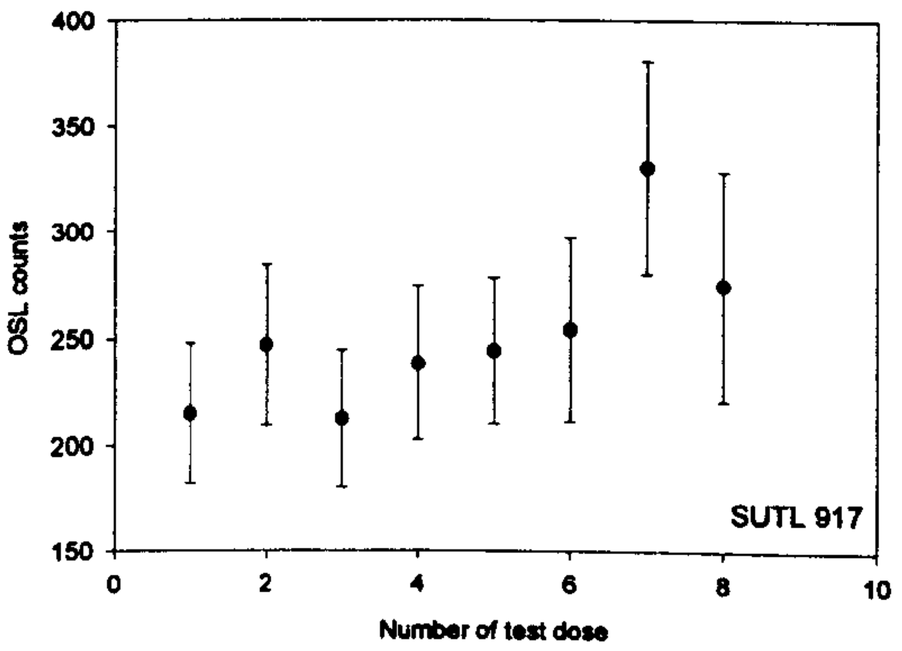
OSL counts
Number of test dose
SUTL 917

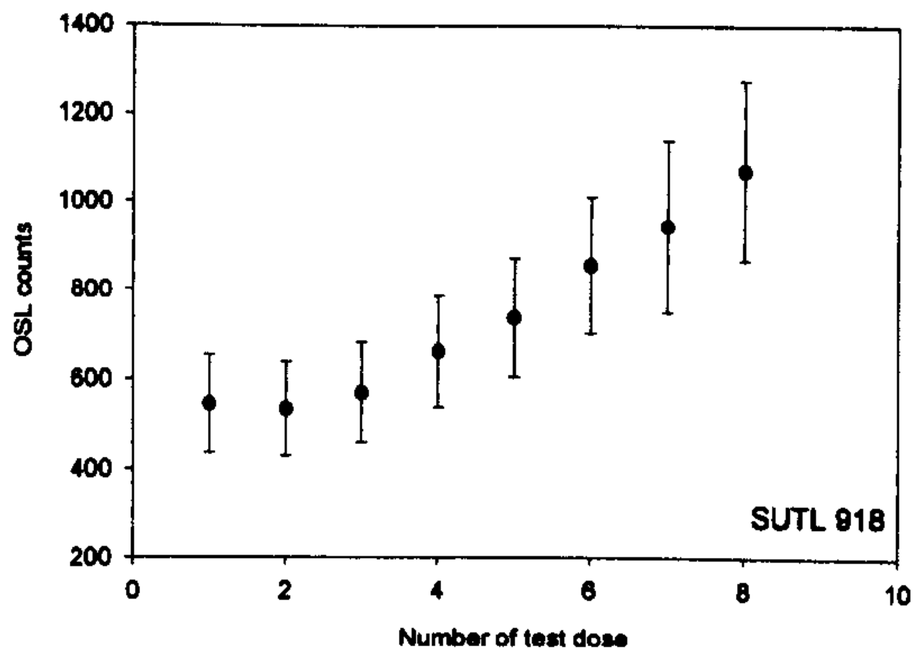
OSL counts
Number of test dose
SUTL 918

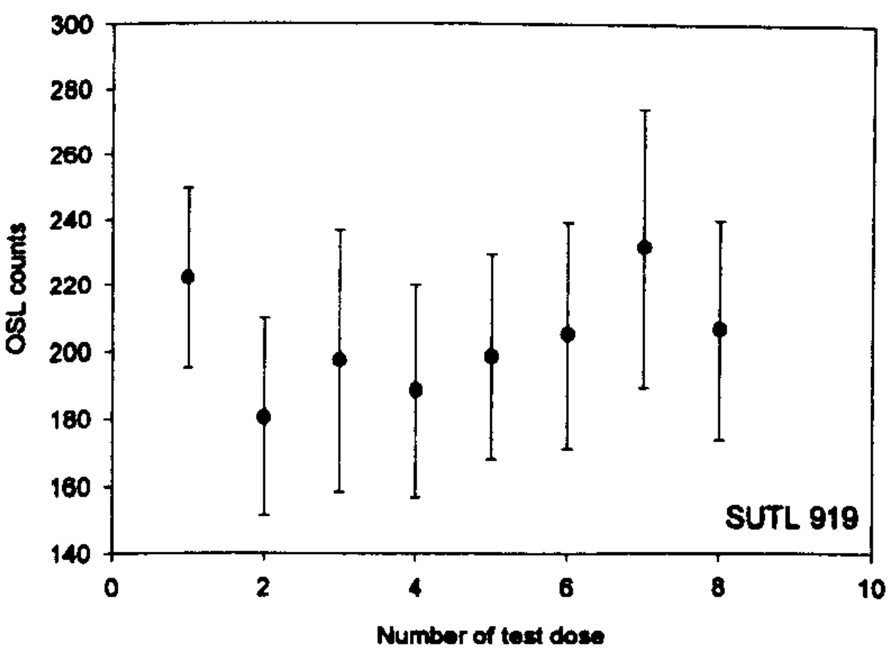
OSL counts
Number of test dose
SUTL 919

SANDHILL

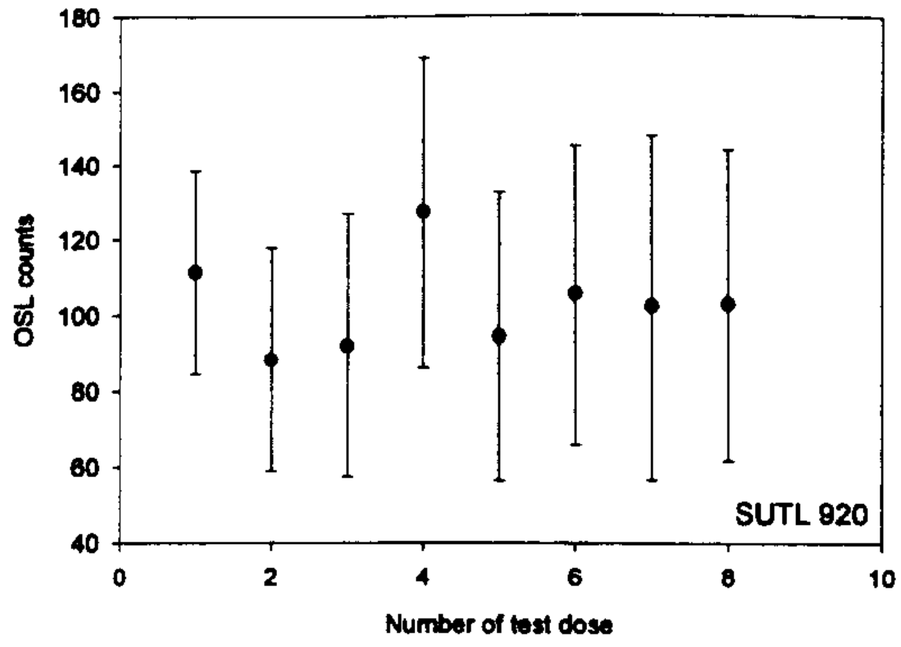
OSL counts
Number of test dose
SUTL 920

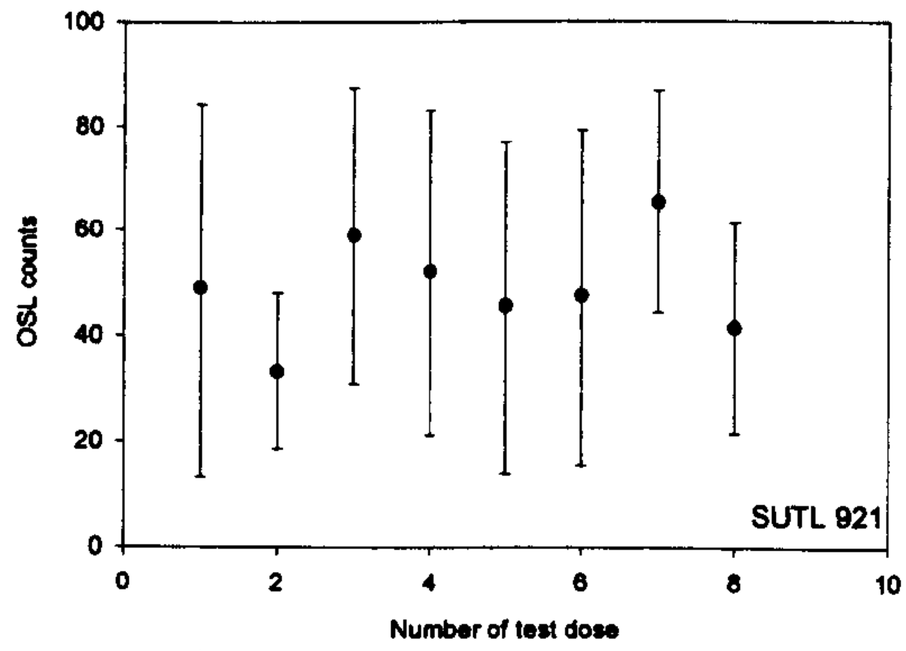
OSL counts
Number of test dose
SUTL 921

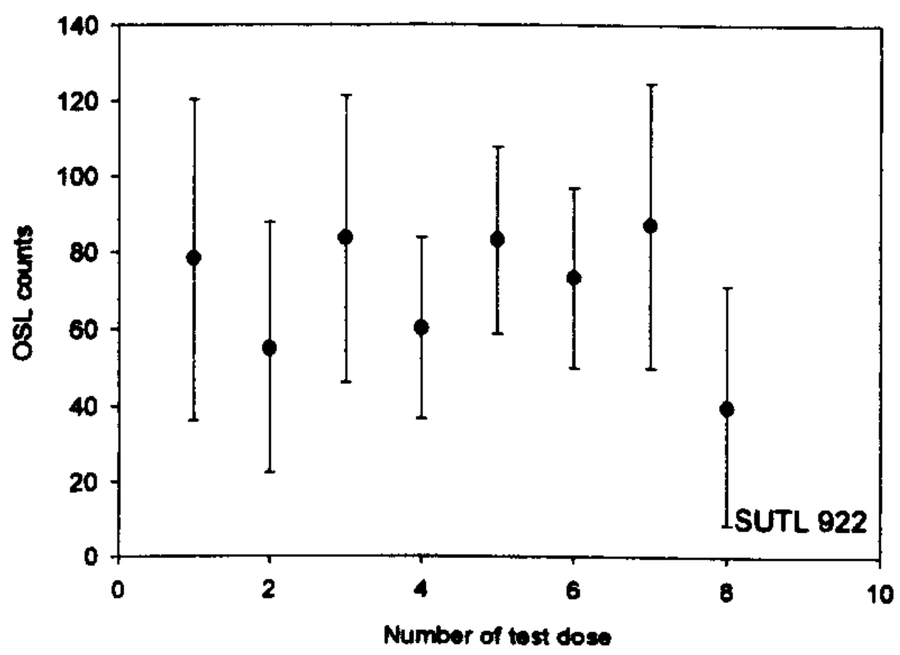
OSL counts
Number of test dose
SUTL 922

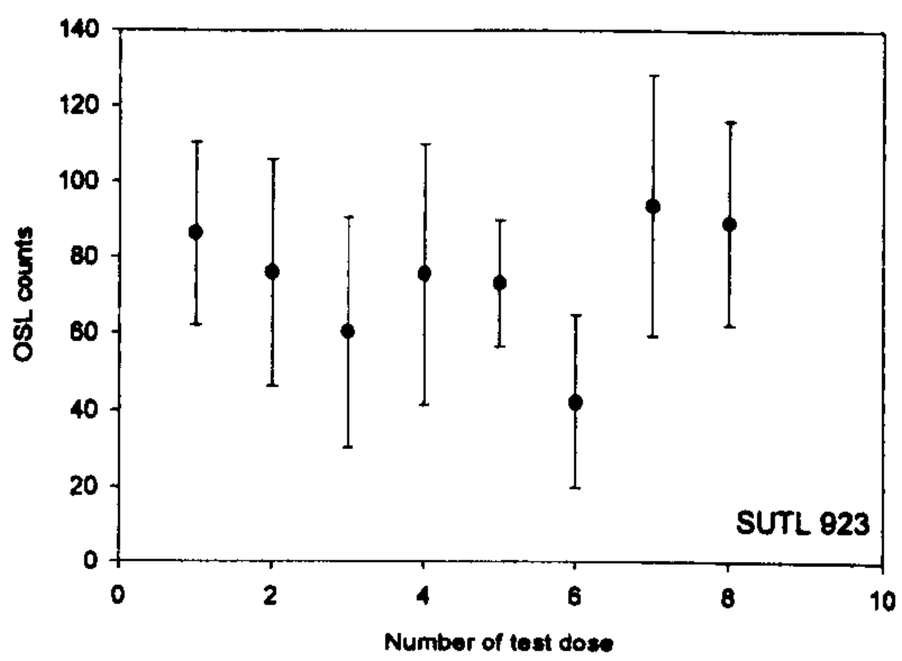
OSL counts
Number of test dose
SUTL 923

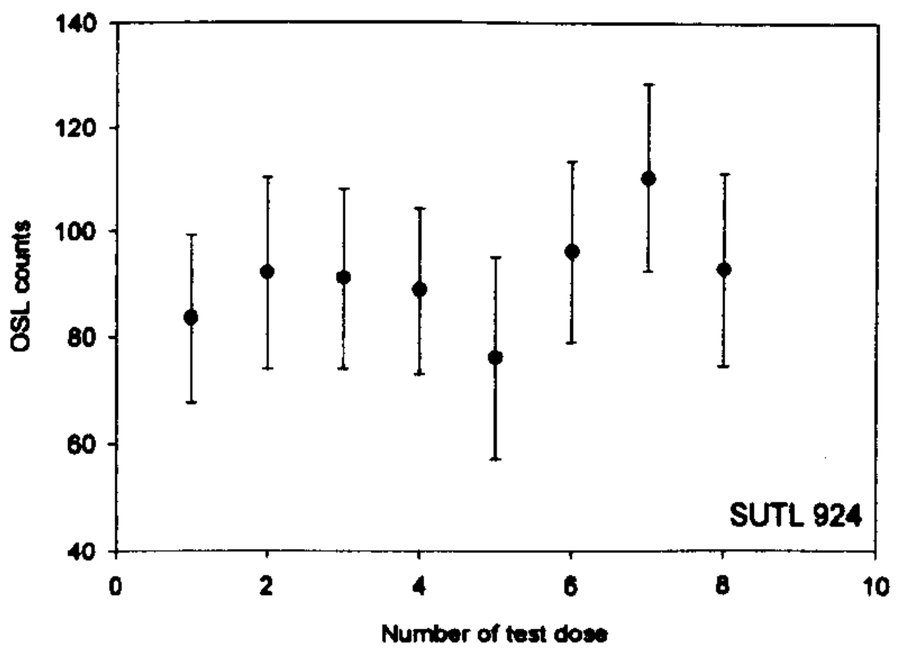
OSL counts
Number of test dose
SUTL 924

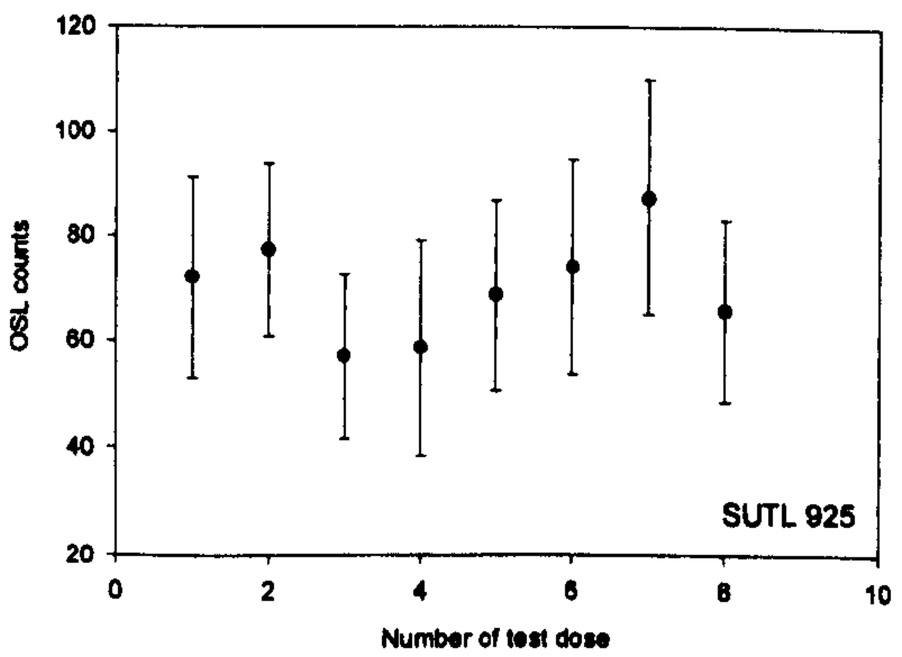
OSL counts
Number of test dose
SUTL 925

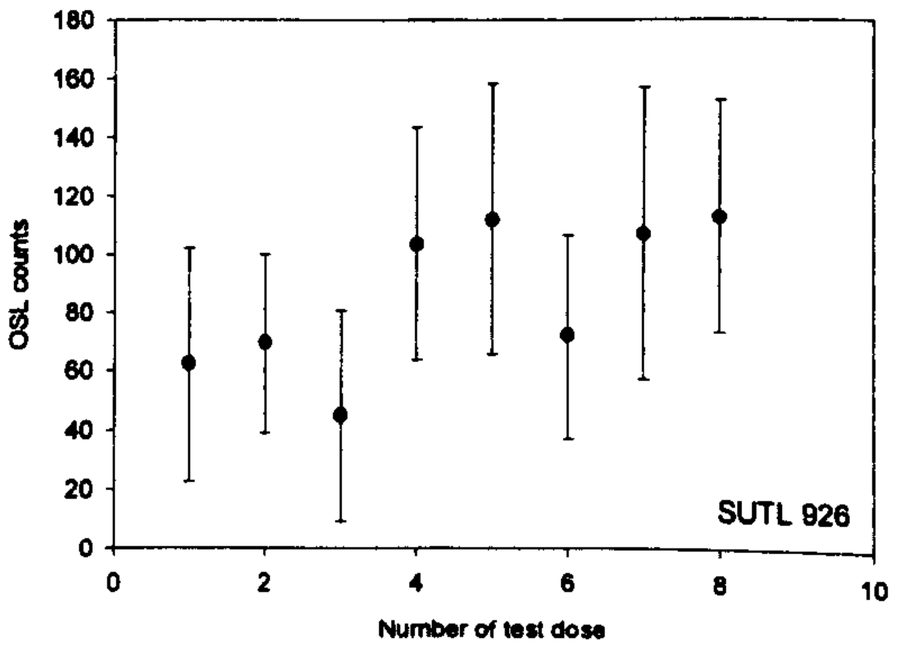
OSL counts
Number of test dose
SUTL 926

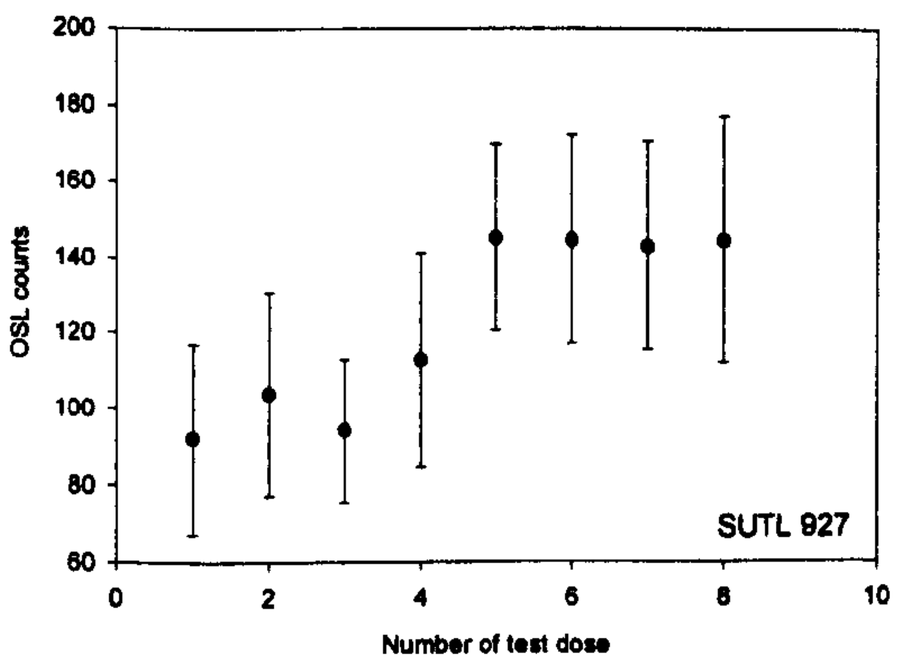
OSL counts
Number of test dose
SUTL 927

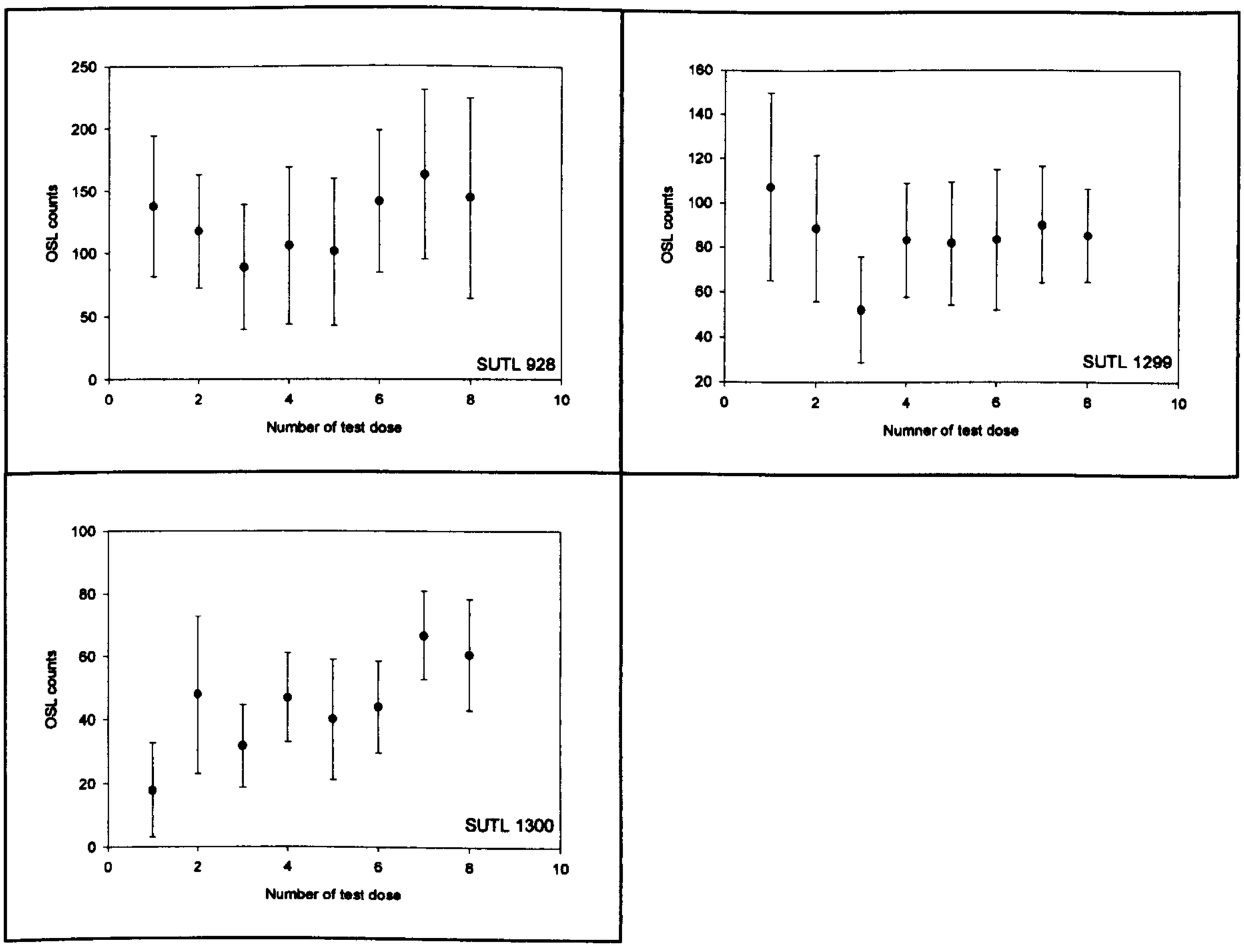

BAY OF SKAILL

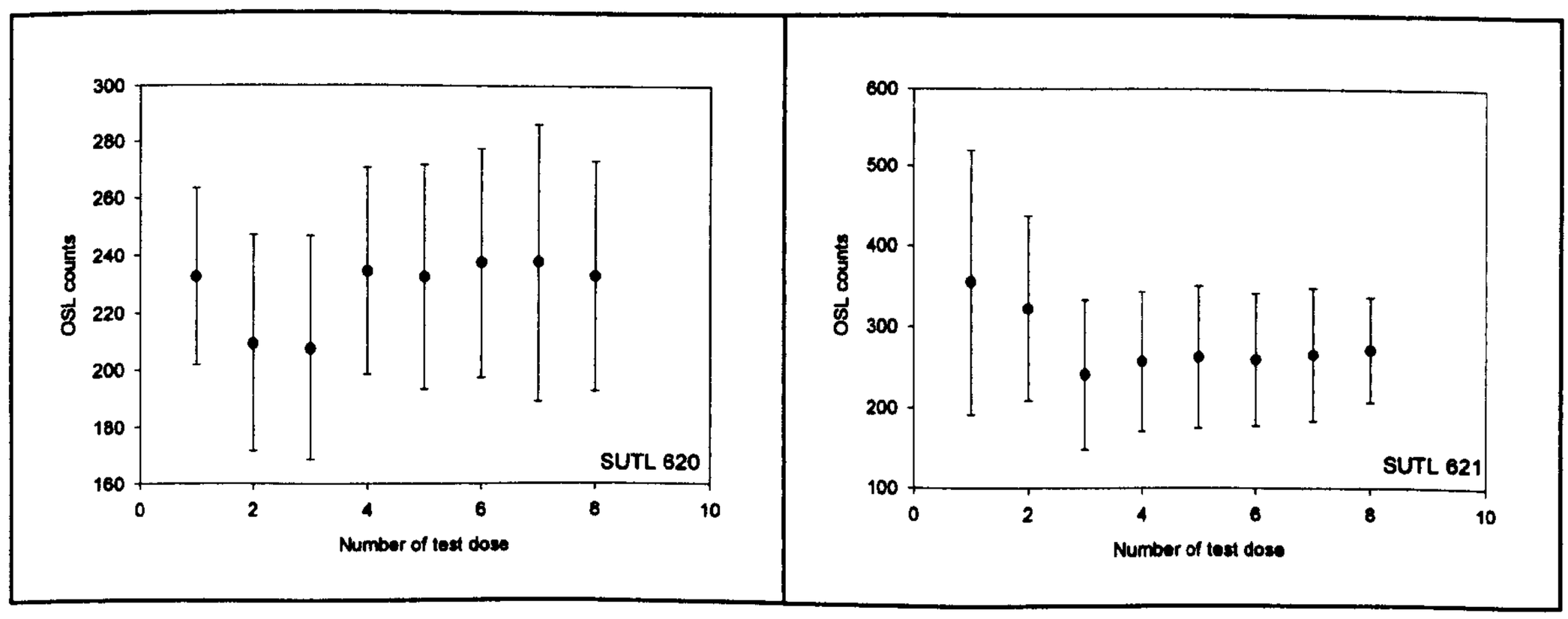

Appendix 5.3

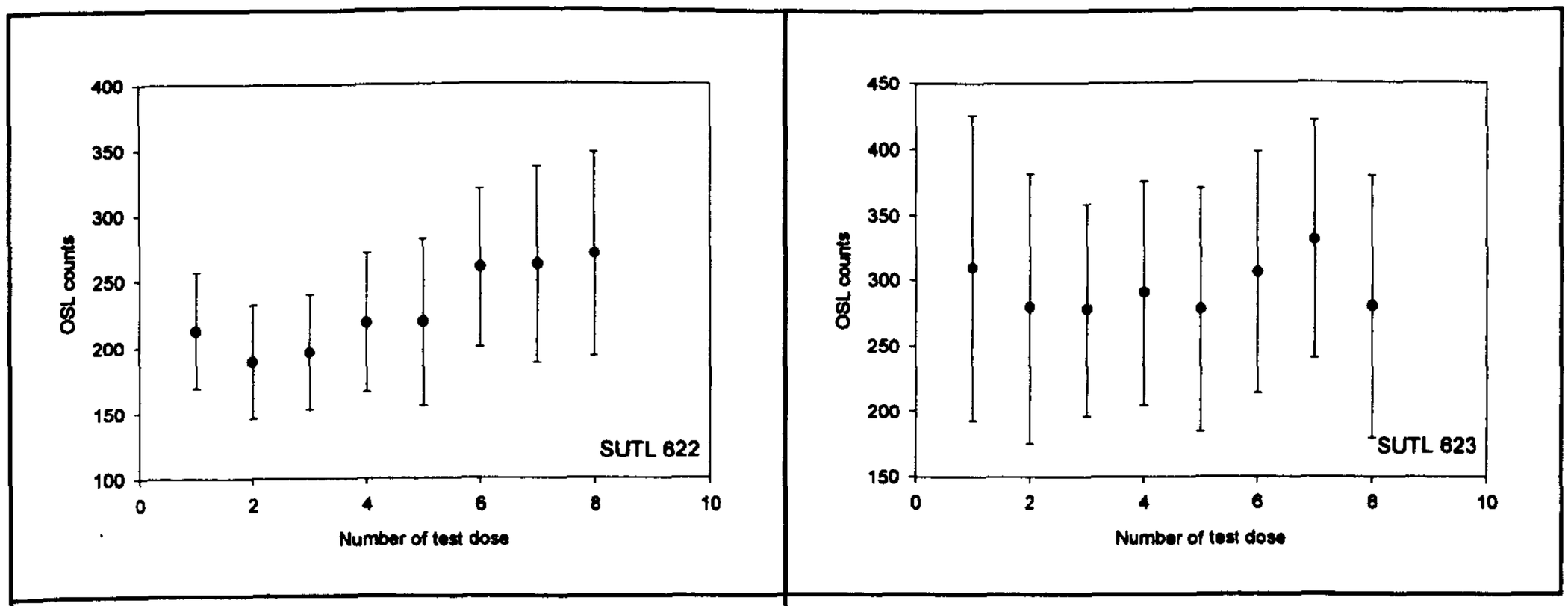
OSL counts
Number of test dose
SUTL 622
SUTL 623

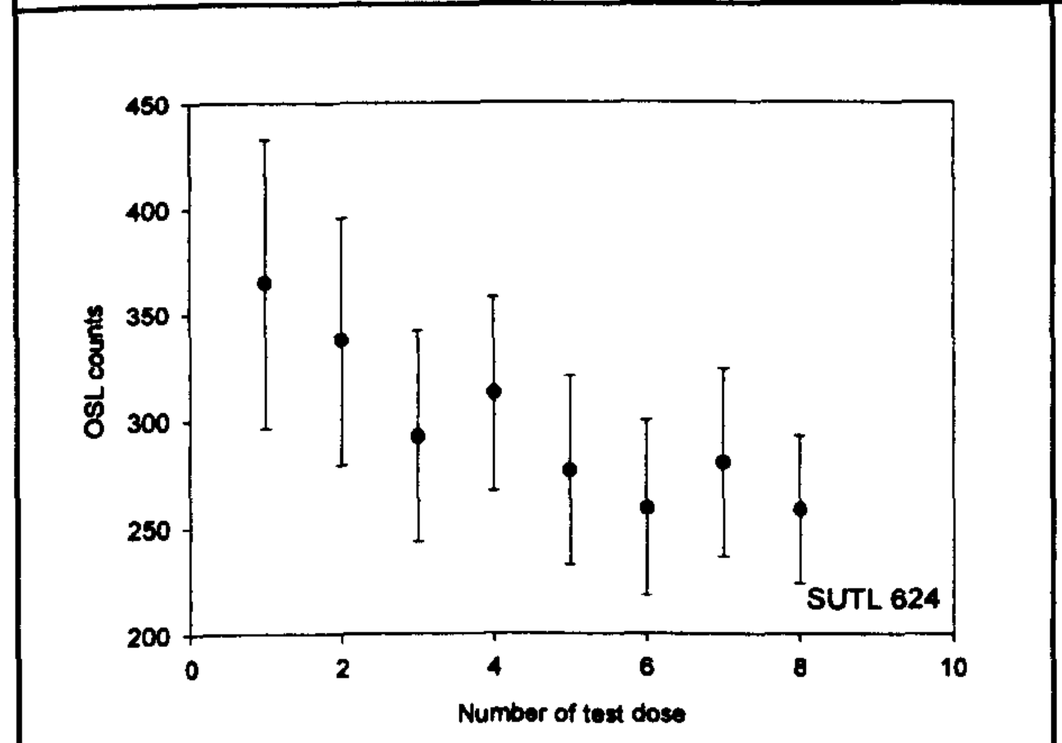
OSL counts
Number of test dose
SUTL 624

Appendix 5.4 – Normalised average test dose response for each preheat temperature per sample

TOFTS NESS

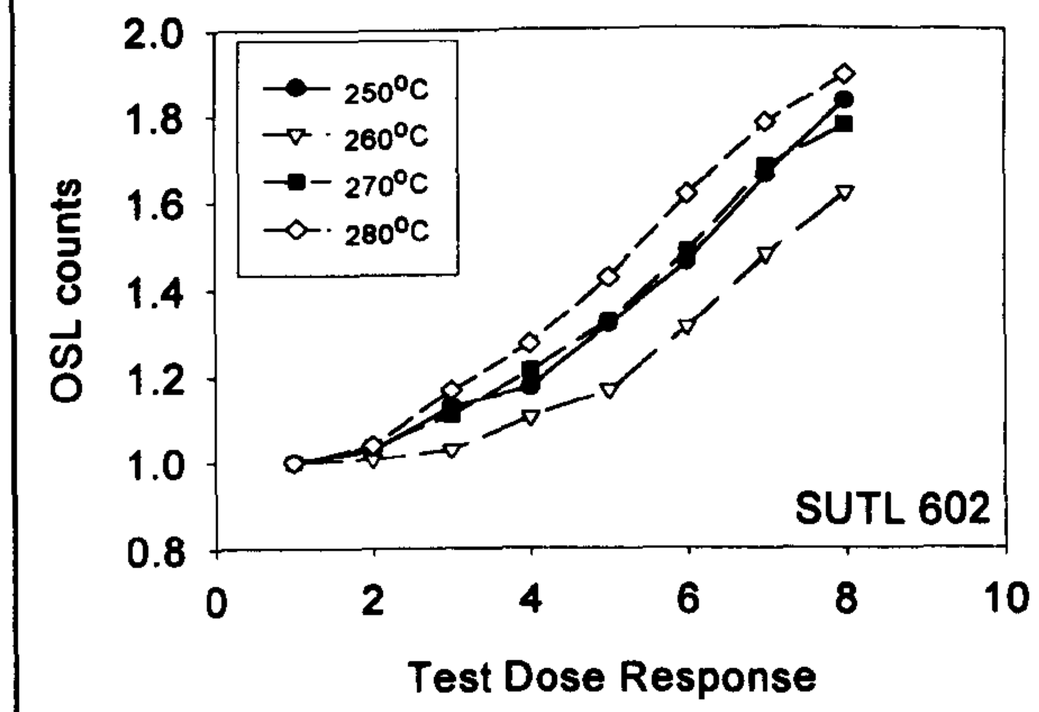

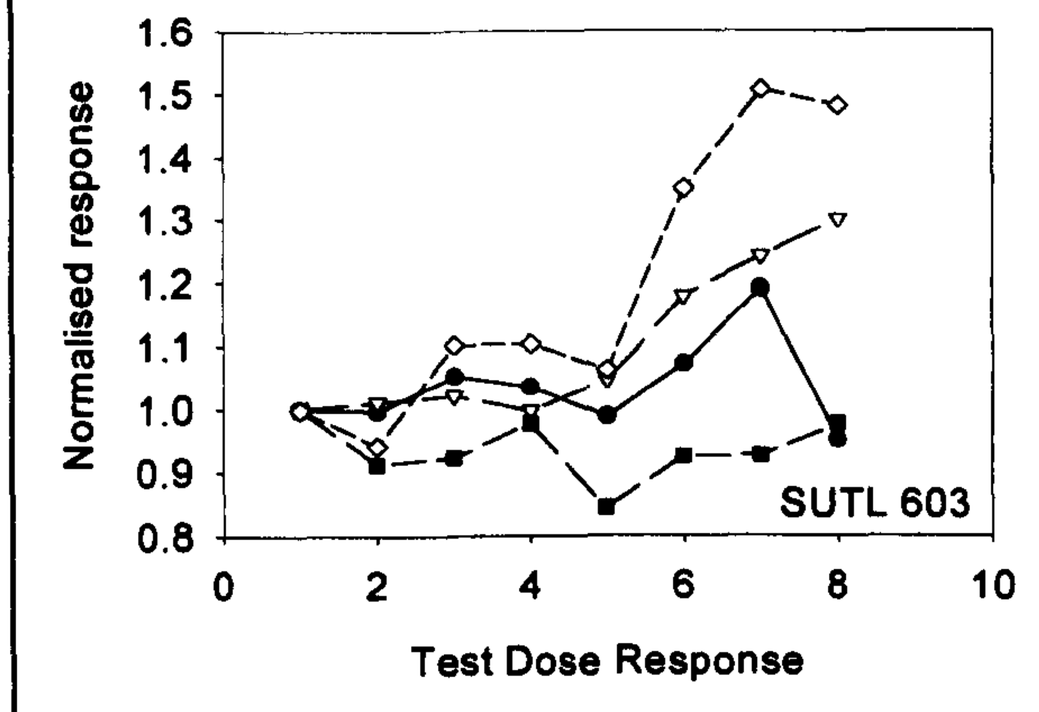

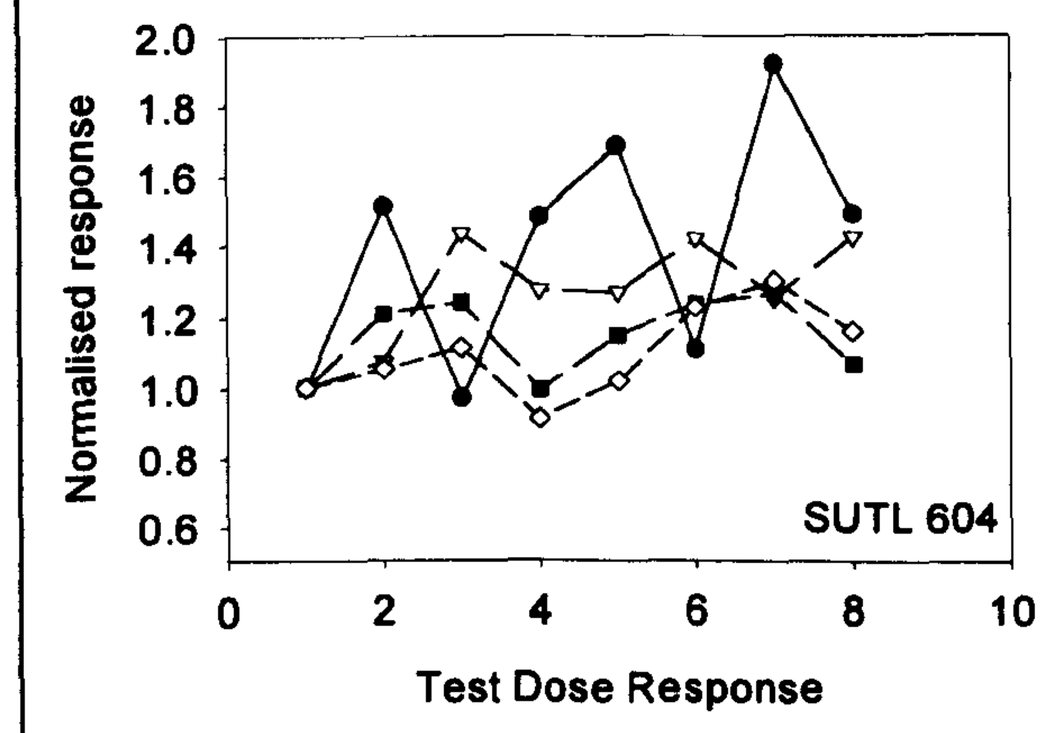

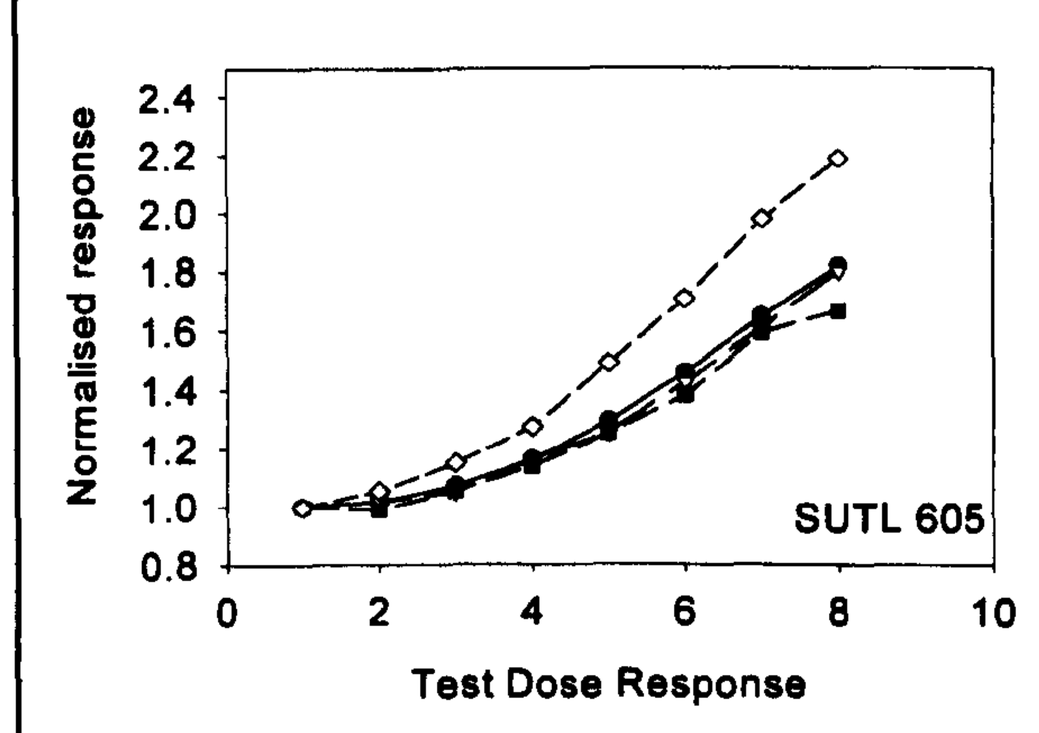

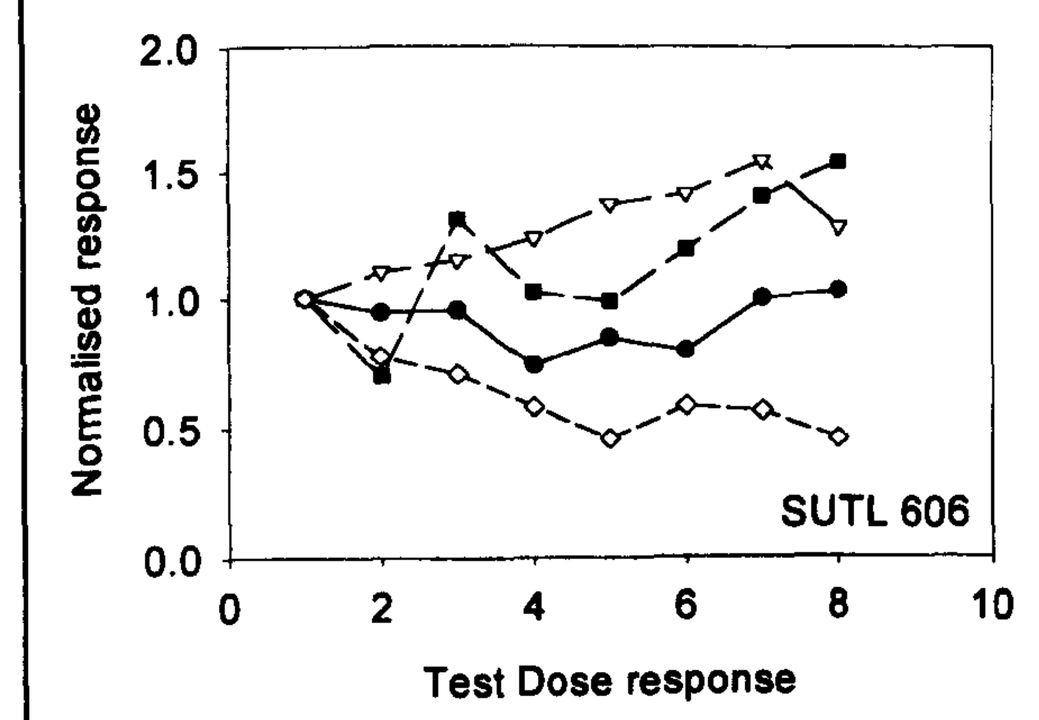

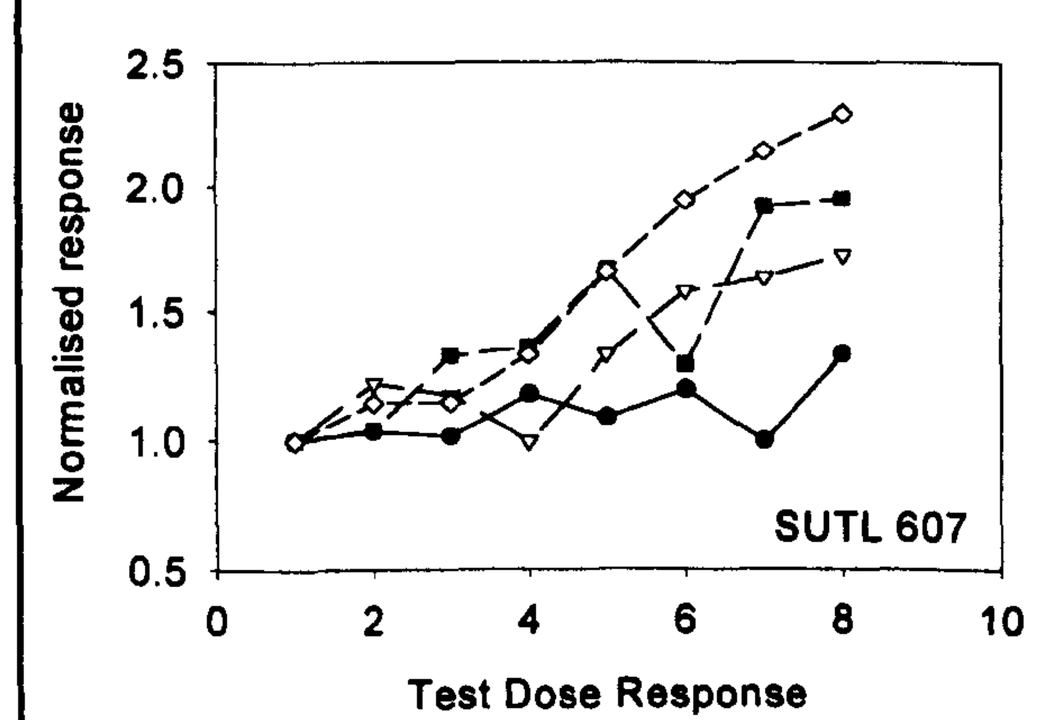

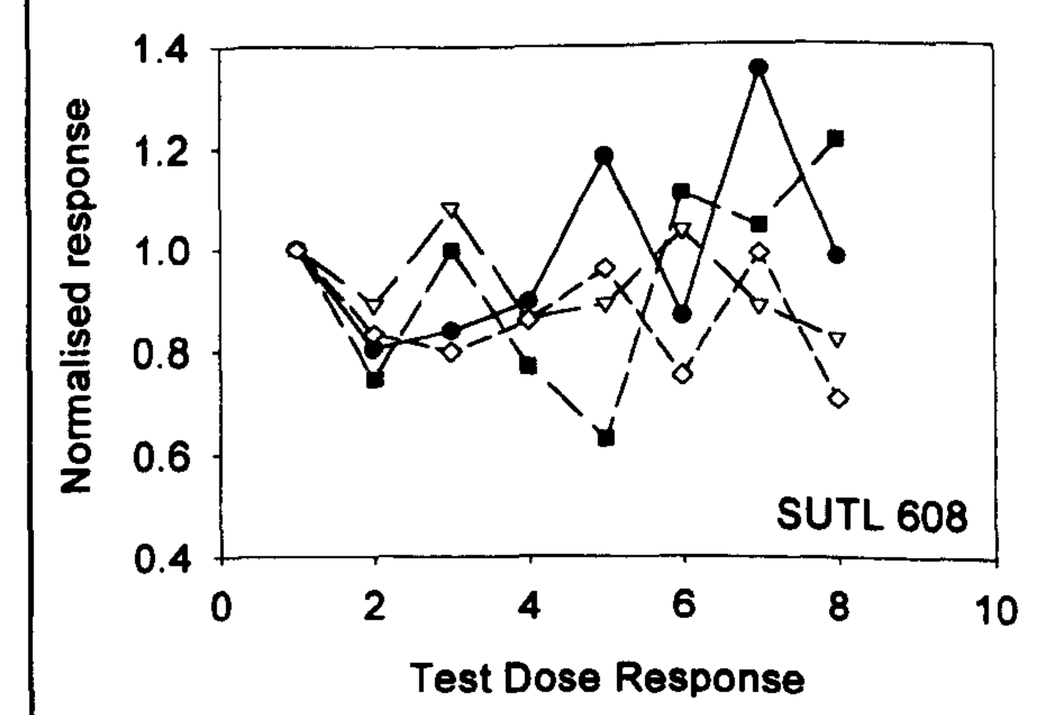

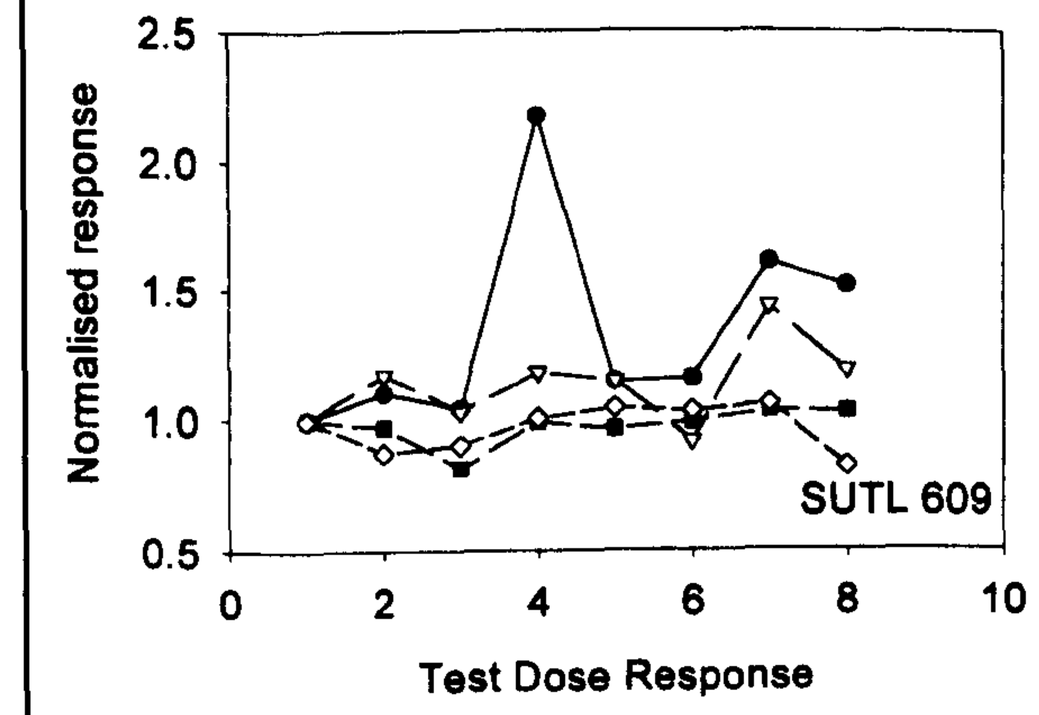

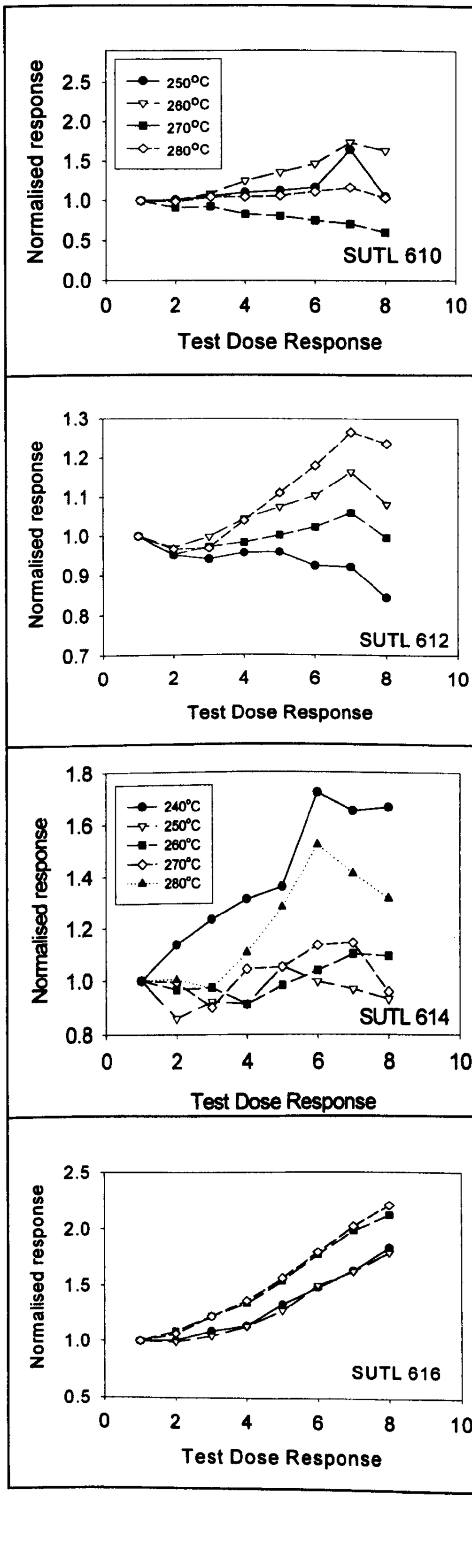
Normalised response
Test Dose Response
250°C
260°C
270°C
280°C
SUTL 610
SUTL 611
SUTL 612
SUTL 613
240°C
250°C
260°C
270°C
280°C
SUTL 614
SUTL 615
SUTL 616
SUTL 617

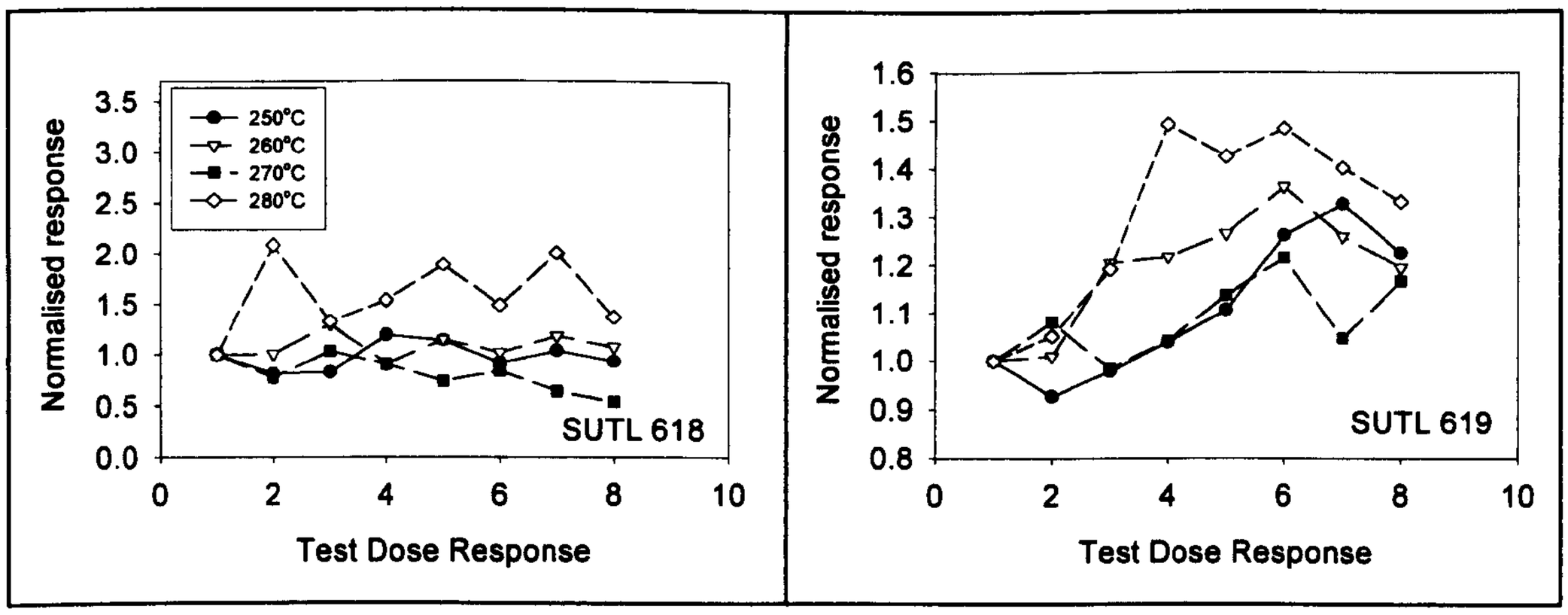

BAY OF LOPNESS

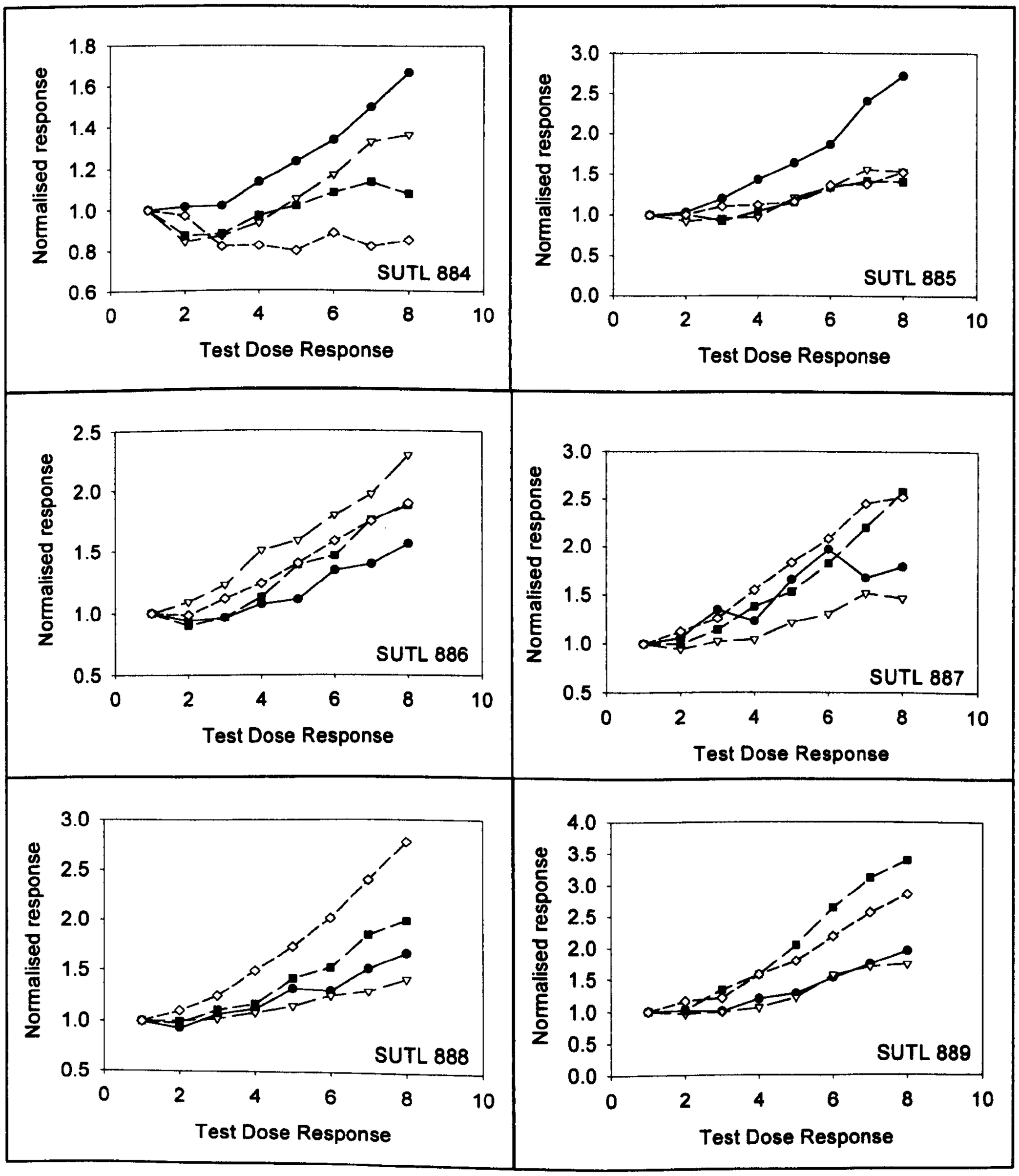

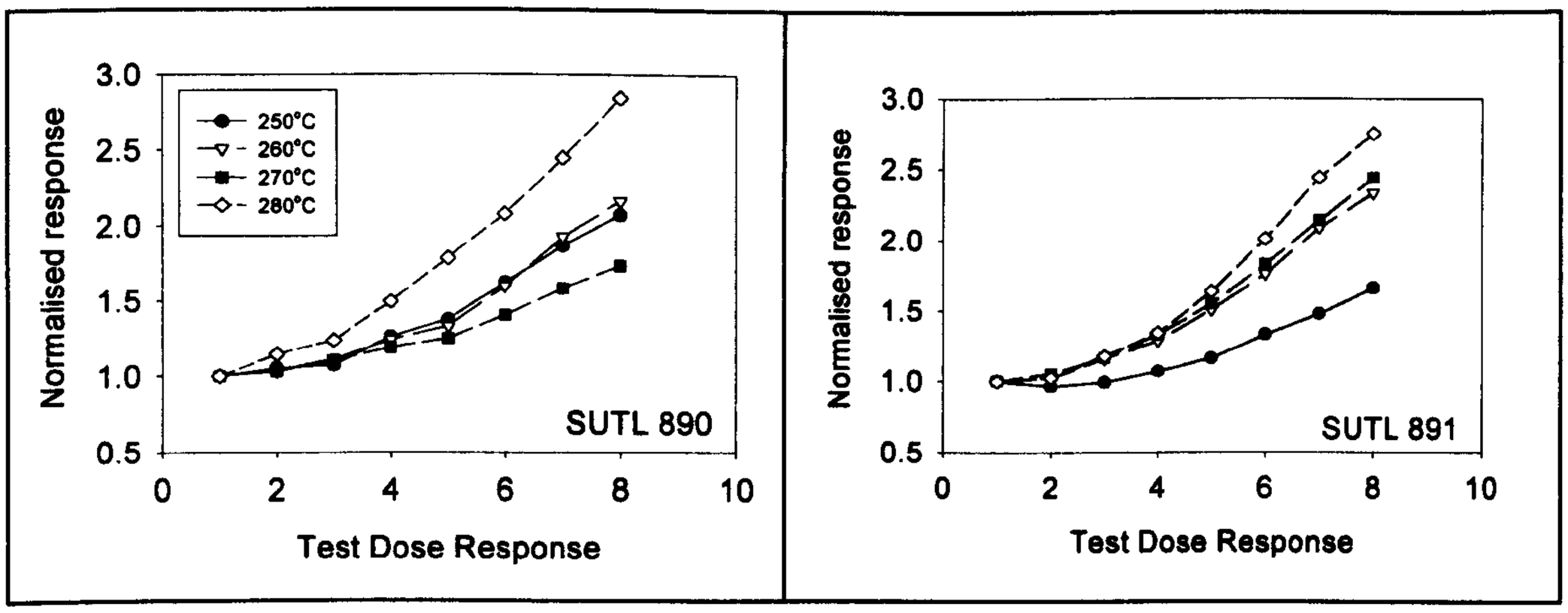
250°C
260°C
270°C
280°C
Normalised response
Test Dose Response
SUTL 890
SUTL 891

QUOYGREW

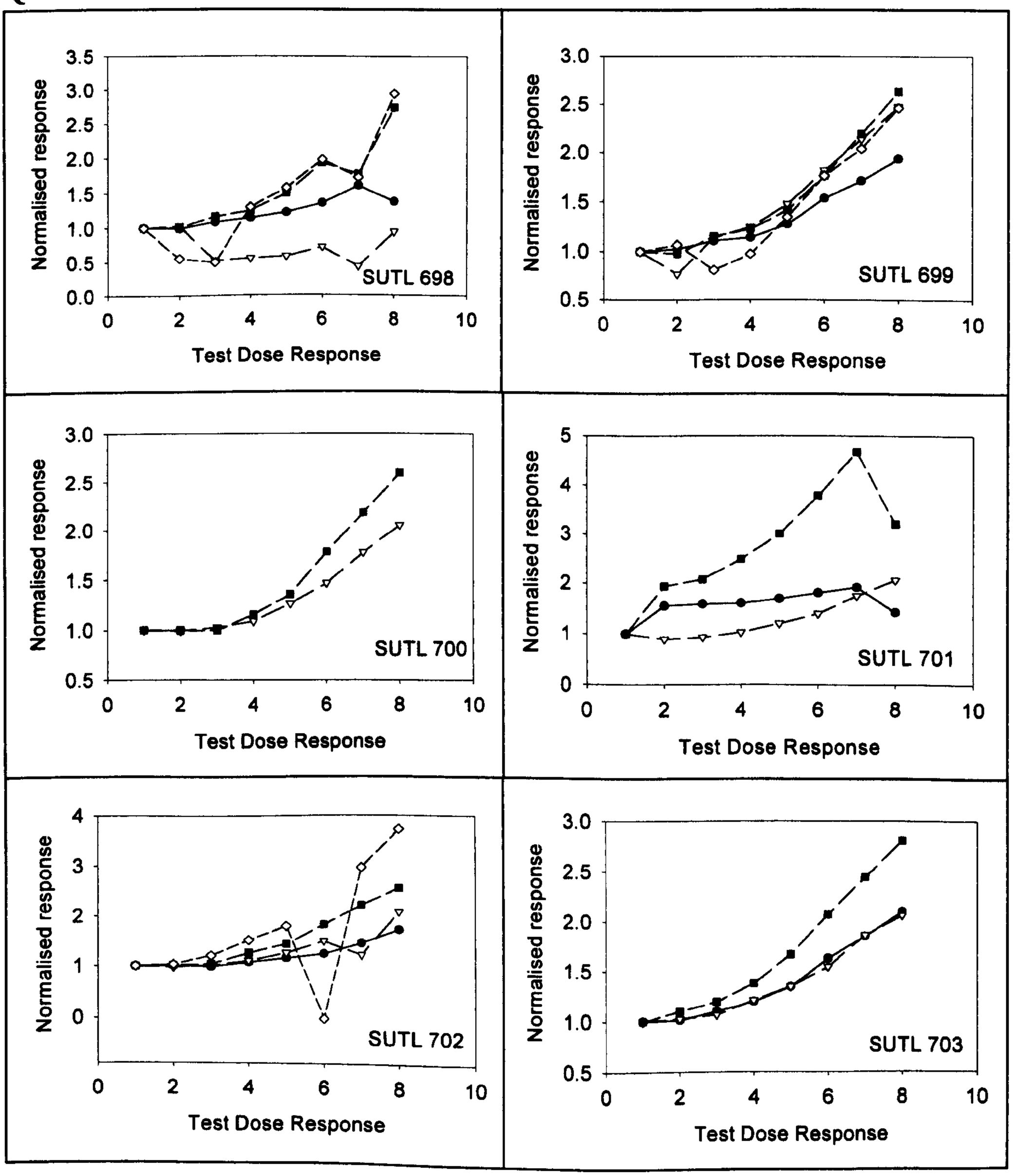
Normalised response
Test Dose Response
SUTL 698
SUTL 699
SUTL 700
SUTL 701
SUTL 702
SUTL 703

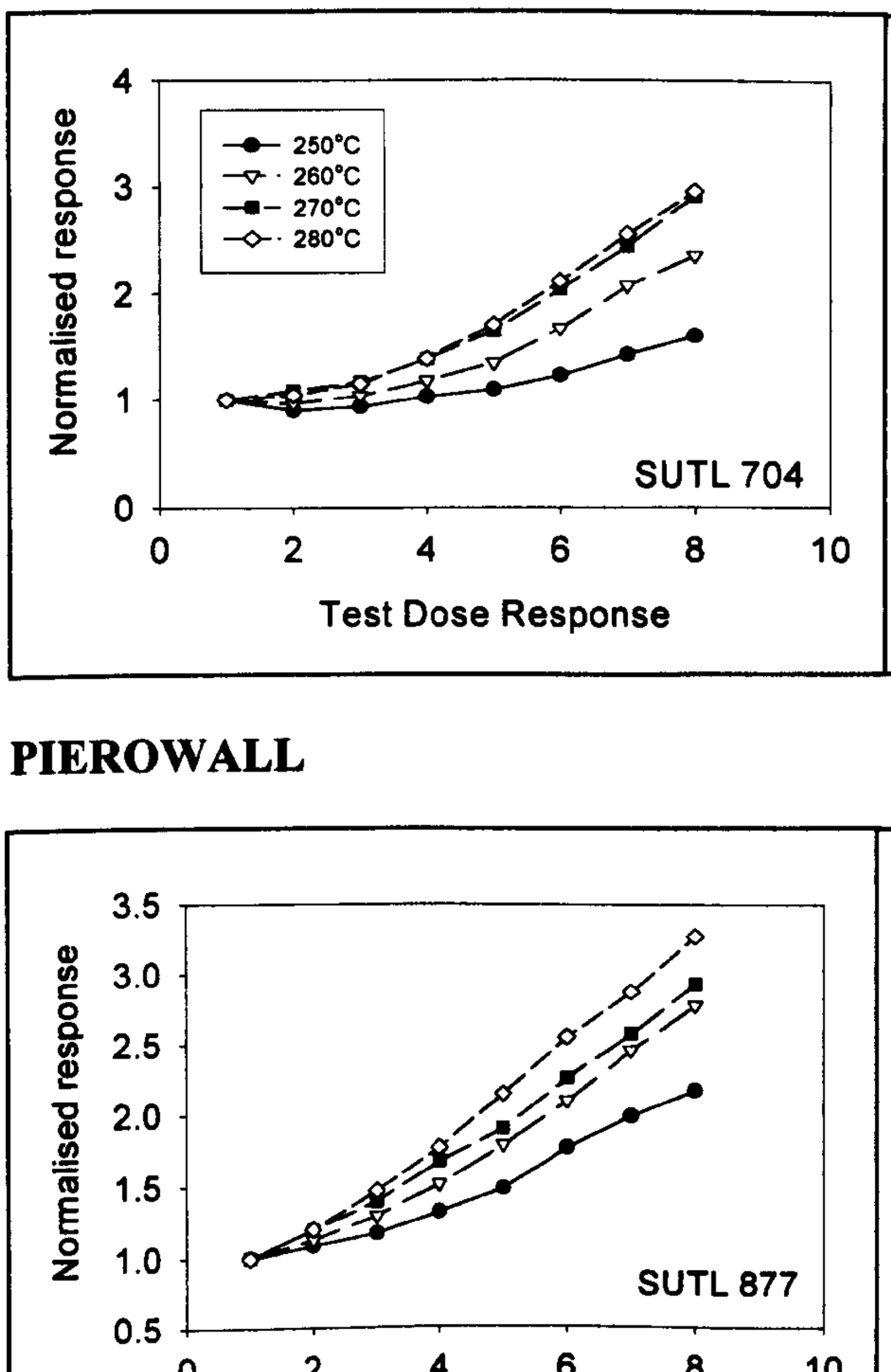
Normalised response
Test Dose Response
250°C
260°C
270°C
280°C
SUTL 704

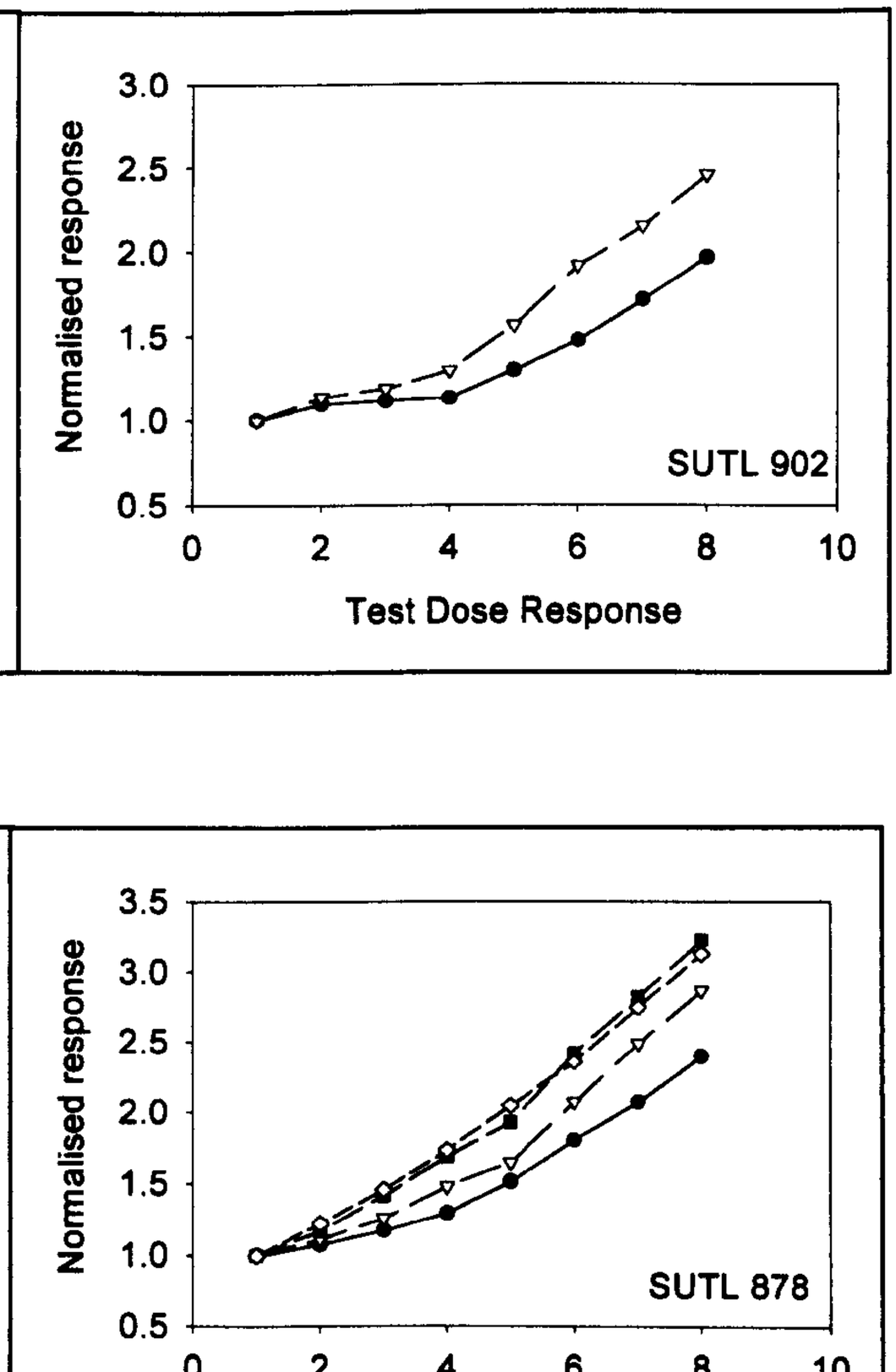
Normalised response
Test Dose Response
SUTL 902

Normalised response
Test Dose Response
SUTL 877

Normalised response
Test Dose Response
SUTL 878

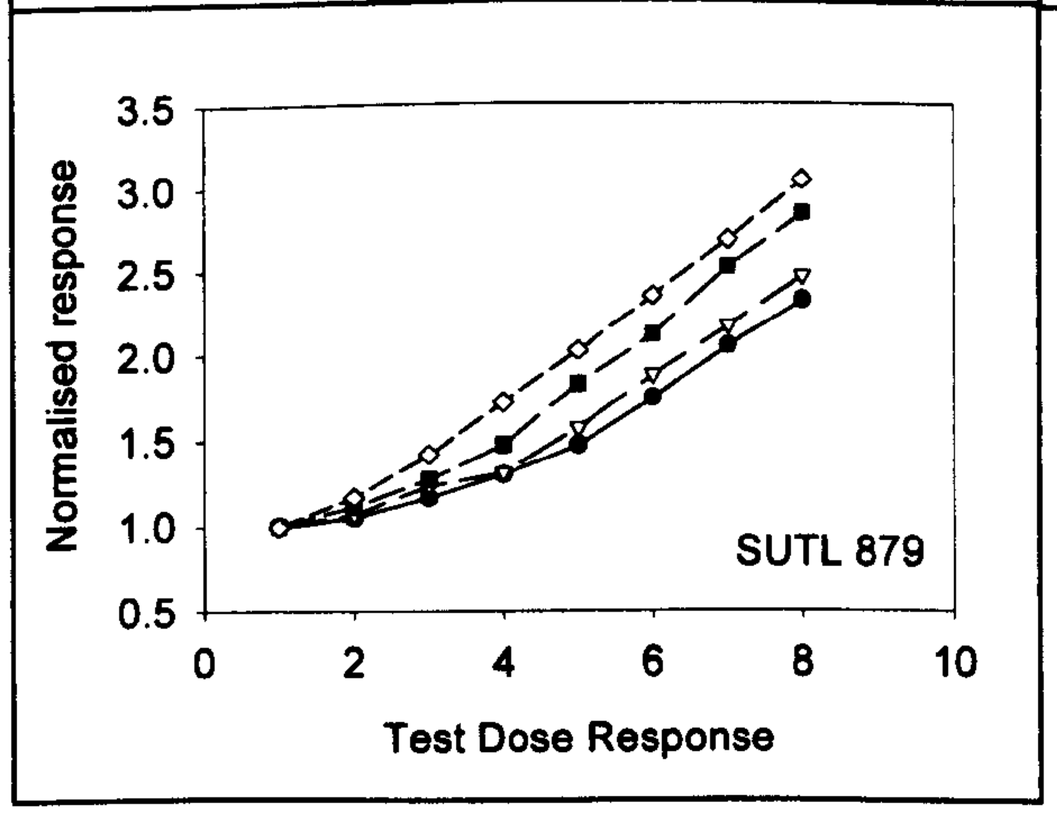
Normalised response
Test Dose Response
SUTL 879

EVERTAFT

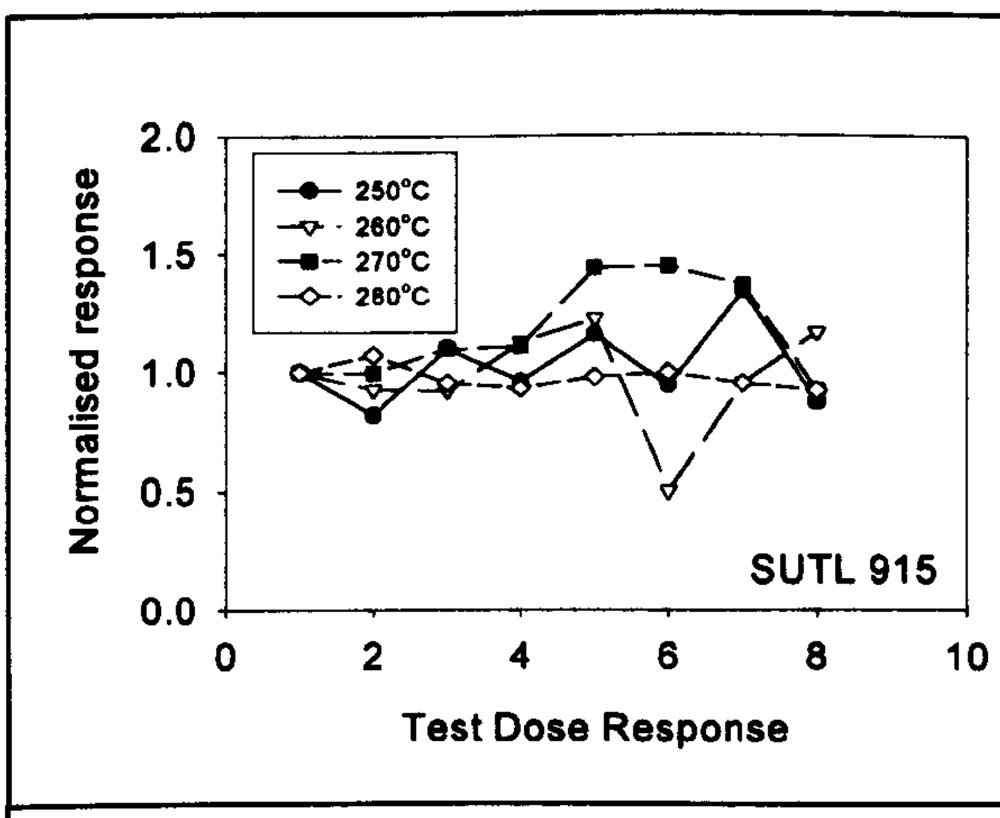
250°C
260°C
270°C
280°C
SUTL 915
Normalised response
Test Dose Response

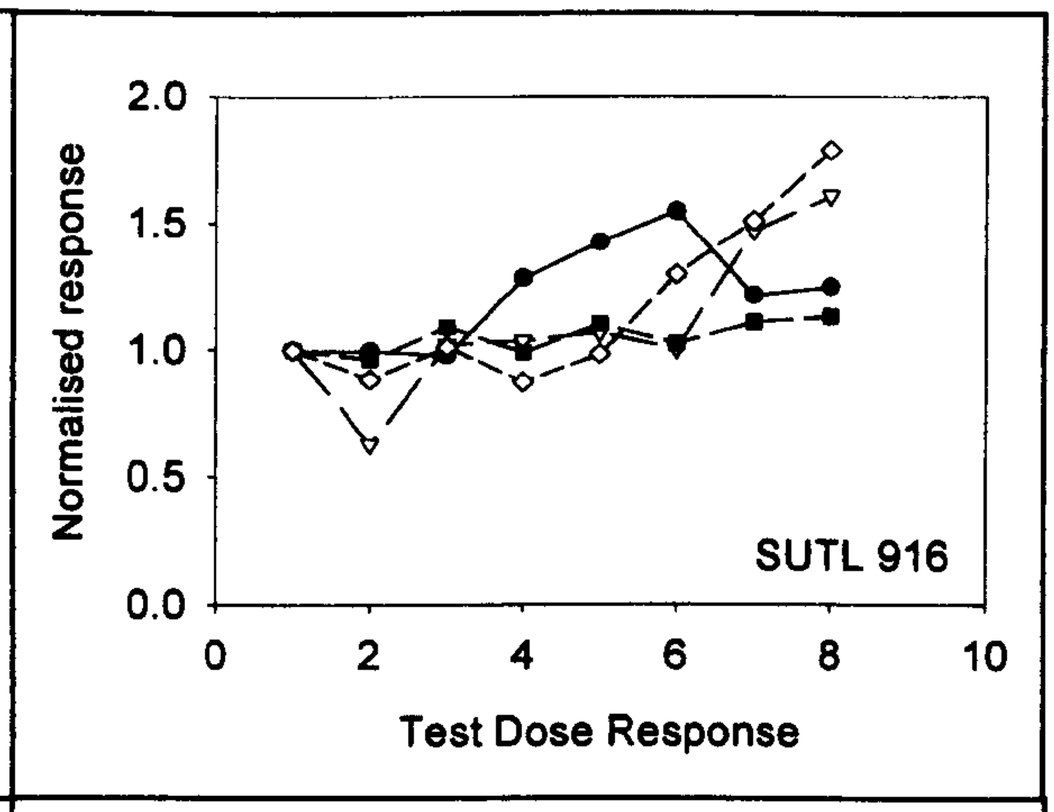
SUTL 916
Normalised response
Test Dose Response

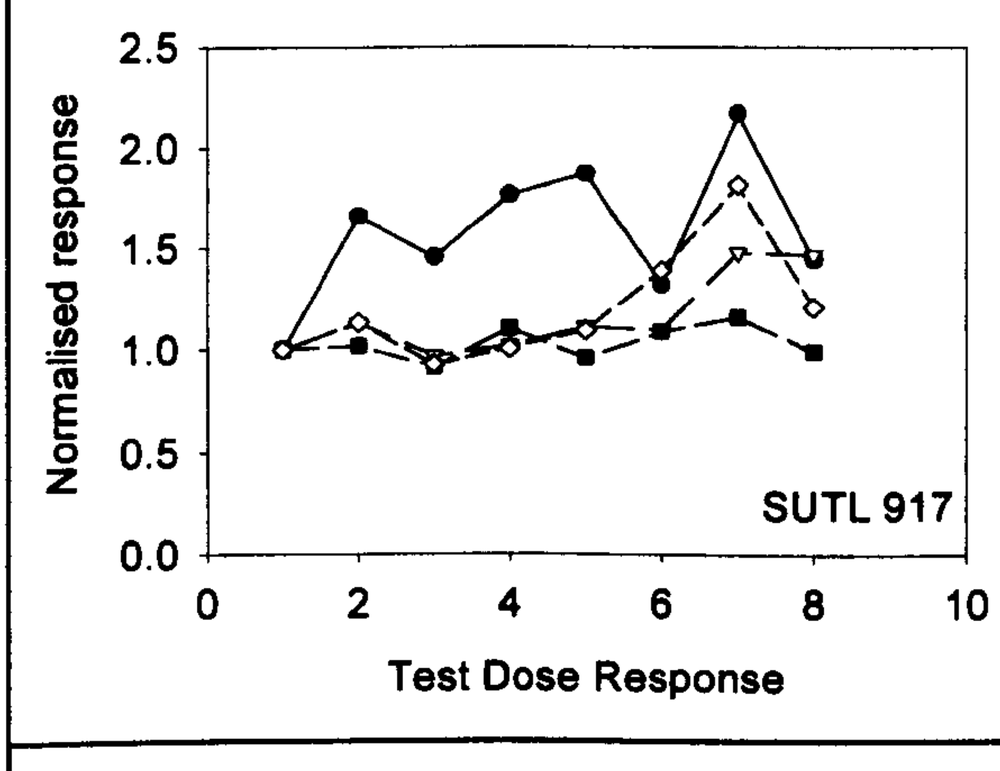
SUTL 917
Normalised response
Test Dose Response

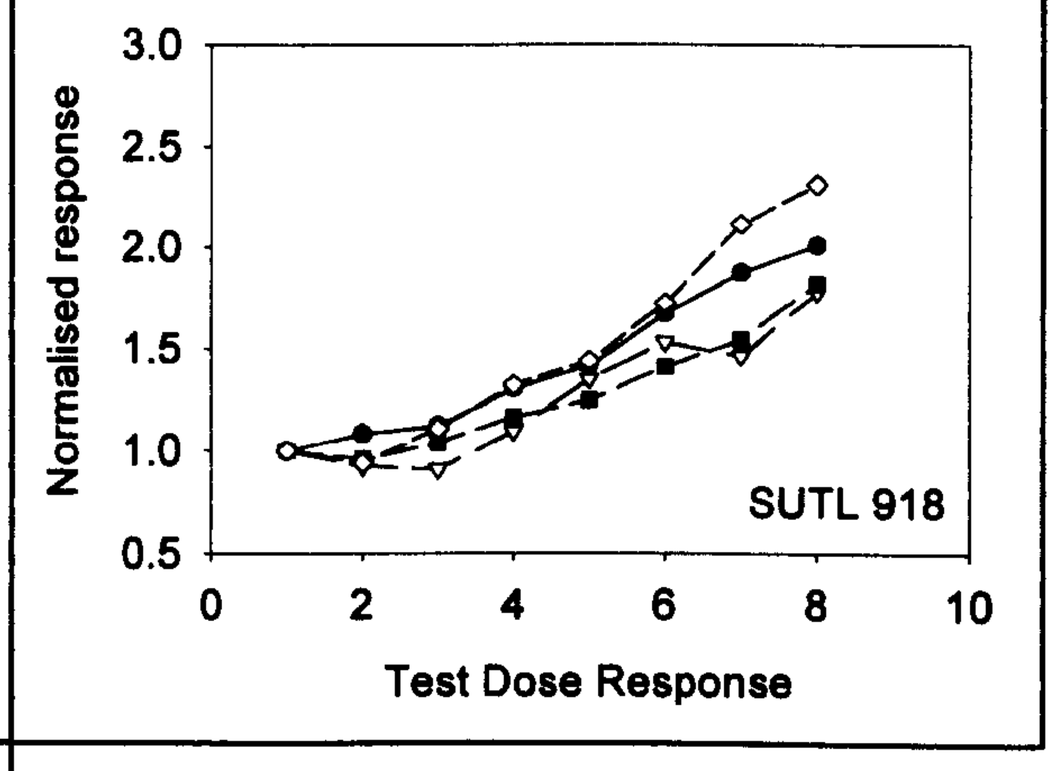
SUTL 918
Normalised response
Test Dose Response

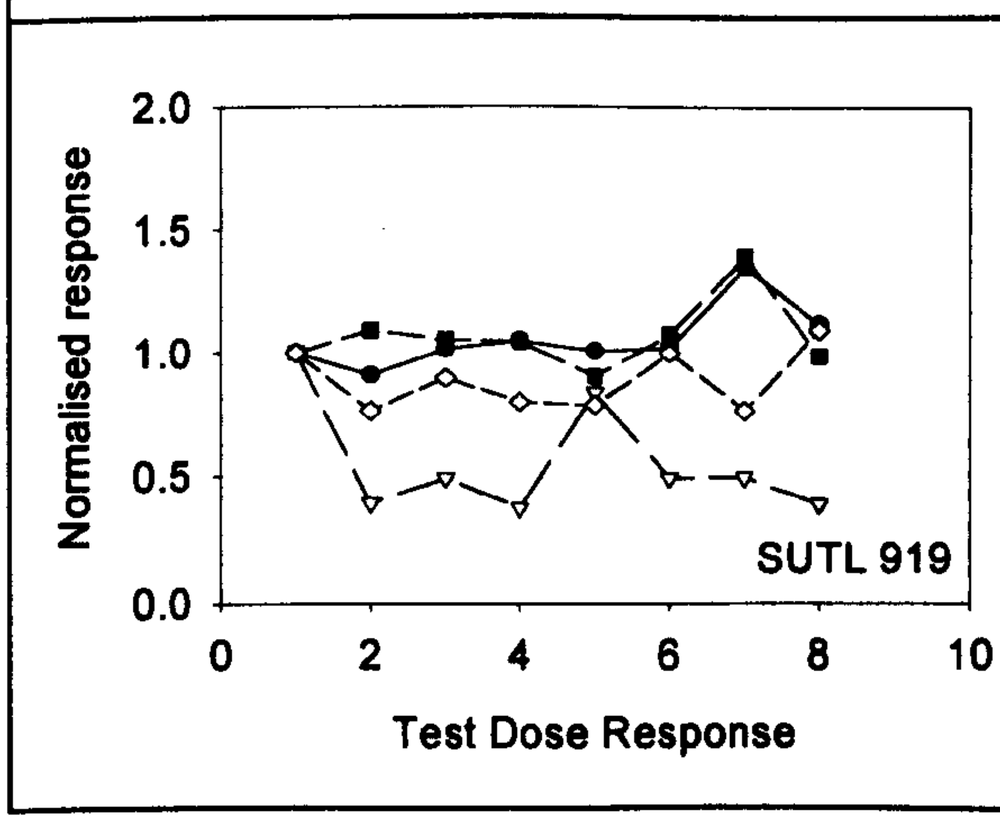
SUTL 919
Normalised response
Test Dose Response

SANDHILL

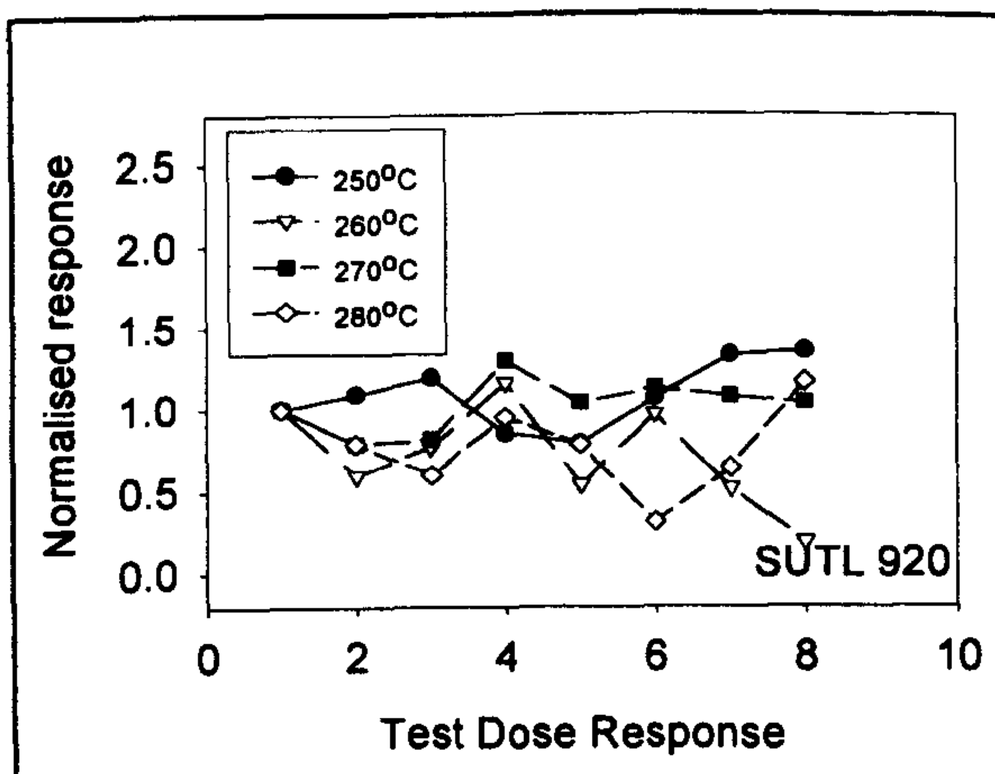
Normalised response
250°C
260°C
270°C
280°C
SUTL 920
Test Dose Response

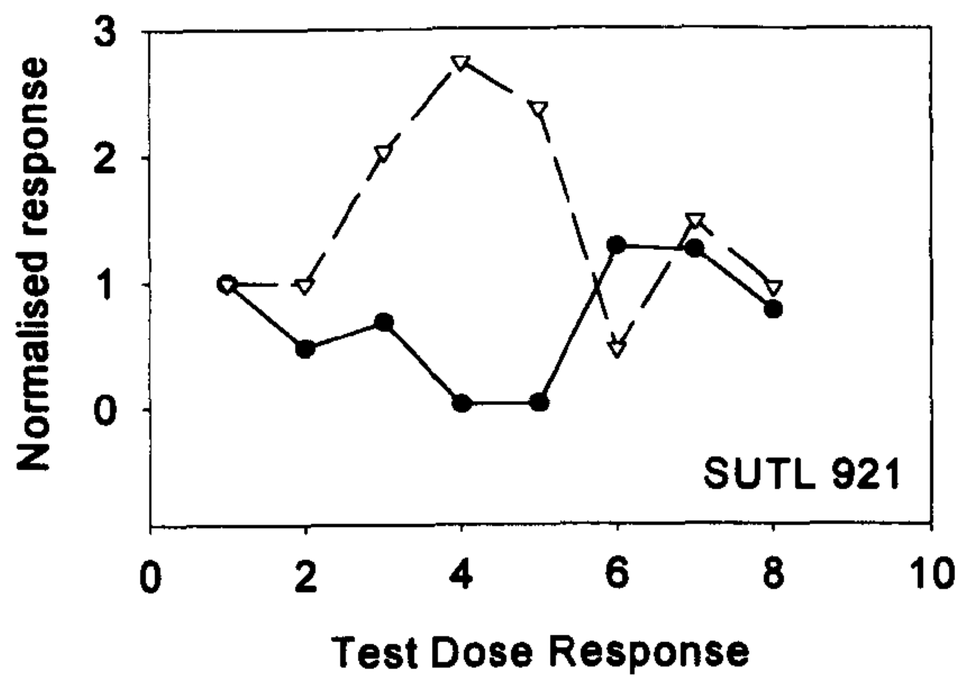
Normalised response
SUTL 921
Test Dose Response

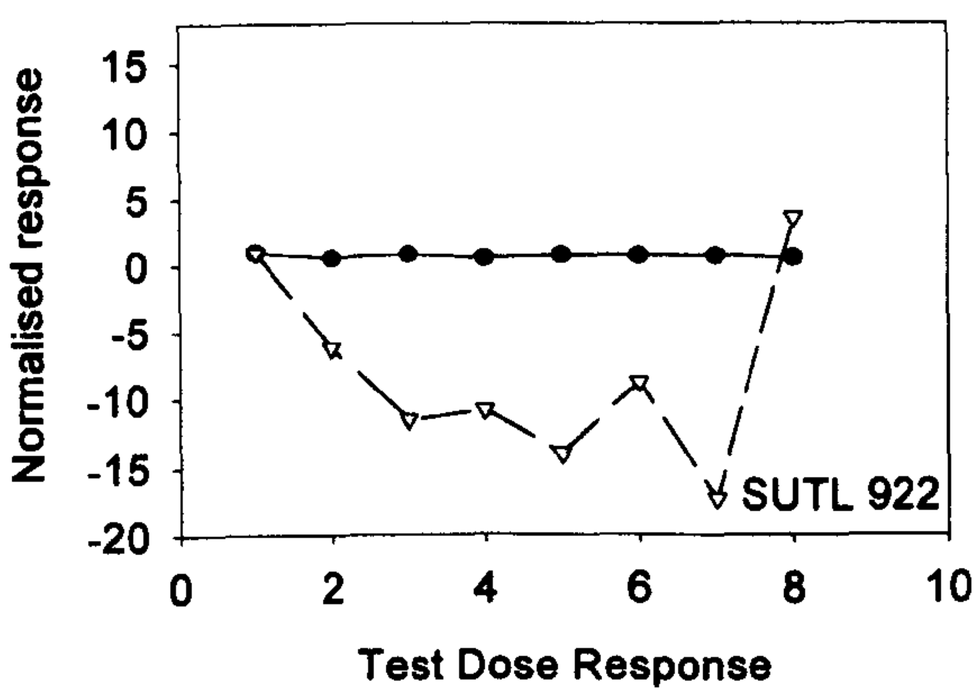
Normalised response
SUTL 922
Test Dose Response

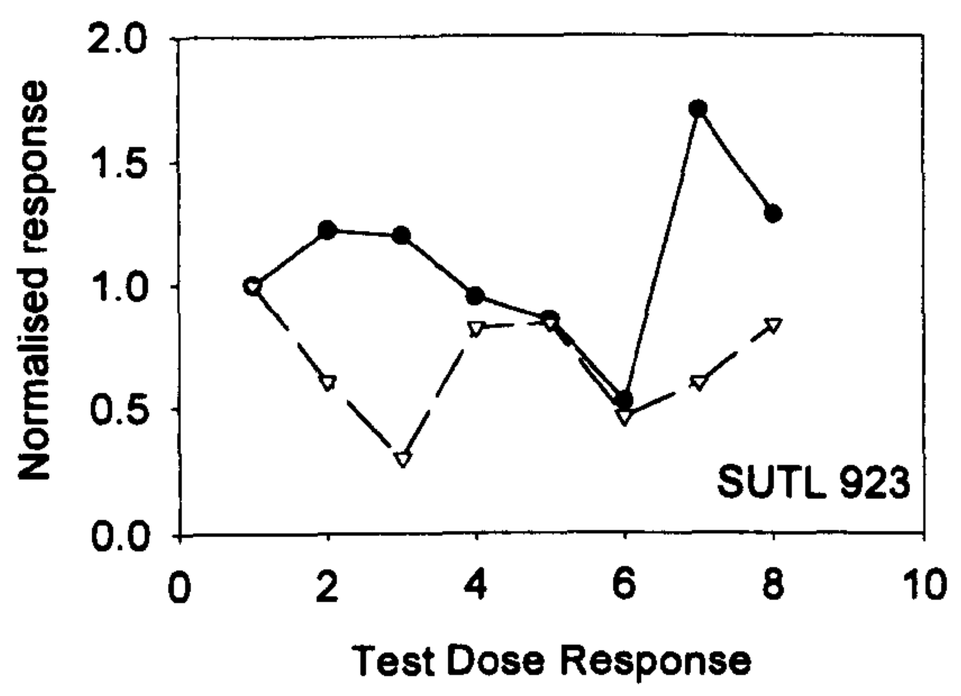
Normalised response
SUTL 923
Test Dose Response

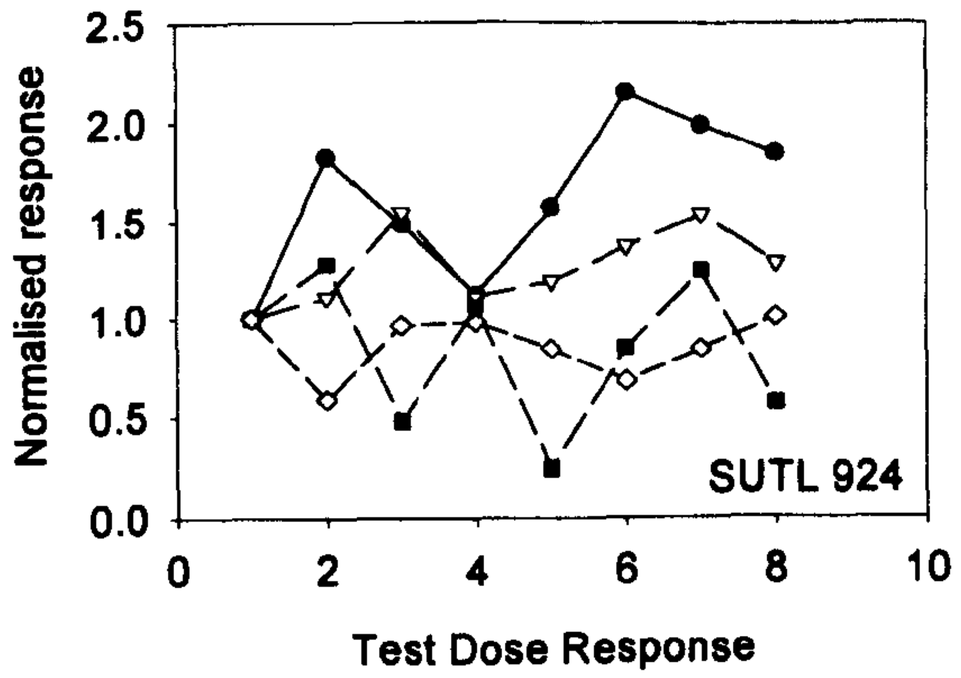
Normalised response
SUTL 924
Test Dose Response

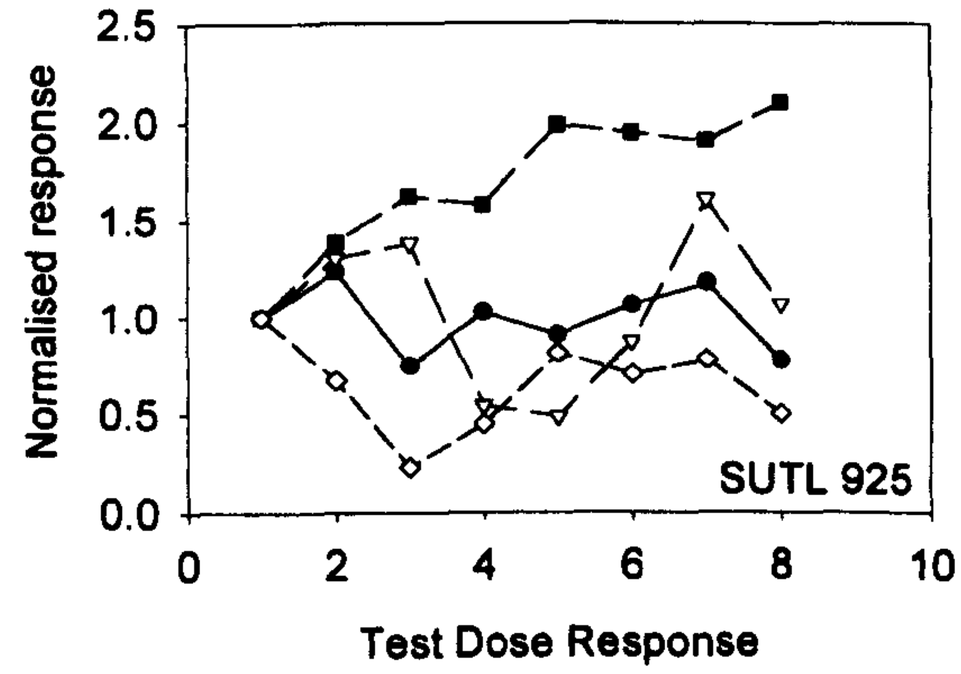
Normalised response
SUTL 925
Test Dose Response

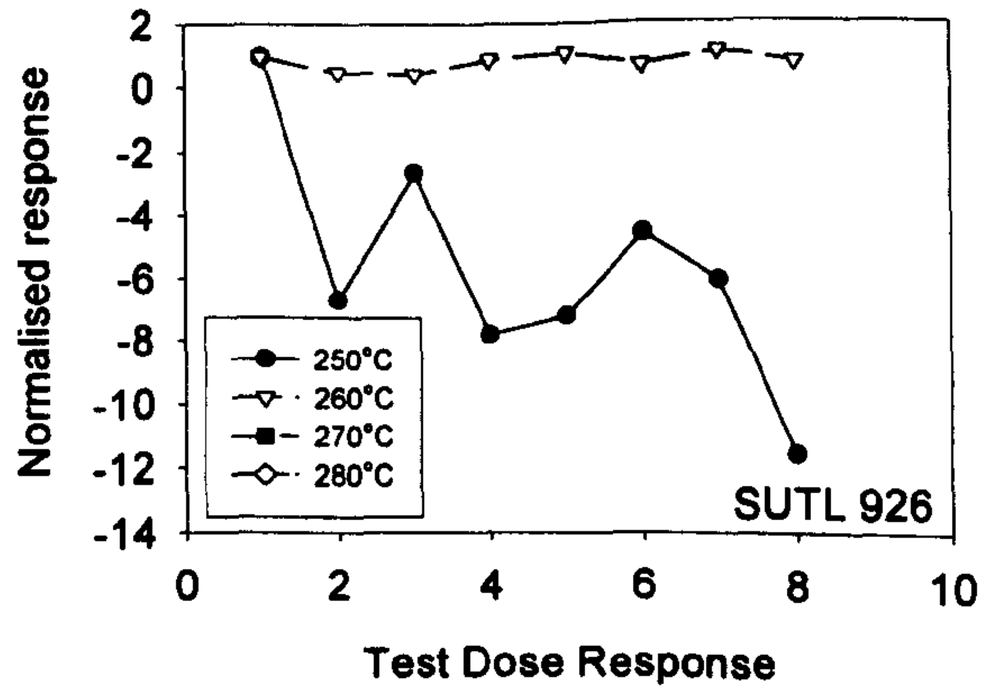
Normalised response
250°C
260°C
270°C
280°C
SUTL 926
Test Dose Response

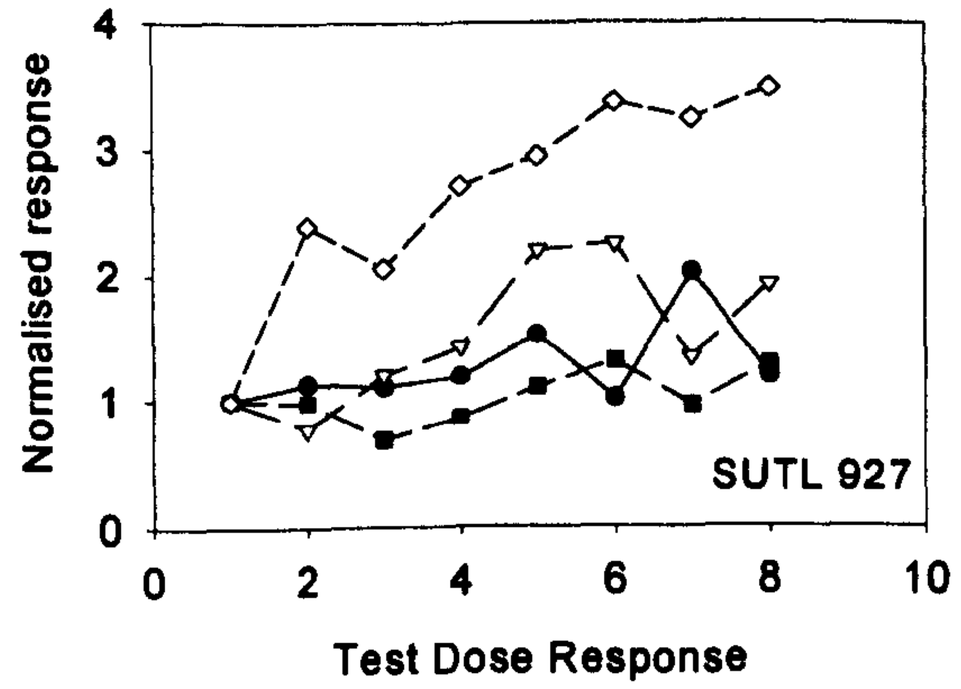
Normalised response
SUTL 927
Test Dose Response

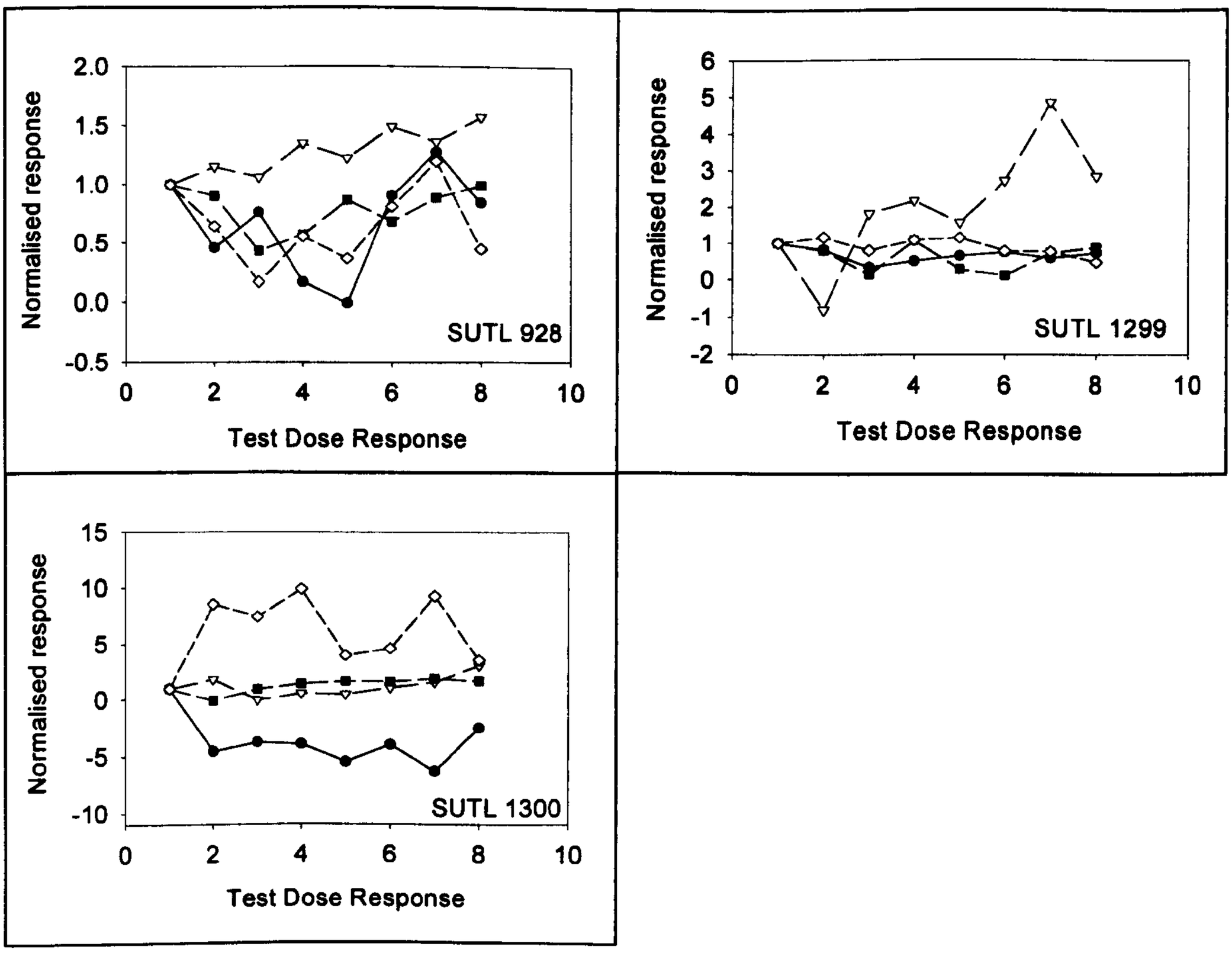

BAY OF SKAILL

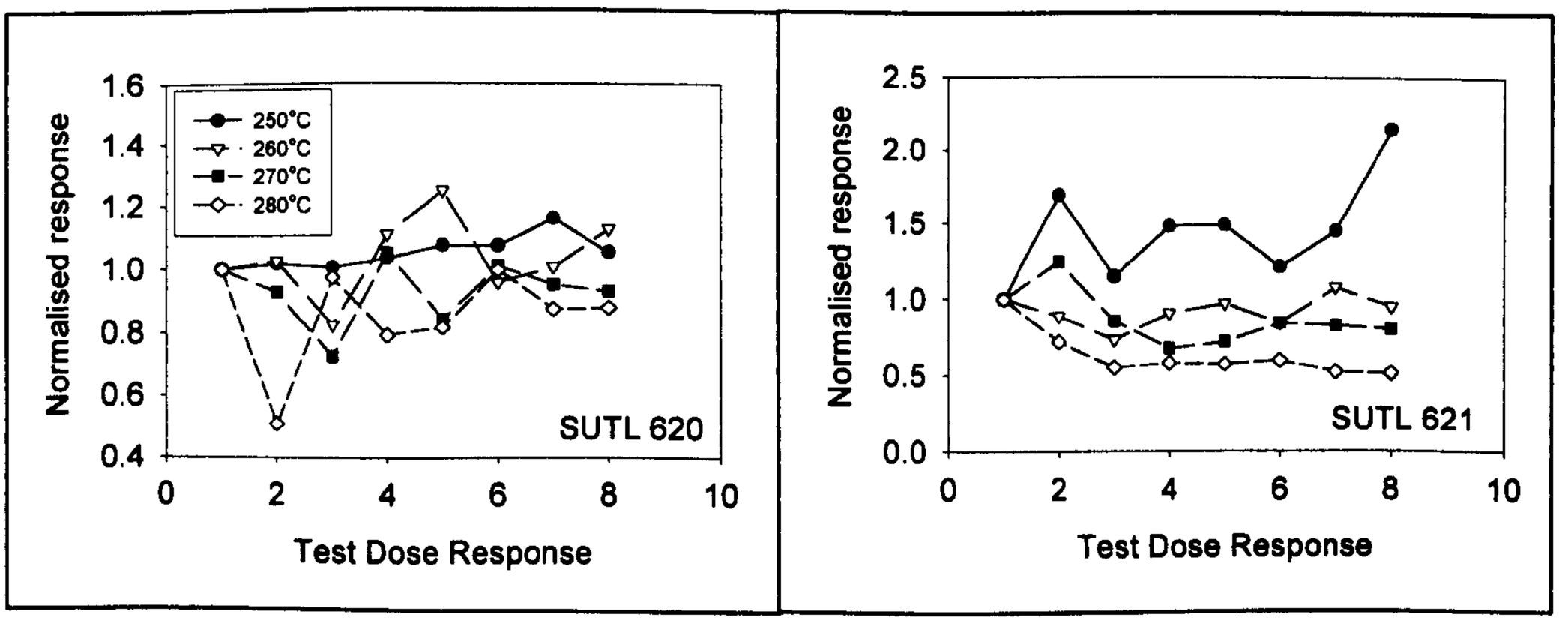

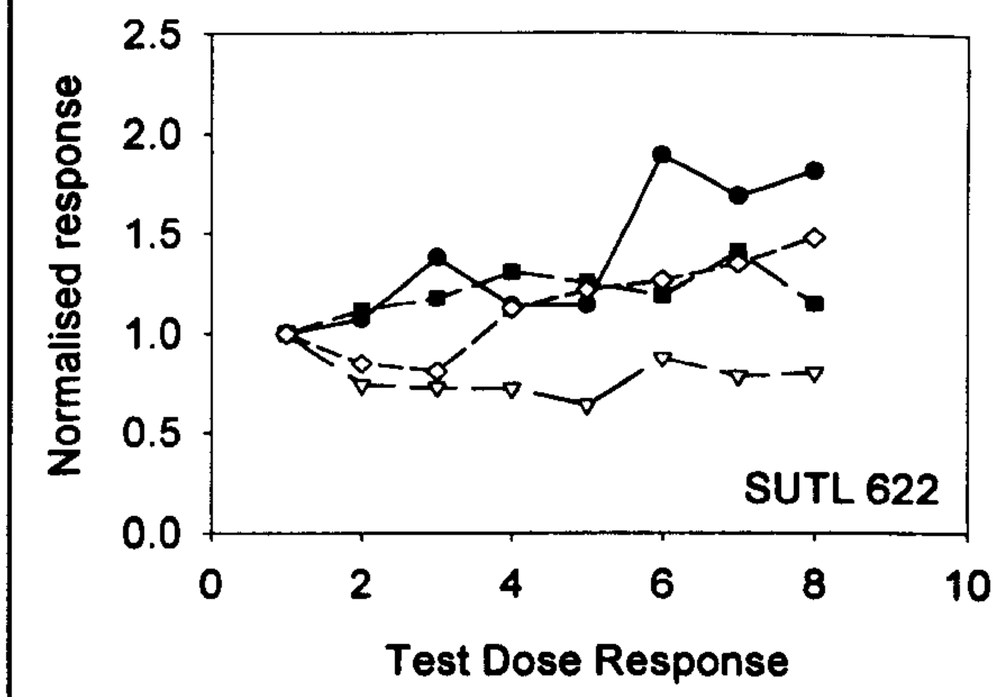
Normalised response
2.5
2.0
1.5
1.0
0.5
0.0
0
2
4
6
8
10
Test Dose Response
SUTL 622

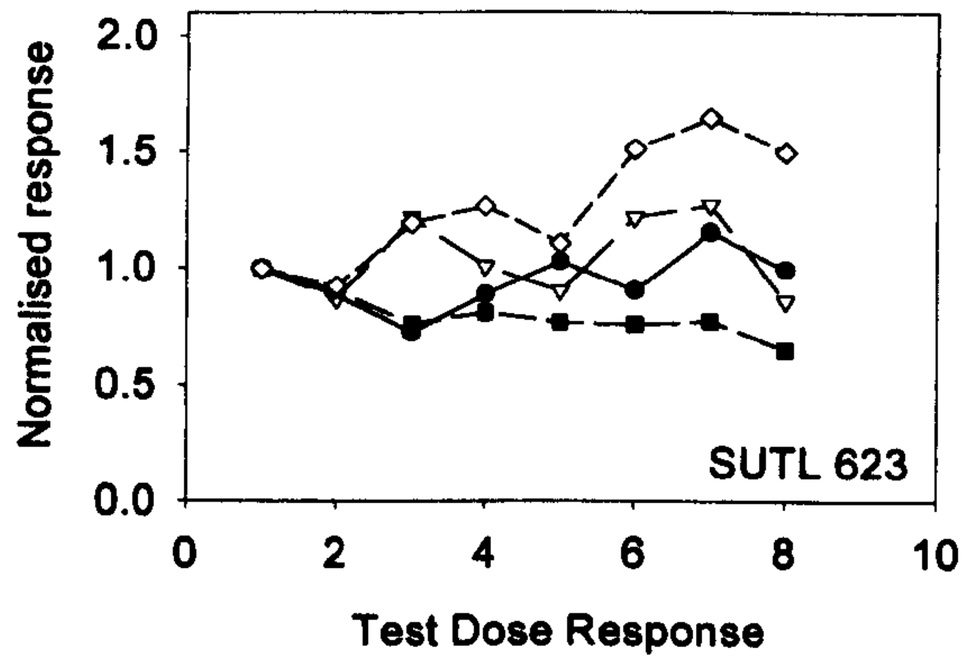
Normalised response
2.0
1.5
1.0
0.5
0.0
0
2
4
6
8
10
Test Dose Response
SUTL 623

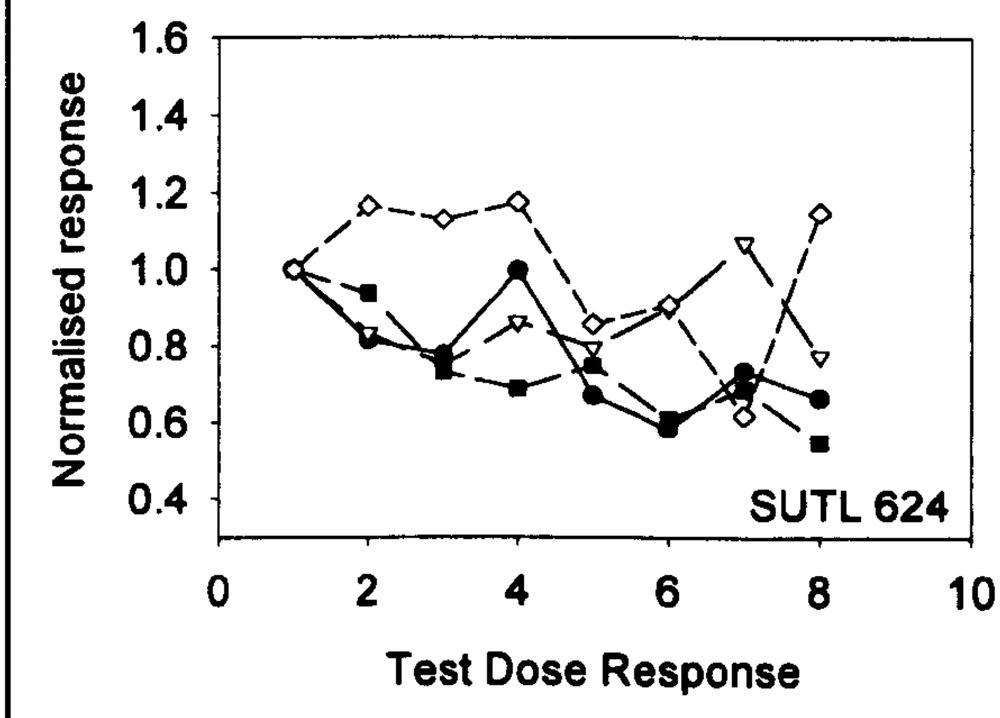
Normalised response
1.6
1.4
1.2
1.0
0.8
0.6
0.4
0
2
4
6
8
10
Test Dose Response
SUTL 624

Appendix 5.5 – Comparison of the D_e of aliquots contaminated with IR sensitive minerals with the D_e of quartz aliquots. Aliquots contaminated with IR sensitive minerals are shaded.

Disc	SUTL 606	SUTL 607	SUTL 609	SUTL 610	SUTL 611
1	0.655 ± 0.731	0.395 ± 0.224	1.127 ± 1.883	0.705 ± 0.248	0.162 ± 0.181
2	3.541 ± 2.438	1.181 ± 1.263	5.854 ± 12.476	1.197 ± 0.353	0.416 ± 0.802
3	0.594 ± 0.188	2.587 ± 5.342	3.478 ± 2.18	0.975 ± 0.094	1.316 ± 0.18
4	0.251 ± 0.227	3.185 ± 1.485	0.776 ± 0.426	1.009 ± 0.264	0.304 ± 0.219
5	0.201 ± 0.915	1.782 ± 1.769	0.667 ± 0.364	0.87 ± 0.571	1.085 ± 1.04
6	0.214 ± 0.221	0.435 ± 0.202	0.471 ± 0.478	1.411 ± 0.942	0.002 ± 3.364
7	0.215 ± 0.57	0.094 ± 0.116	3.277 ± 1.23	0.71 ± 0.545	1.028 ± 1.164
8	0.479 ± 1.426	0.868 ± 0.381	1.256 ± 1.584	0.896 ± 0.203	1.292 ± 0.51
9	0.122 ± 0.083	0.237 ± 0.126	0.629 ± 0.644	1.802 ± 0.229	0.226 ± 1.788
10	0.779 ± 0.087	0.382 ± 0.682	1.032 ± 1.123	0.86 ± 0.481	1.355 ± 0.361
11	2.101 ± 2.041	0.385 ± 0.693	1.653 ± 1.916	1.55 ± 1.08	0.68 ± 0.525
12	0.866 ± 1.046	0.916 ± 0.964	1.255 ± 0.451	0.295 ± 0.215	2.242 ± 0.93
13		0.77 ± 0.298	1.522 ± 1.211	1.128 ± 0.375	3.734 ± 1.426
14		0.418 ± 0.108	0.516 ± 1.046	0.761 ± 0.273	1.569 ± 0.718
15		0.891 ± 0.356	1.45 ± 1.677	0.985 ± 0.145	1.396 ± 0.854
16			0.335 ± 7.59	1.268 ± 0.482	1.074 ± 3.387
17			5.191 ± 5.298	1.228 ± 1.006	1.801 ± 6.258
18			1.751 ± 2.774	0.277 ± 4.862	1.01 ± 0.574
19			0.59 ± 1.194	4.609 ± 2.465	
20			1.899 ± 0.905	1.012 ± 0.579	
21			1.018 ± 0.605	1.464 ± 0.266	
22			1.823 ± 1.354	2.261 ± 0.772	
23			1.786 ± 0.637	1.118 ± 0.923	
24			1.312 ± 0.967	1.152 ± 1.092	
25			0.762 ± 0.407	3.039 ± 0.309	
26				1.385 ± 0.779	
27				1.591 ± 0.411	
Disc	**SUTL 612**	**SUTL 614**	**SUTL 615**	**SUTL 616**	**SUTL 617**
1	2.644 ± 0.439	2.796 ± 2.235	0.148 ±0.138	5.949 ± 4.54	5.835 ± 0.737
2	3.408 ± 0.379	2.427 ± 0.728	1.984 ± 1.234	6.183 ± 3.229	6.714 ± 0.948
3	3.248 ± 0.316	1.801 ± 1.604	0.758 ± 0.859	6.267 ± 2.182	6.069 ± 1.241
4	3.289 ± 0.265	1.686 ± 0.334	0.673 ± 4.311	9.88 ± 3.672	6.178 ± 0.832
5	2.709 ± 0.374	1.324 ± 0.993	0.992 ± 0.204	5.866 ± 1.635	5.449 ± 0.486
6	3.365 ± 0.406	1.451 ± 0.887	1.204 ± 0.671	5.904 ± 2.137	5.631 ± 0.765
7	3.49 ± 0.392	1.517 ± 1.962	2.134 ± 1.62	7.307 ± 2.065	5.295 ± 0.613
8	3.32 ± 1.029	1.88 ± 0.657	1.168 ± 0.816	4.655 ± 1.762	9.864 ± 1.689
9	4.712 ± 1.117	1.421 ± 0.295	0.386 ± 0.385	6.878 ± 0.971	6.185 ± 1.041
10	3.078 ± 0.371	1.926 ± 0.517	1.775 ± 0.247	6.14 ± 4.12	6.759 ± 1.147
11	3.322 ± 0.298	1.338 ± 0.286	2.121 ± 0.494	5.864 ± 3.658	6.694 ± 1.908
12	2.972 ± 0.355	1.657 ± 0.365	1.677 ± 0.751	5.585 ± 1.68	7.756 ± 0.871
13	2.799 ± 0.276	1.627 ± 0.813	1.885 ± 0.663	6.011 ± 2.032	7.13 ± 1.144
14	3.283 ± 0.549	1.666 ± 0.394	1.042 ± 0.123	4.626 ±4.244	5.367 ± 0.977
15	3.622 ± 0.445	2.682 ± 3.584	1.976 ± 1.064	4.285 ± 0.898	6.937 ± 1.865
16	3.295 ± 0.501	0.807 ± 0.647	1.407 ± 0.55	7.155 ± 1.594	5.592 ± 1.257
17	3.352 ± 0.779	1.869 ± 0.318	2.924 ± 2.484	7.183 ±1.841	6.071 ± 3.24
18	3.309 ± 0.835	1.285 ± 0.923	1.429 ± 0.48	7.724 ± 1.143	8.8 ± 1.775
19	3.394 ± 3.388	1.293 ± 0.536	0.327 ± 0.381	8.122 ± 4.411	6.787 ± 1.475
20	3.366 ± 0.52	0.891 ± 0.744	1.652 ± 0.453	7.957 ± 1.99	8.12 ± 2.955
21	3.25 ± 1.633		1.494 ± 1.632	6.865 ± 0.835	7.808 ± 3.67
22	3.998 ± 3.482		1.028 ± 0.275	6.334 ± 2.333	7.338 ± 0.943
23	3.667 ± 0.818		1.699 ± 1.168	5.7 ± 2.18	7.014 ± 0.769
24	5.462 ± 2.336		3.124 ± 0.405	6.674 ± 1.031	5.564 ± 3.076
25	3.57 ± 1.063			9.408 ± 1.856	7.185 ± 1.319
26	3.37 ± 0.566			7.506 ± 1.111	
27	4.272 ± 0.81			5.716 ± 1.818	
28	3.291 ± 1.254			7.93 ± 1.033	
29	2.428 ± 0.671			7.45 ± 1.819	
30	3.315 ± 0.456			7.793 ± 1.139	
31	4.497 ± 0.491				

Disc	SUTL 618	SUTL 619	SUTL 886	SUTL 888	SUTL 889
1	0.685 ± 2.878	0.191 ± 0.138	0.245 ± 0.111	0.466 ± 0.172	0.258 ± 0.059
2	0.736 ± 0.742	0.359 ± 0.121	0.158 ± 0.088	0.224 ± 0.282	0.41 ± 0.132
3	0.13 ± 4.021	0.07 ± 0.062	0.108 ± 0.077	0.178 ± 0.147	0.647 ± 0.22
4	1.125 ± 1.589	0.41 ± 0.16	0.127 ± 0.061	0.188 ± 0.165	0.224 ± 0.171
5	0.761 ± 0.768	0.573 ± 2.072	0.698 ± 0.483	0.224 ± 0.206	0.267 ± 0.134
6	0.462 ± 0.443	0.76 ± 0.164	0.401 ± 0.346	0.332 ± 0.182	0.577 ± 0.352
7	2.608 ± 0.998	2.239 ± 1.78	0.1 ± 0.014	0.727 ± 0.337	0.167 ± 0.352
8	1.321 ± 2.501	1.267 ± 2.194	0.337 ± 1.682	0.275 ± 0.31	0.167 ± 0.064
9	0.574 ± 0.606	1.107 ± 0.384	0.083 ± 0.031	0.092 ± 0.051	0.194 ± 0.046
10	0.365 ± 1.735	0.59 ± 1.661	0.356 ± 0.526	0.356 ± 0.284	0.471 ± 0.965
11	1.366 ± 0.79	1.539 ± 1.199	0.893 ± 0.449	0.285 ± 0.169	0.173 ± 0.057
12	1.055 ± 1.516	2.825 ± 4.909	0.106 ± 0.098	0.221 ± 0.048	0.369 ± 0.186
13	1.698 ± 1.451	0.943 ± 2.061	0.223 ± 0.133	0.535 ± 0.493	0.261 ± 0.089
14	1.101 ± 0.854	1.424 ± 0.344		0.21 ± 0.219	0.32 ± 0.104
15	2.701 ± 0.996	1.454 ± 0.501			0.471 ± 0.139
16	0.896 ± 0.764	1.247 ± 1.042			
17	2.429 ± 3.279	1.909 ± 0.868			
18	1.668 ± 2.054				
19	3.516 ± 4.811				
Disc	**SUTL 891**	**SUTL 699**	**SUTL 700**	**SUTL 701**	**SUTL 915**
1	3.293 ± 0.54	0.173 ± 0.028	0.282 ± 0.058	0.302 ± 0.111	1.121 ± 1.773
2	2.747 ± 0.488	0.201 ± 0.032	0.231 ± 0.031	0.222 ± 0.061	0.392 ± 2.497
3	3.183 ± 0.279	0.214 ± 0.024	0.213 ± 0.044	0.204 ± 0.069	0.586 ± 0.332
4	3.1 ± 0.455	0.301 ± 0.227	0.228 ± 0.032	0.242 ± 0.038	1.372 ± 1.408
5	3.26 ± 0.2	0.227 ± 0.039	0.227 ± 0.029	0.253 ± 0.029	1.578 ± 0.535
6	3143 ± 0.257	0.228 ± 0.019	0.225 ± 0.028	0.27 ± 0.043	4.561 ± 7.707
7	2.92 ± 0.423	0.226 ± 0.026	0.246 ± 0.059	0.278 ± 0.037	1.592 ± 0.836
8	2.879 ± 0.226	0.223 ± 0.034	0.155 ± 0.019	0.284 ± 0.031	0.754 ± 0.388
9	3.224 ± 0.334	0.256 ± 0.032			1.218 ± 0.179
10	2.626 ± 0.285	0.23 ± 0.045			
11	2.834 ± 0.184				
12	2.832 ± 0.26				
Disc	**SUTL 919**	**SUTL 920**	**SUTL 922**	**SUTL 924**	**SUTL 1299**
1	1.595 ± 1.361	0.507 ± 2.893	0.744 ± 0.643	1.117 ± 1.039	0.199 ± 2.748
2	1.196 ± 1.367	1.503 ± 2.959	0.116 ± 14.294	1.025 ± 1.191	0.474 ± 0.119
3	0.734 ± 1.587	1.694 ± 2.259	1.072 ± 5.419	1.211 ± 2.15	0.512 ± 2.543
4	1.37 ± 0.475	0.596 ± 0.523		0.353 ± 1.792	1.072 ± 1.643
5	0.711 ± 1.533				0.774 ± 5.087
6	0.937 ±1.418				1.666 ± 0.988
7	0.268 ± 1.986				
8	1.28 ± 0.644				
9	1.797 ± 0.912				
10	0.67 ± 0.782				
11	1.394 ± 1.542				
12	1.382 ± 0.778				
13	0.988 ± 0.819				
Disc	**SUTL 620**	**SUTL 621**	**SUTL 622**		
1	0.997 ± 0.768	5.352 ± 2.775	2.596 ± 2.362		
2	2.25 ± 0.718	4.162 ± 2.482	2.245 ± 2.085		
3	1.337 ± 0.345	2.894 ± 2.558	2.354 ± 0.775		
4	2.129 ± 1.636	4.833 ± 5.736	2.175 ± 1.232		
5	3.354 ± 3.302	5.883 ± 6.771	1.463 ± 1.576		
6	2.476 ± 2.254	2.997 ± 4.555	1.675 ± 1.847		
7	1.647 ± 1.937	4.117 ± 2.448	3.539 ± 0.86		
8	1.478 ± 1.398	2.648 ± 1.012	2.669 ± 0.704		
9	1.873 ± 2.192	6.059 ± 4.608	0.977 ± 1.054		
10	2.97 ± 1.744	4.347 ± 3.178	2.259 ± 1.218		
11	1.897 ± 1.85	3.058 ± 1.901	1.38 ± 0.743		
12	0.578 ± 0.443				
13					
14					
15					